frontiers | Research Topics

Skeletal stem/progenitor cells and their environment in bone regeneration

Edited by
Celine Colnot, Ling Qin, Noriaki Ono and Brya Matthews

Published in
Frontiers in Physiology

ISSN 1664-8714
ISBN 978-2-8325-4363-4
DOI 10.3389/978-2-8325-4363-4

About Frontiers

Frontiers is more than just an open access publisher of scholarly articles: it is a pioneering approach to the world of academia, radically improving the way scholarly research is managed. The grand vision of Frontiers is a world where all people have an equal opportunity to seek, share and generate knowledge. Frontiers provides immediate and permanent online open access to all its publications, but this alone is not enough to realize our grand goals.

Frontiers journal series

The Frontiers journal series is a multi-tier and interdisciplinary set of open-access, online journals, promising a paradigm shift from the current review, selection and dissemination processes in academic publishing. All Frontiers journals are driven by researchers for researchers; therefore, they constitute a service to the scholarly community. At the same time, the *Frontiers journal series* operates on a revolutionary invention, the tiered publishing system, initially addressing specific communities of scholars, and gradually climbing up to broader public understanding, thus serving the interests of the lay society, too.

Dedication to quality

Each Frontiers article is a landmark of the highest quality, thanks to genuinely collaborative interactions between authors and review editors, who include some of the world's best academicians. Research must be certified by peers before entering a stream of knowledge that may eventually reach the public - and shape society; therefore, Frontiers only applies the most rigorous and unbiased reviews. Frontiers revolutionizes research publishing by freely delivering the most outstanding research, evaluated with no bias from both the academic and social point of view. By applying the most advanced information technologies, Frontiers is catapulting scholarly publishing into a new generation.

What are Frontiers Research Topics?

Frontiers Research Topics are very popular trademarks of the *Frontiers journals series*: they are collections of at least ten articles, all centered on a particular subject. With their unique mix of varied contributions from Original Research to Review Articles, Frontiers Research Topics unify the most influential researchers, the latest key findings and historical advances in a hot research area.

Find out more on how to host your own Frontiers Research Topic or contribute to one as an author by contacting the Frontiers editorial office: frontiersin.org/about/contact

Skeletal stem/progenitor cells and their environment in bone regeneration

Topic editors

Celine Colnot — Institut National de la Santé et de la Recherche Medicale, INSERM U955, France

Ling Qin — University of Pennsylvania, United States

Noriaki Ono — University of Texas Health Science Center at Houston, United States

Brya Matthews — The University of Auckland, New Zealand

Citation

Colnot, C., Qin, L., Ono, N., Matthews, B., eds. (2024). *Skeletal stem/progenitor cells and their environment in bone regeneration*. Lausanne: Frontiers Media SA.

doi: 10.3389/978-2-8325-4363-4

Table of contents

frontiers | Frontiers in Physiology

TYPE Original Research
PUBLISHED 04 January 2023
DOI 10.3389/fphys.2022.1083301

OPEN ACCESS

EDITED BY
Celine Colnot,
Institut National de la Santé et de la Recherche Medicale, INSERM U955, France

REVIEWED BY
Brya Matthews,
The University of Auckland, New Zealand
Melanie Haffner-Luntzer,
University of Ulm, Germany

*CORRESPONDENCE
Evan G. Buettmann,
buettmanne@vcu.edu

SPECIALTY SECTION
This article was submitted to Skeletal Physiology, a section of the journal Frontiers in Physiology

RECEIVED 28 October 2022
ACCEPTED 02 December 2022
PUBLISHED 04 January 2023

CITATION
Buettmann EG, Yoneda S, Hu P, McKenzie JA and Silva MJ (2023), Postnatal Osterix but not DMP1 lineage cells significantly contribute to intramembranous ossification in three preclinical models of bone injury. *Front. Physiol.* 13:1083301. doi: 10.3389/fphys.2022.1083301

Postnatal Osterix but not DMP1 lineage cells significantly contribute to intramembranous ossification in three preclinical models of bone injury

Evan G. Buettmann[1,2,3]*, Susumu Yoneda[1], Pei Hu[1], Jennifer A. McKenzie[1] and Matthew J. Silva[1,2]

[1]Department of Orthopaedic Surgery, Washington University in St. Louis School of Medicine, St. Louis, MO, United States, [2]Department of Biomedical Engineering, Washington University in St. Louis, St. Louis, MO, United States, [3]Department of Biomedical Engineering, Virginia Commonwealth University, Richmond, VA, United States

Murine models of long-bone fracture, stress fracture, and cortical defect are used to discern the cellular and molecular mediators of intramembranous and endochondral bone healing. Previous work has shown that Osterix (Osx^+) and Dentin Matrix Protein-1 ($DMP1^+$) lineage cells and their progeny contribute to injury-induced woven bone formation during femoral fracture, ulnar stress fracture, and tibial cortical defect repair. However, the contribution of pre-existing *versus* newly-derived Osx^+ and $DMP1^+$ lineage cells in these murine models of bone injury is unclear. We addressed this knowledge gap by using male and female 12-week-old, tamoxifen-inducible Osx Cre_ERT2 and DMP1 Cre_ERT2 mice harboring the Ai9 TdTomato reporter allele. To trace pre-existing Osx^+ and $DMP1^+$ lineage cells, tamoxifen (TMX: 100 mg/kg gavage) was given in a pulse manner (three doses, 4 weeks before injury), while to label pre-existing and newly-derived lineage Osx^+ and $DMP1^+$ cells, TMX was first given 2 weeks before injury and continuously (twice weekly) throughout healing. TdTomato positive (TdT^+) cell area and cell fraction were quantified from frozen histological sections of injured and uninjured contralateral samples at times corresponding with active woven bone formation in each model. We found that in uninjured cortical bone tissue, Osx Cre_ERT2 was more efficient than DMP1 Cre_ERT2 at labeling the periosteal and endosteal surfaces, as well as intracortical osteocytes. Pulse-labeling revealed that pre-existing Osx^+ lineage and their progeny, but not pre-existing $DMP1^+$ lineage cells and their progeny, significantly contributed to woven bone formation in all three injury models. In particular, these pre-existing Osx^+ lineage cells mainly lined new woven bone surfaces and became embedded as osteocytes. In contrast, with continuous dosing, both Osx^+ and $DMP1^+$ lineage cells and their progeny contributed to intramembranous woven bone formation, with higher TdT^+ tissue area and cell fraction in Osx^+ lineage *versus* $DMP1^+$ lineage calluses (femoral fracture and ulnar stress fracture). Similarly, Osx^+ and $DMP1^+$ lineage cells and their progeny significantly contributed to endochondral callus regions with continuous dosing only, with higher TdT^+ chondrocyte fraction in Osx^+ *versus* $DMP1^+$ cell lineages. In summary, pre-existing Osx^+ but not $DMP1^+$

lineage cells and their progeny make up a significant amount of woven bone cells (particularly osteocytes) across three preclinical models of bone injury. Therefore, Osx$^+$ cell lineage modulation may prove to be an effective therapy to enhance bone regeneration.

KEYWORDS

osteoblast lineage cells, fracture healing, lineage tracing, stress fracture, osteoprogenitor cells, inducible Cre-LoxP recombination

Introduction

Bone is one of the only tissues in the body that can heal with scarless tissue regeneration. This remarkable capacity for self-repair requires a complex, multi-faceted process that involves growth factors, mechanical cues, and unique populations of cells. Based on these environmental factors, bone healing occurs either *via* endochondral or intramembranous ossification. In endochondral ossification, progenitor cells first differentiate and form a cartilage callus that is later replaced by bone. In contrast, intramembranous ossification results in direct bone formation from progenitor cells, bypassing the cartilage intermediate. Although still unclear, studies indicate that endochondral processes are favored in environments with low oxygen tension, vascular disruption, and some micromotion (non-rigid fixation) (Toyosawa et al., 2004; Marsell and Einhorn, 2011; Bahney et al., 2015; Miller et al., 2015). With nearly 5–10% of fractures progressing to delayed healing or non-union (Woolf and Pfleger, 2003; Einhorn and Gerstenfeld, 2015) and resulting in increased medical cost and loss of productivity (Bonafede et al., 2013), understanding the cellular and molecular mediators of both and endochondral and intramembranous ossification following bone injury is paramount.

Preclinical models of bone injury are critical for dissecting the cellular and molecular processes controlling endochondral and intramembranous ossification. The most common injury model used is the transverse, full fracture ("Einhorn model") first developed by Bonnarens and Einhorn (Bonnarens and Einhorn, 1984). This model has been adapted for use in both the tibia and femur of rats and mice (Bonnarens and Einhorn, 1984; An et al., 1994; Zondervan et al., 2018; Buettmann et al., 2019), and utilizes blunt trauma to induce a mid-diaphyseal fracture that is stabilized with an intramedullary rod. Due to the semi-stable nature of fixation, this model heals by periosteal intramembranous woven bone formation near the callus periphery and endochondral ossification near the fracture site, with both woven bone tissue and cartilage visible by day 14 post-injury (Colnot, 2009; Buettmann et al., 2019). Tissue transplantation studies have determined that cells from the periosteum are the primary contributors to callus formation in this model, with smaller contributions from the adjacent skeletal muscle and marrow (Colnot, 2009; Julien et al., 2022). In contrast, the rodent stress fracture model, developed and characterized in our lab, utilizes forelimb cyclic fatigue loading to create a non-displaced ulnar fracture that heals predominantly by periosteal intramembranous woven bone formation 10–14 days post-injury (Hsieh and Silva, 2002; Uthgenannt et al., 2007; Wohl et al., 2009; Martinez et al., 2010). Bulk RNAseq analysis comparing the transverse, full fracture model *versus* stress fracture model in mice indicates that the stress fracture model has a shorter, less pronounced inflammatory phase and a more enriched osteogenic signature (Coates et al., 2019). Another widely used bone repair model is the monocortical defect injury. In this model, a small monocortical defect (0.4–0.8 mm in diameter) is drilled in the mid-diaphysis of the long-bone (Liu et al., 2018; Buettmann et al., 2019; Li and Helms, 2021). Healing progresses after injury with inflammation followed by small amounts of periosteal cartilage callus formation between days 3 and 7 (Hu and Olsen, 2016; Liu et al., 2018). By days 5–10 after injury, intramedullary intramembranous hard callus formation occurs, followed by resolution at days 14–21. Due to the differing healing modalities among these three bone injury models, their simultaneous utilization can provide insights into the unique cellular and molecular mediators of bone healing (Supplementary Figure S1).

Tracking the cellular mediators of bone healing has been aided by the recent development of many tamoxifen-inducible Cre constructs (Cre_ERT2) that can be crossed with fluorescent transgenic reporters (Ai9, Ai14, mTmG, YFP, etc.), allowing for longitudinal tracking of targeted cell populations that contribute to fracture healing *in vivo* (Feil et al., 2009; Madisen et al., 2010; Abe and Fujimori, 2013; Seime et al., 2015). The emerging role of different skeletal stem cells in fracture repair has been reported by numerous groups and was reviewed recently (Serowoky et al., 2020). We have focused on cells at the later stage of the osteoblast lineage (Osx and later), and used continuous tamoxifen dosing to demonstrate that Osx$^+$ lineage cells and their progeny (labeled in Osterix Cre_ERT2 (Maes et al., 2010) Ai9 (Madisen et al., 2010) mice) contributed greater cell numbers than DMP1$^+$ lineage cells (labeled in Dentin Matrix-Protein 1 Cre_ERT2 (Powell et al., 2011) Ai9 (Madisen et al., 2010) mice) and their progeny to woven bone formation in femoral transverse, ulnar stress fracture, and tibial cortical defects (Buettmann et al., 2019). However, because cells were labeled before and during healing by continuous tamoxifen, we could not determine the contribution of pre-existing *versus* newly differentiated Osx$^+$ and DMP1$^+$ lineage cells and their progeny (herein labeled Osx$^+$ or DMP1$^+$ lineage cells) to fracture callus tissues. More

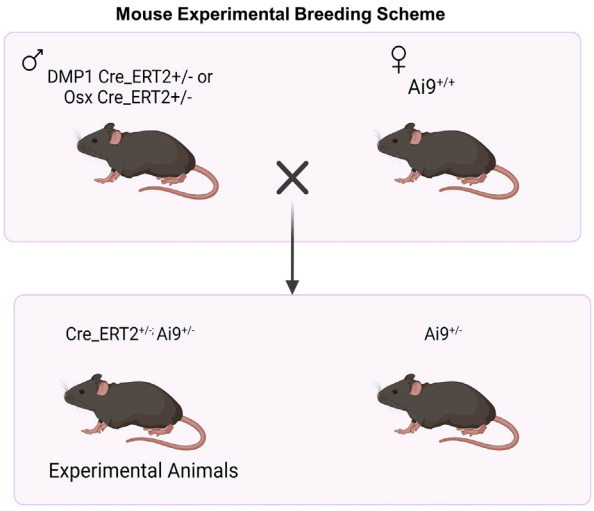

FIGURE 1
Breeding Strategy for Osx$^+$ and DMP1$^+$ Osteoblast Cell Lineage Analysis. For experimental animal generation, male mice hemizygous for inducible Cre (Cre_ERT2$^{+/-}$) were crossed to female mice containing homozygous Ai9 alleles (Ai9$^{+/+}$). Male and female mice hemizygous for Osx or DMP1 Cre_ERT2 and containing the Ai9 allele were utilized for experiments. + = presence of transgene; - = absence of transgene. Figure created in Biorender.

recent work by our lab group used pulse-chase labeling strategies and demonstrated that pre-existing Osx$^+$ and DMP$^+$ lineage cells and their progeny contribute significantly to early lamellar bone formation following anabolic (non-damaging) skeletal loading (Zannit and Silva, 2019; Harris and Silva, 2022). Interestingly, we observed that these lineage-labeled cells, especially DMP1$^+$ lineage cells, are rapidly depleted from the periosteal bone surface when a higher loading stimulus induces woven bone formation (Zannit and Silva, 2019; Harris and Silva, 2022). Together these data indicate that Osx$^+$ and DMP1$^+$ lineage cells play a role in load-induced bone formation and bone healing, however the relative contributions of pre-existing *versus* newly-derived Osx$^+$ and DMP1$^+$ lineage cells and their progeny across various bone injury types remains poorly defined.

Using both continuous and pulse-chase tamoxifen dosing strategies, we sought to determine the role of pre-existing and/or newly-differentiated Osx$^+$ and DMP1$^+$ lineage cells and their progeny in three pre-clinical models of bone repair: transverse femoral fracture, ulnar stress fracture and tibial cortical defect (Supplementary Figure S1). Due to the wider resident bone cell population reported to be targeted with Osx Cre_ERT2 construct (Maes et al., 2010), we hypothesized, that pre-existing Osx$^+$ lineage cells target a greater portion of woven bone regions *versus* pre-existing DMP1$^+$ lineage across all three injury models. Furthermore, we hypothesized that lineage-labeled cells in woven bone callus would be significantly increased with continuous dosing compared to pulse dosing in both Osx Cre_ERT2 Ai9 and DMP1 Cre_ERT2 Ai9 mice.

Methods

Mouse lines

All mouse breeding and experimental protocols were approved by Washington University in St. Louis IACUC. Mouse lines including Osx Cre_ERT2 (Maes et al., 2007), DMP1 Cre_ERT2 (Powell et al., 2011), and Ai9 (RCL-tdTomato) (Madisen et al., 2010) were previously generated and described. Osx Cre_ERT2 and DMP1 Cre_ERT2 breeders were shared from the laboratories of Drs. Henry Kronenberg and Paola Pajevic, respectively. Ai9 (RCL-tdT; Catalog #007909) breeders were purchased from Jackson Laboratories. All mice were obtained from a previously backcrossed C57BL/6J line. To generate inducible Cre reporter mice, male mice hemizygous for Cre were crossed to female mice containing homozygous Ai9 alleles (Figure 1).

Experimental overview and tamoxifen dosing timeline

Tamoxifen (TMX) was mainly administered by oral gavage dissolved in corn oil (Sigma-Aldrich, CAS #10540-29-1; 100 mg/kg). In an initial cohort of mice (~10% of study), TMX was given by chow diet (ENVIGO TD. 130859; ~40 mg/kg daily) for continuous dosing strategies but later discontinued in favor of gavage dosing. We did not observe differences in TdTomato expression during bone healing between tamoxifen administration methods when used continuously (data not shown). Experimental mice harboring Osx Cre_ERT2$^{+/-}$; Ai9$^{+/-}$ ($^+$ = presence of transgene;$^-$= absence of transgene) or DMP1 Cre_ERT2$^{+/-}$; Ai9$^{+/-}$ and given TMX served as Cre reporter mice and are labeled as Osx^{TMX} and DMP1^{TMX}, respectively (Table 1). Mice harboring Cre and Ai9 alleles and only given the vehicle corn oil or chow without tamoxifen were used to assess Cre non-inducible recombination (i.e. "leakiness") and are labeled as Osx^{VEH} or DMP1^{VEH}, respectively. To label pre-existing Osx$^+$ and DMP1$^+$ lineage cells (and their progeny) as well as newly-derived Osx$^+$ and DMP1$^+$ lineage cells and their progeny after bone injury, mice were given TMX continuously (2x weekly; 100 mg/kg) starting at 2 weeks before injury and throughout healing (Figure 2). These mice are referred to as Osx^{TMX};Continuous and DMP1^{TMX};Continuous groups, respectively. To label only pre-existing Osx$^+$ and DMP1$^+$ lineage cells (and their progeny), mice were given three TMX doses 4 weeks before bone injury at 8 weeks of age (Figure 2). These mice are referred to as Osx^{TMX};Pulse and DMP1^{TMX};Pulse groups, respectively. We have previously reported residual tamoxifen effects on bone formation are negligible following a 4-week clearance time (Zannit and Silva, 2019). Male and female mice were used as available and in approximately equal numbers among experimental groups. We utilized both males and females

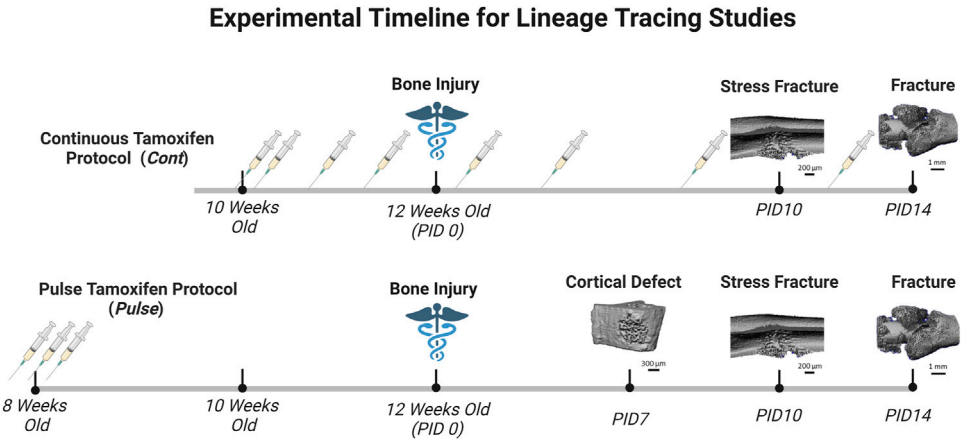

FIGURE 2
Timeline of Pulse Versus Continuous Dosing During Bone Repair. Mice were either given tamoxifen by oral gavage (syringe icon in Figure 2) (TMX; 100 mg/kg) continuously (2 days/wk) starting at 10 weeks old, or pulsed with TMX for three consecutive days starting at 8 weeks old. Then mice underwent bone injury *via* semi-stabilized femoral fracture, ulnar stress fracture or tibial defect injury at 12 weeks. Mice were sacrifice at pre-defined timepoints corresponding with robust woven bone formation for each injury model (microCT reconstruction for woven bone; day 7 defect; day 10 stress fracture; day 14 femoral fracture). Days post-injury (PID) are subsequently labeled. Figure created in Biorender.

TABLE 1 Overview of experimental groups.

Mouse genotype	Treatment(100 mg/kg)	Abbreviation
Osx Cre_ERT2$^{+/-}$; Ai9$^{+/-}$	Tamoxifen in Corn Oil	Osx^{TMX}
Osx Cre_ERT2$^{+/-}$; Ai9$^{+/-}$	Vehicle (Corn Oil)	Osx^{VEH}
DMP1 Cre_ERT2$^{+/-}$; Ai9$^{+/-}$	Tamoxifen in Corn Oil	DMP1^{TMX}
DMP1 Cre_ERT2$^{+/-}$; Ai9$^{+/-}$	Vehicle (Corn Oil)	DMP1^{VEH}

in this study since both mouse sexes have been readily utilized in these inducible Cre lines in previous literature (Buettmann et al., 2019; McKenzie et al., 2019; Harris and Silva, 2022). Mice were group housed under a standard 12-h light/dark cycle and given access to food and water *ad libitum*.

Models of bone repair

For each bone repair model, the right limb was injured whereas the left contralateral limb served as the uninjured control. Mice were given buprenorphine SR LAB (1 mg/kg, s.c.) one hour before injury, and anesthetized during all procedures with isoflurane (1–3% v/v). The right limb was shaved and sterilized with betadine and alcohol (70%) before surgery. Following all bone injury procedures, mice were returned to their cage and placed on electronic heating pads (BeanFarm; Ultratherm) until awake and sternal. Mice were monitored daily for signs of pain and distress and open wounds were quickly resutured and treated with topical triple antibiotic ointment.

Femoral semi-stabilized transverse fracture

Right femurs were prepared for fracture as previously described (McBride-Gagyi et al., 2015; McKenzie et al., 2018). Briefly, a complete (full) transverse bone fracture was made in the femoral mid-diaphysis *via* three-point bending using a custom designed fixture on a materials testing machine (Instron, DynaMight 8841). The fracture was stabilized with a 24-gauge stainless steel pin (Microgroup, #304 H24RW) and the wound sutured with 3–0 nylon sutures in a simple interrupted pattern (Ethicon, #1669H). Immediately after fracture, lateral radiographs at ×3 magnification (Faxitron, Ultrafocus 100) were taken to verify proper fixation of the fracture site. Mice were allowed to heal for 14 days post-injury (PID 14), when the intramembranous woven bone on the callus periphery and cartilage undergoing endochondral ossification near the

fracture line are both visible (Supplementary Figure S1) (Einhorn and Gerstenfeld, 2015; Buettmann et al., 2019).

Ulnar stress fracture

Right ulnas had a stress fracture generated as previously described (Martinez et al., 2010; Buettmann et al., 2019). Briefly, a non-displaced (partial) stress fracture was made in the ulnar mid-diaphysis *via* fatigue loading by cyclic compression on a material testing machine (Instron, DynaMight 8841). Right forelimbs were loaded at a calibrated peak force of 3.1 N to a 50% increase in cyclic displacement from the 10th cycle of loading. Previous work has shown that loading to this average cyclic displacement level in similarly aged wildtype C57BL/6J mice produces a reproducible non-displaced crack on the compressive surface (Buettmann et al., 2019). Mice were allowed to heal for 10 days post-injury (PID 10), when the woven bone response, predominantly formed *via* periosteal intramembranous ossification, is maximal (Supplementary Figure S1) (Uthgenannt et al., 2007; Martinez et al., 2010).

Tibial cortical defect

The right tibia was prepared as previously described (Kim et al., 2007; Liu et al., 2018). Briefly, a 0.78 mm monocortical circular defect was made using a #68 sterilized drill bit attached to a Dremel tool (Bosch Tool Group, Model 395). It was centered on the anterior medial cortex of the tibia and was located 4.3 mm from the tibial plateau. Following drilling, the cortical defect was irrigated with sterile saline with the wound closed using 5-0 nylon sutures (McKesson, #1034511). Mice were allowed to heal for 7 days post-injury (PID 7), when the woven bone response, formed *via* intramembranous ossification, encompasses the entire localized marrow space (Supplementary Figure S1) (Uthgenannt et al., 2007; Martinez et al., 2010).

Frozen histology

Injured and contralateral uninjured limbs were harvested at previously mentioned timepoints (transverse femoral fracture–PID14, ulnar stress fracture–PID10, tibial cortical defect–PID7) and immediately fixed in 4% paraformaldehyde (Electron Microscopy Sciences; #15710) for 24 h. A small subset of transverse femoral fracture femurs (injured + contralateral) were also harvested at days 5 (pulse TMX dosing strategy) and day 7 (continuous TMX dosing strategy) to investigate Osx^+ and $DMP1^+$ lineage cells in the rapidly expanding periosteum and mesenchyme before robust woven bone formation. All specimens underwent standard decalcification for 14 days (14% EDTA, pH 7.0) and subsequent tissue processing (30% sucrose infiltration) followed by embedding and freezing in O.C.T. Compound (Tissue-Tek®; #25608-930). Sections were cut longitudinally at a thickness of 5 μm using the Leica CryoJane Tape-Transfer System and stored at −80°C until use.

Imaging and TdTomato quantification

Slides were rehydrated in deionized water, counterstained using DAPI (Sigma-Aldrich, #D9542, 1:1,000 in DiH_20), and mounted with Fluoromount aqueous mounting media (Thermo Fisher Scientific, #00-4958-02). Sections were subsequently imaged under consistent exposure settings for DAPI and TRITC signal at 20–40× magnification by the Nanozoomer Digital Slide Scanning System (Hamamatsu, S360 System). Images containing both channels (DAPI; TdTomato) were exported using NDP. viewer2 (Hamamatsu, #U12388-01) software with consistent image settings (Contrast = 200%; γ = 1.8).

Contralateral uninjured femur analysis

40X images were randomly taken from each cortical diaphyseal quadrant (ROIs: anterior-proximal; anterior-distal; posterior-proximal; posterior-distal) from uninjured D7 and D14 continuous TMX and vehicle mice from each Cre_ERT2 line. We did not see any differences in TdTomato expression (Cre activation) between uninjured D7 and D14 images. Images were blinded and manually counted for TdTomato positive (TdT^+) osteocytes, periosteal labeled surface and endosteal labeled surface using the FIJI (Schindelin et al., 2012) ROI manager and cell counter plug-in. TdTomato positive (TdT^+) cells were normalized to total number of osteocytes or endosteal/periosteal bone surface length for their respective indices. Indices for all four cortical ROIs were averaged on each specimen for final data statistical analysis. 20x images from the femoral mid-diaphysis and distal femoral growth plate were also captured to qualitatively determine relative targeting of skeletal muscle, marrow cells, and chondrocytes based on cellular morphology and anatomical location (Supplementary Figure S2).

PID14 femur fracture analysis

Woven Bone (Intramembranous Region): Any tissue between the skeletal muscle and cortical bone was considered callus tissue. 40X images were randomly taken from two woven bone regions in the callus (~2.5–3 mm peripheral to the fracture site), one on the anterior side of the bone and the other on the posterior side. Images were blinded and manually counted for TdTomato positive (TdT^+) osteocytes within woven bone (Wo.B). Osteocytes were counted as any cell within the woven bone (Wo.B) tissue, excluding the bone surface and adjacent marrow spaces (marked by clusters of overlapping cells). The multi-layered outline of cells encompassing the perimeter of the woven bone (i.e. expanded periosteal perimeter) was also manually counted for TdT^+ cells using the FIJI (Schindelin et al., 2012) ROI manager and cell counter plug-in. Both

indices were normalized to total Wo. B osteocytes and callus perimeter length, respectively. TdT$^+$ cellular area was also computed automatically by FIJI as per previous methods and normalized to total callus area (Wang et al., 2019; Shihan et al., 2021). In brief, TdT$^+$ cell area was counted automatically by collecting data only on the red channel (split channel function), thresholding to make the image binary (threshold 190), and calculating the thresholded area (particle analysis–no restrictions on size/circularity).

Cartilage (Endochondral Region): 40X images were randomly taken from two cartilage regions anterior and posterior to the fracture site away from the mineralizing woven bone front. TdT$^+$ cartilage cellular area was also computed automatically by FIJI as per exact methods listed for the woven bone region and normalized to total cartilage area. TdT$^+$ cartilage cells per total cartilage cells were calculated for the same images by splitting the red and blue channels, and using particle analysis to automatically count the ratio of TdT$^+$ to DAPI$^+$ cells. In brief, TdT$^+$ cells were counted by binary thresholding (threshold 190), discretizing overlapping cells by watershed analysis, and running particle analysis (size: 20–200 microns; circularity: 0.2-1.0). DAPI$^+$ cells were counted by binary thresholding (threshold 150), discretizing overlapping cells by watershed analysis, and running particle analysis (size: 20–200 microns; circularity: 0.2-1).

PID10 stress fracture analysis

To complement the woven bone analysis for femoral fracture mice, the periosteal stress fracture callus was also analyzed. For this, 10X images were taken that were centered at the stress fracture crack line of the compressive region of the callus (this ROI encompassed the majority of the callus). Images were blinded and manually counted for TdT$^+$ positive osteocytes within woven bone (TdT$^+$ Wo.B Osteocytes) and TdT$^+$ callus perimeter similar to methods used for the femoral woven bone analysis. TdT$^+$ Wo. B cells were calculated for the same images by splitting the red and blue channels and using particle analysis to automatically count the ratio of TdT$^+$ to DAPI$^+$ cells within the 10X callus region, regardless of location. This cell population included the total number of TdT$^+$ woven bone lining cells, woven bone marrow cells and osteocytes. In brief, TdT$^+$ cells were counted by binary thresholding (threshold 150), discretizing overlapping cells by watershed analysis, and running particle analysis (size: 20–200 microns; circularity: 0.2-1). DAPI$^+$ cells were counted by binary thresholding (threshold 20), discretizing overlapping cells by watershed analysis, and running particle analysis (size: 20–200 microns; circularity: 0.2-1).

PID7 tibial cortical defect analysis

To determine if contributions of pre-existing Osx$^+$ and DMP1$^+$ lineage cells differ following marrow-derived intramembranous bone repair, a small number of mice were given cortical defect injuries following pulse TMX regimens. (Cortical defect experiments were not performed under the continuous TMX protocol.) 10X images were taken centered at the PID7 cortical defect site around the anterior medial surface of the tibia and used to investigate TdT$^+$ cells expression within the intramedullary woven bone.

Statistics

Quantitative outcomes of TdTomato cellular expression per tissue area (woven bone or cartilage), per perimeter (callus or bone), or per cell number were analyzed within each inducible Cre line (Osx or DMP1). Due to the smaller sample sizes used (n = 2-4), data normality was first assessed by Q-Q plots and assumed to be normal if not deviating significantly from a straight diagonal line. Depending on outcome, data was compared by unpaired t-test or ANOVA (normally distributed) or Mann-Whitney or Kruskal–Wallis to test for the significant effects of tamoxifen dosing (continuous, pulse, vehicle) in GraphPad Prism Pro Version 9 (La Jolla, CA). The type of statistical test for each figure is noted in the legend. Direct statistical comparisons between Cre lines were avoided due to potential confounding technical differences in Ai9 recombination efficiency between Osx Cre_ERT2 and DMP1 Cre_ERT2 constructs, which may not reflect accurate changes in biology. Mouse sex was not tested as an independent variable because our study wasn't adequately powered to compute male and female differences (so they were pooled for analysis). For added clarity, data points from male and female mice are represented on graphs as diamonds and circles, respectively as noted in each figure's caption. Post-hoc Tukey's (parametric - ANOVA) or Dunn's (non-parametric - Kruskal–Wallis) were used to determine significance differences between individual groups after accounting for multiple comparisons corrections. Statistical significance was defined as $p < 0.05$ and trending values were denoted as $p < 0.10$. Data are presented as mean ± SD with individual sample sizes for each outcome denoted as data points in each graph and in the figure caption.

Results

Inducible Osx Cre_ERT2 under continuous dosing targets a higher percentage of femoral cortical bone cells in uninjured bones compared to inducible DMP1 Cre_ERT2

Uninjured contralateral femurs were first assessed for TdT$^+$ cells in intracortical osteocytes and bone surfaces at the mid-diaphysis following continuous TMX administration for 4 weeks. Overall, Osx^{TMX};Continuous femurs showed greater targeting of cells compared to DMP1^{TMX};Continuous femurs in

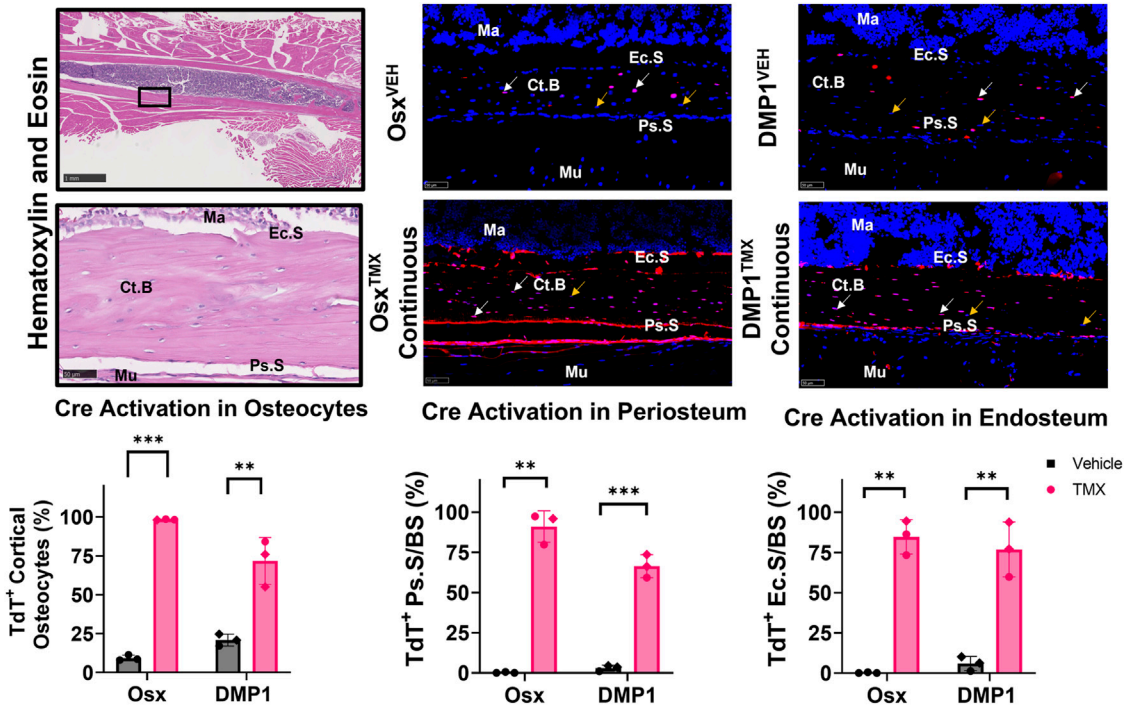

FIGURE 3
Osx Cre_ERT2 has greater diaphyseal cell targeting than DMP1 Cre_ERT2 in uninjured femurs (osteocytes and bone lining cells). 2.5X (scale bar 1 mm) and 40X images (scale bar 50 μm) were randomly taken from each cortical diaphyseal quadrant (Black ROIs) and used for quantification of Cre specificity from uninjured D7 and D14 continuous TMX and vehicle femurs from each Cre_ERT2 line. TdTomato positive (TdT^+) osteocytes (white arrow) were normalized to total number of osteocytes (TdT^+ and TdT^- cells - orange arrow). TdTomato positive endosteal (TdT^+ Ec. S) and periosteal bone surface (TdT^+ Ps. S) were normalized to total bone surface length (BS). Data presented as mean ± SD with $n = 3$ per group. Mouse sex of each data point is represented by shape (circle–female; diamond–male). Effects between continuous and vehicle dosing within each inducible Cre line were compared by Unpaired *t*-test $^*p < 0.05$; $^{**}p < 0.005$; $^{***}p < 0.0005$ Abbreviations: Ma = Marrow; Ct. B = Cortical bone; Mu = Skeletal muscle.

each bone component analyzed (Figure 3). For example, Osx^{TMX}; Continuous femurs had 98% of osteocytes labeled TdT^+ compared to 72% in $DMP1^{TMX}$;Continuous femurs. In addition, Osx^{TMX}; Continuous femurs had 91% and 85% of the periosteal and endosteal surfaces labeled, whereas $DMP1^{TMX}$; Continuous femurs had 66% and 77% of the periosteal and endosteal surfaces labeled, respectively (Figure 3). The majority of TdT^+ labeling was attributed to tamoxifen induction as expected, as both Osx^{TMX};Continuous and $DMP1^{TMX}$;Continuous femurs had significantly increased TdT^+ labeling in all investigated cortical compartments *versus* respective vehicle-treated controls ($p < 0.05$). In the absence of TMX, the periosteal surface and endosteal surface had negligible non-inducible recombination ("leakiness") in either Cre_ERT2 line, however leakiness was readily apparent in intracortical osteocytes. For example, 9.4% of osteocytes were TdT^+ in Osx^{VEH} femurs while in $DMP1^{VEH}$ femurs 21% of osteocytes were TdT^+ (Figure 3).

Qualitative assessment of TdT^+ cell labeling outside the cortical diaphyseal bone in the marrow, skeletal muscle and primary spongiosa was also performed (Supplementary Figure S2). Osx^{TMX};Continuous and $DMP1^{TMX}$;Continuous femurs both showed minimal TdT^+ expression in marrow cells (Supplementary Figure S2; Panel 1). Notably, both $DMP1^{TMX}$; Continuous and $DMP1^{VEH}$ femurs showed robust TdT^+ expression in skeletal muscle cells, indicative of non-inducible recombination at this site (Supplementary Figure S2; Panel 2). Looking at the distal femoral growth plate, a place undergoing endochondral ossification similar to the fracture callus, Osx^{TMX}; Continuous femurs showed greater targeting of growth plate chondrocytes (white arrows) and trabecular bone within the primary spongiosa compared to $DMP1^{TMX}$;Continuous femurs (Supplementary Figure S2; Panel 3). In summary, these results demonstrated that $DMP1^{VEH}$ femurs had greater non-inducible TdTomato expression and hence leakiness in multiple tissue compartments, notably intracortical osteocytes and skeletal muscle, compared to Osx^{VEH}. However following a 4-week period of TMX dosing, Osx Cre_ERT2 caused Cre activation in a greater number of bone cells compared to $DMP1^{TMX}$; Continuous mice, such as intracortical osteocytes, periosteal and endosteal lining cells, and growth plate chondrocytes.

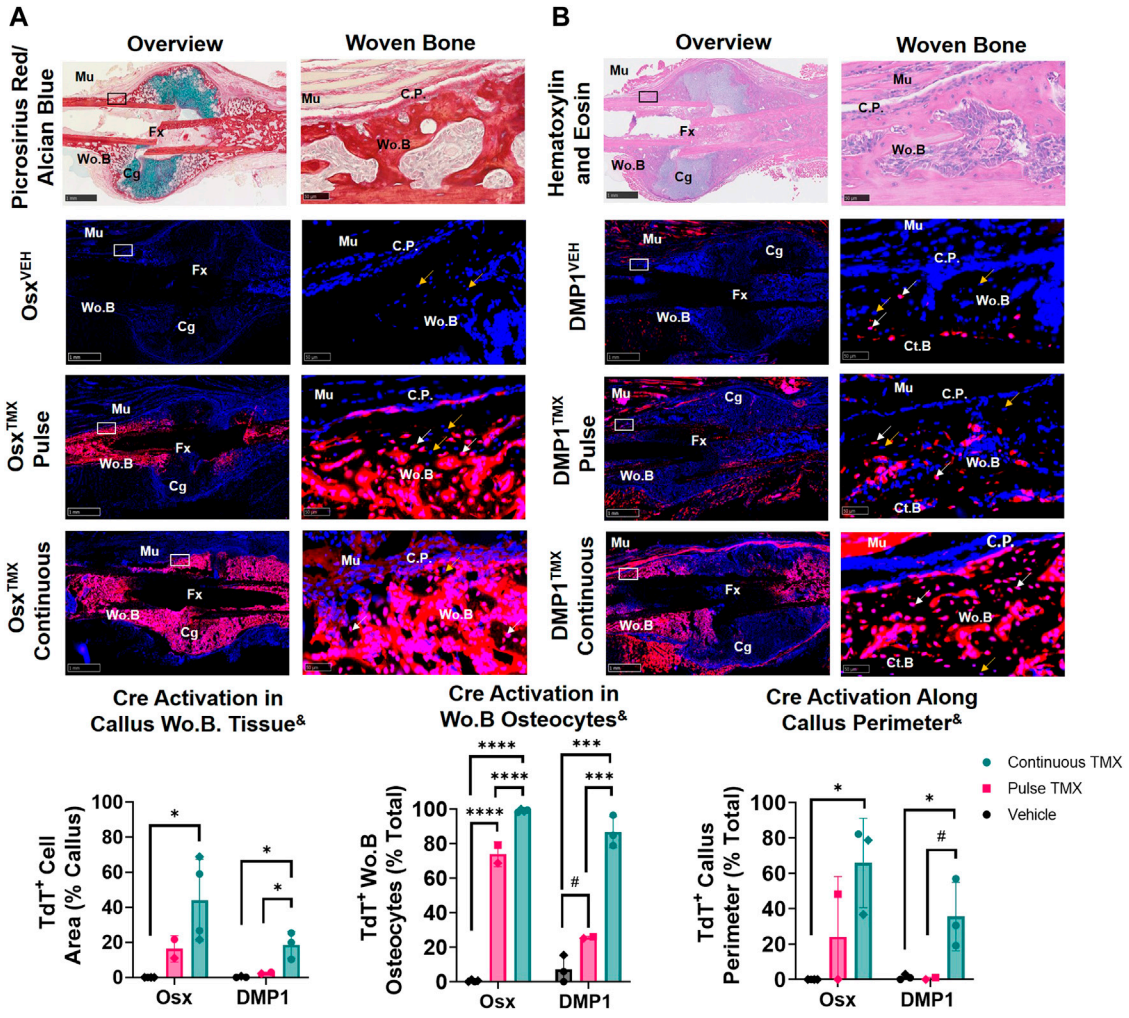

FIGURE 4
Pre-existing Osx$^+$ (panel **(A)**) and DMP1$^+$ (panel **(B)**) lineage cells contribute to varying extents of woven bone osteocytes during transverse fracture healing (intramembranous region). 2.5X (Overview; scale bar 1 mm) and 40X images (woven bone - scale bar 50 μm; black/white ROI boxes) were randomly taken and averaged from two regions of interest at the callus periphery >2 mm from PID14 fracture site (Fx) known to contain predominantly woven bone (Wo.B). TdTomato positive (TdT$^+$) callus area were calculated from automated thresholding for TdT$^+$ area between cortical bone (Ct.B) and skeletal muscle (Mu). Wo.B TdTomato positive (TdT$^+$) osteocytes (white arrow) were normalized to total number of osteocytes (TdT$^+$ and TdT$^-$ cells-orange arrow). TdT$^+$ periosteal callus perimeter was normalized to total callus perimeter length (C.P.). Data presented as mean ± SD with n = 2-4 per group. Mouse sex of each data point is represented by shape (circle–female; diamond–male). $^{\&}$ Significant Tamoxifen Effect by 1-WAY ANOVA. $^{\#}p < 0.10$; $^{*}p < 0.05$; $^{***}p < 0.0005$; $^{****}p < 0.00005$ Significantly Different by Tukey Post-Hoc.

Pulse-chase labeling reveals that pre-existing Osx$^+$ but not DMP1$^+$ lineage cells and their progeny give rise to most intramembranous woven bone osteocytes following femoral fracture

The callus from the fractured femurs was next analyzed for TdTomato expression in woven bone regions at the callus periphery, known to primarily undergo intramembranous ossification, and revealed a large contribution of pre-exisiting Osx$^+$ but not DMP1$^+$ lineage cells. With pulse dosing, Osx^{TMX};Pulse callus had noticeably increased TdT$^+$ stained woven bone area compared to Osx^{VEH} control (16% vs. 0.02%; Figure 4A) but still nearly 3-fold less staining less than Osx^{TMX};Continuous calluses (16% vs. 44%; Figure 4A). Notably, TdT$^+$ osteocytes were significantly more abundant in Osx^{TMX};Pulse calluses (74%) than Osx^{VEH} controls (0.47%) although less abundant than Osx^{TMX}; Continuous femurs (99%, $p < 0.05$; Figure 4A). Lastly, Osx^{TMX}; Pulse femurs also had more TdT$^+$ labeled cells lining the perimeter of the intramembranous woven bone callus compared to Osx^{VEH} (24% vs 0%) but this only reached signficance *versus* vehicle in the Osx^{TMX}; Continuous group (66% vs 0%, $p < 0.05$; Figure 4A). Taken together,

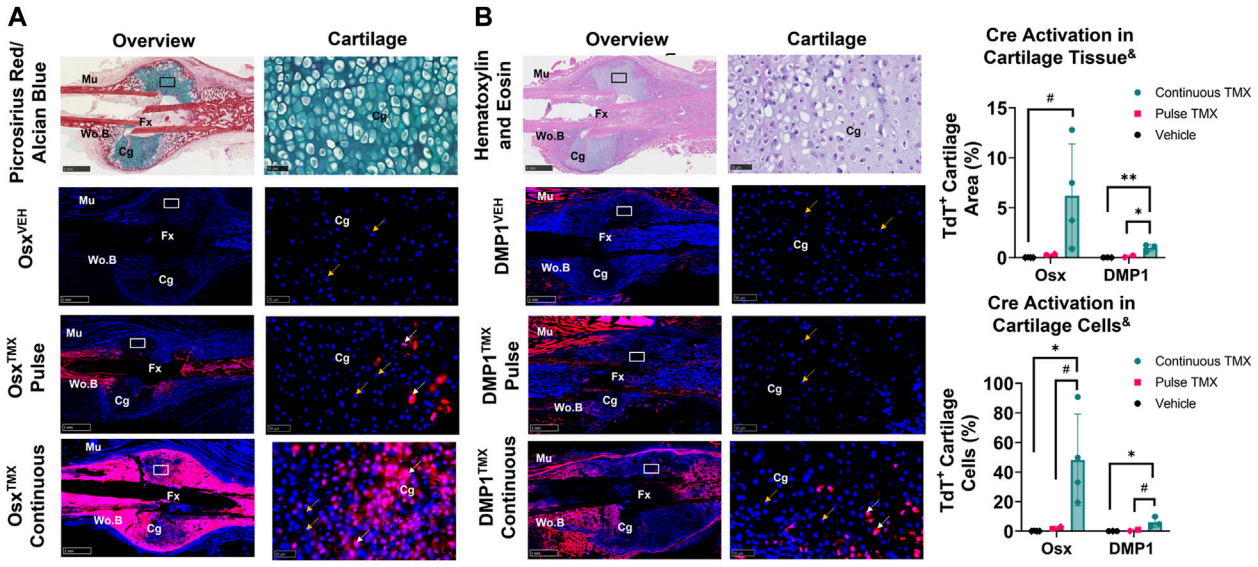

FIGURE 5
Newly-derived but not pre-existing Osx$^+$ (panel **(A)**) and DMP1$^+$ (panel **(B)**) lineage cells and their progeny make up cartilage callus following femoral fracture (endochondral region). 2.5X (Overview; scale bar 1 mm) and 40X images (cartilage - scale bar 50 μm; black/white ROI boxes) were randomly taken and averaged from two regions of interest centered in cartilage regions adjacent to the PID14 fracture site (Fx). TdTomato positive callus area were calculated from automated thresholding for TdT$^+$ area within each field of view. Cartilage TdTomato positive cells (TdT$^+$ Cg cells - white arrow) were thresholded, counted and normalized to total number of DAPI$^+$ chondrocytes (TdT$^+$ and TdT$^-$ cells - orange arrow). Data presented as mean ± SD with n = 2–4 per group. Mouse sex of each data point is represented by shape (circle–female; diamond–male). [&] Significant Tamoxifen Effect by 1-WAY ANOVA. #p < 0.10, *p < 0.05; **p < 0.005; Significantly Different by Tukey Post-Hoc.

these results indicate that pre-existing Osx$^+$ lineage cells and their progeny (identified by pulse-chase labeling) make up about a fifth of intramembranous callus tissue (16%), which is two to three-fold less than the amount labeled by continuous dosing (44%), which captures both pre-existing and newly differentiated Osx$^+$ lineage cells and their progeny. Notably, the majority of intramembranous woven bone osteocytes are derived from pre-existing Osx$^+$ lineage cells and their progeny (74%).

In contrast, DMP1^{TMX}; Pulse calluses demonstrated minimal increases in TdT$^+$ woven bone area that was not significantly different from DMP1^{VEH} controls (2.6% vs. 0.3%; Figure 4B). Moreover, DMP1^{TMX}; Pulse calluses had significantly less TdT$^+$ intramembranous area compared to DMP1^{TMX};Continuous Calluses (2.6% vs 19%; p < 0.05; Figure 4B). Differential TdT$^+$ labeling between DMP1$^{TMX;}$ Continuous and DMP1 $^{TMX;}$ Pulse was even more apparent in woven bone intracortical osteocytes and the callus periphery. For instance, DMP1^{TMX}; Pulse intramembranous calluses showed a trending but non-significant increase in TdT$^+$ osteocytes compared to DMP1^{VEH} controls (26% vs. 7.2%, p < 0.10; Figure 4B) but was signficantly less compared to DMP1^{TMX};Continuous calluses (26% vs. 87%, p < 0.05; Figure 4B). In addition, only DMP1^{TMX};Continuous calluses had signficantly more TdT$^+$ cells lining the periphery of the intramembranous woven bone compared to DMP1^{VEH} (36% vs. 1.3%, p < 0.05; Figure 4B). These DMP1$^+$ lineage results indicate that pre-existing DMP1$^+$ lineage cells contribute minimally to callus formation and only become a small fraction of the total DMP1$^+$ cell lineage population (pre-existing and newly-derived). These pre-existing DMP1 lineage cells only contribute to the initial woven bone osteoblasts and osteocytes (marked by proximity to original cortical bone) during fracture healing.

Comparing Osx and DMP1 Cre_ERT2 models, it appears that most osteocytes within woven bone come from pre-existing Osx$^+$ lineage cells and their progeny and will acquire DMP1$^+$ expression as evidenced by the similar labeling of osteocytes between Osx^{TMX}; Pulse and DMP1^{TMX}; Continuous calluses (74% *versus* 87%). This is further supported when looking at early timepoints of fracture healing such as PID5 and PID7 in pulsed and continuous fracture calluses, respectively (Supplementary Figures S3, S4). For example, by PID5 a greater extent (i.e. longitudinal length) of the expanded periosteum is labeled by pre-existing Osx$^+$ lineage cells than DMP1$^+$ lineage cells (Supplementary Figure S3) resulting in a greater proportion of pre-existing and newly-derived Osx$^+$ lineage cells and their progeny compared to DMP1$^+$ lineage cells and their progeny within woven bone tissue at PID7 (Supplementary Figure S4). Overall, our results indicate that pre-existing Osx$^+$ lineage cells and their progeny, but not DMP1$^+$ lineage cells (and their progeny), contribute to early

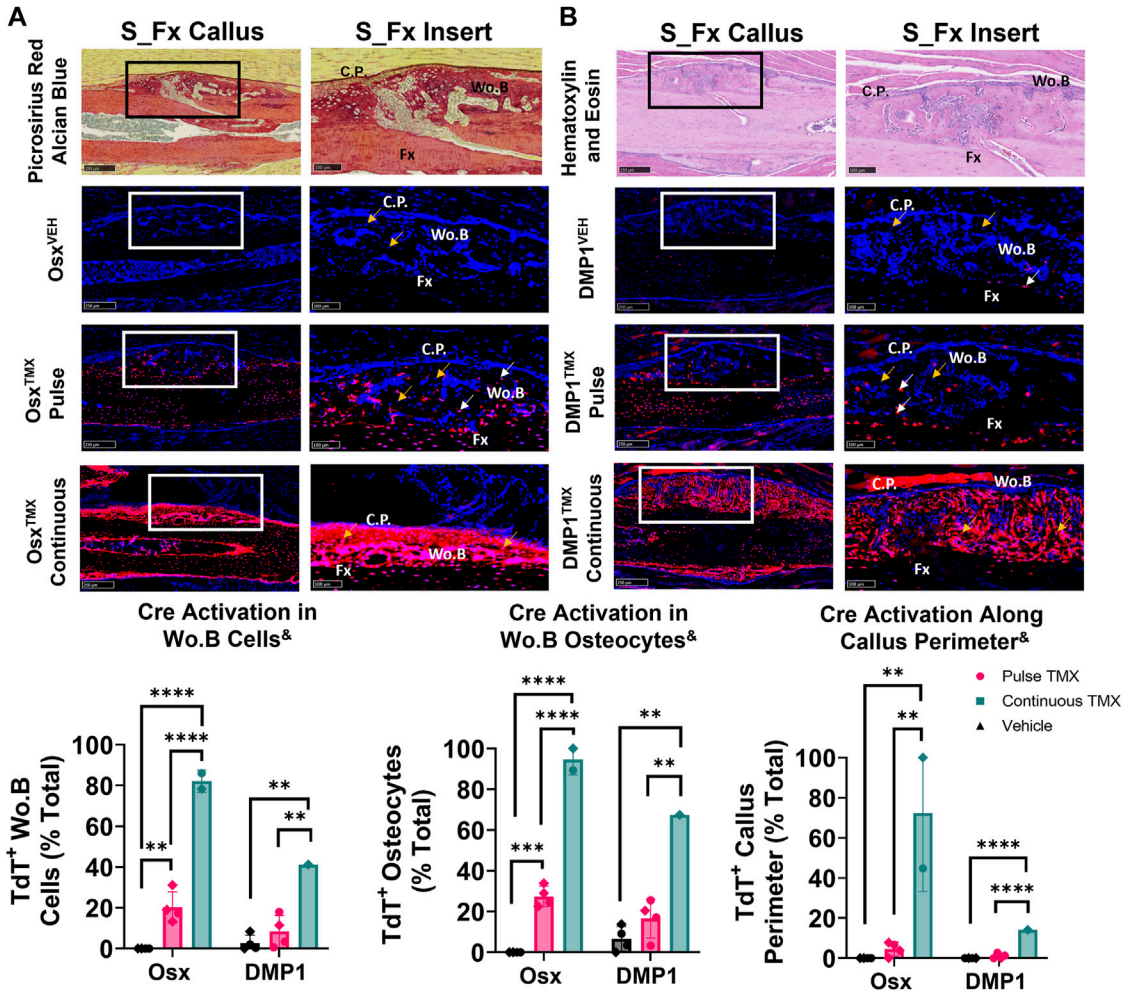

FIGURE 6
Pre-existing Osx$^+$ (panel **(A)**) but not DMP1$^+$ (panel **(B)**) lineage cells and their progeny significantly contribute to woven bone cells during stress fracture. 10X and 20X images (S_Fx insert - scale bar 100 μm) centered around the PID10 stress fracture line (Fx). TdTomato positive cells within the callus were thresholded, counted and normalized to total number DAPI$^+$ callus cells (TdT$^+$ Wo. B Cells). TdTomato positive Wo. B osteocytes (TdT$^+$ Wo. B osteocytes - white arrow) were normalized to total number of osteocytes (TdT$^+$ and TdT$^-$ osteocytes - orange arrow). TdT$^+$ periosteal callus perimeter was normalized to total callus perimeter length (C.P.). Data presented as mean ± SD with n = 1–4 per group. Mouse sex of each data point is represented by shape (circle–female; diamond–male). [&] Significant Tamoxifen Effect by 1-WAY ANOVA. **$p < 0.005$; ****$p < 0.00005$ Significantly Different by Tukey Post-Hoc.

woven bone formation in the fracture callus both by lining new woven bone surfaces and becoming embedded osteocytes.

Newly-derived but not pre-existing Osx$^+$ and DMP1$^+$ lineage cells and their progeny make up cartilage callus following femoral fracture

TdTomato expression in multiple cartilage regions immediately adjacent to the femoral fracture site was averaged to evaluate the role of pre-existing *versus* newly-derived Osx$^+$ and DMP1$^+$ lineage cells and their progeny in endochondral ossification at 14 days post-fracture. Overall, we saw little evidence of pre-existing Osx$^+$ or DMP1$^+$ lineage cells contributing to cartilage formation. For example, with pulse dosing, Osx^{TMX}; Pulse calluses had non-signficant TdT$^+$ stained cartilage callus tissue (0.3% *versus* 0.0%) and cartilage cells (2.3% *versus* 0.1%) compared to Osx^{VEH} control (Figure 5A). However, with continuous tamoxifen dosing there were trending increases in Osx^{TXM};Continuous TdT$^+$ stained callus tissue (6.2 *versus* 0.3%) and cells (48% *versus* 2.3%; $p < 0.10$)

10.3389/fphys.2022.1083301

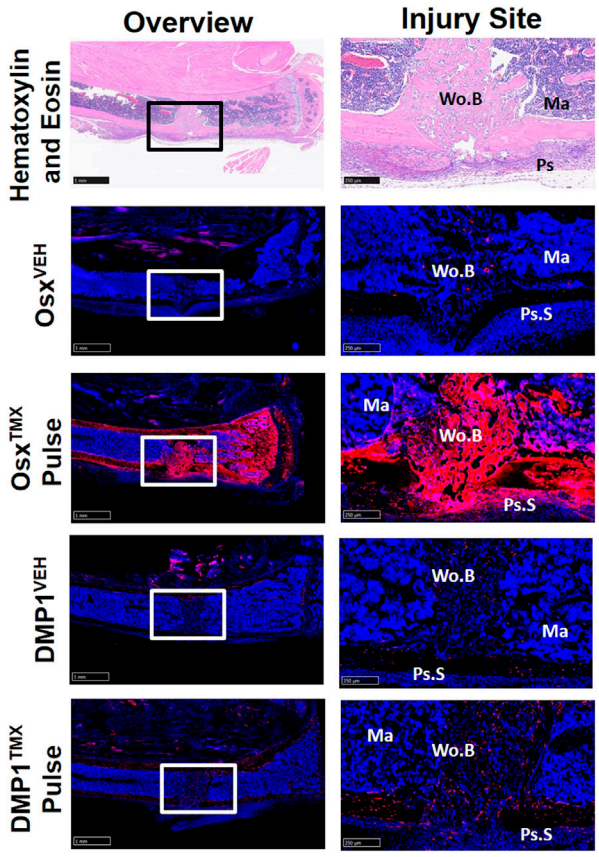

FIGURE 7
Pre-existing Osx$^+$ but not DMP1$^+$ Lineage Cells Contribute to Woven Bone Cells During Cortical Defect Healing. 2.5X images (overview - scale bar 1 mm) and 10X images (ROI at injury site - scale bar 250 μm) centered around the PID7 cortical defect. TdTomato positive (TdT$^+$) cells were highly visible in woven bone (Wo.B) lining cells, osteocytes, damaged marrow (Ma) and expanded periosteal surface cells (Ps.S) from Osx$^{TMX;}$ Pulse mice. DMP1$^{TMX;}$ Pulse mice demonstrated sparse TdT$^+$ signal in woven bone lining cells, osteocytes, and activated periosteal cells.

compared to Osx^{VEH} control (Figure 5A) indicating the majority of Osx$^+$ lineage cartilage cells are newly-derived following fracture.

Similarly, with pulse dosing, DMP1^{TMX}; Pulse calluses had minimal cartilage callus area (0.1% *versus* 0.0%) and cartilage cells (0.7% *versus* 0.0%) targeted compared to DMP1^{VEH} but this was significantly enhanced with continuous tamoxifen expression (Figure 5B). While continuous TMX dosing resulted in significant cartilage labeling compared to vehicle controls in both Cre lines, Osx^{TMX} Continuous femurs, on average, targeted approximately 10-fold more chondrocytes compared to DMP1^{TMX} Continuous femurs (48% *versus* 6.0%). These data indicate that pre-existing Osx$^+$ and DMP1$^+$ lineage cells and their progeny give rise to minimal chondrocytes in the fracture callus. However, it appears that a large portion of total chondrocytes become Osx$^+$ lineage cells once formed in the fracture callus between PID7 and PID14, with an even smaller population of chondrocytes becoming DMP1$^+$ lineage cells near sites of endochondral ossification.

Pre-existing Osx$^+$ but not DMP1$^+$ lineage cells and their progeny contribute a significant but small portion of periosteal woven bone osteocytes following ulnar stress fracture

The ulnar stress fracture model was utilized in each Cre_ERT2 line (Osx and DMP1) with pulse and continuous TMX dosing to further assess the role of each osteoblast cell lineages' contribution to periosteal woven bone intramembranous repair. These results partially mirrored the findings in the intramembranous region of the femoral fracture callus and suggest that pre-existing Osx$^+$ but not DMP1$^+$ lineage cells and their progeny contribute significantly more to woven bone formation following stress fracture. For example, Osx$^{TMX;}$ Pulse stress fracture calluses had signficantly increased TdT$^+$ cells within the woven bone regions of the stress fracture callus compared to Osx^{VEH} control (20% *versus* 0%; $p < 0.05$; Figure 6A). However, the overall TdT$^+$ cell population was significantly less in Osx$^{TMX;}$ Pulse calluses compared to Osx$^{TMX;}$ Continuous Calluses (20% vs 82%; $p < 0.05$; Figure 6A). Stratifying TdT$^+$ cells based on location, the majority of TdT$^+$ cells in Osx$^{TMX;}$ Pulse stress fracture calluses were embedded woven bone osteocytes (24% of Wo. B osteocytes TdT$^+$; $p < 0.05$ compared to 0% in Osx^{VEH}) but not callus peripheral cells in the expanded periosteum (4.6% peripheral cells TdT$^+$; $p > 0.05$ compared to 0% Osx^{VEH}). With continuous TMX dosing, Osx$^{TMX;}$ Continuous calluses showed a significant elevation in TdT$^+$ targeting of woven bone osteocytes (95% of Wo. B osteocytes TdT$^+$; $p < 0.05$) and expanded callus periosteum (72% of peripheral cells TdT$^+$; $p < 0.05$) compared to Osx$^{TMX;}$ Pulse and Osx^{VEH} groups (Figure 6A). These data indicate that pre-existing Osx$^+$ lineage cells and their progeny make up a small but significant portion of total Osx$^+$ lineage cells in intramembranous callus tissue following stress fracture, mainly in the form of woven bone osteocytes. In addition, the majority of intramembranous callus cells acquire Osx$^+$ lineage cell specification after injury.

In contrast, DMP1$^{TMX;}$ Pulse stress fracture calluses showed no significant elevation of TdTomato expression in callus cells (including total cells, osteocytes, or callus perimeter) *versus* DMP1^{VEH} controls (Figure 6B). However, with continuous TMX dosing, DMP1$^{TMX;}$ Continuous stress fracture calluses had significantly elevated TdTomato

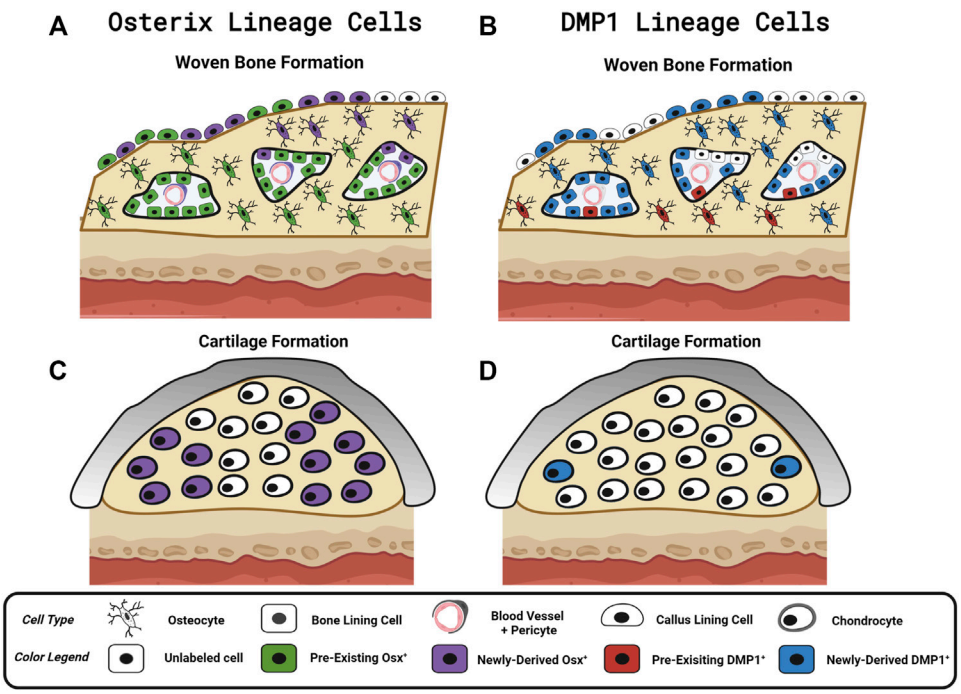

FIGURE 8
Contribution of Osx and DMP1 Cell Lineages to Bone Repair. Model depicting pre-existing (Pulse TMX) and newly-derived (Continuous TMX) Osx and DMP1 cell lineage contributions to woven bone and cartilage formation in response to bone injury. **(A)** Following full fracture, stress fracture, and cortical defect pre-existing Osx$^+$ lineage cells and their progeny (Green) readily become callus lining cells (expanded periosteum), osteocytes and bone lining cells in new woven bone adjacent to the cortical bone surface. Newly-derived Osx$^+$ lineage cells (Purple) then make up the rest of the woven bone osteocytes and woven bone lining cells, including the high cellularity marrow spaces, within the intramembranous ossification region. **(B)** In contrast, pre-existing DMP1$^+$ lineage cells (Red) sparsely populate new woven bone tissue (i.e. woven bone osteocytes and woven bone lining cells). Although the majority of newly-derived post-fracture woven bone osteocytes and woven bone lining cells go on to express DMP1 (Blue), the high cellularity marrow spaces within woven bone (vasculature and pericytes) are not labeled by DMP1 Cre_ERT2. **(C)** Cells in cartilage regions near the femoral fracture site don't arise from pre-existing Osx$^+$ lineage cells or their progeny. With continuous tamoxifen dosing, a high percentage of chondrocytes are labeled by Osx Cre_ERT2. **(D)** Cells in cartilage regions near the femoral fracture site don't arise from pre-existing DMP1$^+$ lineage cells or their progeny. However, with continuous tamoxifen dosing, a small percentage of chondrocytes express DMP1 (less than Osx$^+$ lineage cells). Figure Created in Biorender.

expression in the callus (41% cells TdT$^+$), osteocytes (67% TdT$^+$), and callus perimeter cells (14% TdT$^+$) compared to DMP1$^{TMX;}$ Pulse and DMP1^{VEH} controls (Figure 6B; $p < 0.05$). Comparing Cre lines with continuous dosing, Osx^{TMX}; Continuous had 2-fold greater TdT$^+$ labeling in total stress fracture callus cells *versus* DMP1^{TMX}; Continuous callus (82% vs 41%). Moreover, Osx^{TMX}; Continuous had approximately 1.5-fold greater osteocyte labeling (95% vs. 67%) and nearly 5-fold greater callus peripheral labeling (72% vs. 14%) compared to DMP1^{TMX}; Continuous calluses. Collectively, these data indicate that pre-existing Osx$^+$ but not DMP1$^+$ lineage cells and their progeny contribute a significant number of cells to stress fracture calluses. In addition, although newly-derived Osx$^+$ and DMP1$^+$ lineage cells and their progeny make up the majority of cells in the stress fracture callus, newly-derived Osx$^+$ lineage cells contribute significantly more than newly-derived DMP1$^+$ lineage cells to non-osteocytic populations.

Pre-exisiting Osx$^+$ but not DMP1$^+$ lineage cells and their progeny significantly contribute to cells in the intramedullary woven bone following tibial cortical defect

To investigate the contribution of Osx$^+$ and DMP1$^+$ lineage cells and their progeny in another widely used model of bone repair, a tibial cortical defect was created in Osx^{TMX}; Pulse and DMP1$^{TMX;}$ Pulse mice. With TMX pulsing, TdT$^+$ signal was strongly present in the majority of woven bone cells, including woven bone osteocytes, woven bone lining cells and injured marrow surrounding the defect in Osx^{TMX}; Pulse but not DMP1$^{TMX;}$ Pulse mice (Figure 7). Osx^{VEH} and DMP1^{VEH} defects showed minimal non-inducible expression. In all, this suggests that the majority of woven bone cells following cortical defect arises from pre-existing Osx$^+$ and their progeny but not pre-existing DMP1$^+$ lineage cells and their progeny.

Discussion

We investigated the contributions of pre-existing *versus* newly-derived Osx$^+$ and Dmp1$^+$ lineage cells and their progeny to regenerated tissues in three preclinical models of bone injury using inducible Osx Cre_ERT2 Ai9 and DMP1 Cre_ERT2 Ai9 mice. Using two different tamoxifen dosing regimens: 1) pulse-labeling with washout (4 weeks) before injury or 2) biweekly dosing before (2 weeks) and during bone injury healing, we found across injury models (femoral fracture, ulnar stress fracture, tibial cortical defect) that pre-existing Osx$^+$ lineage cells and their progeny, but not pre-existing DMP1$^+$ lineage cells and their progeny, contributed a significant amount of total TdT$^+$ labeled tissue area and cells *versus* respective vehicle controls (Figure 8). These results support our first hypothesis and demonstrate that pre-existing Osx$^+$ lineage cells and their progeny but not DMP1$^+$ lineage cells and their progeny are a significant source of woven bone forming osteoblasts and osteocytes following bone injury. In addition, continuous tamoxifen administration significantly increased labeling within each inducible Cre line. For example, Osx Cre_ERT2 showing significantly higher targeting of callus tissue with continuous TMX dosing across all scenarios compared to DMP1 Cre_ERT2, supporting our second hypothesis (Figure 8). Importantly, these results suggest that pre-existing Osx$^+$ lineage cells and their progeny are likely critical for postnatal injury-induced bone formation, although their contribution varies based on skeletal site and the type of bone injury.

In the femoral fracture callus at day 14 post-injury, the specific Cre model and tamoxifen dosing regimen led to differential targeting of cells based on callus region. Comparing pulse to continuous dosing allowed us to see the maximum contribution of Osx$^+$ or DMP1$^+$ lineage cells and their progeny to bone healing (pre-existing and newly-derived) within each Cre line. Using this methodology, we saw when comparing Osx^{TMX}; Pulse to Osx ^{TMX}; Continuous, that the majority of Osx$^+$ lineage osteocytes (74% *versus* 99%) and some callus border cells (24% *versus* 66%) and virtually no chondrocytes (2.3% *versus* 48%) were derived from pre-existing Osx$^+$ lineage cells and their progeny (Figure 4A and Figure 5A). Comparing DMP1^{TMX}; Pulse to DMP1^{TMX}; Continuous, we saw that out of all DMP1$^+$ lineage cells involved in femoral fracture, only a small percent of pre-existing DMP1$^+$ lineage cells become osteocytes (26% *versus* 87%), and virtually none become callus border cells (0.5% *versus* 36%) or chondrocytes (0.7% *versus* 6.0%; Figure 4B and Figure 5B). Our DMP1^{TMX}; Pulse results are similar to previous results by Root et al., whom utilized the DMP1 CreERT2; Ai9 mouse crossed to the 2.3 kb Col1 Cre thymidine kinase (tk) mouse (Visnjic et al., 2001) during transcortical fracture healing in 8 week old mice (Root et al., 2020). In this study, the authors used ganciclovir administration (GCV) for 16 days prior to fracture to eliminate the proliferating 2.3Col1 tk$^+$ osteoblast lineage cells, which overlap significantly with pulse-labeled DMP1$^+$ lineage cells (Matic et al., 2016), leaving only transcortical DMP1$^+$ lineage cells prior to injury (Root et al., 2020). Tracing of these pre-labeled transcortical DMP1$^+$ lineage cells following fracture for 7 days revealed minimal contribution of DMP1$^+$ lineage cells to periosteal woven bone, although all DMP1$^+$ lineage cells lining woven bone were 2.3Col1 GFP$^+$, suggesting that they were bone-forming osteoblasts (Root et al., 2020). Similarly, our data also suggest minimal contributions of pre-existing DMP1$^+$ lineage cells (even those that may not be targeted by 2.3Col1 tk) and their progeny to woven bone following transverse fracture.

Looking at Osx and DMP1 CreERT2 lines collectively in our results indicate that pre-existing Osx$^+$ osteoprogenitor lineage cells and their progeny at the time of fracture readily become woven bone callus lining cells, woven bone forming osteoblasts and the majority of embedded osteocytes, whereas pre-existing DMP1$^+$ lineage cells and their progeny are mainly absent from fracture callus tissues (a few become woven bone lining osteoblasts and osteocytes) (Figure 8). Furthermore, the higher percentage of overall Osx$^+$ lineage cells compared to DMP1$^+$ lineage cells in intramembranous callus tissue area (44% *versus* 19%) and chondrocytes (48% *versus* 6.0%), but similar overlap in the percentage of osteocytes (99% *versus* 87%) targeted under continuous dosing regimens suggests that Osx Cre_ERT2 targets a wider population of bone cells that eventually go on to become DMP1$^+$ lineage concurrent with woven bone formation and matrix embedding (i.e. osteocytogenesis in woven bone) (Figure 8). This wider targeting of osteoblast lineage cells using Osx Cre_ERT2 over DMP1 Cre_ERT2 is supported by previously published works that DMP1 is expressed at the mature osteoblast and osteocyte stages of differentiation during matrix mineralization and osteocyte cell embedding (Maes et al., 2007; Lu et al., 2011; Powell et al., 2011; Kim et al., 2012; Kalajzic et al., 2013; Matic et al., 2016; Shiflett et al., 2019).

Based on the continuous dosing regimen labeling pre-existing and newly-derived cells and their progeny, we also found that cells will acquire Osx$^+$ lineage specification and to a lesser degree DMP1$^+$ lineage specification within sites of endochondral ossification at day 14 in the femoral fracture callus (Figure 8). A limitation of this work is that we did not use co-staining to better characterize the identity of these newly-derived Osx$^+$ or DMP1$^+$ lineage cells observed near the cartilage to bone transition zone (e.g., Collagen type II or Collagen X staining). Another limitation is that our study was underpowered to detect differences in these TdT$^+$ cell populations between mouse sexes. As emerging data suggests that mouse sex may differentially regulate the response to tamoxifen (Ceasrine et al., 2019) and lead to biological changes in fracture healing

(particularly cartilage formation) (Haffner-Luntzer et al., 2021), future research is needed to determine if mouse sex significantly alters Cre specificity during bone healing. The similar trends in Cre specificity seen between males and females in our data suggest that mouse sex effects are subtle compared to the tamoxifen dosing regimen and Cre construct used for inducible cell targeting. Non-etheless, the anatomic location of these newly-derived Osx$^+$ and DMP1$^+$ lineage cells and their progeny in both mouse sexes, within the chondrocyte transition zone (near vasculature), are in line with other reports showing that Osx$^+$ lineage cells labeled continuously during fracture healing can demonstrate a hypertrophic chondrocyte phenotype (labeled by Collagen X) (Hu et al., 2017; Buettmann et al., 2019). In addition, DMP1 mRNA has previously been shown via *in situ* hybridization to be weakly expressed in a small number of hypertrophic chondrocytes in the growth plate (Lu et al., 2011) and during fracture repair (Toyosawa et al., 2004). These results, along with our own, are consistent with the trans-differentiation of chondrocytes to osteoblast lineage cells as proposed by others (Bahney et al., 2015; Hu et al., 2017). Our use of pulse-labeling strategies extends these prior results and indicates that chondrocytes likely do not arise from pre-existing Osx$^+$ or DMP1$^+$ lineage cells following bone injury. Therefore, researchers studying conditional gene deletion postnatally during transverse fracture repair would minimize targeting of cartilage cells with Osx Cre_ERT2 or DMP1 Cre_ERT2 mice by using a similar pulse dosing strategy. However, our results differ from Mizoguchi et al., which showed that Osx$^+$ lineage cells labeled at postnatal day 5 (P5), can become fracture callus chondrocytes following bone injury nearly 15 weeks later (Mizoguchi et al., 2014). Overall, this suggests that there is a critical time-window between birth and 8 weeks postnatally in which pre-existing Osx$^+$ osteoprogenitor cells are bipotent *in vivo*.

In order to complement our femoral fracture results, we tested the requirement of pre-existing and newly-derived Osx$^+$ and DMP1$^+$ lineage cells and their progeny to contribute to stress fracture repair. This model heals predominantly by intramembranous ossification (Martinez et al., 2010) and has not been extensively explored in the literature using Cre reporter mice. Our results largely mirror the woven bone results seen at day 14 of healing in the intramembranous region of the femoral fracture callus, with pre-existing Osx$^+$ but not DMP1$^+$ lineage cells and their progeny significantly contributing to callus woven bone cells based on changes from each Cre lines respective vehicle controls (Figure 6). These results reinforce that the stress fracture model largely mirrors the intramembranous processes in the femoral fracture model as we previously reported (Wohl et al., 2009). However, what was striking is that the overall percentage of total Osx$^+$ lineage Wo.B osteocytes labeled in pulse versus continuous dosing was much lower in the stress fracture (~20% total Osx$^+$ lineage Wo.B osteocytes came from pre-existing Osx$^+$ lineage cells) compared to femoral fracture (~75% total Osx$^+$ lineage Wo.B osteocytes came from pre-existing Osx$^+$ lineage cells). In contrast, osteocytes expressing DMP1$^+$ cell lineage between pulse vs. continuous labeling were relatively unchanged (~20–25% total DMP1$^+$ lineage Wo.B osteocytes came from pre-existing DMP1$^+$ lineage cells) between full fracture and stress fracture repair. These findings suggest, that pre-existing Osx$^+$ lineage osteoprogenitors and their progeny contribute less to total callus area and cellularity in the less traumatic ulnar stress fracture than the femoral fracture model. The overall result that pre-existing Osx$^+$ lineage cells contribute more to callus cells than DMP1$^+$ lineage cells with higher degrees of bone damage are consistent with previous reports using anabolic tibial loading at graded force levels (Harris and Silva, 2022), and may potentially reflect the smaller overall cellularity and decreased proliferative processes in stress fracture *versus* full fracture injuries as previously shown (Coates et al., 2019). However, it may also reflect changes in anatomic location (ulna *versus* femur) or slight differences in analysis regions between the two fracture models used in the current study (i.e. majority of callus used to analyze stress fracture vs. callus periphery in transverse fracture).

Despite these differences in pre-existing Osx$^+$ lineage cell recruitment, the full fracture and stress fracture model also show some striking similarities in the types of cells targeted between both inducible Cre drivers. For example, in both models, Osx^{TMX}; Continuous but not DMP1^{TMX}; Continuous labeling results in a strong TdT$^+$ signal within woven bone marrow spaces known as sites of progenitor cell and blood vessel invasion (Figure 4 and Figure 6) that support bone healing (Hausman et al., 2001; Lu et al., 2006; Tomlinson et al., 2013). Furthermore, Osx^{TMX}; Pulse labeling shows much weaker TdT$^+$ signal compared to Osx^{TMX}; Continuous calluses at these woven bone marrow sites. Maes et al. has demonstrated previously that osteoblast precursors labeled instantaneously by Osx Cre (but not Collagen 1 Cre), can take on a pericyte-like profile and co-invade woven bone spaces in the fracture callus, thereby supporting angiogenesis and subsequent bone formation (Maes et al., 2010). This concept was further supported by Buettmann et al., where using continuous dosing in Osx Cre_ERT2 VEGFA$^{fl/fl}$ mice led to decreased femoral fracture and stress fracture angiogenesis and subsequent woven bone formation (Buettmann et al., 2019). Our pulse labeling strategy expands upon these results and suggests that pre-existing Osx$^+$ lineage cells and their progeny, due to reduced TdT$^+$ targeting of Wo.B marrow cells in femoral fracture and ulnar stress fracture, likely do not co-invade with vasculature (neither do more mature DMP1$^+$ lineage cells). Thus, if Osx Cre_ERT2 VEGFA$^{fl/fl}$ mice were pulse-dosed with TMX (rather than continuously dosed as previously performed in Buettmann et al., 2019), we hypothesize that femoral fracture and ulnar stress fracture healing would not be impaired.

Lastly, we showed that pre-existing Osx$^+$ but not DMP1$^+$ lineage cells and their progeny make up a majority of intramedullary woven bone tissue following monocortical defect. In particular, Osx^{TMX}; Pulse showed TdT$^+$ cells

encompassing the majority of woven bone surfaces, osteocytes and even adjacent marrow, whereas these sites were largely void of TdT$^+$ expression in DMP1^{TMX}; Pulse defects (Figure 7). These results indicate that, at 8 weeks age, pre-existing Osx$^+$ lineage cells but not pre-existing DMP1$^+$ lineage cells and their progeny significantly contribute to intramedullary bone formation following cortical defect. Although the exact bone compartment contributing to this differential TdTomato expression is unknown, work by Colnot suggests that both endosteal and marrow derived cellular niches act locally to play a large role in monocortical defect healing (Colnot, 2009). Therefore, it is likely that the pre-existing Osx$^+$ but not pre-existing DMP1$^+$ lineage cells contributing to defect labeling are derived from the endosteum or marrow niche. Although continuous labeling revealed similar endosteal (Figure 3) and minimal marrow (Supplementary Figure S2; Panel 1) targeting in Osx Cre_ERT2 and DMP1 Cre_ERT2 mice, pre-existing lineage cells at these sites were not quantitated in pulse-labeled uninjured specimens, which is a limitation of the current work. Other reports indicate that later pulse labeling (14 days postnatal or after) in Osx Cre_ERT2 and DMP1 Cre_ERT2 labels vascular associated reticular marrow cells and endosteal bone-lining cells that decrease in number over time (Powell et al., 2011; Kim et al., 2012; Park et al., 2012). For example, Matic et al. demonstrated that DMP1$^+$ lineage endosteal bone lining cells decrease by 50–75% 3 weeks following tamoxifen induction (Matic et al., 2016). Therefore, it is possible that the differential Osx$^+$ and DMP1$^+$ lineage cell labeling in the intramedullary woven bone seen in our study is due to a preferential decline in DMP1$^+$ over Osx$^+$ lineage endosteal cells during the 4 weeks between pulse labeling and the cortical defect creation. Another possibility is that Osx Cre_ERT2 targets a marrow or endosteal lineage cell population with higher regenerative capacity overall compared to DMP1 Cre_ERT2. This differential Cre specificity would be in line with previous reports showing that peri-vascular stromal Osx$^+$ lineage cells in the marrow have high regenerative capacity following bone injury (Park et al., 2012; Mizoguchi et al., 2014). Future studies, using dual-labeling strategies, to determine the instantaneous degree of overlap between Osx$^+$ and DMP1$^+$ lineage cells in various bone compartments, would be particularly informative.

In all, we have shown in the current study that pre-existing postnatal Osx$^+$ lineage cells and not pre-existing DMP1$^+$ lineage cells and their progeny contribute significantly to cells populating woven bone in multiple widely used preclinical models of bone injury. This study underscores the importance that pre-existing Osx$^+$ lineage cells play in bone regeneration, especially for early woven bone formation, and suggest that bone targeting therapies to improve healing might target this particular cellular subset. Furthermore, this work provides a tissue and cellular atlas for inducible Cre targeting using the Osx Cre_ERT2 and DMP1 Cre_ERT2 models during bone healing, thereby providing a framework for researchers using these widely available tools in future studies.

Data availability statement

The original contributions presented in the study are included in the article/Supplementary Material, further inquiries can be directed to the corresponding author.

Ethics statement

All animal procedures have been approved by the staff veterinarians of the Washington University in St. Louis Department of Comparative Medicine (DCM) and the Washington University in St. Louis School of Medicine Institutional Animal Care and Use Committee (i.e. WUSTL IACUC).

Author contributions

Study design: MS, JM, EB. Study conduct: EB, JM, PH, SY. Data collection: EB, JM, PH, SY. Data analysis: EB, JM. Data interpretation: EB, JM, SY, PH, MS. Drafting manuscript: EB. Revising manuscript: EB, JM, MS. All authors revised the manuscript critically and approve of the submitted version.

Funding

This work was supported by funding from NIAMS (R01 AR050211 and P30 AR057235) and by the Translational Research Institute for Space Health (TRISH) through Cooperative Agreement NNX16AO69A. Histological images were taken with the Nanozoomer at Alafi Neuroimaging Core (NIH Shared Instrumentation Grant #S10 RR027552).

Acknowledgments

The authors would like to thank the Washington University in St. Louis Musculoskeletal Research Center (MRC) Cores and staff for assistance. Special thanks to Crystal Idleburg for training on frozen decalcified histological processing and sectioning and Madelyn Lorenz on fluorescent frozen histological slide preparation. The authors would also like to thank Heather Zannit, for her assistance in identifying the appropriate tamoxifen pulse-labelling regimen. Histological images were taken with the Nanozoomer at Alafi Neuroimaging Core (S10 RR027552). Inducible Osx Cre-ERT2 were kindly provided by the lab of Henry Kronenberg (Harvard). Inducible Dmp1 Cre-ERT2 from Paola Pajevic (Boston University) were kindly provided by the lab of Alexander Robling (Indiana University Medical School).

Conflict of interest

The authors declare that the research was conducted in the absence of any commercial or financial relationships that could be construed as a potential conflict of interest.

Publisher's note

All claims expressed in this article are solely those of the authors and do not necessarily represent those of their affiliated organizations, or those of the publisher, the editors and the reviewers. Any product that may be evaluated in this article, or claim that may be made by its manufacturer, is not guaranteed or endorsed by the publisher.

Supplementary material

The Supplementary Material for this article can be found online at: https://www.frontiersin.org/articles/10.3389/fphys.2022.1083301/full#supplementary-material

References

Abe, T., and Fujimori, T. (2013). Reporter mouse lines for fluorescence imaging. *Dev. Growth Differ.* 55 (4), 390–405. doi:10.1111/dgd.12062

An, Y., Friedman, R. J., ParenT, T., and Draughn, R. A. (1994). Production of a standard closed fracture in the rat tibia. *J. Orthop. Trauma* 8 (2), 111–115. doi:10.1097/00005131-199404000-00006

Bahney, C. S., Hu, D. P., Miclau, T., and Marcucio, R. S. (2015). The multifaceted role of the vasculature in endochondral fracture repair. *Front. Endocrinol.* 6, 4. doi:10.3389/fendo.2015.00004

Bonafede, M., Espindle, D., and Bower, A. G. (2013). The direct and indirect costs of long bone fractures in a working age US population. *J. Med. Econ.* 16 (1), 169–178. doi:10.3111/13696998.2012.737391

Bonnarens, F., and Einhorn, T. A. (1984). Production of a standard closed fracture in laboratory animal bone. *J. Orthop. Res.* 2 (1), 97–101. doi:10.1002/jor.1100020115

Buettmann, E. G., McKenzie, J. A., Migotsky, N., Sykes, D. A., Hu, P., Yoneda, S., et al. (2019). VEGFA from early osteoblast lineage cells (Osterix+) is required in mice for fracture healing. *J. Bone Min. Res.* 34 (9), 1690–1706. doi:10.1002/jbmr.3755

Ceasrine, A. M., Ruiz-Otero, N., Lin, E. E., Lumelsky, D. N., Boehm, E. D., and Kuruvilla, R. (2019). Tamoxifen improves glucose tolerance in a delivery-sex-and strain-dependent manner in mice. *Endocrinology* 160 (4), 782–790. doi:10.1210/en.2018-00985

Coates, B., McKenzie, J. A., Buettmann, E. G., Liu, X., Gontarz, P. M., Zhang, B., et al. (2019). Transcriptional profiling of intramembranous and endochondral ossification after fracture in mice. *Bone* 127, 577–591. doi:10.1016/j.bone.2019.07.022

Colnot, C. (2009). Skeletal cell fate decisions within periosteum and bone marrow during bone regeneration. *J. Bone Min. Res.* 24 (2), 274–282. doi:10.1359/jbmr.081003

Einhorn, T. A., and Gerstenfeld, L. C. (2015). Fracture healing: Mechanisms and interventions. *Nat. Rev. Rheumatol.* 11 (1), 45–54. doi:10.1038/nrrheum.2014.164

Feil, S., Valtcheva, N., and Feil, R. (2009). Inducible Cre mice. *Methods Mol. Biol.* 530, 343–363. doi:10.1007/978-1-59745-471-1_18

Haffner-Luntzer, M., Fischer, V., and Ignatius, A. (2021). Differences in fracture healing between female and male C57bl/6J mice. *Front. Physiol.* 12, 712494. doi:10.3389/fphys.2021.712494

Harris, T. L., and Silva, M. J. (2022). Dmp1 lineage cells contribute significantly to periosteal lamellar bone formation induced by mechanical loading but are depleted from the bone surface during rapid bone formation. *JBMR Plus* 6 (3), e10593. doi:10.1002/jbm4.10593

Hausman, M. R., Schaffler, M. B., and Majeska, R. J. (2001). Prevention of fracture healing in rats by an inhibitor of angiogenesis. *Bone* 29 (6), 560–564. doi:10.1016/s8756-3282(01)00608-1

Hsieh, Y. F., and Silva, M. J. (2002). *In vivo* fatigue loading of the rat ulna induces both bone formation and resorption and leads to time-related changes in bone mechanical properties and density. *J. Orthop. Res.* 20 (4), 764–771. doi:10.1016/S0736-0266(01)00161-9

Hu, D. P., Ferro, F., Yang, F., Taylor, A. J., Chang, W., Miclau, T., et al. (2017). Cartilage to bone transformation during fracture healing is coordinated by the invading vasculature and induction of the core pluripotency genes. *Development* 144 (2), 221–234. doi:10.1242/dev.130807

Hu, K., and Olsen, B. R. (2016). Osteoblast-derived VEGF regulates osteoblast differentiation and bone formation during bone repair. *J. Clin. Invest.* 126 (2), 509–526. doi:10.1172/JCI82585

Julien, A., Perrin, S., Martinez-Sarra, E., Kanagalingam, A., Carvalho, C., Luka, M., et al. (2022). Skeletal stem/progenitor cells in periosteum and skeletal muscle share a common molecular response to bone injury. *J. Bone Min. Res.* 37 (8), 1545–1561. doi:10.1002/jbmr.4616

Kalajzic, I., Matthews, B. G., Torreggiani, E., Harris, M. A., Divieti Pajevic, P., and Harris, S. E. (2013). *In vitro* and *in vivo* approaches to study osteocyte biology. *Bone* 54 (2), 296–306. doi:10.1016/j.bone.2012.09.040

Kim, J. B., Leucht, P., Lam, K., Luppen, C., Ten Berge, D., Nusse, R., et al. (2007). Bone regeneration is regulated by wnt signaling. *J. Bone Min. Res.* 22 (12), 1913–1923. doi:10.1359/jbmr.070802

Kim, S. W., Pajevic, P. D., Selig, M., Barry, K. J., Yang, J. Y., Shin, C. S., et al. (2012). Intermittent parathyroid hormone administration converts quiescent lining cells to active osteoblasts. *J. Bone Min. Res.* 27 (10), 2075–2084. doi:10.1002/jbmr.1665

Li, Z., and Helms, J. A. (2021). Drill hole models to investigate bone repair. *Methods Mol. Biol.* 2221, 193–204. doi:10.1007/978-1-0716-0989-7_12

Liu, C., Carrera, R., Flamini, V., Kenny, L., Cabahug-Zuckerman, P., George, B. M., et al. (2018). Effects of mechanical loading on cortical defect repair using a novel mechanobiological model of bone healing. *Bone* 108, 145–155. doi:10.1016/j.bone.2017.12.027

Lu, C., Marcucio, R., and Miclau, T. (2006). Assessing angiogenesis during fracture healing. *Iowa Orthop. J.* 26, 17–26.

Lu, Y., Yuan, B., Qin, C., Cao, Z., Xie, Y., Dallas, S. L., et al. (2011). The biological function of DMP-1 in osteocyte maturation is mediated by its 57-kDa C-terminal fragment. *J. Bone Min. Res.* 26 (2), 331–340. doi:10.1002/jbmr.226

Madisen, L., Zwingman, T. A., Sunkin, S. M., Oh, S. W., Zariwala, H. A., Gu, H., et al. (2010). A robust and high-throughput Cre reporting and characterization system for the whole mouse brain. *Nat. Neurosci.* 13 (1), 133–140. doi:10.1038/nn.2467

Maes, C., Kobayashi, T., Selig, M. K., Torrekens, S., Roth, S. I., Mackem, S., et al. (2010). Osteoblast precursors, but not mature osteoblasts, move into developing and fractured bones along with invading blood vessels. *Dev. Cell.* 19 (2), 329–344. doi:10.1016/j.devcel.2010.07.010

Maes, C., Kobayashi, T., and Kronenberg, H. M. (2007). A novel transgenic mouse model to study the osteoblast lineage *in vivo*. *Ann. N. Y. Acad. Sci.* 1116, 149–164. doi:10.1196/annals.1402.060

Marsell, R., and Einhorn, T. A. (2011). The biology of fracture healing. *Injury* 42 (6), 551–555. doi:10.1016/j.injury.2011.03.031

Martinez, M. D., Schmid, G. J., McKenzie, J. A., Ornitz, D. M., and Silva, M. J. (2010). Healing of non-displaced fractures produced by fatigue loading of the mouse ulna. *Bone* 46 (6), 1604–1612. doi:10.1016/j.bone.2010.02.030

Matic, I., Matthews, B. G., Wang, X., Dyment, N. A., Worthley, D. L., Rowe, D. W., et al. (2016). Quiescent bone lining cells are a major source of osteoblasts during adulthood. *STEM CELLS* 34 (12), 2930–2942. doi:10.1002/stem.2474

McBride-Gagyi, S. H., McKenzie, J. A., Buettmann, E. G., Gardner, M. J., and Silva, M. J. (2015). Bmp2 conditional knockout in osteoblasts and endothelial cells does not impair bone formation after injury or mechanical loading in adult mice. *Bone* 81, 533–543. doi:10.1016/j.bone.2015.09.003

McKenzie, J., Smith, C., Karuppaiah, K., Langberg, J., Silva, M. J., and Ornitz, D. M. (2019). Osteocyte death and bone overgrowth in mice lacking fibroblast growth factor receptors 1 and 2 in mature osteoblasts and osteocytes. *J. Bone Min. Res.* 34 (9), 1660–1675. doi:10.1002/jbmr.3742

McKenzie, J. A., Maschhoff, C., Liu, X., Migotsky, N., Silva, M. J., and Gardner, M. J. (2018). Activation of hedgehog signaling by systemic agonist improves fracture healing in aged mice. *J. Orthop. Res.* 37, 51–59. doi:10.1002/jor.24017

Miller, G. J., Gerstenfeld, L. C., and Morgan, E. F. (2015). Mechanical microenvironments and protein expression associated with formation of different skeletal tissues during bone healing. *Biomech. Model. Mechanobiol.* 14 (6), 1239–1253. doi:10.1007/s10237-015-0670-4

Mizoguchi, T., Pinho, S., Ahmed, J., Kunisaki, Y., Hanoun, M., Mendelson, A., et al. (2014). Osterix marks distinct waves of primitive and definitive stromal progenitors during bone marrow development. *Dev. Cell.* 29 (3), 340–349. doi:10.1016/j.devcel.2014.03.013

Park, D., Spencer, J. A., Koh, B. I., Kobayashi, T., Fujisaki, J., Clemens, T. L., et al. (2012). Endogenous bone marrow MSCs are dynamic, fate-restricted participants in bone maintenance and regeneration. *Cell. Stem Cell.* 10 (3), 259–272. doi:10.1016/j.stem.2012.02.003

Powell, W. F., Jr, Barry, K. J., Tulum, I., Kobayashi, T., Harris, S. E., Bringhurst, F. R., et al. (2011). Targeted ablation of the PTH/PTHrP receptor in osteocytes impairs bone structure and homeostatic calcemic responses. *J. Endocrinol.* 209 (1), 21–32. doi:10.1530/JOE-10-0308

Root, S. H., Wee, N. K. Y., Novak, S., Rosen, C. J., Baron, R., Matthews, B. G., et al. (2020). Perivascular osteoprogenitors are associated with transcortical channels of long bones. *STEM CELLS* 38 (6), 769–781. doi:10.1002/stem.3159

Schindelin, J., Arganda-Carreras, I., Frise, E., Kaynig, V., Longair, M., Pietzsch, T., et al. (2012). Fiji: An open-source platform for biological-image analysis. *Nat. Methods* 9 (7), 676–682. doi:10.1038/nmeth.2019

Seime, T., Kolind, M., Mikulec, K., Summers, M. A., Cantrill, L., Little, D. G., et al. (2015). Inducible cell labeling and lineage tracking during fracture repair. *Dev. Growth Differ.* 57 (1), 10–23. doi:10.1111/dgd.12184

Serowoky, M. A., Arata, C. E., Crump, J. G., and Mariani, F. V. (2020). Skeletal stem cells: Insights into maintaining and regenerating the skeleton. *Development* 147 (5), dev179325. doi:10.1242/dev.179325

Shiflett, L. A., Tiede-Lewis, L. M., Xie, Y., Lu, Y., Ray, E. C., and Dallas, S. L. (2019). Collagen dynamics during the process of osteocyte embedding and mineralization. *Front. Cell. Dev. Biol.* 7, 178. doi:10.3389/fcell.2019.00178

Shihan, M. H., Novo, S. G., Le Marchand, S. J., Wang, Y., and Duncan, M. K. (2021). A simple method for quantitating confocal fluorescent images. *Biochem. Biophys. Rep.* 25, 100916. doi:10.1016/j.bbrep.2021.100916

Tomlinson, R. E., McKenzie, J. A., Schmieder, A. H., Wohl, G. R., Lanza, G. M., and Silva, M. J. (2013). Angiogenesis is required for stress fracture healing in rats. *Bone* 52 (1), 212–219. doi:10.1016/j.bone.2012.09.035

Toyosawa, S., KaNataNiN.Shintani, S., KobataM.YukiM.KishinoM., et al. (2004). Expression of dentin matrix protein 1 (DMP1) during fracture healing. *Bone* 35 (2), 553–561. doi:10.1016/j.bone.2004.03.030

Uthgenannt, B., Kramer, M. H., Hwu, J. A., Wopenka, B., and Silva, M. J. (2007). Skeletal self-repair: Stress fracture healing by rapid formation and densification of woven bone. *J. Bone Min. Res.* 22 (10), 1548–1556. doi:10.1359/jbmr.0070614

Visnjic, D., KalajzIc, I., Gronowicz, G., Aguila, H. L., Clark, S. H., Lichtler, A. C., et al. (2001). Conditional ablation of the osteoblast lineage in Col2.3deltatk transgenic mice. *J. Bone Min. Res.* 16 (12), 2222–2231. doi:10.1359/jbmr.2001.16.12.2222

Wang, K., Le, L., Chun, B. M., Tiede-Lewis, L. M., Shiflett, L. A., Prideaux, M., et al. (2019). A novel osteogenic cell line that differentiates into GFP-tagged osteocytes and forms mineral with a bone-like lacunocanalicular structure. *J. Bone Min. Res.* 34 (6), 979–995. doi:10.1002/jbmr.3720

Wohl, G. R., Towler, D. A., and Silva, M. J. (2009). Stress fracture healing: Fatigue loading of the rat ulna induces upregulation in expression of osteogenic and angiogenic genes that mimic the intramembranous portion of fracture repair. *Bone* 44 (2), 320–330. doi:10.1016/j.bone.2008.09.010

Woolf, A. D., and Pfleger, B. (2003). Burden of major musculoskeletal conditions. *Bull. World Health Organ.* 81 (9), 646–656.

Zannit, H. M., and Silva, M. J. (2019). Proliferation and activation of osterix-lineage cells contribute to loading-induced periosteal bone formation in mice. *JBMR Plus* 3 (11), e10227. doi:10.1002/jbm4.10227

Zondervan, R. L., Vorce, M., Servadio, N., and Hankenson, K. D. (2018). Fracture apparatus design and protocol optimization for closed-stabilized fractures in rodents. *J. Vis. Exp.* 138, 58186. doi:10.3791/58186

frontiers | Frontiers in Physiology

TYPE Review
PUBLISHED 02 February 2023
DOI 10.3389/fphys.2023.1087254

OPEN ACCESS

EDITED BY
Celine Colnot,
Institut National de la Santé et de la Recherche Medicale, INSERM U955, France

REVIEWED BY
Noriaki Ono,
University of Texas Health Science Center at Houston, United States
Yuki Matsushita,
Nagasaki University, Japan

*CORRESPONDENCE
Luigi Mancinelli,
LUM39@pitt.edu
Giuseppe Intini,
gii5@pitt.edu

SPECIALTY SECTION
This article was submitted to Skeletal Physiology, a section of the journal Frontiers in Physiology

RECEIVED 02 November 2022
ACCEPTED 19 January 2023
PUBLISHED 02 February 2023

CITATION
Mancinelli L and Intini G (2023), Age-associated declining of the regeneration potential of skeletal stem/progenitor cells. *Front. Physiol.* 14:1087254.
doi: 10.3389/fphys.2023.1087254

Age-associated declining of the regeneration potential of skeletal stem/progenitor cells

Luigi Mancinelli[1,2]* and Giuseppe Intini[1,2,3,4,5]*

[1]Department of Periodontics and Preventive Dentistry, University of Pittsburgh School of Dental Medicine, Pittsburgh, PA, United States, [2]Center for Craniofacial Regeneration, University of Pittsburgh School of Dental Medicine, Pittsburgh, PA, United States, [3]Department of Medicine (Hematology/Oncology), University of Pittsburgh School of Medicine, Pittsburgh, PA, United States, [4]University of Pittsburgh UPMC Hillman Cancer Center, Pittsburgh, PA, United States, [5]McGowan Institute for Regenerative Medicine, University of Pittsburgh, Pittsburgh, PA, United States

Bone fractures represent a significant health burden worldwide, mainly because of the rising number of elderly people. As people become older, the risk and the frequency of bone fractures increase drastically. Such increase arises from loss of skeletal integrity and is also associated to a reduction of the bone regeneration potential. Central to loss of skeletal integrity and reduction of regeneration potential are the skeletal stem/progenitor cells (SSPCs), as they are responsible for the growth, regeneration, and repair of the bone tissue. However, the exact identity of the SSPCs has not yet been determined. Consequently, their functions, and especially dysfunctions, during aging have never been fully characterized. In this review, with the final goal of describing SSPCs dysfunctions associated to aging, we first discuss some of the most recent findings about their identification. Then, we focus on how SSPCs participate in the normal bone regeneration process and how aging can modify their regeneration potential, ultimately leading to age-associated bone fractures and lack of repair. Novel perspectives based on our experience are also provided.

KEYWORDS

skeletal stem/progenitor cells (SSPCs), aging, bone regeneration, Prrx1/Prx1, senescence

1 Introduction

The skeleton is a complex apparatus made of several types of tissues, including bone, endothelium, cartilage, and adipose and hematopoietic tissues. Beyond its primary functions of structural support and movement, the skeleton houses the bone marrow, in which hematopoiesis occurs, and stores or releases minerals (Karsenty and Ferron, 2012). Skeleton, like all the other tissue systems in our body, as time goes by is subjected to a series of detrimental processes which slow down and reduce its physiological functions. Collectively, these processes are defined as "aging". In modern society, the lifespan has increased progressively and, with that, the number of elderly people. As a result, the health burden of bone fractures and skeletal weaknesses has also raised significantly; consequently, scientific interest in skeletal health has increased worldwide. As mentioned, the skeleton is composed of many distinct cell types; yet, skeletal/stem progenitor cells (SSPCs) are fundamental to maintaining and regenerating the skeleton and therefore are the major subject of scientific interest.

To start studying and characterizing the SSPCs' roles in bone homeostasis and diseases, first their identity should be completely unveiled. However, despite various efforts, so far there is no consensus about such identity (Ambrosi et al., 2019). Consequently, we still do not completely understand the basic cellular and molecular mechanisms underlying the bone regenerative

potential and how such potential is affected by aging, leading to impaired healing. This review aims to explore the current knowledge about the aging of SSPCs and their loss of regeneration potential thorough aging. First, we will consider some of the most recent findings about SSPCs' identity. We explore studies performed in both mice and humans, underling the many locations and sources of the SSPCs. These multiple studies suggest that perhaps more than one identity of SSPCs exists, underscoring an heterogeneity in terms of their anatomical location. Then, we focus on the mechanisms of aging that are responsible for the declining of the SSPCs regeneration potential, leading to the age-associated bone weakening, fractures, and impaired repair/regeneration. We describe the significance of employing new technologies, such as single-cell RNA sequencing (scRNA-seq), to better understand the biology of SSPCs, properly identifying them and comparing their functions and disfunctions. Finally, we introduce new perspectives, based on our experience in the field.

2 Identification of SSPCs: A fundamental issue

Stem cells present two fundamental characteristics: the ability to self-renew, which allows for their replenishment, and the capacity to differentiate into multiple cell types, which preside to tissue development and regeneration. Since Haeckel first used the term "stem cell" in the 19th century, these concepts have been largely accepted and experimentally verified, and the scientific community has made significant advancements in this field of research. For instance, stem cells have been identified in different tissues (hematopoietic (Ng and Alexander, 2017), neural (Takagi, 2016), epithelial (Visvader and Smith, 2011), etc.) and somatic cells can now be reprogrammed into pluripotent stem cells (Takahashi and Yamanaka, 2006).

SSPCs were first described simultaneously to the hematopoietic stem cells (HSCs), but their characterization has been much more difficult and controversial than the HSCs, perhaps because of their multiple anatomical locations. All began in the 60' when a series of studies (Tavassoli and Crosby, 1968; Owen and Friedenstein, 1988) showed that bone marrow was able to regenerate bone, stroma and adipocytes, and support hematopoiesis. This ability was imputed to stem cells residing in the bone marrow. It took many years for the bone marrow derived stem cells to earn the name of SSPCs (for a complete revision about the origin of the skeletal stem/progenitor cells name, readers should refer to (Ambrosi et al., 2019)). Before consensus was achieved, SSPCs have been called first "Mesenchymal Stem Cells" (Caplan, 1991) and then "Mesenchymal Stromal Cells" (Dominici et al., 2006); the generic use of these names along with the various assays employed to prove their stem cells qualities, has contributed to generate confusion over the years (Ambrosi et al., 2019).

The employment of powerful and reliable assays is crucial to identify stem cell properties in a putative SSPC population. Such assays should also be changed or updated as new technologies advance. For instance, today it is still common practice to utilize markers that were previously identified and that have not been validated with the new available technologies. With the advent of scRNA-seq, important information and details regarding the transcriptional profile of the analysed cells, which would reveal the expression of genes associated to their regeneration potential and their unique identity, can be unveiled. The ideal scRNA-seq workflow should begin with animal lineage tracing studies that identify putative stem cells. Then, an unbiased and reliable assessment of the transcriptional profile of the putative SSPCs should follow, with the final goal of identifying their surface markers. Once the surface markers have been discovered and validated, SSPCs can be reliably isolated, so that the evaluation and the characterization of their stem cells qualities, both *in vitro* and *in vivo*, can follow (Figure 1). The animal studies should be paralleled by human studies, so that the human homolog putative SSPCs can be isolated, identified, and characterized.

To date, various cell populations, from different regions of the skeleton, have been defined as SSPCs. As mentioned, first came cells isolated from the bone marrow cavity, which many refer to as "mesenchymal stem cells" (MSCs). This is the case, for instance, of Grem1+ cells and Lepr + cells, which have been previously reported to exhibit SSPCs qualities, such as the ability to form bone, cartilage, and adipose tissue (Zhou et al., 2014; Worthley et al., 2015). However, subsequent scRNA-seq analysis revealed lineage biases associated to the identification of these SSPCs (Baryawno et al., 2019; Tikhonova et al., 2019). For instance, expression of Lepr has been demonstrated to mark a wide and heterogeneous population of stromal cells, of which only a subgroup could be considered as authentic SSPCs (Baryawno et al., 2019). Even the expression of Cxcl12, which has been previously shown to largely overlap with the expression of Lepr (Ara et al., 2003), identifies a mixed population of cells that, when needed, for instance upon injury, converts into skeletal stem cell-like (Matsushita et al., 2020). Glioma-associated oncogene 1 (Gli1) is another marker that has been used to identify putative SSPCs of the bone marrow. However, Shy et al. found that Gli1+ cells, which co-express perilipin, a marker of adipocytes, and Lepr, are only present in high quantity in the marrow cavity of mice during embryogenesis (Shi et al., 2017). Postnatally, Gli1+ cells can be found mainly by the trabeculae and the growth plate. Only subsequently, by 9 months of age, Gli1+ cells reappear in the bone marrow, while decreasing by the trabeculae and the growth plate. This finding suggests that the postnatal Gli1+ cells of the bone marrow are stromal cells that derive from the postnatal Gli1+ SSPCs normally residing by the growth plate (Shi et al., 2017). Physiologically, bone marrow residing SSPCs have been described to possess a dual role: to constitute a reservoir of cells of the skeletal lineage for bone growth, and to support hematopoiesis (Bianco et al., 2013; Greenbaum et al., 2013). For instance, bone marrow residing SSPCs expressing CD146, described as adventitial reticular cells (ARCs), have been located by the sinusoids and have been shown to have this dual function (Sacchetti et al., 2007). However, these same studies also described cells that, while representing a reservoir of skeletal cells, are not able to support hematopoiesis (Sacchetti et al., 2007). This finding is also supported by subsequent studies showing that bone marrow residing SSPCs (labelled by the expression of Adiponectin) may have limited functions, as they might only be involved in the repair and regeneration of small and mechanically stable bone defect (Jeffery et al., 2022). A deeper analysis *via* scRNA-seq might be helpful to reveal the exact identity of the bone marrow SSPCs with dual function, to distinguish them from those only able to differentiate in cells of the skeletal lineage.

It is important to note that SSPCs found by the trabeculae and/or the endosteum are sometimes also labelled as SSPCs of the bone marrow. An example is represented by the SSPC population recently characterized by Liu et al. (Liu et al., 2022). These cells, identified by

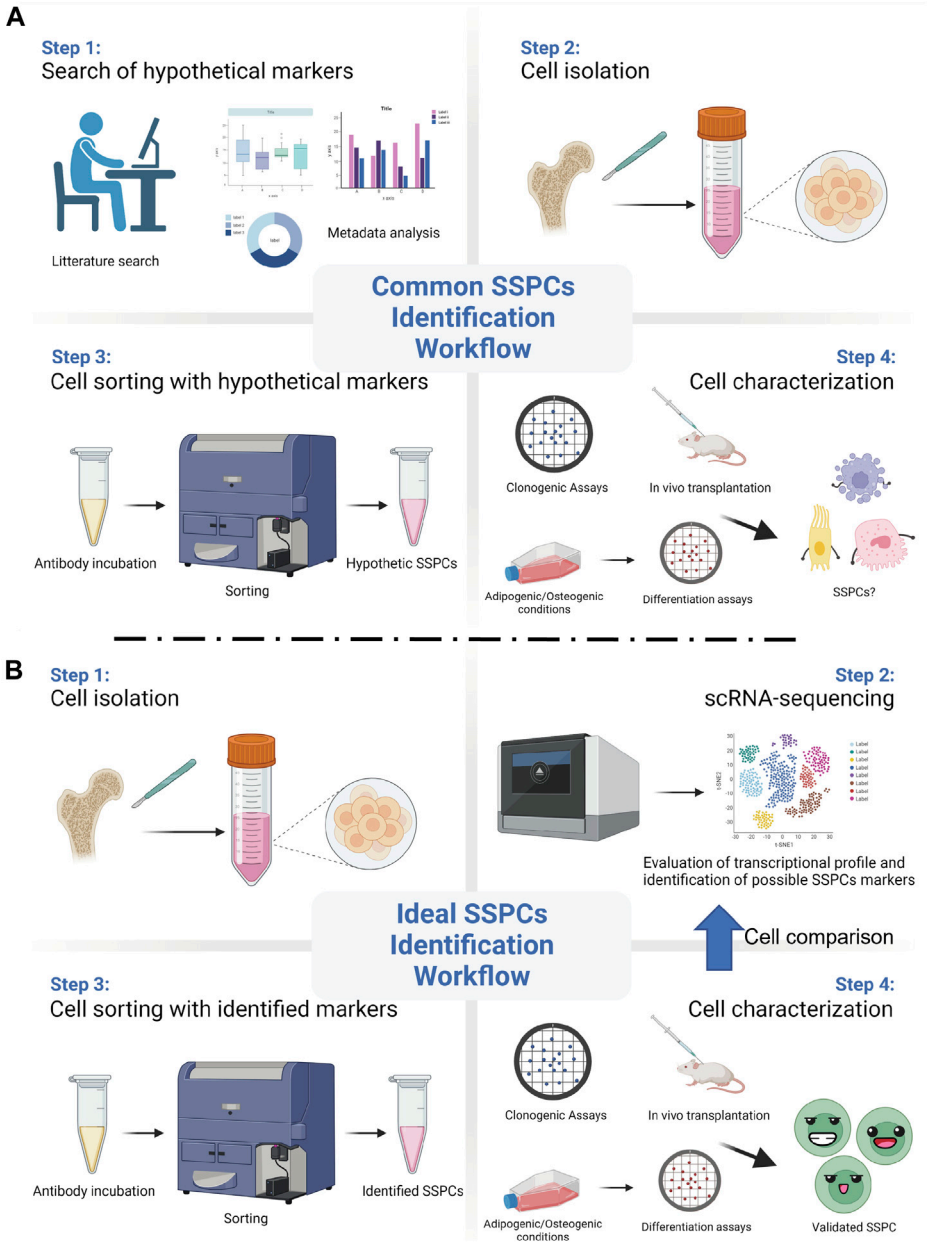

FIGURE 1
Common vs ideal SSPCs identification workflow. **(A)** A common and biased approach starts with the selection of SSPCs markers using previously published data. Then, such markers are used to sort hypothetic SSPCs from the pool of the isolated cells. Different assays are then employed to test the putative SSPCs self-renewal, clonogenic, and differentiation abilities. **(B)** Recent technological advancements, such as single-cell RNA sequencing (scRNA-seq), allows for an unbiased and ideal workflow that starts from the evaluation of the transcriptional profile and the identification of appropriate SSPCs markers right after cell isolation. After sorting them with the identified markers, SSPCs can be tested for their stem cell properties. (*Created with BioRender.com*).

the expression of Paired related homeobox 1 (Prrx1), are defined as "bone marrow Prrx1+ SSPCs" even though they can be found by the trabeculae, the endosteum, and in the bone marrow. In this study the authors showed that genetic ablation of these "bone marrow Prrx1+ SSPCs" leads to an osteoporotic phenotype, reduction of trabecular bone number and bone volume, as well as to impaired bone healing (Liu et al., 2022). Importantly, the authors performed a scRNA-seq analysis of these cells, confirming that they express several markers commonly used to identify SSPCs. However, a scRNA-seq evaluation of the Prrx1 expressing cells isolated exclusively from the bone marrow could have revealed differences, or similarities, between these cells and the Prrx1 expressing cells of the endosteum and the trabeculae. This scRNA-seq approach would identify and validate markers of a specific population of SSPCs, thus providing the opportunity to characterize multiple types of SSPCs (Figure 1).

Being the location where cells in active proliferation mature into osteoblasts, the growth plate, which is responsible for the elongation of the long bones, has been proposed to be another location where SSPCs can be discovered. In fact, similar to what has been shown for the SSPCs of the bone marrow, different population of SSPCs can be found in the growth plate, and, as observed for the SSPCs of the bone marrow, the SSPCs of the growth plate also support bone formation and hematopoiesis

(Chan et al., 2015; Mizuhashi et al., 2018). One of the most referred studies about SSPCs of the growth plate was performed by Chan and colleagues (Chan et al., 2015). Using a "Rainbow mouse" crossed with a mouse carrying a tamoxifen-inducible Cre recombinase under the control of the actin promoter, these authors revealed that within the mouse growth plate there is a clonal region of cells able to form bone, cartilage, and stromal tissue but not muscle, adipose, or hematopoietic tissue (Chan et al., 2015). Then, they isolated from the growth plates putative common progenitor cells by selecting for expression of hematopoietic (CD45 and Ter119), vascular (Tie2), and osteoblastic (Integrin alpha V/ItgaV) markers; they found that cells expressing ItgaV can be fractioned in eight sub-population of cells on the basis of the expression of CD105, Thy, 6C3, and CD200. After testing the ability of these sub-populations to self-renew and give rise to skeletal tissue, and after verifying whether any of these sub-populations was able to generate others, they concluded that CD45-Ter119-Tie2-ItgaV+Thy-6C3-CD105-CD200+ cells are the murine SSPCs of the growth plate. Taking a similar approach, the same authors identified human SSPCs (Chan et al., 2018). Such approach relied on the use of a pre-existing set of markers generated by a metadata analysis to validate the SSPCs' traits of different population of cells. As mentioned above, in reference to the SSPCs identified in the bone marrow, once again an approach utilizing scRNA-seq to identify and validate markers of a putative population of SSPCs may provide the opportunity to widen the search for markers and perhaps identify multiple types of SSPCs (Figure 1). Another noteworthy investigation about SSPCs of the growth plate has been conducted by Mizuhashi et al. (Mizuhashi et al., 2018). This study utilized the panel of SSPCs markers proposed by Chan et al. (Chan et al., 2015) and characterized a unique class of SSPCs, originally unipotent and becoming multipotent at the post-mitotic stage. These cells are characterized by the expression of parathyroid hormone-related protein (PTHrP) and originate from a small subset of PTHrP + chondrocytes precisely located within the resting zone of the post-natal growth plate. The authors tested the self-renew and differentiation abilities of these cells, both *in vitro* and *in vivo*, and claimed their SSPC identity. A further fascinating aspect of these cells is that they are not found during fetal development, as they can be found only after the formation of the growth plate, suggesting that a distinct environment, which could be defined as a niche (see also Section 3.3 hereafter), is required for SSPCs development and self-renewal. Once again, with the final goal of validating a list of genes which could be used to sort and characterize these SSPCs for medical purposes, it would be extremely interesting to investigate through scRNA-seq the complete transcriptional profile of these growth plate SSPCs, characterizing their equalities or differences. Similar findings have been described by Newton and colleagues (Newton et al., 2019), who observed a shift in the clonality of chondrocytes of the growth plate. This shift is accompanied by a marked depletion of chondroprogenitors during the formation of the growth plate, and by the acquisition of self-renewal abilities as soon as the growth plate is formed. To better investigate this phenomenon, the authors used laser capture microdissection and single cell RNA Smart2 sequencing to compare chondroprogenitors isolated at P2 with chondroprogenitors isolated at P28. Interestingly, they found changes in genes related to the extracellular matrix, the oxidative stress, and the regulation of WNT and ERK1/2 pathways (Newton et al., 2019), indicating that gain of stemness is regulated by the niche microenvironment. Furthermore, the authors reported CD73 to be the most upregulated "stem cell surface marker" for these cells, and, consequently, performed experiments using CD73+/CD49e+ cells to study their potential to differentiate in chondrocytes, osteoblasts, and adipocytes (Newton et al., 2019). Leveraging more on the potentials of scRNA-seq analysis could have led the authors to the identifications of additional differences between the P2 and the P28 chondroprogenitor cells.

Another anatomical region that contains dividing cells and that, for this reason, has been of interest in SSPCs research is the periosteum. The periosteum is a thin fibrous membrane that lines the outer surface of bones and is made of fibroblasts, extracellular matrix, blood vessels, nerves, and, in the inner cambium layer, of osteoblasts and SSPCs (for a thorough review of biology and applications of the periosteum, readers may refer to (Lin et al., 2014)). The potential of the periosteum to generate bone after a fracture was firstly reported by Dr. Alexander Watson (Watson, 1845). Additional studies, where loss or damage of the periosteum was associated to lack of fracture repair further supported the initial observations of Dr. Watson (Garcia et al., 2008; Wu et al., 2021). Very recently, a study compared the contribution to the repair of various types of injuries between the bone marrow Adiponectin + SSPCs and the periosteal Gli1+ SSPCs (Jeffery et al., 2022). While, as mentioned above, the Adiponectin + SSPCs of the bone marrow are involved with the repair and regeneration of small and mechanically stable bone defects, the periosteal Gli1+ SSPCs are involved with the repair the bicortical fractures, suggesting that, depending on type of damage and mechanism of repair, distinctive SSPCs are required. Thus, different SSPCs have different abilities which may or may not be necessarily related with their potency. Identifying SSPCs in the periosteum is difficult because the periosteum is thin, with limited cellularity, and difficult to collect. In fact, current methods to extract cells from the periosteum are based on mechanical scraping and subsequent enzymatic digestion; alternatively, periosteal cells have been isolated by means of direct *ex-vivo* tissue culturing of the explanted periosteum (Roberts et al., 2015). To track periosteal SSPCs, studies have used countless markers (for a complete list, we suggest looking at (Perrin and Colnot, 2022)). Gli1 and Prrx1, which, as mentioned above, have been used to identify SSPCs of the bone marrow, along with Axis inhibition protein 2 (Axin2) and Cathepsin K (Ctsk) have also been utilized to mark SSPCs of the periosteum. In fact, expression of both Gli1 and Axin2 has been found to mark cells with skeletogenic potential in mouse embryo and post-natal tissues (Zhao et al., 2015; Maruyama et al., 2016; Ransom et al., 2016). Ctsk, encoding for the cysteine protease cathepsin K and traditionally used as marker of the bone-resorbing osteoclasts, has now been reported to identify an SSPC population of the mouse periosteum (Debnath et al., 2018). Expression of Prrx1, a transcription factor that is highly expressed during limb bud formation and craniofacial development, has been utilized to identify SSPCs in the mouse periosteum (Duchamp de Lageneste et al., 2018), as well as in the mouse periodontium (Bassir et al., 2019) and the mouse calvarial sutures (Wilk et al., 2017).

Calvarial sutures is the latest site in which SSPCs have been found. Indeed, calvarial sutures are synarthrosis composed by fibrous and connective tissue that act not only as connectors between the calvarial bones but also as reservoir of SSPCs (Wilk et al., 2017). For instance, it has been shown that during calvarial bone development putative SSPCs of the calvaria expressing Msx2 are destined to remain undifferentiated within the most central portion of the suture while only cells next to the advancing osteogenic fronts get incorporated into the growing bone (Lana-Elola et al., 2007). This indicates that the fate of SSPCs may depend on their position within the suture. Our group has also shown that putative mouse SSPCs expressing Prrx1 reside in the calvarial suture niche, respond to WNT signalling both *in vitro* and *in vivo* by

differentiating into osteoblasts, are required for calvarial bone regeneration, and, upon heterotopic transplantation, are able to regenerate calvarial bone (Wilk et al., 2017). Others have shown that SSPCs of the calvaria may also express Gli1, Axin2, and Ctsk (Zhao et al., 2015; Maruyama et al., 2016; Debnath et al., 2018). Recently, we have been able to isolate SSPCs resident within the calvaria, and, using scRNA-seq analysis, we have delineated their transcriptional profile. Following a scRNA-seq approach, we compared the expression of all the known potential markers of SSPCs, including CD146, 6C3, CD200, and found that Ctsk, Gli1, Axin2, and Prrx1 are the only four genes whose expression is significantly overlapped in certain cells of the calvaria sutures (manuscript in revision). In this case, the scRNA-seq approach has allowed for a comprehensive analysis, permitting to evaluate the overlap of expression of the many previously proposed markers. Considering the large number of existing studies that describe different putative SSPCs, such comprehensive approach should be used to reach a consensus over the existence of a single or multiple populations of SSPCs within the same anatomical area. Moreover, since calvarial bones are formed *via* intramembraneous ossification and calvarial bone defect are repaired by a similar process, calvarial SSPCs may have to be listed as a class of their own, with a unique biological activity that may differ from that of other SSPCs. ScRNA-seq comparative studies along with functional assays may help understand the similarities and differences between the calvarial SSPCs and the SSPCs of other skeletal segments.

In summary, SSPCs can be found in many different anatomical regions. Since investigations reported that the skeletal system is incredibly plastic (Mizuhashi et al., 2018) and since the activity of different types of SSPCs depends on the necessities (i.e., physiological or regenerative), we suggest that indeed multiple kinds of SSPCs may exist within the same anatomical site or in separate sites and that they act according to the skeleton urgencies. Thus, some of them may contribute more on supporting regeneration rather than hematopoiesis or *vice versa*. Unfortunately, no studies analysing functional similarities and differences in SSPCs have been performed to date. Therefore, comparing all putative populations of SSPCs is, in our opinion, a necessary exercise to identify common features across various SSPCs, finally solving the problem of SSPCs' identification and characterization. scRNA-seq technology, by offering the opportunity to do so, should be systematically utilized for such guided approach to unify the available data.

3 Mechanisms of SSPCs aging and their impact on bone repair

As mentioned above, no consensus exists yet about the identity of SSPCs. Consequently, any consideration about the effects of aging on these cells can either be generic or can only be specific about a certain population of the putative SSPCs so far identified. Here we attempt such analysis, on the basis on the available evidence.

Aging is associated with the degenerative processes that physiologically occur in an organism as time goes by. Degenerative processes become evident after the organism reaches the reproductive age, suggesting that after fulfilling the main purpose of life, which is the perpetuation of the species, an organism is somehow programmed to deteriorate. These processes involve all organs, and cells of the body; thus, bone is not spared. Aged bones present with a lower bone mass, alterations in the number and the architecture of trabeculae (Link et al., 2002; Boutroy et al., 2005; Sornay-Rendu et al., 2007), as well as increase in matrix mineralization, which make them stiffer, but more brittle (Currey, 1990; Grynpas, 1993).

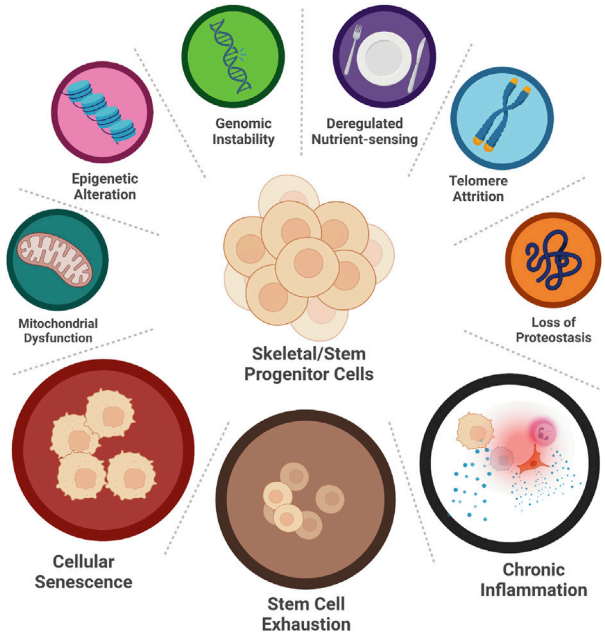

FIGURE 2
Hallmarks of SSPCs aging. Nine hallmarks of aging have been identified: genomic instability, deregulated nutrient-sensing, telomere attrition, loss of proteostasis, epigenetic alteration, mitochondrial dysfunction, cellular senescence, stem cell exhaustion and chronic inflammation. Only three of them, namely cellular senescence, stem cell exhaustion, and chronic inflammation, have been studied in aging SSPCs. (*Created with BioRender.com*).

Aging is a multifactorial process with many driving mechanisms involved; not all of them are fully elucidated and therefore aging, *per se*, is difficult to define. These mechanisms are called aging hallmarks, and, as per today, nine have been identified: genomic instability, deregulated nutrient-sensing, telomere attrition, epigenetic alterations, loss of proteostasis, mitochondrial dysfunction, inflammation, cellular senescence, and stem cell exhaustion (Figure 2) (Lopez-Otin et al., 2013). These hallmarks are highly interconnected: one can be both the cause and the consequence of another, and all together carry on the process of aging. For instance, inflammation can cause genomic instability, which can trigger cellular senescence, which in return can foster inflammation. Moreover, each of them is capable of directly and significantly influence aging, at least experimentally (Lopez-Otin et al., 2013), therefore it is very difficult to understand whether any of them has any dominant role, being responsible for triggering the others. In short, this is also the reason why aging is so difficult to intercept and why it is preferrable to attempt curing age-related diseases instead.

Unfortunately, studies about the aging hallmarks of the SSPCs are limited. Only few of them are available (Figure 2). Hereafter, we explore the results of these studies and report on their significance.

3.1 Stem cells exhaustion

The first aging hallmark constantly found active in the aging tissues where SSPCs reside (i.e., the bone marrow cavity, the growth plate, the

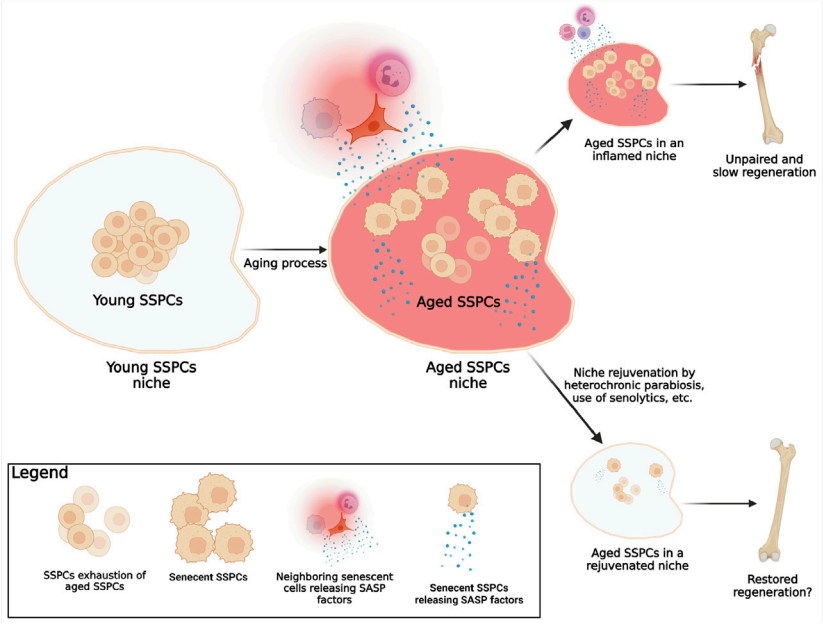

FIGURE 3
Known mechanism of SSPCs aging. In a young organism, the pool of young SSPCs is large, fully functional, and located in a young microenvironment (SSPCs niche) that offers ideal conditions for the SSPCs functions. As the organism becomes older, several mechanisms associated with aging and with a decline of SSPCs regeneration potential are known to happen: 1) the number of the now-aged, but probably still functional, SSPCs reduces (SSPCs exhaustion); 2) some SSPCs become senescent; 3) SSPCs niche conditions change (aged SSPCs niche) due to the chronic inflammation caused by the actively release of SASP factors by both senescent SSPCs within the niche, and neighboring senescent cells (immune, epithelial, endothelial, etc.). In the event of a fracture in elderly individuals the reduced number of SSPCs, the presence of senescent SSPCs, and the chronic inflammation within the aged niche are responsible for the lack of bone formation and fracture healing; a rejuvenation of the niche, by eliminating the inflammation and increasing the number of the functional non-senescent SSPCs, can foster fracture healing. (*Created with BioRender.com*).

periosteum, the calvarial sutures, etc.) is the stem cells exhaustion. This appears to involve all different populations of putative SSPCs identified so far (Martin and Olson, 2000; Farr et al., 2017) (Figure 3). The number of SSPCs available at the site of injury is crucial for proper bone healing and bone regeneration. For instance, our group has demonstrated that a significant reduction of the number of the SSPCs of the calvarial suture impairs calvarial bone regeneration (Wilk et al., 2017); conversely, recently generated data (manuscript in revision) shows that increasing the number of SSPCs *via* suture expansion fosters regeneration of calvarial critical size defects, otherwise unable to spontaneously regenerate. These observations suggest that: 1) a minimal number of SSPCs is required to sustain and promote bone healing; 2) in an aged environment, stem cell exhaustion may be one of the primary reasons for the impaired bone regeneration; 3) the proliferation of SSPCs that occurs in an aged organism after an injury does not reach a proliferative threshold able to sustain regeneration. This may be due to an initial very limited number of cells or to their intrinsic ability to proliferate effectively. Thus, SSPCs may be depleted during aging not only by a reduction of their number, but also by senescence, a mechanism that impairs their vital functions (Figure 3).

3.2 Stem cells senescence

In biology, senescent cells are defined as cells that despite the presence of space, nutrients, and growth factors, stop proliferating but do not die (Hayflick, 1965). Traditionally, telomere shortening has been used to identify senescence (Carlone et al., 2021). This is the reason why studies finding no changes in telomerase activity in SSPCs (Ambrosi et al., 2021), concluded that senescence was not a significant player in aging of SSPCs. However, SSPCs may present other mechanisms by which they become senescent, despite the lack of changes in telomere length and telomerase activity. Two other mechanisms should be considered: 1) telomeres are just DNA ends, and therefore they can acquire damages and mutations that may result in cellular senescence independently from their length or the expression of telomerase (Kruk et al., 1995). Moreover, telomeres are invisible to DNA repair machinery, so their probability to develop a biologically significant mutation is higher when compared to other DNA regions (Griffith et al., 1999); 2) non-telomeric DNA damage accumulation may occur with aging (Burkhalter et al., 2015) (genomic instability) or *via* senescence associated secretory phenotype (SASP) factors released by other nearby senescent cells (Josephson et al., 2019). Unfortunately, no investigation has thoroughly analysed the characteristics of senescent SSPCs, and of course, this is also due to the lack of consensus about their identity. Despite these gaps in the literature, and thanks to few available findings about aged SSPCs and on other types of stem cells (Boyle et al., 2007; Coppe et al., 2010; Sousa-Victor et al., 2014; Ambrosi et al., 2020), we can at least speculate that senescent SSPCs are characterized by cell cycle arrest, apoptosis resistance, alterations in the expression of senescence specific genes such as CDKN1A, CDKN2A (Sharpless and DePinho, 2007), SIRT1, etc., and by the active production and secretion of SASP factors (Josephson et al., 2019). These speculations will require additional investigations; yet, what remains biologically significant in aging, is the existence of a certain number of senescent

SSPCs that may reach a biologically significant threshold. Indeed, a single or few senescent cells may not be biologically significant because they can be eliminated by immune cells; yet, when the number of senescent cells raises exponentially, a series of deleterious events occur: first, since senescent SSPCs do not proliferate (Hayflick, 1965), the regenerative capacity of the tissue is compromised; second, once SSPCs become senescent, they lose their original identity and function, affecting the homeostasis of the tissue; and third, if SSPCs released SASP factors, they also sustain the senescence of other SSPCs in a paracrine fashion, increasing local environment inflammation (Campisi and d'Adda di Fagagna, 2007) (Figure 3).

In conclusion, it is important to distinguish aged from senescent SSPCs. The first are cells present in an old organism that still possess their original identity and are therefore still able to perform their duties as stem cells; the second, originate in response to age-associated factors characteristic of an aged microenvironment, and are non-functional (Figure 3). In other words, when the skeleton becomes older, the number of SSPCs may decrease or their regenerative potential may decline and this may be due to a reduced number of SSPCs, and increased number of senescent SSPCs, or both. Similar with what has been shown with HSCs (Ho et al., 2017), re-creating the original SSPCs cellular microenvironment may induce an increase of their number or may re-establish their function.

3.3 Chronic inflammation: Bad environment makes bad SSPCs

Inflammation is a significant hallmark of aging (Ferrucci and Fabbri, 2018), and it is even more important in the field of aging of SSPCs and age-associated compromised bone healing. Indeed, the first response after a bone fracture is represented by an acute inflammation, which is essential for initiating fracture healing. It has been demonstrated that mice deficient in innate and adaptive immunity have substantially compromised endochondral bone repair (Rapp et al., 2016) and that inhibition of inflammation causes delays in fracture recovering (Gerstenfeld et al., 2003). Inflammation, at the site of injury, is useful not only because its chemotaxis on neutrophils and macrophages, which clean the site from debris, but also for mobilization of SSPCs, providing the topological information about the regenerative activity site. However, a distinguish needs to be made between acute or chronic inflammation. While an inflammation strong in intensity but lasting a relatively short amount of time (acute inflammation) is beneficial for all the reasons said above, a chronic, weak, but non-resolving inflammation is detrimental to fracture healing. There is much evidence that in conditions of chronic inflammation bone healing is impaired (Kayal et al., 2007). Amongst the plethora of conditions that are accompanied by chronic inflammation (i.e., diabetes, Alzheimer's disease, cancer, etc.), there is aging, which probably is the most significant and most subtle among all, because sometimes it's not even considered as a condition.

Low chronic inflammation always accompanies aging, and in fact the term "inflammaging" is commonly used to describe this association (Franceschi and Campisi, 2014). A significant amount of data show how inflammaging is capable of inducing a reduction in bone regeneration potential (Sebastian et al., 2005) and, conversely, how rejuvenation of the inflammatory system in aged animals can accelerate fracture repair (Lu et al., 2005; Xing et al., 2010). Josephson and colleagues firstly demonstrated a direct correlation between the number of SSPCs and the time of healing of a human bone fracture and they identified chronic local inflammation as the main factor responsible for the decline of the SSPCs number and function. As mentioned, while acute inflammation is necessary to engage SSPCs recruitment and support tissue repair, chronic inflammation needs to be reduced, so that homeostasis can be restored.

Recent investigations have supported the concept of inflammaging as the main driving force in SSPCs dysfunction during aging (Ambrosi et al., 2021). This idea is appealing because it also suggests that SASP factors (interleukins and cytokines), by which inflammation exerts its effects, may be able to directly influence stem cell fate. Thus, directly modulating SASP factors, or indirectly modulating their effects, may lead to novel and effective therapeutic strategies in the field of bone regeneration.

Inflammation can also indirectly affect SSPCs functionality by affecting the environment in which they are located. In fact, stem cells reside in a specialized microenvironment (the niche), which, by means of self-renewal-regulating signals, adhesion molecules, and other cell types, conditions the properties and spatial organization of the SSPCs, maintaining their biological health and tissue competency. In addition, the niche provides an isolated space in which stem cells are kept safe from mechanical stimulations and from other damaging agents such as ROS and radiations. Unfortunately, as discussed above, a niche is not able to shield SSPCs from age-associated inflammation. In fact, Song et al. (2012) . Observed that increased SASP factors in aged mice contribute to altering bone marrow niches, which are depleted of osteopontin (OPN), a factor known to preserve the polarity and the physiology of the SSPCs. Yet, not much is known about the effects of aging on the SSPCs niche. This missing information has become particularly significant since more than one SSPCs niche has been described (i.e., the endosteal/bone marrow niche, the periosteal niche, the calvarial suture niche). In fact, it is possible that aging influences the various niches in different and unique ways, highlighting the importance of studies that identify and characterize SSPCs and their niches.

Rejuvenating the niche may sound appealing as a method to increase the number and re-establish the function of SSPCs. However, it may not be an easy task to accomplish. For instance, several studies demonstrated that the exposure to a youthful circulation (i.e., by means of heterochronic parabiosis) can improve bone repair in older animals (Baht et al., 2015; Ma et al., 2022). However, recent findings utilizing the same approach showed no reversion of SSPCs aging and no improvement of bone mass or healing (Ambrosi et al., 2021). These controversial outcomes may be due to the distinct conditions tested (age of mice used, evaluation of bone mass with or without a fracture first, etc.) and not necessarily to lack of efficacy in the rejuvenation strategy. Therefore, the topic of niche rejuvenation, while appealing, needs additional extensive studies. An interesting idea would be based on a multi-intervention strategy: on one side, rejuvenate the niches (i.e., simulating the heterochronic parabiosis with transfusions of blood obtained from young individuals), on the other side reduce the number of senescent SSPCs by means of agents such as senolytics (Kirkland and Tchkonia, 2020) (Figure 3).

4 Conclusion and future perspectives

The latest years have been characterized by significant attempts to identify and describe SSPCs in multiple locations (Sacchetti et al.,

2007; Chan et al., 2015; Wilk et al., 2017; Chan et al., 2018; Debnath et al., 2018; Mizuhashi et al., 2018; Newton et al., 2019; Matsushita et al., 2020). Despite these efforts, we still lack important information about their identity, or different identities, and about the interplay that they have with their niches, both in young individuals as well as during aging. Therefore, future efforts should aim to characterize and compare various putative SSPCs within the same niche and among all niches, with the final goal of generating a register of SSPCs helpful to study their biology and their regeneration potential. Then, each SSPCs type can be studied in relation to aging or other conditions, such as diabetes. Emerging techniques like the scRNA-seq can help clarifying similarities and dissimilarities among putative SSPCs, figuring out biological properties of SSPCs and their unique identity.

The study of aged SSPCs is even more challenging than the young ones, since the old ones are quite rare (Wilk et al., 2017; Ambrosi et al., 2019; Ambrosi et al., 2020). As discussed above, along with the development of aging mechanisms, the chances of SSPCs becoming senescent grow. Thus, in an old organism the number of physiologically competent SSPCs is limited, while the number of senescent ones is higher. From this point of view, given their higher number, senescent SSPCs may be easier to study; yet the difficulty of recognizing them, since they probably share some features of the non-senescent/functional SSPCs from which they derive, remains a crucial problem that needs to be overcome.

Watchful readers may have noticed that, even if we mentioned nine hallmarks of aging, we only discussed three of them. This does not mean that the other ones do not or may not have a significant role during SSPCs aging. Simply, it's just that no exhaustive investigations exist on SSPCs and aging, and this is also probably due to our lack of knowledge about the various SSPCs identity. Therefore, studies conducted in the past years suffer from this limitation; however, they may be still useful in suggesting interesting mechanisms of actions during aging.

As mentioned, given their limited number, studying SSPCs is extremely challenging, and even more so in aged organisms. Since not much is known about SSPCs, no significant strategies able to harness them for bone regeneration exist. In fact, most of the current approaches for bone regenerative therapies focus on the transplantation of bone competent cells or the implantation of osteoconductive or osteoinductive biomaterials (Borrelli et al., 2020). These approaches, which are not exempt from health risks, may not be necessary if the biological regenerative potential of SSPCs is fully exploited, so that they can be harnessed for autotherapies even in the elderly. To reach this goal, the precise identity of the SSPCs needs to be defined.

Author contributions

LM conceptualized the manuscript, analyzed and interpreted the cited studies, wrote the manuscript, and gave final approval. GI contributed to the conceptualization, the analysis, and the interpretation of the cited studies, edited and critically revised the manuscript, and gave final approval.

Funding

Funds were provided by the University of Pittsburgh (to GI) and the National Institutes of Health/National Institute of Dental and Craniofacial Research (Grant # DE026155 to GI).

Conflict of interest

The authors declare that the research was conducted in the absence of any commercial or financial relationships that could be construed as a potential conflict of interest.

Publisher's note

References

Ambrosi, T. H., Goodnough, L. H., and Chan, C. K. F. (2020). Human skeletal stem cell aging. *Aging* 12 (17), 16669–16671. doi:10.18632/aging.104034

Ambrosi, T. H., Longaker, M. T., and Chan, C. K. F. (2019). A revised perspective of skeletal stem cell biology. *Front. Cell Dev. Biol.* 7, 189. doi:10.3389/fcell.2019.00189

Ambrosi, T. H., Marecic, O., McArdle, A., Sinha, R., Gulati, G. S., Tong, X., et al. (2021). Aged skeletal stem cells generate an inflammatory degenerative niche. *Nature* 597 (7875), 256–262. doi:10.1038/s41586-021-03795-7

Ara, T., Itoi, M., Kawabata, K., Egawa, T., Tokoyoda, K., Sugiyama, T., et al. (2003). A role of CXC chemokine ligand 12/stromal cell-derived factor-1/pre-B cell growth stimulating factor and its receptor CXCR4 in fetal and adult T cell development *in vivo*. *J. Immunol.* 170 (9), 4649–4655. doi:10.4049/jimmunol.170.9.4649

Baht, G. S., Silkstone, D., Vi, L., Nadesan, P., Amani, Y., Whetstone, H., et al. (2015). Exposure to a youthful circulaton rejuvenates bone repair through modulation of beta-catenin. *Nat. Commun.* 6, 7131. doi:10.1038/ncomms8131

Baryawno, N., Przybylski, D., Kowalczyk, M. S., Kfoury, Y., Severe, N., Gustafsson, K., et al. (2019). A cellular taxonomy of the bone marrow stroma in homeostasis and leukemia. *Cell* 177 (7), 1915–1932. doi:10.1016/j.cell.2019.04.040

Bassir, S. H., Garakani, S., Wilk, K., Aldawood, Z. A., Hou, J., Yeh, S. A., et al. (2019). Prx1 expressing cells are required for periodontal regeneration of the mouse incisor. *Front. Physiol.* 10, 591. doi:10.3389/fphys.2019.00591

Bianco, P., Cao, X., Frenette, P. S., Mao, J. J., Robey, P. G., Simmons, P. J., et al. (2013). The meaning, the sense and the significance: Translating the science of mesenchymal stem cells into medicine. *Nat. Med.* 19 (1), 35–42. doi:10.1038/nm.3028

Borrelli, M. R., Hu, M. S., Longaker, M. T., and Lorenz, H. P. (2020). Tissue engineering and regenerative medicine in craniofacial reconstruction and facial aesthetics. *J. Craniofac Surg.* 31 (1), 15–27. doi:10.1097/SCS.0000000000005840

Boutroy, S., Bouxsein, M. L., Munoz, F., and Delmas, P. D. (2005). *In vivo* assessment of trabecular bone microarchitecture by high-resolution peripheral quantitative computed tomography. *J. Clin. Endocrinol. Metab.* 90 (12), 6508–6515. doi:10.1210/jc.2005-1258

Boyle, M., Wong, C., Rocha, M., and Jones, D. L. (2007). Decline in self-renewal factors contributes to aging of the stem cell niche in the Drosophila testis. *Cell Stem Cell* 1 (4), 470–478. doi:10.1016/j.stem.2007.08.002

Burkhalter, M. D., Rudolph, K. L., and Sperka, T. (2015). Genome instability of ageing stem cells--Induction and defence mechanisms. *Ageing Res. Rev.* 23, 29–36. doi:10.1016/j.arr.2015.01.004

Campisi, J., and d'Adda di Fagagna, F. (2007). Cellular senescence: When bad things happen to good cells. *Nat. Rev. Mol. Cell Biol.* 8 (9), 729–740. doi:10.1038/nrm2233

Caplan, A. I. (1991). Mesenchymal stem cells. *J. Orthop. Res.* 9 (5), 641–650. doi:10.1002/jor.1100090504

Carlone, D. L., Riba-Wolman, R. D., Deary, L. T., Tovaglieri, A., Jiang, L., Ambruzs, D. M., et al. (2021). Telomerase expression marks transitional growth-associated skeletal progenitor/stem cells. *Stem Cells* 39 (3), 296–305. doi:10.1002/stem.3318

Chan, C. K., Seo, E. Y., Chen, J. Y., Lo, D., McArdle, A., Sinha, R., et al. (2015). Identification and specification of the mouse skeletal stem cell. *Cell* 160 (1-2), 285–298. doi:10.1016/j.cell.2014.12.002

Chan, C. K. F., Gulati, G. S., Sinha, R., Tompkins, J. V., Lopez, M., Carter, A. C., et al. (2018). Identification of the human skeletal stem cell. *Cell* 175 (1), 43–56. doi:10.1016/j.cell.2018.07.029

Coppe, J. P., Desprez, P. Y., Krtolica, A., and Campisi, J. (2010). The senescence-associated secretory phenotype: The dark side of tumor suppression. *Annu. Rev. pathology* 5, 99–118. doi:10.1146/annurev-pathol-121808-102144

Currey, J. D. (1990). Physical characteristics affecting the tensile failure properties of compact bone. *J. Biomech.* 23 (8), 837–844. doi:10.1016/0021-9290(90)90030-7

Debnath, S., Yallowitz, A. R., McCormick, J., Lalani, S., Zhang, T., Xu, R., et al. (2018). Discovery of a periosteal stem cell mediating intramembranous bone formation. *Nature* 562 (7725), 133–139. doi:10.1038/s41586-018-0554-8

Dominici, M., Le Blanc, K., Mueller, I., Slaper-Cortenbach, I., Marini, F., Krause, D., et al. (2006). Minimal criteria for defining multipotent mesenchymal stromal cells. The International Society for Cellular Therapy position statement. *Cytotherapy* 8 (4), 315–317. doi:10.1080/14653240600855905

Duchamp de Lageneste, O., Julien, A., Abou-Khalil, R., Frangi, G., Carvalho, C., Cagnard, N., et al. (2018). Periosteum contains skeletal stem cells with high bone regenerative potential controlled by Periostin. *Nat. Commun.* 9 (1), 773. doi:10.1038/s41467-018-03124-z

Farr, J. N., Xu, M., Weivoda, M. M., Monroe, D. G., Fraser, D. G., Onken, J. L., et al. (2017). Targeting cellular senescence prevents age-related bone loss in mice. *Nat. Med.* 23 (9), 1072–1079. doi:10.1038/nm.4385

Ferrucci, L., and Fabbri, E. (2018). Inflammageing: Chronic inflammation in ageing, cardiovascular disease, and frailty. *Nat. Rev. Cardiol.* 15 (9), 505–522. doi:10.1038/s41569-018-0064-2

Franceschi, C., and Campisi, J. (2014). Chronic inflammation (inflammaging) and its potential contribution to age-associated diseases. *J. Gerontol. A Biol. Sci. Med. Sci.* 69, S4–S9. doi:10.1093/gerona/glu057

Garcia, P., Holstein, J. H., Maier, S., Schaumloffel, H., Al-Marrawi, F., Hannig, M., et al. (2008). Development of a reliable non-union model in mice. *J. Surg. Res.* 147 (1), 84–91. doi:10.1016/j.jss.2007.09.013

Gerstenfeld, L. C., Thiede, M., Seibert, K., Mielke, C., Phippard, D., Svagr, B., et al. (2003). Differential inhibition of fracture healing by non-selective and cyclooxygenase-2 selective non-steroidal anti-inflammatory drugs. *J. Orthop. Res.* 21 (4), 670–675. doi:10.1016/S0736-0266(03)00003-2

Greenbaum, A., Hsu, Y. M., Day, R. B., Schuettpelz, L. G., Christopher, M. J., Borgerding, J. N., et al. (2013). CXCL12 in early mesenchymal progenitors is required for haematopoietic stem-cell maintenance. *Nature* 495 (7440), 227–230. doi:10.1038/nature11926

Griffith, J. D., Comeau, L., Rosenfield, S., Stansel, R. M., Bianchi, A., Moss, H., et al. (1999). Mammalian telomeres end in a large duplex loop. *Cell* 97 (4), 503–514. doi:10.1016/s0092-8674(00)80760-6

Grynpas, M. (1993). Age and disease-related changes in the mineral of bone. *Calcif. Tissue Int.* 53, S57–S64. doi:10.1007/BF01673403

Hayflick, L. (1965). The limited *in vitro* lifetime of human diploid cell strains. *Exp. Cell Res.* 37, 614–636. doi:10.1016/0014-4827(65)90211-9

Ho, T. T., Warr, M. R., Adelman, E. R., Lansinger, O. M., Flach, J., Verovskaya, E. V., et al. (2017). Autophagy maintains the metabolism and function of young and old stem cells. *Nature* 543 (7644), 205–210. doi:10.1038/nature21388

Jeffery, E. C., Mann, T. L. A., Pool, J. A., Zhao, Z., and Morrison, S. J. (2022). Bone marrow and periosteal skeletal stem/progenitor cells make distinct contributions to bone maintenance and repair. *Cell Stem Cell* 29 (11), 1547–1561.e6. doi:10.1016/j.stem.2022.10.002

Josephson, A. M., Bradaschia-Correa, V., Lee, S., Leclerc, K., Patel, K. S., Muinos Lopez, E., et al. (2019). Age-related inflammation triggers skeletal stem/progenitor cell dysfunction. *Proc. Natl. Acad. Sci. U. S. A.* 116 (14), 6995–7004. doi:10.1073/pnas.1810692116

Karsenty, G., and Ferron, M. (2012). The contribution of bone to whole-organism physiology. *Nature* 481 (7381), 314–320. doi:10.1038/nature10763

Kayal, R. A., Tsatsas, D., Bauer, M. A., Allen, B., Al-Sebaei, M. O., Kakar, S., et al. (2007). Diminished bone formation during diabetic fracture healing is related to the premature resorption of cartilage associated with increased osteoclast activity. *J. Bone Min. Res.* 22 (4), 560–568. doi:10.1359/jbmr.070115

Kirkland, J. L., and Tchkonia, T. (2020). Senolytic drugs: From discovery to translation. *J. Intern Med.* 288 (5), 518–536. doi:10.1111/joim.13141

Kruk, P. A., Rampino, N. J., and Bohr, V. A. (1995). DNA damage and repair in telomeres: Relation to aging. *Proc. Natl. Acad. Sci. U. S. A.* 92 (1), 258–262. doi:10.1073/pnas.92.1.258

Lana-Elola, E., Rice, R., Grigoriadis, A. E., and Rice, D. P. (2007). Cell fate specification during calvarial bone and suture development. *Dev. Biol.* 311 (2), 335–346. doi:10.1016/j.ydbio.2007.08.028

Lin, Z., Fateh, A., Salem, D. M., and Intini, G. (2014). Periosteum: Biology and applications in craniofacial bone regeneration. *J. Dent. Res.* 93 (2), 109–116. doi:10.1177/0022034513506445

Link, T. M., Link, T. M., Link, T. M., Saborowski, O., Kisters, K., Kempkes, M., et al. (2002). Changes in calcaneal trabecular bone structure assessed with high-resolution MR imaging in patients with kidney transplantation. *Osteoporos. Int.* 13 (2), 119–129. doi:10.1007/s001980200003

Liu, H., Li, P., Zhang, S., Xiang, J., Yang, R., Liu, J., et al. (2022). Prrx1 marks stem cells for bone, white adipose tissue and dermis in adult mice. *Nat. Genet.* 54 (12), 1946–1958. doi:10.1038/s41588-022-01227-4

Lopez-Otin, C., Blasco, M. A., Partridge, L., Serrano, M., and Kroemer, G. (2013). The hallmarks of aging. *Cell* 153 (6), 1194–1217. doi:10.1016/j.cell.2013.05.039

Lu, C., Miclau, T., Hu, D., Hansen, E., Tsui, K., Puttlitz, C., et al. (2005). Cellular basis for age-related changes in fracture repair. *J. Orthop. Res.* 23 (6), 1300–1307. doi:10.1016/j.orthres.2005.04.003.1100230610

Ma, S., Wang, S., Ye, Y., Ren, J., Chen, R., Li, W., et al. (2022). Heterochronic parabiosis induces stem cell revitalization and systemic rejuvenation across aged tissues. *Cell Stem Cell* 29 (6), 990–1005 e10. doi:10.1016/j.stem.2022.04.017

Martin, J. F., and Olson, E. N. (2000). Identification of a prx1 limb enhancer. *Genesis* 26 (4), 225–229. doi:10.1002/(sici)1526-968x(200004)26:4<225::aid-gene10>3.0.co;2-f

Maruyama, T., Jeong, J., Sheu, T. J., and Hsu, W. (2016). Stem cells of the suture mesenchyme in craniofacial bone development, repair and regeneration. *Nat. Commun.* 7, 10526. doi:10.1038/ncomms10526

Matsushita, Y., Nagata, M., Kozloff, K. M., Welch, J. D., Mizuhashi, K., Tokavanich, N., et al. (2020). A Wnt-mediated transformation of the bone marrow stromal cell identity orchestrates skeletal regeneration. *Nat. Commun.* 11 (1), 332. doi:10.1038/s41467-019-14029-w

Mizuhashi, K., Ono, W., Matsushita, Y., Sakagami, N., Takahashi, A., Saunders, T. L., et al. (2018). Resting zone of the growth plate houses a unique class of skeletal stem cells. *Nature* 563 (7730), 254–258. doi:10.1038/s41586-018-0662-5

Newton, P. T., Li, L., Zhou, B., Schweingruber, C., Hovorakova, M., Xie, M., et al. (2019). A radical switch in clonality reveals a stem cell niche in the epiphyseal growth plate. *Nature* 567 (7747), 234–238. doi:10.1038/s41586-019-0989-6

Ng, A. P., and Alexander, W. S. (2017). Haematopoietic stem cells: Past, present and future. *Cell Death Discov.* 3, 17002. doi:10.1038/cddiscovery.2017.2

Owen, M., and Friedenstein, A. J. (1988). Stromal stem cells: Marrow-derived osteogenic precursors. *Ciba Found. Symp.* 136, 42–60. doi:10.1002/9780470513637.ch4

Perrin, S., and Colnot, C. (2022). Periosteal skeletal stem and progenitor cells in bone regeneration. *Curr. Osteoporos. Rep.* 20, 334–343. doi:10.1007/s11914-022-00737-8

Ransom, R. C., Hunter, D. J., Hyman, S., Singh, G., Ransom, S. C., Shen, E. Z., et al. (2016). Axin2-expressing cells execute regeneration after skeletal injury. *Sci. Rep.* 6, 36524. doi:10.1038/srep36524

Rapp, A. E., Bindl, R., Recknagel, S., Erbacher, A., Muller, I., Schrezenmeier, H., et al. (2016). Fracture healing is delayed in immunodeficient NOD/scid-IL2Rγ-cnull mice. *PLoS One* 11 (2), e0147465. doi:10.1371/journal.pone.0147465

Roberts, S. J., van Gastel, N., Carmeliet, G., and Luyten, F. P. (2015). Uncovering the periosteum for skeletal regeneration: The stem cell that lies beneath. *Bone* 70, 10–18. doi:10.1016/j.bone.2014.08.007

Sacchetti, B., Funari, A., Michienzi, S., Di Cesare, S., Piersanti, S., Saggio, I., et al. (2007). Self-renewing osteoprogenitors in bone marrow sinusoids can organize a hematopoietic microenvironment. *Cell* 131 (2), 324–336. doi:10.1016/j.cell.2007.08.025

Sebastian, C., Espia, M., Serra, M., Celada, A., and Lloberas, J. (2005). MacrophAging: A cellular and molecular review. *Immunobiology* 210 (2-4), 121–126. doi:10.1016/j.imbio.2005.05.006

Sharpless, N. E., and DePinho, R. A. (2007). How stem cells age and why this makes us grow old. *Nat. Rev. Mol. Cell Biol.* 8 (9), 703–713. doi:10.1038/nrm2241

Shi, Y., He, G., Lee, W. C., McKenzie, J. A., Silva, M. J., and Long, F. (2017). Gli1 identifies osteogenic progenitors for bone formation and fracture repair. *Nat. Commun.* 8 (1), 2043. doi:10.1038/s41467-017-02171-2

Song, Z., Zhang, J., Ju, Z., and Rudolph, K. L. (2012). Telomere dysfunctional environment induces loss of quiescence and inherent impairments of hematopoietic stem cell function. *Aging Cell* 11 (3), 449–455. doi:10.1111/j.1474-9726.2012.00802.x

Sornay-Rendu, E., Boutroy, S., Munoz, F., and Delmas, P. D. (2007). Alterations of cortical and trabecular architecture are associated with fractures in postmenopausal women, partially independent of decreased BMD measured by DXA: The OFELY study. *J. Bone Min. Res.* 22 (3), 425–433. doi:10.1359/jbmr.061206

Sousa-Victor, P., Gutarra, S., Garcia-Prat, L., Rodriguez-Ubreva, J., Ortet, L., Ruiz-Bonilla, V., et al. (2014). Geriatric muscle stem cells switch reversible quiescence into senescence. *Nature* 506 (7488), 316–321. doi:10.1038/nature13013

Takagi, Y. (2016). History of neural stem cell research and its clinical application. *Neurol. Med. Chir. (Tokyo)* 56 (3), 110–124. doi:10.2176/nmc.ra.2015-0340

Takahashi, K., and Yamanaka, S. (2006). Induction of pluripotent stem cells from mouse embryonic and adult fibroblast cultures by defined factors. *Cell* 126 (4), 663–676. doi:10.1016/j.cell.2006.07.024

Tavassoli, M., and Crosby, W. H. (1968). Transplantation of marrow to extramedullary sites. *Science* 161 (3836), 54–56. doi:10.1126/science.161.3836.54

Tikhonova, A. N., Dolgalev, I., Hu, H., Sivaraj, K. K., Hoxha, E., Cuesta-Dominguez, A., et al. (2019). The bone marrow microenvironment at single-cell resolution. *Nature* 569 (7755), 222–228. doi:10.1038/s41586-019-1104-8

Visvader, J. E., and Smith, G. H. (2011). Murine mammary epithelial stem cells: Discovery, function, and current status. *Cold Spring Harb. Perspect. Biol.* 3 (2), a004879. doi:10.1101/cshperspect.a004879

Watson, A. (1845). Observations on the formation of bone by the periosteum. *Edinb Med. Surg. J.* 63 (163), 302–307.

Wilk, K., Yeh, S. A., Mortensen, L. J., Ghaffarigarakani, S., Lombardo, C. M., Bassir, S. H., et al. (2017). Postnatal calvarial skeletal stem cells expressing PRX1 reside exclusively in the calvarial sutures and are required for bone regeneration. *Stem Cell Rep.* 8 (4), 933–946. doi:10.1016/j.stemcr.2017.03.002

Worthley, D. L., Churchill, M., Compton, J. T., Tailor, Y., Rao, M., Si, Y., et al. (2015). Gremlin 1 identifies a skeletal stem cell with bone, cartilage, and reticular stromal potential. *Cell* 160 (1-2), 269–284. doi:10.1016/j.cell.2014.11.042

Wu, X. Q., Wang, D., Liu, Y., and Zhou, J. L. (2021). Development of a tibial experimental non-union model in rats. *J. Orthop. Surg. Res.* 16 (1), 261. doi:10.1186/s13018-021-02408-3

Xing, Z., Lu, C., Hu, D., Miclau, T., 3rd, and Marcucio, R. S. (2010). Rejuvenation of the inflammatory system stimulates fracture repair in aged mice. *J. Orthop. Res.* 28 (8), 1000–1006. doi:10.1002/jor.21087

Zhao, H., Feng, J., Ho, T. V., Grimes, W., Urata, M., and Chai, Y. (2015). The suture provides a niche for mesenchymal stem cells of craniofacial bones. *Nat. Cell Biol.* 17 (4), 386–396. doi:10.1038/ncb3139

Zhou, B. O., Yue, R., Murphy, M. M., Peyer, J. G., and Morrison, S. J. (2014). Leptin-receptor-expressing mesenchymal stromal cells represent the main source of bone formed by adult bone marrow. *Cell Stem Cell* 15 (2), 154–168. doi:10.1016/j.stem.2014.06.008

frontiers | Frontiers in Physiology

TYPE Original Research
PUBLISHED 16 February 2023
DOI 10.3389/fphys.2023.1119368

OPEN ACCESS

EDITED BY
Noriaki Ono,
University of Texas Health Science Center at Houston, United States

REVIEWED BY
Rui Yue,
Tongji University, China
Beth Bragdon,
Boston University, United States
Peter Maye,
UCONN Health, United States

*CORRESPONDENCE
Marian F. Young,
myoung@dir.nidcr.nih.gov

SPECIALTY SECTION
This article was submitted to Skeletal Physiology, a section of the journal Frontiers in Physiology

RECEIVED 08 December 2022
ACCEPTED 31 January 2023
PUBLISHED 16 February 2023

CITATION
Shainer R, Kram V, Kilts TM, Li L, Doyle AD, Shainer I, Martin D, Simon CG Jr., Zeng-Brouwers J, Schaefer L, Young MF and Genomics and Computational Biology Core (2023), Biglycan regulates bone development and regeneration. *Front. Physiol.* 14:1119368. doi: 10.3389/fphys.2023.1119368

Biglycan regulates bone development and regeneration

Reut Shainer[1], Vardit Kram[1], Tina M. Kilts[1], Li Li[1], Andrew D. Doyle[2], Inbal Shainer[3], Daniel Martin[4], Carl G. Simon Jr.[5], Jinyang Zeng-Brouwers[6], Liliana Schaefer[6], Marian F. Young[1]* and Genomics and Computational Biology Core

[1]Molecular Biology of Bones and Teeth Section, National Institute of Dental and Craniofacial Research, National Institutes of Health, Bethesda, MD, United States, [2]NIDCR Imaging Core, National Institute of Dental and Craniofacial Research, National Institutes of Health, Bethesda, MD, United States, [3]Department Genes-Circuits-Behavior, Max Planck Institute for Biological Intelligence, Martinsried, Germany, [4]NIDCD/NIDCR Genomics and Computational Biology Core, National Institutes of Health, Bethesda, MD, United States, [5]Biosystems and Biomaterials Division, National Institute of Standards and Technology, Gaithersburg, MD, United States, [6]Pharmazentrum Frankfurt, Institut für Allgemeine Pharmakologie und Toxikologie, Klinikum der Goethe-Universität Frankfurt am Main, Frankfurt, Germany

Endochondral bone development and regeneration relies on activation and proliferation of periosteum derived-cells (PDCs). Biglycan (Bgn), a small proteoglycan found in extracellular matrix, is known to be expressed in bone and cartilage, however little is known about its influence during bone development. Here we link biglycan with osteoblast maturation starting during embryonic development that later affects bone integrity and strength. Biglycan gene deletion reduced the inflammatory response after fracture, leading to impaired periosteal expansion and callus formation. Using a novel 3D scaffold with PDCs, we found that biglycan could be important for the cartilage phase preceding bone formation. The absence of biglycan led to accelerated bone development with high levels of osteopontin, which appeared to be detrimental to the structural integrity of the bone. Collectively, our study identifies biglycan as an influencing factor in PDCs activation during bone development and bone regeneration after fracture.

KEYWORDS

periosteum, biglycan, extracellular matrix, fracture, bone, cartilage

Introduction

Skeletal development proceeds through two different ossification processes. Craniofacial bones develop through intramembranous ossification by direct differentiation of the mesenchymal stem/progenitor cells into osteoblasts. Development of the long bones on the other hand occurs *via* endochondral ossification, in which the mesenchymal stem/progenitor cells differentiate into chondrocytes and lay down a cartilage template, which is later replaced by osteoblasts that are responsible for bone formation (Berendsen and Olsen, 2015; Salhotra et al., 2020).

The periosteum is a thin highly vascularized membrane surrounding the bone that serves as an attachment site for tendons, ligaments and muscles. The periosteum is composed of an external fibrous layer containing fibroblasts and an inner cambium layer containing progenitor cells, known as periosteum derived-cells (PDCs), that allow bone growth and remodeling (Marsell and Einhorn, 2011; Colnot et al., 2012; Roberts et al., 2015).

Bone fracture healing involves a complex sequence of physiological events, which is similar to embryonic bone development except that it has an inflammation phase after the fracture that is necessary for the regeneration progress. In general, fracture healing through endochondral

bone formation involves 4 phases: 1) inflammation, 2) proliferation, 3) callus formation and 4) bone remodeling. The initial fracture leads to a hematoma followed by an inflammatory response. Inflammatory cells migrate to the fracture area and secrete stimulatory factors including IL-1, IL-6, and bone morphogenetic proteins (BMPs) to promote angiogenesis and to recruit skeletal progenitor cells from the periosteum. After the inflammation phase, a callus forms due to a massive proliferation of PDCs leading to cellular condensation and chondrogenic differentiation. Recent evidence show that the periosteum is the major source of progenitor cells needed for the bone repair process (Marecic et al., 2015; Debnath et al., 2018; Duchamp de Lageneste et al., 2018). In the next phase of bone healing, the chondrocytes in the callus become hypertrophic and blood vessels and osteoblasts from periosteal regions enter to replace the cartilage template and form the woven bone. In the final phase of the fracture healing, the woven bone remodels through osteoclast-osteoblast coupling to create the mature lamellar bone.

The extracellular matrix (ECM) of bone plays a pivotal role in tissue integrity and strength. The organic ECM is comprised mainly of collagen type I (90%), which is arranged in fibrils that become mineralized to provide a scaffold for bone cells and ultimately determines the bone strength and integrity. Other components of the ECM are the non-collagenous proteins (10%) which mainly include γ-carboxyglutamic-containing proteins, small integrin-binding ligand N-linked glycoproteins (SIBLINGs) and proteoglycans, including small leucine-rich proteoglycans (SLRPs), that also contribute to bone structure and strength (Lin et al., 2020).

Biglycan (Bgn) is a member of the SLRP family and is highly abundant in the ECM of a variety of tissues, including bone, cartilage and tendon (Fisher et al., 1983; Bianco et al., 1990). During skeletal development, high levels of Bgn mRNA are detected in areas of endochondral and membranous bone formation (Kram et al., 2020). To study the role of Bgn in the skeleton, a knockout (KO) mouse, globally deficient in *Bgn*, was generated. Although *Bgn*-deficient mice appear normal at birth, they display a phenotype characterized by reduced bone mass and age-dependent osteopenia (Xu et al., 1998; Chen et al., 2002). In this study, we explored the role of Bgn from early stages of bone development and during fracture healing. Lack of Bgn influenced embryonic osteoblast differentiation, which later resulted in structural changes in the bone, including reduced integrity and strength. In addition, the fracture healing cascade in *Bgn* KO mice was compromised in multiple ways. Unlike wild-type (WT) mice, *Bgn*-deficient mice showed a reduced response to injury during the inflammatory phase, which led to decreased periosteal expansion, resulting in a smaller callus around the fracture site that then mineralize and remodel faster, generating new bone that was structurally abnormal. Analyzing the expression pattern of Bgn showed that it was dramatically upregulated in the periosteum in response to fracture. Using a novel 3D system, we found that under conditions that stimulate osteogenic differentiation, WT PDCs underwent endochondral ossification by forming cartilage structures *in vitro* followed by mineralization *in vivo*. In the 3D scaffolds containing *Bgn* KO PDCs, cartilage differentiation was reduced which resulted in abnormal accelerated mineralization. Overall, our results demonstrate that *Bgn* deletion impairs bone development and regeneration and may do so by regulating the cartilage phase preceding bone formation.

Materials and methods

Mice

C57BL/6J and C57BL/6-Tg (CAG-EGFP)1Osb/J male mice were obtained from The Jackson Laboratory. *Bgn*-deficient (KO) mice were generated as previously described (Xu et al., 1998) all mice were bred and housed at the NIDCR/NIH/DHHS animal facility with standard conditions and genotyped in our laboratory. All procedures using mice were approved by the NIDCR/NIH/DHHS ACUC (protocol numbers 18-865, 18-871).

Primary culture of PDCs

After euthanasia, femurs and tibias were dissected from 6 to 7 week-old WT or *Bgn* KO male mice. Muscle and connective tissue were removed under sterile conditions and the epiphyses were coated with 5% low melting point agarose (Invitrogen) to protect the cartilage from digestion. PDCs were isolated by 1 h digestion in 3 mg/mL collagenase type II (Gibco) and 4 mg/mL dispase (Gibco) in α-minimal essential medium (αMEM) with 3% glutaMAX (Gibco) at 37°C (van Gastel et al., 2012; van Gastel et al., 2014). The cell suspension was passed through a 70 μm cell strainer (Falcon) and plated in 25 cm^2 flasks with growth medium composed of αMEM (Gibco) supplemented with 20% FBS (Gemini Bio Products), 100 U/mL each of penicillin and streptomycin and 2 mM glutaMAX (Gibco), and the medium was replenished twice a week until cells reached confluence.

Preparation of 3D culture system

When PDC cultures reached 80%–90% confluency (10–14 days post isolation), the cells were trypsinized and seeded in RAFT™ 3D 96 well cell culture plates according to the manufacturer's instructions (RAFT™ 3D Cell Culture bundle Kit, Lonza) at a concentration of 120,000 cells/well. Briefly, cells were seeded in a chilled mixture of collagen solution containing x10 MEM medium, 2 mg/mL rat tail collagen type I and neutralizing solution and incubated for 18 min at 37°C to form a hydrogel. Next, an absorber device was placed on top of the hydrogel for 15 min to condense and concentrate the mix of cells and collagen to create the RAFT™ disc. 0.24 mL/well growth medium was immediately added and thereafter replaced twice a week. To induce osteogenic differentiation, 10^{-8} M dexamethasone, 100 μM L-ascorbic acid phosphate and 2 mM β-glycerophosphate were added to the growth medium containing only 10% FBS for 14 days.

Fractures and 3D scaffold transplantation

For all surgeries, 6–7 week-old WT or *Bgn* KO male mice were anesthetized with 2%–3% isoflurane. 1 mg/kg of buprenorphine SR-LAB (ZooPharm) was administrated subcutaneously before the procedure and 72 h post-surgery. For open stabilized fractures, the right hindleg was shaved and scrubbed with 10% povidone-iodine and alcohol solutions. A 5 mm medial parapatellar incision was created and the patella was dislocated to expose the femoral condyle. A hole was burred into the femoral epiphysis using a 25 gauge (25 G) needle

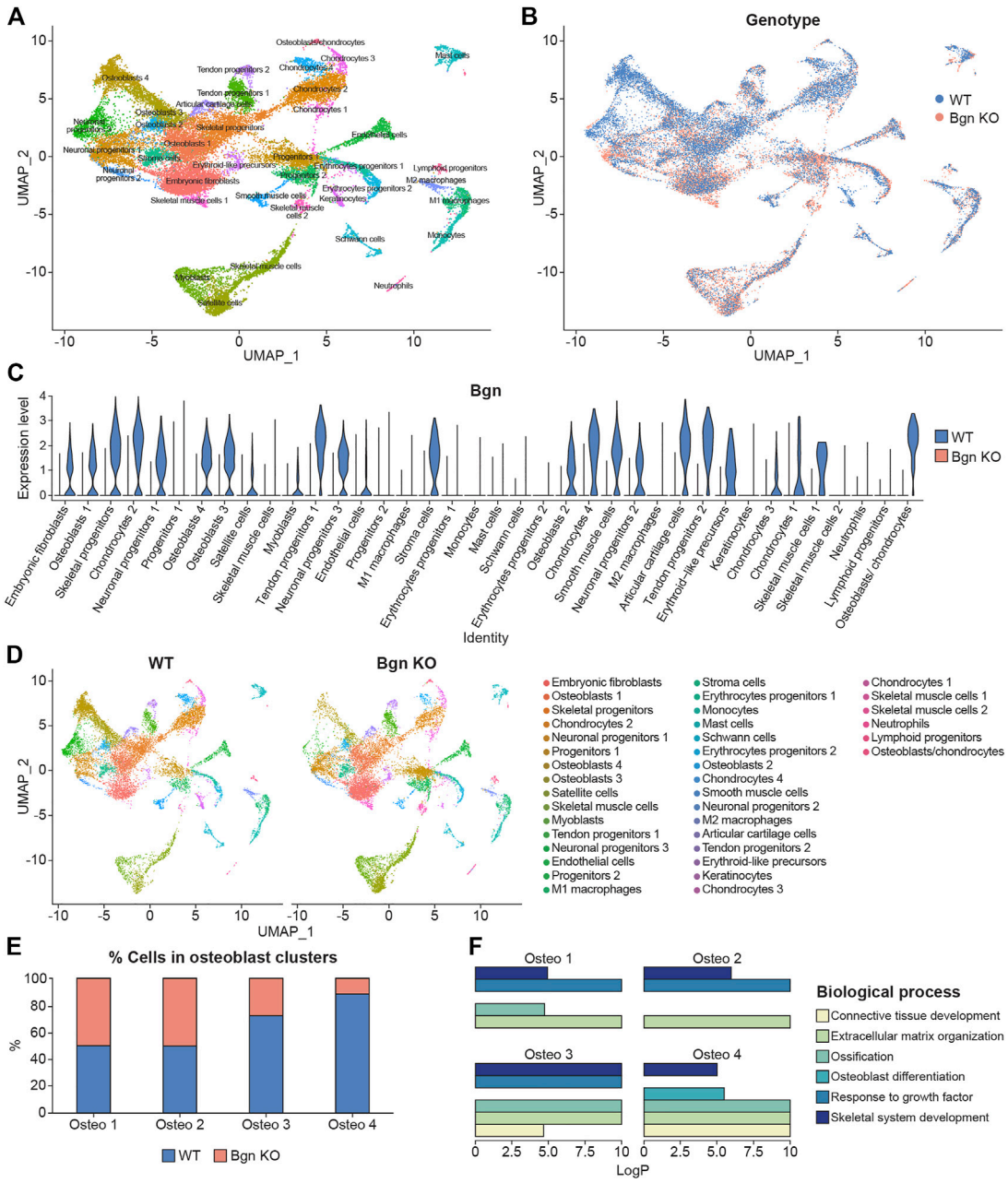

FIGURE 1
Single-cell sequencing of mouse embryonic bones shows Bgn is important for osteoblast differentiation. **(A)** UMAP visualization of transcriptional clusters derived from WT and *Bgn* KO cells (E16.5). Each point represents a single cell, colored according to cell type. The cells were clustered into 38 distinct types, which were defined according to their unique transcriptomes. See also Supplementary Table S1. **(B)** UMAP visualization of the cells, colored according to their genotype origin. See also Supplementary Figure S1A. **(C)** Violin-plot comparison of *Bgn* gene expression in the different clusters, split according to their genotype origin. See also Supplementary Figure S1B. **(D)** UMAP visualization of the 38 clusters, WT compared with *Bgn* KO cells. See also Supplementary Figure S2. **(E)** The percentage of WT and *Bgn* KO cells that populate the osteoblast clusters. **(F)** GO analysis of the genes in the different osteoblast clusters.

and enlarged using a 23 G needle. A 26 G cannula (Millpledge Veterinary) was inserted into the femoral shaft through the burred hole. The muscles and tendons were shifted to expose the bone shaft and a horizontal fracture was created at the center of the shaft using surgical scissors. The soft tissue was repositioned and the protruding end of the needle was cut off. The incision was closed using 5-0 absorbable sutures (Ethicon). X-ray was performed to visualize the fracture (Faxitron® Ultra Focus). For subcutaneous transplantation, a small incision was made in the skin on the back of the mouse. 3D scaffolds with un-differentiated PDCs (that served as control) or differentiated PDCs were implanted subcutaneously and the incision was closed using 5-0 absorbable sutures (Ethicon). The 3D scaffolds were analyzed at time points 0 (the day of implantation), and 4 and 8 weeks after implantation.

Micro-computed tomography (μCT)

The 3D scaffolds recovered after implantation and mice femurs before and after fracture were fixed in Z-fix (170; Anatech, LTD) for 24 h at room temperature (RT) and stored in 70% ethanol. 3D transplants were scanned at 45 kV, 200 μA, 600 ms integration time (IT), 14.8 μm voxel size. Femurs were scanned at 70 kV, 85 μA, 300 ms IT, 10 μm resolution (μCT50; Scanco Medical AG, Brüttisellen, Switzerland). Mineralized tissues were reconstructed using the global approach and segmented by a global thresholding software (Scanco Medical AG, Brüttisellen, Switzerland). Standardized nomenclature was used for the bone parameters measured. For the femurs, trabecular parameters were measured at the secondary spongiosa of the distal metaphysis and cortical parameters were determined in a 1 mm ring at the mid-diaphyseal region according to previously published guidelines (Bouxsein et al., 2010). The callus of the fractured femurs was analyzed along the entire shaft of the bone. Cross section measurements of the callus were calculated based on the entire stack of 2D images.

Histology and imaging

For scanning electron microscopy (SEM), 3D scaffolds were fixed at 4°C overnight with Karnovsky fixative (Electron Microscopy Sciences) followed by three washes with phosphate buffered saline (PBS) and dehydrated in a series of ethanol washes (0, 30, 50, 70, 85, 95, and 100%), with each wash conducted 3 times for a total of 15 min. The samples were then critical point dried (Autosamdri-814, Tousimis), mounted and sputter-coated with gold (75 mA for 60 s, Denton Vacuum Desk II) prior to imaging (2 kV, 10 Ua, S-4700-II FE-SEM, Hitachi). For histology, immunofluorescent and second harmonic generation (SHG) imaging, 3D scaffolds or femurs were decalcified prior to paraffin-embedding.

Femur sections were deparaffinized and rehydrated prior to SHG imaging of type I collagen. SHG imaging was performed on a Nikon A1R MP + HD confocal system using a ×40 Apo LWD objective (N.A. 1.15) in resonant scanning mode (512 × 512, 4X line average scanning). The two-photon beam excitation was provided by a Chameleon Vision II laser tuned to 820 nm (Coherent). The non-descanned detector used a 400–480 band pass emission filter. Z-stacks were taken of the middle 10 or 15 microns of 20 or 30 micron-thick tissue slices, respectively. Image tiles were created in a ~250–500 μm wide by 1800 μm long region centered around the femur center. Femur sections were oriented to match the two-photon beams polarity (parallel with the *Y*-axis). After acquisition, images were denoised using NIS Elements Denoise A.I. software (Nixon). Line scans depicted in figures show SHG signal intensity normalized to the brightest pixels for comparison on a similar scale.

To analyze SHG fibril differences between WT and KO femurs, ctFIRE and curve align standalone plugins for MatLab (Bredfeldt et al., 2014) were used with the following settings: Min fiber length 100 pixels, Max fiber width 15.

For Bgn immunochemistry, deparaffinized and rehydrated sections were incubated for 1 h at 37°C with ABCase (Seikagaku biobusiness corp.), followed by antigen retrieval (Unitrieve, Innovex), and quenching of endogenous peroxidase activity with dual endogenous enzyme block (Dako). The sections were blocked with 10% normal goat serum in PBS for 1 h at 37°C and incubated with Bgn rabbit antisera (from Dr. Larry W. Fisher, NIH, ref. LF-159) 1: 600 diluted in the blocking buffer overnight at 4°C. The sections were washed and incubated with Super PicTure™ Polymer detection kit (Invitrogen) for 20 min at RT and detected with ImmPACT™ AEC (Vector laboratories). Slides were scanned using an Aperio ScanScope slide scanner.

For F4/80, Ym1, and iNOS immunohistochemistry, deparaffinized and rehydrated sections were incubated for 48 h at 55°C with citrate buffer, pH 6.0 (BIOZOL, Germany). The sections were blocked with 3% H_2O_2 in PBS for 10 min and with Protein Block Serum-free solution (Dako, X0909) for 20 min. This was followed by incubation with rat anti-mouse F4/80 antibody (1:250, Biorad, MCA497G), rabbit anti-Ym1 antibody (1:100, Abcam, ab93034) or rabbit anti-iNOS (1:500, Enzo Life Sciences, ADI-905-431–1) diluted in antibody diluent (Dako S3022) overnight at 4°C. The sections were washed and incubated with Histofine Simple Stain Mouse MAX PO (Rat) (Nichirei Biosciences INC, 414311F) for F4/80, or with Histofine Simple Stain Mouse MAX PO (Rabbit) (Nichirei Biosciences INC, 414341F) for Ym1 and iNOS, for 30 min at RT and detected with Vector DAB Substrate (Vector laboratories, SK4100). Mayer's hematoxylin was used as counterstain. The protein expression levels were determined by the reciprocal intensity of the chromogen stain using the open source ImageJ Fiji software (http://fiji.sc/Fiji).

For aggrecan (ACAN) and osteopontin (OPN) immunofluorescence, deparaffinized and rehydrated sections were incubated for 1 h at 37°C with ABCase (Seikagaku biobusiness corp). Following antigen retrieval (Unitrieve, Innovex), and incubation with 0.1% sodium borohydride, the sections were blocked with 10% normal goat serum in PBS for 1 h at 37°C, and incubated 1:200 with either rabbit anti-ACAN antibody (Millipore, ref. AB1031) or rabbit anti-OPN antibody (IBL, ref. 18,621) overnight at 4°C. The sections were washed and incubated with secondary antibody, anti-Rabbit IgG conjugated to Rhodamine Red 1:500 (Jackson, ref. AB_2340614) and DAPI 1:500 (Thermo Fisher Scientific, ref. D21490) for 1 h at RT. Finally, the slides were washed, mounted and imaged by A1R-MP + HD multiphoton confocal system (Nikon). Tiled (2 × 2, 6 × 6 or 7 × 7) Z-stacks (every 1.0 μm) were taken using a ×40 Plan Fluor (N.A 1.3) oil immersion objective in resonant scanning mode (×512512, 4X line average scanning) using the 405 nm and 561 nm lasers. Images were denoised using NIS Elements Denoise A.I. software after acquisition (Nixon). For quantification, we applied a Li threshold and then captured the mean fluorescence intensity of included area of the image using ImageJ Fiji software.

For osteoclast analysis, deparaffinized sections of fractured bones were stained with TRAP (Sigma).

Staining with hematoxylin and eosin (H&E) was performed using standard protocols. For periosteal width analysis, H&E stained slides were scanned using an Aperio ScanScope slide scanner and the entire enlarged periosteum was outlined, measured and the expanded area analyzed by Image Pro 7.0 software (Media Cybernetics Inc., United States). This resulted in five data points for each genotype used.

RNA isolation, qRT-PCR and RNAseq

Femoral shafts were isolated and immediately frozen in liquid nitrogen. The bones were centered in a tissue tube (Covaris) under

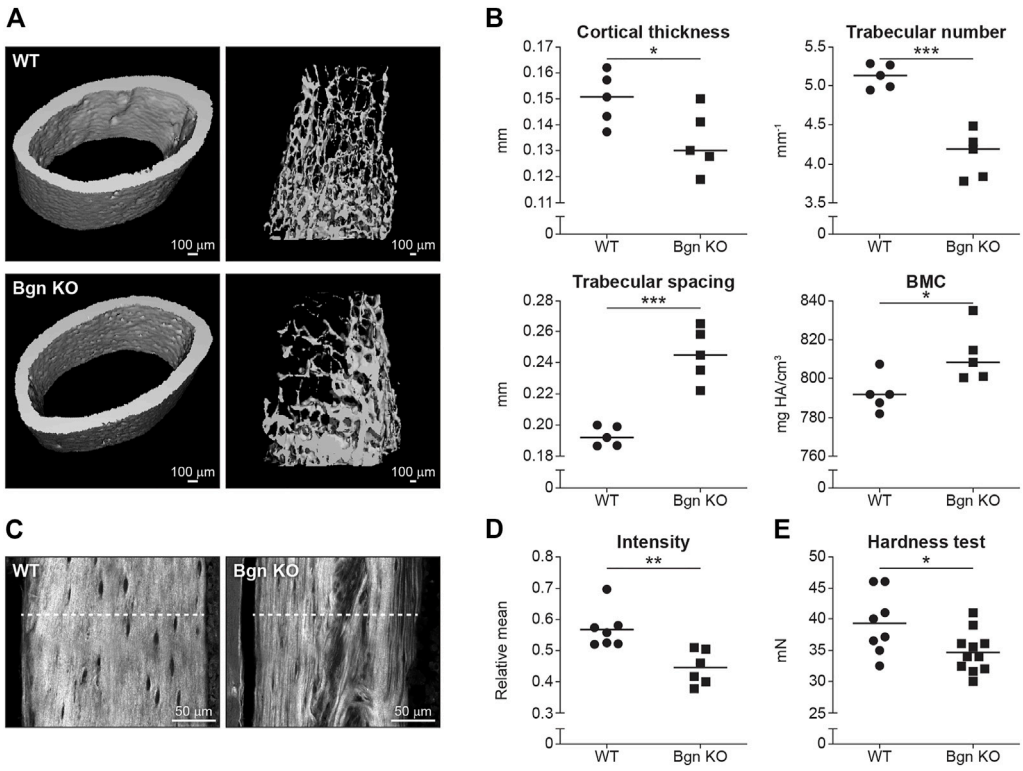

FIGURE 2
Bgn is needed for the structural integrity and the strength of bone. **(A)** 3D µCT reconstruction of femoral mid-diaphyseal cortical bone and the distal femoral metaphyseal bone from WT and *Bgn* KO mice (6 week-old), representative images. **(B)** Quantitative µCT analysis of cortical thickness, trabecular number, trabecular spacing, and Bone Mineral Content (BMC) (n = 5 per group). **(C)** Second harmonic generation (SHG) representative images of the collagen fibers in WT and *Bgn* KO femurs (6 week-old). **(D)** Quantitative SHG analysis of Type I collagen intensity. (n = 6/7 per group). **(E)** Micro indentation analysis of hardness of the femurs of WT and *Bgn* KO 6 week-old mice. (n = 8/11 per group).

liquid nitrogen and crushed using a CP02 cryoPREP Dry Pulverizer. Total mRNA was extracted and purified from the pulverized tissue using TriPure (Sigma, United States) followed by RNeasy mini kit (Qiagen) hybrid protocol.

Total mRNA from cultured cells was extracted and purified using RNeasy mini kit (Qiagen).

Total mRNA was converted to cDNA using iScript cDNA Synthesis Kit (Bio-Rad) and qRT-PCR analysis was performed using iQ SYBR Green Supermix (Bio-Rad). Target gene (Bgn: F: 5′-AGACAAACCGACAGCCTGACAAC-3′, R: 5′-GCCAGCAGCAAGGTGAGTAGC-3′) was normalized to S29 (F: 5′-GGAGTCACCCACGGAGTTCG-3′, R: 5′-GGAAGCAGCTGGCGGCACATG-3′) and relative expression data was calculated using the ΔΔCt method.

For RNA seq procedures, RNA was transcribed by Superscript IV (Thermo Fisher Scientific) and full-length 2nd strand cDNA amplified by LongAmp DNA polymerase (New England BioLabs). Sequencing libraries were prepared using a Nextera XT kit (Illumina), individually barcoded, pooled to a 2 nM final concentration, and sequenced on a NextSeq500 or NextSeq2000 instrument (Illumina) using 37 × 37 paired-end (NextSeq 500) or 55 × 55 (NextSeq 2000) paired-end read configurations. After sequencing, the base-called demultiplexed (fastq) reads from multiple sequencing runs were merged when appropriate and read qualities were determined using FastQC (v0.11.2), aligned to the GENCODE M11 mouse genome (GRCm38.p4) and gene counts generated using STAR (v2.5.2a). Post-alignment qualities were generated with Picard Tools RnaSeqMetrics (v1.129). An expression matrix of raw gene counts was generated using R and filtered to remove low count genes (defined as those with less than five reads in at least one sample). The filtered expression matrix was used to generate a list of differentially expressed genes (DEGs) between the sample groups using three statistical methods: DESeq2, EdgeR, and Limma-voom.

Single cell RNA seq

For single-cell RNA sequencing (scRNA seq), WT and *Bgn* KO embryos (E16.5) were used. After euthanasia, the posterior limbs were dissected and connective tissues were removed under sterile conditions. The bones were dissected into small pieces and digested with 2 mg/mL collagenase IV (Gibco) in Advanced DMEM (supplement with 1% Glutamine) for 40 min at 37°C with manual shaking every 10 min. When the dissociation procedure was complete, the cell-suspension was centrifuged, supernatants were carefully removed and the cell pellet suspended in PBS containing 0.1% BSA. The cells were then filtered using Flowmi filter tips (Bel-Art Products, #H13680-0040) to remove possible undissociated cells and debris. The cells were counted and resuspended to a final concentration of 1 × 10^6 cells/mL.

The single-cell suspension was loaded onto the droplet-based single-cell barcoding system (10x Chromium Controller, 10x Genomics) and a Chromium NextGEM Single Cell 3' Reagent Kit

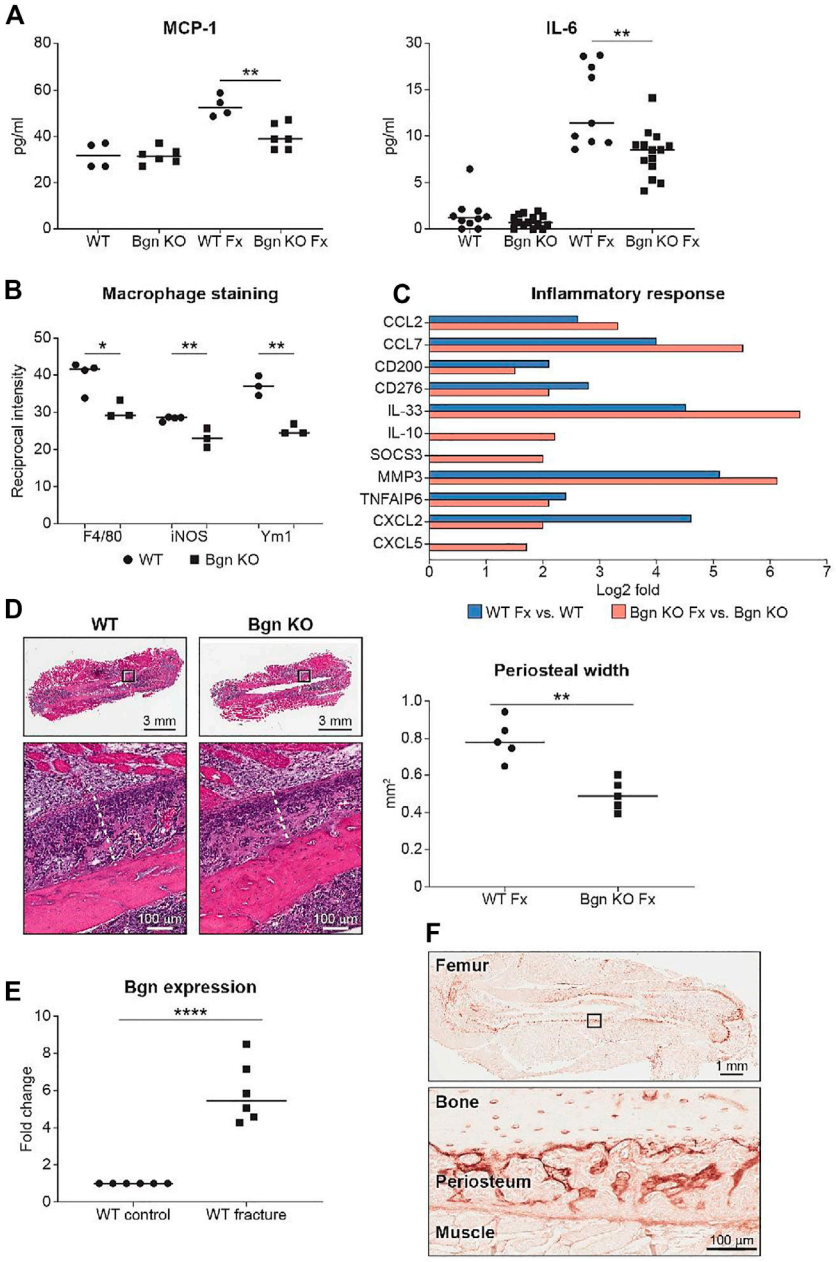

FIGURE 3
Bgn is needed for the inflammatory response after fracture. **(A)** Analysis of systemic cytokine secretion 24 h after fracture (Fx—Fracture). (For MCP-1, *n* = 4/6 per group; for IL-6, *n* = 10/14 per group) **(B)** Quantification of immunostaining for F4/80, iNOS and Ym1 around the fracture site 72 h after fracture (*n* = 3 per group). See also Supplementary Figure S3. **(C)** GO analysis of RNAseq data for genes involved in the inflammatory response before and 72 h after fracture (*n* = 6 per group). **(D)** Representative images and quantification of periosteal width 72 h after fracture (*n* = 5 per group). **(E)** Real-time PCR analysis of *Bgn* gene expression in WT bones before and 3 days after fracture (*n* = 6 per group). **(F)** Immunohistochemistry of Bgn in the periosteum 72 h after fracture, representative images (*n* = 5 per group).

v3.1 (10x Genomics) was used to prepare single-cell, barcoded 3' cDNA libraries according to the manufacturer"s instructions. The libraries were sequenced on a NextSeq2000 instrument (Illumina). The sequenced data was processed by CellRanger (v5.0.0, filtering, barcode and UMI counting) using default command line options and gene-barcode matrices were generated. The sequenced reads were aligned to the mouse genome assembly provided by 10X Genomics (10X Genomics reference mm10-2020-A), based on Ensembl annotation. Downstream data analysis was performed on the CellRanger cell-gene filtered matrix, using the Seurat R package V4 (Hao et al., 2021). Seurat objects were generated for each of the four samples (2 WT, two *Bgn* KO), which were then merged into a single Seurat object. Cells with unusual numbers of genes (<200), UMI count (>15,000) or percentage of mitochondrial genes (>20%) were filtered out. The data was then normalized by the "LogNormalization" method implemented in the Seurat package (scale factor = 10,000) and scaled using Seurat's default settings. The 2,000 top variable genes were identified using the "vst" method implemented in Seurat. Linear

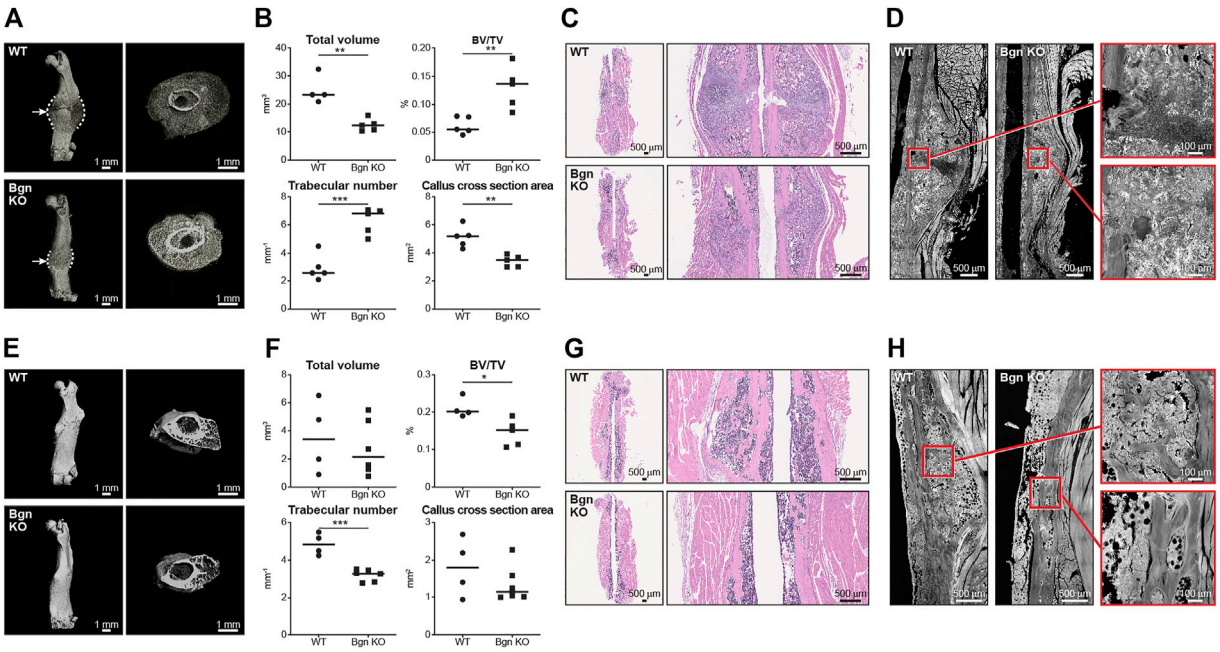

FIGURE 4
Lack of Bgn impairs bone healing after fracture. **(A)** 3D µCT reconstruction of femoral bone and cross section of the callus 2 weeks after fracture, representative images. Dashed lines mark the callus borders. Arrows marks the fracture site. **(B)** Quantitative µCT analysis of callus total volume, BV/TV, trabecular number and callus cross section area 2 weeks after fracture (n = 5 per group). **(C)** H&E staining of the callus area 2 weeks after fracture, representative images (*n* = 5 per group). **(D)** SHG representative images of healing bone 2 weeks after fracture (*n* = 5 per group). **(E)** 3D µCT reconstruction of femoral bone and cross section of the callus 8 weeks after fracture, representative images. **(F)** Quantitative µCT analysis of callus total volume, BV/TV, trabecular number and callus cross section area 8 weeks after fracture (*n* = 4/5 per group). **(G)** H&E staining of the callus area 8 weeks after fracture, representative images (*n* = 4/5 per group). **(H)** SHG representative images of the newly regenerated bone 8 weeks after fracture (*n* = 4/5 per group).

dimensional reduction (PCA) was performed, followed by batch correction using "Harmony" ("RunHarmony" command, using default settings) (Korsunsky et al., 2019). Nearest Neighbor analysis and clustering were performed using the Harmony embeddings. The clusters were visualized using Uniform Manifold Approximation and Projection (UMAP) (Becht et al., 2018). The DEGs between the clusters were identified using the Wilcoxon Rank Sum test implemented in Seurat's "FindAllMarkers" command. The cell identities were then assigned according to the markers identified (Supplementary Tables S1, S2). Cell types that were over clustered were merged (e.g., mast cells). For pseudotime trajectory analysis, a new Seurat object containing the osteoblasts clusters (1–4) and the skeletal progenitor cell was generated. The single cell trajectory and branching point were detected using the reversed graph embedding algorithm implemented in Monocle3 R package (Qiu et al., 2017) using default parameters. The root of the trajectory was defined as the list of the skeletal progenitor cells. The full code for the analysis and figures will be found in https://github.com/ishainer/R_shainer_et_al_2022/. The raw scRNA seq data is available through the NCBI GEO repository, accession number GSE192542, upon publication (token will be given upon reviewer's request).

Serum cytokines evaluation

Mouse serum was analyzed from peripheral blood, obtained by retro-orbital bleeding, 24 h post fracture. Circulating cytokine levels were determined by flow cytometry using a mouse inflammation CBA kit (BD Bioscience, BD 552364) according to the manufacturer's protocol. Briefly, a mix of six bead populations coated with antibodies specific for IL-6, IL-10, MCP-1, IFN-γ, TNF, and IL-12p70 were incubated for 2 h at RT with serum samples and with PE conjugated detection antibodies to form sandwich complexes. PE fluorescence intensity for each of the antibodies was measured by Flow Cytometer and FCAP Array™ software was used to generate the results.

Micro indentation

Femurs were embedded without demineralization in SamplKwick fast cure acrylic compound (Burhler). 7 mm thick cross-sections were cut from the bone's mid-shaft using a diamond saw. The samples were ground and polished with Micro-Mesh sanding sheets followed by 0.25 µm diamond paste. Indents were preformed using HMV-G21DT micro-hardness testing machine (Shimadzu) with a diamond Vickers microindenter tip using 0.05 N of applied force for 10 s before unloading. 3-4 indents were performed for each sample and the results were averaged.

Statistical analysis

Differences were examined by two-tailed Student's t-test for comparing two groups and by either one-way or two-way analysis of variance (ANOVA) test for comparing multiple groups. When

10.3389/fphys.2023.1119368

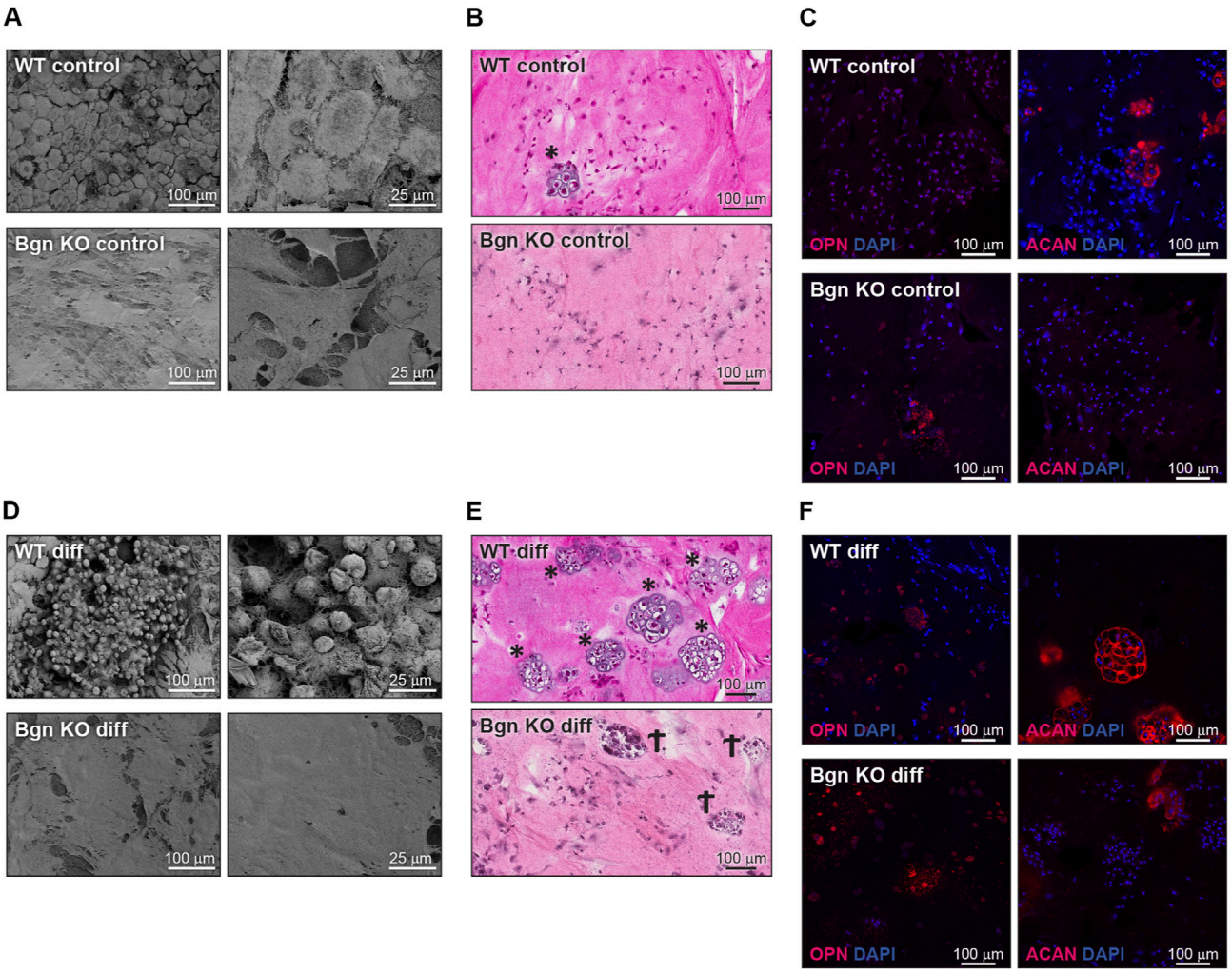

FIGURE 5
Bgn affects cartilage and bone differentiation in 3D culture system. **(A)** SEM images of the ECM secreted by undifferentiated (control) PDCs in the 3D structures, representative images (n = 5 per group). **(B)** H&E staining of the control 3D structures representative images (n = 5 per group). * marks chondrocytes. **(C)** Immunostaining of the control 3D structures stained for ACAN and OPN, representative images. See also Figure S5A-C (n = 5-8 per group). **(D)** SEM images of the ECM secreted by the differentiated PDCs in the 3D structure, representative images (n = 5 per group). **(E)** H&E staining of the differentiated 3D structures, representative images (n = 5 per group). * marks chondrocytes. † marks dead cells. **(F)** Immunostaining of the differentiated 3D structures stained for ACAN and OPN, representative images. See also Supplementary Figures S5A–C (n = 5-8 per group).

significant differences were indicated by ANOVA, group means were compared to establish the source of the differences. $p < 0.05$ was considered statistically significant.

Results

Single-cell sequencing of mouse embryonic bones shows Bgn is important for osteoblast differentiation

Bgn is an abundant matrix component expressed in skeletal tissues throughout bone development and maturation. To study the role of Bgn *in vivo*, a *Bgn*-deficient mouse line was generated (Xu et al., 1998). Although *Bgn* KO mice appear normal at birth, they display a phenotype characterized by reduced bone mass and age-dependent osteopenia. Lechner et al. (2006) measured the expression of *Bgn* mRNA in mouse hindlimbs during development and found that *Bgn* was present at E14, exhibited a striking 5-fold upregulation at E16, before dropping 5-fold by E18. Therefore, to understand when bone defects begin to arise in *Bgn* KO mice, we isolated cells from fetal hindlimbs of WT and *Bgn* KO embryos at 16.5 days of age, where *Bgn* transcript level is at its highest, and performed single-cell RNA sequencing (scRNA seq) analysis using the 10X Genomic's Chromium platform. Clustering analysis of the sequenced cells revealed 38 transcriptionally distinct populations. The top 50 differentially expressed genes within each cluster were used to identify the cell-type represented by each cluster (Figure 1A; Supplementary Table S1). 14,781 WT cells and 15,054 *Bgn* KO cells were analyzed, and both genotypes expressed the same clustering pattern (Figure 1B; Supplementary Figures S1A, S2). *Bgn* was found to be expressed mainly in skeletal progenitor cells, osteoblasts, chondrocytes, stromal cells, embryonic fibroblasts, tendon cells and neuronal progenitor cell clusters (Figure 1C). *Bgn* mRNA wasn't

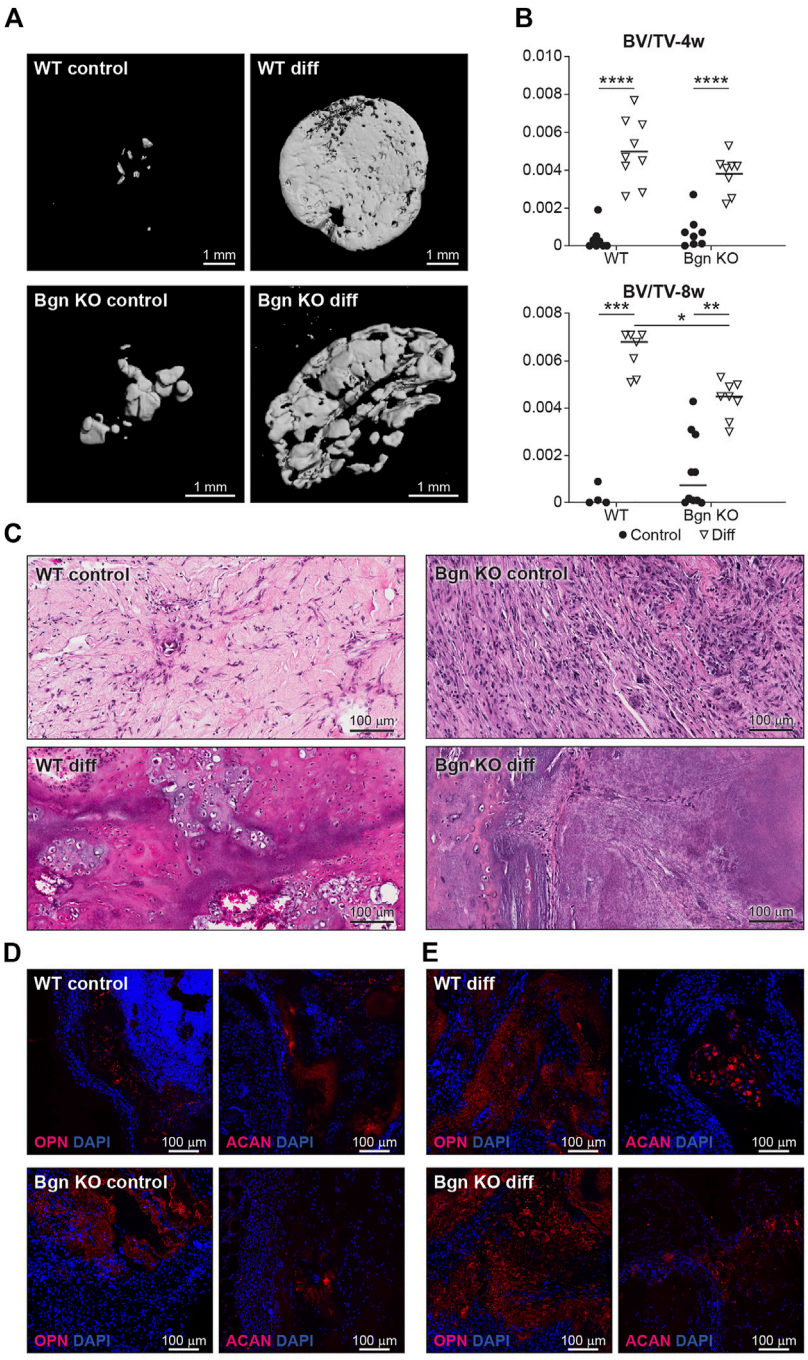

FIGURE 6
Lack of *Bgn* in a 3D culture system result in compromised bone formation. **(A)** 3D µCT reconstruction of the implants 8 weeks after subcutaneous implantation, representative images. **(B)** Quantitative µCT analysis of BV/TV of the 3D structures 4 and 8 weeks after subcutaneous implantation. **(C)** H&E staining of the 3D structures 8 weeks after subcutaneous implantation, representative images. **(D)** Immunostaining of the control 3D structures stain for ACAN and OPN 8 weeks after subcutaneous implantation, representative images. See also Supplementary Figures S5D–F (n = 4-9 per group). **(E)** Immunostaining of the differentiated 3D structures stained for ACAN and OPN 8 weeks after subcutaneous implantation, representative images. See also Supplementary Figures S5D–F (n = 4-9 per group).

detected in *Bgn* KO cells as shown in Figure 1C and Supplementary Figure S1B. All the clusters included cells originating from both WT and *Bgn* KO animals, but the relative distribution of *Bgn* KO and WT cells differed in many of the clusters (Figure 1D; Supplementary Figure S2). From the total analyzed cells, 8.6% were chondrocytes. However, 5.6% came from WT cells and 3% came from *Bgn* KO cells. In addition, from the total analyzed cells, 18.6% were osteoblasts. In this cell type, 12.1% came from WT cells while only 6.5% came from *Bgn* KO cells. More specifically, in osteoblast clusters 1 and 2, the number of WT cells was almost equal to the number of *Bgn* KO cells but in the progression to osteoblast clusters 3 and 4 the number of *Bgn* KO cells dramatically decreased. In particular, osteoblast cluster 4 was

comprised primarily of WT cells (88%) versus *Bgn* KO cells, which represented a minor fraction (12%) (Figures 1D–E; Supplementary Figure S2). Since the total number of cells that was analyzed equally represent both genotypes, the differences in specific cluster distribution most likely reflect the effect of *Bgn* deficiency on cell differentiation. To identify the differences between the 4 osteoblast clusters, enrichment analysis of biological pathways was performed on the differentially expressed genes. While the cells in all osteoblast clusters expressed genes that are involved in the ECM organization and the skeletal system development pathways, the genes specifically associated with the ossification pathway were highly expressed in osteoblast clusters 3 and 4, and genes associated with the osteoblast differentiation pathway were only found in osteoblast cluster 4 (Figure 1F). To further investigate the relationship between the osteoblast clusters, we analyzed their differentiation progress along a pseudotime trajectory using monocle3 (Qiu et al., 2017). The pseudotime trajectory was tested for the four osteoblast clusters, together with the skeletal progenitor cells, that were defined as the trajectory root. The global gene expression changes, enabled the detection of a single branching point leading the cell fate towards osteoblasts 3 and osteoblasts 4 (Supplementary Figures S1C, D), suggesting these clusters differentiate later than osteoblast cluster 2.

Taken together these data suggest that the differentiation and maturation levels of the osteoblasts are more advanced as they progress from osteoblast cluster 1 to osteoblast cluster 4. Cells from embryonic *Bgn* KO bone have less mature osteoblasts, less chondrocytes and more immature embryonic fibroblast cells (Figure 1D; Supplementary Figure S2), suggesting that Bgn is needed for early stages of bone development starting from the origin of the cells that generate the bone.

Biglycan is needed for the structural integrity and the hardness of bone

To understand how the changes we found in the scRNA seq of embryonic bones could affect skeletal development, μCT was performed on mature 6 week-old mice.

Our data showed that there was a reduction in cortical thickness and trabecular number, and an increase in trabecular spacing and bone mineral content (BMC) in *Bgn* KO mice compared with WT mice (Figures 2A, B). Since 90% of the organic ECM of bone is collagen type I, second harmonic generation (SHG) microscopy was used to visualize and quantify the structural integrity of the collagen fibers in the *Bgn*-deficient bones. High collagen signature, as indicated by a consistently high even SHG intensity, with minor spacing between the collagen fibers was observed in the femurs of WT mice, whereas *Bgn* KO femurs showed significantly less of a collagen signature and more spacing between the fibers (Figures 2C, D). To understand how these molecular structural changes were affecting bone hardness, we assessed the strength of the bone by micro-indentation and found a reduction in the hardness of the *Bgn* KO bones compared with WT (Figure 2E). These results correlate with previous observations by Wallace et al. (2006) who used a 4-point bending test to demonstrate a reduction in the bone strength in Bgn KO bones compared to WT. Taken together, our findings show that in the absence of Bgn, compromised bone formation occurs that, ultimately, appears to affect collagen integrity, and subsequently biomechanical phenotype.

Lack of biglycan impairs bone healing

Considering bone defects were discovered in the mature bones of *Bgn* KO mice, we wanted to examine the skeletal remodeling process under the challenge of induced bone fracture. Bone healing involves a complex sequence of physiological events, starting with an inflammatory response at the fracture site, followed by activation and proliferation of skeletal stem cells in the periosteum and in the bone marrow. In the first phase of inflammation, inflammatory chemokines and cytokines are secreted to recruit inflammatory cells. Migration of macrophages into the fracture area has a major impact on the long term outcome of bone healing (Schlundt et al., 2018). Schaefer et al. (2005) previously showed in a sepsis model that Bgn, upon release from the ECM or from macrophages, acts as a proinflammatory factor and can boost inflammation by signaling through toll-like receptor (TLR) 2 and TLR4, which mediate the innate immunity.

To evaluate the onset of inflammation as a result of the injury, serum was obtained from peripheral blood 24 h after fracture. We analyzed the systemic inflammatory cytokine secretion and found a reduction in monocyte chemoattractant protein 1 (MCP-1) and IL-6 secretion in *Bgn* KO mice (Figure 3A). MCP-1 is a chemokine that regulates macrophage infiltration and is highly expressed in the periosteum in response to fracture. To understand how MCP-1 reduction impacts macrophage infiltration, fractured bones were collected 1–3 days after fracture and stained for different macrophage markers. Significant reduction in macrophage infiltration around the fracture site was found in *Bgn* KO compared with WT mice. Lower numbers of both F4/80$^+$ and iNOS$^+$ M1 macrophages were observed as early as 1 day after fracture. While Ym1$^+$ M2-like macrophages were also reduced in *Bgn* KO compared with WT mice, this was not significant until 2 days after injury (Figure 3B; Supplementary Figure S3). RNAseq analysis of the bones 3 days after fracture showed enhanced expression of inflammatory suppressor cytokines, such as IL-10 and SOCS3, in the *Bgn* KO (Figure 3C).

Since the role of the inflammation is to trigger the activation and proliferation of periosteal progenitors, we next measured the size of the periosteum 3 days after fracture and found that the periosteum of *Bgn* KO mice didn't expand to the same extent as the WT after fracture (Figure 3D). The periosteum has a crucial role in bone regeneration and therefore we wanted to determine whether the expanding PDCs express Bgn. mRNA analysis and immunohistochemistry showed that in response to fracture, Bgn expression is upregulated in the bone, particularly in the enlarging periosteum (Figures 3E, F). Since the rapid periosteal expansion leads to callus formation around the fracture site, we measured the callus formation 1, 2 and 8 weeks after fracture. In the earlier time point of 1 week after fracture, there were no significant differences in callus total volume, BV/TV, trabecular number and callus cross section between *Bgn* KO and WT mice (Supplementary Figure S4). However, 2 weeks post fracture, when the full callus is formed, we found that fractured bones from *Bgn* KO mice formed a smaller callus compared with WT mice (Figures 4A–D). μCT analysis demonstrated lower total callus volume and callus cross section area in *Bgn* KO fractured bones, whereas BV/TV and the trabecular number were higher (Figure 4B). In addition, massive cartilage tissue was observed in the WT callus compared with that from *Bgn* KO, as shown by both H&E staining (Figure 4C) and SHG imaging (Figure 4D), suggesting an impaired cartilage phase in the *Bgn* KO mice at this time point compared with the WT. These

results concur with cartilage specific aggrecan (ACAN) staining we previously published (Berendsen et al., 2014). The amount of TRAP staining in the callus was not significantly different between WT and *Bgn* KO bones 2 weeks after fracture (data not shown) indicating that the smaller callus in the KO bones isn't due to higher bone resorption. By week 8, most of the callus formed in the *Bgn* KO fractured bones was resorbed and the bone had prematurely remodeled into mature bone (Figures 4E–H). μCT analysis 8 weeks post fracture showed there was higher BV/TV and trabecular number in the callus of the fractured WT bones compared with *Bgn* KO bones with no significant differences in the callus total volume and cross section area (Figure 4F). Furthermore, analysis of the newly formed bone by both H&E staining and SHG imaging (Figures 4G, H respectively) showed that WT bones developed more uniform and mature collagen fibril-like structures compared with the healing *Bgn* KO bone. Analyzing the SHG images of 8 weeks post fracture bones, revealed that both the collagen fiber length and width were higher in the regenerated *Bgn* KO bones, whereas no differences were found in collagen fiber number (Supplementary Figure S5A). When we analyzed WT and *Bgn* KO in un-fractured bones, there were no differences in the number, length and width of the collagen fibers (Supplementary Figure S5B), however the collagen fiber orientation wasn't normal. A closer look at irregular regions of Bgn KO bones using second harmonic microscopy, showed significant changes in the structure, that may have an overall impact on bone function (Figures 2C, D). We take these observations to indicate that the small callus formed by the *Bgn* KO arises from an abnormal progression of the healing process that results in bone with inferior structure.

Bgn affects cartilage and bone differentiation in 3D culture system

Since PDCs have an important role in the healing process, we decided to study their activity using a 3D culture system in order to more closely mimic the native environment of the cells.

The 3D RAFT™ cell culture is based on rat tail collagen type I, where the cells and the collagen are mixed together to form a 100 μ thick hydrogel disc, in the size of a well in a 96 well plate. After isolation, PDCs from WT and *Bgn* KO mice were allowed to proliferate within the 3D culture system and either maintained with standard culture medium or induced towards osteogenic differentiation for 2 weeks. Analysis of the control (un-differentiated) 3D scaffolds with scanning electron microscopy (SEM) showed discrete differences between the ECM secreted by WT and *Bgn* KO PDCs (Figure 5A). H&E staining of the WT control 3D cultures surprisingly showed some chondrocyte clusters, a finding which was confirmed by aggrecan (ACAN) immunostaining. Neither chondrocytes nor aggrecan staining was detected in *Bgn* KO control 3D structures (Figures 5B, C; Supplementary Figure S6A). Upon osteogenic differentiation in the 3D culture system, WT PDCs seemed to undergo endochondral ossification by secreting ACAN and forming cartilage structures that were incorporated into the matrix (Figures 5D–F; Supplementary Figure S6A). At the same time, evidence of dead chondrocytes was found in the differentiated *Bgn* KO PDCs as shown by H&E staining and low level of ACAN staining (Figures 5E, F; Supplementary Figure S6A). The total number of cells (quantified by DAPI staining) wasn't significantly different between *Bgn* KO and WT 3D constructs (Supplementary Figure S6C).

When the 3D structures were subcutaneously implanted into syngeneic mice, we found that the differentiated PDCs (both WT and KO) created mineralized tissues 4 and 8 weeks post implantation (Figures 6A, B). To understand the composition of the mineralized 3D structures 8 weeks post transplantation, histological analysis was performed. Differentiated WT implants displayed an endochondral ossification pattern with chondrocytes surrounded by bone and blood vessels, which wasn't found in the structures formed by differentiated *Bgn* KO PDCs (Figure 6C). Since the H&E staining of the *Bgn* KO implants was difficult to interpret, immunofluorescence staining for ACAN and OPN was performed. The WT control implants showed again higher expression of ACAN compared with the *Bgn* KO control implants (Figure 6D; Supplementary Figure S6D). As expected, after 8 weeks of implantation, differentiated implants from both genotypes showed some staining for ACAN and intense staining for OPN, however, *Bgn* KO implants demonstrated more robust staining of OPN compared with WT (Figure 6E; Supplementary Figure S6E). No differences were observed in cell number between the samples as quantified by DAPI staining (Supplementary Figure S6F).

The low level of cartilage differentiation coupled with a high level of OPN expression suggest that in the absence of *Bgn*, the cartilage phase preceding bone is compromised, leading to more direct bone differentiation.

Discussion

Bone tissue has the unique ability to heal and regenerate throughout life. This process, which is similar to embryonic endochondral bone development, relies on a complex sequence of physiological events leading to the formation of new bone at the fracture site. The inflammatory response is necessary in the early stages of bone healing to trigger and activate the proliferation of skeletal progenitor cells within the periosteal layer. During healing, the differentiation of progenitor cells into chondrocytes and osteoblasts gives rise to a callus around the fracture site. As the chondrocytes undergo hypertrophy, blood vessels and osteoprogenitor cells are attracted from nearby periosteal regions. The cartilage template is degraded and replaced by woven bone which ultimately remodels to the mature bone (Marsell and Einhorn, 2011; Roberts et al., 2015; Salhotra et al., 2020). In this study, we demonstrate a role for *Bgn* in early stages of bone development, as well as in bone repair.

The *Bgn* gene is located on the X chromosome in mice and humans and is highly expressed during development (Bianco et al., 1990; Fisher et al., 1991; Wilda et al., 2000). Recently, loss-of-function mutations in the human *Bgn* gene were found in Meester-Loeys syndrome (MRLS) (Meester et al., 2017). Clinically, MRLS patients present with early-onset aortic aneurysm and dissection. The males carrying the deletion also have skeletal dysplasia, which is characterized by relatively short stature, phalangeal dysplasia, brachydactyly, hip dislocation and dysplastic epiphyses of the long bones. Like MRLS patients, *Bgn* KO mice also have skeletal abnormalities. *Bgn*-deficient mice acquire early onset osteoporosis-like phenotype with significant decreases to their trabecular bone volume and mineral apposition rate (Xu et al., 1998; Chen et al., 2002), as well as structural abnormalities of collagen fibrils in bone, dermis, and tendon (Corsi et al., 2002). While these studies point to the importance of Bgn in bone, its exact role in skeletal healing and early bone formation was unclear.

Bone is a heterogeneous organ, composed of a variety of cell types. Single-cell sequencing is an advanced technique that can be used to

understand the cellular basis of skeletal development (Greenblatt et al., 2019). In order to detect the onset of possible changes in the cell landscape in *Bgn* KO mice during embryonic development, single cell RNAseq analysis of E16.5 WT and *Bgn* KO embryo hindlimbs was performed for the first time. Seurat's unbiased cluster detection algorithm defined 38 cell populations within the long bone endocortical samples of both WT and *Bgn* KO. Our analysis revealed 4 osteoblast clusters (1–4). Compared to clusters 1 and 2, clusters 3 and 4 expressed elevated levels of osteogenic genes, which were identified by GO analysis, and were sequentially located after cluster 1 on the UMAP pseudo-time trajectory branch. This data suggests that cells in cluster 4 are more committed and mature osteoblasts compared with those found in clusters 1-3. We show that the majority of cells that populate the mature cluster 4 originate from WT samples. We hypothesize that the lower levels of mature osteoblast cells found in *Bgn* KO mice, as early as 16.5 days of embryonic development, together with a reduced number of cells in the chondrocyte clusters, leads to the abnormalities seen in the adult *Bgn* KO bones. Previous *in vitro* studies showed an increased number of osteoclasts in adult *Bgn* KO mice which was presumed to be due to defects in the proliferation and differentiation of osteoblasts and their precursors (Bi et al., 2006). Our studies established, at the single-cell level, the concept that *Bgn* is needed for embryonic bone-cell maturation, and that the absence of Bgn could, later in life, result in defective osteogenesis. Further experiments to validate our findings at the protein level will be needed to confirm this theory. Our lab has previously found that Bgn's core protein enhances canonical Wnt signaling (Berendsen et al., 2011). Moreover, using other skeletal progenitors, we showed that *Bgn* can regulate TGF-β activity (Chen et al., 2002; Bi et al., 2007; Embree et al., 2010). Both pathways could be important mechanisms to modulate *Bgn* skeletal cell differentiation and cell fate.

In mature bones, we show here the importance of *Bgn* to bone integrity, where *Bgn* KO bones have reduced cortical thickness and trabecular number, and an increase in trabecular spacing and bone mineral content (BMC), leading to a more fragile bone that is biomechanically compromised. Additionally. We show that *Bgn* is crucial for normal bone repair in response to injury. Shortly after bone fracture, chemokines and inflammatory cytokines are secreted to recruit inflammatory cells and promote angiogenesis. It was previously shown that *Bgn* can serve as a pro-inflammatory factor in a sepsis model and the mechanistic basis involves TLR 2 and 4 (Schaefer et al., 2005). In the present study, we demonstrate that *Bgn* plays a regulatory role in the immune response during the first phase of fracture healing. Mice lacking *Bgn* had a decreased inflammatory response demonstrated by decreased secretion of inflammatory cytokines, MCP-1 and IL-6, and reduced macrophage infiltration around the fracture site. MCP-1 (also known as CCL2), which has been shown to be expressed in the periosteum around the fracture site during fracture healing (Edderkaoui, 2017), is one of the earliest, highly expressed chemokines in response to fracture and is involved in regulating angiogenesis and macrophage infiltration. IL-1 and IL-6 are believed to be critical cytokines for fracture healing. IL-1, produced by macrophages during the acute phase of inflammation, induces the production of IL-6 in osteoblasts. It also stimulates the formation of the initial cartilaginous callus and promotes angiogenesis around the fracture site. IL-6, also produced during the acute inflammatory phase, stimulates angiogenesis and vascular endothelial growth factor (VEGF) production (Kon et al., 2001; Mountziaris and Mikos, 2008; Marsell and Einhorn, 2011). Fracture healing requires a blood supply and therefore revascularization is essential for successful bone repair. We previously showed that compared with WT controls, *Bgn*-deficient mice have a significant decrease in VEGF gene expression and concomitant smaller vessel size and volume around the fracture site (Berendsen et al., 2014; Myren et al., 2016). The reduced inflammatory response and angiogenesis in the *Bgn* KO mice may be the cause for the observed reduction in periosteal expansion around the fracture site, resulting in the formation of a smaller callus 14 days post fracture. We found that the smaller callus in *Bgn* KO mice has substantially fewer chondrocytes compared with WT, which is in agreement with previous studies showing less aggrecan at the callus site of *Bgn* KO mice compared with WT (Berendsen et al., 2014). μCT analysis 14 days after fracture surprisingly demonstrated higher BV/TV and trabecular number in the *Bgn* KO callus compared with WT, which may indicate that the defective cartilage phase in *Bgn* KO mice forced the healing process to occur through direct bone development. 8 weeks post fracture, the *Bgn* KO callus was almost completely resolved, excluding the possibility the healing process in the KO mice is delayed. We believe that the larger the callus is, the more time it takes for it to resolve and heal. Since *Bgn* KO have a smaller callus, it takes less time for it to fully heal, which does not necessarily mean the process itself is accelerated.

The periosteum is a major source of the heterogenous array of skeletal progenitor cells, important not only in bone development but also during fracture healing. Several studies demonstrated that removal of the periosteum dramatically impairs bone repair (Ozaki et al., 2000; Colnot, 2009). Ozaki et al. showed a delay in cartilage formation after fracture when the periosteum was removed, suggesting that the periosteum and its PDCs are important for mediating chondrogenesis during the endochondral ossification phase in bone repair (Ozaki et al., 2000). In this study, we found that *Bgn* is highly expressed in the expanding periosteum after fracture. *Bgn*-deficient periosteum didn't expand to the same extent as the WT, leading to smaller callus formation. Our results clearly demonstrate the importance of *Bgn* in the early phase of inflammation and during the subsequent periosteal expansion that is required for proper callus formation and proper healing during bone regeneration. These findings suggest that Bgn may influence bone repair by: 1) its pro-inflammatory role in the healing process and/or 2) by directly affecting the PDCs themselves.

Currently, like progenitor cells derived from the bone marrow (BMSCs), it has been challenging to identify markers that are specific for PDCs. In recent years, several markers have been proposed to identify PDCs, including Cathepsin K, periostin and alpha smooth muscle actin (αSMA), and it is likely these markers define subpopulations of the cells within the periosteal layer (Marecic et al., 2015; Debnath et al., 2018; Deveza et al., 2018; Duchamp de Lageneste et al., 2018; Ortinau et al., 2019; Matthews et al., 2021). To understand the role of Bgn on PDCs in their natural heterogenous state, we harvested the periosteum and used the entire cell population. A 3D culture system was employed to further mimic the native environment of the cells. We allowed the cells to proliferate on the 3D structures before subjecting them to osteogenic differentiation. After 2 weeks of differentiation, WT PDC cultures formed ACAN expressing chondrocytes, the cells that provide an essential template for bone repair and bone development. In the 3D cultures containing *Bgn* KO cells, the chondrogenic phase was bypassed and instead the cultures showed expedited bone development, as judged by the high level of

OPN, a marker of early osteogenic differentiation. We further show, using a subcutaneous transplantation approach, that PDCs from WT and *Bgn* KO differentiate differently during endochondral ossification *in vivo*. Histological analysis of the calcified structures showed that compared with WT structures, which developed osteoblasts, chondrocytes and encouraged vascularization necessary for bone development, implants containing *Bgn* KO PDCs differentiated more directly into bone, expressing high levels of OPN. Although OPN is believed to be important for homeostasis of osteoclasts and osteoblasts, elevated levels of OPN are also functionally implicated in bone-related diseases, such as osteoporosis, rheumatoid arthritis, and osteosarcoma (Si et al., 2020). The high level of OPN expressed in the *Bgn* KO PDC cultures during osteogenic differentiation may be harmful to the structural integrity and strength of bone, which could be a potential basis for the early onset osteoporosis phenotype found in this genetic model (Xu et al., 1998).

In conclusion, *Bgn* deletion impairs endochondral bone formation and regeneration. The defective periosteal cells may be the key to the subsequent abnormalities we observed in the healing bone. More investigation will be required in the future to understand how *Bgn* and other ECM proteins influence skeletal stem cell populations during bone development and the periosteal progenitors during regeneration. Better understanding of these processes and their key elements will help in developing better strategies to treat skeletal defects and bone disease.

Data availability statement

The datasets presented in this study can be found in online repositories. The names of the repository/repositories and accession number(s) can be found below: https://www.ncbi.nlm.nih.gov/search/all/?term=GSE192542.

Ethics statement

The animal study was reviewed and approved by NIDCR/NIH/DHHS ACUC. Written informed consent was obtained from the owners for the participation of their animals in this study.

Author contributions

RS and MFY designed experiments and RS performed experiments. RS and TMK conducted mice experiments, VK preformed μCT analysis and provided assistance with experiments, LL prepared histological slides, ADD performed SHG and fluorescent microscopy imaging, IS performed single cell analysis, DM assisted with RNAseq and scRNA seq studies, CGS assisted with SEM, and LS and JZ-B conducted macrophage staining. RS and MFY wrote the manuscript. MFY conceived the overall project idea.

Funding

The research was supported in part by the Intramural Research Program of the NIH, NIDCR Molecular Biology of Bones and Teeth Section (Z01DE000379), Veterinary Resources Core (ZICDE000740) Genomics and Computational Biology Core (ZIC DC000086), Imaging Core (ZIC DE000750) Combined Technical Research Core (ZIC DE000729). This work utilized the computational resources of the NIH HPC Biowulf cluster (http://hpc.nih.gov). IS work was supported by the Alexander von Humboldt foundation research fellowship. LS work was supported by the German Research Council (SFB 1039, project B02, SFB 1177, 259130777, project E02, and the CardioPulmonary Institute (CPI), EXC 2026, Project ID: 390649896.

Acknowledgments

We would like to thank Steve Hudson (NIST) for assisting with the critical point dryer, Yankel Gabet (TAU) for generating a new μCT script and to Megan Noonan (NIDCR) for experimental assistance. Certain equipment, instruments, or materials are identified in this paper to adequately specify the experimental details. Such identification does not imply a recommendation by NIST, nor does it imply the materials are necessarily the best available for the purpose. This manuscript is a contribution of NIST and therefore is not subject to copyright in the United States.

Conflict of interest

The authors declare that the research was conducted in the absence of any commercial or financial relationships that could be construed as a potential conflict of interest.

Publisher's note

All claims expressed in this article are solely those of the authors and do not necessarily represent those of their affiliated organizations, or those of the publisher, the editors and the reviewers. Any product that may be evaluated in this article, or claim that may be made by its manufacturer, is not guaranteed or endorsed by the publisher.

Supplementary material

The Supplementary Material for this article can be found online at: https://www.frontiersin.org/articles/10.3389/fphys.2023.1119368/full#supplementary-material

References

Becht, E., Mcinnes, L., Healy, J., Dutertre, C. A., Kwok, I. W. H., Ng, L. G., et al. (2018). Dimensionality reduction for visualizing single-cell data using umap. *Nat. Biotechnol.* 37, 38–44. doi:10.1038/nbt.4314

Berendsen, A. D., Fisher, L. W., Kilts, T. M., Owens, R. T., Robey, P. G., Gutkind, J. S., et al. (2011). Modulation of canonical Wnt signaling by the extracellular matrix component biglycan. *Proc. Of Natl. Acad. Of Sci.* 108, 17022–17027. doi:10.1073/pnas.1110629108

Berendsen, A. D., and Olsen, B. R. (2015). Bone development. *Bone* 80, 14–18. doi:10.1016/j.bone.2015.04.035

Berendsen, A. D., Pinnow, E. L., Maeda, A., Brown, A. C., Mccartney-Francis, N., Kram, V., et al. (2014). Biglycan modulates angiogenesis and bone formation during fracture healing. *Matrix Biol.* 35, 223–231. doi:10.1016/j.matbio.2013.12.004

Bi, Y., Ehirchiou, D., Kilts, T. M., Inkson, C. A., Embree, M. C., Sonoyama, W., et al. (2007). Identification of tendon stem/progenitor cells and the role of the extracellular matrix in their niche. *Nat. Med.* 13, 1219–1227. doi:10.1038/nm1630

Bi, Y., Nielsen, K. L., Kilts, T. M., Yoon, A., Karsdal, A., Wimer, H. F., et al. (2006). Biglycan deficiency increases osteoclast differentiation and activity due to defective osteoblasts. *Bone* 38, 778–786. doi:10.1016/j.bone.2005.11.005

Bianco, P., Fisher, L. W., Young, M. F., Termine, J. D., and Robey, P. G. (1990). Expression and localization of the two small proteoglycans biglycan and decorin in developing human skeletal and non-skeletal tissues. *J. Of Histochem. Cytochem.* 38, 1549–1563. doi:10.1177/38.11.2212616

Bouxsein, M. L., Boyd, S. K., Christiansen, B. A., Guldberg, R. E., Jepsen, K. J., and Müller, R. (2010). Guidelines for assessment of bone microstructure in rodents using micro–computed tomography. *J. Of Bone And Mineral Res.* 25, 1468–1486. doi:10.1002/jbmr.141

Bredfeldt, J. S., Liu, Y., Pehlke, C. A., Conklin, M. W., Szulczewski, J. M., Inman, D. R., et al. (2014). Computational segmentation of collagen fibers from second harmonic generation images of breast cancer. *J. Biomed. Opt.* 19, 16007. doi:10.1117/1.JBO.19.1.016007

Chen, X.-D., Shi, S., Xu, T., Robey, P. G., and Young, M. F. (2002). Age-related osteoporosis in biglycan-deficient mice is related to defects in bone marrow stromal cells. *J. Of Bone And Mineral Res.* 17, 331–340. doi:10.1359/jbmr.2002.17.2.331

Colnot, C. (2009). Skeletal cell fate decisions within periosteum and bone marrow during bone regeneration. *J. Of Bone And Mineral Res. Official J. Of Am. Soc. Bone And Mineral Res.* 24, 274–282. doi:10.1359/jbmr.081003

Colnot, C., Zhang, X., and Tate, M. L. K. (2012). Current insights on the regenerative potential of the periosteum: Molecular, cellular, and endogenous engineering approaches. *J. Of Orthop. Res.* 30, 1869–1878. doi:10.1002/jor.22181

Corsi, A., Xu, T., Chen, X.-D., Boyde, A., Liang, J., Mankani, M., et al. (2002). Phenotypic effects of biglycan deficiency are linked to collagen fibril abnormalities, are synergized by decorin deficiency, and mimic ehlers-danlos-like changes in bone and other connective tissues. *J. Of Bone And Mineral Res.* 17, 1180–1189. doi:10.1359/jbmr.2002.17.7.1180

Debnath, S., Yallowitz, A. R., Mccormick, J., Lalani, S., Zhang, T., Xu, R., et al. (2018). Discovery of A periosteal stem cell mediating intramembranous bone formation. *Nature* 562, 133–139. doi:10.1038/s41586-018-0554-8

Deveza, L., Ortinau, L., Lei, K., and Park, D. (2018). Comparative analysis of gene expression identifies distinct molecular signatures of bone marrow- and periosteal-skeletal stem/progenitor cells. *Plos One* 13, E0190909. doi:10.1371/journal.pone.0190909

Duchamp De Lageneste, O., Julien, A., Abou-Khalil, R., Frangi, G., Carvalho, C., Cagnard, N., et al. (2018). Periosteum contains skeletal stem cells with high bone regenerative potential controlled by periostin. *Nat. Commun.* 9, 773. doi:10.1038/s41467-018-03124-z

Edderkaoui, B. (2017). Potential role of chemokines in fracture repair. *Front. Endocrinol.* 8, 39. doi:10.3389/fendo.2017.00039

Embree, M. C., Kilts, T. M., Ono, M., Inkson, C. A., Syed-Picard, F., Karsdal, M. A., et al. (2010). Biglycan and fibromodulin have essential roles in regulating chondrogenesis and extracellular matrix turnover in temporomandibular joint osteoarthritis. *Am. J. Pathol.* 176, 812–826. doi:10.2353/ajpath.2010.090450

Fisher, L. W., Heegaard, A. M., Vetter, U., Vogel, W., Just, W., Termine, J. D., et al. (1991). Human biglycan gene. Putative promoter, intron-exon junctions, and chromosomal localization. *J. Of Biol. Chem.* 266, 14371–14377. doi:10.1016/s0021-9258(18)98694-1

Fisher, L. W., Termine, J. D., Dejter, S. W., Whitson, S. W., Yanagishita, M., Kimura, J. H., et al. (1983). Proteoglycans of developing bone. *J. Of Biol. Chem.* 258, 6588–6594. doi:10.1016/s0021-9258(18)32453-0

Greenblatt, M. B., Ono, N., Ayturk, U. M., Debnath, S., and Lalani, S. (2019). The unmixing problem: A guide to applying single-cell rna sequencing to bone. *J. Of Bone And Mineral Res.* 34, 1207–1219. doi:10.1002/jbmr.3802

Hao, Y., Hao, S., Andersen-Nissen, E., Mauck, W. M., 3rd, Zheng, S., Butler, A., et al. (2021). Integrated analysis of multimodal single-cell data. *Cell* 184, 3573–3587. E29. doi:10.1016/j.cell.2021.04.048

Kon, T., Cho, T. J., Aizawa, T., Yamazaki, M., Nooh, N., Graves, D., et al. (2001). Expression of osteoprotegerin, receptor activator of nf-kappab ligand (osteoprotegerin ligand) and related proinflammatory cytokines during fracture healing. *J. Bone Min. Res.* 16, 1004–1014. doi:10.1359/jbmr.2001.16.6.1004

Korsunsky, I., Millard, N., Fan, J., Slowikowski, K., Zhang, F., Wei, K., et al. (2019). Fast, sensitive and accurate integration of single-cell data with Harmony. *Nat. Methods* 16, 1289–1296. doi:10.1038/s41592-019-0619-0

Kram, V., Shainer, R., Jani, P., Meester, J. A. N., Loeys, B., and Young, M. F. (2020). Biglycan in the skeleton. *J. Of Histochem. Cytochem.* 68, 747–762. doi:10.1369/0022155420937371

Lechner, B. E., Lim, J. H., Mercado, M. L., and Fallon, J. R. (2006). Developmental regulation of biglycan expression in muscle and tendon. *Muscle Nerve* 34, 347–355. doi:10.1002/mus.20596

Lin, X., Patil, S., Gao, Y.-G., and Qian, A. (2020). The bone extracellular matrix in bone formation and regeneration. *Front. Pharmacol.* 11, 757. doi:10.3389/fphar.2020.00757

Marecic, O., Tevlin, R., Mcardle, A., Seo, E. Y., Wearda, T., Duldulao, C., et al. (2015). Identification and characterization of an injury-induced skeletal progenitor. *Proc. Natl. Acad. Sci. U. S. A.* 112, 9920–9925. doi:10.1073/pnas.1513066112

Marsell, R., and Einhorn, T. A. (2011). The Biology of fracture healing. *Injury* 42, 551–555. doi:10.1016/j.injury.2011.03.031

Matthews, B. G., Novak, S., Sbrana, F. V., Funnell, J. L., Cao, Y., Buckels, E. J., et al. (2021). Heterogeneity of murine periosteum progenitors involved in fracture healing. *Elife* 10, E58534. doi:10.7554/eLife.58534

Meester, J. A. N., Vandeweyer, G., Pintelon, I., Lammens, M., Van Hoorick, L., De Belder, S., et al. (2017). Loss-of-function mutations in the X-linked biglycan gene cause A severe syndromic form of thoracic aortic aneurysms and dissections. *Genet. Med. Official J. Of Am. Coll. Of Med. Genet.* 19, 386–395. doi:10.1038/gim.2016.126

Mountziaris, P. M., and Mikos, A. G. (2008). Modulation of the inflammatory response for enhanced bone tissue regeneration. *Tissue Eng. Part B, Rev.* 14, 179–186. doi:10.1089/ten.teb.2008.0038

Myren, M., Kirby, D. J., Noonan, M. L., Maeda, A., Owens, R. T., Ricard-Blum, S., et al. (2016). Biglycan potentially regulates angiogenesis during fracture repair by altering expression and function of endostatin. *Matrix Biol.* 52–54, 141–150. doi:10.1016/j.matbio.2016.03.008

Ortinau, L. C., Wang, H., Lei, K., Deveza, L., Jeong, Y., Hara, Y., et al. (2019). Identification of functionally distinct Mx1+Asma+ periosteal skeletal stem cells. *Cell Stem Cell* 25, 784–796. E5. doi:10.1016/j.stem.2019.11.003

Ozaki, A., Tsunoda, M., Kinoshita, S., and Saura, R. (2000). Role of fracture hematoma and periosteum during fracture healing in rats: Interaction of fracture hematoma and the periosteum in the initial step of the healing process. *J. Of Orthop. Sci.* 5, 64–70. doi:10.1007/s007760050010

Qiu, X., Mao, Q., Tang, Y., Wang, L., Chawla, R., Pliner, H. A., et al. (2017). Reversed graph embedding resolves complex single-cell trajectories. *Nat. Methods* 14, 979–982. doi:10.1038/nmeth.4402

Roberts, S. J., Van Gastel, N., Carmeliet, G., and Luyten, F. P. (2015). Uncovering the periosteum for skeletal regeneration: The stem cell that lies beneath. *Bone* 70, 10–18. doi:10.1016/j.bone.2014.08.007

Salhotra, A., Shah, H. N., Levi, B., and Longaker, M. T. (2020). Mechanisms of bone development and repair. *Nat. Rev. Mol. Cell Biol.* 21, 696–711. doi:10.1038/s41580-020-00279-w

Schaefer, L., Babelova, A., Kiss, E., Hausser, H.-J., Baliova, M., Krzyzankova, M., et al. (2005). The matrix component biglycan is proinflammatory and signals through toll-like receptors 4 and 2 in macrophages. *J. Of Clin. Investigation* 115, 2223–2233. doi:10.1172/JCI23755

Schlundt, C., El Khassawna, T., Serra, A., Dienelt, A., Wendler, S., Schell, H., et al. (2018). Macrophages in bone fracture healing: Their essential role in endochondral ossification. *Bone* 106, 78–89. doi:10.1016/j.bone.2015.10.019

Si, J., Wang, C., Zhang, D., Wang, B., and Zhou, Y. (2020). Osteopontin in bone metabolism and bone diseases. *Med. Sci. Monit.* 26, E919159. doi:10.12659/MSM.919159

Van Gastel, N., Stegen, S., Stockmans, I., Moermans, K., Schrooten, J., Graf, D., et al. (2014). Expansion of murine periosteal progenitor cells with fibroblast growth factor 2 reveals an intrinsic endochondral ossification Program mediated by bone morphogenetic protein 2. *Stem Cells* 32, 2407–2418. doi:10.1002/stem.1783

Van Gastel, N., Torrekens, S., Roberts, S. J., Moermans, K., Schrooten, J., Carmeliet, P., et al. (2012). Engineering vascularized bone: Osteogenic and proangiogenic potential of murine periosteal cells. *Stem Cells* 30, 2460–2471. doi:10.1002/stem.1210

Wallace, J. M., Rajachar, R. M., Chen, X.-D., Shi, S., Allen, M. R., Bloomfield, S. A., et al. (2006). The mechanical phenotype of biglycan-deficient mice is bone- and gender-specific. *Bone* 39, 106–116. doi:10.1016/j.bone.2005.12.081

Wilda, M., Bächner, D., Just, W., Geerkens, C., Kraus, P., Vogel, W., et al. (2000). A comparison of the expression pattern of five genes of the family of small leucine-rich proteoglycans during mouse development. *J. Of Bone And Mineral Res.* 15, 2187–2196. doi:10.1359/jbmr.2000.15.11.2187

Xu, T., Bianco, P., Fisher, L. W., Longenecker, G., Smith, E., Goldstein, S., et al. (1998). Targeted disruption of the biglycan gene leads to an osteoporosis-like phenotype in mice. *Nat. Genet.* 20, 78–82. doi:10.1038/1746

frontiers | Frontiers in Physiology

TYPE Review
PUBLISHED 28 February 2023
DOI 10.3389/fphys.2023.1137063

OPEN ACCESS

EDITED BY
Ling Qin,
University of Pennsylvania, United States

REVIEWED BY
Nick Van Gastel,
Université catholique de Louvain, Belgium
Yuki Matsushita,
Nagasaki University, Japan

*CORRESPONDENCE
Dongsu Park,
Dongsu.park@bcm.edu

SPECIALTY SECTION
This article was submitted to Skeletal Physiology, a section of the journal Frontiers in Physiology

RECEIVED 03 January 2023
ACCEPTED 16 February 2023
PUBLISHED 28 February 2023

CITATION
Solidum JGN, Jeong Y, Heralde F III and Park D (2023), Differential regulation of skeletal stem/progenitor cells in distinct skeletal compartments.
Front. Physiol. 14:1137063.
doi: 10.3389/fphys.2023.1137063

Differential regulation of skeletal stem/progenitor cells in distinct skeletal compartments

Jea Giezl Niedo Solidum[1,2], Youngjae Jeong[2], Francisco Heralde III[1] and Dongsu Park[2,3]*

[1]Department of Biochemistry and Molecular Biology, College of Medicine, University of the Philippines Manila, Manila, Philippines, [2]Department of Molecular and Human Genetics, Houston, TX, United States, [3]Center for Skeletal Biology, Baylor College of Medicine, Houston, TX, United States

Skeletal stem/progenitor cells (SSPCs), characterized by self-renewal and multipotency, are essential for skeletal development, bone remodeling, and bone repair. These cells have traditionally been known to reside within the bone marrow, but recent studies have identified the presence of distinct SSPC populations in other skeletal compartments such as the growth plate, periosteum, and calvarial sutures. Differences in the cellular and matrix environment of distinct SSPC populations are believed to regulate their stemness and to direct their roles at different stages of development, homeostasis, and regeneration; differences in embryonic origin and adjacent tissue structures also affect SSPC regulation. As these SSPC niches are dynamic and highly specialized, changes under stress conditions and with aging can alter the cellular composition and molecular mechanisms in place, contributing to the dysregulation of local SSPCs and their activity in bone regeneration. Therefore, a better understanding of the different regulatory mechanisms for the distinct SSPCs in each skeletal compartment, and in different conditions, could provide answers to the existing knowledge gap and the impetus for realizing their potential in this biological and medical space. Here, we summarize the current scientific advances made in the study of the differential regulation pathways for distinct SSPCs in different bone compartments. We also discuss the physical, biological, and molecular factors that affect each skeletal compartment niche. Lastly, we look into how aging influences the regenerative capacity of SSPCs. Understanding these regulatory differences can open new avenues for the discovery of novel treatment approaches for calvarial or long bone repair.

KEYWORDS

periosteum, bone marrow, growth plate, bone regeneration, skeletal stem/progenitor cells, sutures, skeletal compartments, homeostasis

1 Introduction

The skeletal system is among the largest of the human organ systems, constituting up to 15% of the total human body weight (Su et al., 2019). It allows functional body movement, protects internal organs, and serves as reservoir for minerals (Mizokami et al., 2017; Su et al., 2019); bones also have extra-skeletal endocrine functions (Su et al., 2019) that are essential for overall body homeostasis and systemic health (Ambrosi et al., 2019). Skeletal system functions are affected by skeletal shape, strength, and stiffness, which substantially change with the stage of development and age (Sheehan et al., 2018).

Advancing age is a key risk factor for degenerative bone and cartilage disorders, such as osteoporosis and osteoarthritis (Raisz and Seeman, 2001; Su et al., 2019; Jeong and Park, 2020), which lead to decreased mobility and diminished quality of life (Lee et al., 2014). However, bone mass, strength, and vitality are affected by other factors aside from age (Demontiero et al., 2012; Nandiraju and Ahmed, 2019). Alterations in cellular components, hormonal, biochemical, and vasculature status, which can be brought about by metabolic disorders, are examples of intrinsic factors (Demontiero et al., 2012), whereas nutrition, physical activity, injury, and comorbidities are some of the contributing extrinsic factors (Demontiero et al., 2012; Sheehan et al., 2018). Congenital or acquired skeletal deformities also affect the form and function of the skeletal system due to geometric abnormalities of the bones and articulating surfaces (Sheehan et al., 2018).

Some age-related defects in bones and cartilage have been attributed to changes in the populations and functions of stem cells in skeletal tissues (Jeong and Park, 2020). These molecular and functional changes in skeletal stem/progenitor cells (SSPCs) lead to a negative bone balance with reduced bone remodeling coupled with continued, or even accelerated, bone resorption (Demontiero et al., 2012). By itself, stem cell regeneration of large skeletal defects is difficult and often lead to the delay or failure of bone repair (Vidal et al., 2020). Confounded by aging and age-related diseases (e.g., diabetes), incidence of bone fractures and failure of large bone defect repair is further amplified. (Clark et al., 2017; Wu et al., 2021).

Currently, the goals of therapies for degenerative bone conditions are fracture prevention and decreased bone resorption through antiresorptive agents. For the reconstruction of critical-sized bone defects, transplantation of an autologous free vascularized bone flap containing the patient's cells, growth factors, and a vascularization bed is the current gold standard approach (Vidal et al., 2020). However, these vascularized bone flaps are of finite supply, and their harvest can result in significant morbidity and anatomical incompatibility. Prosthetic and bio-matrix materials are also unable to restore complex sensory and motor functions, do not expand with age, and present a risk of failure and infection (Borrelli et al., 2020; Tang et al., 2021). Recently, in the field of tissue engineering and regenerative medicine, the use of SSPCs in combination with scaffolds and growth factors has been introduced to facilitate bone regeneration (Miller et al., 2017; Borrelli et al., 2020; Tang et al., 2021). Therefore, a better understanding of the properties and regulation of SSPCs with respect to their locations and skeletal compartments, as well as the effects of age, can potentially facilitate the discovery of new approaches to bone defect reconstruction and degenerative bone disease therapy.

SSPCs are essential for skeletal development, bone remodeling, and bone repair and are characterized by the capacity for self-renewal and multipotency (Matsushita et al., 2020c). Traditionally, they have been known to reside within the bone marrow (BM), but recent scientific advancements identified distinct SSPC populations in various skeletal compartments such as the growth plate (GP), periosteum, and calvarial sutures (Matsushita et al., 2020c; Jeong and Park, 2020) (Figure 1). Adult SSPCs are heterogeneous, and each population potentially contributes to bone maintenance and regeneration in a different manner (Ortinau and Park, 2021). The cellular and matrix environment of each distinct SSPC population is also believed to regulate SSPC stemness and to direct its roles at different stages of development, homeostasis, and regeneration (Matsushita et al., 2020c). However, it is largely unknown how these SSPCs are regulated, and which specific roles they play in these biological

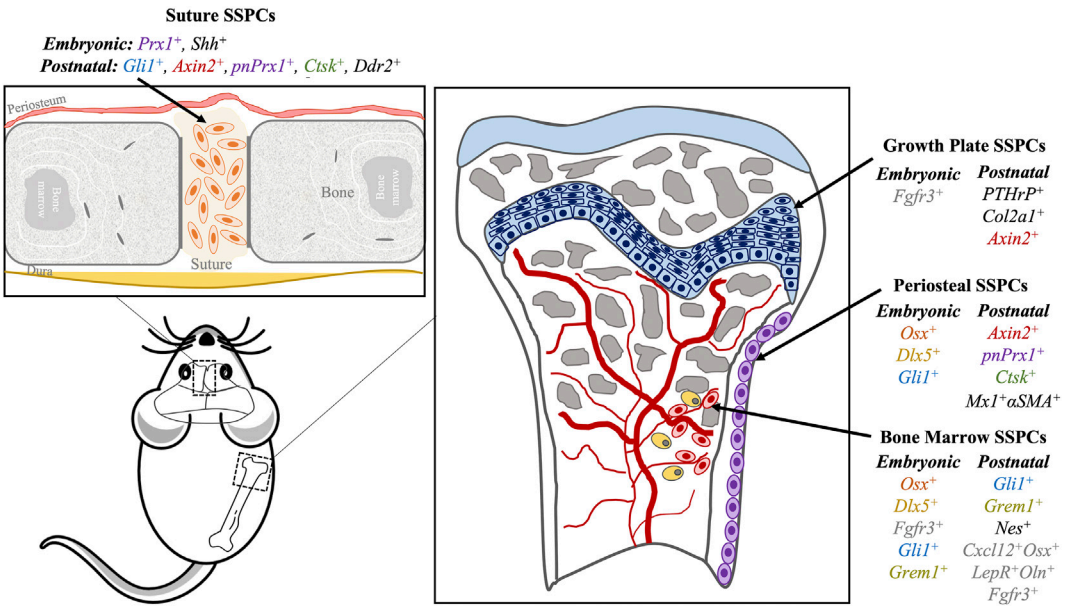

FIGURE 1
Skeletal stem progenitor cells (SPPCs) in different bone compartments in mice. Several markers of SSPCs per location (suture, growth plate, periosteum, bone marrow) are summarized here. Similar markers have similar text colors (i.e., *Axin2, Ctsk, pnPrx1 and Gli1*).

processes (Iaquinta et al., 2019; Ortinau and Park, 2021). In this review, we present the different regulation mechanisms during the development and repair of the distinct SSPC populations in major compartments, namely, the suture, GP, periosteum, and BM. We also discuss the currently known changes that occur in the regulation pathways of SSPCs with aging.

2 Embryogenic cellular origins and location of SSPCs

The musculoskeletal system develops from various embryonic origins, including: 1) the paraxial mesoderm, 2) the parietal layer of the lateral plate mesoderm, and 3) the neural crest cells (NCCs), which undergo mesenchymal condensation to begin bone formation (Figures 2, 3) (Mitchell and Sharma, 2009). Most facial bones, the cranial vault, clavicle, and calvarial frontal bones originate from NCCs through the intramembranous ossification process. By contrast, most of the remaining bones in the skull and all perpendicular bones develop from mesoderm-derived (MDD) cells through the endochondral ossification process (Chung et al., 2009; Sadler and Langman, 2012; Schoenwolf et al., 2015; Moore et al., 2016). Some intriguing tissues include the clavicle originating from NCCs but forms through mixed intramembranous and endochondral ossification, and the calvarial parietal bones which originate from MDD but are formed through the intramembranous ossification process (Percival and Richtsmeier, 2013). Intramembranous bones develop *via* direct osteoblast differentiation within the mesenchyme, while endochondral bones develop with an intermediate cartilage structure before being replaced by or transformed into bones (Sadler and Langman, 2012; Schoenwolf et al., 2015; Moore et al., 2016; Galea et al., 2021; Shu et al., 2021). Furthermore, mesodermal cells from different embryonic origins show different transcriptomic signatures and differentiation potentials, suggesting that tissue-specific SSPCs with different embryonic origins are present in different bones and that they require differential regulation pathways for bone regeneration (Sacchetti et al., 2016).

Intramembranous bone formation begins with the expression of *Runx2* driving SSPCs into the osteoblast lineage (Pazhanisamy, 2013) (Figure 2). This is followed by the sequential expression of *osterix* (*Osx*), *type I collagen*, *Bglap* (or *osteocalcin*), and *Spp1* (or *osteopontin*), which are the core osteoblast differentiation factors. As osteoblasts become surrounded by bone matrix, they express late markers such as the *dentin matrix protein 1* (*Dmp1*). Lastly, the expression of the osteocyte marker *sclerostin* is observed (Pazhanisamy, 2013; Galea et al., 2021). In endochondral bone formation, however, *Sox9* initiates chondrocyte commitment in the pre-condensing mesenchyme. During early chondrocyte development, *Sox9, Sox5*, and *Sox6* are highly expressed and subsequently drive the expression of early cartilaginous matrix components *type II collagen* (*Col II*) and *aggrecan* (Galea et al., 2021). During the terminal hypertrophic stage of endochondral ossification, co-expression of cartilaginous (*type X collagen*) and osteoblastic (*Runx2*, *Osx*, *bone sialoprotein*) markers is observed. *Sox9* expression persists in early hypertrophic chondrocytes and induces the expression of *type X collagen* while inhibiting *Runx2* activity. Later on, the degradation of *Sox9* protein relieves the inhibition of *Runx2*, thus allowing for chondrocyte-osteoblast transformation and subsequent mineralization (Taher et al., 2011; Galea et al., 2021). Overall, endochondral and intramembranous ossification use distinct molecular signals responsible for the different types of bone formation.

The expression of regulatory genes in specific cell types and locations in the body may also account for the differences in SSPC functionality. For example, a mandibular injury site undergoes osteogenic regeneration through *Homeobox* non-

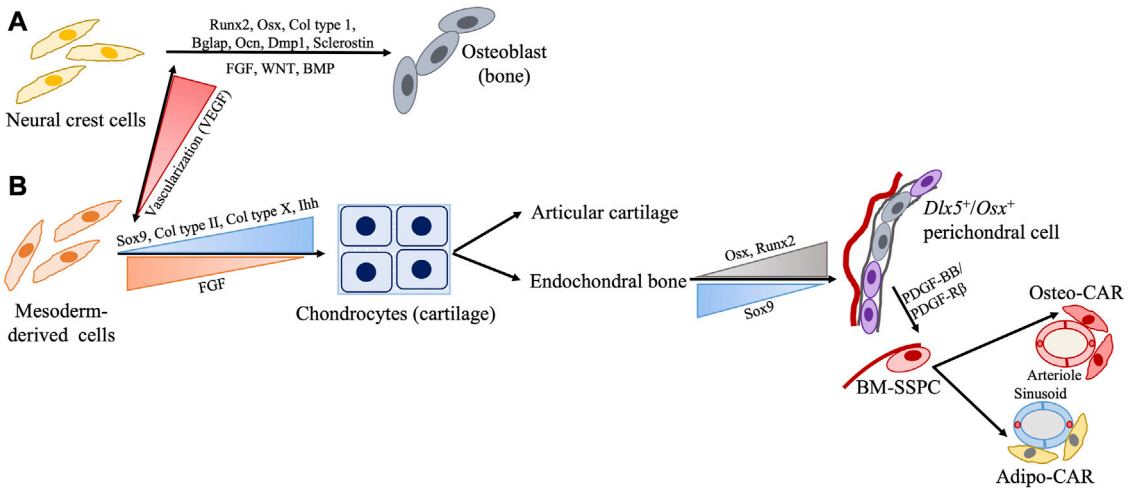

FIGURE 2
Schematic representation of SSPC regulation during development from embryonic cell origin **(A)** neural crest cells (NCC) and **(B)** mesoderm-derived cells (MDD). Generally, bones NCC form *via* intramembranous ossification while bones from the MDD form *via* endochondral ossification with few interesting exceptions such as NCC-derived clavicle forming *via* endochondral and MDD-derived parietal bone forming *via* intramembranous processes. Presence or absence of adequate vascularization may play a role in this.

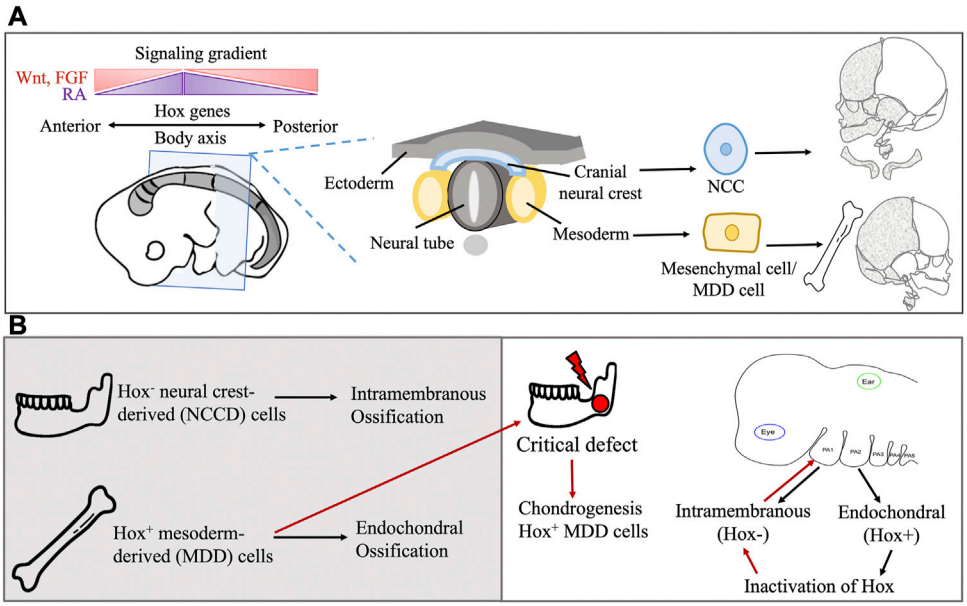

FIGURE 3
(A) Embryonic origin of extracranial and craniofacial bone and the role of Hox genes in directional differentiation. Hox genes also interact with regulatory gene, transcription factors and signaling molecule gradient for patterning of the body axis. **(B)** The Hox gene confers spatial regulation and affects the type of bone ossification during development and transplantation in bone defect.

expressing (*Hox*$^{-}$) neural crest-derived (NCD) cells, while tibial or long bone injuries ossify with *Hox*$^{+}$ MDD cells (Lappin et al., 2006) (Figure 3). *Hox* genes encode the Hox proteins, which are master regulators of embryonic development, but these genes continue to be expressed throughout postnatal life. In humans, they control body proportions, vertebral segments, and proper spatial development of organs and limbs (Lappin et al., 2006; Rux and Wellik, 2017). Upon transplantation of MDD cells to a mandibular injury site, *Hox*$^{+}$ MDD cells remain *Hox*$^{+}$, while inherently *Hox*$^{-}$ NCD cells transplanted to the tibial injury site become *Hox*$^{+}$. This indicates a sense of positional identity that is unchanged with transplantation, and this positional identity is also seen in facial bone development (Leucht et al., 2008). The first pharyngeal arch (PA) cells, which are *Hox*$^{-}$, form most of the facial bones in an intramembranous manner. The second PA cells, which are *Hox*$^{+}$, form the hyoid, styloid, and stapes bones in an endochondral manner (Weber et al., 2021). Inactivation of *Hox* genes in the second PA results in intramembranous ossification, while their overexpression in the first PA results in second PA-like elements (Bonaventure, 2001; Kitazawa et al., 2022). Overall, these findings suggest that embryonic cell origin may confer a differentiation bias to SSPCs.

Although some distinct SSPCs may come from the same embryonic cells, they undergo further development in their distinct skeletal compartments. With the complex development in each compartment, dynamic and specialized microenvironments are also formed (Kurenkova et al., 2020). Most likely, these microenvironments provide an additional layer of unique regulation to each SSPC population aside from what is offered by embryonic cell origin (Donsante et al., 2021) (Table 1). Parallel niches may therefore be progressively altered, explaining the different properties and functions of distinct SSPCs through time and condition, which will be discussed later.

3 Differences in the regulation of calvarial and long bone development and remodeling

Calvarial bone formation begins around the third week of gestation (Jha et al., 2018). At this stage, NCCs expand and form a condensed mesenchyme. Capillaries then begin to surround the mesenchymal condensation which may serve as a vehicle for nutrient supply, osteoblastic factor transport, and conduit of additional NCCs and SSPCs (Percival and Richtsmeier, 2013; van Gastel et al., 2020). Next, the cells in the mesenchyme center start to differentiate directly into osteoblastic cells and generate an osteoid (calvarial bone primordia) which later become mineralized bones (Ishii et al., 2015; Kenkre and Bassett, 2018). The Bone Morphogenic Protein (BMP 2/4/7) signaling pathway and its immediate-early effector homeodomain transcriptional factor (*Msx2*) play major roles in the early specification of the calvarial bone primordia from NCCs by positively controlling the expression of *Runx2*. Transcription factor *Foxc1*, on the other hand, negatively regulates *Msx2* and *Bmp2/4* and positively regulates *Noggin* to prevent premature differentiation of the frontal bone primordia, thus promoting apical migration of undifferentiated progenitor cells. Wnt signaling is a key regulator in the early specification of primordia that favors the osteogenic lineage. Wntless, a Wnt ligand transporter, found in the cranial surface ectoderm and underlying mesenchyme, promotes expression of the Wnt ligands (Wnt5a/11/4/3a/16) and secretion of Wnt protein, activating *Twist1*

TABLE 1 Summary of the regulations of distinct skeletal stem//progenitor cells (SSPCs) in different skeletal compartments during development, remodeling and aging.

Skeletal Stem//Progenitor cells	Molecular regulators	Development	Remodeling	Aging
Suture	EphA4	-Directs embryonic osteoprogenitor cell migration Ting et al. (2009); Ishii et al. (2015)	?	-Closes between the second and third decade of life Libby et al. (2017)
	Twist1, FGF, Notch	-Maintains cell stemness Bonaventure (2001); Ishii et al. (2015)	?	
	BMP2/4/7, FGF-2, FGFR-1, IGF-2, Ptn, Sparc, Oc (from dura mater)	-Promotes interstitial bone formation during brain and skull growth Wan D C et al. (2008)	-Potentially the same	
	TGFβ	-Maintains a continuous osteogenic lineage commitment Ishii et al. (2015)	-Promotes osteogenic differentiation Wilk et al. (2017)	
		- Triggers interstitial bone production Wang et al. (2020)		
Gli1$^+$	Hh, BMP/Bmpr1a	-Promotes osteogenic differentiation adding osteoblasts in the osteogenic font for interstitial growth Zhao et al. (2015)	-Promotes osteogenic differentiation Zhao et al. (2015)	-
	Hh/RANKL	?	-Stimulates osteoclast differentiation and resorption activity Guo et al. (2018)	
Axin2$^+$ Maruyama et al. (2010); Maruyama et al. (2017); Maruyama et al. (2021)	BMP/Bmpr1a/Rapb1	-Suppresses osteogenesis and maintains cell stemness	?	-
	FGF/FGFR1	-Enhances osteoblast proliferation and differentiation	?	
	Wnt/β-catenin	-Mediates BMP/FGF balance	-Promotes cell fate switch between osteoblast and chondrogenic lineage cells during injury, thus may promote osteochondral regeneration.	
	Wnt3	?	-Increased calvarial bone regeneration	
pnPrx1$^+$ Wilk et al. (2017)	Wnt	-Inhibited by *Dkk1* and *Sost*	-Promotes osteogenic differentiation	-
Ctsk$^+$	Bmp 1/2, Runx2, Sox9 Debnath et al. (2018)	?	-Potentially promotes osteogenic differentiation	?
Ddr2$^+$ Greenblatt et al. (2021)	Myc, Runx2, Klf4, Nes1, Msx1/2, Acta2, Lgr5, and Lrig1	-Potentially maintains stem cell quiescence and suture patency	?	?
	Sox9, Col2a1, and Acan	?	-Potentially promotes endochondral ossification	
Growth Plate				-Closes near puberty Setiawati and Rahardjo (2019)
Fgfr3+ (embryonic)	IHh	-Promotes chondrocyte proliferation	-	-
		-Promotes chondrocyte hypertrophy Mizuhashi et al. (2018); Ağırdil (2020)		
PTHrP+ (postnatal)	PTHrP	-Suppresses hypertrophic differentiation of proliferating	-Same as development	-

(Continued on following page)

TABLE 1 (*Continued*) Summary of the regulations of distinct skeletal stem//progenitor cells (SSPCs) in different skeletal compartments during development, remodeling and aging.

Skeletal Stem//Progenitor cells	Molecular regulators	Development	Remodeling	Aging
		chondrocytes Mizuhashi et al. (2018)		
	PTHrP, Runx2, BMP, IHh, TGFβ	-Promotes chondrocyte proliferation		
		-Promotes chondrocyte hypertrophy Mizuhashi et al. (2018); Ağırdil (2020)		
Col2a1+ (postnatal)	Notch Zieba et al. (2020)	-Maintains SSPC population and functions	-Notch2 allows hypertrophy and mineralization of proliferating chondrocytes.	
		-Notch 1 Promotes chondrocyte proliferation, GP organization and hypertrophy		
	mTORC1, IGF-1	-Increased number and thickness of multi-columnar clones Newton et al. (2019)	?	-
	Gsα, Gq/G11α	-Maintains quiescence of resting chondrocytes Guo et al. (2009); Chagin et al. (2014)		
Axin2$^+$ (postnatal)	Wnt/β-catenin	-Physiologically inhibited in the resting zone. Maintenance of SSPCs in the resting zone	-Same as development	-
		-Promotes chondrocyte proliferation and hypertrophy in the proliferating zone Hallett et al. (2021)		
Periosteum	OSTN/CNP/GC-B signaling (towards growth plate)	-	-Chondrocyte proliferation and maturation Watanabe-Takano et al. (20199	?
	IHh	-Regulates chondrocyte proliferation and differentiation Wang et al. (2020)	-Same as development	?
	PGE2, Postn (from mechanical loading)	-	-Higher mineralization and apposition rate Galea et al. (2011); Bivi et al. (2013); Gerbaix et al. (2015)	-Decreased loading causes bone resorption and osteocyte apoptosis Lloyd et al. (2012)
Dlx5+, *Osx*+, *Gli1*+ (embryonic)	HIF-1α, VEGF	-Absence may promote expansion in periosteum and inhibition of migration to BM Nagao et al. (2017)	-	-
Ctsk$^+$ (postnatal)	Bmp, Runx2, Sox9, Wnt Debnath et al. (2018)	?	?	?
	LKB1	- May promote quiescence Han et al. (2019)	?	
	mTORC1	- Promotes appositional growth Han et al. (2019)	-Activated, couple with VEGF. Potential mechanism for osteochondral regeneration Wan C et al. (2008); Wan et al. (2010)	
Axin2$^+$(postnatal)	Wnt	? (Possibly similar with *Axin2*$^+$ Su-SSPC) Maruyama et al. (2016); Ransom et al. (2016)	?	?
Mx1$^+$α*SMA*$^+$(postnatal)	CCR5/CCL5	?	-Facilitates immediate migration to injury site Ortinau et al. (2019)	?

(Continued on following page)

TABLE 1 (*Continued*) Summary of the regulations of distinct skeletal stem//progenitor cells (SSPCs) in different skeletal compartments during development, remodeling and aging.

Skeletal Stem//Progenitor cells	Molecular regulators	Development	Remodeling	Aging
pnPrx1^{+}	TGFβ	-Inhibits adipogenesis Du et al. (2013)	?	?
	Prx1	-Inhibits the expression of *Osx* and *Runx2, and inhibits* osteogenic differentiation Lu et al. (2011)	-Reserved stem cells Duchamp de Lageneste et al. (2018); Esposito et al. (2020)	
	BMP/Cxcl12	?	-Activates injury induced SSPCs Esposito et al. (2020)	
	Postn, Sostdc1	-Maintains SSPCs pool Bonnet et al. (2013); Collette et al. (2013)	-Maintains SSPCs pool used for regeneration Bonnet et al. (2013); Collette et al. (2013)	
			-Inhibition hastens the expansion and differentiation of SSPCs Collette et al. (2013)	
	Notch/Jagged1 signaling	?	-Periosteal expansion of cortical bone young Youngstrom et al. (2016)	
Bone Marrow	Notch Vanderbeck and Maillard (2019); Sottoriva and Pajcini (2021)	-Maintains BM niche, promotes HSC maintenance, and promotes megakaryocyte/ erythroid cell development	-Regulates hematopoietic recovery	?
	NO, IL-1, IL-6 (from M1 macrophage)	-May facilitate establishment and maintenance of BM niche Genin et al. (2015)	?	-Sustained exposure to inflammatory molecules Franceschi et al. (2018); Josephson et al. (2019)
	MAF/Runx2, Cbfβ, Forkhead box P1/CEBPβ	-Promotes osteogenesis, inhibits adipogenesis Wu et al. (2014); Wu et al. (2017); Li et al. (2017)	?	-Reduction of factors with aging releases inhibition to adipogenesis Li et al. (2017)
	MAF/PPARγ	?	?	-Promotes adipogenesis Li et al. (2017)
	RANKL/OPG	-	-Promotes osteoclastogenesis Weitzmann (2013); Zhang et al. (2020)	-Increased OPG production results in osteoclast differentiation Li et al. (2015)
	G-CSF (from B-lymphocytes)	-	-Promotes osteogenesis Weitzmann (2013); Zhang et al. (2020)	?
	IL-17 (from Th17 cells)	-	- Promotes osteogenesis in the long bones but suppression in calvarial bone Wang et al. (2020)	-Sustained exposure to inflammatory molecules Franceschi et al. (2018); Josephson et al. (2019)
	BMP2, TGFβ, osteopontin (from M2 macrophage)	-	-Promotes osteogenesis Chen et al. (2020)	-Sustained effects similar to remodeling
	IL-1α, TGFβ, ROS (from activated neutrophils)	-	-SSPCs differentiation into osteoblasts Nam et al. (2012); Lee (2013)	-Promotes negative bone balance or exhaustion of proliferating or differentiating cells Owusu-Ansah and Banerjee (2009); Chakkalakal et al. (2012)
Dlx5^{+} (embryonic)	HIF-1α, VEGF	-Promotes angiogenesis needed for migration of BM-SSPCs from perichondrium to BM Nagao et al. (2017); Matsushita et al. (2022)	-	-
	IHh		-	-

(Continued on following page)

TABLE 1 (*Continued*) Summary of the regulations of distinct skeletal stem//progenitor cells (SSPCs) in different skeletal compartments during development, remodeling and aging.

Skeletal Stem//Progenitor cells	Molecular regulators	Development	Remodeling	Aging
Cxcl12^{+}*Adiponectin*$^{+}$ (*Dlx5*$^{+}$; adipogenic progenitor/Adipo-CAR; postnatal)	Gs/cAMP/β-adrenergic signaling	?	-Potentially promotes BM adipocyte lipolysis, pre-adipocyte-like CAR cells differentiation, and osteogenesis Bachman et al. (2002); Lohse et al. (2003)	?
	Wnt/BMP/Bmpr1b signaling	?	- Potentially promotes pre-adipocyte-like CAR cells differentiation and osteogenesis Merrell and Stanger (2016); Matsushita et al. (2020a)	
	Cxcl12	?	-Attracts osteoblast and osteoclast progenitors into the BM Li et al. (2009); Yang et al. (2015)	
	Adiponectin	?	-Facilitates migration of osteoblast progenitors and repels osteoclast progenitors into injury site Li et al. (2009); Yang et al. (2015)	

Gli1 - Zinc finger protein glioma-associated oncogene 1; Axin2 - Axis inhibition protein 2; pnPrx1 - Postnatal Paired-related homeobox protein; Ctsk - Cathepsin k; Ddr2 - Discoidin domain-containing receptor 2; Fgfr3 - Fibroblast growth factor 3; PTHrP - Parathyroid hormone-related protein; Col2a1 - Collagen type 2 alpha1; Dlx5 - Distal-less homeobox 5; Osx - Osterix; Mx1 - Myxovirus resistance 1; α*SMA - α-Smooth muscle actin; Nes - Nestin; Grem1 - Gremlin 1; Cxcl12 - CXC motif chemokine ligand 12; LepR - Leptin receptor; Oln - Osteolectin*; EphA4 - Ephrin A receptor 4; FGF(R) - Fibroblast growth factor (receptor); BMP(r)- Bone morphogenic protein (receptor); IGF - Insulin-like growth factor; Ptn - Pleiotrophin; Sparc - Secreted protein acidic and cysteine rich; Oc/Ocn - Osteocalcin; TGFβ - Transforming growth factor-β; (I)Hh - (Indian) Hedgehog; RANKL – Receptor activator of NF-κB Ligand; Runx2 - Runt-related transcription factor 2; Sox9 - Sex-determining region Y-box transcription factor 9; Myc - Myelocytomatosis oncogene; Klf4 - Kruppel-like factor 4; Acta2 - Actin alpha 2; Lgr5 - Leucine-rich repeat-containing G-protein coupled receptor 5; Lrig1 - Leucine rich repeats and immunoglobulin like domains 1; Acan - Aggrecan; Gs - Guanine nucleotide-binding protein G subunit; Gq/G11α - G proteins Gqα and G11α; OSTN - Osteocrin; CNP - C-type natriuretic peptide; GC-B - Guanylate cyclase-B; PGE2 - Prostaglandin E2; Postn - Periostin; HIF-1α - hypoxia inducible factor-1α; VEGF - vascular endothelial growth factor; LKB1 - liver kinase b1; mTORC1 - mammalian target of rapamycin complex 1; CCL5 - CC motif chemokine ligand 5; CCR5 - CC motif chemokine receptor 5; Sostdc1 - Sclerostin domain-containing protein 1; NO - Nitric oxide; CEBPβ - CCAAT/enhancer-binding protein beta; Cbfβ - Core binding factor beta; MAF - Musculoaponeurotic fibrosarcoma; PPARγ - Peroxisome proliferator-activated receptor γ; cAMP - Cyclic adenosine monophosphate; OPG - Osteoprotegerin; G-CSF - Granulocyte colony-stimulating factor.; IL- Interleukin; ROS - Reactive oxygen species; Wnt - Wingless-related integration site.

and then *β-catenin* downstream. *B-catenin* promotes the osteogenic lineage but represses the chondrogenic lineage in the cranial mesenchyme. Interestingly, a haploid deficiency of *Fgfr1* in suture cells switches their fate to form ectopic chondrocytes in the suture mesenchyme, suggesting that local Fibroblast growth factor (FGF) signals are necessary for their direct intramembranous ossification (Maruyama et al., 2010).

Once the primordia are established, osteogenic precursors migrate, through the EphrinA (EphA) signaling, to the edge of the growing bone, where they contribute to the apical expansion of the calvarial rudiments. Wnt signaling is still a prerequisite at this point for the final phase of osteoblast differentiation; TGF-β signaling, on the other hand, is required to maintain a continuous osteogenic lineage commitment (Ishii et al., 2015). Between calvarial bones, cranial sutures develop while allowing calvarial expansion for brain growth (Sadler and Langman, 2012). A study by Deckelbaum et al. (2012) identified a group of Sonic hedgehog (Shh)-responsive cells in the head mesoderm as precursors of the coronal suture. These cells migrate first to the supraorbital ridge transiently expressing *En1*, a vertebrate homolog of the *Drosophila* transcription factor *engrailed*, before apically migrating together with the calvarial rudiments to form the coronal suture (Deckelbaum et al., 2012). Other embryonic origins of the suture precursor cells still need to be identified.

Long bone formation becomes visible by the end of the fourth week of gestation. Limbs initiate with small bud formation as outpocketing from the ventrolateral body wall. These limb buds generate a core of mesenchymal cells from the somatic layer of the lateral plate mesoderm covered by a layer of ectoderm. An apical ectodermal ridge (AER) is located at the distal end of the limb and induces rapid mesenchymal cell proliferation without differentiation. FGF signals in the so-called progress zone control proximal to distal limb growth (Bonaventure, 2001; Sadler and Langman, 2012; Schoenwolf et al., 2015; Moore et al., 2016). A unique feature of endochondral bone formation is the moment when the cells move further from the influence of the AER, causing local FGF levels to decrease and allowing the mesenchymal cells to differentiate into cartilage. This is where endochondral ossification begins, and skeletal compartments subsequently develop (Figure 2). GP formation starts off with early cartilage development through chondrocyte proliferation and differentiation of *Fgfr3*$^{+}$ cells in the mesenchymal condensation (Ono and Kronenberg, 2016; Zieba et al., 2020; Matsushita et al., 2022). The proliferating chondrocytes become mature and later organize, through Notch signaling, at both sides of long bones as a tri-layer GP consisting of resting, proliferating, and hypertrophic chondrocyte zones (Ono and Kronenberg, 2016; Zieba et al., 2020). The remaining cells form the outer layer called the perichondrium. All of the mesenchymal condensations in the forming limbs still remain avascular at this

point (Percival and Richtsmeier, 2013). The spatio-temporal differences on angiogenesis may also explain the unique ossification processes with avascular state limiting supply of osteogenic factors and SSPCs that would promote osteogenesis (Percival and Richtsmeier, 2013; van Gastel et al., 2020). Eventually, hypoxic condition in limb forming cells promotes vascular invasion to the perichondrium leading to osteoblast differentiation, and development of perichondrium to periosteum and articular soft tissues (Percival and Richtsmeier, 2013). The periosteum becomes a layer of connective tissue housing the proliferating progenitor cells with chondrogenic and osteogenic differentiation properties, while the osteoblasts differentiating mostly from *Dlx5*$^{+}$ cells of the periosteum form a bony collar around the shaft of limb bones (Vanderbeck and Maillard, 2019; Sottoriva and Pajcini, 2021; Matsushita et al., 2022). Subsequently, the marrow cavity forms as long bones develop, and blood vessels invade the cartilage template from the osteogenic perichondrium, which are maintained through Notch signaling (Vanderbeck and Maillard, 2019; Sottoriva and Pajcini, 2021). Blood-borne hematopoietic progenitors and BM stromal cells then seed this environment. While most of the BM stromal cells originate from the outer perichondral *Dlx5*$^{+}$ cells, a minimal contribution of inner perichondrial *Osx*$^{+}$ cells and cartilage *Fgfr3*$^{+}$ cells implicate that BM stroma may have transitions from primitive progenitor cells in early postnatal development to definitive SSPCs in adult bone homeostasis, respectively. This is exemplified by the transition of fetal *Osx*$^{+}$ SSPCs to more long term postnatal *Osx*$^{+}$ BM SSPCs, and a shift from a more proliferative fetal *Dlx5*$^{+}$ SSPCs to a more quiescent postnatal *Dlx5*$^{+}$ BM-SSPCs. (Mizoguchi et al., 2014; Matsushita et al., 2022). With age, a subset of BM stoma cells further shifts towards adipocyte development (Taher et al., 2011; Bianco and Robey, 2015).

The difference between calvarial vs. long bone is apparently observed in bone injury healing. In general, all bones heal through three overlapping processes, namely, inflammation, bone formation, and bone remodeling (Sheen and Garla, 2021). Immediately after bone injury, a hematoma develops, leading to inflammation of the injury site. Inflammatory cells migrate into the injury site and secrete various cytokines and growth factors like tumor necrosis factor-α (TNF-α), BMPs, and interleukins, subsequently attracting more inflammatory and osteogenic progenitor cells (Wang et al., 2020; Sheen and Garla, 2021). Bone regeneration then begins with callus formation and a gradual decrease in inflammation. A unique process of long bone fracture healing is the fibrocartilaginous callus formation that first appears at days 5–11. During this process, vascular endothelial growth factor (VEGF) allows angiogenesis, and BMP drives the differentiation of SSPCs into chondroblasts, osteoblasts, and fibroblasts. At the same time, woven bones begin to appear adjacent to the periosteal layer (Wang et al., 2020; Sheen and Garla, 2021). Later on, on days 11–28, when Sox9 protein is degraded, inhibition of osteogenic *Runx2* is relieved, and a bony callus then forms as chondrocytes calcify with calcium–phosphate crystals, which is followed by bone replacement by osteoblasts (Sadler and Langman, 2012; Schoenwolf et al., 2015; Moore et al., 2016; Galea et al., 2021). In contrast, calvarial injury repair is normally completed by repeated cycle of bone resorption by osteoclasts and bone formation by osteoblasts without forming fibrocartilaginous callus (Lim et al., 2013; Wang et al., 2020), although some recent studies show endochondral ossification upon scaffold induced calvarial injury repair (Ko and Sumner, 2021). Macrophage-colony stimulating factor and receptor activator of nuclear factor kappa-B ligand (RANKL) are two critical cytokines for osteoclast differentiation (Castillo et al., 2017; Wang et al., 2020). These factors recruit osteoclast precursors, activate their fusion to form multinucleated pre-osteoclasts, and induce downstream signaling molecules (e.g., mitogen-activated protein kinase, TNF-receptor-associated factor 6, NF-κB, and c-fos) and key transcription factors (e.g., nuclear factor of activated T-cells [NFATc1]) that regulate osteoclast gene expression (Kenkre and Bassett, 2018).

In summary, calvarial and long bone development and remodeling leads to different bone morphologies and histologic characteristics. Although not all the regulatory pathways involved are the same (Table 1), Notch, BMP, TGFβ, Hedgehog (Hh) and Wnt/β-catenin signaling pathways play a key role in embryogenesis and regulation within the different bone compartments (Sottoriva and Pajcini, 2021). In addition, the balance between proliferation and differentiation is important in the development and remodeling of these compartments.

3.1 Unique regulation of calvarial suture SSPCs (Su-SSPCs)

Sutures of calvarial bones are unique structures that function as fibrous joints to facilitate calvarial bone movements and as brain cushions to absorb mechanical forces (Wang et al., 2020). With the growth of the brain, the meningeal and cutaneous periosteal layers grow in an ectocranial direction displacing the calvarial bones with them. The tensile physiological forces are then produced and serve as a stimuli to trigger interstitial bone production (Jin et al., 2016). During this process, skeletal stem/progenitor cells in sutures (Su-SSPCs) are a major contributor to calvarial bone growth in response to such forces (Wang et al., 2020) and express specific factors (e.g., *Runx2, Nel-like Molecule-1* [*NELL-1*], *TGFβ1*, and *FGF-2*) (Figure 4). Further, recent studies demonstrate that sutures act as the major sites of calvarial interstitial bone growth (Lana-Elola et al., 2007; Opperman et al., 2009; Jin et al., 2016) and constitute a unique microenvironment for adult craniofacial SSPCs (Zhao et al., 2015; Doro et al., 2017).

The specific embryonic origin of progenitor cells for suture is unknown. However, an integrated transcriptome and network analysis conducted by Holmes et al. (2020), and a single-cell resolution analysis performed by Farmer et al. (2021), identified *Lgr5, Lrig1*, *Prx1, Erg, Six2,* and *Pthlh*, as potential embryogenic Su-SSPCs markers. *Prx1* and *Shh* are also detectable in postnatal Su-SSPCs (Holmes et al., 2020; Farmer et al., 2021). The relationship between embryonic osteoprogenitor cells and postnatal Su-SSPCs, and the timing of the transition, remain to be explored (Holmes et al., 2020). Currently, four markers have been verified to label Su-SSPCs, namely,: 1) *zinc finger protein glioma-associated oncogene 1* (*Gli1*$^{+}$), 2) *axis inhibition protein 2* (*Axin2*$^{+}$), 3) *cathepsin k* (*Ctsk*$^{+}$), and 4) *paired-related homeobox protein 1* (*Prx1*$^{+}$)-expressing cells (Zhao et al., 2015; Maruyama et al., 2016; Wilk et al., 2017; Debnath et al., 2018; Li et al., 2021). While it is not clear whether these four markers label the same Su-SSPC subset or they are mutually

distinguishable, there has been a significant advance in the signaling pathways and potential interplay mechanisms in the regulation of Su-SSPCs.

A heterozygous loss of function mutation in *Twist1*, a basic helix–loop–helix transcription factor, results in reduced *Jagged1* expression and causes suture cells to become osteogenic (*Notch2* with *Runx2* expression) and original osteogenic cells to invade the suture (Yen et al., 2010; Ishii et al., 2015). In addition, this phenotype can be augmented by an accompanying specific *FGF* and *Gli3* mutations because a compound *Twist1-Gli3* mutation results in aberrant *Runx2* expression in sutural cells (Ishii et al., 2015). Interestingly, compound *Twist1-EphA4* heterozygotes show loss of the osteogenic-non osteogenic boundary integrity of the coronal suture, suggesting the role of *EphA4* in the migration of osteogenic cells to the leading edges of bone fronts (Ting et al., 2009; Ishii et al., 2015).

The *Fgfr* and *Gli3* signaling is known to maintain cell stemness during limb development. Consistently, a missense mutation in *Fgfr2* leads to suture mesenchyme ossification (Bonaventure, 2001; Ishii et al., 2015). Physiologically controlled by Hh signaling, *Gli3* acts like one end of a transcriptional switch with *Gli1* and *Gli2* transcription factors, and suppresses osteogenic differentiation. Without Hh signaling, non-mutated *Gli3* is active, inhibits transcription of certain genes (e.g., *Gli1, Gli2, Ptch1, Ccnd1, Igf2, Myc*, and *Bcl2*), and maintains cell stemness (McCubrey et al., 2014). *Gli1*$^+$ Su-SSPCs, therefore, contribute to calvarial bone formation through Hh signaling regulation. Treatment with IHh significantly upregulates *Gli1*$^+$ Su-SSPCs differentiation, whereas IHh signaling antagonist GDC0449 significantly downregulates *Gli1*$^+$ Su-SSPCs differentiation (Zhao et al., 2015). In injury experiments, *IHh* knock-out resulted in decreased bone volume and osteoporosis (Zhao et al., 2015). More recently, Greenblatt and others knocked out *Twist1* in *Ctsk*$^+$ lineage cells to create a craniosynostosis model. Unexpectedly, they observed that the cells expressing *Discoidin domain-containing receptor 2 (DDR2)* populate the suture with a corresponding decrease in *Ctsk*$^+$ Su-SSPCs, and proposed that these are a distinct population of Su-SSPCs (Greenblatt et al., 2021).

The BMP and Wnt pathways are also fundamental to the development of calvarial bones and sutures (Maruyama et al., 2010; Ishii et al., 2015). In *Axin2*$^+$ Su-SSPCs, BMP signaling in presence of both *Axin2* and *type 1a BMP receptor* (*Bmpr1a*) expression suppresses early neonatal osteogenesis and maintains their stemness. *Rap1b*, a signaling effector of *Axin2*, mediates the balance between chondrogenic BMP to osteogenic FGF effect in the postnatal Wnt signaling pathway (Maruyama et al., 2010; Maruyama et al., 2017; Maruyama et al., 2021). Postnatal *Prx1*$^+$ (pn*Prx1*$^+$) Su-SSPCs also respond to Wnt signaling. Transcription factor profiling under physiologic conditions showed high levels of Wnt inhibitors, *Dkk1* and *Sost*, in pn*Prx1*$^+$ Su-SSPCs. Furthermore, inactivated Wnt signaling maintains the undifferentiated quiescent status of pn*Prx1*$^+$ Su-SSPCs, suggesting that Wnt signaling activation allows calvarial bone development and remodeling through pn*Prx1*$^+$ Su-SSPCs differentiation (Wilk et al., 2017). Given that pn*Prx1*$^+$ SSPCs are also found in the periosteum of long bones (Esposito et al., 2020), it is possible that pn*Prx1*$^+$ periosteal SSPCs are present and contribute to the observed long bone injury remodeling process as well.

Below the sutures, there is a fibrous membrane called the dura mater that provides paracrine signals for skull bone expansion and healing upon injury (Levi et al., 2011; Wang et al., 2020). The dura mater cells release BMP that serves as a stimuli to suture cells during brain and bone expansion (Levi et al., 2011) (Jin et al., 2016). After an injury, there is upregulation of *BMP2/4/7*, *FGF-2*, *FGFR-1*, *IGF-2* and *Ptn*, osteogenic markers *Sparc* and *Oc*, and osteoclast activity markers *Acp5*, *Ctsk, Mmp2,* and *Mmp14* in dura mater cells (Wan D. C. et al., 2008). Additionally, the absence of dura leads to fusion of the coronal suture, supporting the regulatory role and interaction of the dura with Su-SSPCs (Opperman et al., 2009). As sutures close, the reservoir of Su-SSPCs is lost. Given this closure or fusion of calvarial sutures happens physiologically during adulthood or prematurely with craniosynostosis, spontaneous repair of the critical-sized calvarial defect is a rare phenomenon in adults. To our knowledge, there is only one reported total re-ossification case in the adult age to date (González-Bonet, 2021).

In summary, the *Twist1* regulatory network, *EphA4* signaling, Hh/*Gli* pathway, and FGF receptors are uniquely involved in the development and patency of calvarial sutures. However, much still remains to be determined with regard to the regulatory mechanisms and their interactions, as well as the cellular processes in place. Su-SSPCs contribute to bone healing after injury; however, a slower rate is observed in the healing of defects in the calvarial periosteum compared to long bone periosteum (Lim et al., 2013). The absence of muscles and tendon attachments in the cranial region, which provides an additional layer of regulation, may be one of the reasons for this delay of healing.

3.2 Unique regulation of growth plate SSPCs (GP-SSPCs)

The GP consists of cartilaginous tissue that has a critical role in endochondral bone formation and elongation (Matsushita et al., 2020b). It is composed of three different layers with the resting zone on top (Ono and Kronenberg, 2016). It has long been thought that cells in the resting zone do not divide (Gibson, 1998; Shapiro et al., 2005), but recent studies demonstrated that, upon formation of the highly vascularized secondary ossification center, a postnatal SSPC niche is established in the resting zone located at the epiphysis of long bones (Mizuhashi et al., 2018; Newton et al., 2019).

Ono and others discovered postnatal chondrocyte cell populations expressing *PTHrP–mCherry* in the resting zone with SSPC markers ([CD45$^-$Ter119$^-$CD31$^-$CD51$^+$CD90$^-$] CD105$^-$CD200$^+$ mouse SSCs, CD105$^-$CD200$^-$ pre-bone, cartilage and stromal progenitors [pre-BCSPs], and CD105$^+$ BCSPs). These *PTHrP*$^+$ SSPCs give rise to transit-amplifying chondrocytes in the proliferating zone and to columnar chondrocytes from the early postnatal age decreasing until 6 months. The columnar chondrocytes undergo hypertrophy and subsequently differentiate into osteoblasts and *Cxcl12*$^+$ BMSCs beneath the GP (Mizuhashi et al., 2018). Similarly, Zhou and others observed migration of perinatal GP chondrocytes to the metaphysis just below the GP which form new osteoblasts in the BM and periosteum until 2 months of age, with significant decrease in contribution after adolescence (Shu et al., 2021). Resting *PTHrP*$^+$ SSPCs secrete PTHrP, which binds to the receptors expressed on the

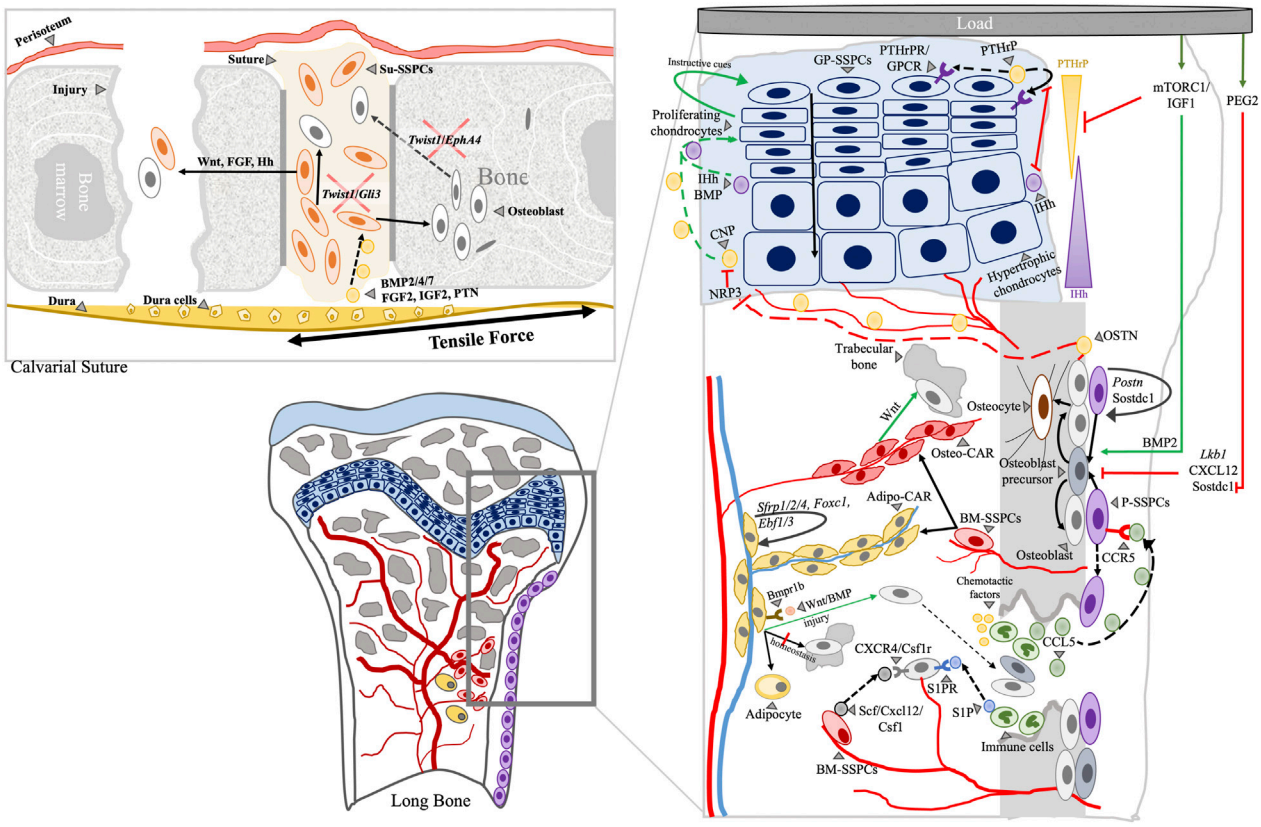

FIGURE 4
Schematic representation of plausible interactions of cellular components and molecular regulators at various skeletal compartments during bone remodeling and aging. Calvarial and long bone skeletal compartments are shown. Arrowhead: label; Black solid arrow: fate; Black dashed arrow: movement/migration; Red line: negative regulation; Green arrow: positive regulation; Arrows indicate directions of interactions or positive regulation.

proliferating chondrocytes. This suppresses their hypertrophic differentiation and delays the production of IHh derived from pre-hypertrophic chondrocytes. As proliferation progresses, the distance between the resting and the hypertrophic zones increases, which naturally releases the PTHrP-induced IHh suppression. Despite the presence of IHh, BMP acts as a downstream regulator of proliferation; IHh and BMP act in a positive feedback loop, allowing an increased rate of chondrocyte proliferation and inhibition of the development of terminally differentiated chondrocytes. *Runx2* also positively regulates *IHh* expression and promotes chondrocyte proliferation (Mizuhashi et al., 2018; Ağırdil, 2020). Consistent with calvarial sutures, local FGF antagonizes BMP activity, which results in the downregulation of proliferation, and promotion of differentiation and columnar chondrocyte formation in the area (Mizuhashi et al., 2018; Ağırdil, 2020; Matsushita et al., 2020b).

Another GP-SSPC population, *Col2a1*$^+$, was identified using a multicolor fluorescent reporter and *Col2a1-CreER*. *Col2a1*$^+$ SSPCs were present but few at E14.5 and early postnatal age, only increasing markedly at P30. The mammalian target of rapamycin complex 1 (mTORC1) signaling shifts the cell division of resting zone *Col2a1*$^+$ SSPCs from asymmetric to symmetric, which results in increased number and thickness of multi-columnar clones. Activation of mTORC1 may be a response to changes in local energy and oxygen levels (Newton et al., 2019). Moreover, insulin-like growth factor 1 (IGF-1) signaling induces mTOR signaling activity and suppresses PTHrP production (Ağırdil, 2020). Since the GP is expected to be highly active during early human development until puberty, it is logical that increase of GP-SSPCs for bone formation would be triggered by mTOR-activating factors such as physical loading and muscle hypertrophy due to an active lifestyle and a protein-rich diet. *Axin2*$^+$ cells were also identified in the outermost layer of the GP acting as chondroprogenitors (Matsushita et al., 2020b). While in the resting zone, Wnt-inhibitory environment allows the maintenance of *PTHrP*$^+$ GP-SSPCs and activation promotes cell proliferation without columnar formation (Hallett et al., 2021), Wnt activation in the GP periphery promotes chondrocyte formation of *Axin2*$^+$ GP-SSPCs (Matsushita et al., 2020b). This possibly explains GP lateral expansion, but the physiological triggers of activation of Wnt/β-catenin remain to be investigated.

G-protein-coupled receptors (GPCRs) also regulate the self-renewal and differentiation capabilities of resting zone chondrocytes. Global ablation of Gsα (*Col2a1-creER; Gnas f/f*) causes premature differentiation of stem-like resting chondrocytes. When combined with the inactivation of Gq/G11α, a more severe phenotype with GP fusion occurs (Guo et al., 2009). These results suggest that PTH/PTHrP receptor-mediated protein stimulatory subunit-α (Gsα) and Gq/G11α synergistically maintain the quiescence of resting chondrocytes and their differentiation into

columnar chondrocytes (Chagin et al., 2014). However, details of this regulatory mechanism, and whether this occurs without a trigger in resting chondrocytes, are yet to be determined.

Recently, periosteal cells were reported to interact with GP cells and regulate their endochondral bone formation. Periosteal osteoblast-derived *Osteocrin* (*OSTN*) inhibits *Natriuretic peptide receptor 3 (NPR3)* expressed in the GP hypertrophic chondrocytes. *OSTN* released by periosteal osteoblasts is delivered to the GP possibly through the epiphyseal and metaphyseal arteries supplying the ends of the GP. When active, *NPR3* causes the degradation of C-type natriuretic peptide (CNP) of the CNP-guanylate cyclase (GC)-B signaling pathway which is expressed in proliferating and pre-hypertrophic zones of the GP. Given that CNP promotes chondrocyte proliferation and maturation, the inhibition of *NPR3* by *OSTN* from periosteal osteoblasts produces a pro-chondrogenic effect (Potter et al., 2006; Watanabe-Takano et al., 2019). Periosteal osteoblast production of *OSTN* decreases with age, entirely downregulated by 3-month in mice (Watanabe-Takano et al., 2019). With GP chondrocytes forming BM and periosteal bone, positive feedback loop between the periosteal and GP cells seems to be in play contributing to bone elongation during early postnatal development.

In summary, long bone elongation *via* endochondral ossification is highly complex and structured, with chondrocytes taking a central role in the process. Being an analogous structure to calvarial sutures, similarities in regulations are evident. The GP eventually closes near the end of puberty (Setiawati and Rahardjo, 2019) and is regulated by the same pathways mentioned above. A decrease in the proliferative capacity of the SSPCs in the resting zone, together with decreased production of extracellular matrix (ECM), leads to GP closure and a limited contribution of trabecular osteoblasts in adult life (Ağırdil, 2020).

3.3 Unique regulation of periosteal SSPCs (P-SSPCs)

The periosteum, composed of the fibrous outer layer and cambium inner layer, covers the outer surface of the cortical bone. Periosteal SSPCs and osteoblasts are considered to be housed in the cambium layer (Matsushita et al., 2020c) and contribute to bone thickening and cortical maintenance during development and homeostasis (Serowoky et al., 2020). In addition, these periosteal cells are required for bone appositional growth, which occurs throughout life due to stress from increased muscle activity or weight.

Recently, *Ctsk*$^+$ cells with the SSPC immunophenotype (CD45$^-$ TER119$^-$ CD31$^-$ THY$^-$ 6C3$^-$ CD200$^+$ CD105$^-$) were identified and located in the periosteum of postnatal long bones and calvaria (Chan et al., 2015; Debnath et al., 2018). However, the *Ctsk* gene transcribes cathepsin K, a thiol protease that is highly expressed in osteoclastic cells. Thus, it should be noted that *Ctsk* is not a specific P-SSPC marker and *Ctsk*$^+$ cells include tartrate-resistant acid phosphatase (TRAP)-positive osteoclastic cells in the BM and TRAP-negative SSPCs and osteoprogenitor cells in the periosteum (Debnath et al., 2018; Zhang et al., 2022). *Axin2-CreER* also labels a subpopulation of postnatal P-SSPCs (Maruyama et al., 2016; Ransom et al., 2016), but non-specifically marks the endosteal cell population as well (~42%) (Ransom et al., 2016). Aside from Wnt signaling, *liver kinase b1* (*LKB1*), a master serine/threonine kinase and known tumor suppressor that links energy homeostasis and cell growth through the mTORC1 pathway, may also play a role in the maintenance of *Ctsk*$^+$ P-SSPCs. Studied in osteosarcoma formation, deletion of *LKB1* in *Ctsk*$^+$ P-SSPCs resulted in increased mTORC1 activity, subsequently causing an osteogenic tumor-like phenotype (Han et al., 2019). Therefore, the presence of *LKB1* may promote P-SSPC quiescence, while mTORC1 activation promotes appositional growth. The involvement of mTORC1 in both GP- and P-SSPCs suggests the importance of both axial and lateral bone growth during bone development.

In an attempt to define a specific marker for more immature osteogenic progenitor cells in adult bones, Park et al. defined *Mx1-Cre* as an efficient labeling model for osteogenic stem/progenitor cells (Park et al., 2012). In a subsequent study, they showed that double labeling of *Mx1-Cre* with *αSMA*GFP$^+$ allows selective labeling of endogenous P-SSPCs (Ortinau et al., 2019). This P-SSPC population expresses CCR5, which results in their migration to injury sites with increased CCL5 from immune cells. Further, they showed that immune cells specifically from the macrophage lineage seem to play an important role in supporting periosteal niches. A deficiency in cytokine colony-stimulating factor 1 (CSF-1) in mononuclear cells, macrophages, and osteoclasts lead to a significant reduction of *Nestin*-, *Osx*-expressing, and *Leptin receptor (LepR)*-traced cells (Gao et al., 2019), which further supports the presence of interactions among cells within skeletal compartments.

Mx1$^+$*αSMA*$^{GFP^+}$ P-SSPCs are present in long bones and calvaria, and they overlap with pn*Prx1*$^+$ periosteal cells (Ortinau et al., 2019). Consistently, most *Prx1*$^+$ SSPCs are present in the long bone periosteum during embryonic and postnatal development. *Prx1*$^+$ cells are present during embryonic development restricted to the mesoderm which becomes mesenchymal cells postnatally without losing their embryonic tissue specification and thus have SSPC properties (Du et al., 2013; Bragdon et al., 2022). These pn*Prx1*$^+$ P-SSPCs are known to inhibit adipogenesis by activating TGFβ signaling (Du et al., 2013). Furthermore, pn*Prx1* expression and osteogenic activity of pn*Prx1*$^+$ P-SSPCs are induced in long bone injuries. Gene ontology study showed that they serve as a subset of reserve stem cells with the expression of stemness and limb development genes that can be engaged in tissue remodeling following injury (Duchamp de Lageneste et al., 2018). Injury-induced postnatal expression of *Prx1* in the periosteum is regulated by the BMP/CXCL12 interaction. Increases in BMP2 after injury result in a decrease in CXCL12 and *Prx1*, and *vice versa*. On day 14 post-injury, BMP2 upregulation leads to a decrease of CXCL12 expression and downregulation of *Prx1*, allowing cells to commit to callus maturation and osteogenic differentiation (Esposito et al., 2020).

The regenerative potential of P-SSPCs was also shown to be controlled by *Periostin (Postn)*. A microarray analysis of pn*Prx1*$^+$ P-SSPCs isolated from non-injured and injured bone identified that the *Postn* gene, expressed within the periosteum, is important for both intramembranous and endochondral re-ossification (Duchamp de Lageneste et al., 2018). *Postn* is a matricellular protein regulating cell-cell and cell-matrix interactions (Bonnet et al., 2009; Bonnet et al., 2013) and, when knocked out, causes reduced callus size, abnormal repair of unicortical bone defects that

heal through direct bone formation, reduced bone volume throughout the repair, and local deficiency in the P-SSPC pool. *Postn* and its linked genes contribute to P-SSPC activation, niche regulation, and production of ECM proteins in response to bone injury (Duchamp de Lageneste et al., 2018). Similar to *Postn*, *Sclerostin domain-containing protein 1* (*Sostdc1*), a BMP and Wnt signaling antagonist primarily expressed in the periosteum, also maintains the P-SSPC pool (Semënov et al., 2005; Yanagita, 2005). The absence of *Sostdc1* hastens the expansion and differentiation P-SSPCs during bone healing (Collette et al., 2013).

Under normal homeostatic conditions, P-SSPCs provide a cellular source for the maintenance and growth of periosteal bones inherently through intramembranous ossification. However, these cells are able to undergo endochondral fracture repair with the formation of cartilage intermediates. $Mx1^{+}\alpha SMA^{GFP+}$ P-SSPCs demonstrated this plasticity triggered by injury (Ortinau et al., 2019). Although the exact mechanism as to how this occurs is yet unknown, extracellular lipids, the hypoxia-inducible factor-1α (HIF-1α) and the BMP signaling pathways may be involved in this process (Hanada et al., 2001; Eyckmans et al., 2009; van Gastel et al., 2020; Zhang et al., 2022). The avascular state of the injury limits serum supply and creates extracellular lipid scarcity which activates FoxO signaling and pro-chondrogenic *Sox9* expression in the P-SSPCs (van Gastel et al., 2020). During bone repair, the HIF-1α pathway, required for normal skeletal development, is also activated (Wan C. et al., 2008) and is coupled with the action of VEGF, which is released by hypertrophic chondrocytes as well as osteoblast and undifferentiated cells near the injury (Wan C. et al., 2008; Wan et al., 2010; Nagao et al., 2017). This can initiate the invasion of blood vessels and facilitate GP- and P-SPPCs regulatory interactions. VEGF which is known to be a chondrocyte survival factor during development and bone formation (Nagao et al., 2017) could initially support the cartilage intermediate formation until enough vasculature and lipid levels are present for subsequent osteogenesis of remaining adjacent P-SSPCs.

In summary, postnatal P-SSPCs are heterogenous populations with unique regulatory mechanisms. Due to their proximity with the GP and BM niches, P-SSPCs may interact with cells from other compartments, thus affecting their regulation and contribution to osteochondrogenic bone regeneration. The identification of other regulatory factors or selective control mechanisms of P-SSPCs will present promising new approaches for bone regeneration.

3.4 Unique regulation of bone marrow SSPCs (BM-SSPCs)

The BM contains distinct SSPC populations with self-renewal and multi-lineage differentiation potentials (Herrmann and Jakob, 2019). BM-SSPCs are critical niche constituents with hematopoiesis-supportive function (Dominici et al., 2006), and are spatially associated with hematopoietic stem cells (HSCs) (Méndez-Ferrer et al., 2010). The BM is more prominent in long bones as compared to the calvarial bones, and the interaction between BM-SSPCs and HSCs is also more pronounced in long bones (Sadr et al., 1980; Chan et al., 2009; Chan et al., 2013; Ma et al., 2015).

As mentioned earlier, BM forms during bone development with blood vessels invading through a layer of committed osteogenic cells. Osx^{+} and $Dlx5^{+}$ osteogenic precursor cells populate the forming fetal marrow with the development of the blood vessels (Maes et al., 2010; Liu et al., 2013; Matsushita et al., 2022). While both cells contribute to fetal periosteum and marrow stroma development, Osx^{+} cells are transient as their number dramatically declined after 13 weeks, leaving $Dlx5^{+}$ cells as the major BM-SSPCs with the role of regulating BM space formation (Mizoguchi et al., 2014; Matsushita et al., 2022). $Fgfr3^{+}$ cells contributing to the fetal cartilage template and fetal GP also form BM-SSPCs in embryonic trabecular bone formation, together with a subset of Osx^{+} and $Dlx5^{+}$ cells. Mechanistically, IHh secreted by $Fgfr3^{+}$ cells bind to the *Ptch1* of $Dlx5^{+}$ BM-SSPCs to promote BM space formation. Similar to its effect on GP chondrocytes, secreted IHh also promotes proliferation of $Fgfr3^{+}$ BM chondrocytes which may differentiate into osteoblasts (Matsushita et al., 2022).

Postnatally, $Dlx5^{+}$ cells localize in the mid-diaphysis retaining its BM-SSPC properties but with adipogenic tendencies to become $Perilipin^{+}$ marrow adipocytes in adult bones. Interestingly, a subset of $Fgfr3^{+}$ cells develop into postnatal metaphyseal BM-SSPCs with osteogenic tendencies contributing to *alkaline phosphatase*-expressing osteoblasts (Shu et al., 2021; Matsushita et al., 2022). These cells may be the same population as the $PTHrP^{+}$ GP hypertrophic chondrocytes that turns into $Cxcl12^{+}$ BM-SSPCs beyond the GP (Mizuhashi et al., 2018). Separately, postnatal $LepR^{+}$ BM-SSPCs with *Osx* expression are responsible for new osteoblasts in adult BM and in the metaphyseal area (Mizoguchi et al., 2014; Shu et al., 2021). While a portion of the this cell population differentiate to trabecular osteoblasts, some cells remain unchanged in the metaphyseal stroma with long term SSPCs properties, and a portion change into BM reticular cells (Maes et al., 2010; Liu et al., 2013; Mizoguchi et al., 2014; Matsushita et al., 2020c; Matsushita et al., 2020a). These BM-SSPCs proliferate along the developing blood vessels regulated by the endothelial cell-derived PDGF-BB signaling pathway through PDGFRβ of the precursor cells, which subsequently become perivascular cells that establish the BM stroma (Bianco et al., 2013). These cells are marked as $CD45^{-}/CD34^{-}/CD146^{+}$, with the *Osx* expression confirming its osteogenic origin (Liu et al., 2013). Consistently, a perivascular cell marker *Nestin-GFP* also labels BM-SSPCs with stem cell functions at E15.5 and postnatal to adulthood, supporting the idea that at least a subset of BM-SSPCs has BM perivascular location (Méndez-Ferrer et al., 2010; Wei and Frenette, 2018).

$Gli1^{+}$ metaphyseal mesenchymal progenitors (MMPs) located beneath the GP express SSPC markers CD146, CD44, CD106, and CD140a (PDGFRα), and may possibly label the same population of unchanged postnatal Osx^{+} osteogenic precursor cells in the metaphyseal region. Both cells migrate from the perichondrium to the BM at E15.5–16.5, suggesting cell population overlap even during embryonic development (Shi et al., 2017; Matsushita et al., 2022). Proliferation and osteoblast differentiation of $Gli1^{+}$ MMPs is driven by β-catenin and *Hh* signaling from the pre-hypertrophic chondrocytes of the GP. Without β-catenin (e.g., GP closure), adipogenesis is favored and *LepR* expression is observed. These early $Gli1^{+}$ progenitor cells also disappear from their position in aged

mice and do not contribute to major *Cxcl12*$^{+}$ stromal cells (Shi et al., 2017), implicating that they are more likely osteochondrogenic progenitor cells rather than SSCs. Populations of SSPCs that express *Gremlin1* (*Grem1*), a secreted BMP antagonist, were also identified in the embryonic and postnatal mice (Chan et al., 2015; Worthley et al., 2015). Postnatal *Grem1*$^{+}$ cells in the BM metaphysis, just under the GP, define a population of osteochondroreticular (OCR) stem cells with self-renewal, and osteoblasts, chondrocytes, and reticular BM-SSPC differentiation capacity during early development. Interestingly, these OCR stem cells do not differentiate into adipocytes. Deletion of *Grem1* results in BM hypoplasia with early hematopoietic failure (Rowan et al., 2020). From its properties and location, overlap with *Fgfr3*$^{+}$ BM-SSPCs is possible, but is yet to be established.

3.4.1 Unique adipogenic regulation of BM-SSPCs

In the postnatal and adult mouse BM, most perivascular BM-SSPCs acquire marker expression such as *LepR* and *Mx1*, with the latter labelling not only stromal cells but HSCs as well (Park et al., 2012; Zhou et al., 2014). In addition, BM-SSPCs distinctly express cytokines responsible for the retention of hematopoietic progenitors such as CXCL12 or stromal cell-derived factor 1 (SDF1), stem cell factor (SCF) (Wei and Frenette, 2018). *LepR*$^{+}$ cells are observed only in postnatal perisinusoidal or periarteriolar BM-SSPCs (Zhou et al., 2014; Shen et al., 2021) that are largely overlapping with the *Cxcl12*-abundant reticular (CAR) cells (Matsushita et al., 2020a). In addition, CAR cells have subclusters and have been reclassified into osteo-CAR (*Cxcl12*$^{+}$*Osx*$^{+}$) and adipo-CAR cells (*Cxcl12*$^{+}$*LepR*$^{+}$), having pre-osteogenic and pre-adipogenic tendencies respectively (Matsushita et al., 2020a; Baccin et al., 2020; Shen et al., 2021). Recently, a mechanosensitive *LepR*$^{+}$ *Osteolectin*$^{+}$ (*Oln*$^{+}$) cell population, a potential subset of the osteo-CAR population, has also been discovered, and are distinguishable from adipo-CAR population. They contribute to bone formation during injury and mechanical loading through the mechanosensitive ion channel, Piezo1 (Shen et al., 2021). The *Fgfr3*$^{+}$ metaphyseal and *Dlx5*$^{+}$ diaphyseal BM-SSPCs were also proposed to represent osteo- and adipo-CAR cells, respectively, implying that these two CAR cell populations developed from two distinct origin sharing the same marker rather than coming from a single progenitor (Matsushita et al., 2022). Further, these osteo- and adipo-CAR cells have a distinct periarteriolar and perisinusoidal location respectively, implicating their heterogeneity. Osteo-CAR cells contributes to cortical bone formation during homeostasis and injury regeneration, while adipo-CAR only minorly contributes during injury repair (Matsushita et al., 2020a; Baccin et al., 2020; Shen et al., 2021). During homeostasis, adipo-CAR cells express potent Wnt inhibitors such as *Sfrp1*, *Sfrp2*, and *Sfrp4,* suggesting a role for *Cxcl12* in the inhibition of CAR cell differentiation (Matsushita et al., 2020a). *Foxc1* and *Early B-cell factor1/3* (*Ebf1/Ebf3*) also contribute to this inhibition and are important in the maintenance of BM-SSPCs. Deficiency of *Foxc1* or *Ebf1/3* in *LepR*$^{+}$ cells results in osteosclerotic BM, impaired HSC niche function, and fibrotic conversion of the BM-SSPCs (Seike et al., 2018; Omatsu et al., 2022). Upon injury, activation of Wnt signaling may stimulate production of BMP, which interacts with type Ib receptor Bmpr (Bmpr1b) (Muruganandan et al., 2009). Additionally, pre-adipogenic factors are inhibited, which may further stimulate their osteogenic differentiation (Abdallah, 2017). However, whether this plasticity is due to a bipotential capacity or presence of a quiescent osteogenic progenitor subset is still unknown.

Reconciling rare adipocytes in the young postnatal marrow, Zhong et al. (2020) reported a group of non-proliferative cells expressing adipocyte genes (e.g., *adiponectin* [*Adipoq*]) called marrow adipogenic lineage precursor (MALP) cells. These MALPs lack significant lipid stores usually seen in adult adipocytes and lack adipocyte progenitor markers such as *SCA1* and *CD34*. Interestingly, MALPs form a vast 3D network structure inside the BM that allows cell-to-cell contact and BM environment interaction which may be important for marrow vasculature maintenance and suppression of osteogenic differentiation. Early adiponectin studies reported that adiponectin can facilitate the migration of osteoblast progenitors to the endosteal injury site through increasing sphingosine1 phosphate (S1P) (Li et al., 2009; Holland et al., 2011) since osteoblasts are reported to express the S1P receptor (Sartawi et al., 2017). Conversely, adiponectin repels osteoclast progenitors and osteoclasts from injury sites, allowing structured intramembranous bone repair (Yang et al., 2015). However, recent studies showed that the removal of *Adipoq-Cre*$^{+}$ cells resulted in disruption of sinusoidal vessels and a significant increase in bone trabeculae in the marrow space (Zhong et al., 2020). Further, *Adipoq-Cre*$^{+}$ MALPs highly express *Cxcl12*, *Scf*, and Csf1 (Zhong et al., 2020; Yu et al., 2021) needed for HSC retention, hematopoietic regeneration after injury, and osteoclast activation, respectively (Peled et al., 1999; Zhou et al., 2017; Yu et al., 2021). These factors attract osteoblast and osteoclast progenitors expressing CXCR4 into the BM, supporting a role of *Adipoq-Cre*$^{+}$ cells in the bone marrow function. Whether MALPs and adipo-CAR cells overlap or are distinct cell populations is still unknown. Further elucidation of the role of adipo-CAR cells during homeostasis may therefore reveal novel functions in BM maintenance and osteoblast regulation (Ortinau and Park, 2021).

3.4.2 Unique hematopoietic regulation of BM-SSPCs

The BM is an essential environment for HSPCs. In particular, BM-HSCs are in a fluid condition and require the niche interaction with perivascular SSPCs through adhesion proteins (e.g., *Scdf1* and E-selectin) for their long-term maintenance (Sipkins et al., 2005). Conversely, HSPCs contribute to the maintenance, as well as the activation, of their niche cells and BM-SSPCs *via* their inflammatory cells. Th1 cells secrete TNFα, which mediates increased RANKL expression by macrophages and B-lymphocytes (Lam et al., 2000; Castillo et al., 2017). These increased RANKL expression from B-lymphocytes can control osteoclastogenesis (Walsh and Choi, 2014; Toni et al., 2020). Further, B-lymphocytes have spontaneous production of granulocyte-colony stimulating factor (G-CSF) throughout life and increased Osteoprotegerin (OPG) production with age (Li et al., 2015) with boosts under the stress or inflammatory conditions (Corcione and Pistoia, 1997). Depending on the expression levels of G-CSF and OPG, osteogenesis (high G-CSF, low OPG) or osteoclastogenesis (low G-CSF, high OPG) may be favored (Weitzmann, 2013; Zhang et al., 2020). Therefore, B-lymphocytes are an important regulator of

SSPCs by contribute to bone healing after injury and excessive bone resorption during aging.

M1 macrophages also contribute to SSPC maintenance and activation. They secrete reactive oxygen species (ROS), nitric oxide (NO), and several proinflammatory cytokines (e.g., IL-1, IL-2, IL-6, TNFα, and IFNγ) (Genin et al., 2015). NO allows vasodilation which may increase the migration of cells through and from the BM (Bianco, 2011). Together with factors such as IL-1 and IL-6, which decrease osteogenic differentiation, these macrophages further help in the establishment of the BM niche and maintenance of BM-SSPCs. On the other hand, M2 macrophages secrete pro-osteogenic molecules BMP2, TGFβ, and osteopontin (Chen et al., 2020). Additionally, activated neutrophils produce IL-1α and TGFβ directly causing BM-SSPC differentiation into osteoblasts (Al-Hakami et al., 2020) and inhibition of ECM production (Bastian et al., 2018).

Overall, the interaction of HSPCs and BM-SSPCs does not only affect the BM niche but bone turnover as well. While the identity of BM-SSPCs remains elusive, the regulation mechanisms of BM-SSPCs appear to be highly connected to factors released from the GP chondrocyte and BM inflammatory cells, suggesting that cellular and molecular regulators interact across skeletal compartments (Figure 4).

4 Regulations during aging

The elderly population has poor capacity for skeletal regeneration and a limited physiologic SSPC reserve (Lee et al., 2014) leading to degenerative conditions (Jeong and Park, 2020). SSPCs from older individuals have similar clonogenicity, but impaired osteochondrogenic differentiation, as compared to younger individuals (Ambrosi et al., 2020). Changes in hormones and sustained pro-inflammatory stimuli in aging might alter epigenetics regulators (Beerman and Rossi, 2015; Josephson et al., 2019). A recent study showing the downregulation of histone deacetylase *Sirtuin1* in aged human SSPCs supports this hypothesis (Ambrosi et al., 2020). Moreover, downregulation of osteogenic genes (e.g., Wnt signaling), and upregulation of fibroblast-like ECM- and cellular senescence-related genes, were seen in aged human SSPCs, suggesting skewing towards stromal/fibroblastic states (Ambrosi et al., 2020). Excess or continuous inflammation in the elderly, and low-grade chronic inflammation associated with degenerative and cardiometabolic diseases, are known to inhibit the regeneration of various tissues including bones (Franceschi et al., 2018; Josephson et al., 2019). Activation of Nuclear factor-kappa B (NF-κB), a regulator of innate immunity, resulted in increased expression of the senescence genes *Cdkn1a* and *Cdkn2a*, suggesting its central role as a mediator of a pro-inflammatory state and SSPC aging (Albensi, 2019) (Josephson et al., 2019). Extensive proliferation may also lead to cellular exhaustion. Sustained FGF2 signaling in SSPCs and increased neutrophil-related ROS in HSC cause loss of quiescence and impaired regenerative capacity of SSPCs (Owusu-Ansah and Banerjee, 2009; Chakkalakal et al., 2012).

With age, the rest of the BM undergoes adipocyte conversion where fat cells progressively increase in number. Adipocytes then inhibit BM-SSPC functions (Bianco, 2011). Normally, adipogenesis involves sequential expression of *CCAAT enhancer-binding protein beta* (*C/EBPβ*), *gamma* (*C/EBPγ*), *alfa* (*C/EBPα*), and finally *peroxisome proliferator-activated receptor gamma* (*PPARγ*) from progenitor cells. Several transcription factors direct age-related shifts in BM-SSPC differentiation. MAF bZIP transcription factor (MAF), a binding partner of *Runx2*, is increased in the young but decreased in the old. With age, reduced MAF promotes adipogenesis through upregulation of *PPARγ* and the suppression of osteogenesis (Nishikawa et al., 2010). *Forkhead box P1* (*FOXP1*) also declines with age, losing its anti-adipocyte interaction with *C/EBPβ* and pro-osteogenic repression of Notch signaling pathway, all leading to bone loss (Li et al., 2017). Core-binding factor subunit beta (CBFβ) is another key co-factor of *Runx2* that is reduced with aging. Normally, CBFβ inhibits adipogenic gene expression and enhances Wnt/β-catenin signaling (Wu et al., 2014; Wu et al., 2017). An increase of BM adipocytes with age is also associated with the gradual decrease of *Adipoq*$^{+}$ expression, potentially facilitating MALPs differentiation to adipocyte cells. Expression of *Cxcl12* is also reduced, further leading to BM atrophy and adipogenesis (Zhang et al., 2021). Furthermore, BM adipocytes may also inhibit BM-SSPCs function by physically blocking blood flow through the sinusoid. The larger-sized adipocytes can compress the sinusoid, leading to its collapse (Bachman et al., 2002).

Unlike most bones, cranial bones are rarely affected by osteoporosis. However, the same mechanisms leading to this condition can also reduce cranial bone mass density and regeneration capacity (Cotofana et al., 2018; Hudieb et al., 2021). Radiographic and histologic studies showed a decreased computed volume of the calvaria and a lateral expansion of the skull, favoring a skeletonized facial appearance in elderly individuals (Cotofana et al., 2018). Increased soft tissue laxity and decreased fat (Cotofana et al., 2016) can contribute to increased bone resorption in elder individuals due to decreased mechanical loading. The tensile strength of the dura also decreases with age; alterations in collagen fiber organization may cause this change in dura properties, which ultimately affects the ECM of the tissue (Zwirner et al., 2019; Panteleichuk et al., 2021). The osteogenic activity of the dura also tends to be less active with age (Wan D. C. et al., 2008), probably due to the absence of skull growth-induced mechanical strain (Wang et al., 2020).

Further understanding of which cellular and molecular changes SSPCs undergo during stress, aging, and pro-inflammatory conditions, and which regulatory mechanisms control these changes, will offer new approaches to the treatment of bone diseases through the ages.

5 Conclusion and future directions

Calvarial and long bones are unique types of bone that are distinctively regulated but show subtle similarities in the involved pathways. In both types of bone, multiple types of distinct SSPCs are present and interact with each other to achieve skeletal development. Despite improvements in our understanding of SSPCs, the different functional responses and regulations of SSPCs in various locations, especially during injury, have not been thoroughly studied. Although some essential molecular regulators are shared by distinct SSPCs, their effect on differentiation, cell fate, or tissue type formation of distict SSPCs can be different. As such, local SSPCs contribute uniquely to their bone development, homeostasis, and regeneration. Different conditions (e.g., injury, stress, aging) result in different regulations as

well. Studies looking into these differences are currently inadequate. Possible regulatory differences directing the rate of defect or injury healing in the craniofacial area and long bones have not been extensively investigated despite this long-observed difference.

Long bone is important for addressing the mechanical loading throughout life, while craniofacial deformities are important not only for the physiology of the organs in the craniofacial area but also for the quality of life of patients in general. Thus, studies pertinent to enhancing healing of both long bones and craniofacial bones may have to be given equal importance. The unique effect of the limited presence of ligaments, tendons, and muscles in the craniofacial area, as compared to long bones, is an interesting area of research. Characterization of the heterogenous SSPC population in the BM, and the regulatory mechanisms by which they contribute to BM maintenance, could be continued and expanded as a research initiative. Single-cell approaches together with *in vivo,* and *ex vivo* functional studies appear to be a powerful approach to facilitate SSPC characterization and biology. Additionally, the single-cell approach would allow further analyses on differential gene expression and the regulatory mechanisms established between cell populations, skeletal compartments, and cell conditions (development vs. injury vs. aging).

Advancements in SSPC research and interest in the aging bone have allowed the discovery of more unique populations such as those adipocyte marker-expressing cells that do not undergo adipogenesis, but rather unexpectedly remains undifferentiated in the marrow with marrow stroma and cortical bone maintenance roles. Further research could also be done to deepen our understanding of how each multiple types of SSPCs relate to each in the context of development, regeneration, and aging. These differences are necessary for designing specific tissue engineering and regenerative medicine therapies for bone repair.

Author contributions

Conceptualization, JS, FH, and DP; methodology, JS, FH, and DP; writing—original draft preparation, JS and YJ; writing—review and editing, JS, YJ, FH, and DP; supervision, DP. All authors have read and agreed to the published version of the manuscript.

Funding

This work was supported by the Bone Disease Program of Texas Award and the NIAMS and NIDCR of the National Institutes of Health, under award numbers R01AR072018, R01DE031288, R01DE031162 to DP and T32DK060445 to YJ. JS is supported in part through the MD-PhD Research Enrichment Program from the Department of Science and Technology-Philippine Council for Health Research and Development, and Science Education Institute.

Conflict of interest

The authors declare that the research was conducted in the absence of any commercial or financial relationships that could be construed as a potential conflict of interest.

Publisher's note

References

Abdallah, B. M. (2017). Marrow adipocytes inhibit the differentiation of mesenchymal stem cells into osteoblasts via suppressing BMP-signaling. *J. Biomed. Sci.* 24, 11. doi:10.1186/s12929-017-0321-4

Ağırdil, Y. (2020). The growth plate: A physiologic overview. *EFORT Open Rev.* 5, 498–507. doi:10.1302/2058-5241.5.190088

Albensi, B. C. (2019). What is nuclear factor kappa B (NF-κB) doing in and to the mitochondrion? *Front. Cell Dev. Biol.* 7, 154. doi:10.3389/fcell.2019.00154

Al-Hakami, A., Alqhatani, S. Q., Shaik, S., Jalfan, S. M., Dhammam, M. S. A., Asiri, W., et al. (2020). Cytokine physiognomies of MSCs from varied sources confirm the regenerative commitment post-coculture with activated neutrophils. *J. Cell. Physiology* 235, 8691–8701. doi:10.1002/jcp.29713

Ambrosi, T. H., Goodnough, L. H., Steininger, H. M., Hoover, M. Y., Kim, E., Koepke, L. S., et al. (2020). Geriatric fragility fractures are associated with a human skeletal stem cell defect. *Aging Cell* 19, e13164. doi:10.1111/acel.13164

Ambrosi, T. H., Longaker, M. T., and Chan, C. K. F. (2019). A revised perspective of skeletal stem cell biology. *Front. Cell Dev. Biol.* 7, 189. doi:10.3389/fcell.2019.00189

Baccin, C., Al-Sabah, J., Velten, L., Helbling, P. M., Grünschläger, F., Hernández-Malmierca, P., et al. (2020). Combined single-cell and spatial transcriptomics reveal the molecular, cellular and spatial bone marrow niche organization. *Nat. Cell Biol.* 22, 38–48. doi:10.1038/s41556-019-0439-6

Bachman, E. S., Dhillon, H., Zhang, C.-Y., Cinti, S., Bianco, A. C., Kobilka, B. K., et al. (2002). betaAR signaling required for diet-induced thermogenesis and obesity resistance. *Science* 297, 843–845. doi:10.1126/science.1073160

Bastian, O. W., Croes, M., Alblas, J., Koenderman, L., Leenen, L. P. H., and Blokhuis, T. J. (2018). Neutrophils inhibit synthesis of mineralized extracellular matrix by human bone marrow-derived stromal cells *in vitro*. *Front. Immunol.* 9, 945. doi:10.3389/fimmu.2018.00945

Beerman, I., and Rossi, D. J. (2015). Epigenetic control of stem cell potential during homeostasis, aging, and disease. *Cell Stem Cell* 16, 613–625. doi:10.1016/j.stem.2015.05.009

Bianco, P. (2011). Bone and the hematopoietic niche: A tale of two stem cells. *Blood* 117, 5281–5288. doi:10.1182/blood-2011-01-315069

Bianco, P., Cao, X., Frenette, P. S., Mao, J. J., Robey, P. G., Simmons, P. J., et al. (2013). The meaning, the sense and the significance: Translating the science of mesenchymal stem cells into medicine. *Nat. Med.* 19, 35–42. doi:10.1038/nm.3028

Bianco, P., and Robey, P. G. (2015). Skeletal stem cells. *Development* 142, 1023–1027. doi:10.1242/dev.102210

Bivi, N., Pacheco-Costa, R., Brun, L. R., Murphy, T. R., Farlow, N. R., Robling, A. G., et al. (2013). Absence of Cx43 selectively from osteocytes enhances responsiveness to mechanical force in mice: Osteocytic CX43 and mechanotransduction. *J. Orthop. Res.* 31, 1075–1081. doi:10.1002/jor.22341

Bonaventure, J. (2001). Skeletal development in human. Atlas of Genetics and cytogenetics in oncology and haematology. Available at: https://atlasgeneticsoncology.org/teaching/30075/skeletal-development-in-human (Accessed May 5, 2022).

Bonnet, N., Gineyts, E., Ammann, P., Conway, S. J., Garnero, P., and Ferrari, S. (2013). Periostin deficiency increases bone damage and impairs injury response to fatigue loading in adult mice. *PLoS ONE* 8, e78347. doi:10.1371/journal.pone.0078347

Bonnet, N., Standley, K. N., Bianchi, E. N., Stadelmann, V., Foti, M., Conway, S. J., et al. (2009). The matricellular protein Periostin is required for Sost inhibition and the anabolic response to mechanical loading and physical activity. *J. Biol. Chem.* 284, 35939–35950. doi:10.1074/jbc.M109.060335

Borrelli, M. R., Hu, M. S., Longaker, M. T., and Lorenz, H. P. (2020). Tissue engineering and regenerative medicine in craniofacial reconstruction and facial aesthetics. *J. Craniofacial Surg.* 31, 15–27. doi:10.1097/SCS.0000000000005840

Bragdon, B. C., Bennie, A., Molinelli, A., Liu, Y., and Gerstenfeld, L. C. (2022). Post natal expression of Prx1 labels appendicular restricted progenitor cell populations of multiple tissues. *J. Cell. Physiology* 237, 2550–2560. doi:10.1002/jcp.30728

Castillo, L. M., Guerrero, C. A., and Acosta, O. (2017). Expression of typical osteoclast markers by PBMCs after PEG-induced fusion as a model for studying osteoclast differentiation. *J. Mol. Hist.* 48, 169–185. doi:10.1007/s10735-017-9717-4

Chagin, A. S., Vuppalapati, K. K., Kobayashi, T., Guo, J., Hirai, T., Chen, M., et al. (2014). G-protein stimulatory subunit alpha and Gq/11α G-proteins are both required to maintain quiescent stem-like chondrocytes. *Nat. Commun.* 5, 3673. doi:10.1038/ncomms4673

Chakkalakal, J. V., Jones, K. M., Basson, M. A., and Brack, A. S. (2012). The aged niche disrupts muscle stem cell quiescence. *Nature* 490, 355–360. doi:10.1038/nature11438

Chan, C. K. F., Chen, C.-C., Luppen, C. A., Kim, J.-B., DeBoer, A. T., Wei, K., et al. (2009). Endochondral ossification is required for haematopoietic stem-cell niche formation. *Nature* 457, 490–494. doi:10.1038/nature07547

Chan, C. K. F., Lindau, P., Jiang, W., Chen, J. Y., Zhang, L. F., Chen, C.-C., et al. (2013). Clonal precursor of bone, cartilage, and hematopoietic niche stromal cells. *Proc. Natl. Acad. Sci. U.S.A.* 110, 12643–12648. doi:10.1073/pnas.1310212110

Chan, C. K. F., Seo, E. Y., Chen, J. Y., Lo, D., McArdle, A., Sinha, R., et al. (2015). Identification and specification of the mouse skeletal stem cell. *Cell* 160, 285–298. doi:10.1016/j.cell.2014.12.002

Chen, K., Jiao, Y., Liu, L., Huang, M., He, C., He, W., et al. (2020). Communications between bone marrow macrophages and bone cells in bone remodeling. *Front. Cell Dev. Biol.* 8, 598263. doi:10.3389/fcell.2020.598263

Chung, I.-H., Yamaza, T., Zhao, H., Choung, P.-H., Shi, S., and Chai, Y. (2009). Stem cell property of postmigratory cranial neural crest cells and their utility in alveolar bone regeneration and tooth development: Neural crest cells in bone regeneration. *STEM CELLS* 27, 866–877. doi:10.1002/stem.2

Clark, D., Nakamura, M., Miclau, T., and Marcucio, R. (2017). Effects of aging on fracture healing. *Curr. Osteoporos. Rep.* 15, 601–608. doi:10.1007/s11914-017-0413-9

Collette, N. M., Yee, C. S., Murugesh, D., Sebastian, A., Taher, L., Gale, N. W., et al. (2013). Sost and its paralog Sostdc1 coordinate digit number in a Gli3-dependent manner. *Dev. Biol.* 383, 90–105. doi:10.1016/j.ydbio.2013.08.015

Corcione, A., and Pistoia, V. (1997). B-Cell-Derived granulocyte-colony stimulating factor (G-CSF). *Methods* 11, 143–147. doi:10.1006/meth.1996.0398

Cotofana, S., Fratila, A., Schenck, T., Redka-Swoboda, W., Zilinsky, I., and Pavicic, T. (2016). The anatomy of the aging face: A review. *Facial plast. Surg.* 32, 253–260. doi:10.1055/s-0036-1582234

Cotofana, S., Gotkin, R. H., Ascher, B., Morozov, S. P., Gombolevsky, V. A., Laipan, A. S., et al. (2018). Calvarial volume loss and facial aging: A computed tomographic (CT)-Based study. *Aesthetic Surg. J.* 38, 1043–1051. doi:10.1093/asj/sjy096

Debnath, S., Yallowitz, A. R., McCormick, J., Lalani, S., Zhang, T., Xu, R., et al. (2018). Discovery of a periosteal stem cell mediating intramembranous bone formation. *Nature* 562, 133–139. doi:10.1038/s41586-018-0554-8

Deckelbaum, R. A., Holmes, G., Zhao, Z., Tong, C., Basilico, C., and Loomis, C. A. (2012). Regulation of cranial morphogenesis and cell fate at the neural crest-mesoderm boundary by engrailed 1. *Development* 139, 1346–1358. doi:10.1242/dev.076729

Demontiero, O., Vidal, C., and Duque, G. (2012). Aging and bone loss: New insights for the clinician. *Ther. Adv. Musculoskelet.* 4, 61–76. doi:10.1177/1759720X11430858

Dominici, M., Le Blanc, K., Mueller, I., Slaper-Cortenbach, I., Marini, F. C., Krause, D. S., et al. (2006). Minimal criteria for defining multipotent mesenchymal stromal cells. The International Society for Cellular Therapy position statement. *Cytotherapy* 8, 315–317. doi:10.1080/14653240600855905

Donsante, S., Palmisano, B., Serafini, M., Robey, P. G., Corsi, A., and Riminucci, M. (2021). From stem cells to bone-forming cells. *IJMS* 22, 3989. doi:10.3390/ijms22083989

Doro, D. H., Grigoriadis, A. E., and Liu, K. J. (2017). Calvarial suture-derived stem cells and their contribution to cranial bone repair. *Front. Physiol.* 8, 956. doi:10.3389/fphys.2017.00956

Du, B., Cawthorn, W. P., Su, A., Doucette, C. R., Yao, Y., Hemati, N., et al. (2013). The transcription factor paired-related homeobox 1 (Prrx1) inhibits adipogenesis by activating transforming growth factor-β (TGFβ) signaling. *J. Biol. Chem.* 288, 3036–3047. doi:10.1074/jbc.M112.440370

Duchamp de Lageneste, O., Julien, A., Abou-Khalil, R., Frangi, G., Carvalho, C., Cagnard, N., et al. (2018). Periosteum contains skeletal stem cells with high bone regenerative potential controlled by Periostin. *Nat. Commun.* 9, 773. doi:10.1038/s41467-018-03124-z

Esposito, A., Wang, L., Li, T., Miranda, M., and Spagnoli, A. (2020). Role of Prx1-expressing skeletal cells and Prx1-expression in fracture repair. *Bone* 139, 115521. doi:10.1016/j.bone.2020.115521

Eyckmans, J., Roberts, S. J., Schrooten, J., and Luyten, F. P. (2009). A clinically relevant model of osteoinduction: A process requiring calcium phosphate and BMP/Wnt signalling. *J. Cell. Mol. Med.* 14, 1845–1856. doi:10.1111/j.1582-4934.2009.00807.x

Farmer, D. T., Mlcochova, H., Zhou, Y., Koelling, N., Wang, G., Ashley, N., et al. (2021). The developing mouse coronal suture at single-cell resolution. *Nat. Commun.* 12, 4797. doi:10.1038/s41467-021-24917-9

Franceschi, C., Garagnani, P., Parini, P., Giuliani, C., and Santoro, A. (2018). Inflammaging: A new immune–metabolic viewpoint for age-related diseases. *Nat. Rev. Endocrinol.* 14, 576–590. doi:10.1038/s41574-018-0059-4

Galea, G. L., Sunters, A., Meakin, L. B., Zaman, G., Sugiyama, T., Lanyon, L. E., et al. (2011). *Sost* down-regulation by mechanical strain in human osteoblastic cells involves PGE2 signaling via EP4. *FEBS Lett.* 585, 2450–2454. doi:10.1016/j.febslet.2011.06.019

Galea, G. L., Zein, M. R., Allen, S., and Francis West, P. (2021). Making and shaping endochondral and intramembranous bones. *Dev. Dyn.* 250, 414–449. doi:10.1002/dvdy.278

Gao, B., Deng, R., Chai, Y., Chen, H., Hu, B., Wang, X., et al. (2019). Macrophage-lineage TRAP+ cells recruit periosteum-derived cells for periosteal osteogenesis and regeneration. *J. Clin. Investigation* 129, 2578–2594. doi:10.1172/JCI98857

Genin, M., Clement, F., Fattaccioli, A., Raes, M., and Michiels, C. (2015). M1 and M2 macrophages derived from THP-1 cells differentially modulate the response of cancer cells to etoposide. *BMC Cancer* 15, 577. doi:10.1186/s12885-015-1546-9

Gerbaix, M., Vico, L., Ferrari, S. L., and Bonnet, N. (2015). Periostin expression contributes to cortical bone loss during unloading. *Bone* 71, 94–100. doi:10.1016/j.bone.2014.10.011

Gibson, G. (1998). Active role of chondrocyte apoptosis in endochondral ossification. *Microsc. Res. Tech.* 43, 191–204. doi:10.1002/(SICI)1097-0029(19981015)43:2<191:AID-JEMT10>3.0.CO;2-T

González-Bonet, L. G. (2021). Spontaneous cranial bone regeneration after a craniectomy in an adult. *World Neurosurg.* 147, 67–69. doi:10.1016/j.wneu.2020.12.056

Greenblatt, M., Bok, S., Yallowitz, A., McCormick, J., Cung, M., Sun, J., et al. (2021). *A multi-stem cell basis for craniosynostosis and calvarial mineralization*. In Review. doi:10.21203/rs.3.rs-1061838/v1

Guo, X., Mak, K. K., Taketo, M. M., and Yang, Y. (2009). The Wnt/beta-catenin pathway interacts differentially with PTHrP signaling to control chondrocyte hypertrophy and final maturation. *PLoS ONE* 4, e6067. doi:10.1371/journal.pone.0006067

Guo, Y., Yuan, Y., Wu, L., Ho, T.-V., Jing, J., Sugii, H., et al. (2018). BMP-IHH-mediated interplay between mesenchymal stem cells and osteoclasts supports calvarial bone homeostasis and repair. *Bone Res.* 6, 30. doi:10.1038/s41413-018-0031-x

Hallett, S. A., Matsushita, Y., Ono, W., Sakagami, N., Mizuhashi, K., Tokavanich, N., et al. (2021). Chondrocytes in the resting zone of the growth plate are maintained in a Wnt-inhibitory environment. *eLife* 10, e64513. doi:10.7554/eLife.64513

Han, Y., Feng, H., Sun, J., Liang, X., Wang, Z., Xing, W., et al. (2019). Lkb1 deletion in periosteal mesenchymal progenitors induces osteogenic tumors through mTORC1 activation. *J. Clin. Investigation* 129, 1895–1909. doi:10.1172/JCI124590

Hanada, K., Solchaga, L. A., Caplan, A. I., Hering, T. M., Goldberg, V. M., Yoo, J. U., et al. (2001). BMP-2 induction and TGF-?1 modulation of rat periosteal cell chondrogenesis. *J. Cell. Biochem.* 81, 284–294. doi:10.1002/1097-4644(20010501)81:2<284:aid-jcb1043>3.0.co;2-d

Herrmann, M., and Jakob, F. (2019). Bone marrow niches for skeletal progenitor cells and their inhabitants in health and disease. *CSCR* 14, 305–319. doi:10.2174/1574888X14666190123161447

Holland, W. L., Miller, R. A., Wang, Z. V., Sun, K., Barth, B. M., Bui, H. H., et al. (2011). Receptor-mediated activation of ceramidase activity initiates the pleiotropic actions of adiponectin. *Nat. Med.* 17, 55–63. doi:10.1038/nm.2277

Holmes, G., Gonzalez-Reiche, A. S., Lu, N., Zhou, X., Rivera, J., Kriti, D., et al. (2020). Integrated transcriptome and network analysis reveals spatiotemporal dynamics of calvarial suturogenesis. *Cell Rep.* 32, 107871. doi:10.1016/j.celrep.2020.107871

Hudieb, M., Haddad, A., Bakeer, M., Alkhazaaleh, A., AlKhader, M., Taani, D., et al. (2021). Influence of age on calvarial critical size defect dimensions: A radiographic and histological study. *J. Craniofacial Surg.* 32, 2896–2900. doi:10.1097/SCS.0000000000007690

Iaquinta, M. R., Mazzoni, E., Bononi, I., Rotondo, J. C., Mazziotta, C., Montesi, M., et al. (2019). Adult stem cells for bone regeneration and repair. *Front. Cell Dev. Biol.* 7, 268. doi:10.3389/fcell.2019.00268

Ishii, M., Sun, J., Ting, M.-C., and Maxson, R. E. (2015). "The development of the calvarial bones and sutures and the pathophysiology of craniosynostosis," in *Current topics in developmental biology* (Elsevier), 131–156. doi:10.1016/bs.ctdb.2015.07.004

Jeong, Y., and Park, D. (2020). Targeting periosteal SSCs for aged bone defects. *Aging* 12, 3124–3125. doi:10.18632/aging.102869

Jha, R. T., Magge, S. N., and Keating, R. F. (2018). "Diagnosis and surgical options for craniosynostosis," in *Principles of neurological surgery* (Elsevier), 148–169.e7. doi:10.1016/B978-0-323-43140-8.00009-3

Jin, S.-W., Sim, K.-B., and Kim, S.-D. (2016). Development and growth of the normal cranial vault: An embryologic review. *J. Korean Neurosurg. Soc.* 59, 192–196. doi:10.3340/jkns.2016.59.3.192

Josephson, A. M., Bradaschia-Correa, V., Lee, S., Leclerc, K., Patel, K. S., Muinos Lopez, E., et al. (2019). Age-related inflammation triggers skeletal stem/progenitor cell dysfunction. *Proc. Natl. Acad. Sci. U.S.A.* 116, 6995–7004. doi:10.1073/pnas.1810692116

Kenkre, J., and Bassett, J. (2018). The bone remodelling cycle. *Ann. Clin. Biochem.* 55, 308–327. doi:10.1177/0004563218759371

Kitazawa, T., Minoux, M., Ducret, S., and Rijli, F. M. (2022). Different ectopic Hoxa2 expression levels in mouse cranial neural crest cells result in distinct craniofacial anomalies and homeotic phenotypes. *JDB* 10, 9. doi:10.3390/jdb10010009

Ko, F. C., and Sumner, D. R. (2021). How faithfully does intramembranous bone regeneration recapitulate embryonic skeletal development? *Dev. Dyn.* 250, 377–392. doi:10.1002/dvdy.240

Kurenkova, A. D., Medvedeva, E. V., Newton, P. T., and Chagin, A. S. (2020). Niches for skeletal stem cells of mesenchymal origin. *Front. Cell Dev. Biol.* 8, 592. doi:10.3389/fcell.2020.00592

Lam, J., Takeshita, S., Barker, J. E., Kanagawa, O., Ross, F. P., and Teitelbaum, S. L. (2000). TNF-α induces osteoclastogenesis by direct stimulation of macrophages exposed to permissive levels of RANK ligand. *J. Clin. Invest.* 106, 1481–1488. doi:10.1172/JCI11176

Lana-Elola, E., Rice, R., Grigoriadis, A. E., and Rice, D. P. C. (2007). Cell fate specification during calvarial bone and suture development. *Dev. Biol.* 311, 335–346. doi:10.1016/j.ydbio.2007.08.028

Lappin, T. R. J., Grier, D. G., Thompson, A., and Halliday, H. L. (2006). HOX genes: Seductive science, mysterious mechanisms. *Ulst. Med. J.* 75, 23–31.

Lee, Y.-K., Lee, Y.-J., Ha, Y.-C., and Koo, K.-H. (2014). Five-year relative survival of patients with osteoporotic hip fracture. *J. Clin. Endocrinol. Metabolism* 99, 97–100. doi:10.1210/jc.2013-2352

Lee, Y. (2013). The role of interleukin-17 in bone metabolism and inflammatory skeletal diseases. *BMB Rep.* 46, 479–483. doi:10.5483/BMBRep.2013.46.10.141

Leucht, P., Kim, J.-B., Amasha, R., James, A. W., Girod, S., and Helms, J. A. (2008). Embryonic origin and Hox status determine progenitor cell fate during adult bone regeneration. *Development* 135, 2845–2854. doi:10.1242/dev.023788

Levi, B., Nelson, E. R., Li, S., James, A. W., Hyun, J. S., Montoro, D. T., et al. (2011). Dura mater stimulates human adipose-derived stromal cells to undergo bone formation in mouse calvarial defects. *Stem Cells* 29, 1241–1255. doi:10.1002/stem.670

Li, B., Wang, Y., Fan, Y., Ouchi, T., Zhao, Z., and Li, L. (2021). Cranial suture mesenchymal stem cells: Insights and advances. *Biomolecules* 11, 1129. doi:10.3390/biom11081129

Li, C., Kong, Y., Wang, H., Wang, S., Yu, H., Liu, X., et al. (2009). Homing of bone marrow mesenchymal stem cells mediated by sphingosine 1-phosphate contributes to liver fibrosis. *J. Hepatology* 50, 1174–1183. doi:10.1016/j.jhep.2009.01.028

Li, H., Liu, P., Xu, S., Li, Y., Dekker, J. D., Li, B., et al. (2017). FOXP1 controls mesenchymal stem cell commitment and senescence during skeletal aging. *J. Clin. Investigation* 127, 1241–1253. doi:10.1172/JCI89511

Li, Y., Terauchi, M., Vikulina, T., Roser-Page, S., and Weitzmann, N. M. (2015). B cell production of both OPG and RANKL is significantly increased in aged mice. *TOBONEJ* 6, 8–17. doi:10.2174/1876525401406010008

Libby, J., Marghoub, A., Johnson, D., Khonsari, R. H., Fagan, M. J., and Moazen, M. (2017). Modelling human skull growth: A validated computational model. *J. R. Soc. Interface.* 14, 20170202. doi:10.1098/rsif.2017.0202

Lim, J., Lee, J., Yun, H.-S., Shin, H.-I., and Park, E. K. (2013). Comparison of bone regeneration rate in flat and long bone defects: Calvarial and tibial bone. *Tissue Eng. Regen. Med.* 10, 336–340. doi:10.1007/s13770-013-1094-9

Liu, Y., Strecker, S., Wang, L., Kronenberg, M. S., Wang, W., Rowe, D. W., et al. (2013). Osterix-cre labeled progenitor cells contribute to the formation and maintenance of the bone marrow stroma. *PLoS ONE* 8, e71318. doi:10.1371/journal.pone.0071318

Lloyd, S. A., Lewis, G. S., Zhang, Y., Paul, E. M., and Donahue, H. J. (2012). Connexin 43 deficiency attenuates loss of trabecular bone and prevents suppression of cortical bone formation during unloading. *J. Bone Min. Res.* 27, 2359–2372. doi:10.1002/jbmr.1687

Lohse, M. J., Engelhardt, S., and Eschenhagen, T. (2003). What is the role of β-adrenergic signaling in heart failure? *Circulation Res.* 93, 896–906. doi:10.1161/01.RES.0000102042.83024.CA

Lu, X., Beck, G. R., Gilbert, L. C., Camalier, C. E., Bateman, N. W., Hood, B. L., et al. (2011). Identification of the homeobox protein Prx1 (MHox, Prrx-1) as a regulator of osterix expression and mediator of tumor necrosis factor α action in osteoblast differentiation. *J. Bone Min. Res.* 26, 209–219. doi:10.1002/jbmr.203

Ma, J., Yang, F., Both, S. K., Prins, H.-J., Helder, M. N., Pan, J., et al. (2015). Bone forming capacity of cell- and growth factor-based constructs at different ectopic implantation sites: Bone Formation at Different Ectopic Sites. *J. Biomed. Mat. Res.* 103, 439–450. doi:10.1002/jbm.a.35192

Maes, C., Kobayashi, T., Selig, M. K., Torrekens, S., Roth, S. I., Mackem, S., et al. (2010). Osteoblast precursors, but not mature osteoblasts, move into developing and fractured bones along with invading blood vessels. *Dev. Cell* 19, 329–344. doi:10.1016/j.devcel.2010.07.010

Maruyama, T., Jeong, J., Sheu, T.-J., and Hsu, W. (2016). Stem cells of the suture mesenchyme in craniofacial bone development, repair and regeneration. *Nat. Commun.* 7, 10526. doi:10.1038/ncomms10526

Maruyama, T., Jiang, M., Abbott, A., Yu, H.-M. I., Huang, Q., Chrzanowska-Wodnicka, M., et al. (2017). Rap1b is an effector of Axin2 regulating crosstalk of signaling pathways during skeletal development: RAP1B in AXIN2-MEDIATED skeletal development and disease. *J. Bone Min. Res.* 32, 1816–1828. doi:10.1002/jbmr.3171

Maruyama, T., Mirando, A. J., Deng, C.-X., and Hsu, W. (2010). The balance of WNT and FGF signaling influences mesenchymal stem cell fate during skeletal development. *Sci. Signal.* 3, ra40. doi:10.1126/scisignal.2000727

Maruyama, T., Stevens, R., Boka, A., DiRienzo, L., Chang, C., Yu, H.-M. I., et al. (2021). BMPR1A maintains skeletal stem cell properties in craniofacial development and craniosynostosis. *Sci. Transl. Med.* 13, eabb4416. doi:10.1126/scitranslmed.abb4416

Matsushita, Y., Chu, A. K. Y., Tsutsumi-Arai, C., Orikasa, S., Nagata, M., Wong, S. Y., et al. (2022). The fate of early perichondrial cells in developing bones. *Nat. Commun.* 13, 7319. doi:10.1038/s41467-022-34804-6

Matsushita, Y., Nagata, M., Kozloff, K. M., Welch, J. D., Mizuhashi, K., Tokavanich, N., et al. (2020a). A Wnt-mediated transformation of the bone marrow stromal cell identity orchestrates skeletal regeneration. *Nat. Commun.* 11, 332. doi:10.1038/s41467-019-14029-w

Matsushita, Y., Ono, W., and Ono, N. (2020b). Growth plate skeletal stem cells and their transition from cartilage to bone. *Bone* 136, 115359. doi:10.1016/j.bone.2020.115359

Matsushita, Y., Ono, W., and Ono, N. (2020c). Skeletal stem cells for bone development and repair: Diversity matters. *Curr. Osteoporos. Rep.* 18, 189–198. doi:10.1007/s11914-020-00572-9

McCubrey, J. A., Steelman, L. S., Bertrand, F. E., Davis, N. M., Sokolosky, M., Abrams, S. L., et al. (2014). GSK-3 as potential target for therapeutic intervention in cancer. *Oncotarget* 5, 2881–2911. doi:10.18632/oncotarget.2037

Méndez-Ferrer, S., Michurina, T. V., Ferraro, F., Mazloom, A. R., MacArthur, B. D., Lira, S. A., et al. (2010). Mesenchymal and haematopoietic stem cells form a unique bone marrow niche. *Nature* 466, 829–834. doi:10.1038/nature09262

Merrell, A. J., and Stanger, B. Z. (2016). Adult cell plasticity *in vivo*: De-differentiation and transdifferentiation are back in style. *Nat. Rev. Mol. Cell Biol.* 17, 413–425. doi:10.1038/nrm.2016.24

Miller, M. Q., Park, S. S., and Christophel, J. J. (2017). Applying regenerative medicine techniques in facial plastic and reconstructive surgery: The bar has been set high. *npj Regen. Med.* 2 (20), 20–017. doi:10.1038/s41536-017-0025-0

Mitchell, B., and Sharma, R. (2009). "How does an embryo form?" in *Embryology* (Elsevier), 1–8. doi:10.1016/B978-0-7020-3225-7.50004-X

Mizoguchi, T., Pinho, S., Ahmed, J., Kunisaki, Y., Hanoun, M., Mendelson, A., et al. (2014). Osterix marks distinct waves of primitive and definitive stromal progenitors during bone marrow development. *Dev. Cell* 29, 340–349. doi:10.1016/j.devcel.2014.03.013

Mizokami, A., Kawakubo-Yasukochi, T., and Hirata, M. (2017). Osteocalcin and its endocrine functions. *Biochem. Pharmacol.* 132, 1–8. doi:10.1016/j.bcp.2017.02.001

Mizuhashi, K., Ono, W., Matsushita, Y., Sakagami, N., Takahashi, A., Saunders, T. L., et al. (2018). Resting zone of the growth plate houses a unique class of skeletal stem cells. *Nature* 563, 254–258. doi:10.1038/s41586-018-0662-5

Moore, K. L., Persaud, T. V. N., and Torchia, M. G. (2016). *The developing human: Clinically oriented embryology* 10th edition. Philadelphia, PA: Elsevier.

Muruganandan, S., Roman, A. A., and Sinal, C. J. (2009). Adipocyte differentiation of bone marrow-derived mesenchymal stem cells: Cross talk with the osteoblastogenic program. *Cell. Mol. Life Sci.* 66, 236–253. doi:10.1007/s00018-008-8429-z

Nagao, M., Hamilton, J. L., Kc, R., Berendsen, A. D., Duan, X., Cheong, C. W., et al. (2017). Vascular endothelial growth factor in cartilage development and osteoarthritis. *Sci. Rep.* 7, 13027. doi:10.1038/s41598-017-13417-w

Nam, D., Mau, E., Wang, Y., Wright, D., Silkstone, D., Whetstone, H., et al. (2012). T-lymphocytes enable osteoblast maturation via IL-17F during the early phase of fracture repair. *PLoS ONE* 7, e40044. doi:10.1371/journal.pone.0040044

Nandiraju, D., and Ahmed, I. (2019). Human skeletal physiology and factors affecting its modeling and remodeling. *Fertil. Steril.* 112, 775–781. doi:10.1016/j.fertnstert.2019.10.005

Newton, P. T., Li, L., Zhou, B., Schweingruber, C., Hovorakova, M., Xie, M., et al. (2019). A radical switch in clonality reveals a stem cell niche in the epiphyseal growth plate. *Nature* 567, 234–238. doi:10.1038/s41586-019-0989-6

Nishikawa, K., Nakashima, T., Takeda, S., Isogai, M., Hamada, M., Kimura, A., et al. (2010). Maf promotes osteoblast differentiation in mice by mediating the age-related switch in mesenchymal cell differentiation. *J. Clin. Invest.* 120, 3455–3465. doi:10.1172/JCI42528

Omatsu, Y., Aiba, S., Maeta, T., Higaki, K., Aoki, K., Watanabe, H., et al. (2022). Runx1 and Runx2 inhibit fibrotic conversion of cellular niches for hematopoietic stem cells. *Nat. Commun.* 13, 2654. doi:10.1038/s41467-022-30266-y

Ono, N., and Kronenberg, H. M. (2016). Bone repair and stem cells. *Curr. Opin. Genet. Dev.* 40, 103–107. doi:10.1016/j.gde.2016.06.012

Opperman, L. A., Passarelli, R. W., Morgan, E. P., Reintjes, M., and Ogle, R. C. (2009). Cranial sutures require tissue interactions with dura mater to resist osseous obliteration *in vitro*. *J. Bone Min. Res.* 10, 1978–1987. doi:10.1002/jbmr.5650101218.1987

Ortinau, L. C., and Park, D. (2021). Do adipogenic stromal cells undergo lineage plasticity in response to bone injury? *BioEssays* 43, 2000296. doi:10.1002/bies.202000296

Ortinau, L. C., Wang, H., Lei, K., Deveza, L., Jeong, Y., Hara, Y., et al. (2019). Identification of functionally distinct Mx1+αSMA+ periosteal skeletal stem cells. *Cell Stem Cell* 25, 784–796.e5. doi:10.1016/j.stem.2019.11.003

Owusu-Ansah, E., and Banerjee, U. (2009). Reactive oxygen species prime Drosophila haematopoietic progenitors for differentiation. *Nature* 461, 537–541. doi:10.1038/nature08313

Panteleichuk, A. B., Shmeleva, A. A., Kadzhaya, M. V., Hnatiuk, O. P., Karakhim, S. I., Dovbeshko, G. I., et al. (2021). Quantitative evaluation of the regenerated dura mater in a decompressive skull trepanation model in rats. *Int. J. Morphol.* 39, 1731–1736. doi:10.4067/S0717-95022021000601731

Park, D., Spencer, J. A., Koh, B. I., Kobayashi, T., Fujisaki, J., Clemens, T. L., et al. (2012). Endogenous bone marrow MSCs are dynamic, fate-restricted participants in bone maintenance and regeneration. *Cell Stem Cell* 10, 259–272. doi:10.1016/j.stem.2012.02.003

Pazhanisamy, S. (2013). Adult stem cell and embryonic stem cell markers. *MATER METHODS* 3. doi:10.13070/mm.en.3.200

Peled, A., Petit, I., Kollet, O., Magid, M., Ponomaryov, T., Byk, T., et al. (1999). Dependence of human stem cell engraftment and repopulation of NOD/SCID mice on CXCR4. *Science* 283, 845–848. doi:10.1126/science.283.5403.845

Percival, C. J., and Richtsmeier, J. T. (2013). Angiogenesis and intramembranous osteogenesis: Angiogenesis and intramembranous osteogenesis. *Dev. Dyn.* 242, 909–922. doi:10.1002/dvdy.23992

Potter, L. R., Abbey-Hosch, S., and Dickey, D. M. (2006). Natriuretic peptides, their receptors, and cyclic guanosine monophosphate-dependent signaling functions. *Endocr. Rev.* 27, 47–72. doi:10.1210/er.2005-0014

Raisz, L. G., and Seeman, E. (2001). Causes of age-related bone loss and bone fragility: An alternative view. *J. Bone Min. Res.* 16, 1948–1952. doi:10.1359/jbmr.2001.16.11.1948

Ransom, R. C., Hunter, D. J., Hyman, S., Singh, G., Ransom, S. C., Shen, E. Z., et al. (2016). Axin2-expressing cells execute regeneration after skeletal injury. *Sci. Rep.* 6, 36524. doi:10.1038/srep36524

Rowan, S. C., Jahns, H., Mthunzi, L., Piouceau, L., Cornwell, J., Doody, R., et al. (2020). Gremlin 1 depletion *in vivo* causes severe enteropathy and bone marrow failure. *J. Pathol.* 251, 117–122. doi:10.1002/path.5450

Rux, D. R., and Wellik, D. M. (2017). *Hox* genes in the adult skeleton: Novel functions beyond embryonic development: *Hox* Genes in the Adult Skeleton. *Dev. Dyn.* 246, 310–317. doi:10.1002/dvdy.24482

Sacchetti, B., Funari, A., Remoli, C., Giannicola, G., Kogler, G., Liedtke, S., et al. (2016). No identical "mesenchymal stem cells" at different times and sites: Human committed progenitors of distinct origin and differentiation potential are incorporated as adventitial cells in microvessels. *Stem Cell Rep.* 6, 897–913. doi:10.1016/j.stemcr.2016.05.011

Sadler, T. W., and Langman, J. (2012). *Langman's medical embryology* 12th ed. Philadelphia: Wolters Kluwer Health/Lippincott Williams and Wilkins.

Sadr, A. M., Cardenas, F., and Tavassoli, M. (1980). Functional potential of ectopic marrow autotransplants. *Experientia* 36, 605–606. doi:10.1007/BF01965828

Sartawi, Z., Schipani, E., Ryan, K. B., and Waeber, C. (2017). Sphingosine 1-phosphate (S1P) signalling: Role in bone biology and potential therapeutic target for bone repair. *Pharmacol. Res.* 125, 232–245. doi:10.1016/j.phrs.2017.08.013

Schoenwolf, G. C., Bleyl, S. B., Brauer, P. R., and Francis-West, P. H. (2015). *Larsen's human embryology* Fifth edition. Philadelphia, PA: Churchill Livingstone.

Seike, M., Omatsu, Y., Watanabe, H., Kondoh, G., and Nagasawa, T. (2018). Stem cell niche-specific Ebf3 maintains the bone marrow cavity. *Genes Dev.* 32, 359–372. doi:10.1101/gad.311068.117

Semënov, M., Tamai, K., and He, X. (2005). SOST is a ligand for LRP5/LRP6 and a Wnt signaling inhibitor. *J. Biol. Chem.* 280, 26770–26775. doi:10.1074/jbc.M504308200

Serowoky, M. A., Arata, C. E., Crump, J. G., and Mariani, F. V. (2020). Skeletal stem cells: Insights into maintaining and regenerating the skeleton. *Development* 147, dev179325. doi:10.1242/dev.179325

Setiawati, R., and Rahardjo, P. (2019). "Bone development and growth," in *Osteogenesis and bone regeneration*. Editors H. Yang doi:10.5772/intechopen.82452

Shapiro, I. M., Adams, C. S., Freeman, T., and Srinivas, V. (2005). Fate of the hypertrophic chondrocyte: Microenvironmental perspectives on apoptosis and survival in the epiphyseal growth plate. *Birth Defect Res. C* 75, 330–339. doi:10.1002/bdrc.20057

Sheehan, F. T., Brainerd, E. L., Troy, K. L., Shefelbine, S. J., and Ronsky, J. L. (2018). Advancing quantitative techniques to improve understanding of the skeletal structure-function relationship. *J. NeuroEngineering Rehabil.* 15, 25. doi:10.1186/s12984-018-0368-9

Sheen, J. R., and Garla, V. V. (2021). Fracture healing overview *StatPearls* (treasure island (FL): StatPearls publishing). Available at: http://www.ncbi.nlm.nih.gov/books/NBK551678/(Accessed January 10, 2022).

Shen, B., Tasdogan, A., Ubellacker, J. M., Zhang, J., Nosyreva, E. D., Du, L., et al. (2021). A mechanosensitive peri-arteriolar niche for osteogenesis and lymphopoiesis. *Nature* 591, 438–444. doi:10.1038/s41586-021-03298-5

Shi, Y., He, G., Lee, W.-C., McKenzie, J. A., Silva, M. J., and Long, F. (2017). Gli1 identifies osteogenic progenitors for bone formation and fracture repair. *Nat. Commun.* 8, 2043. doi:10.1038/s41467-017-02171-2

Shu, H. S., Liu, Y. L., Tang, X. T., Zhang, X. S., Zhou, B., Zou, W., et al. (2021). Tracing the skeletal progenitor transition during postnatal bone formation. *Cell Stem Cell* 28, 2122–2136.e3. doi:10.1016/j.stem.2021.08.010

Sipkins, D. A., Wei, X., Wu, J. W., Runnels, J. M., Côté, D., Means, T. K., et al. (2005). *In vivo* imaging of specialized bone marrow endothelial microdomains for tumour engraftment. *Nature* 435, 969–973. doi:10.1038/nature03703

Sottoriva, K., and Pajcini, K. V. (2021). Notch signaling in the bone marrow lymphopoietic niche. *Front. Immunol.* 12, 723055. doi:10.3389/fimmu.2021.723055

Su, N., Yang, J., Xie, Y., Du, X., Chen, H., Zhou, H., et al. (2019). Bone function, dysfunction and its role in diseases including critical illness. *Int. J. Biol. Sci.* 15, 776–787. doi:10.7150/ijbs.27063

Taher, L., Collette, N. M., Murugesh, D., Maxwell, E., Ovcharenko, I., and Loots, G. G. (2011). Global gene expression analysis of murine limb development. *PLoS ONE* 6, e28358. doi:10.1371/journal.pone.0028358

Tang, G., Liu, Z., Liu, Y., Yu, J., Wang, X., Tan, Z., et al. (2021). Recent trends in the development of bone regenerative biomaterials. *Front. Cell Dev. Biol.* 9, 665813. doi:10.3389/fcell.2021.665813

Ting, M.-C., Wu, N. L., Roybal, P. G., Sun, J., Liu, L., Yen, Y., et al. (2009). *EphA4* as an effector of *Twist1* in the guidance of osteogenic precursor cells during calvarial bone growth and in craniosynostosis. *Development* 136, 855–864. doi:10.1242/dev.028605

Toni, R., Di Conza, G., Barbaro, F., Zini, N., Consolini, E., Dallatana, D., et al. (2020). Microtopography of immune cells in osteoporosis and bone lesions by endocrine disruptors. *Front. Immunol.* 11, 1737. doi:10.3389/fimmu.2020.01737

van Gastel, N., Stegen, S., Eelen, G., Schoors, S., Carlier, A., Daniëls, V. W., et al. (2020). Lipid availability determines fate of skeletal progenitor cells via SOX9. *Nature* 579, 111–117. doi:10.1038/s41586-020-2050-1

Vanderbeck, A. N., and Maillard, I. (2019). Notch in the niche: New insights into the role of Notch signaling in the bone marrow. *Haematologica* 104, 2117–2119. doi:10.3324/haematol.2019.230854

Vidal, L., Kampleitner, C., Brennan, M. Á., Hoornaert, A., and Layrolle, P. (2020). Reconstruction of large skeletal defects: Current clinical therapeutic strategies and future directions using 3D printing. *Front. Bioeng. Biotechnol.* 8, 61. doi:10.3389/fbioe.2020.00061

Walsh, M. C., and Choi, Y. (2014). Biology of the RANKL-RANK-OPG system in immunity, bone, and beyond. *Front. Immunol.* 5, 511. doi:10.3389/fimmu.2014.00511

Wan, C., Gilbert, S. R., Wang, Y., Cao, X., Shen, X., Ramaswamy, G., et al. (2008). Activation of the hypoxia-inducible factor-1alpha pathway accelerates bone regeneration. *Proc. Natl. Acad. Sci. U.S.A.* 105, 686–691. doi:10.1073/pnas.0708474105

Wan, C., Shao, J., Gilbert, S. R., Riddle, R. C., Long, F., Johnson, R. S., et al. (2010). Role of HIF-1α in skeletal development: HIF-1α in skeletal development. *Ann. N. Y. Acad. Sci.* 1192, 322–326. doi:10.1111/j.1749-6632.2009.05238.x

Wan, D. C., Kwan, M. D., Gupta, D. M., Wang, Z., Slater, B. J., Panetta, N. J., et al. (2008). Global age-dependent differences in gene expression in response to calvarial injury. *J. Craniofacial Surg.* 19, 1292–1301. doi:10.1097/SCS.0b013e3181843609

Wang, D., Gilbert, J. R., Zhang, X., Zhao, B., Ker, D. F. E., and Cooper, G. M. (2020). Calvarial versus long bone: Implications for tailoring skeletal tissue engineering. *Tissue Eng. Part B Rev.* 26, 46–63. doi:10.1089/ten.teb.2018.0353

Watanabe-Takano, H., Ochi, H., Chiba, A., Matsuo, A., Kanai, Y., Fukuhara, S., et al. (2019). Periosteum-derived Osteocrin regulates bone growth through both endochondral ossification and intramembranous ossification. *Dev. Biol.* doi:10.1101/697094

Weber, M., Wehrhan, F., Deschner, J., Sander, J., Ries, J., Möst, T., et al. (2021). The special developmental biology of craniofacial tissues enables the understanding of oral and maxillofacial physiology and diseases. *IJMS* 22, 1315. doi:10.3390/ijms22031315

Wei, Q., and Frenette, P. S. (2018). Niches for hematopoietic stem cells and their progeny. *Immunity* 48, 632–648. doi:10.1016/j.immuni.2018.03.024

Weitzmann, M. N. (2013). The role of inflammatory cytokines, the RANKL/OPG Axis, and the immunoskeletal interface in physiological bone turnover and osteoporosis. *Scientifica* 2013, 125705–125729. doi:10.1155/2013/125705

Wilk, K., Yeh, S.-C. A., Mortensen, L. J., Ghaffarigarakani, S., Lombardo, C. M., Bassir, S. H., et al. (2017). Postnatal calvarial skeletal stem cells expressing PRX1 reside exclusively in the calvarial sutures and are required for bone regeneration. *Stem Cell Rep.* 8, 933–946. doi:10.1016/j.stemcr.2017.03.002

Worthley, D. L., Churchill, M., Compton, J. T., Tailor, Y., Rao, M., Si, Y., et al. (2015). Gremlin 1 identifies a skeletal stem cell with bone, cartilage, and reticular stromal potential. *Cell* 160, 269–284. doi:10.1016/j.cell.2014.11.042

Wu, A.-M., Bisignano, C., James, S. L., Abady, G. G., Abedi, A., Abu-Gharbieh, E., et al. (2021). Global, regional, and national burden of bone fractures in 204 countries and territories, 1990–2019: A systematic analysis from the global burden of disease study 2019. *Lancet Healthy Longev.* 2, e580–e592. doi:10.1016/S2666-7568(21)00172-0

Wu, M., Li, C., Zhu, G., Wang, Y., Jules, J., Lu, Y., et al. (2014). Deletion of core-binding factor β (Cbfβ) in mesenchymal progenitor cells provides new insights into Cbfβ/Runxs complex function in cartilage and bone development. *Bone* 65, 49–59. doi:10.1016/j.bone.2014.04.031

Wu, M., Wang, Y., Shao, J.-Z., Wang, J., Chen, W., and Li, Y.-P. (2017). Cbfβ governs osteoblast–adipocyte lineage commitment through enhancing β-catenin signaling and suppressing adipogenesis gene expression. *Proc. Natl. Acad. Sci. U.S.A.* 114, 10119–10124. doi:10.1073/pnas.1619294114

Yanagita, M. (2005). BMP antagonists: Their roles in development and involvement in pathophysiology. *Cytokine and Growth Factor Rev.* 16, 309–317. doi:10.1016/j.cytogfr.2005.02.007

Yang, L., Han, Z., Tian, L., Mai, P., Zhang, Y., Wang, L., et al. (2015). Sphingosine 1-phosphate receptor 2 and 3 mediate bone marrow-derived monocyte/macrophage motility in cholestatic liver injury in mice. *Sci. Rep.* 5, 13423. doi:10.1038/srep13423

Yen, H.-Y., Ting, M.-C., and Maxson, R. E. (2010). Jagged1 functions downstream of Twist1 in the specification of the coronal suture and the formation of a boundary between osteogenic and non-osteogenic cells. *Dev. Biol.* 347, 258–270. doi:10.1016/j.ydbio.2010.08.010

Youngstrom, D. W., Dishowitz, M. I., Bales, C. B., Carr, E., Mutyaba, P. L., Kozloff, K. M., et al. (2016). Jagged1 expression by osteoblast-lineage cells regulates trabecular bone mass and periosteal expansion in mice. *Bone* 91, 64–74. doi:10.1016/j.bone.2016.07.006

Yu, W., Zhong, L., Yao, L., Wei, Y., Gui, T., Li, Z., et al. (2021). Bone marrow adipogenic lineage precursors promote osteoclastogenesis in bone remodeling and pathologic bone loss. *J. Clin. Investigation* 131, e140214. doi:10.1172/JCI140214

Zhang, N., Hu, L., Cao, Z., Liu, X., and Pan, J. (2022). Periosteal skeletal stem cells and their response to bone injury. *Front. Cell Dev. Biol.* 10, 812094. doi:10.3389/fcell.2022.812094

Zhang, X., Robles, H., Magee, K. L., Lorenz, M. R., Wang, Z., Harris, C. A., et al. (2021). A bone-specific adipogenesis pathway in fat-free mice defines key origins and adaptations of bone marrow adipocytes with age and disease. *eLife* 10, e66275. doi:10.7554/eLife.66275

Zhang, Z., Yuan, W., Deng, J., Wang, D., Zhang, T., Peng, L., et al. (2020). Granulocyte colony stimulating factor (G-CSF) regulates neutrophils infiltration and periodontal tissue destruction in an experimental periodontitis. *Mol. Immunol.* 117, 110–121. doi:10.1016/j.molimm.2019.11.003

Zhao, H., Feng, J., Ho, T.-V., Grimes, W., Urata, M., and Chai, Y. (2015). The suture provides a niche for mesenchymal stem cells of craniofacial bones. *Nat. Cell Biol.* 17, 386–396. doi:10.1038/ncb3139

Zhong, L., Yao, L., Tower, R. J., Wei, Y., Miao, Z., Park, J., et al. (2020). Single cell transcriptomics identifies a unique adipose lineage cell population that regulates bone marrow environment. *eLife* 9, e54695. doi:10.7554/eLife.54695

Zhou, B. O., Yu, H., Yue, R., Zhao, Z., Rios, J. J., Naveiras, O., et al. (2017). Bone marrow adipocytes promote the regeneration of stem cells and haematopoiesis by secreting SCF. *Nat. Cell Biol.* 19, 891–903. doi:10.1038/ncb3570

Zhou, B. O., Yue, R., Murphy, M. M., Peyer, J. G., and Morrison, S. J. (2014). Leptin-receptor-expressing mesenchymal stromal cells represent the main source of bone formed by adult bone marrow. *Cell Stem Cell* 15, 154–168. doi:10.1016/j.stem.2014.06.008

Zieba, J. T., Chen, Y.-T., Lee, B. H., and Bae, Y. (2020). Notch signaling in skeletal development, homeostasis and pathogenesis. *Biomolecules* 10, 332. doi:10.3390/biom10020332

Zwirner, J., Scholze, M., Waddell, J. N., Ondruschka, B., and Hammer, N. (2019). Mechanical properties of human dura mater in tension – an analysis at an age range of 2 to 94 years. *Sci. Rep.* 9, 16655. doi:10.1038/s41598-019-52836-9

frontiers | Frontiers in Physiology

TYPE Perspective
PUBLISHED 17 March 2023
DOI 10.3389/fphys.2023.1148414

OPEN ACCESS

EDITED BY
Noriaki Ono,
University of Texas Health Science Center at Houston, United States

REVIEWED BY
Daniel Lucas,
Cincinnati Children's Hospital Medical Center, United States

*CORRESPONDENCE
Helen C. O'Neill,
honeill@bond.edu.au

SPECIALTY SECTION
This article was submitted to Skeletal Physiology, a section of the journal Frontiers in Physiology

RECEIVED 20 January 2023
ACCEPTED 10 March 2023
PUBLISHED 17 March 2023

CITATION
O'Neill HC and Lim HK (2023), Skeletal stem/progenitor cells provide the niche for extramedullary hematopoiesis in spleen.
Front. Physiol. 14:1148414.
doi: 10.3389/fphys.2023.1148414

Skeletal stem/progenitor cells provide the niche for extramedullary hematopoiesis in spleen

Helen C. O'Neill* and Hong Kiat Lim

Clem Jones Centre for Regenerative Medicine, Bond University, Gold Coast, QLD, Australia

In bone marrow, the niche which supports hematopoiesis and nurtures hematopoietic stem cells (HSCs) contains perivascular reticular cells representing a subset of skeletal stem/progenitor cells (SSPCs). These stromal cells which provide the niche are lost or become inadequate during stress, disease or ageing, such that HSCs leave bone marrow and enter spleen and other peripheral sites to initiate extramedullary hematopoiesis and particularly myelopoiesis. Spleen also maintains niches for HSCs under steady-state conditions, evident since neonatal and adult spleen contain HSCs in low number and provide low-level hematopoiesis. In spleen, HSCs are found in the sinusoidal-rich red pulp region also in the vicinity of perivascular reticular cells. These cells resemble to some extent the known stromal elements reflecting HSC niches in bone marrow, and are investigated here for their characteristics as a subset of SSPCs. The isolation of spleen stromal subsets and the generation of cell lines which support HSCs and myelopoiesis *in vitro* has led to the identification of perivascular reticular cells which are unique to spleen. Analysis of gene and marker expression, as well as differentiative potential, identifies an osteoprogenitor cell type, reflective of one of several subsets of SSPCs described previously in bone, bone marrow and adipose tissue. The combined information supports a model for HSC niches in spleen involving perivascular reticular cells as SSPCs having osteogenic, stroma-forming capacity. These associate with sinusoids in red pulp to form niches for HSCs and to support the differentiation of hematopoietic progenitors during extramedullary hematopoiesis.

KEYWORDS

skeletal stem/progenitor cells, stromal cells, extramedullary hematopoiesis, hematopoietic niche, spleen

Introduction

Mesenchymal or skeletal stem and progenitor cells have now been described in many tissue sites including bone and bone marrow (Chan et al., 2009; Lv et al., 2014), and also within the vasculature of many tissues including kidney, heart and adipose tissue (Craig et al., 2022). The definitive skeletal stem cell was recently isolated from growth plates of adult and fetal bone of humans and mice, and has osteogenic, chondrogenic and stroma forming capacity (Chan et al., 2015; Chan et al., 2018). The classification of skeletal stem/progenitor cells (SSPCs) now replaces the spurious 'mesenchymal stem cells' commonly isolated as fibroblast-like cells which grow out of cultures of bone marrow (Pittenger et al., 1999; Pittenger et al., 2019). While early studies showed that culture-derived mesenchymal

precursors could form stroma which support hematopoietic stem cell (HSC) maintenance (Calvi et al., 2003; Zhang et al., 2003), more recent studies confirm an important role for these cells in the formation and regulation of HSC niches and hematopoiesis in bone marrow (Comazzetto et al., 2021). Distinct subsets of perivascular reticular cells in bone marrow have now been described as important stromal elements of the HSC niche which supports hematopoiesis (Sacchetti et al., 2007; Corselli et al., 2013; Crane et al., 2017). More recent identification of subsets of SSPCs now confirms a heterogeneity of subsets isolatable from either the skeletal growth plate (Chan et al., 2015; Chan et al., 2018), or as bone marrow subsets of skeletal progenitors (Zhou et al., 2014; Baccin et al., 2020; Tournaire et al., 2020; Matsushita et al., 2021; Shen et al., 2021), and also within the pericyte and adventitial cell populations that surround blood vessels in vascularised tissues (Sacchetti et al., 2016; Wang et al., 2020; Xu et al., 2021; Craig et al., 2022). It is therefore of interest to determine whether the same SSPCs reside in bone and bone marrow as in other tissue sites, and whether their role in supporting hematopoiesis is restricted to bone marrow or is a feature of many tissue sites. A recent study has identified distinct bone-forming capacity of SSPCs located in bone marrow as opposed to periosteum (Jeffery et al., 2022). Periosteal SSPCs contribute to only transient formation of trabecular bone at fracture sites, but regenerate stromal cells expressing hematopoietic niche factors (Jeffery et al., 2022). Their important role in HSC niche formation, suggests a tight linkage between the mesenchymal and hematopoietic systems at the level of stem cell maintenance.

While bone marrow is the main site for hematopoiesis in adults, increasing evidence points to a role for spleen in the maintenance and differentiation of HSCs. Analysis of HSC niches in spleen and delineation of the mechanisms by which they regulate hematopoiesis, is important in terms of utilisation of spleen as an alternate site for hematopoiesis when bone marrow is compromised by disease or ageing. A history of work from this lab has considered the potential for re-engineering HSC niches in spleen in order to increase hematopoietic cell production (Tan and Watanabe, 2017; O'Neill et al., 2019). If unique stromal cells can be isolated and used to expand HSCs *in vitro*, or provided as an ectopic niche for the same purpose *in vivo*, then the potential exists to enhance hematopoiesis. This article investigates the stromal cells which support hematopoiesis in spleen, and the evidence that perivascular reticular cells which provide the niche for HSCs are reflective of a subset of mesenchymal SSPCs. Regeneration or expansion of HSC niches could represent future therapy for patients undergoing HSC transplantation, myeloablative treatment or involution of lymphoid tissue with ageing. It is therefore important to fully characterise SSPCs in spleen, their growth and differentiative capacity, and the mechanisms by which they support the maintenance of HSCs.

The hematopoietic stem cell niche

Schofield introduced the concept of the hematopoietic 'niche' in the 1970s after observing that once HSCs were removed from the bone marrow microenvironment they quickly lost capacity to self-renew and to reconstitute the hematopoietic system (Schofield, 1978). The 'niche' is now described as a microenvironment comprising non-hematopoietic stromal cells, extracellular matrix and soluble regulatory factors that contribute to stem cell dormancy, quiescence, self-renewal and differentiation, so regulating the fate of HSCs (Crane et al., 2017; Comazzetto et al., 2021; Sánchez-Lanzas et al., 2022). Over time, three main stromal cell types were found to contribute to the HSC niche in bone marrow, namely, endosteal, vascular and perivascular cells (Kiel and Morrison, 2008; Bianco, 2011; Nagasawa et al., 2011; Corselli et al., 2013). It is now clear that interconnected cellular microenvironments provide the niche for HSCs in adult tissue. HSC in bone marrow have been associated most commonly with sinusoidal blood vessels, less commonly with arterioles, with only small numbers of primitive HSCs associated with the endosteum of bone (Crane et al., 2017). HSCs in the vicinity of the vasculature associate with reticular stromal cells which provide CXCL12 for HSC maintenance (Sugiyama et al., 2006a; Ding et al., 2012; Greenbaum et al., 2013). A dichotomy of periarteriolar and perisinusoidal reticular cells (Kunisaki et al., 2013; Acar et al., 2015) along with endothelial cells provide a source of stem cell factor (SCF) for HSC proliferation (Ding et al., 2012; Greenbaum et al., 2013). Current data no longer supports a periarteriolar niche for quiescent HSC (Kokkaliaris et al., 2020), although HSC dependent on periarteriolar niches have been reported during postnatal development (Isern et al., 2014; Asada et al., 2017a). Recent modelling identifies the motility of HSC within the bone marrow niche (Upadhaya et al., 2020), and the close proximity of HSC to a multitude of cell types (Gomariz et al., 2018).

A role for osteoblastic cells in HSC maintenance in bone marrow was first demonstrated in studies varying the number of these cells experimentally (Calvi et al., 2003). Constitutive expression of an active form of parathyroid hormone (PTH) or the PTH-related protein receptor (PPR) gave a marked increase in both the number of osteoblastic cells and the number of HSCs (Calvi et al., 2003). Osteoblasts maintain HSCs through secretion of cytokines like angiopoietin-1 (ANGPT1), thrombopoietin (THPO) and osteopontin (SPP1) which bind to cell surface receptors on HSCs (Nilsson et al., 2005; Qian et al., 2007; Lilly et al., 2011). They also express Jagged 1 which engages with Notch receptors on HSCs, so inhibiting differentiation and enhancing HSC self-renewal (Calvi et al., 2003; Qian et al., 2007; Lilly et al., 2011). Similarly, *Spp1*$^{-/-}$ mice showed a marked increase in the number of HSCs cycling, consistent with osteopontin (SPP1) as an inhibitor of HSC proliferation (Nilsson et al., 2005). However, the direct involvement of osteoblastic cells was challenged when researchers failed to observe a change in HSC numbers after depletion of osteoblasts using ganciclovir treatment or biglycan deficiency (Visnjic et al., 2004; Kiel et al., 2007). *In vivo* imaging studies also revealed few HSCs in direct contact with bone cells (Lo Celso et al., 2009). A vascular niche was also described in the vicinity of blood vessels in bone marrow. This is associated with rapid mobilisation of HSCs into the bloodstream after administration of granulocyte colony stimulating factor (G-CSF) as a mobilising agent (Kiel et al., 2005). Vascular niches also function to support hematopoiesis during embryogenesis since HSCs self-renew and differentiate at a stage of foetal development when bone marrow cavities are not yet formed (Huber et al., 2004). The role of vascular endothelial cells as regulators of hematopoietic integrity was demonstrated by conditionally deleting the signalling molecule vascular endothelial growth factor receptor 2 (VEGFR2) in adult

Vegfr2$^{-/-}$ mice. This impeded development of sinusoidal endothelial cells after irradiation and prevented reconstitution of the hematopoietic system (Hooper et al., 2009).

Mesenchymal perivascular reticular cells expressing high levels of the chemokine CXCL12 have now been identified as probably the most important element of the HSC niche in bone marrow. Several subsets were first characterised and described variably as CXCL12-abundant reticular (CAR) cells (Sugiyama et al., 2006b), nestin^{+} mesenchymal stem cells (Mendez-Ferrer et al., 2010) and leptin receptor^{+} stromal cells (Ding et al., 2012). CAR cells in bone marrow were characterised as bipotent adipo-osteogenic progenitors, developing around sinusoids and maintaining HSCs in an undifferentiated state (Sugiyama et al., 2006b; Omatsu et al., 2010). Conditional ablation of CAR cells using transgenic mice with the diphtheria toxin receptor gene inserted into *Cxcl12* led to a reduction in both HSCs and myeloid differentiation (Omatsu et al., 2010). HSCs have also been localised to nestin^{+} mesenchymal stem cells situated near arterioles in bone marrow (Mendez-Ferrer et al., 2010). On conditional ablation of these cells from mice, HSC numbers decreased so indicating their importance in forming a perivascular niche in bone marrow (Mendez-Ferrer et al., 2010). Leptin receptor^{+} stromal cells expressing high levels of CXCL12 were identified as perivascular cells surrounding sinusoids. All three described subsets reflect an important source of SCF (Ding et al., 2012), a cytokine that signals the c-Kit tyrosine kinase receptor on hematopoietic stem/progenitor cells (McNiece and Briddell, 1995). Loss of the HSC pool in *Scf*$^{-/-}$ mice, highlights the importance of SCF produced by perivascular reticular cells in HSC maintenance (Ding et al., 2012). It is now however very clear that this population is heterogeneous and that several distinct cell types may exist each with distinct roles in hematopoiesis.

Many studies now support the identification of bone marrow stromal cells as subsets of perisinusoidal and periarteriolar stroma. The former commonly have adipogenic differentiative potential and form perisinusoidal niches for HSC, while periarteriolar stromal cells show osteogenic differentiative potential and increase in number upon mechanical stimulation or fracture of bone (Zhou et al., 2014; Baccin et al., 2020; Shen et al., 2021). Transcriptional profiling of bone marrow stromal cells has revealed considerable remodelling under stress which impacts hematopoietic output (Tikhonova et al., 2019), in particular skewing of cells towards adipogenesis. Recently a cell-based protein expression analysis of stromal cells in homeostatic bone marrow revealed 28 distinct subsets of cells of which 14 expressed regulators of hematopoiesis (Severe). Most subsets were sensitive to irradiation conditioning used for HSC transplantation, except some CD73-expressing stromal cells which express factors which enable HSC engraftment (Severe et al. (2019).

The spleen in hematopoiesis

A hematopoietic role for spleen was first indicated by early evidence documenting survival of lethally irradiated mice where the spleen had been shielded with lead (Rugh and Grupp, 1960). We now understand that during adult life, spleen undergoes extramedullary hematopoiesis at times of physiological stress or infection (Kim, 2010), or when bone marrow is compromised through disease or damage (Yamamoto et al., 2013). Movement of HSCs and hematopoietic progenitors between bone marrow, blood and spleen occurs with induction of pregnancy (Nakada et al., 2014), such that spleens of pregnant mice contain higher numbers of HSCs and also expanded HSC niches (Nakada et al., 2014; Inra et al., 2015). The peripheral blood of pregnant mice also contains increased numbers of HSCs, multipotential progenitors, and myeloid progenitors (He et al., 2009; Oguro et al., 2017). When G-CSF is used to mobilize HSCs out of bone marrow, into blood and then spleen (Morrison et al., 1997), migrating HSCs localise around the sinusoids in the splenic red pulp region (Kiel et al., 2005). This is also seen with blood loss and pregnancy (Inra et al., 2015).

Extramedullary hematopoiesis also occurs as a natural process during fetal development which is later activated during pregnancy, stress and infection (Kim, 2010). The active nature of the process is evident since the low number of HSCs present in murine spleen in the steady-state increases quickly following inflammation (Wolber et al., 2002; Massberg et al., 2007). Passive hematopoiesis also occurs in steady-state adult spleen or following bone marrow failure with ageing (Kim, 2010), and several species, including pigs, baboons and humans retain a low number of HSCs in spleen under resting or steady-state conditions (Dor et al., 2006; Tan and O'Neill, 2010). Moreover, in cell tracing experiments, spleen cells from resting neonatal and resting adult mice can provide hematopoietic reconstitution of lethally irradiated host mice following adoptive transfer (Tan and O'Neill, 2010). Evidence of a role for spleen in steady-state hematopoiesis raises question about splenic niches for HSCs and whether the same niche elements support the maintenance of HSCs in both the resting and inflammatory states.

The dynamic role of spleen in provisioning extramedullary hematopoiesis during stress relies on the rapid expansion of the stromal cells forming the niche (Kiel et al., 2005; Inra et al., 2015; Oda et al., 2018). HSC in spleen have been located in the red pulp region in the vicinity of sinusoids (Inra et al., 2015). Mesenchymal progenitor-like cells expressing Tlx1, a transcription factor for spleen organogenesis, have been described as essential elements of the HSC niche located in the red pulp region (Dear et al., 1995; Oda et al., 2018). Further studies by Inra et al. (2015) identified stromal cells which produce CXCL12 and SCF upon induction of extramedullary hematopoiesis. Tcf21, a marker unique to splenic stromal cells, was used to identify perisinusoidal reticular cells in red pulp proximal to HSC and producing SCF and CXCL12 (Oda et al., 2018). Conditional deletion of *Scf* from endothelial cells and of *Scf* and *Cxcl12* from *Tcf21*-expressing stroma, reduced extramedullary hematopoiesis in spleen without affecting hematopoiesis in bone marrow. Perisinusoidal reticular cells in spleen resemble bone marrow HSC niche elements through their expression of PDGFRα/β and the production of CXCL12 and SCF (Oda et al., 2018), but remain distinct through expression of *Tlx1* and *Tcf21*.

Hematopoietic support capacity of splenic stroma cells

A history of work in this lab has identified the capacity of specific splenic stromal cells to support hematopoiesis and particularly myelopoiesis *in vitro* (O'Neill et al., 2014). Despite the limitations of *in vitro* analyses using cell lines, the findings of those studies have

been highly reproducible over many years and reinforced by different experimental approaches. Long-term cultures of spleen were first shown to support continuous production of myeloid cells arising from progenitors maintained within culture (Ni and O'Neill, 1997; O'Neill et al., 2004). Cell production in cultures depended on a mesenchymal stromal cell layer which proliferated slowly and could be readily maintained (Despars et al., 2004; Despars and O'Neill, 2006a). In particular, stroma-dependent cultures of 6-day old murine spleen support the maintenance of small hematopoietic progenitors, and the continuous production of a distinct class of large, dendritic-like cells which have antigen presenting capacity (O'Neill et al., 2011; Periasamy et al., 2009; Ni and O'Neill, 1999; Periasamy et al., 2013). An original STX3 stromal line was isolated from one culture which had ceased support of myelopoiesis after multiple passages *in vitro* due to loss of progenitors (Ni and O'Neill, 1998). Interestingly, myelopoiesis was again supported when STX3 stroma was overlaid with lineage-depleted (Lin^-) cells derived from bone marrow which are highly enriched for HSCs and hematopoietic progenitors (Despars and O'Neill, 2006a). A series of studies on cell production identified production of a majority population of myeloid cells as large MHC-II^- dendritic-like cells (Periasamy and O'Neill, 2013; Tan et al., 2011). These cells are highly efficient in endocytosis and cross-presentation of antigen for $CD8^+$ T cell activation, but do not activate $CD4^+$ T cells as do cells of the common dendritic lineage (Periasamy and O'Neill, 2013; Tan et al., 2011). They represent a population of antigen presenting cells unique to spleen. The highly reproducible nature of cell production in long-term cultures and in co-cultures over splenic stroma, is supported by evidence for an *in vivo* equivalent antigen presenting cell subset in murine and human spleen (Hey and O'Neill, 2016).

In order to better characterise spleen stroma and how it supports myelopoiesis *in vitro*, STX3 was cloned to form multiple cloned cell lines (Despars and O'Neill, 2006a; Despars and O'Neill, 2006b). These included the 5G3 clone, as a supporter of *in vitro* hematopoiesis, and 3B5 as a non-supporter. The 5G3 clone supports production of $MHCII^-$ dendritic-like cells in a highly reproducible, contact-dependent manner similar to the parent line (Periasamy et al., 2009; Periasamy and O'Neill, 2013). Since co-cultures maintained long-term myelopoiesis, the possibility that they maintain self-renewing HSCs or hematopoietic progenitor cells, was investigated. Various progenitor subsets from bone marrow and spleen were sorted and tested for capacity to seed 5G3 stroma for myelopoiesis. When the $Flt3^-c\text{-}Kit^+Lin^-Sca\text{-}1^+$ subset of long-term HSC from bone marrow, and the $Flt3^+c\text{-}Kit^+Lin^-Sca\text{-}1^+$ subset of short-term HSC were overlaid on 5G3 stroma, production of $MHCII^-$ dendritic-like cells was supported (Petvises and O'Neill, 2014a). However, no production was observed in co-cultures overlaid with myeloid dendritic progenitors (MDPs) or common dendritic progenitors (CDPs). These unique spleen-derived dendritic-like cells must therefore derive from a lineage distinct from that of common dendritic cells, plasmacytoid dendritic cells or monocytes (Petvises and O'Neill, 2014b).

It is now clear that the progenitors which seed 5G3 splenic stroma for *in vitro* myelopoiesis reflect HSCs endogenous to spleen, and that the process of myelopoiesis reflects extramedullary hematopoiesis. During development, HSCs and hematopoietic progenitors first appear in murine spleen at embryonic day 18.5, while progenitors of common DC appear at 4 days after birth (Petvises and O'Neill, 2014c). This raises the possibility that hematopoietic progenitors in spleen are laid down during ontogeny, and that myelopoiesis in steady-state adult spleen can occur as an active process not dependent on inflammatory signalling. Hence, we tested whether *in vitro* hematopoiesis in 5G3 co-cultures was dependent on inflammation by assessing the importance of Toll-like receptor signalling to cell production (Periasamy et al., 2013). Co-cultures established with bone marrow progenitors derived from mutant $MyD88^{-/-}$ and $Trif^{-/-}$ mice, which lack the adapter proteins MyD88 and TRIF crucial for Toll-like receptor signalling, were found to be equivalent supporters of myelopoiesis with production of $MHCII^-$ dendritic-like cells. Myelopoiesis *in vitro* occurs independently of Toll-like receptor signalling and inflammation (Periasamy et al., 2013).

One model is that the splenic stromal microenvironment supports restricted and directed differentiation of endogenous hematopoietic progenitors to give antigen presenting cells unique to the spleen microenvironment. Indeed, studies to date on the *in vivo* tissue distribution of these cells confirms them to be a novel subset limited to spleen (Tan et al., 2011). Indeed, such an $MHCII^-$ antigen presenting cell type could be positioned to receive antigen entering spleen from blood for rapid induction of a CD8 T cell response to manage blood-borne infections or cancers. Antigen presentation by MHCII to CD4 T cells would not be desirable in this location due to high cytokines levels directly entering blood.

Characterisation of spleen stromal cell lines

Most information on the stromal cell contribution to spleen development and hematopoiesis comes from conditional deletion studies using mutant mice, combined with immunocytochemical identification of changes in cell and tissue composition. These indirect studies are highly informative, but the definition of stromal cell function needs to be supported by studies on isolated cells. The purification of stromal cells through cell dissociation is however fraught with difficulty and is limited by known marker expression. Early studies to isolate mesenchymal stem cells showed that culturing bone marrow stroma was sufficient to capture these rare cells amongst stroma which grew *in vitro* (Muraglia et al., 2000). Such stromal cell studies are rare for bone marrow and almost non-existent for spleen.

As a prelude to *ex vivo* characterisation of splenic stromal cells which support hematopoiesis, stromal cells lines were analysed for characteristics indicating their lineage origin. Cell surface phenotyping of several cloned lines including 5G3 and 3B5 showed expression of the CD105, CD29, CD90 and PDPN (gp38) markers of SSPCs, and the PDGFRA, CD106 and CD51 markers of perivascular reticular cells (O'Neill et al., 2019; Lim et al., 2018). Absence of CD31, CD54 and CD45 expression ruled out an endothelial or hematopoietic lineage origin. Transcriptome analysis of stromal lines confirmed the mesenchymal origin of cells and their resemblance to mesenchymal stem cells through expression of *Col1a1, Sca1, Pdpn, Cd164, Cd90, Cd29* and *Cd106* (O'Neill et al., 2019). High expression of genes like *Mmp3, Cxcl12, Pdgfrb, Pdgfra, Nkx2-5, Itgav* and *Scf* reflected perivascular reticular cells described in bone marrow (Ding et al., 2012), although absence of *Nes, Mcam, Lepr*

and *Nte5* expression distinguished them from their bone marrow counterparts (Ding et al., 2012; Asada et al., 2017b).

Production of CXCL12 and SCF by 5G3 stromal cells is consistent with their capacity to support hematopoiesis (Lim et al., 2018). Their important role in hematopoiesis was confirmed through addition of inhibitors of HSC signalling to co-cultures. Inhibitors for Notch and Wnt signalling pathways or inhibitors of SCF and CXCL12 receptor uptake, block *in vitro* cell differentiation of HSCs over 5G3 stroma (Lim et al., 2018). Expression of adhesion molecules like VCAM1 by stroma is also consistent with their interaction with HSCs expressing VLA-4, a signalling pathway which supports HSC maintenance and differentiation (Ulyanova et al., 2005; Martinez-Agosto et al., 2007; Castagnaro et al., 2013). Stroma also express SPP1 consistent with their role in hematopoiesis since SPP1 binding to CD44 on HSC maintains their quiescent state (Nilsson et al., 2005; Stier et al., 2005). In sum, our work shows that spleen contains stromal cells reflecting perivascular reticular cells and SSPCs which express receptors for signalling HSCs.

Identification of splenic stromal cells as osteoprogenitors

A collection of recent studies now identifies SSPCs as a heterogeneous population of multi-lineage progenitors with distinct differentiative capacity. The skeletal stem cell isolated from both fetal bone of mice and humans is multipotent with capacity to form osteoblasts, chondrocytes and stromal cells, but not adipocytes (Chan et al., 2013; Chan et al., 2015; Chan et al., 2018). Mesenchymal stem cells have been isolated from mouse bone marrow which also have osteo-chondrogenic differentiative capacity and these cells were also shown to support maintenance of cord blood-derived primitive HSC when stroma was grown *in vitro* (Matsuoka et al., 2015). A multitude of studies on bone marrow stromal cells which support hematopoiesis favour the existence of mesenchymal cells which are adipogenic and retain some osteogenic differentiative potential (Shen et al., 2008). In organs outside of bone and bone marrow such as adipose tissue, microvascular pericytes and adventitial perivascular cells are observed to include multi-lineage progenitors which are active in tissue turnover in response to pathological remodelling. SSPC subsets have been isolated as perivascular cells which exist in the tunica adventitia of arteries and veins (Xu et al., 2021), and several distinct populations were identified through marker expression. Of interest here are the PDGFRA-expressing cells which are distinct as SSPCs in that they have restricted osteogenic capacity (Wang et al., 2020), and thus differ from the SSPC subset dominant in bone which reflects a progenitor with osteogenic, chondrogenic and stroma-forming differentiative capacity (Chan et al., 2015; Chan et al., 2018).

Very few studies have been performed on spleen to identify any inherent SSPC subsets. However, the isolated spleen stromal lines 5G3 and 3B5 were found to resemble skeletal progenitors since they have osteogenic differentiative capacity when cultured under mineralisation conditions, but lacked capacity for chondrogenesis or adipogenesis (O'Neill et al., 2019). These stromal lines were also shown to express genes reflecting early osteogenic precursors like *Spp1, Col1a2, Mmp2, Bmp2, Cdh11* and *Fn*, although not genes of mature osteoblasts including *Sp7, Cbfa1, Alpl, Bglap2* and *Ibsp* (O'Neill et al., 2019). This evidence raises the hypothesis that spleen contains a unique perisinusoidal niche comprising stromal cells resembling osteoprogenitors that support extramedullary hematopoiesis. The unexpected finding of an osteoblastic progenitor cell in spleen suggests a specific subset of SSPCs with an important function in supporting HSCs and their differentiation in proximity to sinusoids in the red pulp.

Using information on the phenotype of splenic stromal cell lines which support hematopoiesis, we undertook a large project to identify and isolate multiple stromal fractions *ex vivo*, assess their phenotype, and to test their growth and hematopoietic support capacity. These same subsets were also tested for capacity to form a spleen stromal graft when transplanted under the kidney capsule. Since long-term stromal cultures were best established with neonatal 6-day spleens, neonatal tissues were used for cell isolation. Spleens were fractionated to remove red blood cells and hematopoietic cells, and then sorted on the basis of expression of markers for mesenchymal stem cells (CD29, PDPN, CD105, PDGFRA, CD90), endothelial cells (CD31, VCAM1), perivascular reticular cells (CD146, MAdCAM1) and mature spleen stromal cells (SCA1, CD51, ER-TR7) (Lim and O'Neill, 2019). On the basis of capacity to form a confluent monolayer of stromal cells by 28 days, only subsets expressing the CD29, PDPN, CD105, PDGFRA and CD90 markers of mesenchymal stem cells, or lacking the endothelial markers CD31 and VCAM1, formed confluent monolayers (Lim and O'Neill, 2019). Other fractionations based on mature stromal markers (SCA1, CD51, ER-TR7) or perivascular reticular cell markers (CD146, MAdCAM1) were less informative. Each of the cell lines which grew acquired the same phenotype after 28 days of culture, reflecting mesenchymal stem/progenitor cells as $SCA1^{+}$ $PDPN^{+}$ $CD51^{+}$ $CD105^{+}$ $PDGFRA^{+}$ $CD90^{+}$ $ER\text{-}TR7^{-}$ (Lim and O'Neill, 2019). Indeed, this outgrowth of a common mesenchymal cell type was demonstrated previously in culture of bone marrow stroma, with outgrowth of a common similar mesenchymal stem cell type (Muraglia et al., 2000).

Cell lines derived *in vitro* from 28-day cultures of spleen stromal fractions were also shown to support hematopoiesis when overlaid with hematopoietic stem/progenitor cells (Lim and O'Neill, 2019). Most established stroma supported the production of myeloid cells equivalent to those produced in control 5G3 stromal cultures, although cell production levels were lower and more variable. Several stromal subsets, including the $SCA1^{lo}CD90^{lo}CD105^{+}CD51^{+}CD140A^{+}$ and $SCA1^{lo}CD90^{-}CD105^{+}CD51^{lo}CD140A^{lo}$ cells, were identified to grow well and to produce monolayers which were strong supporters of myelopoiesis (Lim and O'Neill, 2019).

These same fractionated stromal subsets were also tested *in vivo* for capacity to form stromal grafts when transplanted under the kidney capsule. Previously it had been shown that spleen capsular tissue could engraft to form a spleen graft which became filled with hematopoietic cells from the host (Tan and Watanabe, 2014). Extensive experiments were performed using dissociated capsular tissue and fractionation of specific subsets based on marker expression. However, engraftment was found to be universally unsuccessful using dissociated and fractionated splenic stromal cells. Subsequent experiments involving engraftment of several long-term stromal lines into NOD/SCID host kidney were found to be successful (O'Neill et al., 2019). These stromal lines formed ectopic niches for hematopoiesis, evident specifically by the presence

of myeloid cells similar to those produced in *in vitro* co-cultures of hematopoietic progenitors above stroma, and because HSC could be detected within ectopic grafts (Adolfsson et al., 2005).

Conclusion and outlook

This report describes an SSPC subset in spleen which presents as perivascular reticular cells which support extramedullary hematopoiesis and specifically myelopoiesis. Extramedullary hematopoiesis is an important alternative pathway for hematopoiesis which occurs following stress, infection and bone marrow compromise. This perivascular stromal cell type plays an important role in remodelling of spleen and HSC niches after stress and with ageing and disease. It remains an important cell target for regenerative medicine to replace or amplify damaged niches. Indeed, ageing of SSPCs and the niche they provide for HSCs in bone marrow has been identified as a cause for decline or skewing of blood and bone lineages (Ambrosi et al., 2021).

Mesenchymal stromal cells which form HSC niches in spleen are distinct from those which form niches in bone marrow, raising questions around the equivalence of HSC subsets maintained in those organs and their hematopoietic contribution. Splenic stromal cells which form HSC niches reflect SSPC with osteogenic capacity and are associated with sinusoids in the red pulp region. They differ from the most common stromal subset of perisinusoidal stroma which supports HSC quiescence in bone marrow and which has adipogenic differentiative capacity. Splenic perisinusoidal reticular cells do not express the LepR and Nestin markers of stroma which form the HSC niche in bone marrow, and are distinct through expression of Tlx1 and Tcf21. Stromal niche elements in bone marrow and spleen express markers of mesenchymal progenitors and produce high levels of SCF and CXCL12.

As a secondary lymphoid organ, the spleen has remarkable capacity to undergo continuous remodelling of the stromal microenvironment to facilitate immune responses (Golub et al., 2018). Spleen also has remarkable regenerative capacity (Tan and Watanabe, 2014; Tan and Watanabe, 2017), such that spleen tissue fragments can be successfully grafted under murine kidney capsule for development of ectopic spleen tissue showing both red and white pulp formation and full hematopoietic reconstitution (Tan and Watanabe, 2014). Engraftment of stromal fractions isolated by enrichment based on cell surface markers has also led to identification of two cell types necessary for spleen regeneration. A spleen organiser cell was identified as an endothelial-like CD31$^+$MAdCAM-1$^+$ cell, and a second cell type was found to be a mesenchymal PDGFRβ$^+$ cell, consistent with the requirement of a mesenchymal stromal cell in formation of niches for HSCs (Tan and Watanabe, 2014; Tan and Watanabe, 2017; Deng et al., 2018). Indeed, the remarkable regenerative capacity of spleen could contribute to recovery of HSC niches following myeloablative damage. The effect of myeloablation or irradiation on splenic niches for HSCs is not well documented, despite common use of these procedures.

Data availability statement

The original contributions presented in the study are included in the article, further inquiries can be directed to the corresponding author.

Author contributions

All authors listed have made a substantial, direct, and intellectual contribution to the work and approved it for publication.

Funding

This work was supported by project grants to HO from the Australian Research Council (#DP13010307) and the National Health and Medical Research Foundation of Australia (#585443). HL was supported by an Australian National University Postgraduate Scholarship.

Conflict of interest

The authors declare that the research was conducted in the absence of any commercial or financial relationships that could be construed as a potential conflict of interest.

Publisher's note

References

Acar, M., Kocherlakota, K. S., Murphy, M. M., Peyer, J. G., Oguro, H., Inra, C. N., et al. (2015). Deep imaging of bone marrow shows non-dividing stem cells are mainly perisinusoidal. *Nature* 526 (7571), 126–130. doi:10.1038/nature15250

Adolfsson, J., Mansson, R., Buza-Vidas, N., Hultquist, A., Liuba, K., Jensen, C. T., et al. (2005). Identification of Flt3+ lympho-myeloid stem cells lacking erythro-megakaryocytic potential a revised road map for adult blood lineage commitment. *Cell* 121 (2), 295–306. doi:10.1016/j.cell.2005.02.013

Ambrosi, T. H., Marecic, O., McArdle, A., Sinha, R., Gulati, G. S., Tong, X., et al. (2021). Aged skeletal stem cells generate an inflammatory degenerative niche. *Nature* 597 (7875), 256–262. doi:10.1038/s41586-021-03795-7

Asada, N., Kunisaki, Y., Pierce, H., Wang, Z., Fernandez, N. F., Birbrair, A., et al. (2017). Differential cytokine contributions of perivascular haematopoietic stem cell niches. *Nat. Cell Biol.* 19 (3), 214–223. doi:10.1038/ncb3475

Asada, N., Takeishi, S., and Frenette, P. S. (2017). Complexity of bone marrow hematopoietic stem cell niche. *Int. J. Hematol.* 106 (1), 45–54. doi:10.1007/s12185-017-2262-9

Baccin, C., Al-Sabah, J., Velten, L., Helbling, P. M., Grünschläger, F., Hernández-Malmierca, P., et al. (2020). Combined single-cell and spatial transcriptomics reveal the molecular, cellular and spatial bone marrow niche organization. *Nat. Cell Biol.* 22 (1), 38–48. doi:10.1038/s41556-019-0439-6

Bianco, P. (2011). Bone and the hematopoietic niche: A tale of two stem cells. *Blood* 117 (20), 5281–5288. doi:10.1182/blood-2011-01-315069

Calvi, L. M., Adams, G. B., Weibrecht, K. W., Weber, J. M., Olson, D. P., Knight, M. C., et al. (2003). Osteoblastic cells regulate the haematopoietic stem cell niche. *Nature* 425 (6960), 841–846. doi:10.1038/nature02040

Castagnaro, L., Lenti, E., Maruzzelli, S., Spinardi, L., Migliori, E., Farinello, D., et al. (2013). Nkx2-5(+)islet1(+) mesenchymal precursors generate distinct spleen stromal cell subsets and participate in restoring stromal network integrity. *Immunity* 38 (4), 782–791. doi:10.1016/j.immuni.2012.12.005

Chan, C. K., Chen, C. C., Luppen, C. A., Kim, J. B., DeBoer, A. T., Wei, K., et al. (2009). Endochondral ossification is required for haematopoietic stem-cell niche formation. *Nature* 457 (7228), 490–494. doi:10.1038/nature07547

Chan, C. K. F., Gulati, G. S., Sinha, R., Tompkins, J. V., Lopez, M., Carter, A. C., et al. (2018). Identification of the human skeletal stem cell. *Cell* 175 (1), 43–56. doi:10.1016/j.cell.2018.07.029

Chan, C. K., Lindau, P., Jiang, W., Chen, J. Y., Zhang, L. F., Chen, C. C., et al. (2013). Clonal precursor of bone, cartilage, and hematopoietic niche stromal cells. *Proc. Natl. Acad. Sci. U. S. A.* 110 (31), 12643–12648. doi:10.1073/pnas.1310212110

Chan, C. K., Seo, E. Y., Chen, J. Y., Lo, D., McArdle, A., Sinha, R., et al. (2015). Identification and specification of the mouse skeletal stem cell. *Cell* 160 (1-2), 285–298. doi:10.1016/j.cell.2014.12.002

Comazzetto, S., Shen, B., and Morrison, S. J. (2021). Niches that regulate stem cells and hematopoiesis in adult bone marrow. *Dev. Cell* 56 (13), 1848–1860. doi:10.1016/j.devcel.2021.05.018

Corselli, M., Chin, C. J., Parekh, C., Sahaghian, A., Wang, W., Ge, S., et al. (2013). Perivascular support of human hematopoietic stem/progenitor cells. *Blood* 121 (15), 2891–2901. doi:10.1182/blood-2012-08-451864

Craig, D. J., James, A. W., Wang, Y., Tavian, M., Crisan, M., and Péault, B. M. (2022). Blood vessel resident human stem cells in Health and disease. *Stem Cells Transl. Med.* 11 (1), 35–43. doi:10.1093/stcltm/szab001

Crane, G. M., Jeffery, E., and Morrison, S. J. (2017). Adult haematopoietic stem cell niches. *Nat. Rev. Immunol.* 17 (9), 573–590. doi:10.1038/nri.2017.53

Dear, T. N., Colledge, W. H., Carlton, M. B., Lavenir, I., Larson, T., Smith, A. J., et al. (1995). The Hox11 gene is essential for cell survival during spleen development. *Development* 121 (9), 2909–2915. doi:10.1242/dev.121.9.2909

Deng, M., Luo, K., Hou, T., Luo, F., Xie, Z., Zhang, Z., et al. (2018). IGFBP3 deposited in the human umbilical cord mesenchymal stem cell-secreted extracellular matrix promotes bone formation. *J. Cell Physiol.* 233 (8), 5792–5804. doi:10.1002/jcp.26342

Despars, G., Ni, K., Bouchard, A., O'Neill, T. J., and O'Neill, H. C. (2004). Molecular definition of an *in vitro* niche for dendritic cell development. *Exp. Hematol.* 32 (12), 1182–1193. doi:10.1016/j.exphem.2004.08.013

Despars, G., and O'Neill, H. C. (2006). Heterogeneity amongst splenic stromal cell lines which support dendritic cell hematopoiesis. *vitro Cell. Dev. Biol. Animal* 42 (7), 208–215. doi:10.1290/0602016.1

Despars, G., and O'Neill, H. C. (2006). Splenic endothelial cell lines support development of dendritic cells from bone marrow. *Stem Cells* 24 (6), 1496–1504. doi:10.1634/stemcells.2005-0530

Ding, L., Saunders, T. L., Enikolopov, G., and Morrison, S. J. (2012). Endothelial and perivascular cells maintain haematopoietic stem cells. *Nature* 481 (7382), 457–462. doi:10.1038/nature10783

Dor, F. J., Ramirez, M. L., Parmar, K., Altman, E. L., Huang, C. A., Down, J. D., et al. (2006). Primitive hematopoietic cell populations reside in the spleen: Studies in the pig, baboon, and human. *Exp. Hematol.* 34 (11), 1573–1582. doi:10.1016/j.exphem.2006.06.016

Golub, R., Tan, J., Watanabe, T., and Brendolan, A. (2018). Origin and immunological functions of spleen stromal cells. *Trends Immunol.* 39 (6), 503–514. doi:10.1016/j.it.2018.02.007

Gomariz, A., Helbling, P. M., Isringhausen, S., Suessbier, U., Becker, A., Boss, A., et al. (2018). Quantitative spatial analysis of haematopoiesis-regulating stromal cells in the bone marrow microenvironment by 3D microscopy. *Nat. Commun.* 9 (1), 2532. doi:10.1038/s41467-018-04770-z

Greenbaum, A., Hsu, Y. M., Day, R. B., Schuettpelz, L. G., Christopher, M. J., Borgerding, J. N., et al. (2013). CXCL12 in early mesenchymal progenitors is required for haematopoietic stem-cell maintenance. *Nature* 495 (7440), 227–230. doi:10.1038/nature11926

O'Neill, H. C., Griffiths, K. L., Periasamy, P., Hinton, R. A., Hey, Y. Y., Tan, J. K. H., et al. (2011). Spleen as a site for hematopoiesis of a distinct antigen presenting cell type. *Stem Cells Int.*, 2011, 954275. doi:10.4061/2011/954275

He, S., Nakada, D., and Morrison, S. J. (2009). Mechanisms of stem cell self-renewal. *Annu. Rev. Cell Dev. Biol.* 25, 377–406. doi:10.1146/annurev.cellbio.042308.113248

Hey, Y. Y., and O'Neill, H. C. (2016). Antigen presenting properties of a myeloid dendritic-like cell in murine spleen. *PLOS ONE* 11 (9), e0162358. doi:10.1371/journal.pone.0162358

Hooper, A. T., Butler, J. M., Nolan, D. J., Kranz, A., Iida, K., Kobayashi, M., et al. (2009). Engraftment and reconstitution of hematopoiesis is dependent on VEGFR2-mediated regeneration of sinusoidal endothelial cells. *Cell Stem Cell* 4 (3), 263–274. doi:10.1016/j.stem.2009.01.006

Huber, T. L., Kouskoff, V., Joerg Fehling, H., Palis, J., and Keller, G. (2004). Haemangioblast commitment is initiated in the primitive streak of the mouse embryo. *Nature* 432 (7017), 625–630. doi:10.1038/nature03122

Inra, C. N., Zhou, B. O., Acar, M., Murphy, M. M., Richardson, J., Zhao, Z., et al. (2015). A perisinusoidal niche for extramedullary haematopoiesis in the spleen. *Nature* 527 (7579), 466–471. doi:10.1038/nature15530

Isern, J., García-García, A., Martín, A. M., Arranz, L., Martín-Pérez, D., Torroja, C., et al. (2014). The neural crest is a source of mesenchymal stem cells with specialized hematopoietic stem cell niche function. *Elife* 3, e03696. doi:10.7554/eLife.03696

Jeffery, E. C., Mann, T. L. A., Pool, J. A., Zhao, Z., and Morrison, S. J. (2022). Bone marrow and periosteal skeletal stem/progenitor cells make distinct contributions to bone maintenance and repair. *Cell Stem Cell* 29 (11), 1547–1561.e6. doi:10.1016/j.stem.2022.10.002

Kiel, M. J., and Morrison, S. J. (2008). Uncertainty in the niches that maintain haematopoietic stem cells. *Nat. Rev. Immunol.* 8 (4), 290–301. doi:10.1038/nri2279

Kiel, M. J., Radice, G. L., and Morrison, S. J. (2007). Lack of evidence that hematopoietic stem cells depend on N-cadherin-mediated adhesion to osteoblasts for their maintenance. *Cell Stem Cell* 1 (2), 204–217. doi:10.1016/j.stem.2007.06.001

Kiel, M. J., Yilmaz, O. H., Iwashita, T., Yilmaz, O. H., Terhorst, C., and Morrison, S. J. (2005). SLAM family receptors distinguish hematopoietic stem and progenitor cells and reveal endothelial niches for stem cells. *Cell* 121 (7), 1109–1121. doi:10.1016/j.cell.2005.05.026

Kim, C. H. (2010). Homeostatic and pathogenic extramedullary hematopoiesis. *J. Blood Med.* 1, 13–19. doi:10.2147/JBM.S7224

Kokkaliaris, K. D., Kunz, L., Cabezas-Wallscheid, N., Christodoulou, C., Renders, S., Camargo, F., et al. (2020). Adult blood stem cell localization reflects the abundance of reported bone marrow niche cell types and their combinations. *Blood* 136 (20), 2296–2307. doi:10.1182/blood.2020006574

Kunisaki, Y., Bruns, I., Scheiermann, C., Ahmed, J., Pinho, S., Zhang, D., et al. (2013). Arteriolar niches maintain haematopoietic stem cell quiescence. *Nature* 502 (7473), 637–643. doi:10.1038/nature12612

Lilly, A. J., Johnson, W. E., and Bunce, C. M. (2011). The haematopoietic stem cell niche: New insights into the mechanisms regulating haematopoietic stem cell behaviour. *Stem Cells Int.* 2011, 274564. doi:10.4061/2011/274564

Lim, H. K., and O'Neill, H. C. (2019). Identification of stromal cells in spleen which support myelopoiesis. *Front. Cell Dev. Biol.* 7, 1. doi:10.3389/fcell.2019.00001

Lim, H. K., Periasamy, P., and O'Neill, H. C. (2018). *In vitro* murine hematopoiesis supported by signaling from a splenic stromal cell line. *Stem Cells Int.*, 2018, 9896142. doi:10.1155/2018/9896142

Lo Celso, C., Fleming, H. E., Wu, J. W., Zhao, C. X., Miake-Lye, S., Fujisaki, J., et al. (2009). Live-animal tracking of individual haematopoietic stem/progenitor cells in their niche. *Nature* 457 (7225), 92–96. doi:10.1038/nature07434

Lv, F. J., Tuan, R. S., Cheung, K. M., and Leung, V. Y. (2014). Concise review: The surface markers and identity of human mesenchymal stem cells. *Stem Cells* 32 (6), 1408–1419. doi:10.1002/stem.1681

Martinez-Agosto, J. A., Mikkola, H. K. A., Hartenstein, V., and Banerjee, U. (2007). The hematopoietic stem cell and its niche: A comparative view. *Genes Dev.* 21, 3044–3060. doi:10.1101/gad.1602607

Massberg, S., Schaerli, P., Knezevic-Maramica, I., Köllnberger, M., Tubo, N., Moseman, E. A., et al. (2007). Immunosurveillance by hematopoietic progenitor cells trafficking through blood, lymph, and peripheral tissues. *Cell* 131 (5), 994–1008. doi:10.1016/j.cell.2007.09.047

Matsuoka, Y., Nakatsuka, R., Sumide, K., Kawamura, H., Takahashi, M., Fujioka, T., et al. (2015). Prospectively isolated human bone marrow cell-derived MSCs support primitive human CD34-negative hematopoietic stem cells. *Stem Cells* 33 (5), 1554–1565. doi:10.1002/stem.1941

Matsushita, Y., Ono, W., and Ono, N. (2021). Bone regeneration via skeletal cell lineage plasticity: All hands mobilized for emergencies: Quiescent mature skeletal cells can be activated in response to injury and robustly participate in bone regeneration through cellular plasticity. *Bioessays* 43 (1), e2000202. doi:10.1002/bies.202000202

McNiece, I. K., and Briddell, R. A. (1995). Stem cell factor. *J. Leukoc. Biol.* 58 (1), 14–22. doi:10.1002/jlb.58.1.14

Mendez-Ferrer, S., Michurina, T. V., Ferraro, F., Mazloom, A. R., MacArthur, B. D., Lira, S. A., et al. (2010). Mesenchymal and haematopoietic stem cells form a unique bone marrow niche. *Nature* 466 (7308), 829–834. doi:10.1038/nature09262

Morrison, S. J., Wright, D. E., and Weissman, I. L. (1997). Cyclophosphamide/granulocyte colony-stimulating factor induces hematopoietic stem cells to proliferate prior to mobilization. *Proc. Natl. Acad. Sci.* 94 (5), 1908–1913. doi:10.1073/pnas.94.5.1908

Muraglia, A., Cancedda, R., and Quarto, R. (2000). Clonal mesenchymal progenitors from human bone marrow differentiate *in vitro* according to a hierarchical model. *J. Cell Sci.* 113 (7), 1161–1166. doi:10.1242/jcs.113.7.1161

Nagasawa, T., Omatsu, Y., and Sugiyama, T. (2011). Control of hematopoietic stem cells by the bone marrow stromal niche: The role of reticular cells. *Trends Immunol.* 32 (7), 315–320. doi:10.1016/j.it.2011.03.009

Nakada, D., Oguro, H., Levi, B. P., Ryan, N., Kitano, A., Saitoh, Y., et al. (2014). Oestrogen increases haematopoietic stem-cell self-renewal in females and during pregnancy. *Nature* 505 (7484), 555–558. doi:10.1038/nature12932

Ni, K., and O'Neill, H. C. (1998). Hemopoiesis in long-term stroma-dependent cultures from lymphoid tissue: Production of cells with myeloid/dendritic characteristics. *Vitro Cell Dev. Biol. Anim.* 34 (4), 298–307. doi:10.1007/s11626-998-0006-0

Ni, K., and O'Neill, H. C. (1997). Long-term stromal cultures produce dendritic-like cells. *Br. J. Haematol.* 97 (4), 710–725. doi:10.1046/j.1365-2141.1997.00135.x

Ni, K., and O'Neill, H. (1999). Spleen stromal cells support haemopoiesis and *in vitro* growth of dendritic cells from bone marrow. *Br. J. Haematol.* 105 (1), 58–67. doi:10.1111/j.1365-2141.1999.01294.x

Nilsson, S. K., Johnston, H. M., Whitty, G. A., Williams, B., Webb, R. J., Denhardt, D. T., et al. (2005). Osteopontin, a key component of the hematopoietic stem cell niche and regulator of primitive hematopoietic progenitor cells. *Blood* 106 (4), 1232–1239. doi:10.1182/blood-2004-11-4422

O'Neill, H. C., Griffiths, K. L., Periasamy, P., Hinton, R. A., Petvises, S., Hey, Y. Y., et al. (2014). Spleen stroma maintains progenitors and supports long-term hematopoiesis. *Curr. Stem Cell Res. Ther.* 9 (4), 354–363. doi:10.2174/1574888x09666140421115836

O'Neill, H. C., Lim, H. K., Periasamy, P., Kumarappan, L., Tan, J. K. H., and O'Neill, T. J. (2019). Transplanted spleen stromal cells with osteogenic potential support ectopic myelopoiesis. *PLoS One* 14 (10), e0223416. doi:10.1371/journal.pone.0223416

O'Neill, H. C., Wilson, H. L., Quah, B., Abbey, J. L., Despars, G., and Ni, K. (2004). Dendritic cell development in long-term spleen stromal cultures. *Stem Cells* 22 (4), 475–486. [pii]. doi:10.1634/stemcells.22-4-475

Oda, A., Tezuka, T., Ueno, Y., Hosoda, S., Amemiya, Y., Notsu, C., et al. (2018). Niche-induced extramedullary hematopoiesis in the spleen is regulated by the transcription factor Tlx1. *Sci. Rep.* 8 (1), 8308. doi:10.1038/s41598-018-26693-x

Oguro, H., McDonald, J. G., Zhao, Z., Umetani, M., Shaul, P. W., and Morrison, S. J. (2017). 27-Hydroxycholesterol induces hematopoietic stem cell mobilization and extramedullary hematopoiesis during pregnancy. *J. Clin. Invest.* 127 (9), 3392–3401. doi:10.1172/JCI94027

Omatsu, Y., Sugiyama, T., Kohara, H., Kondoh, G., Fujii, N., Kohno, K., et al. (2010). The essential functions of adipo-osteogenic progenitors as the hematopoietic stem and progenitor cell niche. *Immunity* 33 (3), 387–399. doi:10.1016/j.immuni.2010.08.017

Periasamy, P., and O'Neill, H. C. (2013). Stroma-dependent development of two dendritic-like cell types with distinct antigen presenting capability. *Exp. Hematol.* 41 (3), 281–292. doi:10.1016/j.exphem.2012.11.003

Periasamy, P., Petvises, S., and O'Neill, H. C. (2013). Development of two distinct dendritic-like APCs in the context of splenic stroma. *Front. Immunol.* 4, 73. doi:10.3389/fimmu.2013.00073

Periasamy, P., Tan, J. K. H., Griffiths, K. L., and O' Neill, H. C. (2009). Splenic stromal niches support hematopoiesis of dendritic-like cells from precursors in bone marrow and spleen. *Exp. Hematol.* 37 (9), 1060–1071. doi:10.1016/j.exphem.2009.06.001

Petvises, S., and O'Neill, H. C. (2014). Characterisation of dendritic cells arising from progenitors endogenous to murine spleen. *PLoS One* 9 (2), e88311. doi:10.1371/journal.pone.0088311

Petvises, S., and O'Neill, H. C. (2014). Distinct progenitor origin distinguishes a lineage of dendritic-like cells in spleen. *Front. Immunol.* 4, 501. doi:10.3389/fimmu.2013.00501

Petvises, S., and O'Neill, H. C. (2014). Distinct progenitor origin distinguishes a lineage of dendritic-like cells in spleen. *Front. Immunol.* 4, 501. doi:10.3389/fimmu.2013.00501

Pittenger, M. F., Discher, D. E., Péault, B. M., Phinney, D. G., Hare, J. M., and Caplan, A. I. (2019). Mesenchymal stem cell perspective: Cell biology to clinical progress. *NPJ Regen. Med.* 4, 22. doi:10.1038/s41536-019-0083-6

Pittenger, M. F., Mackay, A. M., Beck, S. C., Jaiswal, R. K., Douglas, R., Mosca, J. D., et al. (1999). Multilineage potential of adult human mesenchymal stem cells. *Science* 284, 143–147. doi:10.1126/science.284.5411.143

Qian, H., Buza-Vidas, N., Hyland, C. D., Jensen, C. T., Antonchuk, J., Mansson, R., et al. (2007). Critical role of thrombopoietin in maintaining adult quiescent hematopoietic stem cells. *Cell Stem Cell* 1 (6), 671–684. doi:10.1016/j.stem.2007.10.008

Rugh, R., and Grupp, E. (1960). Splenic radioprotective agent: Particulate or diffusible? *Radiat. Res.* 13 (5), 657–660. doi:10.2307/3571028

Sacchetti, B., Funari, A., Michienzi, S., Di Cesare, S., Piersanti, S., Saggio, I., et al. (2007). Self-renewing osteoprogenitors in bone marrow sinusoids can organize a hematopoietic microenvironment. *Cell* 131 (2), 324–336. doi:10.1016/j.cell.2007.08.025

Sacchetti, B., Funari, A., Remoli, C., Giannicola, G., Kogler, G., Liedtke, S., et al. (2016). No identical "mesenchymal stem cells" at different times and sites: Human committed progenitors of distinct origin and differentiation potential are incorporated as adventitial cells in microvessels. *Stem Cell Rep.* 6 (6), 897–913. doi:10.1016/j.stemcr.2016.05.011

Sánchez-Lanzas, R., Kalampalika, F., and Ganuza, M. (2022). Diversity in the bone marrow niche: Classic and novel strategies to uncover niche composition. *Br. J. Haematol.* 199 (5), 647–664. doi:10.1111/bjh.18355

Schofield, R. (1978). The relationship between the spleen colony-forming cell and the haemopoietic stem cell. *Blood Cells* 4 (1-2), 7–25.

Severe, N., Karabacak, N. M., Gustafsson, K., Baryawno, N., Courties, G., Kfoury, Y., et al. (2019). Stress-Induced changes in bone marrow stromal cell populations revealed through single-cell protein expression mapping. *Cell Stem Cell* 25 (4), 570–583. doi:10.1016/j.stem.2019.06.003

Shen, B., Tasdogan, A., Ubellacker, J. M., Zhang, J., Nosyreva, E. D., Du, L., et al. (2021). A mechanosensitive peri-arteriolar niche for osteogenesis and lymphopoiesis. *Nature* 591 (7850), 438–444. doi:10.1038/s41586-021-03298-5

Shen, H., Tesar, B. M., Walker, W. E., and Goldstein, D. R. (2008). Dual signaling of MyD88 and TRIF is critical for maximal TLR4-induced dendritic cell maturation. *J. Immunol.* 181 (3), 1849–1858. doi:10.4049/jimmunol.181.3.1849

Stier, S., Ko, Y., Forkert, F., Lutz, C., Neuhaus, T., Grunewald, E., et al. (2005). Osteopontin is a hematopoietic stem cell niche component that negatively regulates stem cell pool size. *J. Exp. Med.*, 201(11), 1781–1791. doi:10.1084/Jem.20041992

Sugiyama, T., Kohara, H., Noda, M., and Nagasawa, T. (2006). Maintenance of the hematopoietic stem cell pool by CXCL12-CXCR4 chemokine signaling in bone marrow stromal cell niches. *Immunity* 25, 977–988. doi:10.1016/j.immuni.2006.10.016

Sugiyama, T., Kohara, H., Noda, M., and Nagasawa, T. (2006). Maintenance of the hematopoietic stem cell pool by CXCL12-CXCR4 chemokine signaling in bone marrow stromal cell niches. *Immunity* 25 (6), 977–988. doi:10.1016/j.immuni.2006.10.016

Tan, J. K., and O'Neill, H. C. (2010). Investigation of murine spleen as a niche for hematopoiesis. *Transplantation* 89 (2), 140–145. doi:10.1097/TP.0b013e3181c42f70

Tan, J. K., Quah, B. J., Griffiths, K. L., Periasamy, P., Hey, Y. Y., and O'Neill, H. C. (2011). Identification of a novel antigen cross-presenting cell type in spleen. *J. Cell Mol. Med.* 15 (5), 1189–1199. doi:10.1111/j.1582-4934.2010.01089.x

Tan, J. K., and Watanabe, T. (2014). Murine spleen tissue regeneration from neonatal spleen capsule requires lymphotoxin priming of stromal cells. *J. Immunol.* 193 (3), 1194–1203. doi:10.4049/jimmunol.1302115

Tan, J. K., and Watanabe, T. (2017). Stromal cell subsets directing neonatal spleen regeneration. *Sci. Rep.* 7, 40401. doi:10.1038/srep40401

Tikhonova, A. N., Dolgalev, I., Hu, H., Sivaraj, K. K., Hoxha, E., Cuesta-Domínguez, Á., et al. (2019). The bone marrow microenvironment at single-cell resolution. *Nature* 569 (7755), 222–228. doi:10.1038/s41586-019-1104-8

Tournaire, G., Stegen, S., Giacomini, G., Stockmans, I., Moermans, K., Carmeliet, G., et al. (2020). Nestin-GFP transgene labels skeletal progenitors in the periosteum. *Bone* 133, 115259. doi:10.1016/j.bone.2020.115259

Ulyanova, T., Scott, L. M., Priestley, G. V., Jiang, Y., Nakamoto, B., Koni, P. A., et al. (2005). VCAM-1 expression in adult hematopoietic and nonhematopoietic cells is controlled by tissue-inductive signals and reflects their developmental origin. *Blood* 106 (1), 86–94. doi:10.1182/blood-2004-09-3417

Upadhaya, S., Krichevsky, O., Akhmetzyanova, I., Sawai, C. M., Fooksman, D. R., and Reizis, B. (2020). Intravital imaging reveals motility of adult hematopoietic stem cells in the bone marrow niche. *Cell Stem Cell* 27 (2), 336–345. doi:10.1016/j.stem.2020.06.003

Visnjic, D., Kalajzic, Z., Rowe, D. W., Katavic, V., Lorenzo, J., and Aguila, H. L. (2004). Hematopoiesis is severely altered in mice with an induced osteoblast deficiency. *Blood* 103 (9), 3258–3264. doi:10.1182/blood-2003-11-4011

Wang, Y., Xu, J., Meyers, C. A., Gao, Y., Tian, Y., Broderick, K., et al. (2020). PDGFRα marks distinct perivascular populations with different osteogenic potential within adipose tissue. *Stem Cells* 38 (2), 276–290. doi:10.1002/stem.3108

Wolber, F. M., Leonard, E., Michael, S., Orschell-Traycoff, C. M., Yoder, M. C., and Srour, E. F. (2002). Roles of spleen and liver in development of the murine hematopoietic system. *Exp. Hematol.* 30 (9), 1010–1019. S0301472X02008810 [pii]. doi:10.1016/s0301-472x(02)00881-0

Xu, J., Wang, Y., Gomez-Salazar, M. A., Hsu, G. C., Negri, S., Li, Z., et al. (2021). Bone-forming perivascular cells: Cellular heterogeneity and use for tissue repair. *Stem Cells* 39 (11), 1427–1434. doi:10.1002/stem.3436

Yamamoto, R., Morita, Y., Ooehara, J., Hamanaka, S., Onodera, M., Rudolph, K. L., et al. (2013). Clonal analysis unveils self-renewing lineage-restricted progenitors generated directly from hematopoietic stem cells. *Cell* 154 (5), 1112–1126. doi:10.1016/j.cell.2013.08.007

Zhang, J., Niu, C., Ye, L., Huang, H., He, X., Tong, W. G., et al. (2003). Identification of the haematopoietic stem cell niche and control of the niche size. *Nature* 425 (6960), 836–841. doi:10.1038/nature02041

Zhou, B. O., Yue, R., Murphy, M. M., Peyer, J. G., and Morrison, S. J. (2014). Leptin-receptor-expressing mesenchymal stromal cells represent the main source of bone formed by adult bone marrow. *Cell Stem Cell* 15 (2), 154–168. doi:10.1016/j.stem.2014.06.008

frontiers | Frontiers in Physiology

TYPE Original Research
PUBLISHED 30 March 2023
DOI 10.3389/fphys.2023.1145763

OPEN ACCESS

EDITED BY
Celine Colnot,
Institut National de la Santé et de la Recherche Medicale, INSERM U955, France

REVIEWED BY
Noriaki Ono,
University of Texas Health Science Center at Houston, United States
Brya Matthews,
The University of Auckland, New Zealand

*CORRESPONDENCE
Yuji Mishina,
mishina@umich.edu

SPECIALTY SECTION
This article was submitted to Skeletal Physiology, a section of the journal Frontiers in Physiology

RECEIVED 16 January 2023
ACCEPTED 21 March 2023
PUBLISHED 30 March 2023

CITATION
Omi M, Koneru T, Lyu Y, Haraguchi A, Kamiya N and Mishina Y (2023), Increased BMP-Smad signaling does not affect net bone mass in long bones.
Front. Physiol. 14:1145763.
doi: 10.3389/fphys.2023.1145763

Increased BMP-Smad signaling does not affect net bone mass in long bones

Maiko Omi[1], Tejaswi Koneru[1], Yishan Lyu[1], Ai Haraguchi[1], Nobuhiro Kamiya[2] and Yuji Mishina[1]*

[1]Department of Biologic and Materials Sciences and Prosthodontics, University of Michigan School of Dentistry, Ann Arbor, MI, United States, [2]Department of Budo and Sport Studies, Faculty of Budo and Sport Studies, Tenri University, Nara, Japan

Bone morphogenetic proteins (BMPs) have been used for orthopedic and dental application due to their osteoinductive properties; however, substantial numbers of adverse reactions such as heterotopic bone formation, increased bone resorption and greater cancer risk have been reported. Since bone morphogenetic proteins signaling exerts pleiotropic effects on various tissues, it is crucial to understand tissue-specific and context-dependent functions of bone morphogenetic proteins. We previously reported that loss-of-function of bone morphogenetic proteins receptor type IA (BMPR1A) in osteoblasts leads to more bone mass in mice partly due to inhibition of bone resorption, indicating that bone morphogenetic protein signaling in osteoblasts promotes osteoclast function. On the other hand, hemizygous constitutively active (ca) mutations for BMPR1A (*caBmpr1a*$^{wt/+}$) in osteoblasts result in higher bone morphogenetic protein signaling activity and no overt skeletal changes in adult mice. Here, we further bred mice for heterozygous null for *Bmpr1a* (*Bmpr1a*$^{+/-}$) and homozygous mutations of *caBmpr1a* (*caBmpr1a*$^{+/+}$) crossed with *Osterix*-Cre transgenic mice to understand how differences in the levels of bone morphogenetic protein signaling activity specifically in osteoblasts contribute to bone phenotype. We found that *Bmpr1a*$^{+/-}$, *caBmpr1a*$^{wt/+}$ and *caBmpr1a*$^{+/+}$ mice at 3 months of age showed no overt bone phenotypes in tibiae compared to controls by micro-CT and histological analysis although BMP-Smad signaling is increased in both *caBmpr1a*$^{wt/+}$ and *caBmpr1a*$^{+/+}$ tibiae and decreased in the *Bmpr1a*$^{+/-}$ mice compared to controls. Gene expression analysis demonstrated that slightly higher levels of bone formation markers and resorption markers along with levels of bone morphogenetic protein-Smad signaling, however, there was no significant changes in TRAP positive cells in tibiae. These findings suggest that changes in bone morphogenetic protein signaling activity within differentiating osteoblasts does not affect net bone mass in the adult stage, providing insights into the concerns in the clinical setting such as high-dose and unexpected side effects of bone morphogenetic protein application.

KEYWORDS

bone morphogenetic protein, BMPR1A, osteoblast lineage cells, bone formation, bone resorption

1 Introduction

Bone morphogenetic proteins (BMPs) were first described in 1965 as potent bone inducers due to their activities to form ectopic bones when implanted subcutaneously (Urist, 1965). Preclinical studies have demonstrated BMPs' osteoinductive properties, especially for BMP-2, BMP-7 at 100–300 ng/mL *in vitro* and around 12 mg/site for new bone formation *in vivo* (8 mL of 1.5 mg/mL of recombinant human BMP-2) (Sampath and Reddi, 1981; Wozney et al., 1988; Luyten et al., 1989; Wozney, 1992; FDA, 2002). The United States Food and Drug Administration (FDA) has approved BMP-2 and BMP-7 for clinical use in non-union fractures long bone open-fractures, spinal fusion, and alveolar ridge augmentation (Gupta and Khan, 2005; Garrison et al., 2007; White et al., 2007). Genetic studies of human disorders fibrodysplasia ossificans progressiva (Shore et al., 2006) and chondrodysplasia (Thomas et al., 1996) indicate the importance of BMP signaling in the skeleton.

BMPs belong to the transforming growth factor-β (TGF-β) gene superfamily (Massague, 1998; Kishigami and Mishina, 2005) and signal through transmembrane serine/threonine kinase receptors. Upon ligand binding, BMP type I and BMP II receptors form heteromultimers (Wrana et al., 1994), and a constitutively active type II receptor kinase phosphorylates a GS box (a short stretch of the glycine- and serine-rich domain next to the transmembrane domains) in the type I receptor kinase to activate its activity. Activated BMP type I receptor kinases phosphorylate their downstream targets, Smad1, Smad5, and Smad9 proteins, and then interact with Smad4 to translocate into the nucleus (Chen et al., 2004). A point mutation in the GS box, for example, Q233D for BMPR1A and Q207D for ACVR1, makes type 1 receptor kinase activity constitutively active, however, type II receptors are still required for active Smad signaling (Bagarova et al., 2013).

BMP receptor type IA (BMPR1A) is abundantly expressed in bone and is activated by BMP-2 and BMP-4 ligands. Conventional knockout of *Bmp2*, *Bmp4* and *Bmpr1a* in mice results in embryonic lethality during gastrulation, which is before bone development, because BMPs are critical for the development of key organs including the heart and brain (Mishina et al., 1995; Winnier et al., 1995; Zhang and Bradley, 1996; Mishina et al., 1999). We previously inactivated *Bmpr1a* in an mature osteoblast-specific manner using *Og2*-Cre mice (Mishina et al., 2002; Mishina et al., 2004) and *Col1a1*-Cre mice (Kamiya et al., 2008a; Kamiya et al., 2008b). We also reported osteoblast-specific disruption of *Acvr1a* (Kamiya et al., 2011). It is interesting that in many cases the mutant mice exhibit more bone volume than littermate controls with some exceptions (Mishina et al., 2004; Kamiya et al., 2008a; Kamiya et al., 2008b; Kamiya et al., 2011). In contrast, gain-of-function of *Bmpr1a* in osteoblasts did not alter bone mass (Kamiya et al., 2020). Taken together with the facts that disruption of *Bmp2* and augmentation of *Bmp4* mutant mice both reduced bone mass (Okamoto et al., 2006; Tsuji et al., 2006), the mechanism of BMP signaling in controlling bone mass can be complicated and is not straightforward (Lowery and Rosen, 2018).

Along with the clinical use of BMP-2, it has been emerged that its efficacy and complications may be actual concerns (Woo, 2012a; b; 2013), including bone resorption and osteolysis (Pradhan et al., 2006). In fact, a phase I randomized study showed that the healing of open tibial fractures was not significantly accelerated by a BMP-2 loaded absorbable collagen sponge (Aro et al., 2011) presumably due to the increase in bone resorption (Seeherman et al., 2010). Additionally, various complications have been documented after spinal surgeries (Mroz et al., 2010; Carragee et al., 2011; Dmitriev et al., 2011; Williams et al., 2011), including vertebral resorption and osteolysis (Pradhan et al., 2006).

Studies from mouse genetics have demonstrated that BMPs and their signaling have pleiotropic roles in the different types of cells in the skeletal system, including mesenchymal cells, chondrocytes, osteoblasts, osteoclasts, and osteocytes (Kamiya and Mishina, 2011). To understand the clinical outcomes from BMP therapy, it is critical to define the roles of BMP signaling in bones in a cell type-dependent manner. We are interested to differentiate the impacts of BMP signaling in the early to late osteoblasts at physiologic levels. It is of interest that augmented BMP signaling in bone cells would affect bone resorption and bone mass, leading to a new insight into the potential use of BMPs in a clinical setting. To supplement our previous gene disruption studies, we conditionally activated the BMP-Smad signaling through BMPR1A in mice (*caBmpr1a*) using *Col1-CreERT* to report that a small upregulation of BMP-Smad signaling in osteoblasts does not show overt bone phenotypes (Kamiya et al., 2008b; Kamiya et al., 2020). In this study, we used a *Osterix*-Cre (Rodda and McMahon, 2006) to avoid possible impacts of tamoxifen treatments on bone phenotype. We bred *caBmpr1a* hemizygous mice to generate homozygous mice for the *caBmpr1a* transgene to further increase BMP-Smad signaling activity in *Osterix*-expressing cells to investigate alterations in bone phenotypes.

2 Materials and methods

2.1 Animals

Generation of the null mice for *Bmpr1a* (B6; 129S7-*Bmpr1a*^{tm1Bhr}/Mmnc, available at MMRRC, #016131-UNC) was previously described (Mishina et al., 1995). The heterozygous null of *Bmpr1a* were crossed with mice carrying the Tet-off *Osterix-Cre* (Tg (Sp7-tTA,tetO-EGFP/cre)1Amc, available at Jax Mice, #006361) (Rodda and McMahon, 2006) to obtain *Bmpr1a*$^{+/-}$;*Osx-Cre* and *Bmpr1a*$^{+/+}$;*Osx-Cre* mice. Mice conditionally expressing a constitutively active form of *Bmpr1a* (*caBmpr1a*) (B6; 129S7-Tg (CAG-lacZ,-BMPR1A*,-EGFP) 1Mis/Mmjax, available at Jax Mice, #012436) (Kamiya et al., 2008b; Komatsu et al., 2013), which has a mutation in Q233D, were bred with mice carrying *Osx-Cre* to generate *caBmpr1a* hemizygous (*caBmpr1a*$^{wt/+}$;*Osx-Cre*) and homozygous (*caBmpr1a*$^{+/+}$;*Osx-Cre*) mice. Resulting mice showed ligand-independent activation of BMP-Smad signaling after Cre recombination. Because *caBmpr1a* transgenic line was generated through random transgenesis and we have not identified the inserted region, we differentiated hemizygous mice from homozygous mice by genomic real-time quantitative PCR using a custom designed TaqMan primer set

(Yang et al., 2021) and on some occasions, genotyping results are confirmed by breeding with wild type mice. Activation of Osterix-Cre during embryogenesis did not cause lethality or overt morphogenic changes; therefore, we decided not to suppress Cre activity during embryogenesis, and mice were kept on regular diet and never treated with Doxycycline. All mice were kept in a mixed background of 129S7 and C57BL6/J and housed in a 12 h light/dark cycle with *ad libitum* access to food and water. All mouse experiments in this manuscript were approved by the Institutional Animal Care and Use Committee (IACUC) at the University of Michigan, Ann Arbor, and were conducted accordance with ARRIVE guidelines.

2.2 Micro-computed tomography (micro-CT)

Tibiae were harvested from 3-month-old male mice and fixed with 4% paraformaldehyde. The samples were placed in a 19 mm diameter specimen holder and scanned over the entire length of the tibia using a micro-CT system (μCT100 Scanco Medical, Bassersdorf, Switzerland) with voxel size 10 μm, 70 kVp, 114 μA, 0.5 mm AL filter, and integration time 500 ms. A 0.5 mm region of trabecular compartment was analyzed immediately below the growth plate using a fixed global threshold of 26% (260 on a grayscale of 0–1,000, or 569 mg HA/ccm); and a 0.3 mm region of cortical compartment at the midpoint was analyzed using a fixed global threshold of 36% (360 on a grayscale of 0–1,000, or 864 mg HA/ccm). Trabecular bone volume fraction (BV/TV), trabecular thickness (Tb. Th), trabecular number (Tb. N), trabecular separation (Tb. Sp), cortical bone volume fraction (BV/TV), cortical porosity, cortical thickness, bone mineral density (BMD), tissue mineral density (TMD), sub-periosteal area and sub-endosteal area were analyzed using an evaluation software from the manufacture.

2.3 Histology and histomorphometry

Samples were decalcified with 14% EDTA and a series of paraffin bone sections was made at 5 μm followed by hematoxylin and eosin (H&E) staining. For TRAP staining, decalcified samples were embedded in OCT to make 10 μm sections and stained with TRAP solution containing Naphthol AS-BI phosphoric acid, 2.5 M acetate buffer, 0.67 M tartrate solution. We used tibial sections for static histomorphometry. These measurements were made in a blinded, non-biased manner using ImageJ (Egan et al., 2012). The secondary spongiosa restricted to a square area 200 μm distal to the growth plate of the proximal tibia were used as regions of interest (ROIs). We followed the Report of the American Society of Bone and Mineral Research Histomorphometry Nomenclature Committee (Dempster et al., 2013) for measurements.

2.4 Immunohistochemistry

Tibiae were decalcified with 14% EDTA for 2 weeks before paraffin embedding. Deparaffinized sections were treated with 0.01 M citric acid (pH 6.0) for 20 min for antigen retrieval. The sections were treated with 3% hydrogen peroxide and blocking solution, then incubated with the primary phospho-Smad1/5/9 (pSmad1/5/9) antibody (Cell Signaling, cat # 13820, 1:100) at 4°C for 16 h. The sections were then reacted with HRP-conjugated goat anti-rabbit IgG (Abcam, cat # ab64241, no dilution). The ROIs were confined to the trabecular bone under the growth plate of the proximal tibia. The ratio of the number of pSmad1/5/9-positive cells to total cells located on the trabecular bone surface was quantified using ImageJ (Crowe and Yue, 2019).

2.5 Quantitative reverse transcription-polymerase chain reaction (qRT-PCR)

Bone marrow was flushed out from bones and the flushed tibia was used for RNA extraction using TRIzol reagent (Ambion). From 500 ng of RNA, cDNA was generated using SuperScript II cDNA Synthesis (Invitrogen). Gene expression levels were compared between different genotypes using Applied Biosystems ViiA7 platform. Endogenous GAPDH was used to normalize expression levels of each gene. The specificity of amplification was confirmed by checking melting curves. The primers for the SYBR Green quantification method are shown in Supplementary Table S1.

2.6 Cell culture and immunofluorescence staining

Bone marrow stromal cells (BMSCs) were isolated from bone marrows from the tibia of mice at 4 weeks old. Briefly, both ends of each tibia were cut, and bone marrow was flushed out by centrifugation. The collected bone marrow was cultured in 10% FBS/Dulbecco's Modified Eagle Medium (DMEM) supplemented with antibiotics. BMSCs were seeded on glass coverslips in 24-well plates (5×10^4 cells/well) and maintained in DMEM without FBS for 5 h. Cells were stimulated with 100 ng/mL of recombinant human BMP-2 (rhBMP-2, R&D, cat # 335-BM) for 30 min and then fixed in 4% paraformaldehyde for 20 min. Cells were sequentially incubated in 5% bovine serum albumin for 60 min and pSmad1/5/9 antibody at 4°C 16 h. Alexa Fluor 594 donkey anti-rabbit IgG (1:200, Invitrogen, cat # A32754) was used for fluorescent detection as a secondary antibody. Slides were mounted with ProLong Gold antifade reagent (Invitrogen, cat# P36934). The mean intensity for the red fluorescence per nuclei was measured using ImageJ (Shi et al., 2016).

2.7 Statistical analysis

Statistical analyses were done using one-way analysis of variance (ANOVA) among four groups and followed by a Tukey test. All experiments were done with three biological replicates or more per group. The results are expressed as the mean ± SD.

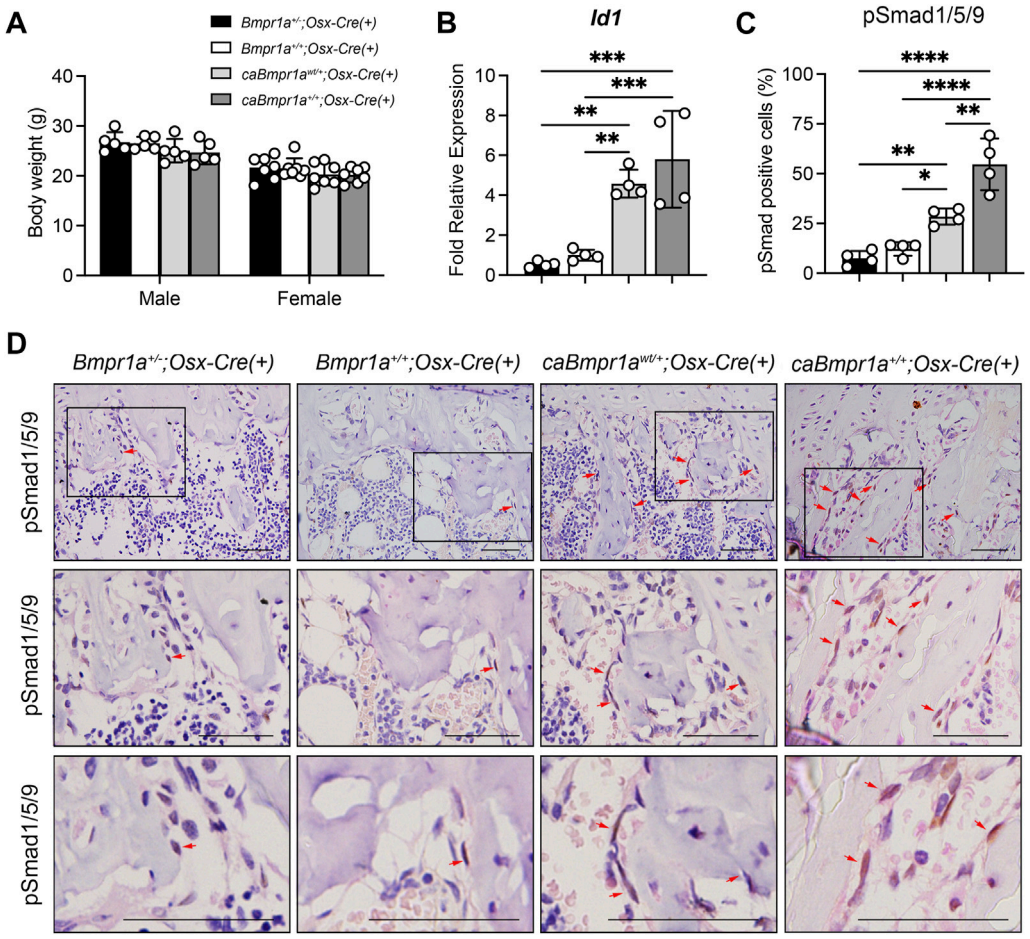

FIGURE 1
Genotype dependent upregulation of BMP-Smad signaling activity. **(A)** Body weight of the mice at 12 weeks of age (male: n = 5 for each group, female: n = 7 for each group). **(B)** Expression levels of *Id1*, a target gene of BMP signaling, in tibiae were measured at 12 weeks of age (n = 4 male for each group). **(C, D)** Immunohistochemical detection of phosphorylated form of Smad1/5/9 in tibiae at 12 weeks of age. pSmad1/5/9-positive cells (brown staining) were marked by red arrows. Higher magnification photos are also shown. Scale bar = 50 μm **(D)**. The ratio of pSmad1/5/9-positive cells (brown + blue) to total cells (blue) on the bone surface of the trabecular bone was analyzed (n = 4 male for each group) **(C)**. ****$p < 0.0001$, ***$p < 0.001$, **$p < 0.01$, and *$p < 0.05$.

3 Results

3.1 Increase in BMP signaling activity in *caBmpr1a* mutant mice

To compare impacts of 4 different levels of BMP-Smad signaling in osteoblasts on adult long bone phenotypes, we set up breeding using conventional null allele for *Bmpr1a* and conditional constitutively activated *Bmpr1a* transgenic mouse line (*caBmpr1a*) to generate *Bmpr1a*$^{+/-}$, *Bmpr1a*$^{+/+}$ (wild type), *caBmpr1a*$^{wt/+}$ and *caBmpr1a*$^{+/+}$ mice, which we previously generated in our group (Mishina et al., 1995; Kamiya et al., 2008b; Komatsu et al., 2013). To achieve osteoblast-specific expression of *caBmpr1a*, we used *Osterix-Cre* mouse line of which Cre activity can be suppressed by Doxycycline for stage-specific genomic manipulation (Rodda and McMahon, 2006; Song et al., 2012). However, induction of *caBmpr1a* expression during embryogenesis did not lead to lethality or overt morphogenetic changes, we decided to keep breeding pairs and resulting pups on regular chow to maintain Cre activity throughout the experiments. To avoid misleading of the phenotypes that could be caused by presence of *Osterix-Cre*, but without Cre-dependent recombination (Razidlo et al., 2010; Davey et al., 2012; Wang et al., 2015), we selected mice carrying *Osterix-Cre* in 4 different genotypes of mice for comparisons.

At 12 weeks of age, the body weights of *Bmpr1a*$^{+/-}$;*Osx-Cre*, *caBmpr1a*$^{wt/+}$;*Osx-Cre* and *caBmpr1a*$^{+/+}$;*Osx-Cre* mice were close to each other including controls (*Bmpr1a*$^{+/+}$;*Osx-Cre*) in both sexes (Figure 1A). The levels of *Id1*, one of the direct targets of BMP-Smad signaling, upregulated in both *caBmpr1a*$^{wt/+}$;*Osx-Cre* (4.6-fold) and *caBmpr1a*$^{+/+}$;*Osx-Cre* (5.8-fold) tibiae, and downregulated in the *Bmpr1a*$^{+/-}$;*Osx-Cre* (0.5-fold) at 3 months compared to controls (Figure 1B). For canonical BMP signaling, the levels of phosphorylated forms of Smad1/5/9 in osteoblast lineage cells (brown-stained cells at the bone surface) were significantly higher in both the trabecular bone of the

10.3389/fphys.2023.1145763

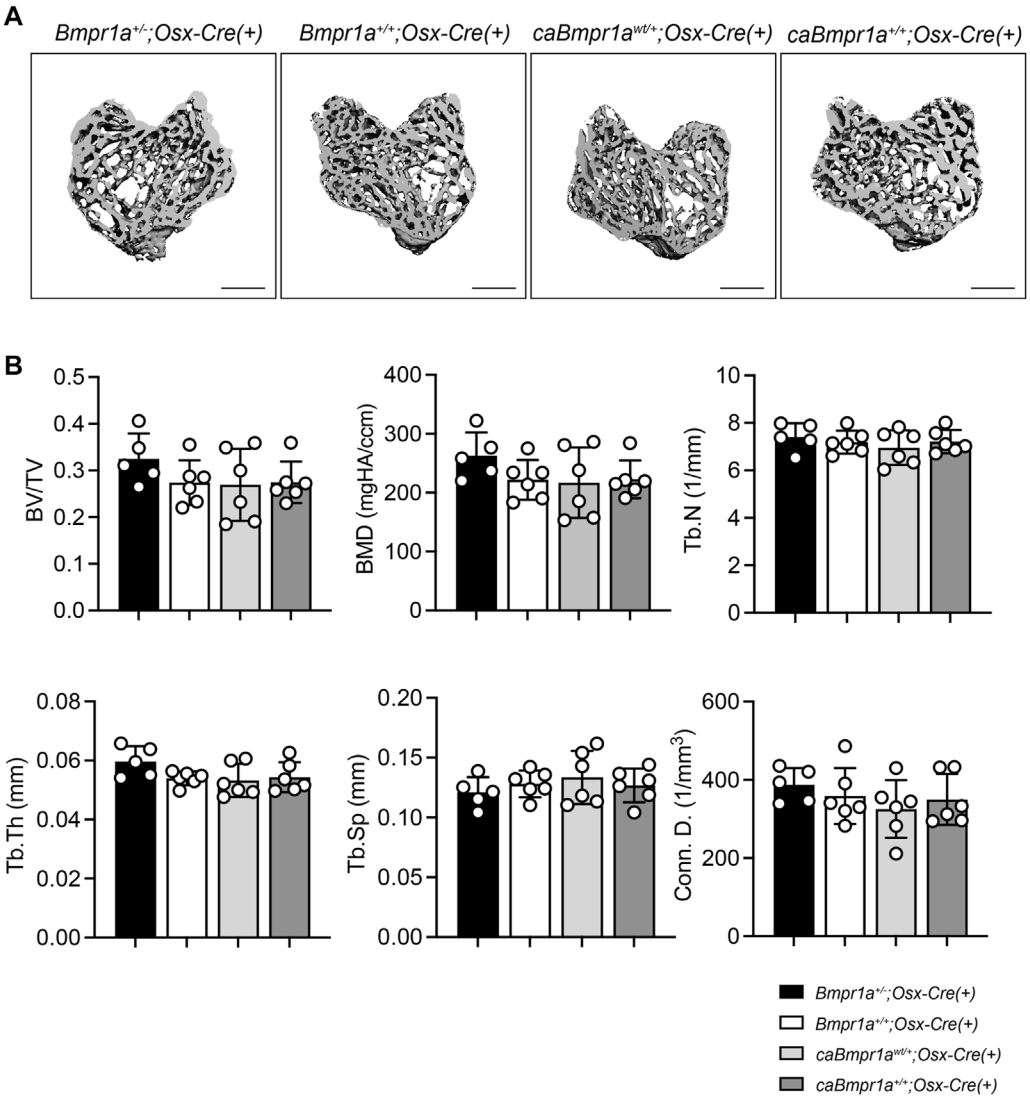

FIGURE 2
Micro-CT analysis for trabecular compartments of the male mouse tibia at 12 weeks of age. **(A)** Micro-CT based 3D images of the mouse proximal tibia. Scale bar = 500 μm. **(B)** Bone volume (BV/TV), bone mineral density (BMD), trabecular number (Tb.N), trabecular thickness (Tb.Th), trabecular space (Tb.Sp) and connective density (Conn.D.) were analyzed (n = 5 male for *Bmpr1a*$^{+/-}$*;Osx-Cre* mice, n = 6 male for *Bmpr1a*$^{+/+}$*;Osx-Cre, caBmpr1a*$^{wt/+}$*;Osx-Cre, caBmpr1a*$^{+/+}$*;Osx-Cre* mice).

caBmpr1a$^{wt/+}$*;Osx-Cre* (2.3-fold) and *caBmpr1a*$^{+/+}$*;Osx-Cre* (4.5-fold) tibiae and lower in the *Bmpr1a*$^{+/-}$*;Osx-Cre* (0.6-fold) at 3 months compared to controls (Figures 1C, D).

3.2 No overt skeletal changes in *Bmpr1a* heterozygous null and *caBmpr1a* mutant mice

Micro-CT analysis for the trabecular compartments of the tibia at 3 months showed no overt differences in BV/TV, BMD, Tb.N, Tb.Th, Tb.Sp and Conn.D among groups (Figures 2A, B). For the cortical compartments of the tibia, there were no overt differences in BV/TV, TMD, thickness, porosity, and sub-periosteal area while sub-endosteal area of the *caBmpr1a*$^{+/+}$*;Osx-Cre* tibia was smaller than controls (Figures 3A, B). Morphometric assessment of H&E-stained tibiae revealed no overt differences in BA/TA, Tb.N, Tb.Th and Tb.Sp among groups (Figures 4A, B). In terms of osteoblast number (N.Ob/BS), osteoclast number (N.Oc/BS), osteoblast surface (Ob.S/BS) and osteoclast surface (Oc.S/BS), there were no significant differences among groups.

3.3 Modest changes in gene expression of bone formation and bone resorption markers in *Bmpr1a* heterozygous null and *caBmpr1a* mutant mice

Quantitative reverse transcribed (RT)-PCR of the tibia showed that the *caBmpr1a*$^{wt/+}$*;Osx-Cre* and *caBmpr1a*$^{+/+}$*;Osx-Cre* tibiae exhibited higher expression of bone formation markers such as

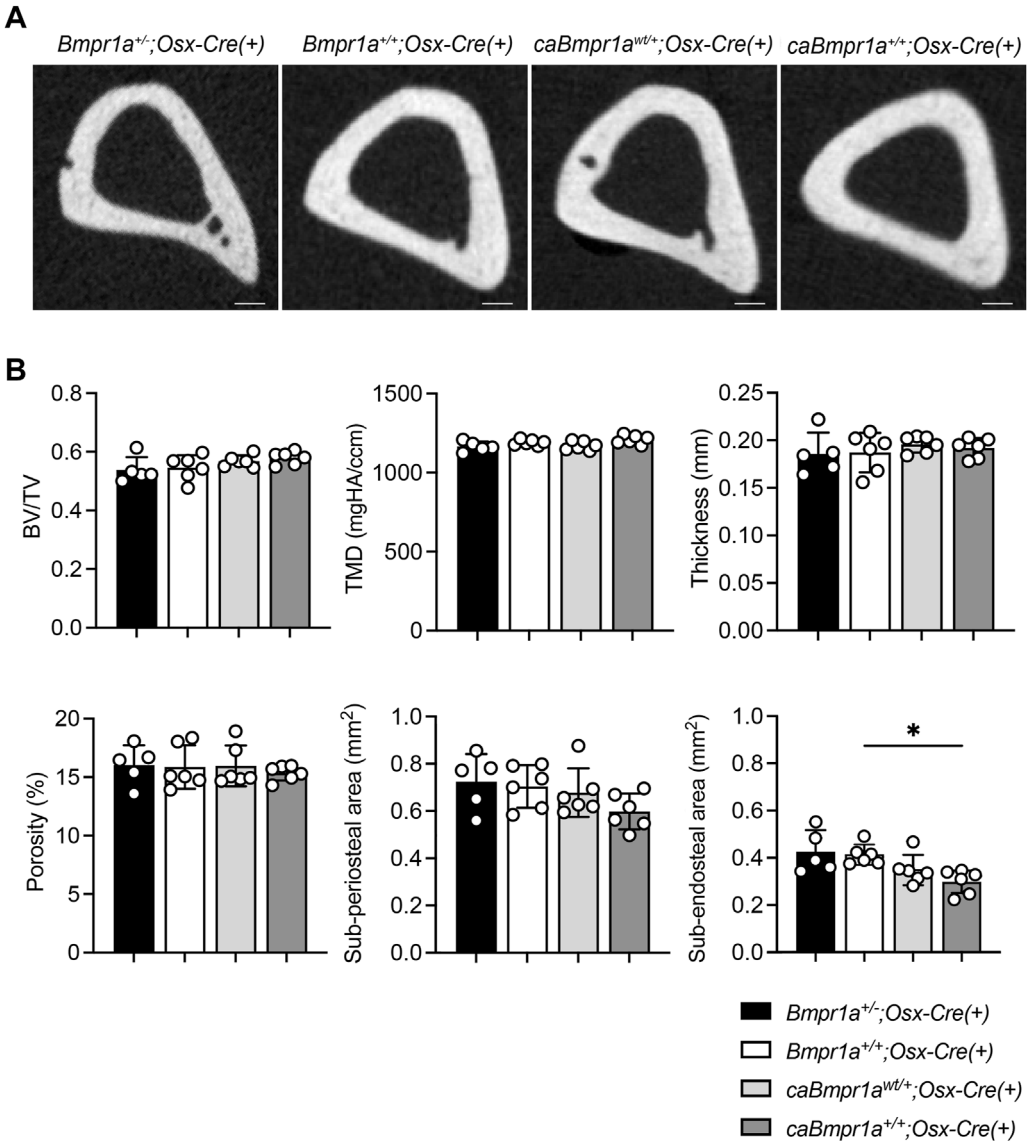

FIGURE 3
Micro-CT analysis for cortical compartments of the male mouse tibia at 12 weeks of age. **(A)** Micro-CT based 2D images of the mouse proximal tibia. Scale bar = 200 μm. **(B)** Bone volume (BV/TV), tissue mineral density (TMD), thickness, porosity, sub-periosteal (total) area and sub-endosteal (marrow) area were analyzed (n = 5 male for *Bmpr1a*$^{+/-}$*;Osx-Cre* mice, n = 6 male for *Bmpr1a*$^{+/+}$*;Osx-Cre, caBmpr1a*$^{wt/+}$*;Osx-Cre, caBmpr1a*$^{+/+}$*;Osx-Cre* mice). $^{**}p < 0.01$.

Col1a1 and *Runx2* than the *Bmpr1a*$^{+/-}$*;Osx-Cre* tibiae (Figure 5A). In terms of bone resorption markers, expression levels of *Opg*, a decoy receptor for RANKL which inhibits osteoclastogenesis, were lower in the *caBmpr1a*$^{wt/+}$*;Osx-Cre* and *caBmpr1a*$^{+/+}$*;Osx-Cre* mice than the *Bmpr1a*$^{+/-}$*;Osx-Cre* mice (Figure 5B).

3.4 Increased BMP signaling activity in *caBmpr1a* mutant mice in ligand-dependent and ligand-independent manners

To investigate the BMP signaling activity in each group, phosphorylation levels of Smad1/5/9 (pSmad1/5/9) in bone marrow stromal cells (BMSCs) isolated from tibiae were determined by immunofluorescence intensity of pSmad1/5/9 signal in nucleus after 5 h in culture. BMSCs from the *caBmpr1a*$^{wt/+}$*;Osx-Cre* and *caBmpr1a*$^{+/+}$*;Osx-Cre* tibiae exhibited higher pSmad1/5/9 levels than those from the *Bmpr1a*$^{+/-}$*;Osx-Cre* and *Bmpr1a*$^{+/+}$*;Osx-Cre* tibiae without BMP-2 stimulation (Figure 6). With BMP-2 stimulation, BMSCs from the all groups exhibited higher levels of pSmad1/5/9 than those without BMP-2 stimulation. In the presence of BMP-2, BMSCs from the *caBmpr1a*$^{wt/+}$*;Osx-Cre* and *caBmpr1a*$^{+/+}$*;Osx-Cre* tibiae exhibited higher levels of pSmad1/5/9 than those from the *Bmpr1a*$^{+/-}$*;Osx-Cre* and *Bmpr1a*$^{+/+}$*;Osx-Cre* tibiae.

10.3389/fphys.2023.1145763

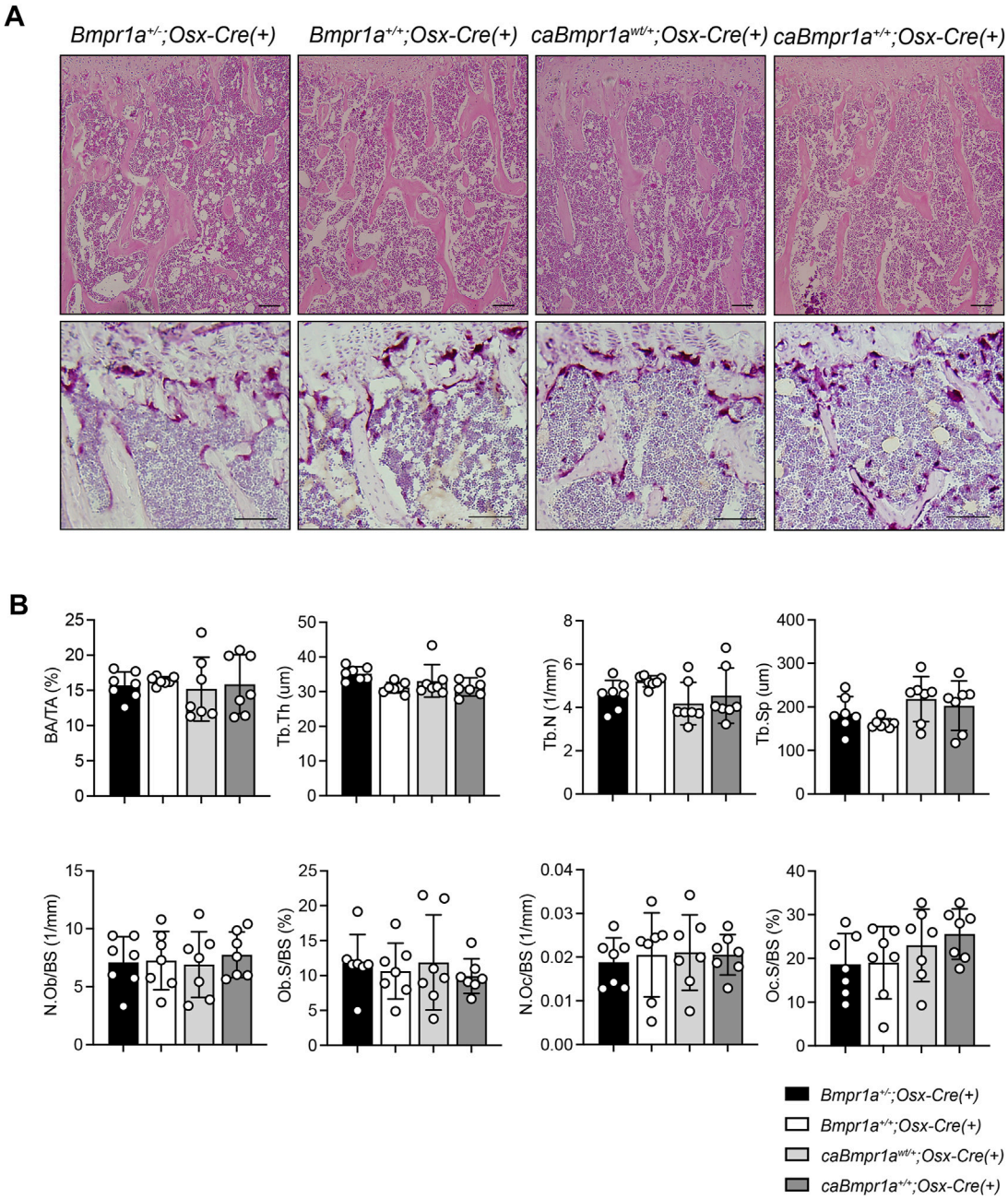

FIGURE 4
(A) Top, H&E staining of the mouse proximal tibia. Scale bar = 100 μm. Bottom, TRAP staining of the mouse proximal tibia. Scale bar = 50 μm. **(B)** Bone area/tissue area (BA/TA), trabecular thickness (Tb.Th), trabecular number (Tb.N), trabecular space (Tb.Sp), osteoblast number/bone surface (N.Ob/BS), osteoblast surface/bone surface (Ob.S/BS), osteoclast number/bone surface (N.Oc/BS), osteoclast surface/bone surface (OcS/BS) were analyzed (n = 7 male for each group). ***p < 0.001, **p < 0.01.

4 Discussion

4.1 Overall findings

Upon the discover of BMPs as potent inducers for ectopic bones formation (Urist, 1965), BMPs have been regarded as a golden standard biological means to increase bone mass. However, after over 2 decades of clinical trials and genetic investigations using animal models conducted by our group and others, outcomes of BMP treatment are much more complicated than initially anticipated. We previously demonstrated loss of function of BMP signaling mediated by BMPR1A in osteoblasts results in augmentation of orthotopic bone mass, while osteoblast-specific enhancement of BMPR1A-Smad signaling transgenic mouse line (in which BMPR1A signaling is constitutively activated in early to late osteoblasts) does not cause overt bone phenotypes (Mishina et al., 2004; Kamiya et al., 2008a; Kamiya et al., 2008b; Shi et al., 2018; Kamiya et al., 2020). To gain further insight into the levels of BMP signaling in osteoblasts and bone

10.3389/fphys.2023.1145763

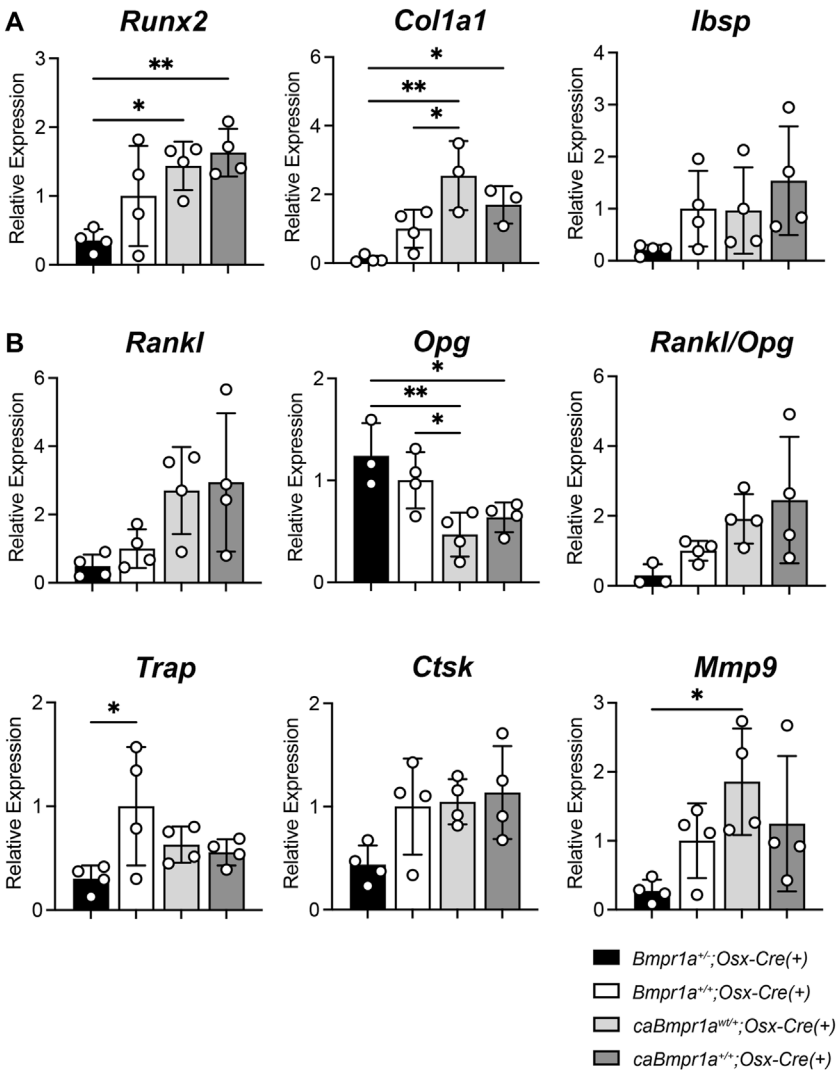

FIGURE 5
Gene expression for bone formation and bone resorption markers in the male mouse tibia at 12 weeks of age. **(A)** Bone formation marker genes (*Runx2, Col1a1, Ibsp*) were analyzed. (n = 4 each group). **(B)** Bone resorption marker genes (*Rankl, Opg, Trap, Ctsk, Mmp9*) were analyzed (n = 4 male for each group). $^{**}p < 0.01$ and $^{*}p < 0.05$.

phenotypes, we took an advantage of the Tet-off *Osx-Cre* mouse line to prepare mouse lines with four different levels of BMP-Smad signaling in osteoblasts without necessitating tamoxifen injection. As expected, BMP dependent signal, as denoted by phosphorylated Smad 1/5/9, as well as specific target gene *Id1*, was downregulated in *Bmpr1a*$^{+/-}$ mice and is elevated more in homozygous mice for *caBmpr1a* transgene (*caBmpr1a*$^{+/+}$*;Osx-Cre* mice) than in heterozygous mice (*caBmpr1a*$^{wt/+}$*; Osx-Cre* mice). However, it is noted that bone mass was not changed in the homozygous transgenic mice. Bone phenotypes were unchanged regarding trabecular and cortical bone structures and static bone parameters for osteoblasts and osteoclasts. The only change we noticed is a small reduction of sub-endosteal area in homozygous mice for the *caBmpr1a* transgene when compared with *Bmpr1a*$^{+/+}$ mice also carrying *Osx-Cre*. It is noted that both markers for bone formation (*Runx2*, *Col1a1*) and resorption (*Mmp9*, *Opg*, tendency for *Rankl*) were significantly augmented by the upregulated BMP signaling in both hemizygous and homozygous *caBmpr1a* mice, which presumably did not alter the balance of bone metabolic kinetics nor net bone mass. Expression levels of most of the aforementioned genes were not changed between *Bmpr1a*$^{+/-}$ and *Bmpr1a*$^{+/+}$ mice and taken together the facts of no significant changes of levels of pSmad1/5/9 (Figure 1B), *Id1* expression (Figure 1C), and response to BMP-2 in culture (Figure 6), these suggest that one copy of *Bmpr1a* is enough to transduce enough levels of BMP-Smad signaling in *Osterix*-expressing cells. These data suggest that a small upregulation of BMP-Smad signaling in *Osterix*-expressing cells does not alter bone phenotypes and also suggest experimental and clinical outcomes of increased bone mass by BMP treatment is due to its impact on other types of cells such as mesenchymal stem cells.

We previously reported that heterozygous conditional mutations of *caBmpr1a* using 3.2-kb Col1-CreER^{TM} mice results in no overt changes in net bone mass with modest changes in osteoblast and osteoclast activities at 34 weeks of age (Kamiya et al., 2020). In this study, we used *Osterix*-Cre (*Osx*-Cre) transgenic mice which are widely used to target

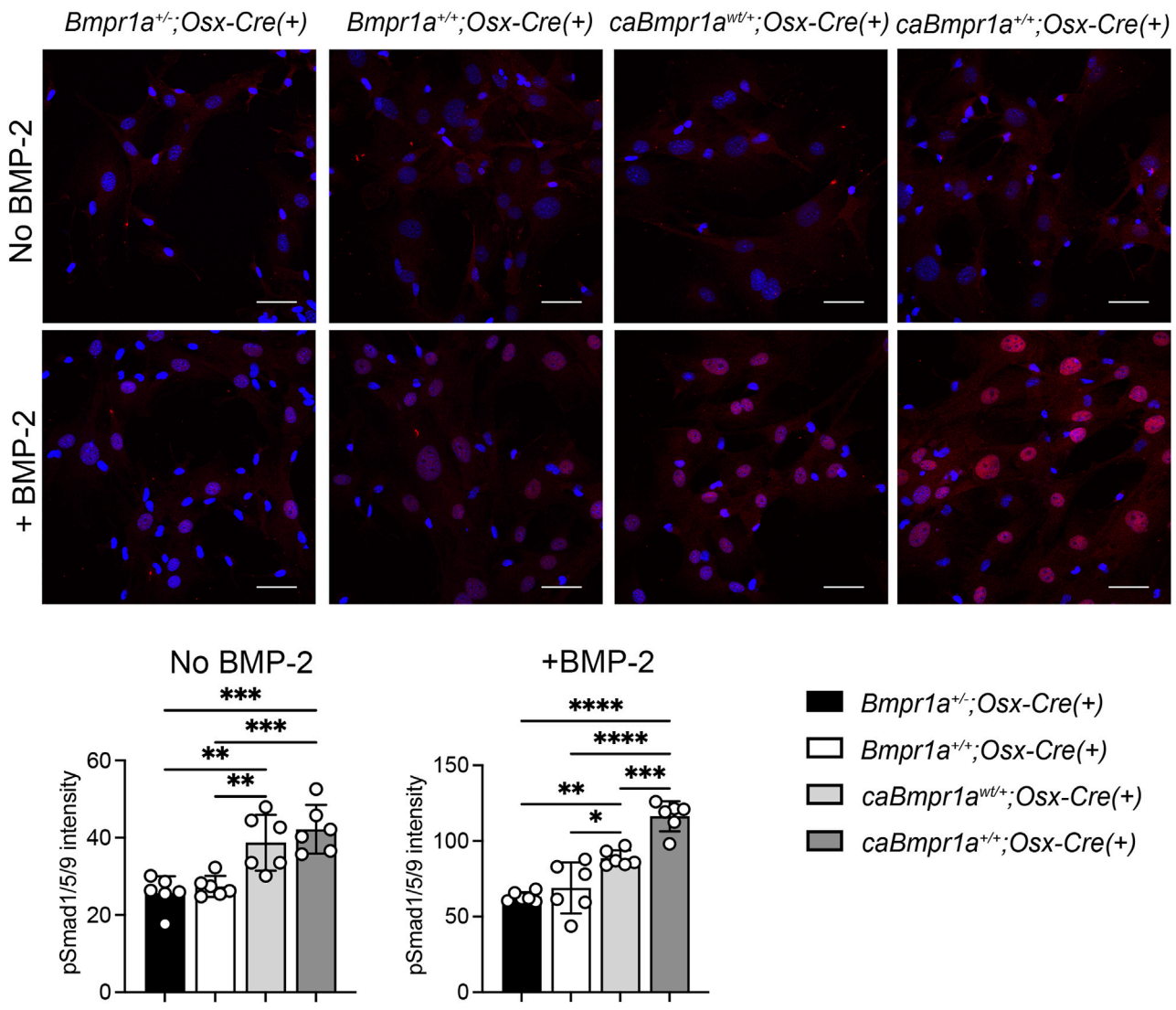

FIGURE 6
Immunofluorescence detection of phosphorylated form of Smad1/5/9 in bone marrow stromal cells (BMSCs) from the mouse tibia. BMSCs were incubated with/without 100 ng/mL of rhBMP-2 for 30 min. Intensity of pSmad1/5/9 (red) in the nucleus was measured (n = 6 male for each group). Scale bar = 50 μm ****$p < 0.0001$, ***$p < 0.001$, and **$p < 0.01$.

immature to mature osteoblasts; they can generate GFP/Cre fusion protein under the control of the Osterix (Sp7) promoter along with a tetracycline responsive element (Rodda and McMahon, 2006). One advantage of use of *Osx*-Cre is to avoid use of tamoxifen, which may affect bone phenotypes (Broulik, 2000). Because we and others reported that *Osx*-Cre mice without any floxed regions show some bone phenotypes including a cortical bone phenotype and minor craniofacial defects (Razidlo et al., 2010; Davey et al., 2012; Wang et al., 2015), we used mice carrying *Osx*-Cre but wildtype for *Bmpr1a* as controls to compare bone phenotypes and molecular changes.

Unlike an early-stage embryonic lethality caused by conventional homozygous deletion of *Bmpr1a* (Mishina et al., 1995), we have not noticed developmental defects in heterozygous mutant mice ($Bmpr1a^{+/-}$). In the adult stage, some of the *Bmpr1a* heterozygous null mice showed an abnormality in glucose metabolism such as higher glucose response and lower insulin levels in the heterozygous mice (Scott et al., 2009); however, the mutation did not cause overt bone abnormalities as reported here. There is a formal possibility that the absence of bone phenotypes in $Bmpr1a^{+/-}$ mice may be due to reduced BMPR1A-Smad signaling in other types of cells, because this is a global knockout. Although less likely, this possibility can be addressed by using of a conditional allele of *Bmpr1a* (Mishina et al., 2002), which we previously generated, in combination with *Osx*-Cre.

One of the limitations of the current study is that only male mice were used to limit possible confounding effects of sex hormones in female mice. We previously reported that heterozygous conditional mutations of *caBmpr1a* using 3.2-kb Col1-CreER™ mice resulted in no overt changes in net bone mass both males and females (Kamiya et al., 2020). Thus, we expect to see no overt changes in net bone mass in female mice. Although less likely, there is a formal possibility that mice used in this study may demonstrate different bone

phenotypes when they age. In the previous study, we analyzed bone phenotypes at 34 weeks after birth (Kamiya et al., 2020), of which phenotypes are similar with these at 12 weeks old. For the cases of loss-of-function studies, when we delete *Bmpr1a* in an osteoblast-specific manner using *Osteocalcin*-Cre, the mutant mice showed age-dependent outcomes, i.e., lower bone mass at 1 month of age, and higher bone mass at 10 months than littermate controls (Mishina et al., 2004). In contrast, when we used 3.2-kb Col1-CreER™, the mutant mice consistently showed higher bone mass as late-stage embryos, at weaning stages and at 22 weeks old after birth (Kamiya et al., 2008a; Kamiya et al., 2008b; Kamiya and Mishina, 2011). However, future studies would be needed to determine the gender dependence using different age groups. Another limitation may be associated with low sample size (n = 4 to 7 per genotype for microCT analyses). For the animal experiments, the number of mice in each group was determined according to our previous reports (Kamiya et al., 2020). In this study, we observed statistically significant changes in BMP dependent signal, as denoted by pSmad1/5/9 levels, as well as specific target gene *Id1* expression levels in both heterozygous and homozygous mice for *caBmpr1a* although these mice displayed no overt bone phenotypes. Thus, we expect that increases in the sample size do not affect the overall conclusion of this study. However, larger sample sizes may be needed to detect subtle differences among groups.

4.2 Clinical aspects

In the clinic, a high dose of BMP-2, such as 12 mg in a concentration of 1.5 mg/mL (FDA, 2002), has been used for fracture repair to induce a bone formation in patients expecting it functions through osteoblasts. However, such high doses of BMPs may introduce unexpected adverse effects (i.e., bone resorption, inflammation, ectopic ossification), likely due to interacting with other types of cells rather than osteoblastic cells (Kim et al., 2013). It is assumed that such clinical side effects are caused by the effects of high dose BMPs on non-bone tissues. Thus, the dosage administered and the way to distribute BMPs are important to be considered for better treatment of BMP-2 therapy. A dose-response with exogenous BMPs would be desired to investigate the multifaceted functions of BMPs *in vivo*. It is noted that BMPs can directly control cartilage formation to positively affect endochondral bone formation by increasing the size of bone templates (Kamiya, 2012; Zhang et al., 2022).

Recently several lines of evidence for BMP-6 as an alternative treatment for orthopedic conditions have been accumulated. BMP-6 is superior to BMP-2 and BMP-7 in its activity to stimulate bone formation *in vitro* and *in vivo* (Vukicevic and Grgurevic, 2009; Song et al., 2010) because it can activate all three type I receptors for BMPs. Additionally, unlike BMP-2 and BMP-7, BMP-6 is resistant to Noggin, a major BMP antagonist found in bones (Song et al., 2010), allowing the use of low BMP-6 concentration with autologous blood coagulum (ABC) (Sampath and Vukicevic, 2020). In human, an autologous bone graft substrate (ABGS), an improved version of ABC (Grgurevic et al., 2019), has been tested for patients with distal radial fracture (Phase I) (Durdevic et al., 2020), and for patients receiving high tibial osteotomy (Phase I/II) (Chiari et al., 2020). In this therapy, ABGS containing 250 μg rhBMP-6 per mL into the fracture site between two ends and was proven safe and efficacious. This is a highly promising avenue for human applications due to the reduced BMP concentration that can reduce adverse reactions.

5 Conclusion

In this study, we bred several lines of mutant mouse lines such as conventional knockout allele of *Bmpr1a* and the constitutively activated BMPR1A allele to generate mice with 4 different doses of BMP-Smad signaling in early to late osteoblasts and investigated the impact of different levels of BMP signaling on endogenous long bones in adults. While alterations in expression levels of bone formation and resorption markers were noted at transcriptional levels, the net bone mass was unchanged in the mutant mice. This study clearly demonstrated a discrepancy between physiological functions of BMP-Smad signaling and expected outcomes in the clinical setting, which provides a new insight in considering a better and more efficient therapeutic regime to mitigate potential side effects by using high dose of BMPs.

Data availability statement

The original contributions presented in the study are included in the article/Supplementary Materials, further inquiries can be directed to the corresponding author.

Ethics statement

The animal study was reviewed and approved by the Institutional Animal Care and Use Committee (IACUC) at the University of Michigan.

Author contributions

MO, NK, and YM contributed to conception, design, and data analysis, drafted the manuscript. MO, TK, YL, and AH contributed to histological and molecular analyses. NK and YM provided critical materials. All approved the final version of the manuscript. MO and YM take responsibility for the integrity of the data analysis.

Funding

This study is supported by the National Institutes of Health NIDCR R01DE020843 to YM. The micro-CT core at the University of Michigan School of Dentistry is funded in part by NIH/NCRR S10RR026475-01. The Histology Core is supported by a core grant from the NIAMS P30 AR069620 to Karl Jepsen, PI; David H. Kohn, Core Director. The content is solely the responsibility of the authors and does not necessarily represent the official views of the NIH.

Acknowledgments

We gratefully acknowledge the University of Michigan School of Dentistry Molecular Biology Core for assistance in

quantitative RT-PCR analysis (Taocong Jin), the University of Michigan School of Dentistry Histology Core for assistance in preparation of histology (Chris Strayhorn), and the University of Michigan School of Dentistry micro-CT Core (Michelle Lynch) for assistance in micro-CT analysis. We also thank Mr. Benton Swanson for critical reading of the manuscript.

Conflict of interest

The authors declare that the research was conducted in the absence of any commercial or financial relationships that could be construed as a potential conflict of interest.

Publisher's note

Supplementary material

The Supplementary Material for this article can be found online at: https://www.frontiersin.org/articles/10.3389/fphys.2023.1145763/full#supplementary-material

References

Aro, H. T., Govender, S., Patel, A. D., Hernigou, P., Perera de Gregorio, A., Popescu, G. I., et al. (2011). Recombinant human bone morphogenetic protein-2: A randomized trial in open tibial fractures treated with reamed nail fixation. *J. Bone Jt. Surg. Am.* 93, 801–808. doi:10.2106/JBJS.I.01763

Bagarova, J., Vonner, A. J., Armstrong, K. A., Borgermann, J., Lai, C. S., Deng, D. Y., et al. (2013). Constitutively active ALK2 receptor mutants require type II receptor cooperation. *Mol. Cell Biol.* 33, 2413–2424. doi:10.1128/MCB.01595-12

Broulik, P. D. (2000). Tamoxifen prevents bone loss in castrated male mice. *Horm. Metab. Res.* 32, 181–184. doi:10.1055/s-2007-978618

Carragee, E. J., Hurwitz, E. L., and Weiner, B. K. (2011). A critical review of recombinant human bone morphogenetic protein-2 trials in spinal surgery: Emerging safety concerns and lessons learned. *Spine J.* 11, 471–491. doi:10.1016/j.spinee.2011.04.023

Chen, D., Zhao, M., and Mundy, G. R. (2004). Bone morphogenetic proteins. *Growth factors* 22, 233–241. doi:10.1080/08977190412331279890

Chiari, C., Grgurevic, L., Bordukalo-Niksic, T., Oppermann, H., Valentinitsch, A., Nemecek, E., et al. (2020). Recombinant human BMP6 applied within autologous blood coagulum accelerates bone healing: Randomized controlled trial in high tibial osteotomy patients. *J. Bone Min. Res.* 35, 1893–1903. doi:10.1002/jbmr.4107

Crowe, A. R., and Yue, W. (2019). Semi-quantitative determination of protein expression using immunohistochemistry staining and analysis: An integrated protocol. *Bio Protoc.* 9, e3465. doi:10.21769/BioProtoc.3465

Davey, R. A., Clarke, M. V., Sastra, S., Skinner, J. P., Chiang, C., Anderson, P. H., et al. (2012). Decreased body weight in young Osterix-Cre transgenic mice results in delayed cortical bone expansion and accrual. *Transgenic Res.* 21, 885–893. doi:10.1007/s11248-011-9581-z

Dempster, D. W., Compston, J. E., Drezner, M. K., Glorieux, F. H., Kanis, J. A., Malluche, H., et al. (2013). Standardized nomenclature, symbols, and units for bone histomorphometry: A 2012 update of the report of the ASBMR histomorphometry nomenclature committee. *J. Bone Min. Res.* 28, 2–17. doi:10.1002/jbmr.1805

Dmitriev, A. E., Lehman, R. A., Jr., and Symes, A. J. (2011). Bone morphogenetic protein-2 and spinal arthrodesis: The basic science perspective on protein interaction with the nervous system. *Spine J.* 11, 500–505. doi:10.1016/j.spinee.2011.05.002

Durdevic, D., Vlahovic, T., Pehar, S., Miklic, D., Oppermann, H., Bordukalo-Niksic, T., et al. (2020). A novel autologous bone graft substitute comprised of rhBMP6 blood coagulum as carrier tested in a randomized and controlled Phase I trial in patients with distal radial fractures. *Bone* 140, 115551. doi:10.1016/j.bone.2020.115551

Egan, K. P., Brennan, T. A., and Pignolo, R. J. (2012). Bone histomorphometry using free and commonly available software. *Histopathology* 61, 1168–1173. doi:10.1111/j.1365-2559.2012.04333.x

FDA (2002). *InFUSE bone graft/LT-CAGE lumbar tapered fusion device*. Rockville, MD: Summary of Safety and Effective Data Premarket Approval Application P000058.

Garrison, K. R., Donell, S., Ryder, J., Shemilt, I., Mugford, M., Harvey, I., et al. (2007). Clinical effectiveness and cost-effectiveness of bone morphogenetic proteins in the non-healing of fractures and spinal fusion: A systematic review. *Health Technol. Assess.* 11, 1–150. doi:10.3310/hta11300

Grgurevic, L., Oppermann, H., Pecin, M., Erjavec, I., Capak, H., Pauk, M., et al. (2019). Recombinant human bone morphogenetic protein 6 delivered within autologous blood coagulum restores critical size segmental defects of ulna in rabbits. *JBMR Plus* 3, e10085. doi:10.1002/jbm4.10085

Gupta, M. C., and Khan, S. N. (2005). Application of bone morphogenetic proteins in spinal fusion. *Cytokine Growth Factor Rev.* 16, 347–355. doi:10.1016/j.cytogfr.2005.02.004

Kamiya, N., Atsawasuwan, P., Joiner, D. M., Waldorff, E. I., Goldstein, S., Yamauchi, M., et al. (2020). Controversy of physiological vs. pharmacological effects of BMP signaling: Constitutive activation of BMP type IA receptor-dependent signaling in osteoblast lineage enhances bone formation and resorption, not affecting net bone mass. *Bone* 138, 115513. doi:10.1016/j.bone.2020.115513

Kamiya, N., Kaartinen, V. M., and Mishina, Y. (2011). Loss-of-function of ACVR1 in osteoblasts increases bone mass and activates canonical Wnt signaling through suppression of Wnt inhibitors SOST and DKK1. *Biochem. Biophys. Res. Commun.* 414, 326–330. doi:10.1016/j.bbrc.2011.09.060

Kamiya, N., and Mishina, Y. (2011). New insights on the roles of BMP signaling in bone-A review of recent mouse genetic studies. *Biofactors* 37, 75–82. doi:10.1002/biof.139

Kamiya, N. (2012). The role of BMPs in bone anabolism and their potential targets SOST and DKK1. *Curr. Mol. Pharmacol.* 5, 153–163. doi:10.2174/1874467211205020153

Kamiya, N., Ye, L., Kobayashi, T., Lucas, D. J., Mochida, Y., Yamauchi, M., et al. (2008a). Disruption of BMP signaling in osteoblasts through type IA receptor (BMPRIA) increases bone mass. *J. Bone Min. Res.* 23, 2007–2017. doi:10.1359/jbmr.080809

Kamiya, N., Ye, L., Kobayashi, T., Mochida, Y., Yamauchi, M., Kronenberg, H. M., et al. (2008b). BMP signaling negatively regulates bone mass through sclerostin by inhibiting the canonical Wnt pathway. *Development* 135, 3801–3811. doi:10.1242/dev.025825

Kim, H. K., Oxendine, I., and Kamiya, N. (2013). High-concentration of BMP2 reduces cell proliferation and increases apoptosis via DKK1 and SOST in human primary periosteal cells. *Bone* 54, 141–150. doi:10.1016/j.bone.2013.01.031

Kishigami, S., and Mishina, Y. (2005). BMP signaling and early embryonic patterning. *Cytokine Growth Factor Rev.* 16, 265–278. doi:10.1016/j.cytogfr.2005.04.002

Komatsu, Y., Yu, P. B., Kamiya, N., Pan, H., Fukuda, T., Scott, G. J., et al. (2013). Augmentation of Smad-dependent BMP signaling in neural crest cells causes craniosynostosis in mice. *J. Bone Min. Res.* 28, 1422–1433. doi:10.1002/jbmr.1857

Lowery, J. W., and Rosen, V. (2018). The BMP pathway and its inhibitors in the skeleton. *Physiol. Rev.* 98, 2431–2452. doi:10.1152/physrev.00028.2017

Luyten, F. P., Cunningham, N. S., Ma, S., Muthukumaran, N., Hammonds, R. G., Nevins, W. B., et al. (1989). Purification and partial amino acid sequence of osteogenin, a protein initiating bone differentiation. *J. Biol. Chem.* 264, 13377–13380. doi:10.1016/s0021-9258(18)80003-5

Massague, J. (1998). TGF-beta signal transduction. *Annu. Rev. Biochem.* 67, 753–791. doi:10.1146/annurev.biochem.67.1.753

Mishina, Y., Crombie, R., Bradley, A., and Behringer, R. R. (1999). Multiple roles for activin-like kinase-2 signaling during mouse embryogenesis. *Dev. Biol.* 213, 314–326. doi:10.1006/dbio.1999.9378

Mishina, Y., Hanks, M. C., Miura, S., Tallquist, M. D., and Behringer, R. R. (2002). Generation of Bmpr/Alk3 conditional knockout mice. *Genesis* 32, 69–72. doi:10.1002/gene.10038

Mishina, Y., Starbuck, M. W., Gentile, M. A., Fukuda, T., Kasparcova, V., Seedor, J. G., et al. (2004). Bone morphogenetic protein type IA receptor signaling regulates postnatal osteoblast function and bone remodeling. *J. Biol. Chem.* 279, 27560–27566. doi:10.1074/jbc.M404222200

Mishina, Y., Suzuki, A., Ueno, N., and Behringer, R. R. (1995). Bmpr encodes a type I bone morphogenetic protein receptor that is essential for gastrulation during mouse embryogenesis. *Genes Dev.* 9, 3027–3037. doi:10.1101/gad.9.24.3027

Mroz, T. E., Wang, J. C., Hashimoto, R., and Norvell, D. C. (2010). Complications related to osteobiologics use in spine surgery: A systematic review. *Spine (Phila Pa 1976)* 35, S86–S104. doi:10.1097/BRS.0b013e3181d81ef2

Okamoto, M., Murai, J., Yoshikawa, H., and Tsumaki, N. (2006). Bone morphogenetic proteins in bone stimulate osteoclasts and osteoblasts during bone development. *J. Bone Min. Res.* 21, 1022–1033. doi:10.1359/jbmr.060411

Pradhan, B. B., Bae, H. W., Dawson, E. G., Patel, V. V., and Delamarter, R. B. (2006). Graft resorption with the use of bone morphogenetic protein: Lessons from anterior lumbar interbody fusion using femoral ring allografts and recombinant human bone morphogenetic protein-2. *Spine (Phila Pa 1976)* 31, E277–E284. doi:10.1097/01.brs.0000216442.12092.01

Razidlo, D. F., Whitney, T. J., Casper, M. E., McGee-Lawrence, M. E., Stensgard, B. A., Li, X., et al. (2010). Histone deacetylase 3 depletion in osteo/chondroprogenitor cells decreases bone density and increases marrow fat. *PLoS One* 5, e11492. doi:10.1371/journal.pone.0011492

Rodda, S. J., and McMahon, A. P. (2006). Distinct roles for Hedgehog and canonical Wnt signaling in specification, differentiation and maintenance of osteoblast progenitors. *Development* 133, 3231–3244. doi:10.1242/dev.02480

Sampath, T. K., and Reddi, A. H. (1981). Dissociative extraction and reconstitution of extracellular matrix components involved in local bone differentiation. *Proc. Natl. Acad. Sci. U. S. A.* 78, 7599–7603. doi:10.1073/pnas.78.12.7599

Sampath, T. K., and Vukicevic, S. (2020). Biology of bone morphogenetic protein in bone repair and regeneration: A role for autologous blood coagulum as carrier. *Bone* 141, 115602. doi:10.1016/j.bone.2020.115602

Scott, G. J., Ray, M. K., Ward, T., McCann, K., Peddada, S., Jiang, F. X., et al. (2009). Abnormal glucose metabolism in heterozygous mutant mice for a type I receptor required for BMP signaling. *Genesis* 47, 385–391. doi:10.1002/dvg.20513

Seeherman, H. J., Li, X. J., Bouxsein, M. L., and Wozney, J. M. (2010). rhBMP-2 induces transient bone resorption followed by bone formation in a nonhuman primate core-defect model. *J. Bone Jt. Surg. Am.* 92, 411–426. doi:10.2106/JBJS.H.01732

Shi, C., Iura, A., Terajima, M., Liu, F., Lyons, K., Pan, H., et al. (2016). Deletion of BMP receptor type IB decreased bone mass in association with compromised osteoblastic differentiation of bone marrow mesenchymal progenitors. *Sci. Rep.* 6, 24256. doi:10.1038/srep24256

Shi, C., Mandair, G. S., Zhang, H., Vanrenterghem, G. G., Ridella, R., Takahashi, A., et al. (2018). Bone morphogenetic protein signaling through ACVR1 and BMPR1A negatively regulates bone mass along with alterations in bone composition. *J. Struct. Biol.* 201, 237–246. doi:10.1016/j.jsb.2017.11.010

Shore, E. M., Xu, M., Feldman, G. J., Fenstermacher, D. A., Cho, T. J., Choi, I. H., et al. (2006). A recurrent mutation in the BMP type I receptor ACVR1 causes inherited and sporadic fibrodysplasia ossificans progressiva. *Nat. Genet.* 38, 525–527. doi:10.1038/ng1783

Song, K., Krause, C., Shi, S., Patterson, M., Suto, R., Grgurevic, L., et al. (2010). Identification of a key residue mediating bone morphogenetic protein (BMP)-6 resistance to noggin inhibition allows for engineered BMPs with superior agonist activity. *J. Biol. Chem.* 285, 12169–12180. doi:10.1074/jbc.M109.087197

Song, L., Liu, M., Ono, N., Bringhurst, F. R., Kronenberg, H. M., and Guo, J. (2012). Loss of wnt/β-catenin signaling causes cell fate shift of preosteoblasts from osteoblasts to adipocytes. *J. Bone Min. Res.* 27, 2344–2358. doi:10.1002/jbmr.1694

Thomas, J. T., Lin, K., Nandedkar, M., Camargo, M., Cervenka, J., and Luyten, F. P. (1996). A human chondrodysplasia due to a mutation in a TGF-beta superfamily member. *Nat. Genet.* 12, 315–317. doi:10.1038/ng0396-315

Tsuji, K., Bandyopadhyay, A., Harfe, B. D., Cox, K., Kakar, S., Gerstenfeld, L., et al. (2006). BMP2 activity, although dispensable for bone formation, is required for the initiation of fracture healing. *Nat. Genet.* 38, 1424–1429. doi:10.1038/ng1916

Urist, M. R. (1965). Bone: Formation by autoinduction. *Science* 150, 893–899. doi:10.1126/science.150.3698.893

Vukicevic, S., and Grgurevic, L. (2009). BMP-6 and mesenchymal stem cell differentiation. *Cytokine Growth Factor Rev.* 20, 441–448. doi:10.1016/j.cytogfr.2009.10.020

Wang, L., Mishina, Y., and Liu, F. (2015). Osterix-Cre transgene causes craniofacial bone development defect. *Calcif. Tissue Int.* 96, 129–137. doi:10.1007/s00223-014-9945-5

White, A. P., Vaccaro, A. R., Hall, J. A., Whang, P. G., Friel, B. C., and McKee, M. D. (2007). Clinical applications of BMP-7/OP-1 in fractures, nonunions and spinal fusion. *Int. Orthop.* 31, 735–741. doi:10.1007/s00264-007-0422-x

Williams, B. J., Smith, J. S., Fu, K. M., Hamilton, D. K., Polly, D. W., Jr., Ames, C. P., et al. (2011). Does bone morphogenetic protein increase the incidence of perioperative complications in spinal fusion? A comparison of 55,862 cases of spinal fusion with and without bone morphogenetic protein. *Spine (Phila Pa 1976)* 36, 1685–1691. doi:10.1097/BRS.0b013e318216d825

Winnier, G., Blessing, M., Labosky, P. A., and Hogan, B. L. (1995). Bone morphogenetic protein-4 is required for mesoderm formation and patterning in the mouse. *Genes Dev.* 9, 2105–2116. doi:10.1101/gad.9.17.2105

Woo, E. J. (2013). Adverse events after recombinant human BMP2 in nonspinal orthopaedic procedures. *Clin. Orthop. Relat. Res.* 471, 1707–1711. doi:10.1007/s11999-012-2684-x

Woo, E. J. (2012a). Adverse events reported after the use of recombinant human bone morphogenetic protein 2. *J. Oral Maxillofac. Surg.* 70, 765–767. doi:10.1016/j.joms.2011.09.008

Woo, E. J. (2012b). Recombinant human bone morphogenetic protein-2: Adverse events reported to the manufacturer and user facility device experience database. *Spine J.* 12, 894–899. doi:10.1016/j.spinee.2012.09.052

Wozney, J. M., Rosen, V., Celeste, A. J., Mitsock, L. M., Whitters, M. J., Kriz, R. W., et al. (1988). Novel regulators of bone formation: Molecular clones and activities. *Science* 242, 1528–1534. doi:10.1126/science.3201241

Wozney, J. M. (1992). The bone morphogenetic protein family and osteogenesis. *Mol. Reprod. Dev.* 32, 160–167. doi:10.1002/mrd.1080320212

Wrana, J. L., Attisano, L., Wieser, R., Ventura, F., and Massague, J. (1994). Mechanism of activation of the TGF-beta receptor. *Nature* 370, 341–347. doi:10.1038/370341a0

Yang, J., Kitami, M., Pan, H., Nakamura, M. T., Zhang, H., Liu, F., et al. (2021). Augmented BMP signaling commits cranial neural crest cells to a chondrogenic fate by suppressing autophagic beta-catenin degradation. *Sci. Signal* 14, eaaz9368. doi:10.1126/scisignal.aaz9368

Zhang, H., and Bradley, A. (1996). Mice deficient for BMP2 are nonviable and have defects in amnion/chorion and cardiac development. *Development* 122, 2977–2986. doi:10.1242/dev.122.10.2977

Zhang, M., Niibe, K., Kondo, T., Limraksasin, P., Okawa, H., Miao, X., et al. (2022). Rapid and efficient generation of cartilage pellets from mouse induced pluripotent stem cells by transcriptional activation of BMP-4 with shaking culture. *J. Tissue Eng.* 13, 20417314221114616. doi:10.1177/20417314221114616

frontiers | Frontiers in Physiology

TYPE Review
PUBLISHED 13 July 2023
DOI 10.3389/fphys.2023.1220555

OPEN ACCESS

EDITED BY
Ling Qin,
University of Pennsylvania, United States

REVIEWED BY
Archana Sanjay,
University of Connecticut Health Center, United States
Anna Urciuolo,
University of Padua, Italy

*CORRESPONDENCE
Yuji Mishina,
mishina@umich.edu
W. Benton Swanson,
wbentons@umich.edu

RECEIVED 10 May 2023
ACCEPTED 05 July 2023
PUBLISHED 13 July 2023

CITATION
Woodbury SM, Swanson WB and Mishina Y (2023), Mechanobiology-informed biomaterial and tissue engineering strategies for influencing skeletal stem and progenitor cell fate. *Front. Physiol.* 14:1220555. doi: 10.3389/fphys.2023.1220555

Mechanobiology-informed biomaterial and tissue engineering strategies for influencing skeletal stem and progenitor cell fate

Seth M. Woodbury[1,2,3], W. Benton Swanson[1]* and Yuji Mishina[1]*

[1]Yuji Mishina Laboratory, University of Michigan School of Dentistry, Department of Biologic and Materials Science & Prosthodontics, Ann Arbor, MI, United States, [2]University of Michigan College of Literature, Science, and Arts, Department of Chemistry, Ann Arbor, MI, United States, [3]University of Michigan College of Literature, Science, and Arts, Department of Physics, Ann Arbor, MI, United States

Skeletal stem and progenitor cells (SSPCs) are the multi-potent, self-renewing cell lineages that form the hematopoietic environment and adventitial structures of the skeletal tissues. Skeletal tissues are responsible for a diverse range of physiological functions because of the extensive differentiation potential of SSPCs. The differentiation fates of SSPCs are shaped by the physical properties of their surrounding microenvironment and the mechanical loading forces exerted on them within the skeletal system. In this context, the present review first highlights important biomolecules involved with the mechanobiology of how SSPCs sense and transduce these physical signals. The review then shifts focus towards how the static and dynamic physical properties of microenvironments direct the biological fates of SSPCs, specifically within biomaterial and tissue engineering systems. Biomaterial constructs possess designable, quantifiable physical properties that enable the growth of cells in controlled physical environments both *in-vitro* and *in-vivo*. The utilization of biomaterials in tissue engineering systems provides a valuable platform for controllably directing the fates of SSPCs with physical signals as a tool for mechanobiology investigations and as a template for guiding skeletal tissue regeneration. It is paramount to study this mechanobiology and account for these mechanics-mediated behaviors to develop next-generation tissue engineering therapies that synergistically combine physical and chemical signals to direct cell fate. Ultimately, taking advantage of the evolved mechanobiology of SSPCs with customizable biomaterial constructs presents a powerful method to predictably guide bone and skeletal organ regeneration.

KEYWORDS

mechanobiology, biomaterials, tissue engineering, skeletal tissue, stem cell, progenitor cell, microenvironment, dynamic stress

1 Introduction

Skeletal stem and progenitor cells are the multipotent, self-renewing cell lineages found in the bone marrow stroma that are broadly responsible for the repair, regeneration, and remodeling of skeletal tissue and cartilage (Bianco and Robey, 2015; Matsushita et al., 2020). SSPCs have the potential to differentiate into various cell types such as bone, cartilage, and fat cells (Figure 1). They are also involved in establishing and managing the microvascular network of bone, shaping the hematopoietic environment, and regulating the differentiation

of osteoclasts and osteoblasts for bone resorption or deposition, respectively (Bianco and Robey, 2015; Li et al., 2022). Thus, it is paramount to focus on manipulating and strategically utilizing these different behaviors of SSPCs when designing effective techniques to guide bone and skeletal tissue regeneration predictably.

The versatile range of functions that SSPCs possess results from their high sensitivity to the specific chemical and physical microenvironment in which they develop (Kurenkova et al., 2020). The physical microenvironment varies in different types of skeletal tissues and each type hosts unique combinations of cell phenotypes (Figure 1). The physical microenvironment plays an impactful role in the development and remodeling of these tissues by influencing SSPC behavior and differentiation. Moreover, mechanical loading forces imposed on these physical microenvironments also contribute to skeletal tissue remodeling and development. Bone mineral density has been well-demonstrated to increase in the bones of subjects who consistently impose mechanical loading on their appendicular skeletal tissues through weight-bearing exercises (Calbet et al., 1998; Benedetti et al., 2018). Osteocytes were traditionally thought to be the only mechanotransducers in skeletal tissues responsible for this behavior, but modern evidence has proven that SSPCs are also important mechanotransducers that play a significant role in sensing mechanical loading forces and remodeling the tissue (Simmons

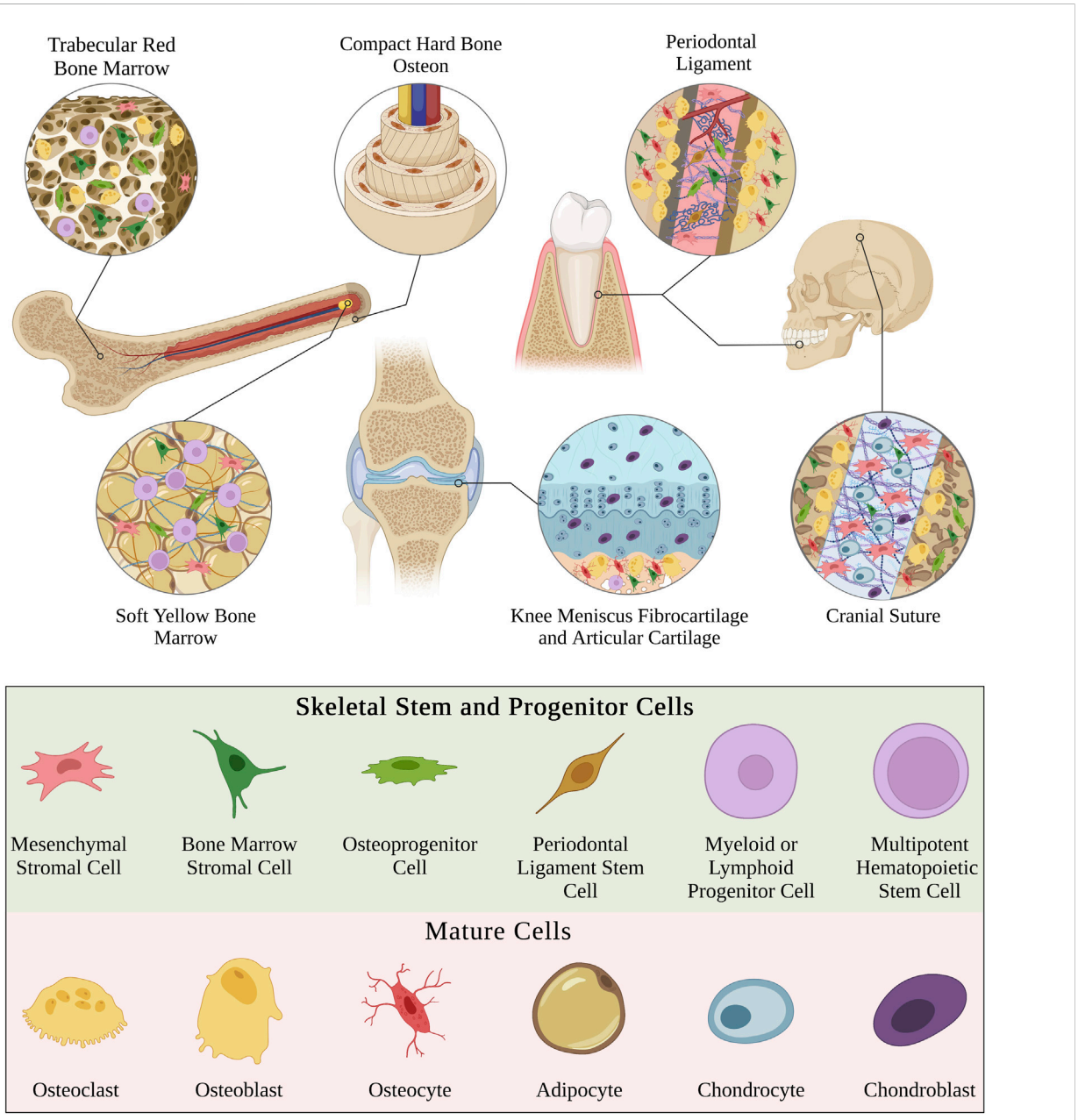

FIGURE 1
Schematic highlighting diverse examples of different types of skeletal tissues. Note that the physical microenvironment is unique in each type of skeletal tissue and therefore contains different combinations, quantities, and distributions of cell phenotypes. The cell phenotypes displayed throughout this figure are depicted in the bottom legend. This legend holds for the rest of the figures within this manuscript. Figure created with BioRender.com.

et al., 2003; Jagodzinski et al., 2004; Li et al., 2004; Scaglione et al., 2008; Grellier et al., 2009). However, the mechanisms by which mechanical forces and physical microenvironments elicit specific SSPC responses have historically remained elusive partially due to the lack of tools to engineer microenvironments with well-controlled physical properties to study SSPC response behaviors (Naqvi and McNamara, 2020). This review aims to highlight important biochemistry mechanisms involved in SSPC mechanotransduction and how tissue engineering strategies have been used to control and study SSPC mechanobiology in different microenvironments.

Mechanobiology is a rapidly emerging field concerned with how cells sense, process, and respond to mechanical information resulting from the extracellular environment (Jansen et al., 2015). It has flourished coinciding with the development and characterization of novel biomaterials and biomaterial construct fabrication methods; engineered biomaterial constructs act as extracellular microenvironments with well-controlled physical properties that allow tissue engineers to study the effects of these properties on the behaviors of different cell types (Hanson et al., 2014; Shafiq et al., 2021). Recent improvements in the understanding of SSPC mechanobiology have lent themselves to inform the next-generation of therapeutic biomaterials and tissue engineering strategies, which account for both physical and chemical cues to guide skeletal tissue and bone regeneration with higher degrees of predictability (Cha et al., 2012; Rahmati et al., 2020). Herein, this review divides biomaterial and tissue engineering physical properties into two main classes (i.e., static or dynamic physical properties) as microenvironment design considerations that guide SSPC behavior and fate.

2 Skeletal stem and progenitor cell classification in this review

There is a history of controversy and debate over what exactly constitutes a *bona fide* skeletal stem or progenitor cell due to different reported detection methods, isolation, and functional evaluation (Ambrosi et al., 2019). Bone and skeletal tissues are made up of many heterogeneous stem and progenitor cell lineages that work in conjunction to recruit active hematopoiesis and maintain the integrity of the skeleton (Bianco and Robey, 2015; Serowoky et al., 2020; Li et al., 2022). Several terminologies have been used synonymously in the literature to refer to different sets and subsets of these heterogenous SSPC populations including: 'multipotent mesenchymal stem/stromal cells' (MSCs), 'bone marrow mesenchymal stem/stromal cells' (BMSCs), and 'skeletal stem cells' (SSCs) (Derubeis and Cancedda, 2004; Lindner et al., 2010; Bianco and Robey, 2015; Bhat et al., 2021). Despite being used interchangeably, these terminologies do not mean the same thing and their broad definitions that lack specificity has created an inconsistency in the literature (Ambrosi et al., 2019).

The ISCT minimal criteria for defining the MSC phenotype (Dominici et al., 2006) is an enormously broad definition encompassing cell lineages that have been isolated from many tissues including skeletal, muscular, cardiac, and adipose (Covas et al., 2008; Orbay et al., 2012; Garikipati et al., 2018; Pilato et al., 2018; Pittenger et al., 2019). MSCs isolated from different tissue sources have been experimentally shown to have different transcriptomic profiles and vastly differing differentiation properties (Sacchetti et al., 2016). Importantly, transplanted MSCs isolated from non-skeletal tissues lacked *in-vivo* osteogenic potential and failed to form any histology-proven bone (Sacchetti et al., 2016). Thus, there has been a push towards using the more specific terminology of BMSC or SSC when referring to the subset of MSCs that have been isolated from skeletal tissues, which do demonstrate *in-vivo* osteogenic potential after transplantation and form histology-proven bone (Sacchetti et al., 2007; Bianco et al., 2008; Bianco and Robey, 2015; Sacchetti et al., 2016). Skeletal stem cells defined in this context are an important step toward establishing a definition for a *bona fide* SSPC population, but there are still further caveats within this broad classification. For example, specific markers like Axin2 are expressed in lineages isolated from craniofacial skeletal tissues but are nearly absent in lineages isolated from appendicular skeletal tissues (Maruyama et al., 2016). The different phenotypes among these skeletal stem cell lineages result in different differentiation capacities, functions, and abilities to form hematopoietic and adventitial structures (Ambrosi et al., 2019).

There have been recent evidence-based proposals to enact better criteria for defining a *bona fide* SSPC population and more nomenclature that further specify subsets of SSPC lineages (Ambrosi et al., 2019). Future investigations should be more conscious of how they define the SSPC lineages that they use. This review acknowledges this problem but will broadly define SSPCs as all the heterogeneous stem cell lineages isolated from skeletal tissues that meet the minimum criteria of being multi-potent, self-renewing, and necessary in facilitating the hematopoietic environment or regulating the structural state of bone tissue. Thus, SSPCs in this context include all aforementioned terminologies and others relevant to the regeneration of skeletal tissues since their mechanosensitive mechanisms and microenvironmental response behaviors are generally conserved.

3 Relevant biochemistry in skeletal tissue mechanotransduction

Mechanotransduction is at the heart of mechanobiology as it describes the biomolecular mechanisms by which a cell converts a mechanical input into a biochemical signal output dictating a cellular response (Jaalouk and Lammerding, 2009; Martino et al., 2018). SSPCs are particularly mechanosensitive as recent investigations have revealed and elucidated several mechanisms of mechanotransduction that result in their awareness and unique behaviors in different physical microenvironments. The following subsections present a brief introductory overview of the currently understood major mechanotransduction pathways, and their relevance to SSPCs, which are generally conserved in other cell phenotypes as well. These biomolecules and pathways are especially well-studied for SSPCs subject to engineered artificial microenvironments, making them an essential knowledge precursor to designing tissue engineering strategies that guide SSPC proliferation and regeneration.

3.1 Focal adhesion kinase

Focal adhesion kinase (FAK) is a non-receptor protein tyrosine kinase found within the cytosol that is referred to as protein-tyrosine kinase-2 (PTK2) in humans (Zachary, 1997; Mitra et al., 2005). FAK is involved in many biochemical pathways controlling cell motility, focal adhesion to the extracellular matrix, cell stiffness, and actin cytoskeleton dynamics (Mitra et al., 2005; Fabry et al., 2011; Yu et al., 2018; Scott et al., 2021). FAK is associated with most of these pathways as a molecular sensor of force that initiates biochemical signals to yield a specific SSPC response. More specifically, FAK acts as a tension sensor between F-actin fibers in the cytoskeleton and the integrins involved in focal adhesions to the extracellular matrix (Bauer et al., 2019; Scott et al., 2021). FAK possesses this ability through its three-domain structure consisting of a kinase active domain sandwiched between a FERM domain, associated with the cell membrane at the focal adhesion, and a FAT domain, associated with the F-actin cytoskeleton fiber (Mitra et al., 2005). The kinase domain is in contact with the FERM domain in the native FAK conformation, blocking the active site of the kinase domain from phosphorylation and subsequent activation (Bauer et al., 2019). Sufficiently high tension between the focal adhesion and F-actin cytoskeleton reversibly unfolds and elongates FAK due to the FERM and FAT domains being pulled in separate directions, exposing the kinase domain. This event causes FAK to become phosphorylated and allows for complexation with Src protein-tyrosine kinase, leading to the subsequent phosphorylation and activation of FAK. In the absence of sufficiently high tension or once the cell relaxes the F-actin cytoskeleton tension in response to FAK activation, FAK will close back into its native low-energy conformation and become inactive (Zhou et al., 2015; Bell and Terentjev, 2017; Bauer et al., 2019). This intricate mechanism is involved in SSPC detection of the stiffness, surface texture, and dimensionality of their environment. Ultimately, the activation of FAK leads to the phosphorylation of many substrates that induce several downstream signaling pathways (Schlaepfer et al., 2004); SSPCs are influenced by the activation state of FAK to craft a unique response to their physical microenvironment (Biggs and Dalby, 2010).

3.2 RhoA/ROCK GTPases

GTPases are a class of proteins that hydrolyze GTP to GDP and transduce signals by cycling between GTP-bound active states and GDP-bound inactive states (Etienne-Manneville and Hall, 2002). Rho-family GTPases are a subset of GTPases that are generally involved with cell migration by the remodeling of cellular architecture, which in SSPCs plays an integral role in controlling differentiation and proliferation (Sadok and Marshall, 2014). The most investigated Rho GTPase pathway in SSPC mechanobiology is the Ras-homolog gene family member A (RhoA)/Rho-associated coiled-coil containing protein kinases (ROCK) pathway (Strzelecka-Kiliszek et al., 2017). The RhoA/ROCK pathway transduces signals in response to changes in the F-actin cytoskeletal network as it is affected by F-actin polymerization or depolymerization events, which provides a steady feedback mechanism for SSPCs to regulate their cytoskeleton dynamics and stability (Arnsdorf et al., 2009; Chen and Jacobs, 2013; Martino et al., 2018). The RhoA/ROCK pathway can additionally be activated in response to FAK activation to propagate downstream signals but can also feed into the phosphoryl activation of FAK. In general, the activation of these pathways starts with RhoA activating ROCK to promote the synthesis of stress fibers, which are contractile actin filaments in the cytoskeleton (Tojkander et al., 2012; Scott et al., 2021). Stress fiber formation results in increased cytoskeletal tension that forcibly opens nuclear pores allowing for the nuclear translocation of YAP/TAZ (Section 3.3), which promotes osteogenesis in SSPCs (Elosegui-Artola et al., 2017; Strzelecka-Kiliszek et al., 2017). For the simplicity of this review, it suffices to consider the RhoA/ROCK pathway as a common mediator signal in the mechanotransduction pathways that signal downstream events to occur involved with cell migration, SSPC differentiation fate, and SSPC proliferation via their modulation of cytoskeletal dynamics and interactions with other signaling molecules.

3.3 YAP/TAZ

Yes-activated protein (YAP) and transcriptional co-activator with PDZ-binding motif (TAZ) are homologous transcriptional co-activator proteins that influence the expression of genes controlling cell differential fate in SSPCs (Heng et al., 2020). More specifically, YAP/TAZ is heavily implicated in controlling SSPC specification towards adipogenic, osteogenic, or chondrogenic fate through mechanotransduction pathways that promote or inhibit YAP nuclear translocation (i.e., activation) from the cytoplasm or the phosphoryl tagging of YAP for cytosolic degradation (Karystinou et al., 2015; Chang et al., 2017; Pan et al., 2018; Scott et al., 2021). It has been well demonstrated that YAP nuclear translocation and activation inhibit chondrogenesis and adipogenesis, but its role in osteogenesis is conflicting and likely more nuanced. Some evidence suggests that the nuclear translocation of YAP inhibits osteogenesis because of YAP complexation and inhibition of Runx2, a vital transcription factor for osteogenesis (Sen et al., 2015; Chang et al., 2018). However, more recent studies are increasingly associating YAP nuclear translocation with promoting osteogenesis due to YAP binding transcriptional enhancer-associated domain (TEAD) to initiate the transcription of genes related to osteogenesis (Kegelman et al., 2018; Pan et al., 2018; Swanson et al., 2022). The role of YAP in promoting osteogenesis in SSPCs is probably more nuanced than previously thought as activator protein 2a (AP2a) competes with Runx2 to bind YAP in the nucleus, allowing Runx2 to remain free to promote the transcription of genes for osteogenesis (Lin et al., 2018). Furthermore, the AP2a-YAP complexes were shown to interact with the BARX1 promoter to inhibit BARX1 transcription; since BARX1 inhibits osteogenic differentiation, this event helped to promote osteogenesis (Lin et al., 2018). Ultimately, YAP is a complex protein involved in the late stages of the mechanotransduction pathway for SSPCs which favors osteogenic differentiation during nuclear translocation under the right conditions (e.g., AP2a presence), but may inhibit osteogenesis if these conditions are not met (Sen et al., 2015; Kegelman et al., 2018; Lin et al., 2018).

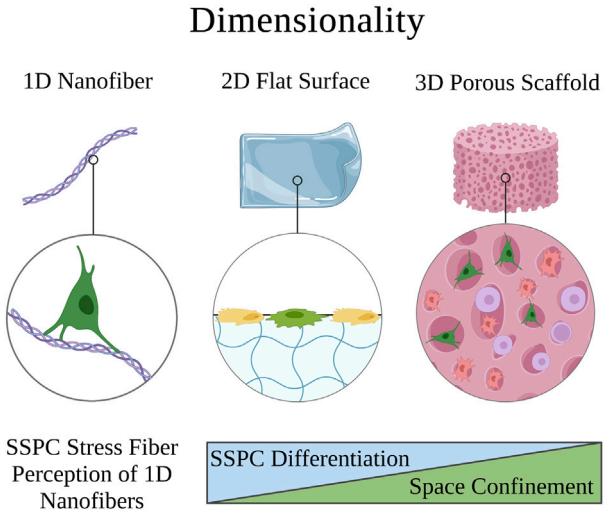

FIGURE 2
Visual overview of how the perceived microenvironment dimensionality affects SSPC behavior. SSPCs form focal adhesions to surfaces to perceive their dimension. Single nanofibers can be approximated as 1D surfaces and are still perceivable to SSPCs through one or more focal adhesions. 2D microenvironments generally allow SSPCs to spread their shape out into a pancake structure, which promotes differentiation. On the contrary, 3D microenvironments typically confine SSPCs to a more rounded shape, which is associated with maintaining stemness or sometimes promoting adipogenesis or chondrogenesis. A legend depicting the cell phenotypes can be found at the bottom of Figure 1. Figure created with BioRender.com.

3.4 Piezo1/2

The Piezo1/2 ion channels similarly play an important role in the mechanism of mechanotransduction in SSPCs. These transmembrane proteins are composed of numerous transmembrane domains and large extracellular domains, forming a mechanically sensitive complex (Qin et al., 2021). When subjected to mechanical stimuli, such as fluid shear stress or stretching, Piezo1/2 channels experience conformational changes that allow the influx of calcium ions into the cell (Qin et al., 2021). This rise in intracellular calcium triggers a cascade of downstream signaling events, including the activation of various intracellular pathways involved in cell proliferation, differentiation, and gene expression (Fang et al., 2021; Qin et al., 2021).

In the context of SSPCs and bone differentiation, the Piezo1/2 mechanism of mechanotransduction has significant implications. Mechanical forces exerted on skeletal stem cells through physical activity or external loading influence their fate determination and lineage commitment. Activation of Piezo1/2 channels in response to these forces leads to an increase in intracellular calcium levels, initiating a series of molecular events that regulate osteogenic differentiation (Zhou et al., 2020; Ma et al., 2022). This calcium signaling, in conjunction with other signaling pathways, promotes the expression of osteogenic genes and the activation of transcription factors that drive the differentiation of skeletal stem cells into osteoblasts, the bone-forming cells (Li et al., 2019; Zhou et al., 2020; Ma et al., 2022). Consequently, the Piezo1/2 mechanism serves as a critical link between mechanical cues and the regulation of skeletal stem cell behavior, ultimately impacting bone remodeling, adaptation to mechanical stress, and overall skeletal health.

4 Static biomaterial strategies

Static biomaterial strategies in this context are defined to be biomaterial systems with fixed physical properties that do not inherently change over most periods of time. Such is often the case with non-active biomaterial constructs, whose properties are determined strictly by their material properties and method of fabrication. For example, titanium dental implants have the fixed material properties of titanium but can be 3D-printed with different structures and surface topologies to affect osseointegration differently (Lee et al., 2022). These subsections explore commonly controlled properties in non-active biomaterial constructs that have been demonstrated to influence the mechanobiology of SSPCs.

4.1 Dimensionality

Biomaterial constructs are typically two-dimensional (2D; e.g., flat nanofibrous surface) or three-dimensional (3D; e.g., spherical nanofibrous pore) but can also be effectively unidimensional (1D) in the case of single nanofibers (Fang et al., 2022) (Figure 2). The dimensionality of the extracellular environment is sensed by SSPCs by influencing the confinement of their cytoskeletal shape (Robey and Riminucci, 2020; Fang et al., 2022). Specifically, SSPCs spread out on 2D surfaces into 'pancake' structures due to a lack of confining static forces in all dimensions (Robey and Riminucci, 2020). This spread, flat shape in SSPCs has been demonstrated to cause increased RhoA activity promoting osteogenesis through the actin-myosin-generated tension in the cytoskeleton (McBeath et al., 2004; Hodge and Ridley, 2016). The increased activity of RhoA increases the activity of ROCK downstream which phosphorylates myosin light-chain kinase and inhibits myosin phosphatase to increase myosin activity (Totsukawa et al., 2000; Scott et al., 2021). This promotes stress fiber formation generating force to open the nuclear pores for YAP nuclear translocation resulting in the promotion of osteogenesis (Tojkander et al., 2012; Elosegui-Artola et al., 2017; Zarka et al., 2022). Conversely, culturing SSPCs in 3D structures allows them to maintain a more rounded, confined shape due to the confining static forces in all dimensions (Remuzzi et al., 2020). This results in the cytoplasmic retention of YAP from the observed decrease in nuclear pore diameter; consequently, there is an upregulation of genes associated with stemness in SSPCs (Heng et al., 2020; Remuzzi et al., 2020). These results ultimately present a fundamental biomaterial strategy to influence SSPCs in a bone tissue engineering context by choosing 2D or 3D biomaterial constructs as the desired platform. Additionally, it suggests that the sensed dimensionality of the microenvironment in different skeletal tissues and regions evolved to purposefully play a role in guiding necessary SSPC shape and fate (Figure 2).

4.2 Porosity and pore size

Porosity is typically associated with 3D biomaterial scaffolds and refers to the average volume of void space (pores) in a given bulk volume of the scaffold. The pores are oftentimes size-controlled with modern porous scaffold fabrication techniques (Loh and Choong, 2013; Chen et al., 2020; Swanson and Ma, 2020). Historically, pores

were thought to facilitate the success of tissue engineering constructs by enabling cell and tissue ingrowth rather than fibrous encapsulation (Nunes et al., 1997; Koh and Atala, 2004). More recent evidence suggests that pores may alter the mechanical strain and density of cells, affecting regenerative responses among other potential mechanisms (Swanson et al., 2022). Both the porosity and pore size of biomaterial scaffolds have been demonstrated to affect SSPC behaviors (Figure 3) (Swanson et al., 2022).

SSPCs are most abundantly observed in the bone marrow located in the trabecular bone, which is extremely porous with an average porosity of 79.3%, indicating this evolved design plays a role in the biology of SSPCs (Renders et al., 2007). Scaffolds with higher porosities, given fixed pore size, have been demonstrated to increase SSPC proliferation, migration, and osteogenic differentiation (Aarvold et al., 2013; Dawson et al., 2018). This is hypothesized to be mainly a consequence of increased surface area, which has been demonstrated to lower focal adhesion down-regulating the FAK/RhoA/YAP pathway which promotes gene expression for osteogenesis and osteogenic differentiation (Chang et al., 2018; Dawson et al., 2018). Nonetheless, lower porosity scaffolds do still promote SSPC proliferation compared to non-porous biomaterials, and could perhaps serve useful in applications where maintaining SSPC stemness is crucial such as cranial-suture regeneration, where it is advantageous to maintain a stem cell population rather than purely facilitate osteoblast differentiation (Swanson et al., 2021).

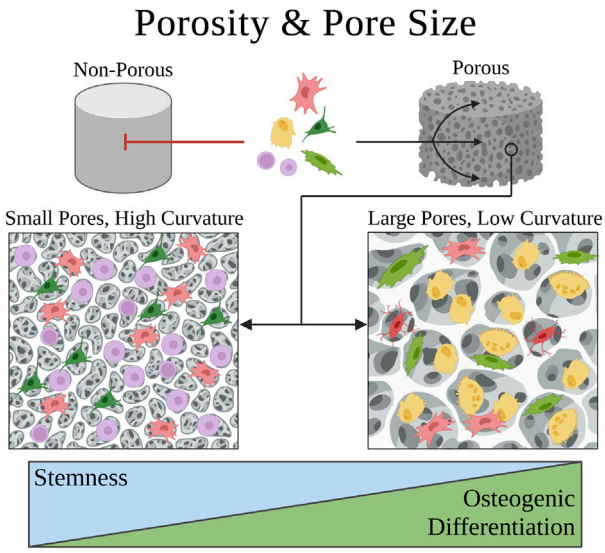

FIGURE 3
Schematic of how porosity and pore size affect SSPC penetration into a biomaterial and their differential behavior within a biomaterial construct, respectively. SSPCs require a porous biomaterial microenvironment for integration and migration within the construct. The pore size within the biomaterial dictates the principal curvature of the surface, which dictates the degree of confinement imposed on SSPCs. Small pores have high principal curvature and thus impose more shape confinement on SSPCs to promote proliferation and the maintenance of stemness. Conversely, larger pores have lower principal curvatures and impose less shape confinement on SSPCs to promote differentiation and osteogenesis. A legend depicting the cell phenotypes can be found at the bottom of Figure 1. Figure created with BioRender.com.

The specific geometric design of pores provides additional design criteria to tune the cell-biomaterial interface (Figure 3). For example, spherical macropores introduce curvature in the biomaterial matrix, where pore size (diameter) influences the curvature experienced by cells in contact with the matrix (Figure 3). It has been demonstrated that the principal curvature of a surface differentially induces cytoskeletal strain and the reorganization of SSPC cytoskeletons (Swanson et al., 2022). The pore size determines the constraint and static force exerted on SSPC cytoskeletons, which was shown to modulate if SSPCs differentiated or maintained stemness via regulation of the YAP/TAZ pathway (Swanson et al., 2022). Sufficiently small pores (<125 μm diameter) with high principal curvature facilitated the upregulation of YAP phosphorylation and its premature degradation in the cytosol to cause maintenance of SSPC stemness within the cell-biomaterial construct. On the contrary, sufficiently large pores (>250 μm diameter) promoted YAP/TAZ complexation and translocation to nuclear targets to induce robust osteogenic differentiation both *in-vivo* and *in-vitro* (Swanson et al., 2022). This is an especially interesting result considering that human trabecular bone has been observed to have a pore size distribution from 50 μm to 850 μm, further suggesting that SSPCs evolved to be mechanosensitive to pore size (Doktor et al., 2011).

4.3 Surface topography

Surface topography in a biomaterial context is defined as the interface between the cells and biomaterial, which is often designed to exhibit specific architectures on the micro- and nanometer dimensions or to be a smooth surface (Swanson and Ma, 2020; Vermeulen et al., 2021). SSPCs reside in the trabecular bone, which has a spongy surface topography and interpenetrating extracellular matrix of fibrous collagen type I (Liu and Ma, 2004; McNamara, 2017). Thus, biomaterial strategies that seek to mimic the surface topography of the physical microenvironment in which SSPCs are naturally observed in the bone commonly aim to recreate this nanofibrous surface topography, which has been shown to facilitate cell and protein adhesion compared to smooth matrices (Figure 4) (Vasita and Katti, 2006). Chang et al., 2018 isolated SSPCs from bone marrow and individually cultured cells on either an electrospun, nanofibrous gelatin methacrylate hydrogel (resembles collagen) or a smooth-surface gelatin methacrylate hydrogel. The authors found that SSPCs cultured on nanofibers exhibited higher alkaline phosphatase activity suggesting that nanofibers promote SSPC differentiation and osteogenesis compared to smooth-surface topographies.

Investigation into the mechanism of action led the authors to propose that SSPCs cultured on nanofibers had less focal adhesion causing lower FAK activity and consequently, lower RhoA/ROCK activity (Chang et al., 2018). They further suggested that this downregulation of RhoA/ROCK led to less cellular actin polymerization necessary to translocate YAP from the cytoplasm to the nucleus, ultimately lowering nuclear YAP expression in SSPCs cultured on nanofibers. Because YAP is known to complex with and inhibit Runx2, a vital transcription factor for initiating osteogenic differentiation and osteogenesis, the authors concluded that the decrease in nuclear YAP resulted in increased free Runx2 to initiate

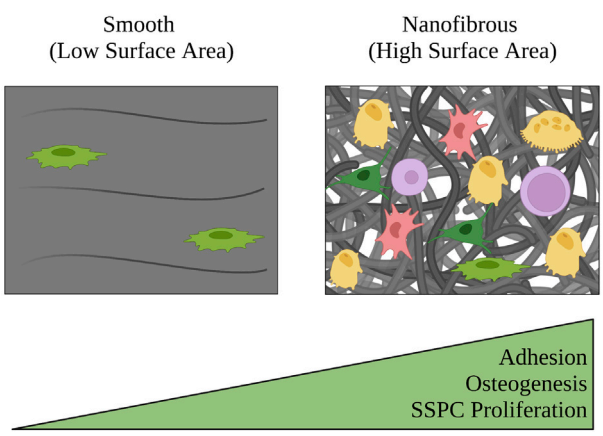

FIGURE 4
Depiction of how the surface topology of a microenvironment affects SSPC proliferation and behavior. Nanofibers are an ideal surface topology for SSPCs because they maximize surface area. This promotes cell adhesion, proliferation, and generally SSPC differentiation towards an osteogenic fate. A legend depicting the cell phenotypes can be found at the bottom of Figure 1. Figure created with BioRender.com.

the synthesis of alkaline phosphatase causing the enhanced differentiation of SSPCs on nanofibers (Zaidi et al., 2004; Chang et al., 2018). This suggests that the collagen nanofibers found in trabecular bone serve the same effect on the mechanobiology of SSPCs. These results have been extensively replicated with nanofibrous surfaces also created from chitosan, poly-*L*-lactic acid, carbon nanotubules, and other biomaterials where a similar upregulation of Runx2 activity is observed, which promotes alkaline phosphatase and osteocalcin expression as biomarkers of osteogenesis and bone maturation (Ho et al., 2015; Zhang et al., 2016; Das et al., 2018; Yu et al., 2020). There is overwhelming evidence in the literature to suggest that fibrous, and particularly nanofibrous, biomaterials with high surface areas are crucial to SSPC adhesion, proliferation, and differentiation to facilitate osteogenesis (Figure 4); therefore, smooth biomaterial constructs should probably be avoided for skeletal tissue regeneration.

4.4 Matrix stiffness

Extracellular matrix and biomaterial stiffness are typically defined by Young's Modulus, which describes the magnitude of stress needed to strain a material a given distance. SSPCs and most other stem cells sense the stiffness of their extracellular environment by forming focal adhesions and stress fibers to the surrounding substrates of their microenvironment; this event is followed by constriction of the cellular actin cytoskeleton to generate tension in these adhesion connections and therefore the material of the substrate (Guilak et al., 2009; Burridge and Guilluy, 2016; Smith et al., 2017; 2018; Naqvi and McNamara, 2020). If the material is soft with a low Young's Modulus, this tension exerted by the cell on the material will cause the material to strain toward the cell, allowing the cell to maintain a more rounded shape (Figure 5). Conversely, if the material is stiff with a high Young's Modulus, the tension exerted by the cell on the material will strain the cell in the directions of the focal adhesions and stress fibers, causing the cell to stretch out into a flatter pancake shape (Figure 5) (Engler et al., 2006; Sun et al., 2018a; Piroli and Jabbarzadeh, 2018). This is important in the context of influencing SSPC differential fate via the FAK/Rho/YAP mechanotransduction pathway (Dupont et al., 2011; Cai et al., 2021; Li et al., 2021; Scott et al., 2021). Specifically, soft biomaterials have been well demonstrated to guide SSPCs toward adipogenesis, soft to medium stiffness biomaterials promote chondrogenesis, and stiff to rigid biomaterials guide SSPCs toward osteogenesis (Flynn and Woodhouse, 2008; Young et al., 2013; Olivares-Navarrete et al., 2017; Sun et al., 2018b; Smith et al., 2018; Zhang et al., 2018; Roncada et al., 2022; Tang et al., 2022).

Quantitatively, the stiffness of these biomaterials tends to dictate SSPC differential fate in the direction of which natural tissue extracellular matrix Young's Modulus it most closely resembles, which makes intuitive sense. That is, biomaterials promoting adipogenesis typically have a Young's Modulus in the range of that of adipose tissue (0.5–2 kPa), biomaterials promoting chondrogenesis typically have a Young's Modulus in the range of cartilage tissue (500–2000 kPa or 0.5–2 MPa), and biomaterials promoting osteogenesis typically have a Young's Modulus above these ranges (Rho et al., 1993; Comley and Fleck, 2010; Cox and Erler, 2011; Handorf et al., 2015; Kabir et al., 2021). Ultimately, human SSPCs have evolved to sense the mechanical properties of their extracellular microenvironment as a mechanism to guide proper differentiation in skeletal tissues. Biomaterials that seek to regenerate skeletal tissues can take advantage of this evolved mechanobiology by mimicking their Young's Moduli (Kozaniti et al., 2022).

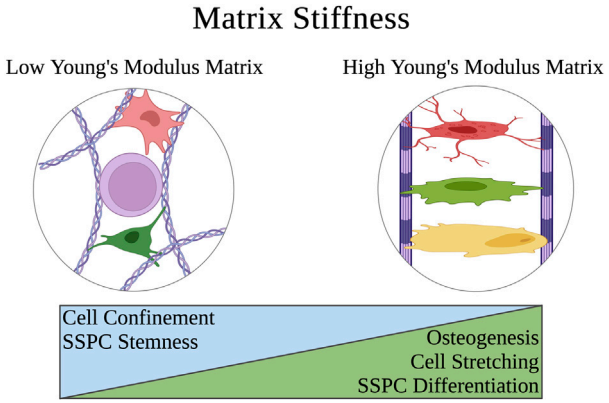

FIGURE 5
Schematic of how the extracellular matrix stiffness of a physical microenvironment affects SSPC shape confinement and therefore their behavior. Soft matrices have a low Young's modulus that allows SSPCs to easily deform the matrix when creating cytoskeletal tension on the matrix at the points of stress fiber adhesion. This allows the SSPCs to maintain a rounded, confined shape that is associated with maintaining stemness. On the contrary, rigid matrices with a high Young's modulus resist deformation when SSPCs exert tension on them which instead causes the SSPC to deform and spread its shape out into a pancake structure. This promotes differentiation and osteogenesis. A legend depicting the cell phenotypes can be found at the bottom of Figure 1. Figure created with BioRender.com.

5 Dynamic biomaterial and tissue engineering strategies

Dynamic strategies in this context are defined to be biomaterial systems with the capacity for inducible changes in their physical properties that effectively change the microenvironment or exert dynamic forces over short periods of time. This requires active biomaterials that can change their physical properties in response to chemical or physical stimuli, such as a piezoelectric material that elongates in an electric field to exert an increased surface tension force along an anchored cell. Additionally, inherently dynamic properties like viscoelasticity are also relevant because they determine how cells physically remodel the microenvironment in time. This can also involve artificial systems that are not necessarily biomaterial in nature but serve the purpose of simulating a dynamic environment (e.g., a dynamic-pressure chamber on a cell culture). Such dynamic strategies are much more limited in the literature but are nonetheless important because they provide an informative basis for how SSPCs respond to acute microenvironment changes and forces, such as those experienced in physical exercise. SSPCs live in a highly dynamic environment and are known to remodel skeletal tissue in response to dynamic forces (Liu et al., 2022); mechanobiological investigations of this phenomenon are necessary to achieve a better understanding of skeletal tissue biology and to design next-generation tissue engineering strategies.

5.1 Mechanical loading systems

Mechanical loading systems are engineered *in-vitro* systems that use the aid of powered machines (e.g., microfluidic injector) or utilities (e.g., vacuum pump) to exert dynamic forces on cultured cells. These devices are oftentimes used to study the behavior of different cells in response to varied magnitudes and exposures to mechanical loading forces, usually compressive or shear forces (Figure 6). Historically, osteocytes were thought to be the dynamic force sensors in the bone because osteons in the hard cortical bone, where the osteocytes reside, receive most of the mechanical loading during physical movement which directly compresses and strains the osteocytes (Weinbaum et al., 1994; Burger and Klein-Nulend, 1999; Taylor et al., 2007; Hart et al., 2017). Although osteocytes are indeed dynamic force sensors that play a role in remodeling skeletal tissue in response to dynamic loading forces, there was a surge of discoveries in the early 2000s demonstrating that SSPCs are also mechanosensitive and aid in the remodeling process with respect to dynamic forces and mechanical loading (Simmons et al., 2003; Jagodzinski et al., 2004; Li et al., 2004; Scaglione et al., 2008; Grellier et al., 2009). This was studied and proved in many cases using mechanical loading systems. Grellier et al., 2009 adapted a parallel-plate culture flow chamber to exert 12 dynes/cm^2 of laminar fluid shear stress on a flat layer of cultured human-derived SSPCs for 30 and 90 min. They observed an increase in alkaline phosphatase mRNA and connexin43 gene expression, which are associated with osteoblastic lineages and activity (Guillotin et al., 2004). These results suggested that SSPCs are responsive to fluid flow and are specifically driven towards an osteoblastic differential fate in response to shear stress from fluid flow, which thereby promotes osteogenesis. Other studies have adopted similar fluid flow systems and experimental setups with SSPCs to support that mechanical loading in the form of fluid shear stress does induce osteogenic differentiation in SSPCs (Yourek et al., 2010; Sun et al., 2022). SSPC mechanosensitive behavior to fluid shear stress has been demonstrated to result from cell-shape elongation activating the Rho/ROCK/YAP pathway, TRPV4 and Piezo1 mechanosensitive ion channels, and primary cilia, which all collectively transduce the shear stress mechanical signals (Hu et al., 2017; Johnson et al., 2018; Li et al., 2019).

Similarly, Jagodzinski et al., 2004 adopted a cell stretching system to cyclically strain a cultured monolayer of SSPCs longitudinally. They found that a cyclic mechanical strain of 8% applied for 2-h durations three times a day, over 3 days, was able to commit SSPCs to an osteogenic differential fate and acted as a stronger differentiation factor than dexamethasone, a small molecule previously shown to promote SSPC differentiation towards osteoblast fate (Byers et al., 1999). Lohberger et al., 2014 replicated these findings with a similar experiment utilizing the Flexcell FX-5000 Tension System, a mechanical loading system that a computer-controlled vacuum to strain cells adhering to a silicon membrane (Figure 6). For 7 days, they applied continuous cycles consisting of 10 s of mini strain cycles (i.e., five back-to-back cycles of 10% elongation held for 2 s) followed by 30 s of relaxation. They found that the mechanically stimulated groups of SSPCs deposited higher amounts of calcium and alkaline phosphatase into the culture while also increasing their expression of osteogenesis-specific markers (e.g., SPARC, BMP2, SSP1, BGLAP, Col1A1) suggesting that this group of SSPCs was driven towards osteogenic differential fate (Lohberger et al., 2014). Ultimately, the emergence of mechanical loading systems has allowed researchers to investigate the rich mechanobiology that results from the dynamic mechanical environment of bones and movement. There has been overwhelming evidence in the past few decades demonstrating that SSPCs have evolved to be highly sensitive to dynamic mechanical changes in their environment. In most cases, cyclic mechanical loading promotes osteogenesis in SSPCs and guides them to differentiate into osteoblasts (Liu et al., 2022). This is crucial for bone remodeling and serves as a mechanism for bone strengthening and density increases in response to repeated physical activity and exercise.

5.2 Active biomaterials

Active biomaterials are a relatively new class of biomaterials that have tunable physicochemical properties in both space and time (Özkale et al., 2021). This review will specifically focus on the subset of active biomaterial constructs that modulate their physical environment in response to external stimuli. These biomaterials are a useful tool for studying how dynamic changes in local mechanical properties influence the mechanobiology of SSPCs in 2D microenvironments (e.g., flat biomaterial sheet) or 3D microenvironments (e.g., porous scaffolds); furthermore, such biomaterial constructs are implantable, which allows for this mechanobiology to be studied with the added complexity of an *in-vivo* microenvironment, unlike the mechanical loading systems (Özkale et al., 2021). One of the most common examples in the

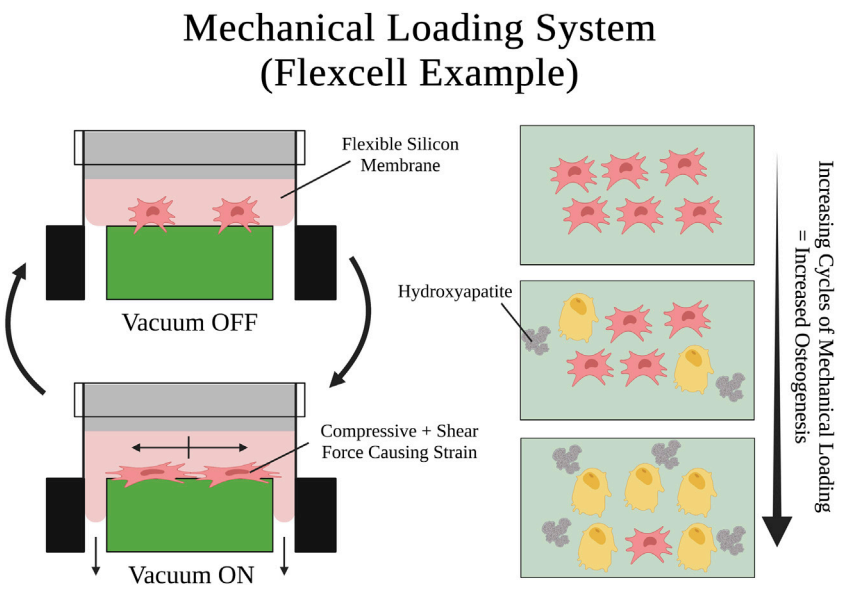

FIGURE 6
Visual schematic of an example mechanical loading system setup and a mechanical loading cycle using Flexcell®. SSPCs are elongated by the shear and compressive tension that the silicon membrane exerts on them when it is pulled by the vacuum. Many repeated cycles of this mechanical loading on SSPCs promotes osteogenic differentiation and mineralization (i.e., hydroxyapatite deposition). A legend depicting the cell phenotypes can be found at the bottom of Figure 1. Figure created with BioRender.com.

literature of active biomaterials that dynamically modulate their physical environment are hydrogels that can stiffen and soften their tensile modulus (Rosales et al., 2017; Lee et al., 2018; Günay et al., 2019). Rosales et al., 2017 created hyaluronic acid-based hydrogels that photodegrade in response to 365 nm light, softening the matrix, and photocrosslinking in response to 400–500 nm light to re-stiffen the matrix. They cultured SSPCs within these hydrogels and found cell area and nuclear YAP/TAZ concentration both positively correlated with increasing hydrogel stiffness, demonstrating that the reversible softening and stiffening of the hydrogel effectively controls the flux of YAP/TAZ between the cell nucleus and cytoplasm. Lee et al., 2018 replicated these findings with SSPCs utilizing a hydrogel made from polyacrylamide and azobenzene, which photoswitches between trans and cis conformations in the presence and absence of blue light, respectively, changing if the matrix is stiff or soft. The SSPC cells and their nuclei were shown to spread more on the stiff matrix than the soft matrix, and the extent of spreading was reversible based on the hydrogel.

More recently, Chen and Lv, 2022 advanced this concept by developing a dynamic hydrogel made from methacrylated gelatin, sodium alginate with calcium carbonate, and D-(+)-gluconic acid δ-lactone that gradually increased in stiffness from 14.63 ± 1.18 kPa to 68.37 ± 4.99 kPa within 7 days (Chen and Lv, 2022). They demonstrated *in-vitro* with SSPCs that this dynamic stiffening promoted osteogenesis more than static hydrogels that were strictly soft or stiff. Moreover, they investigated the regenerative efficacy of this dynamic biomaterial *in-vivo* within calvarial defect models and compared it with soft and stiff static hydrogels. Interestingly, they found that this dynamic stiffening biomaterial significantly enhanced angiogenesis, extracellular matrix remodeling, and bone formation in the critical-sized calvarial defects over 4, 8, and 12 weeks compared to the static soft or stiff hydrogels (Chen and Lv, 2022). The authors hypothesized that the dynamic stiffening environment promoted the expression of extracellular matrix proteins and the secretion of cytokines due to the flattening of SSPCs and subsequent YAP nuclear translocation and activation, committing them to osteogenic differential fates and promoting extracellular matrix remodeling (Lin et al., 2020; Chen and Lv, 2022). Although the exact mechanisms were not investigated, it is obvious from this experiment that SSPCs are sensitive to subtle, gradual changes in the mechanical microenvironment, and this appears to promote their activity with respect to differentiation and participation in remodeling their microenvironment. Ultimately, active biomaterials and dynamic microenvironments may confer unique advantages in bone regeneration because of their ability to activate more mechanisms in SSPCs that favor osteogenesis and other conducive processes for quality bone formation like angiogenesis and extracellular matrix remodeling (Montoya et al., 2021).

5.3 Viscoelasticity and stress relaxation

By definition, when stress is applied to biomaterials with viscoelastic properties they undergo an instantaneous, reversible elastic strain followed by a time-dependent, irreversible viscous strain (i.e., plastic deformation) that continues to increase as long as the applied stress force is greater than the biomaterial viscous force (Cohen et al., 1998; Ryeol Choi et al., 2008). Moreover, viscoelastic materials undergo stress relaxation to decrease their tensile stress and internal energy over time when held at a fixed length that puts the

body under tensile stress (McHugh et al., 1992). Many biomaterials used in skeletal tissue engineering, namely, hydrogels, have viscoelastic properties (Wu et al., 2022). Chaudhuri et al., 2016 were among the first thoroughly investigate how the viscoelastic stress relaxation rate influences SSPC fate and activity. They fixed the initial elastic modulus at 9 kPa or 17 kPa for all hydrogels and found that hydrogels that were able to relax their internal stress more rapidly (i.e., 1 min relaxation time) caused enhanced YAP nuclear translocation in SSPCs which promoted adipogenesis in the 9 kPa hydrogels, and osteogenesis in the 17 kPa hydrogels.

The authors investigated the mechanism of this behavior and demonstrated that faster matrix stress relaxation promoted SSPC spreading and dynamic shape manipulation to increase YAP nuclear translocation. This occurs because of a positive feedback loop where SSPCs repeat cycles of exerting strain on the hydrogel followed by stress relaxation (Chaudhuri et al., 2016). Each cycle of stress relaxation relieves the tension initially exerted by the cytoskeleton. This change in the cytoskeleton dynamics is transduced by the actomyosin and Rho signaling pathways to create more focal adhesions around the new plastic-deformed biomaterial by the pre-existing focal adhesions. The SSPCs repeat the cycles and continue to reinforce their focal adhesions which stretches their shape and nuclear pores for YAP nuclear translocation (Chaudhuri et al., 2016). Other studies have replicated these results *in-vivo*, *in-vitro*, and with SSPC spheroids arriving at the common conclusion that fast stress relaxing viscoelastic biomaterials promote SSPC proliferation, migration, differential fate towards osteogenesis, and fusion with surrounding tissues *in-vivo*, and mature bone formation (Darnell et al., 2017; Wu et al., 2022). The ability for the extracellular matrix to be plastically deformed and remodeled by SSPCs in viscoelastic biomaterials because of their ability to dissipate internal stress imposed by cell pulling forces, leading to plastic deformations, as opposed to purely elastic biomaterials, appears to be highly conducive to osteogenesis and bone regeneration. This is likely because such biomaterials imitate the malleable, fast-relaxing viscoelastic properties of type I collagen that lend themselves to dynamic physicochemical remodeling by SSPCs (Yamashita et al., 2002). Ultimately, the field of tissue engineering can benefit by accounting for these dynamic properties like viscoelasticity and stress relaxation.

5.4 Elasticity

It is worth mentioning that highly elastic biomaterials, such as poly(ester)urethane or poly(lactide-co-caprolactone), have been demonstrated to promote chondrogenesis with SSPCs (Jung et al., 2009; Camarero-Espinosa et al., 2020). Cartilage tissues exhibit viscoelastic properties, but they are best described as mostly elastic because they store significant amounts of elastic energy and do not stress-relax very rapidly. These properties primarily derive from type II collagen, which makes up a significant portion of most cartilage tissues, especially articular cartilage (Silver et al., 2002). Thus, SSPCs and chondrocytes in cartilage cannot physically remodel their microenvironment as easily by exerting cycles of stain followed by microenvironment stress-relaxation, as is possible in bone with type I collagen. This clearly plays a role in the mechanobiology driving SSPCs toward chondrogenesis in elastic microenvironments, but the exact mechanisms driving this chondrogenic fate have not been thoroughly investigated or well understood (Jung et al., 2009; Somoza et al., 2014; Camarero-Espinosa et al., 2020). Nonetheless, biomaterials with static and dynamic properties resembling native skeletal tissues drive SSPC differential fate toward the specific progenitors and cell types present in those tissues, as observed with viscoelastic biomaterials promoting osteogenesis and elastic biomaterials promoting chondrogenesis (Jung et al., 2009; Darnell et al., 2017; Camarero-Espinosa et al., 2020; Wu et al., 2022).

5.5 Mechanotransduction-growth factor interactions

Growth factors, such as transforming growth factor-beta (TGF-β) and platelet-derived growth factor (PDGF), facilitate cell proliferation, differentiation, and extracellular matrix synthesis (Caplan and Correa, 2011; Li et al., 2014; Wu et al., 2016; Kwak and Lee, 2019). Meanwhile, mechanotransduction signaling involves the conversion of mechanical forces into biochemical signals, triggering cellular responses and modulating tissue remodeling. By integrating these two approaches, the synergistic effects of growth factors and mechanotransduction signaling can be harnessed to enhance cell behavior, promote tissue maturation, and optimize the mechanical properties of engineered tissues (Dang et al., 2018). This integration holds great promise for advancing tissue engineering strategies, allowing the creation of functional and biomimetic tissues for various regenerative medicine applications, and is an area of active investigation where matrix-derived cues and soluble factors synergistically influence differentiation trajectories of SSPCs (Kusuma et al., 2017).

The differentiation status of SSPCs has been shown to influence their paracrine activity with distinct changes occurring during osteogenic, chondrogenic, and adipogenic lineage commitment (Choi et al., 2010). In fact, conditioned media from osteogenic SSPCs cultures, both mechanically induced and chemically induced, enhances the differentiation process in recipient cells *in-vitro* (Frith et al., 2013). In particular, mechanical loading has been shown to increase angiogenic paracrine factors within various SSPC populations, namely, MMP2, TGF, and FGF (Kasper et al., 2007). Other studies have similarly shown that limiting cell spreading (and cytoskeletal architecture) depleted VEGF, IGF, and EGF secretion (Kilian et al., 2010; Abdeen et al., 2014). These matrix-derived cues within the engineered cell microenvironment further tune the regenerative trajectory towards specific, predictable tissue fates.

6 Discussion

Skeletal tissues contain heterogeneous physical microenvironments that are sensed by SSPCs to guide their differentiation fate (Miller et al., 2015; Chen et al., 2020). Understanding how the static and dynamic physical properties of native and biomaterial microenvironments are transduced by SSPCs is an important step toward developing more predictable, quality

regenerative therapies for skeletal tissues. Certain physical properties for biomaterial designs aimed to engineer skeletal tissues appear to have a universally desirable option; for example, nanofibrous surface topologies of the SSPC microenvironment universally promote adhesion and proliferation (Nemati et al., 2019; Yu et al., 2020). In contrast, flat surface topologies are not as adhesive and limit cell proliferation and migration in general. However, most properties and design considerations lie on a spectrum where the ideal design depends on the goal of the tissue outcome. Matrix stiffness is an example of this because it lies on a continuous numerical spectrum where soft substrates promote adipogenesis, medium-stiffness substrates promote chondrogenesis, and stiff substrates promote osteogenesis (Park et al., 2011; Assis-Ribas et al., 2018). Similarly, there is good evidence that microenvironment viscoelasticity is a mechanical cue for determining whether SSPCs commit to a chondrogenic fate, which occurs in elastic materials, or an osteogenic fate, which occurs in rapid stress-relaxing viscoelastic materials (Chaudhuri et al., 2016; Begum et al., 2020).

Several factors such as pore size and perceived microenvironment dimensionality control whether SSPCs maintain a round shape and their stemness, or if they flatten out and differentiate (Clause et al., 2010). In fact, most microenvironment physical factors influence SSPC shape and thus it is important to consider the balance between these microenvironmental properties when designing biomaterials and tissue engineering strategies for skeletal tissue regeneration. Oftentimes these mechanical properties may redundantly command SSPC shape and mechanotransduction. For example, macroporous trabecular bone with a relatively stiff but fast-relaxing viscoelastic, nanofibrous extracellular matrix promotes SSPC spreading and therefore differentiation and osteogenesis (Oftadeh et al., 2015). This can be further enhanced with mechanical loading in the form of weight-bearing exercise, which further strains SSPCs through compressive force and shear fluid flow throughout the porous bone to stimulate higher rates of osteogenesis through similar redundant cell-shape spreading mechanobiology pathways (Zernicke et al., 2006). Ultimately, these physical cues work in combination with each other, as native skeletal tissues have carefully evolved to reproducibly guide the SSPCs toward their desired fates with controlled combinations of physical and chemical cues.

From an engineering perspective, it is interesting to consider the cases where different physical microenvironmental cues may conflict with each other in determining skeletal tissue outcomes. For example, consider a small-pore scaffold made from a purely elastic biomaterial with a stiff tensile modulus. The small pores would be predicted to encourage the SSPCs to maintain a rounded shape, promoting stemness, while the elastic properties of the biomaterial may also contribute to a generally more rounded SSPC shape but usually favor chondrogenesis (Begum et al., 2020; Swanson et al., 2022). In contradiction, the stiff tensile modulus tends to cause SSPCs to spread their shape which promotes osteogenic fate. But to what degree will the SSPCs spread out? Will it maintain stemness or be driven to osteogenic or chondrogenic fates? Perhaps the outcome will change if the biomaterial can actively stiffen and soften or impose artificial mechanical loading on the SSPCs.

These are important questions to investigate which will yield a greater understanding of the underlying mechanobiology of how SSPCs sense and respond to complex combinations of physical cues in their microenvironment and which properties of the microenvironment are more important in dictating SSPC differential fate. Understanding how combinations of physical microenvironment properties work synergistically to drive SSPC behavior will inform the next-generation of optimized biomaterial niches and tissue engineering strategies for regenerating skeletal tissues with higher degrees of quality and predictability. This ultimately provides tissue engineers with a control panel of physical property design customizations that can be used to control SSPC differential fate and behavior, allowing for the possibility of precisely and reproducibly engineering specific skeletal tissues that are of interest to the engineer (e.g., articular cartilage, trabecular bone) (Figure 7). Note that some design variables are independent and always applicable (e.g., dimensionality, surface topology) while other design variables are conditionally applicable depending on the choice of an independent variable (Figure 7). For example, the depicted biomaterial designed by the control panel is macroporous and thus requires the pore size to be specified (Figure 7). If the biomaterial was not macroporous then the pore size variable would not be applicable.

Among the important physical strategies for producing desirable SSPC regenerative outcomes, the studies presented on active biomaterials and mechanical loading systems suggest that dynamic physical environments and mechanical loading are universally advantageous strategies for promoting angiogenesis, migration, proliferation, and differentiation (Rosales et al., 2017; Lee et al., 2018; Günay et al., 2019; Chen and Lv, 2022). This is a relatively new area of biomaterials, tissue engineering, and mechanobiology that is ripe for exploration. Mechanisms of mechanotransduction for these dynamic properties are still under investigation especially as new tools and methods are developed for studying mechanobiology (Mohammed et al., 2019). With respect to tissue engineering, there is a lack of methods to controllably impose reversible, specific, known mechanical loading forces on 3D skeletal tissue and SSPC microenvironments *in-vivo*. An active biomaterial scaffold would be ideal for this task because they are 3D and usually implantable, but few constructs have been synthesized that can reversibly impose mechanical loading *in-vivo* to external stimuli on demand. Developing an active biomaterial tool to quantitatively investigate dynamic mechanobiology for SSPCs in a complex *in-vivo* environment would help quantify the desirable dynamic properties and mechanical loading forces necessary for a healthy skeletal microenvironment. It would be a useful tool to investigate how fluid flow through porous environments, in response to mechanical compression, mediates nutrient exchange and influences SSPC fate with shear stress *in-vivo*. Finally, it would help inform a new class of regenerative engineering strategies that utilize dynamics and statics to modulate SSPC mechanobiology for tissue repair and regeneration.

Equally crucial to developing new biomaterial constructs and tools is paramount mapping out the intricate molecular mechanisms by which SSPC mechanotransduction occurs in both static and dynamic microenvironments. Significant progress has been made on this in the past two decades with the emergence of novel tools and methods in molecular biology for studying proteomics and gene

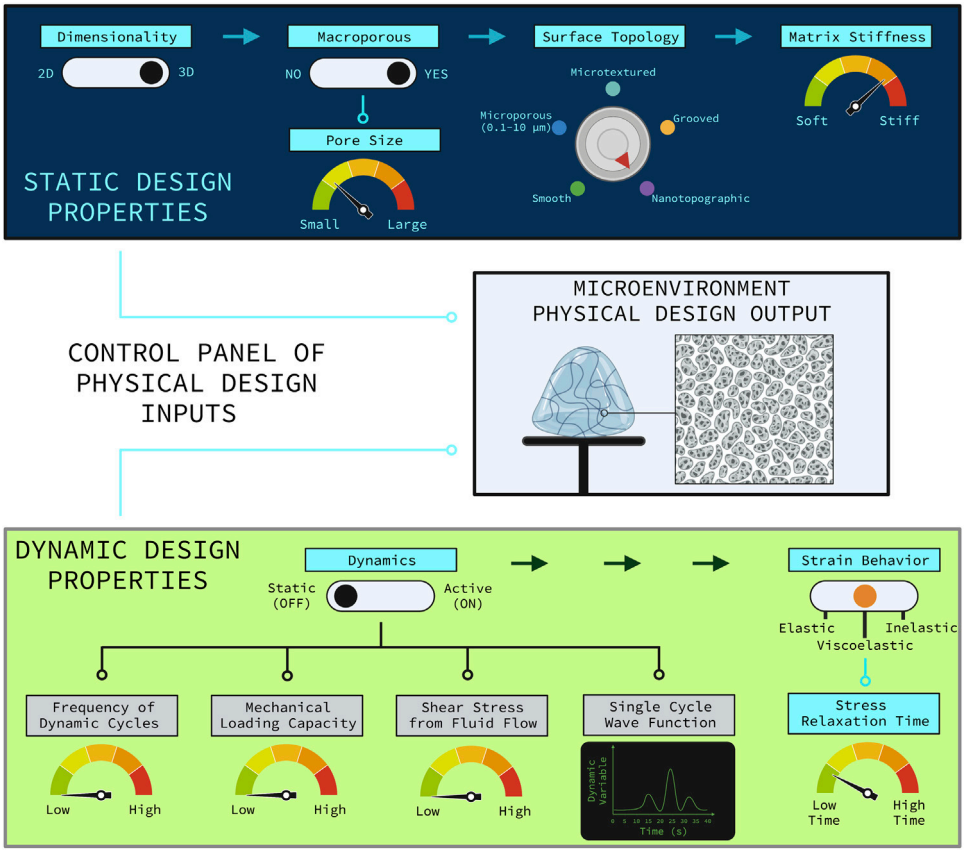

FIGURE 7
Control panel representation of the relevant physical design parameters for designing a biomaterial construct for tissue engineering. The control panel is divided into the static physical design properties (top, blue panel) and the dynamic physical design properties (bottom, green panel). The rational combination of independent and dependent design variables as illustrated allow for various combinations of unique biomaterial environments to guide SSPC trajectories in predictable ways. Design variable names are colored blue if they are applicable or grey if they are not applicable. The independent design variables are horizontally distributed with the arrows at the top of each panel. Design variables that are conditionally dependent on the choice of an independent variable are connected by nodes to the independent variable that it is conditionally dependent on. If an independent variable choice makes the conditionally dependent variable(s) applicable then the node(s) turn light blue; otherwise, the nodes are black meaning that the conditionally dependent variable(s) are not applicable. The hypothetical biomaterial physical microenvironment depicted in the middle box was designed with this control panel to be non-active with fast-relaxing viscoelastic properties, three-dimensional, macroporous with smaller sized macropores, nanotopographic (i.e., nanofibrous), and relatively stiff. Note that utilizing a non-active biomaterial significantly hinders the potential to customize the biomaterial, which generally sacrifices a degree of regenerative outcome predictability and efficacy. It is also important to note that the many static and dynamic physical properties of a microenvironment act in combination to holistically influence SSPC behavior and fate. Figure created with BioRender.com.

expression, but there is still ambiguity with the role of even the most well-studied central biomolecules in mechanotransduction. As previously mentioned, there is a history of controversy and debate as to whether YAP nuclear translocation promotes or inhibits osteogenesis (Kegelman et al., 2018; Pan et al., 2018). Most recent studies have arrived at the consensus that YAP nuclear translocation does generally promote osteogenesis, but it is unknown why many of the groups investigating nanofibrous surface topologies found that osteogenesis was promoted from a lack of YAP nuclear translocation, even though cell-shape spreading was observed (Zaidi et al., 2004; Chang et al., 2018). This dilemma suggests that other mechanotransduction pathways feed into stimulating osteogenesis not necessarily reliant on YAP. For example, Chaudhuri et al., 2016 found the same range of nuclear YAP levels in SSPCs cultured in their 9 kPa and 17 kPa viscoelastic hydrogels but observed the SSPCs differentiate towards adipogenesis in the soft hydrogel and osteogenesis in the stiffer hydrogel. Thus, nuclear YAP levels were surprisingly decoupled from SSPC fate, even though it is known to likely stimulate osteogenesis and inhibit adipogenesis (Chaudhuri et al., 2016). This demonstrates that YAP mechanotransduction and signaling are still not completely understood, and it probably plays a much more non-canonical and nuanced role in SSPC differential fate. Additionally, nuclear YAP immunohistostaining is not sufficient by itself to evaluate how SSPCs respond to physical cues or if this is what triggers their differentiation. Future investigations should look for other mechanotransduction pathways and systematically probe the behavior of known biomolecules that play a role in SSPC mechanobiology by studying their proteomics and spatiotemporal omics when SSPCs are exposed to different physical environments.

7 Conclusion

Next-generation tissue engineering strategies require an understanding of the underlying mechanobiology by which biomaterial and microenvironment physical properties influence SSPC behavior. Culturing SSPCs in artificial biomaterial microenvironments with known physical properties, both *in-vitro* and *in-vivo*, and evaluating their phenotypic outcomes has shed some perspective on how native skeletal tissues and biological materials reproducibly guide SSPC fate. Furthermore, this has led to an increased understanding of the molecular mechanisms by which skeletal organs and cells transduce mechanical stimuli. These mechanical stimuli derive from the physical properties of the microenvironment, which can be broadly categorized as static or dynamic. These properties all work in conjunction to control SSPC behavior and therefore it is paramount to consider how different combinations of all the static and dynamic physical properties in a microenvironment dictate SSPC outcomes when engineering novel strategies to regenerate skeletal tissues with precision and predictability. There are still many questions and challenges ahead in this interdisciplinary collaboration to understand and engineer the SSPC physicochemical microenvironment, but significant progress has been established in just the past decade and the field only continues to grow.

Author contributions

SW conceived the topic of research, performed the literature search, and drafted the manuscript. WS assisted with the literature search and edited and revised the writing. YM edited and revised the writing. All authors contributed to the article and approved the submitted version.

Funding

This work was supported by grants from the NIH (R01DE027662 to YM and F30DE029359 to WS).

Acknowledgments

Thank you to the publisher and the editors for the invitation to write this review.

Conflict of interest

The authors declare that the research was conducted in the absence of any commercial or financial relationships that could be construed as a potential conflict of interest.

Publisher's note

References

Aarvold, A., Smith, J. O., Tayton, E. R., Lanham, S. A., Chaudhuri, J. B., Turner, I. G., et al. (2013). The effect of porosity of a biphasic ceramic scaffold on human skeletal stem cell growth and differentiation *in vivo*. *J. Biomed. Mat. Res. A* 101, 3431–3437. doi:10.1002/jbm.a.34646

Abdeen, A. A., Weiss, J. B., Lee, J., and Kilian, K. A. (2014). Matrix composition and mechanics direct proangiogenic signaling from mesenchymal stem cells. *Tissue Eng. Part A* 20, 2737–2745. doi:10.1089/ten.tea.2013.0661

Ambrosi, T. H., Longaker, M. T., and Chan, C. K. F. (2019). A revised perspective of skeletal stem cell biology. *Front. Cell. Dev. Biol.* 7, 189. doi:10.3389/fcell.2019.00189

Arnsdorf, E. J., Tummala, P., Kwon, R. Y., and Jacobs, C. R. (2009). Mechanically induced osteogenic differentiation – The role of RhoA, ROCKII and cytoskeletal dynamics. *J. Cell. Sci.* 122, 546–553. doi:10.1242/jcs.036293

Assis-Ribas, T., Forni, M. F., Winnischofer, S. M. B., Sogayar, M. C., and Trombetta-Lima, M. (2018). Extracellular matrix dynamics during mesenchymal stem cells differentiation. *Dev. Biol.* 437, 63–74. doi:10.1016/j.ydbio.2018.03.002

Bauer, M. S., Baumann, F., Daday, C., Redondo, P., Durner, E., Jobst, M. A., et al. (2019). Structural and mechanistic insights into mechanoactivation of focal adhesion kinase. *Proc. Natl. Acad. Sci.* 116, 6766–6774. doi:10.1073/pnas.1820567116

Begum, R., Perriman, A. W., Su, B., Scarpa, F., and Kafienah, W. (2020). Chondroinduction of mesenchymal stem cells on cellulose-silk composite nanofibrous substrates: The role of substrate elasticity. *Front. Bioeng. Biotechnol.* 8, 197. doi:10.3389/fbioe.2020.00197

Bell, S., and Terentjev, E. M. (2017). Focal adhesion kinase: The reversible molecular mechanosensor. *Biophys. J.* 112, 2439–2450. doi:10.1016/j.bpj.2017.04.048

Benedetti, M. G., Furlini, G., Zati, A., and Letizia Mauro, G. (2018). The effectiveness of physical exercise on bone density in osteoporotic patients. *Biomed. Res. Int.* 2018, 4840531. doi:10.1155/2018/4840531

Bhat, S., Viswanathan, P., Chandanala, S., Prasanna, S. J., and Seetharam, R. N. (2021). Expansion and characterization of bone marrow derived human mesenchymal stromal cells in serum-free conditions. *Sci. Rep.* 11, 3403. doi:10.1038/s41598-021-83088-1

Bianco, P., Robey, P. G., and Simmons, P. J. (2008). Mesenchymal stem cells: Revisiting history, concepts, and assays. *Cell. Stem Cell.* 2, 313–319. doi:10.1016/j.stem.2008.03.002

Bianco, P., and Robey, P. G. (2015). Skeletal stem cells. *Development* 142, 1023–1027. doi:10.1242/dev.102210

Biggs, M. J. P., and Dalby, M. J. (2010). Focal adhesions in osteoneogenesis. *Proc. Inst. Mech. Eng. H.* 224, 1441–1453. doi:10.1243/09544119JEIM775

Burger, E. H., and Klein-Nulend, J. (1999). Mechanotransduction in bone—Role of the lacunocanalicular network. *FASEB J.* 13, S101–S112. doi:10.1096/fasebj.13.9001.s101

Burridge, K., and Guilluy, C. (2016). Focal adhesions, stress fibers and mechanical tension. *Exp. Cell. Res.* 343, 14–20. doi:10.1016/j.yexcr.2015.10.029

Byers, R. J., Brown, J., Brandwood, C., Wood, P., Staley, W., Hainey, L., et al. (1999). Osteoblastic differentiation and mRNA analysis of STRO-1-positive human bone marrow stromal cells using primary *in vitro* culture and poly (A) PCR. *J. Pathol.* 187, 374–381. doi:10.1002/(SICI)1096-9896(199902)187:3<374:AID-PATH257>3.0.CO;2-V

Cai, X., Wang, K. C., and Meng, Z. (2021). Mechanoregulation of YAP and TAZ in cellular homeostasis and disease progression. *Front. Cell. Dev. Biol.* 9, 673599. doi:10.3389/fcell.2021.673599

Calbet, J. A. L., Moysi, J. S., Dorado, C., and Rodríguez, L. P. (1998). Bone mineral content and density in professional tennis players. *Calcif. Tissue Int.* 62, 491–496. doi:10.1007/s002239900467

Camarero-Espinosa, S., Tomasina, C., Calore, A., and Moroni, L. (2020). Additive manufactured, highly resilient, elastic, and biodegradable poly(ester)urethane scaffolds with chondroinductive properties for cartilage tissue engineering. *Mat. Today Bio* 6, 100051. doi:10.1016/j.mtbio.2020.100051

Caplan, A. I., and Correa, D. (2011). PDGF in bone formation and regeneration: New insights into a novel mechanism involving MSCs. *J. Orthop. Res. Off. Publ. Orthop. Res. Soc.* 29, 1795–1803. doi:10.1002/jor.21462

Cha, C., Liechty, W. B., Khademhosseini, A., and Peppas, N. A. (2012). Designing biomaterials to direct stem cell fate. *ACS Nano* 6, 9353–9358. doi:10.1021/nn304773b

Chang, B., Ma, C., and Liu, X. (2018). Nanofibers regulate single bone marrow stem cell osteogenesis via FAK/RhoA/YAP1 pathway. *ACS Appl. Mat. Interfaces* 10, 33022–33031. doi:10.1021/acsami.8b11449

Chang, C. C., Chen, C. Y., Chang, G. D., Chen, T. H., Chen, W. L., Wen, H. C., et al. (2017). Hyperglycemia and advanced glycation end products (AGEs) suppress the differentiation of 3T3-L1 preadipocytes. *Oncotarget* 8, 55039–55050. doi:10.18632/oncotarget.18993

Chaudhuri, O., Gu, L., Klumpers, D., Darnell, M., Bencherif, S. A., Weaver, J. C., et al. (2016). Hydrogels with tunable stress relaxation regulate stem cell fate and activity. *Nat. Mat.* 15, 326–334. doi:10.1038/nmat4489

Chen, H., Han, Q., Wang, C., Liu, Y., Chen, B., and Wang, J. (2020a). Porous scaffold design for additive manufacturing in orthopedics: A review. *Front. Bioeng. Biotechnol.* 8, 609. doi:10.3389/fbioe.2020.00609

Chen, J. C., and Jacobs, C. R. (2013). Mechanically induced osteogenic lineage commitment of stem cells. *Stem Cell. Res. Ther.* 4, 107. doi:10.1186/scrt318

Chen, X., Hughes, R., Mullin, N., Hawkins, R. J., Holen, I., Brown, N. J., et al. (2020b). Mechanical heterogeneity in the bone microenvironment as characterized by atomic force microscopy. *Biophys. J.* 119, 502–513. doi:10.1016/j.bpj.2020.06.026

Chen, Z., and Lv, Y. (2022). Gelatin/sodium alginate composite hydrogel with dynamic matrix stiffening ability for bone regeneration. *Compos. Part B Eng.* 243, 110162. doi:10.1016/j.compositesb.2022.110162

Choi, Y. A., Lim, J., Kim, K. M., Acharya, B., Cho, J. Y., Bae, Y. C., et al. (2010). Secretome analysis of human BMSCs and identification of SMOC1 as an important ECM protein in osteoblast differentiation. *J. Proteome Res.* 9, 2946–2956. doi:10.1021/pr901110q

Clause, K. C., Liu, L. J., and Tobita, K. (2010). Directed stem cell differentiation: The role of physical forces. *Cell. Commun. Adhes.* 17, 48–54. doi:10.3109/15419061.2010.492535

Cohen, N. P., Foster, R. J., and Mow, V. C. (1998). Composition and dynamics of articular cartilage: Structure, function, and maintaining healthy state. *J. Orthop. Sports Phys. Ther.* 28, 203–215. doi:10.2519/jospt.1998.28.4.203

Comley, K., and Fleck, N. A. (2010). A micromechanical model for the Young's modulus of adipose tissue. *Int. J. Solids Struct.* 47, 2982–2990. doi:10.1016/j.ijsolstr.2010.07.001

Covas, D. T., Panepucci, R. A., Fontes, A. M., Silva, W. A., Orellana, M. D., Freitas, M. C. C., et al. (2008). Multipotent mesenchymal stromal cells obtained from diverse human tissues share functional properties and gene-expression profile with CD146+ perivascular cells and fibroblasts. *Exp. Hematol.* 36, 642–654. doi:10.1016/j.exphem.2007.12.015

Cox, T. R., and Erler, J. T. (2011). Remodeling and homeostasis of the extracellular matrix: Implications for fibrotic diseases and cancer. *Dis. Model. Mech.* 4, 165–178. doi:10.1242/dmm.004077

Dang, M., Saunders, L., Niu, X., Fan, Y., and Ma, P. X. (2018). Biomimetic delivery of signals for bone tissue engineering. *Bone Res.* 6, 25–12. doi:10.1038/s41413-018-0025-8

Darnell, M., Young, S., Gu, L., Shah, N., Lippens, E., Weaver, J., et al. (2017). Substrate stress-relaxation regulates scaffold remodeling and bone formation *in vivo*. *Adv. Healthc. Mat.* 6, 1601185. doi:10.1002/adhm.201601185

Das, P., Ojah, N., Kandimalla, R., Mohan, K., Gogoi, D., Dolui, S. K., et al. (2018). Surface modification of electrospun PVA/chitosan nanofibers by dielectric barrier discharge plasma at atmospheric pressure and studies of their mechanical properties and biocompatibility. *Int. J. Biol. Macromol.* 114, 1026–1032. doi:10.1016/j.ijbiomac.2018.03.115

Dawson, E. R., Suzuki, R. K., Samano, M. A., and Murphy, M. B. (2018). Increased internal porosity and surface area of hydroxyapatite accelerates healing and compensates for low bone marrow mesenchymal stem cell concentrations in critically-sized bone defects. *Appl. Sci.* 8, 1366. doi:10.3390/app8081366

Derubeis, A. R., and Cancedda, R. (2004). Bone marrow stromal cells (BMSCs) in bone engineering: Limitations and recent advances. *Ann. Biomed. Eng.* 32, 160–165. doi:10.1023/b:abme.0000007800.89194.95

Doktor, T., Kytýř, D., Valach, J., and Jiroušek, O. (2011). Pore size distribution of human trabecular bone - comparison of intrusion measurements with image analysis. Available at: http://hdl.handle.net/11104/0197299 (Accessed January 22, 2023).

Dominici, M., Le Blanc, K., Mueller, I., Slaper-Cortenbach, I., Marini, F., Krause, D., et al. (2006). Minimal criteria for defining multipotent mesenchymal stromal cells. The International Society for Cellular Therapy position statement. *Cytotherapy* 8, 315–317. doi:10.1080/14653240600855905

Dupont, S., Morsut, L., Aragona, M., Enzo, E., Giulitti, S., Cordenonsi, M., et al. (2011). Role of YAP/TAZ in mechanotransduction. *Nature* 474, 179–183. doi:10.1038/nature10137

Elosegui-Artola, A., Andreu, I., Beedle, A. E. M., Lezamiz, A., Uroz, M., Kosmalska, A. J., et al. (2017). Force triggers YAP nuclear entry by regulating transport across nuclear pores. *Cell.* 171, 1397–1410.e14. doi:10.1016/j.cell.2017.10.008

Engler, A. J., Sen, S., Sweeney, H. L., and Discher, D. E. (2006). Matrix elasticity directs stem cell lineage specification. *Cell.* 126, 677–689. doi:10.1016/j.cell.2006.06.044

Etienne-Manneville, S., and Hall, A. (2002). Rho GTPases in cell biology. *Nature* 420, 629–635. doi:10.1038/nature01148

Fabry, B., Klemm, A. H., Kienle, S., Schäffer, T. E., and Goldmann, W. H. (2011). Focal adhesion kinase stabilizes the cytoskeleton. *Biophys. J.* 101, 2131–2138. doi:10.1016/j.bpj.2011.09.043

Fang, H., Zhu, D., Yang, Q., Chen, Y., Zhang, C., Gao, J., et al. (2022). Emerging zero-dimensional to four-dimensional biomaterials for bone regeneration. *J. Nanobiotechnology* 20, 26. doi:10.1186/s12951-021-01228-1

Fang, X. Z., Zhou, T., Xu, J. Q., Wang, Y. X., Sun, M. M., He, Y. J., et al. (2021). Structure, kinetic properties and biological function of mechanosensitive Piezo channels. *Cell. Biosci.* 11, 13. doi:10.1186/s13578-020-00522-z

Flynn, L., and Woodhouse, K. A. (2008). Adipose tissue engineering with cells in engineered matrices. *Organogenesis* 4, 228–235. doi:10.4161/org.4.4.7082

Frith, J. E., Titmarsh, D. M., Padmanabhan, H., and Cooper-White, J. J. (2013). Microbioreactor array screening of wnt modulators and microenvironmental factors in osteogenic differentiation of mesenchymal progenitor cells. *PLOS ONE* 8, e82931. doi:10.1371/journal.pone.0082931

Garikipati, V. N. S., Singh, S. P., Mohanram, Y., Gupta, A. K., Kapoor, D., and Nityanand, S. (2018). Isolation and characterization of mesenchymal stem cells from human fetus heart. *PLoS ONE* 13, e0192244. doi:10.1371/journal.pone.0192244

Grellier, M., Bareille, R., Bourget, C., and Amédée, J. (2009). Responsiveness of human bone marrow stromal cells to shear stress. *J. Tissue Eng. Regen. Med.* 3, 302–309. doi:10.1002/term.166

Guilak, F., Cohen, D. M., Estes, B. T., Gimble, J. M., Liedtke, W., and Chen, C. S. (2009). Control of stem cell fate by physical interactions with the extracellular matrix. *Cell. Stem Cell.* 5, 17–26. doi:10.1016/j.stem.2009.06.016

Guillotin, B., Bourget, C., Remy-Zolgadri, M., Bareille, R., Fernandez, P., Conrad, V., et al. (2004). Human primary endothelial cells stimulate human osteoprogenitor cell differentiation. *Cell. Physiol. biochem. Int. J. Exp. Cell. Physiol. biochem. Pharmacol.* 14, 325–332. doi:10.1159/000080342

Günay, K. A., Ceccato, T. L., Silver, J. S., Bannister, K. L., Bednarski, O. J., Leinwand, L. A., et al. (2019). PEG-anthracene hydrogels as an on-demand stiffening matrix to study mechanobiology. *Angew. Chem. Int. Ed. Engl.* 58, 9912–9916. doi:10.1002/anie.201901989

Handorf, A. M., Zhou, Y., Halanski, M. A., and Li, W. J. (2015). Tissue stiffness dictates development, homeostasis, and disease progression. *Organogenesis* 11, 1–15. doi:10.1080/15476278.2015.1019687

Hanson, S., D'Souza, R. N., and Hematti, P. (2014). Biomaterial–mesenchymal stem cell constructs for immunomodulation in composite tissue engineering. *Tissue Eng. Part A* 20, 2162–2168. doi:10.1089/ten.tea.2013.0359

Hart, N. H., Nimphius, S., Rantalainen, T., Ireland, A., Siafarikas, A., and Newton, R. U. (2017). Mechanical basis of bone strength: Influence of bone material, bone structure and muscle action. *J. Musculoskelet. Neuronal Interact.* 17, 114–139.

Heng, B. C., Zhang, X., Aubel, D., Bai, Y., Li, X., Wei, Y., et al. (2020). Role of YAP/TAZ in cell lineage fate determination and related signaling pathways. *Front. Cell. Dev. Biol.* 8, 735. doi:10.3389/fcell.2020.00735

Ho, M. H., Yao, C. J., Liao, M. H., Lin, P. I., Liu, S. H., and Chen, R. M. (2015). Chitosan nanofiber scaffold improves bone healing via stimulating trabecular bone production due to upregulation of the Runx2/osteocalcin/alkaline phosphatase signaling pathway. *Int. J. Nanomedicine* 10, 5941–5954. doi:10.2147/IJN.S90669

Hodge, R. G., and Ridley, A. J. (2016). Regulating Rho GTPases and their regulators. *Nat. Rev. Mol. Cell. Biol.* 17, 496–510. doi:10.1038/nrm.2016.67

Hu, K., Sun, H., Gui, B., and Sui, C. (2017). TRPV4 functions in flow shear stress induced early osteogenic differentiation of human bone marrow mesenchymal stem cells. *Biomed. Pharmacother. Biomedecine Pharmacother.* 91, 841–848. doi:10.1016/j.biopha.2017.04.094

Jaalouk, D. E., and Lammerding, J. (2009). Mechanotransduction gone awry. *Nat. Rev. Mol. Cell. Biol.* 10, 63–73. doi:10.1038/nrm2597

Jagodzinski, M., Drescher, M., Zeichen, J., Hankemeier, S., Krettek, C., Bosch, U., et al. (2004). Effects of cyclic longitudinal mechanical strain and dexamethasone on osteogenic differentiation of human bone marrow stromal cells. *Eur. Cell. Mat.* 7, 35–41. doi:10.22203/ecm.v007a04

Jansen, K. A., Donato, D. M., Balcioglu, H. E., Schmidt, T., Danen, E. H. J., and Koenderink, G. H. (2015). A guide to mechanobiology: Where biology and physics meet. *Biochim. Biophys. Acta BBA - Mol. Cell. Res.* 1853, 3043–3052. doi:10.1016/j.bbamcr.2015.05.007

Johnson, G. P., Stavenschi, E., Eichholz, K. F., Corrigan, M. A., Fair, S., and Hoey, D. A. (2018). Mesenchymal stem cell mechanotransduction is cAMP dependent and regulated by adenylyl cyclase 6 and the primary cilium. *J. Cell. Sci.* 131, jcs222737. doi:10.1242/jcs.222737

Jung, Y., Kim, S. H., Kim, Y. H., and Kim, S. H. (2009). The effects of dynamic and three-dimensional environments on chondrogenic differentiation of bone marrow stromal cells. *Biomed. Mat. Bristol Engl.* 4, 055009. doi:10.1088/1748-6041/4/5/055009

Kabir, W., Di Bella, C., Choong, P. F. M., and O'Connell, C. D. (2021). Assessment of native human articular cartilage: A biomechanical protocol. *CARTILAGE* 13, 427S–437S. doi:10.1177/1947603520973240

Karystinou, A., Roelofs, A. J., Neve, A., Cantatore, F. P., Wackerhage, H., and De Bari, C. (2015). Yes-associated protein (YAP) is a negative regulator of chondrogenesis in mesenchymal stem cells. *Arthritis Res. Ther.* 17, 147. doi:10.1186/s13075-015-0639-9

Kasper, G., Dankert, N., Tuischer, J., Hoeft, M., Gaber, T., Glaeser, J. D., et al. (2007). Mesenchymal stem cells regulate angiogenesis according to their mechanical environment. *Stem Cells* 25, 903–910. doi:10.1634/stemcells.2006-0432

Kegelman, C. D., Mason, D. E., Dawahare, J. H., Horan, D. J., Vigil, G. D., Howard, S. S., et al. (2018). Skeletal cell YAP and TAZ combinatorially promote bone development. *FASEB J.* 32, 2706–2721. doi:10.1096/fj.201700872R

Kilian, K. A., Bugarija, B., Lahn, B. T., and Mrksich, M. (2010). Geometric cues for directing the differentiation of mesenchymal stem cells. *Proc. Natl. Acad. Sci.* 107, 4872–4877. doi:10.1073/pnas.0903269107

Koh, C. J., and Atala, A. (2004). Tissue engineering, stem cells, and cloning: Opportunities for regenerative medicine. *J. Am. Soc. Nephrol.* 15, 1113–1125. doi:10.1097/01.ASN.0000119683.59068.F0

Kozaniti, F. K., Deligianni, D. D., Georgiou, M. D., and Portan, D. V. (2022). The role of substrate topography and stiffness on MSC cells functions: Key material properties for biomimetic bone tissue engineering. *Biomimetics* 7, 7. doi:10.3390/biomimetics7010007

Kurenkova, A. D., Medvedeva, E. V., Newton, P. T., and Chagin, A. S. (2020). Niches for skeletal stem cells of mesenchymal origin. *Front. Cell. Dev. Biol.* 8, 592. doi:10.3389/fcell.2020.00592

Kusuma, G. D., Carthew, J., Lim, R., and Frith, J. E. (2017). Effect of the microenvironment on mesenchymal stem cell paracrine signaling: Opportunities to engineer the therapeutic effect. *Stem Cells Dev.* 26, 617–631. doi:10.1089/scd.2016.0349

Kwak, E. A., and Lee, N. Y. (2019). Synergetic roles of TGF-β signaling in tissue engineering. *Cytokine* 115, 60–63. doi:10.1016/j.cyto.2018.12.010

Lee, I. N., Dobre, O., Richards, D., Ballestrem, C., Curran, J. M., Hunt, J. A., et al. (2018). Photoresponsive hydrogels with photoswitchable mechanical properties allow time-resolved analysis of cellular responses to matrix stiffening. *ACS Appl. Mat. Interfaces* 10, 7765–7776. doi:10.1021/acsami.7b18302

Lee, U. L., Yun, S., Lee, H., Cao, H. L., Woo, S. H., Jeong, Y. H., et al. (2022). Osseointegration of 3D-printed titanium implants with surface and structure modifications. *Dent. Mat. Off. Publ. Acad. Dent. Mat.* 38, 1648–1660. doi:10.1016/j.dental.2022.08.003

Li, A., Xia, X., Yeh, J., Kua, H., Liu, H., Mishina, Y., et al. (2014). PDGF-AA promotes osteogenic differentiation and migration of mesenchymal stem cell by down-regulating PDGFRα and derepressing BMP-smad1/5/8 signaling. *PLoS ONE* 9, e113785. doi:10.1371/journal.pone.0113785

Li, Q., Xu, R., Lei, K., and Yuan, Q. (2022). Insights into skeletal stem cells. *Bone Res.* 10, 61–17. doi:10.1038/s41413-022-00235-8

Li, X., Han, L., Nookaew, I., Mannen, E., Silva, M. J., Almeida, M., et al. (2019). Stimulation of Piezo1 by mechanical signals promotes bone anabolism. *eLife* 8, e49631. doi:10.7554/eLife.49631

Li, Y. J., Batra, N. N., You, L., Meier, S. C., Coe, I. A., Yellowley, C. E., et al. (2004). Oscillatory fluid flow affects human marrow stromal cell proliferation and differentiation. *J. Orthop. Res. Off. Publ. Orthop. Res. Soc.* 22, 1283–1289. doi:10.1016/j.orthres.2004.04.002

Li, Y., Wang, J., and Zhong, W. (2021). Regulation and mechanism of YAP/TAZ in the mechanical microenvironment of stem cells (Review). *Mol. Med. Rep.* 24, 506. doi:10.3892/mmr.2021.12145

Lin, C., Xu, K., He, Y., Tao, B., Yuan, Z., Li, K., et al. (2020). A dynamic matrix potentiates mesenchymal stromal cell paracrine function via an effective mechanical dose. *Biomater. Sci.* 8, 4779–4791. doi:10.1039/D0BM01012J

Lin, X., Yang, H., Wang, L., Li, W., Diao, S., Du, J., et al. (2018). AP2a enhanced the osteogenic differentiation of mesenchymal stem cells by inhibiting the formation of YAP/RUNX2 complex and BARX1 transcription. *Cell. Prolif.* 52, e12522. doi:10.1111/cpr.12522

Lindner, U., Kramer, J., Rohwedel, J., and Schlenke, P. (2010). Mesenchymal stem or stromal cells: Toward a better understanding of their biology? *Transfus. Med. Hemotherapy* 37, 75–83. doi:10.1159/000290897

Liu, P., Tu, J., Wang, W., Li, Z., Li, Y., Yu, X., et al. (2022). Effects of mechanical stress stimulation on function and expression mechanism of osteoblasts. *Front. Bioeng. Biotechnol.* 10, 830722. doi:10.3389/fbioe.2022.830722

Liu, X., and Ma, P. X. (2004). Polymeric scaffolds for bone tissue engineering. *Ann. Biomed. Eng.* 32, 477–486. doi:10.1023/b:abme.0000017544.36001.8e

Loh, Q. L., and Choong, C. (2013). Three-dimensional scaffolds for tissue engineering applications: Role of porosity and pore size. *Tissue Eng. Part B Rev.* 19, 485–502. doi:10.1089/ten.teb.2012.0437

Lohberger, B., Kaltenegger, H., Stuendl, N., Payer, M., Rinner, B., and Leithner, A. (2014). Effect of cyclic mechanical stimulation on the expression of osteogenesis genes in human intraoral mesenchymal stromal and progenitor cells. *Biomed. Res. Int.* 2014, 189516. doi:10.1155/2014/189516

Ma, N., Chen, D., Lee, J. H., Kuri, P., Hernandez, E. B., Kocan, J., et al. (2022). Piezo1 regulates the regenerative capacity of skeletal muscles via orchestration of stem cell morphological states. *Sci. Adv.* 8, eabn0485. doi:10.1126/sciadv.abn0485

Martino, F., Perestrelo, A. R., Vinarský, V., Pagliari, S., and Forte, G. (2018). Cellular mechanotransduction: From tension to function. *Front. Physiol.* 9, 824. doi:10.3389/fphys.2018.00824

Maruyama, T., Jeong, J., Sheu, T. J., and Hsu, W. (2016). Stem cells of the suture mesenchyme in craniofacial bone development, repair and regeneration. *Nat. Commun.* 7, 10526. doi:10.1038/ncomms10526

Matsushita, Y., Ono, W., and Ono, N. (2020). Skeletal stem cells for bone development and repair: Diversity matters. *Curr. Osteoporos. Rep.* 18, 189–198. doi:10.1007/s11914-020-00572-9

McBeath, R., Pirone, D. M., Nelson, C. M., Bhadriraju, K., and Chen, C. S. (2004). Cell shape, cytoskeletal tension, and RhoA regulate stem cell lineage commitment. *Dev. Cell.* 6, 483–495. doi:10.1016/S1534-5807(04)00075-9

McHugh, M. P., Magnusson, S. P., Gleim, G. W., and Nicholas, J. A. (1992). Viscoelastic stress relaxation in human skeletal muscle. *Med. Sci. Sports Exerc.* 24, 1375–1382. doi:10.1249/00005768-199212000-00011

McNamara, L. M. (2017). "2.10 bone as a material," in *Comprehensive biomaterials II.* Editor P. Ducheyne (Oxford: Elsevier), 202–227. doi:10.1016/B978-0-12-803581-8.10127-4

Miller, G. J., Gerstenfeld, L. C., and Morgan, E. F. (2015). Mechanical microenvironments and protein expression associated with formation of different skeletal tissues during bone healing. *Biomech. Model. Mechanobiol.* 14, 1239–1253. doi:10.1007/s10237-015-0670-4

Mitra, S. K., Hanson, D. A., and Schlaepfer, D. D. (2005). Focal adhesion kinase: In command and control of cell motility. *Nat. Rev. Mol. Cell. Biol.* 6, 56–68. doi:10.1038/nrm1549

Mohammed, D., Versaevel, M., Bruyère, C., Alaimo, L., Luciano, M., Vercruysse, E., et al. (2019). Innovative tools for mechanobiology: Unraveling outside-in and inside-out mechanotransduction. *Front. Bioeng. Biotechnol.* 7, 162. doi:10.3389/fbioe.2019.00162

Montoya, C., Du, Y., Gianforcaro, A. L., Orrego, S., Yang, M., and Lelkes, P. I. (2021). On the road to smart biomaterials for bone research: Definitions, concepts, advances, and outlook. *Bone Res.* 9, 12–16. doi:10.1038/s41413-020-00131-z

Naqvi, S. M., and McNamara, L. M. (2020). Stem cell mechanobiology and the role of biomaterials in governing mechanotransduction and matrix production for tissue regeneration. *Front. Bioeng. Biotechnol.* 8, 597661. doi:10.3389/fbioe.2020.597661

Nemati, S., Kim, S., Shin, Y. M., and Shin, H. (2019). Current progress in application of polymeric nanofibers to tissue engineering. *Nano Converg.* 6, 36. doi:10.1186/s40580-019-0209-y

Nunes, C. R., Simske, S. J., Sachdeva, R., and Wolford, L. M. (1997). Long-term ingrowth and apposition of porous hydroxylapatite implants. *J. Biomed. Mat. Res.* 36, 560–563. doi:10.1002/(SICI)1097-4636(19970915)36:4<560:AID-JBM15>3.0.CO;2-E

Oftadeh, R., Perez-Viloria, M., Villa-Camacho, J. C., Vaziri, A., and Nazarian, A. (2015). Biomechanics and mechanobiology of trabecular bone: A review. *J. Biomech. Eng.* 137, 0108021–01080215. doi:10.1115/1.4029176

Olivares-Navarrete, R., Lee, E. M., Smith, K., Hyzy, S. L., Doroudi, M., Williams, J. K., et al. (2017). Substrate stiffness controls osteoblastic and chondrocytic differentiation of mesenchymal stem cells without exogenous stimuli. *PLoS ONE* 12, e0170312. doi:10.1371/journal.pone.0170312

Orbay, H., Tobita, M., and Mizuno, H. (2012). Mesenchymal stem cells isolated from adipose and other tissues: Basic biological properties and clinical applications. *Stem Cells Int.* 2012, 461718. doi:10.1155/2012/461718

Özkale, B., Sakar, M. S., and Mooney, D. J. (2021). Active biomaterials for mechanobiology. *Biomaterials* 267, 120497. doi:10.1016/j.biomaterials.2020.120497

Pan, J. X., Xiong, L., Zhao, K., Zeng, P., Wang, B., Tang, F. L., et al. (2018). YAP promotes osteogenesis and suppresses adipogenic differentiation by regulating β-catenin signaling. *Bone Res.* 6, 18–12. doi:10.1038/s41413-018-0018-7

Park, J. S., Chu, J. S., Tsou, A. D., Diop, R., Tang, Z., Wang, A., et al. (2011). The effect of matrix stiffness on the differentiation of mesenchymal stem cells in response to TGF-β. *Biomaterials* 32, 3921–3930. doi:10.1016/j.biomaterials.2011.02.019

Pilato, C. A., Stadiotti, I., Maione, A. S., Saverio, V., Catto, V., Tundo, F., et al. (2018). Isolation and characterization of cardiac mesenchymal stromal cells from endomyocardial bioptic samples of arrhythmogenic cardiomyopathy patients. *J. Vis. Exp.* 2018, 57263. doi:10.3791/57263

Piroli, M. E., and Jabbarzadeh, E. (2018). Matrix stiffness modulates mesenchymal stem cell sensitivity to geometric asymmetry signals. *Ann. Biomed. Eng.* 46, 888–898. doi:10.1007/s10439-018-2008-8

Pittenger, M. F., Discher, D. E., Péault, B. M., Phinney, D. G., Hare, J. M., and Caplan, A. I. (2019). Mesenchymal stem cell perspective: Cell biology to clinical progress. *Npj Regen. Med.* 4, 22–15. doi:10.1038/s41536-019-0083-6

Qin, L., He, T., Chen, S., Yang, D., Yi, W., Cao, H., et al. (2021). Roles of mechanosensitive channel Piezo1/2 proteins in skeleton and other tissues. *Bone Res.* 9, 44–17. doi:10.1038/s41413-021-00168-8

Rahmati, M., Silva, A., Reseland, E., E. J., Heyward, C. A., and Haugen, J. H. (2020). Biological responses to physicochemical properties of biomaterial surface. *Chem. Soc. Rev.* 49, 5178–5224. doi:10.1039/D0CS00103A

Remuzzi, A., Bonandrini, B., Tironi, M., Longaretti, L., Figliuzzi, M., Conti, S., et al. (2020). Effect of the 3D artificial nichoid on the morphology and mechanobiological response of mesenchymal stem cells cultured *in vitro*. *Cells* 9, 1873. doi:10.3390/cells9081873

Renders, G. A. P., Mulder, L., van Ruijven, L. J., and van Eijden, T. M. G. J. (2007). Porosity of human mandibular condylar bone. *J. Anat.* 210, 239–248. doi:10.1111/j.1469-7580.2007.00693.x

Rho, J. Y., Ashman, R. B., and Turner, C. H. (1993). Young's modulus of trabecular and cortical bone material: Ultrasonic and microtensile measurements. *J. Biomech.* 26, 111–119. doi:10.1016/0021-9290(93)90042-d

Robey, P. G., and Riminucci, M. (2020). "Chapter 2 - skeletal stem cells: Tissue-specific stem/progenitor cells of cartilage, bone, stroma, and marrow adipocytes," in *Principles of bone biology*. Editors J. P. Bilezikian, T. J. Martin, T. L. Clemens, and C. J. Rosen (London: Academic Press), 45–71. doi:10.1016/B978-0-12-814841-9.00002-6

Roncada, T., Bonithon, R., Blunn, G., and Roldo, M. (2022). Soft substrates direct stem cell differentiation into the chondrogenic lineage without the use of growth factors. *J. Tissue Eng.* 13, 20417314221122121. doi:10.1177/20417314221122121

Rosales, A. M., Vega, S. L., DelRio, F. W., Burdick, J. A., and Anseth, K. S. (2017). Hydrogels with reversible mechanics to probe dynamic cell microenvironments. *Angew. Chem. Int. Ed.* 56, 12132–12136. doi:10.1002/anie.201705684

Ryeol Choi, H., Jung, K., Choon Koo, J., Nam, J., and Lee, Y. (2008). "Chapter 25 - micro-annelid-like robot actuated by artificial muscles based on dielectric elastomers," in *Dielectric elastomers as electromechanical transducers*. Editors F. Carpi, D. De Rossi, R. Kornbluh, R. Pelrine, and P. Sommer-Larsen (Amsterdam: Elsevier), 259–269. doi:10.1016/B978-0-08-047488-5.00025-3

Sacchetti, B., Funari, A., Michienzi, S., Di Cesare, S., Piersanti, S., Saggio, I., et al. (2007). Self-renewing osteoprogenitors in bone marrow sinusoids can organize a hematopoietic microenvironment. *Cell.* 131, 324–336. doi:10.1016/j.cell.2007.08.025

Sacchetti, B., Funari, A., Remoli, C., Giannicola, G., Kogler, G., Liedtke, S., et al. (2016). No identical "mesenchymal stem cells" at different times and sites: Human committed progenitors of distinct origin and differentiation potential are incorporated as adventitial cells in microvessels. *Stem Cell. Rep.* 6, 897–913. doi:10.1016/j.stemcr.2016.05.011

Sadok, A., and Marshall, C. J. (2014). Rho GTPases: Masters of cell migration. *Small GTPases* 5, e29710. doi:10.4161/sgtp.29710

Scaglione, S., Wendt, D., Miggino, S., Papadimitropoulos, A., Fato, M., Quarto, R., et al. (2008). Effects of fluid flow and calcium phosphate coating on human bone marrow stromal cells cultured in a defined 2D model system. *J. Biomed. Mat. Res. A* 86, 411–419. doi:10.1002/jbm.a.31607

Schlaepfer, D. D., Mitra, S. K., and Ilic, D. (2004). Control of motile and invasive cell phenotypes by focal adhesion kinase. *Biochim. Biophys. Acta BBA - Mol. Cell. Res.* 1692, 77–102. doi:10.1016/j.bbamcr.2004.04.008

Scott, K. E., Fraley, S. I., and Rangamani, P. (2021). A spatial model of YAP/TAZ signaling reveals how stiffness, dimensionality, and shape contribute to emergent outcomes. *Proc. Natl. Acad. Sci.* 118, e2021571118. doi:10.1073/pnas.2021571118

Sen, B., Xie, Z., Uzer, G., Thompson, W. R., Styner, M., Wu, X., et al. (2015). Intranuclear actin regulates osteogenesis. *Stem Cells* 33, 3065–3076. doi:10.1002/stem.2090

Serowoky, M. A., Arata, C. E., Crump, J. G., and Mariani, F. V. (2020). Skeletal stem cells: Insights into maintaining and regenerating the skeleton. *Development* 147, dev179325. doi:10.1242/dev.179325

Shafiq, M., Ali, O., Han, S. B., and Kim, D. H. (2021). Mechanobiological strategies to enhance stem cell functionality for regenerative medicine and tissue engineering. *Front. Cell. Dev. Biol.* 9, 747398. doi:10.3389/fcell.2021.747398

Silver, F. H., Bradica, G., and Tria, A. (2002). Elastic energy storage in human articular cartilage: Estimation of the elastic modulus for type II collagen and changes associated with osteoarthritis. *Matrix Biol.* 21, 129–137. doi:10.1016/S0945-053X(01)00195-0

Simmons, C. A., Matlis, S., Thornton, A. J., Chen, S., Wang, C. Y., and Mooney, D. J. (2003). Cyclic strain enhances matrix mineralization by adult human mesenchymal stem cells via the extracellular signal-regulated kinase (ERK1/2) signaling pathway. *J. Biomech.* 36, 1087–1096. doi:10.1016/s0021-9290(03)00110-6

Smith, L., Cho, S., and Discher, D. E. (2017). Mechanosensing of matrix by stem cells: From matrix heterogeneity, contractility, and the nucleus in pore-migration to cardiogenesis and muscle stem cells *in vivo*. *Semin. Cell. Dev. Biol.* 71, 84–98. doi:10.1016/j.semcdb.2017.05.025

Smith, L. R., Cho, S., and Discher, D. E. (2018). Stem cell differentiation is regulated by extracellular matrix mechanics. *Physiology* 33, 16–25. doi:10.1152/physiol.00026.2017

Somoza, R. A., Welter, J. F., Correa, D., and Caplan, A. I. (2014). Chondrogenic differentiation of mesenchymal stem cells: Challenges and unfulfilled expectations. *Tissue Eng. Part B Rev.* 20, 596–608. doi:10.1089/ten.teb.2013.0771

Strzelecka-Kiliszek, A., Mebarek, S., Roszkowska, M., Buchet, R., Magne, D., and Pikula, S. (2017). Functions of Rho family of small GTPases and Rho-associated coiled-coil kinases in bone cells during differentiation and mineralization. *Biochim. Biophys. Acta BBA - Gen. Subj.* 1861, 1009–1023. doi:10.1016/j.bbagen.2017.02.005

Sun, M., Chi, G., Li, P., Lv, S., Xu, J., Xu, Z., et al. (2018a). Effects of matrix stiffness on the morphology, adhesion, proliferation and osteogenic differentiation of mesenchymal stem cells. *Int. J. Med. Sci.* 15, 257–268. doi:10.7150/ijms.21620

Sun, M., Chi, G., Xu, J., Tan, Y., Xu, J., Lv, S., et al. (2018b). Extracellular matrix stiffness controls osteogenic differentiation of mesenchymal stem cells mediated by integrin α5. *Stem Cell. Res. Ther.* 9, 52. doi:10.1186/s13287-018-0798-0

Sun, Y., Wan, B., Wang, R., Zhang, B., Luo, P., Wang, D., et al. (2022). Mechanical stimulation on mesenchymal stem cells and surrounding microenvironments in bone regeneration: Regulations and applications. *Front. Cell. Dev. Biol.* 10, 808303. doi:10.3389/fcell.2022.808303

Swanson, W. B., and Ma, P. X. (2020). "1.4.7 - textured and porous biomaterials," in *Biomaterials science*. Editors W. R. Wagner, S. E. Sakiyama-Elbert, G. Zhang, and M. J. Yaszemski (London: Academic Press), 601–622. doi:10.1016/B978-0-12-816137-1.00039-8

Swanson, W. B., Omi, M., Woodbury, S. M., Douglas, L. M., Eberle, M., Ma, P. X., et al. (2022). Scaffold pore curvature influences μsc fate through differential cellular organization and YAP/TAZ activity. *Int. J. Mol. Sci.* 23, 4499. doi:10.3390/ijms23094499

Swanson, W. B., Omi, M., Zhang, Z., Nam, H. K., Jung, Y., Wang, G., et al. (2021). Macropore design of tissue engineering scaffolds regulates mesenchymal stem cell differentiation fate. *Biomaterials* 272, 120769. doi:10.1016/j.biomaterials.2021.120769

Tang, W., Qi, J., Wang, Q., Qu, Y., Fu, S., and Luan, J. (2022). Investigating the adipogenic effects of different tissue-derived decellularized matrices. *Front. Bioeng. Biotechnol.* 10, 872897. doi:10.3389/fbioe.2022.872897

Taylor, A. F., Saunders, M. M., Shingle, D. L., Cimbala, J. M., Zhou, Z., and Donahue, H. J. (2007). Mechanically stimulated osteocytes regulate osteoblastic activity via gap junctions. *Am. J. Physiol. Cell. Physiol.* 292, C545–C552. doi:10.1152/ajpcell.00611.2005

Tojkander, S., Gateva, G., and Lappalainen, P. (2012). Actin stress fibers – assembly, dynamics and biological roles. *J. Cell. Sci.* 125, 1855–1864. doi:10.1242/jcs.098087

Totsukawa, G., Yamakita, Y., Yamashiro, S., Hartshorne, D. J., Sasaki, Y., and Matsumura, F. (2000). Distinct roles of ROCK (Rho-kinase) and MLCK in spatial regulation of MLC phosphorylation for assembly of stress fibers and focal adhesions in 3T3 fibroblasts. *J. Cell. Biol.* 150, 797–806. doi:10.1083/jcb.150.4.797

Vasita, R., and Katti, D. S. (2006). Nanofibers and their applications in tissue engineering. *Int. J. Nanomedicine* 1, 15–30. doi:10.2147/nano.2006.1.1.15

Vermeulen, S., Honig, F., Vasilevich, A., Roumans, N., Romero, M., Dede Eren, A., et al. (2021). Expanding biomaterial surface topographical design space through natural surface reproduction. *Adv. Mat.* 33, 2102084. doi:10.1002/adma.202102084

Weinbaum, S., Cowin, S. C., and Zeng, Y. (1994). A model for the excitation of osteocytes by mechanical loading-induced bone fluid shear stresses. *J. Biomech.* 27, 339–360. doi:10.1016/0021-9290(94)90010-8

Wu, D. T., Diba, M., Yang, S., Freedman, B. R., Elosegui-Artola, A., and Mooney, D. J. (2022). Hydrogel viscoelasticity modulates migration and fusion of mesenchymal stem cell spheroids. *Bioeng. Transl. Med.* 8, e10464. doi:10.1002/btm2.10464

Wu, M., Chen, G., and Li, Y. P. (2016). TGF-β and BMP signaling in osteoblast, skeletal development, and bone formation, homeostasis and disease. *Bone Res.* 4, 16009. doi:10.1038/boneres.2016.9

Yamashita, J., Li, X., Furman, B. R., Rawls, H. R., Wang, X., and Agrawal, C. M. (2002). Collagen and bone viscoelasticity: A dynamic mechanical analysis. *J. Biomed. Mat. Res.* 63, 31–36. doi:10.1002/jbm.10086

Young, D. A., Choi, Y. S., Engler, A. J., and Christman, K. L. (2013). Stimulation of adipogenesis of adult adipose-derived stem cells using substrates that mimic the stiffness of adipose tissue. *Biomaterials* 34, 8581–8588. doi:10.1016/j.biomaterials.2013.07.103

Yourek, G., McCormick, S. M., Mao, J. J., and Reilly, G. C. (2010). Shear stress induces osteogenic differentiation of human mesenchymal stem cells. *Regen. Med.* 5, 713–724. doi:10.2217/rme.10.60

Yu, D., Wang, J., Qian, K., Yu, J., and Zhu, H. (2020). Effects of nanofibers on mesenchymal stem cells: Environmental factors affecting cell adhesion and osteogenic differentiation and their mechanisms. *J. Zhejiang Univ. Sci. B* 21, 871–884. doi:10.1631/jzus.B2000355

Yu, H., Gao, M., Ma, Y., Wang, L., Shen, Y., and Liu, X. (2018). Inhibition of cell migration by focal adhesion kinase: Time-dependent difference in integrin-induced signaling between endothelial and hepatoblastoma cells. *Int. J. Mol. Med.* 41, 2573–2588. doi:10.3892/ijmm.2018.3512

Zachary, I. (1997). Focal adhesion kinase. *Int. J. Biochem. Cell. Biol.* 29, 929–934. doi:10.1016/S1357-2725(97)00008-3

Zaidi, S. K., Sullivan, A. J., Medina, R., Ito, Y., van Wijnen, A. J., Stein, J. L., et al. (2004). Tyrosine phosphorylation controls Runx2-mediated subnuclear targeting of YAP to repress transcription. *EMBO J.* 23, 790–799. doi:10.1038/sj.emboj.7600073

Zarka, M., Haÿ, E., and Cohen-Solal, M. (2022). YAP/TAZ in bone and cartilage biology. *Front. Cell. Dev. Biol.* 9, 788773. doi:10.3389/fcell.2021.788773

Zernicke, R., MacKay, C., and Lorincz, C. (2006). Mechanisms of bone remodeling during weight-bearing exercise. *Appl. Physiol. Nutr. Metab. Physiol. Appl. Nutr. Metab.* 31, 655–660. doi:10.1139/h06-051

Zhang, X. R., Hu, X. Q., Jia, X. L., Yang, L. K., Meng, Q. Y., Shi, Y. Y., et al. (2016). Cell studies of hybridized carbon nanofibers containing bioactive glass nanoparticles using bone mesenchymal stromal cells. *Sci. Rep.* 6, 38685. doi:10.1038/srep38685

Zhang, Y., Xing, Y., Li, J., Zhang, Z., Luan, H., Chu, Z., et al. (2018). Osteogenesis-related behavior of mc3t3-E1 cells on substrates with tunable stiffness. *Biomed. Res. Int.* 2018, 4025083. doi:10.1155/2018/4025083

Zhou, J., Aponte-Santamaría, C., Sturm, S., Bullerjahn, J. T., Bronowska, A., and Gräter, F. (2015). Mechanism of focal adhesion kinase mechanosensing. *PLoS Comput. Biol.* 11, e1004593. doi:10.1371/journal.pcbi.1004593

Zhou, T., Gao, B., Fan, Y., Liu, Y., Feng, S., Cong, Q., et al. (2020). Piezo1/2 mediate mechanotransduction essential for bone formation through concerted activation of NFAT-YAP1-ß-catenin. *eLife* 9, e52779. doi:10.7554/eLife.52779

frontiers | Frontiers in Physiology

TYPE Original Research
PUBLISHED 04 September 2023
DOI 10.3389/fphys.2023.1231352

OPEN ACCESS

EDITED BY
Paola Divieti Pajevic,
Boston University, United States

REVIEWED BY
Noriaki Ono,
University of Texas Health Science Center at Houston, United States
Dongsu Park,
Baylor College of Medicine, United States

*CORRESPONDENCE
Ivo Kalajzic,
ikalaj@uchc.edu
Brya G. Matthews,
brya.matthews@auckland.ac.nz

RECEIVED 30 May 2023
ACCEPTED 22 August 2023
PUBLISHED 04 September 2023

CITATION
Cao Y, Kalajzic I and Matthews BG (2023), CD51 labels periosteal injury-responsive osteoprogenitors. *Front. Physiol.* 14:1231352. doi: 10.3389/fphys.2023.1231352

CD51 labels periosteal injury-responsive osteoprogenitors

Ye Cao[1], Ivo Kalajzic[2]* and Brya G. Matthews[1,2]*

[1]Department of Molecular Medicine and Pathology, University of Auckland, Auckland, New Zealand, [2]Center for Regenerative Medicine and Skeletal Development, School of Dental Medicine, UConn Health, Farmington, CT, United States

The periosteum is a critical source of skeletal stem and progenitor cells (SSPCs) that form callus tissue in response to injury. There is yet to be a consensus on how to identify SSPCs in the adult periosteum. The aim of this study was to understand how potential murine periosteal SSPC populations behave *in vivo* and in response to injury. We evaluated the *in vivo* differentiation potential of Sca1^{-}CD51^{+} and Sca1^{+}CD51^{+} cells following transplantation. *In vitro*, the Sca1^{+}CD51^{+} population appears to be more primitive multipotent cells, but after transplantation, Sca1^{-}CD51^{+} cells showed superior engraftment, expansion, and differentiation into chondrocytes and osteoblasts. Despite representing a clear population with flow cytometry, we identified very few Sca1^{+}CD51^{+} cells histologically. Using a periosteal scratch injury model, we successfully mimicked the endochondral-like healing process seen in unstable fractures, including the expansion and osteochondral differentiation of αSMA^{+} cells following injury. CD51^{+} cells were present in the cambium layer of resting periosteum and expanded following injury. Sca1^{+}CD51^{-} cells were mainly localized in the outer periosteal layer. We found that injury increased colony-forming unit fibroblast (CFU-F) formation in the periosteum and led to rapid expansion of CD90^{+} cells. Several other populations, including Sca1^{-}CD51^{+} and CD34^{+} cells, were expanded by day 7. Mice with enhanced fracture healing due to elevated Notch signaling mediated by NICD1 overexpression showed significant expansion of CD51^{+} and CD34^{hi} cells in the early stages of healing, suggesting these populations contribute to more rapid healing. In conclusion, we demonstrate that periosteal injury leads to the expansion of various SSPC populations, but further studies are required to confirm their lineage hierarchy in the adult skeletal system. Our data indicate that CD51^{+} skeletal progenitor cells are injury-responsive and show good engraftment and differentiation potential upon transplantation.

KEYWORDS

periosteum, fracture, Notch, SCA1, CD51, CD34

1 Introduction

The periosteum is a critical source of skeletal stem and progenitor cells (SSPCs) that form callus tissue in response to injury. Fracture healing is delayed when periosteum is seriously damaged or removed, and periosteum retention can allow regeneration of areas of bone that would otherwise fail to regenerate (Zhang et al., 2005; Tate et al., 2007). Periosteal SSPCs usually remain quiescent during adulthood, but these cells can become active and proliferate extensively following fracture. Following this initial expansion

phase, callus forms via a combination of endochondral-like callus formation and direct bone formation occurs beginning towards the end of the first week following injury in mice. This callus later becomes completely mineralized and is ultimately remodeled. Several key signaling pathways regulate periosteal response following healing, including Notch signaling (Dishowitz et al., 2012; Matthews et al., 2014; Novak et al., 2020). Overexpressing Notch 1 intracellular domain (NICD1) in αSMA$^+$ cells improves the progression of fracture healing and mineralization *in vivo* when induced around the time of fracture (Novak et al., 2020). Both genetic and pharmacological inhibition of Notch signaling lead to impairments in fracture healing (Dishowitz et al., 2013; Wang et al., 2016; Novak et al., 2020). These results indicate that activation of Notch signaling promotes bone healing.

While it is well-accepted that the periosteum houses tissue-resident SSPCs, the identity of the population or populations that contribute to healing is still controversial. Numerous lineage-tracing reporters and cell surface markers have been proposed to prospectively identify SSPCs (Cao et al., 2020). Periosteal cells expressing periostin, cathepsin K, and paired-related homeobox 1 (Prx1) contribute to bone and cartilage during fracture healing (Kawanami et al., 2009; Wilk et al., 2017; Debnath et al., 2018; Duchamp de Lageneste et al., 2018; Julien et al., 2022; Chai et al., 2023). αSMA-CreER labels long-term, self-renewing osteochondral progenitors within the adult periosteum (Grcevic et al., 2012; Matthews et al., 2014; Matthews et al., 2021). It is also enriched in Mx1+ periosteal progenitor cells (Ortinau et al., 2019). The majority of injury-responsive periosteal progenitor cells are αSMA+, these cells rapidly expand and contribute to the majority of bone and a reasonable amount of cartilage formation (Grcevic et al., 2012; Matthews et al., 2014; Matthews et al., 2021).

Cell surface markers are useful for identifying SSPCs as they can be combined to refine populations and can be applied to many systems without the need for transgenic animals. Adult periosteum is enriched for many putative SSPC markers compared to bone marrow and endosteum in both humans and mice (Tournaire et al., 2020; Matthews et al., 2021; Cao et al., 2022). Similar marker combinations have been proposed for growth plate resident skeletal stem cells and periosteal stem cells, with presence of CD51, absence of CD90 and 6C3, and variable expression of CD105 and CD200, and these populations expand in response to fracture, particularly about a week after injury (Chan et al., 2015; Marecic et al., 2015; Debnath et al., 2018). We previously separated periosteal populations on the basis of Sca1 and CD51 expression. *In vitro*, Sca1$^+$CD51$^+$ and Sca1$^-$CD51$^+$ cells were both enriched for colony forming unit fibroblasts (CFU-F), but Sca1$^+$CD51$^+$ cells are multipotent progenitors, and Sca1$^-$CD51$^+$ cells are more restricted to osteoblast lineage differentiation (Matthews et al., 2021).

The aim of this study was to understand how potential periosteal SSPC populations behave *in vivo* and in response to injury. In particular we focus on Sca1$^-$CD51$^+$ and Sca1$^+$CD51$^+$ cells following transplantation. Using a periosteal scratch injury model, we successfully mimicked the fracture healing process, and investigated the response of these and other populations to injury. We also defined a population of progenitors that is the basis for enhanced healing due to NICD1 overexpression.

2 Materials and methods

2.1 Mice

All animals were obtained from either Vernon Jansen Unit at the University of Auckland or from UConn Health. All the handling and surgical procedures involving animals were approved by the University of Auckland Animal Ethics Committee (approval numbers 001940 and 002735), and UConn Health Institutional Animal Care and Use Committee (animal protocol number AP-200271-1023). Mice were housed in a controlled environment (12-h light/dark cycle, 22°C ± 2°C, and 55% ± 5% humidity) with *ad libitum* access to food and water.

The transgenic mice used in this study are listed in Table 1. αSMACreER/Tom/Col2.3GFP mice were generated using either Ai9 or A14 reporter animals (a gift from the University of Otago) (Madisen et al., 2010). To generate CAG-tdTomato mice with tdTomato (Tom) expression from the Rosa26 locus in all cells, Ai9 mice were bred with female HprtCre mice (Sinder et al., 2020). CAG-Tom mice were crossed with Col2.3GFP to generate CAG-Tom/Col2.3GFP donor cells for transplantation. αSMACreER mice were bred with Rosa^{NICD1} to generate αSMACreER/NICD1 (homozygous for NICD1) as described previously (Novak et al., 2020). All strains except NSG were maintained on a C57Bl/6J background. CreER was activated by administration of tamoxifen in corn oil (75 μg/g i.p.), the timing of tamoxifen for different studies is indicated in the figures or legends.

2.2 Periosteal cell isolation

Periosteum was isolated from the hind limbs and single cell suspensions generated similar to previous studies (Matthews et al., 2014). Briefly, tibias and femurs were roughly dissected, the epiphyses cut off, and bone marrow was flushed out with PBS. Remaining muscle was removed, then periosteum scraped, collected in a tube and enzymatically digested with either 0.2% collagenase P, 0.2% dispase II (Gibco, Life Technologies Corporation, Cat: 17105-041), 5% FBS or 0.05% collagenase P, 0.2% hyaluronidase (Sigma Aldrich, St Louis, MO, United States) in PBS for 1 hour at 37°C, 120 rpm. Tubes were mixed every 15 min to spread the tissues evenly in the digestion solution. The cell solution was then diluted in PBS, passed through cell strainer mesh, centrifuged, washed in 40 mL PBS, then resuspended.

2.3 Flow cytometry and cell sorting

Flow cytometry on periosteal cells was performed in a similar manner to our previous studies (Matthews et al., 2021). For detailed analysis of periosteal response to injury, we used a panel containing 15 cell surface markers in addition to GFP and tdTomato on the Cytek Northern Lights spectral cytometer, and a simpler panel on a BD LSRII. These and other reagents used are shown in Supplementary Tables S1–S3. TruStain blocking reagents were used in spectral cytometry analysis for 30 min at 4°C in the dark prior to the full stain. Antibody master mix was prepared for each panel by adding the brilliant violet antibodies to 5 μL Brilliant Stain

TABLE 1 Mouse lines used in this study.

Mouse line	Official name	Source/References
αSMACreER	B6.Cg-Tg(Acta2-cre/ERT2)1Ikal	Grcevic et al. (2012)
Col2.3GFP	B6.Cg-Tg(Col1a1*2.3-GFP)1Rowe/J	Kalajzic et al. (2002)
Ai9	B6.Cg-Gt(ROSA)26Sor$^{tm9(CAG-tdTomato)Hze}$/J	Jax: 007909
Ai14	B6.Cg-Gt(ROSA)26Sor$^{tm14(CAG-tdTomato)Hze}$/J	Jax: 007914
NSG	NOD.Cg-Prkdc^{scid} Il2rgt^{m1Wjl}/SzJ	Jax: 005557
Rosa^{NICD1}	Gt(ROSA)26Sor$^{tm1(Notch1)Dam/J}$	Jax: 008159
HprtCre	129S1/Sv-Hprt$^{tm1(CAGcre)Mnn}$/J	Jax: 004302

TABLE 2 Donor cell (Tom$^+$) counts pre and post transplantation.

	Cells/implant	Cells/ossicle
Sca1$^-$CD51$^+$	6,760 ± 759	11,504 ± 2,771
Sca1$^+$CD51$^+$	6,700 ± 670	3,677 ± 1,347

Buffer (BD Biosciences, United States). The rest of the antibodies from the panel were then added to make up a final volume of 50 µL master mix. The cells were incubated for 30 min at 4°C in the dark with the master mix. DAPI (50 ng/mL final concentration) was added to each tube prior to analysis for dead cell exclusion.

Cell sorting was performed on a BD FACS Aria II using simplified stains. Cells were sorted with 100 µm or 130 µm nozzles into tubes containing αMEM 20% FBS.

2.4 Subcutaneous cell transplantation

Freshly sorted cells were combined with cultured bone marrow stromal cells (BMSCs) for subcutaneous transplant. Cells were sorted from samples generated from 2–3 animals. We sorted all available cells with the goal of obtaining 5,000 cells/population for transplant, and ultimately each implant contained 4,900–8,000 cells (Table 2). BMSCs from C57Bl/6 mice were cultured for 7 days prior to transplantation as previously described (Matthews et al., 2014). Following detachment with accutase, 750,000 BMSCs were added to the sorted populations, centrifuged, and resuspended prior to making gels for transplantation. Collagen gels (5 mg/mL, 100 µL volume) were made by mixing Rat Tail High Concentration Collagen I (Corning, United States, catalog 354249) with a suitable volume of 1M NaOH and cells in αMEM 10% FBS. Gels were incubated in a Petri dish at 37°C for at least 30 min prior to transplant. Transplantation was performed in isoflurane anesthetized NSG mice. The back of the mice was shaved and cleaned with 1% chlorhexidine, then a small incision created and pre-made collagen gels were placed in subcutaneous pockets on the flanks. Each recipient mouse received up to 2 implants in separate pockets. Mice were subcutaneously delivered up to 1 mg/kg body weight of buprenorphine twice a day over the first 2 days for post-operative analgesia.

2.5 Periosteal scratch injury

The periosteal injury was performed under isoflurane anesthesia using a 25 G needle to poke through the skin and muscle and scratch the surface of tibia and femur. Both unilateral and bilateral injuries were performed. Buprenorphine analgesia was provided as described above.

2.6 Histology and immunostaining

Ossicles were dissected, fixed overnight in 4% paraformaldehyde, then washed with PBS prior to X-ray imaging. After X-ray, they were incubated in 30% sucrose overnight, and embedded in cryomatrix. 7 µm cryosections were collected at ~30 µm intervals for the whole visible ossicle. Following DAPI staining, imaging was performed on a Zeiss Axioscan using the ×10 objective. Labeled cell counting was performed on all sections based on fluorescence colocalization with DAPI signal using ImageJ as described previously (Matthews et al., 2021). All sections from each ossicle were pooled, and the average donor cell numbers for each population were calculated. Labeled cell surface/bone surface measurements were performed on the central three sections of each ossicle. In order to measure the cell surface/bone surface, bone surface was drawn for each section along the inner (endosteal) and outer (periosteal) bone surfaces, Tom$^+$ cell surface was drawn individually for each Tom$^+$ cell, and added up as total Tom$^+$ cell surface, GFP$^+$ cell surface was drawn individually for each cell co-expressing Tom and GFP, and added up as total GFP$^+$ cell surface. Tom$^+$ cell surface/bone surface, and GFP$^+$ cell surface/bone surface were calculated. At least three ossicles were analyzed for each transplanted population.

Mouse long bones were dissected and fixed in 4% PFA for 48–72 h, followed by sucrose overnight prior to embedding in cryomatrix, and sectioning with a tape transfer system as previously described (Dyment et al., 2016). For immunostaining, we utilized rat anti-Sca1 (ThermoFisher, catalog 14-5981, 1:100) and rabbit anti-CD51 (Abcam, catalog ab179475, 1:1,000) combined with the secondary antibodies donkey anti-rat Alexa-Fluor 647 (Jackson Immunoresearch, catalog J1712605153) and goat anti-rabbit Alexa Fluor 750 (ThermoFisher, catalog A-21039), all 1:500. Briefly, sections were permeabilized with 0.1% Triton X in PBS for 15 min, followed by 1 h incubation in Blocking Solution (5% BSA in 0.1% Tween 20/PBS (PBST)) with either 10% Normal

Donkey Serum or Normal Goat Serum depending on which species the secondaries were raised in) at room temperature. After blocking, sections were incubated with primary antibody cocktail (made up in 1% BSA in PBST with either 2% Normal Donkey Serum or Normal Goat Serum) at 4°C overnight. Sections were incubated for 1 h in secondary antibody cocktail, then counterstained with 100 ng/mL DAPI for 5 min. Slides were washed three times in PBST for 5 min between each step. Following the last wash, slides were cover slipped with 50% glycerol in PBS.

After fluorescent imaging, histochemical staining was performed on the same section. Safranin O staining was performed as follows: sections were stained with Wiegert's hematoxylin for 5 min, washed with tap water for 5 min, followed by distilled water for 1 min, stained with 0.2% Fast green for 15 min, washed with 1% acetic acid, then stained with 0.1% Safranin O for 1 min, washed with water for 5 min, and cover slipped with 50% glycerol in water.

2.7 *In vitro* assays

CFU-F assays were performed on freshly sorted cells. Cells were seeded at 20–50 cells/cm^2 in αMEM 20% FBS and maintained in a humidified incubator at 37°C with 5% CO_2 and 5% O_2. Half media change was performed on day 4. Colonies were either fixed in 10% formalin and stained with crystal violet or underwent differentiation on day 7.

We induced differentiation of primary colonies using a combined osteogenic/adipogenic medium: αMEM 50 μg/mL ascorbate-2-phosphate, 5 mM β-glycerophosphate, 0.5 μM rosiglitazone, 1 μM insulin, and 10% FBS, and maintained at 37°C with 5% CO_2. On differentiation day 2, plates were fixed in 10% formalin, stained for ALP, followed by Oil Red O, then crystal violet, as previously described (Matthews et al., 2014; Matthews et al., 2021).

2.8 Statistics

Data were analyzed using GraphPad Prism 9 (GraphPad Software, San Diego, CA) with *t*-test, one-way, or two-way analysis of variance (ANOVA) with appropriate *post hoc* tests. Exact n values are listed in figure legends. Values represent the number of biological replicates. In most flow cytometry experiments, 2-3 mice were pooled to generate a biological replicate. Flow and CFU-F data were generated with flow or sorts performed on the same day. Paired tests were used for flow cytometry datasets where different populations from one sample were evaluated. Each graph is presented as the mean ± standard error of the mean (SEM). $p < 0.05$ was considered as statistically significant.

3 Results

3.1 Sca1$^-$CD51$^+$ show superior expansion to Sca1$^+$CD51$^+$ cells upon *in vivo* transplantation

We previously demonstrated that periosteal Sca1$^+$CD51$^+$ were enriched for cells capable of CFU-F formation and differentiation towards osteogenic and adipogenic lineages (Matthews et al., 2021). Sca1$^-$CD51$^+$ cells showed slightly lower CFU-F frequency and their differentiation was limited to the osteogenic lineage. We characterized the *in vivo* growth and differentiation capabilities of these populations following subcutaneous transplantation of CAG-Tom/Col2.3GFP donor cells (Figure 1A). We found ossicles from all the transplanted populations. The size and structure of the ossicles did not vary between the populations macroscopically (Figure 1B). All ossicles were comprised of an outer fibrous capsule/periosteal layer, bone, and central marrow compartments. Cells derived from the Sca1$^-$CD51$^+$ population survived and expanded well following transplantation, whereas the ossicles formed from the Sca1$^+$CD51$^+$ population contained fewer Tom$^+$ donor cells within the sections we evaluated than we originally sorted for implantation (Table 2).

Tom$^+$ cells were identified in all sections evaluated, with some expression of Col2.3GFP, indicating the ability of transplanted cells to engraft and undergo osteogenic differentiation (Figures 1C, D). Compared to Sca1$^+$CD51$^+$ donor cells, Sca1$^-$CD51$^+$ donor cells demonstrated higher engraftment (Figures 1E, F; Table 2), in contrast with our *in vitro* results (Matthews et al., 2021). Around 60% of the periosteum and endosteum surface was covered by cells derived from the Sca1$^-$CD51$^+$ population, and some of these cells differentiated into Col2.3GFP$^+$ osteoblasts, covering 15% and 35% of the periosteum, and endosteum surface, respectively. Ossicles formed with Sca1$^-$CD51$^+$ cells contained bone, cartilage and a limited amount of bone marrow. Tom$^+$ donor cells contributed to osteoblasts and chondrocytes, but it was unclear if they contributed to bone marrow stromal cells due to the limited amount of marrow present (Figure 1C). Despite lower engraftment, Sca1$^+$CD51$^+$ cells contributed to endosteal osteoblasts, endosteal and periosteal surface construction, and stromal cells in the bone marrow (Figure 1D). Ossicles formed with Sca1$^+$CD51$^+$ cells displayed a phenotype similar to ossicles formed from BMSCs only, containing bone marrow and endosteum partially covered by osteoblasts inside the cortical ring, and an outer fibrous capsule/periosteum. Approximately 20% and 40% of the periosteum and endosteum surface was covered by labeled cells, respectively (Figure 1E). Sca1$^+$CD51$^+$ derived Col2.3GFP$^+$ osteoblasts covered around 15% of the endosteum surface, but they rarely formed osteoblasts on the periosteal surface (Figure 1F). These results indicate that Sca1$^-$CD51$^+$ cells show effective engraftment, expansion and differentiation towards osteogenic and chondrogenic lineages, while Sca1$^+$CD51$^+$ cells show poorer engraftment, in contrast to our previous *in vitro* studies, but are capable of osteogenic and stromal differentiation.

3.2 Evaluation of potential periosteal SSPC populations in mice following injury

Next, we evaluated the response of these and other periosteal SSPC populations to injury. We evaluated the periosteum response following scratch injury at different time points with histology (n = 3–5 per group) (Figure 2A). This model enables damage to the periosteum without exposure of the bone marrow. We utilized adult αSMACreER/Tom/Col2.3GFP mice in order to localize the long-

10.3389/fphys.2023.1231352

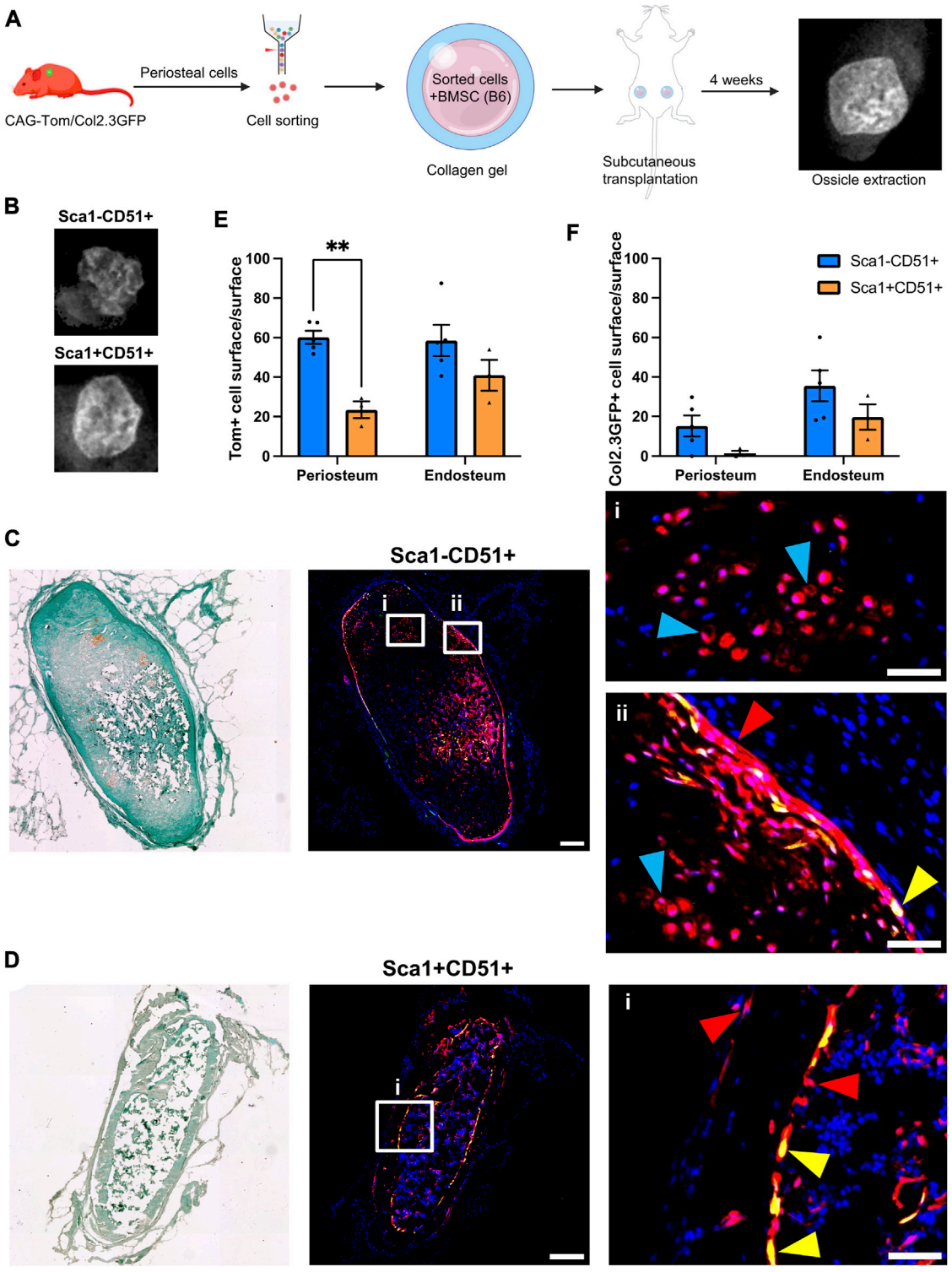

FIGURE 1
Periosteal Sca1^{-}CD51^{+} cells contribute to osteoblasts and chondrocytes in ectopic bone **(A)** Experimental design. Periosteal donor cells were isolated from CAG-Tom/Col2.3GFP animals. Sorted populations (4,900–8,000 cells) were mixed with 750,000 bone marrow stromal cells (BMSCs) from wild type animals. After 4 weeks, implants were extracted. Representative image of BMSC only ossicle is shown. Figure partially created with BioRender. **(B)** X-rays of representative ossicles formed from the Sca1^{-}CD51^{+}, and Sca1^{+}CD51^{+} cells. Representative sections showing cells derived from sorted **(C)** Sca1^{-}CD51^{+} and **(D)** Sca1^{+}CD51^{+} populations in ossicles. Magnified images indicating the red Tom^{+} donor cells (red arrowheads), and yellow donor cell-derived osteoblasts (yellow arrowheads) and chondrocytes (blue arrowheads) are shown in (i,ii). Sections were counterstained with DAPI. **(E)** tdTomato^{+} (donor), and **(F)** Col2.3GFP^{+} periosteum and (where present) endosteum surface was calculated (n = 4–5 implants/group). $^{**}p < 0.01$ (t-test). Tom, tdTomato; DAPI, 4′,6-diamidino-2-phenylindole. Scale bars are 200 μm **(C,D)**, and 50 μm (i, ii).

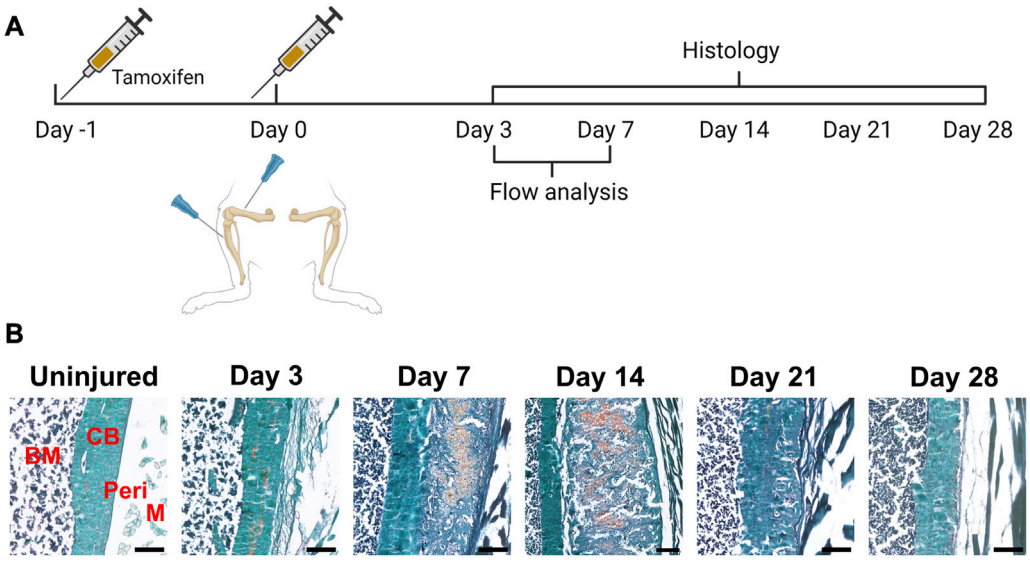

FIGURE 2
Time course of periosteal response to scratch injury. **(A)** Experimental design for histology and flow analysis of αSMACreER/Tom/Col2.3GFP mice following periosteal injury, created with BioRender. **(B)** Brightfield imaging of safranin O and fast green stained femur sections showing periosteal response following local injury at different time points (n = 3–5). BM, bone marrow; CB, cortical bone; Peri, periosteum (injured periosteum and healing response); M, muscle. Scale bars are 200 μm.

term periosteal progenitor cells labelled by αSMA, and osteoblasts labelled by Col2.3GFP. We successfully mimicked the endochondral healing process with the periosteal scratch injury (Figure 2B; Supplementary Figure S1). The periosteum layer was very thin without injury, but it was obviously thickened by day 3 following the scratch. Fibrocartilage formation was observed by day 7 between the bone surface and the thickened periosteum, meanwhile, new woven bone was found at the periphery of the injury, indicating the start of peripheral intramembranous bone formation. By day 14, bone formation gradually took over, with marrow infiltration filling the spaces between bone and cartilage tissues. Remodeling was underway by day 21, and by day 28, marrow infiltration almost disappeared, but there was still thickened periosteum and some areas of active remodeling at the injury site compared to uninjured bones. These results suggest that periosteum alone is healed through an endochondral process similar to semi-stabilized fracture (Matthews et al., 2014; Novak et al., 2020; Matthews et al., 2021). We also confirmed that cells labeled by αSMACreER dramatically expanded with periosteum injury by histology (Figure 3), consistent with our previous fracture studies (Matthews et al., 2014; Matthews et al., 2021). These cells were rapidly activated with periosteum expansion, contributed to new bone, cartilage and fibroblast formation, and were retained in the periosteum for at least a month after injury.

In order to characterize murine periosteal progenitor populations *in vivo* following injury, we performed spectral flow cytometry analysis at day 3 (inflammation stage) and day 7 (fibrocartilage stage). All events from each sample were recorded for analysis, and the average event numbers from different groups are shown in Table 3. Although the proportion of non-hematopoietic (Lin-) cells did not change with injury (Figure 4A), both live cell yields and Lin^- cell yields were enriched by day 3 and 7 compared to the uninjured group following injury (Table 3), indicating the expansion of the total periosteal cells, and Lin^- periosteal cells following injury consistent with the histology data.

We compared the expression of two transgenes and individual markers within the Lin^- populations at different time points following injury. Very few $αSMA^+$ cells (around 3%) were present in the periosteum without injury (Figure 4B), which is consistent with our previous findings (Matthews et al., 2014; Matthews et al., 2021). After injury, the expression of αSMA significantly increased by day 3 and further at day 7. The proportion of $Col2.3GFP^+$ osteoblasts was also increased after injury. The enrichment of $αSMA^+$ cells and $Col2.3GFP^+$ cells were also confirmed by histology (Figure 3). The frequency of $CD24^+$ and $PDGFRα^+$ cells significantly dropped by day 3 and was further decreased on day 7 (Figure 4C). CD90 expression was enriched at day 3 and day 7 compared to the uninjured group. Strong enrichment of CD200 and CD34 was also observed by day 7 post injury. In a different experiment using wild-type mice, the proportions of $Sca1^+CD51^+$ and $Sca1^-CD51^+$ cells were also increased at day 7 following injury (Figure 4D).

3.3 Localization of injury-responsive periosteal populations

We performed multicolor histology in αSMACreER/Tom/Col2.3GFP animals to localize selected injury-responsive periosteal progenitor populations. The contralateral uninjured femurs were used as the uninjured controls. Prior to injury, Sca1 was mainly expressed in the outer fibrous layer of the periosteum, next to muscle, whereas CD51 was mainly located in the inner cambium layer adjacent to bone (Figure 5; Supplementary Figure S2). By day 3 and day 7, in the periosteum, both Sca1 and CD51 cells were enriched with the expansion of periosteum

10.3389/fphys.2023.1231352

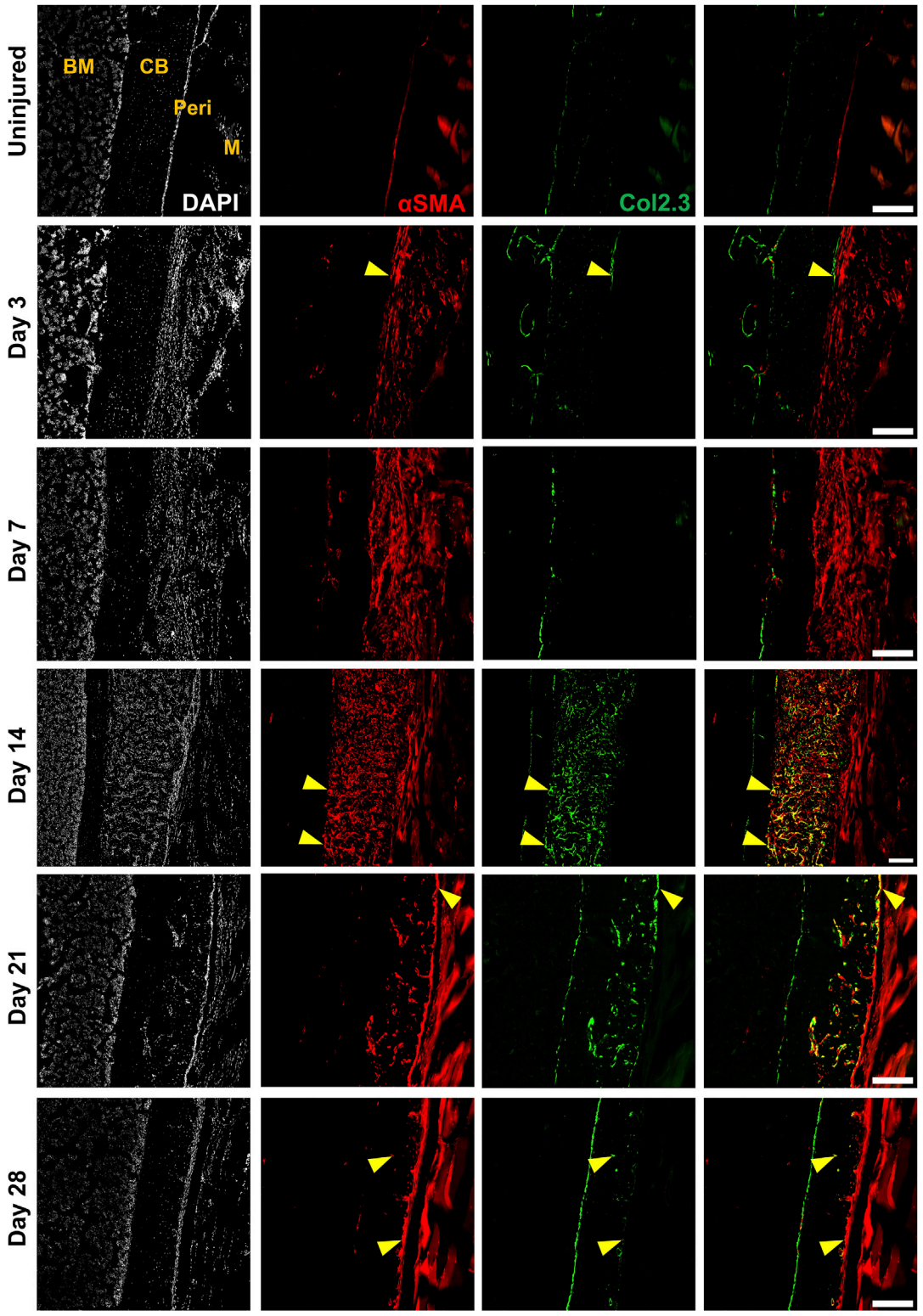

FIGURE 3
Alpha smooth muscle actin (αSMA) identifies injury-responsive periosteal stem and progenitor populations. Representative histology showing periosteum injury response compared to the uninjured femur at day 3 (n = 3), 7 (n = 4), 14 (n = 3), 21 (n = 4), and 28 (n = 2) following injury in αSMACreER/Tom/Col2.3GFP mice. DAPI (white), αSMA (red), Col2.3 (green) were labelled. αSMA cells rapidly expanded as soon as the injury occurred, these cells contributed to periosteum healing by giving rise to Col2.3GFP labelled osteoblasts (yellow arrowheads). BM, bone marrow; CB, cortical bone; Peri, periosteum (injured periosteum and healing response); M, muscle. Scale bars are 200 μm. DAPI, 4′,6-diamidino-2-phenylindole.

TABLE 3 Periosteal Lin$^-$ fraction event numbers isolated from different groups.

	Live cells	Lin- cells
Uninjured	207,347 ± 51,916	3,782 ± 1,197
Day 3	249,889 ± 25,504	5,621 ± 954
Day 7	353,219 ± 57,394	7,125 ± 564

Data shown as mean ± SEM.

(Figure 5). In contrast to flow analysis which consistently showed the presence of a Sca1$^+$CD51$^+$ population (Figure 4D), histologically, very few Sca1$^+$CD51$^+$ cells were present in the periosteum without injury, and these two markers were mostly expressed in separate layers after injury (Figure 5; Supplementary Figure S2). The highest CD51$^+$ expression was found on post injury day 14, these cells were observed in the new bone, and inner periosteum area, but they were rarely present in the outer layer of the periosteum (Figures 5, 6). Some of these CD51$^+$ cells also expressed Col2.3GFP (Figures 6A, B), but such co-expression disappeared a week later (Figures 6C, D), indicating that Sca1$^-$CD51$^+$ cells probably contribute to bone formation through forming osteoblasts, but they subsequently lose CD51 expression during maturation, suggesting that CD51 is present on osteoblast progenitors, and newly-formed osteoblasts, but not mature osteoblasts. This differs from our previous flow results showing 30%–60% of Col2.3GFP$^+$ osteoblasts express CD51 (Matic et al., 2016; Matthews et al., 2021). Both CD51$^+$ and Sca1$^+$ cells were rare at post injury day 21, when periosteum shrunk, and the remodeling was mostly complete. By day 28, CD51$^+$ cells returned to their original location in uninjured bones. CD51 may be expressed on the osteocytes, and in trans-cortical channels, but the majority of CD51$^+$ cells resided in the inner layer of the periosteum. Unlike CD51, most Sca1$^+$ cells resided in the outer periosteal layer during the whole healing process, except for at day 14 when some Sca1$^+$ cells were present in the marrow infiltration area inside the new bone, indicating a potential stromal support function. CD51 and Sca1 were generally absent in fibrocartilage regions of the callus, and were never expressed on cells with chondrocyte morphology (Supplementary Figure S3). Our transplantation study showed that some Sca1$^-$CD51$^+$ cells were capable of chondrocyte formation, however, suggesting downregulation of CD51 during chondrocyte maturation. Overall, these results illustrate spatial separation of Sca1$^+$ and

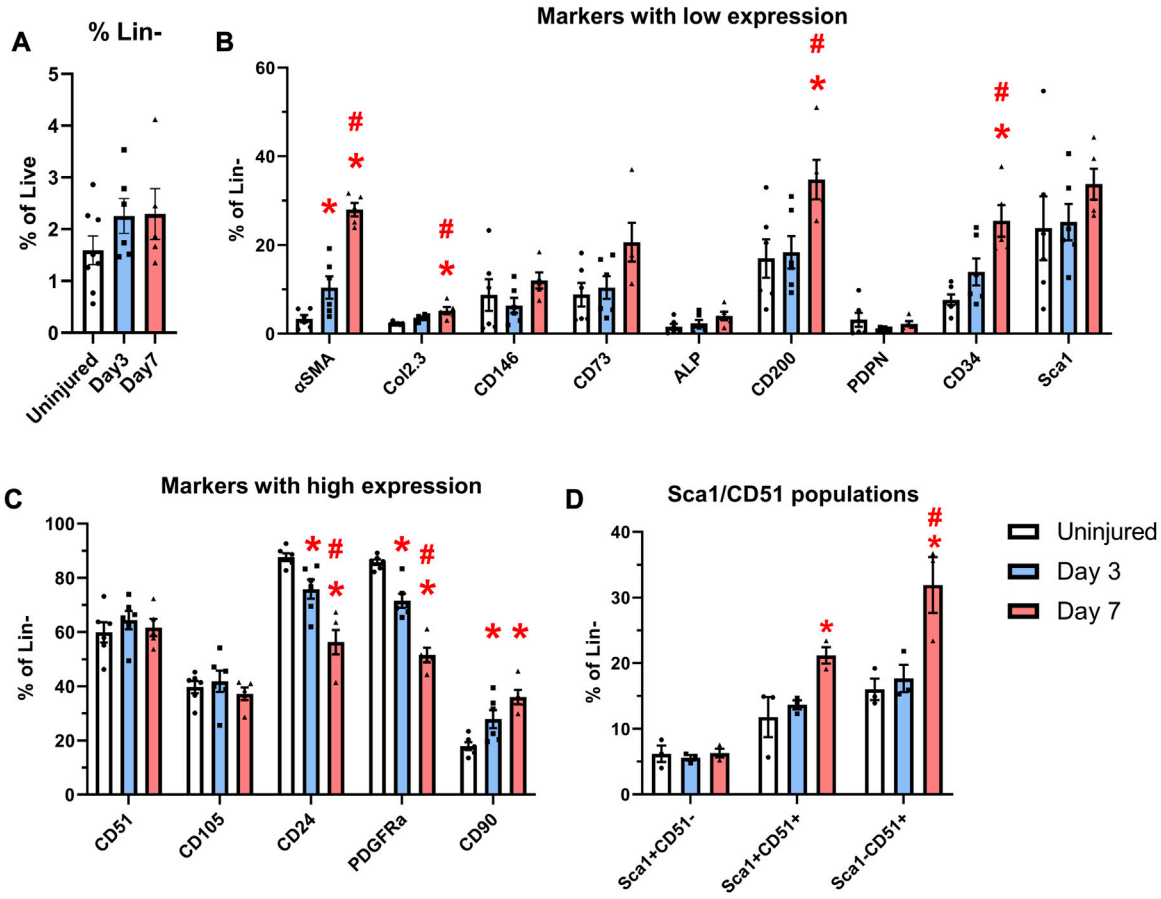

FIGURE 4
Expansion of cells expressing markers including CD90 and CD34 occurs after injury. αSMACreER/Tom/Col2.3GFP mice were treated with tamoxifen at day −1 and day 0, and had periosteal cells isolated 3 and 7 days later, uninjured αSMACreER/Tom/Col2.3GFP mice were treated with tamoxifen 1 and 2 days before harvesting. **(A)** The frequency of CD45/Ter119/CD31$^-$ (Lin$^-$) cells (n = 6–8). Expression of cell surface markers with low **(B)**, and high **(C)** expression in the periosteum following injury (n = 5-6). **(D)** Expression of populations expressing Sca1 and CD51 in a separate cohort of B6 mice (n = 3). *p < 0.05 compared to uninjured, #p < 0.05 compared to day 3 with one way ANOVA followed by Tukey's *post hoc* test.

10.3389/fphys.2023.1231352

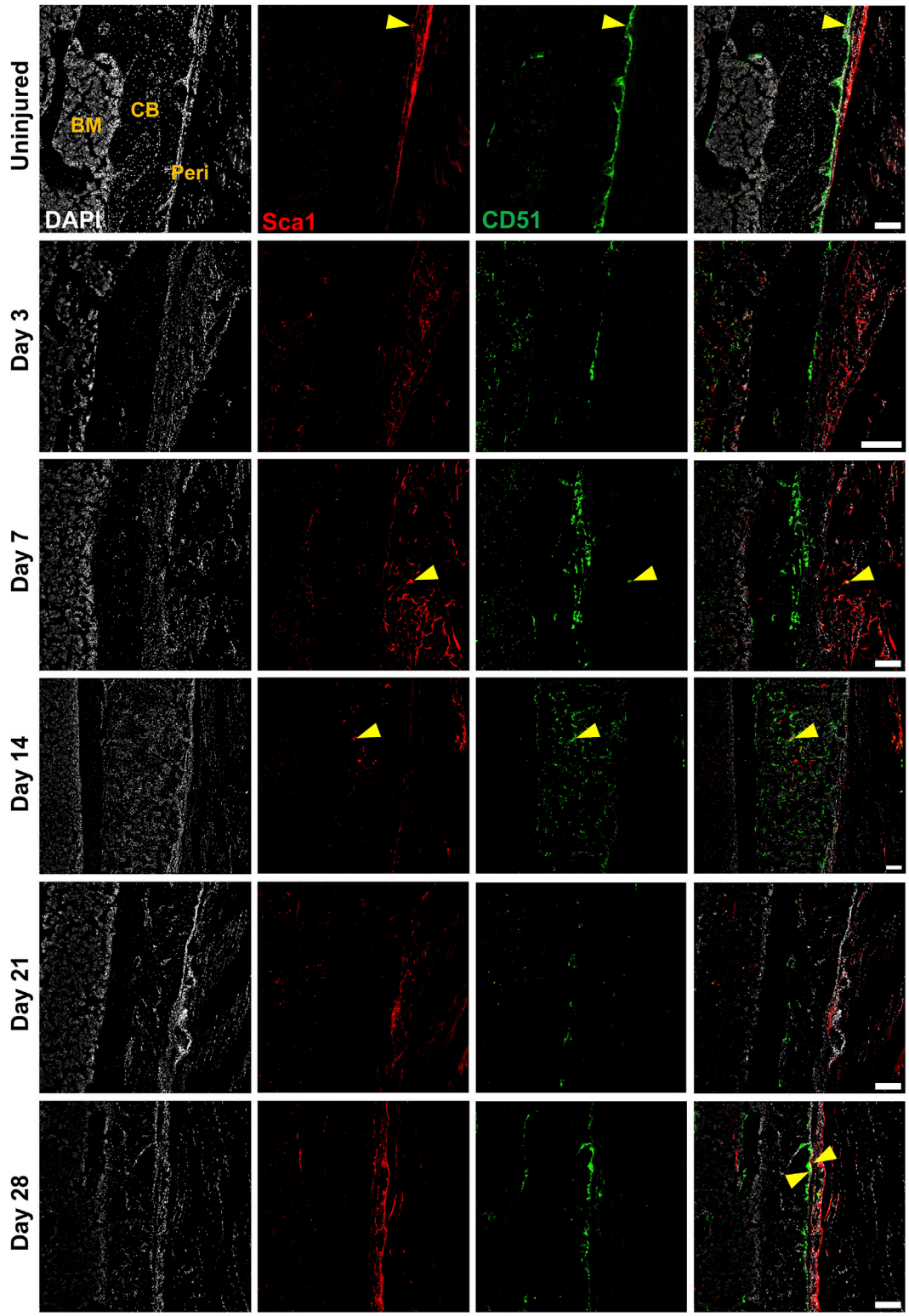

FIGURE 5
CD51$^+$ periosteal cells expand in response to local injury. Representative histology showing periosteum injury response compared to the uninjured femur at day 3 (n = 3), 7 (n = 4), 14 (n = 3), 21 (n = 4), and 28 (n = 2) following injury. Sca1$^+$ cells mainly resided in the outer layer of the periosteum and did not contribute much to healing; CD51 cells localized in the inner layer of the periosteum, contributed to bone and periosteum formation. Sca1$^+$CD51$^+$ cells (yellow arrowheads) were rare without injury and may decrease with injury. BM, bone marrow; CB, cortical bone; Peri, periosteum (injured periosteum and healing response). Scale bars are 200 μm. DAPI, 4′,6-diamidino-2-phenylindole.

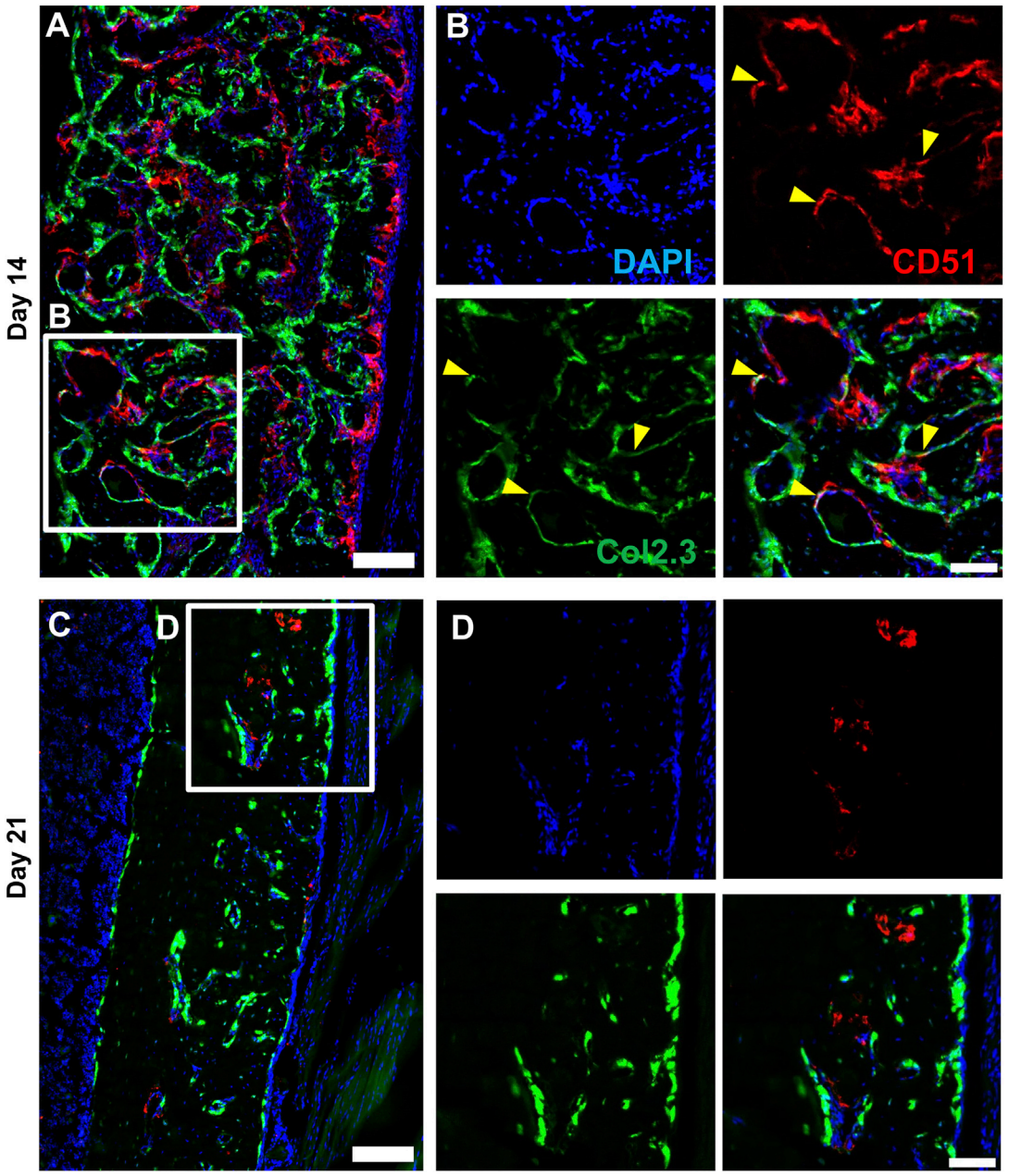

FIGURE 6
CD51 expression is detectable in some osteoblasts during active bone formation. Representative histology showing the localization of CD51 in relation to Col2.3GFP$^+$ osteoblasts on day 14 **(A,B)** and day 21 **(C,D)** following injury (n = 3–4). DAPI (white), Col2.3 (green), CD51 (red) were labelled. CD51 labelled osteoblasts (yellow arrowheads) were found on day 14 post injury, but these cells disappeared on day 21. Scale bars are 200 μm **(A,C)** or 100 μm **(B,D)**. DAPI, 4′,6-diamidino-2-phenylindole.

CD51$^+$ periosteal cells, with Sca1$^+$ cells primarily present in the fibrous layer while CD51$^+$ are cambium-resident and more closely-associated with tissue formation and remodeling.

3.4 Sca1$^+$CD51$^+$ and CD34$^+$ cell expansion in a model of enhanced healing

Activation of Notch signaling stimulates fracture healing. In this experiment, we utilized αSMACreER/NICD1 animals that have an established enhanced fracture healing phenotype with the expansion of cells and osteoprogenitor during the early stage of fracture healing (Novak et al., 2020). All mice received three doses of tamoxifen to activate NICD1 expression in Cre$^+$ animals and SSPC populations were evaluated at day 3 post injury (Figure 7A). Mice with overexpressed NICD1 did not show a significant change in Lin$^-$ cells compared to wild type mice (Figures 7B, C). NICD1 overexpression led to expansion of CD34^{hi} and Sca1$^+$CD51$^+$ cells compared to wild-type (WT) Cre$^-$ controls (Figures 7D–F). We found that CD34^{med} and CD34^{hi} cells had

10.3389/fphys.2023.1231352

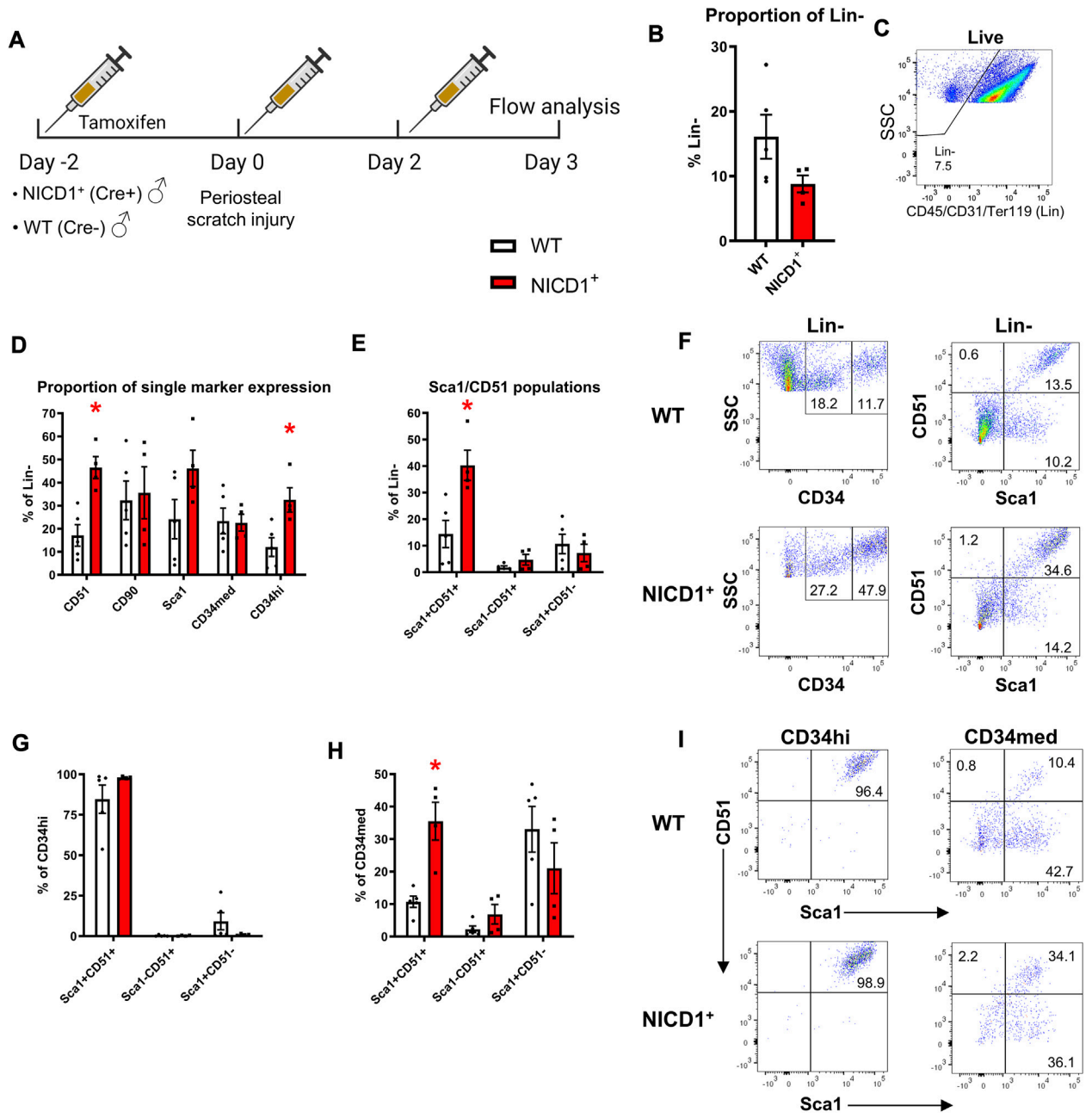

FIGURE 7
CD34^{hi} cells are stimulated with NICD1 overexpression following periosteal injury. **(A)** Experimental design of flow cytometry analysis on αSMACreER/NICD1 animals following periosteal injury (n = 4–5), partially created with BioRender. **(B)** The proportion of hematopoietic lineage negative (Lin$^-$) from WT (Cre$^-$) and NICD1$^+$ (Cre$^+$) mice, representative flow plot shown in **(C)**. **(D)** The proportion of single marker expression within the Lin$^-$ fraction. **(E)** The proportion of Sca1/CD51 populations within Lin$^-$. **(F)** Representative flow plots showing gating strategy of CD34^{med} and CD34^{hi} populations, and Sca1/CD51 populations within periosteal Lin$^-$ of WT and NICD1$^+$ mice. **(G)** The frequency of Sca1/CD51 populations within CD34^{hi} cells. **(H)** The frequency of Sca1/CD51 populations within CD34^{med} cells. **(I)** Representative flow plots showing Sca1/CD51 populations within CD34^{hi} and CD34^{med} populations of WT and NICD1$^+$ mice. *p < 0.05 compared to WT with unpaired t-test. Percentages are specific to the sample. WT, wild type; NICD1, Notch intracellular domain 1.

distinct cell surface marker phenotypes. CD34^{hi} cells were almost 100% Sca1$^+$CD51$^+$ (Figures 7G–I) while CD34^{med} contained all populations from the Sca1/CD51 combination.

In *ex vivo* assays, periosteal Lin$^-$ cells isolated from WT mice showed greater CFU-F forming ability at day 3 post scratch injury than those from uninjured mice (Figures 8A, B). CD34$^-$ cells contributed minimally to CFU-F formation *in vitro*, whereas the CD34$^+$ population formed around 4× more CFU-F than the Lin$^-$ cells without injury (Figure 8B). Three days post injury, the frequency of CFU-F formation in periosteal CD34$^+$ cells was almost doubled compared to uninjured CD34$^+$ cells, indicating better expansion and proliferation potential of skeletal progenitor cells during the early stages of the periosteum healing

10.3389/fphys.2023.1231352

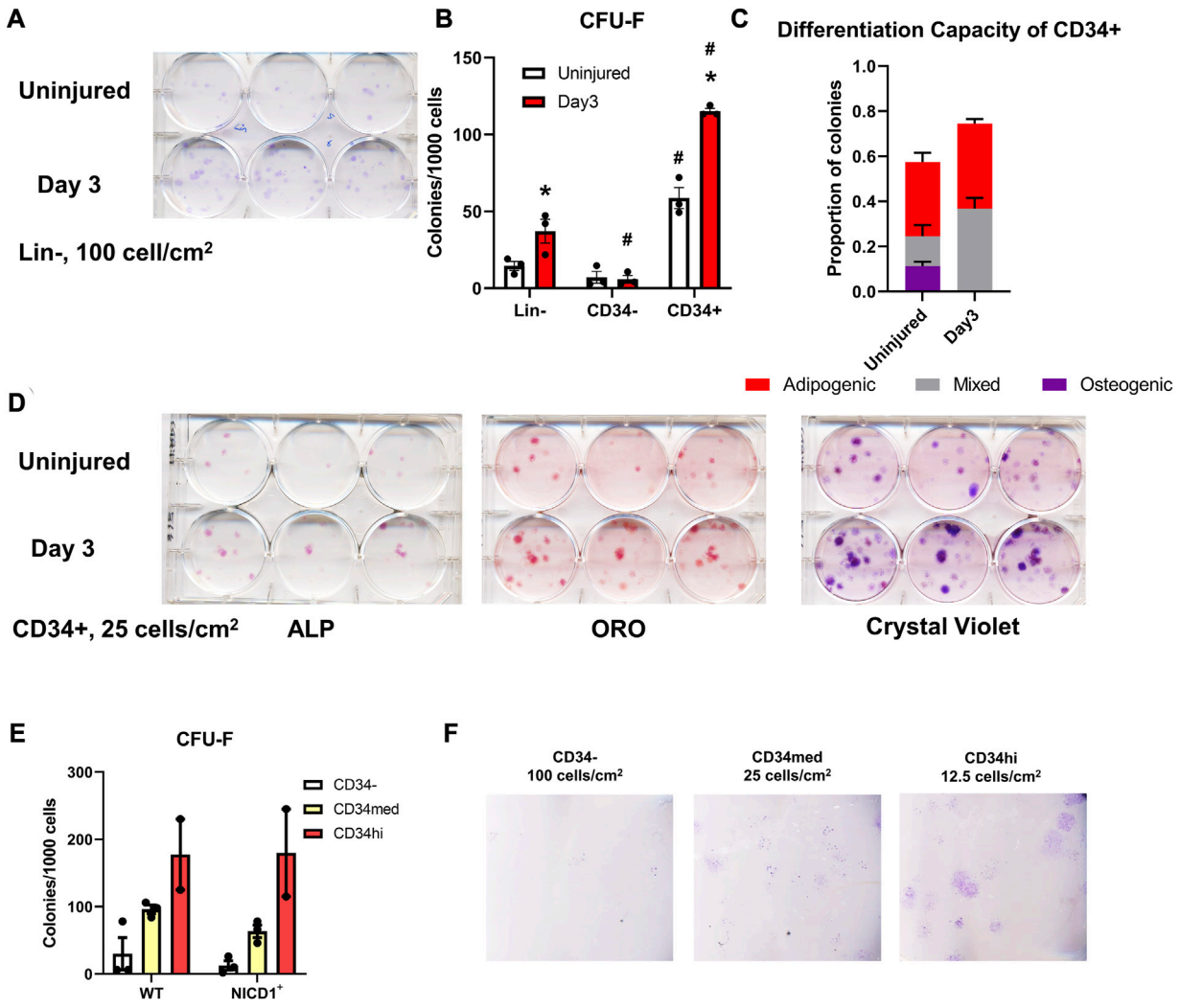

FIGURE 8
Injury enhances CFU-F formation overall and in CD34⁺ cells. Unilateral periosteal injury was performed on WT mice, and periosteal cells were harvested 3 days after injury, the uninjured cells were isolated from the matched uninjured legs (n = 3). **(A)** Representative plate image showing CFU-F of periosteal Lin-populations from uninjured and day 3 injury, stained with crystal violet, and **(B)** quantification of CFU-F for each population. CFU-Fs from the CD34⁺ cells were differentiated with dual-lineage media, and stained with alkaline phosphate (ALP, for osteogenesis), and oil red O (ORO, for adipogenesis), and the stained colonies were quantified **(C)**, representative stained colonies are shown in **(D)**. **(E,F)** Unilateral periosteal injury was performed on αSMACreER/NICD1 mice as indicated in Figure 7A, and periosteal cells sorted at day 3. **(E)** Quantification of CFU-F for CD34 populations in WT and NICD1+ animals (n = 2–3), and representative plate images with crystal violet staining of CFU-Fs are shown in **(F)**. Two-way ANOVA with Tukey's *post hoc* test: *p < 0.05 compared to uninjured, #p < 0.05 compared to Lin⁻ within the same time point. Lin⁻: hematopoietic lineage negative.

process. We also examined the differentiation capacity of the CD34⁺ cells with or without injury. CD34⁺ cells from injured periosteum formed adipocytes rapidly, therefore, in order to fairly compare their differentiation potential, cells were fixed and stained at day 2 post differentiation when massive adipocyte colonies were observed. We found that some periosteal CD34⁺ cells with and without injury were bi-potent, containing colonies with osteogenic, adipogenic, and combined potentials (Figures 8C, D). It is not surprising that some colonies were undifferentiated on day 2 after differentiation induction. These results suggest that the periosteal CD34⁺ cells are immature progenitors that can be stimulated with periosteum injury.

To better understand the functions of different CD34 populations, we isolated CD34⁻, CD34^{med}, and CD34^{hi} populations from αSMACreER/NICD1 mice 3 days after periosteum injury and investigated their colony-forming potential (Figures 8E, F). CD34^{hi} cells exhibited the best CFU-F formation ability, but NICD1 overexpression did not alter the CFU-F formation. These results suggest that the expression of CD34 and CD51 is rapidly stimulated with injury when NICD1 is overexpressed around the time of injury. CD34⁺ cells exhibit better expansion, proliferation and differentiation potential following periosteal injury.

4 Discussion

In this study we sought to identify injury-responsive stem and progenitor populations in adult murine periosteum. Our studies

indicate that CD51 is expressed on periosteal stem and progenitor cells. Many groups use CD51 as one of the markers for skeletal stem and progenitor phenotype (Chan et al., 2009; Pinho et al., 2013; Chan et al., 2015; Green et al., 2021). We have previously reported that all periosteal SSPCs capable of CFU-F formation expressed CD51, although CD51 also labelled a large portion of osteoblasts *in vivo* (Matthews et al., 2021). We separated CD51$^+$ cells on the basis of Sca1 expression, which in our previous study enabled separation of Sca1$^+$CD51$^+$ CFU-F with multilineage differentiation potential from Sca1$^-$CD51$^+$ cells which formed fewer CFU-F and showed restricted potential to the osteoblast lineage (Matthews et al., 2021). Surprisingly, Sca1$^-$CD51$^+$ cells isolated from resting periosteum showed much greater engraftment and expansion *in vivo* than the Sca1$^+$CD51$^+$ cells that appear more stem-like *in vitro*. Notably, we previously observed good engraftment and contribution to new bone formation when mature osteoblasts or bone lining cells identified by *Dmp1* expression were transplanted (Matic et al., 2016). While this ectopic bone formation model does not directly replicate any clinical scenario, this data suggest that progenitor cells may be more effective than stem cells for transplantation in scenarios where rapid expansion and tissue formation are required to enable one-off skeletal regeneration.

Consistent with our previous flow data (Matthews et al., 2021), immunostaining results confirmed that Sca1 expression is enriched in the periosteum. However, these cells rarely co-expressed CD51, and resided primarily in the outer periosteum which thought to house fibroblasts rather than stem and progenitor cells. Single cell RNAseq analysis of periosteal cells suggested that Sca1 is a differentiated periosteal cell marker (Debnath et al., 2018). There appears to be differences in sensitivity between flow and immunostaining studies which make it difficult to localize the Sca1$^+$CD51$^+$ population *in vivo*. *In vivo*, CD51$^+$ cells demonstrated cambium layer localization, which is more consistent with what we expected from periosteal stem and progenitor cells. Notably, we rarely found CD51$^+$ osteoblasts *in vivo* except during the most active phase of bone formation in the callus suggesting that CD51 is downregulated as osteogenic differentiation progresses. Single cell RNAseq analysis of bone marrow cells suggested that CD51 is enriched in Col2.3Cre labelled cells compared to cells expressing LepRCre and VE-CadCre (Tikhonova et al., 2019). Among the three clusters deriving from the Col2.3Cre$^-$ labelled cells, CD51 is downregulated in the cluster that appears most likely to represent true osteoblasts based on high expression of *Ibsp* and *Bglap*. This agrees with our data that CD51 expression diminishes with osteoprogenitor maturation. Another single cell RNAseq analysis of bone marrow stroma also suggested that CD51 expression is enriched in the osteogenic lineage cell cluster (cluster 7) (Baryawno et al., 2019). Both studies show fairly low expression of CD51 in around a third of cells within osteoblast clusters, consistent with our previous flow analysis of Col2.3GFP$^+$ endosteal cells (Matic et al., 2016; Matthews et al., 2021).

We utilized a periosteal scratch injury as an alternative to creating a full fracture. Consistent with previous reports, this model recapitulated the healing process following generation of a semi-stabilized fracture, despite the absence of instability (Colnot, 2009; Hagiwara et al., 2015). The early phases of healing showed a remarkably similar time course to full fracture healing, although the final remodeling stage appeared to progress more quickly, presumably because repositioning and remodeling of the original cortical bone was not required. Consistent with our previous findings in fracture, αSMA labels periosteal progenitor cells that expand dramatically after injury and give rise to osteoblasts, chondrocytes, and osteocytes (Matthews et al., 2021). We reasoned that stem and progenitor cells that are critical for healing should begin to expand in the early stages of fracture prior to the initiation of fibrocartilage formation. The only marker apart from αSMA-derived cells that showed consistent expansion at day 3 was CD90. CD90 is considered a marker of osteochondrogenic progenitors in fetal and neonatal skeletal tissues, and more immature stem and progenitor are often reported to be CD90$^-$ (Chan et al., 2009; Chan et al., 2015; Debnath et al., 2018). We have found that CD90 enriches for periosteal CFU-F in both mice and humans (Matthews et al., 2021; Cao et al., 2022). A study using single cell RNAseq on cells from resting periosteum showed co-expression of CD90 with Sca1 and CD34 in what their analysis identified as an undefined non-osteoblastic mature periosteal cell type (Debnath et al., 2018). We did not find any difference in CD90$^+$ cell response in our model of enhanced healing.

Several cell populations, including Sca1$^+$CD51$^+$, Sca1$^-$CD51$^+$ and CD34$^+$ cells showed enhanced expansion by day 7 after injury. This is consistent with other studies showing strong expansion of various proposed SSPC populations by about a week after fracture (Marecic et al., 2015; Debnath et al., 2018). We noted the appearance of a CD34^{hi} population primarily after injury. CD34 was traditionally considered a negative marker for SSPCs (Viswanathan et al., 2019), but more thorough analyses suggest that CD34 is present in at least some SSPC types *in vivo* including those in the periosteum, but is downregulated in culture (Ball et al., 2011; Abdallah et al., 2015; Cao et al., 2022). Julien et al. reported the skeletal stem/progenitor cluster is highly enriched for CD34 compared to the macrophages or osteoclasts cluster from single-cell RNAseq analysis (Julien et al., 2022). In this study, we found that the CD34$^+$ population was relatively rare in intact adult periosteum, but its expression increased significantly by day 7 following local injury. Periosteal CD34$^+$ cells expanded and differentiated faster 3 days after injury, these cells were osteogenic and adipogenic *in vitro*. CD34^{hi} cells in particular were much more common in our Notch-mediated model of enhanced healing. Future studies will be needed to address localization of the CD34$^+$ populations, however strong expression of CD34 in other cell types including endothelial cells complicates this analysis.

Notch signaling controls bone growth and homeostasis in mice and humans. Dishowitz et al. (2013) inhibited Notch signaling systemically using Mx1Cre; dnMAML mice which led to impaired fracture healing with prolonged inflammation. A different model of impaired Notch signaling, Prx1Cre; RBPjk$^{fl/fl}$, had fracture non-union (Wang et al., 2016). Pharmacological Notch1 inhibition also impaired fracture healing, albeit to a lesser extent (Novak et al., 2020). Conversely, overexpressing NICD1 in αSMA$^+$ cells at the early stages of fracture accelerates the progression of fracture healing in male mice (Novak et al., 2020). Using similar injury-related activation of NICD1, we found that the frequency of cells expressing CD51 was enriched with NICD1 overexpression at day 3 following periosteal injury.

$Sca1^+CD51^+$ and $CD34^{hi}$ cells were also highly enriched with NICD1 overexpression. These results indicate that greater or earlier expansion of $CD51^+$, $Sca1^+CD51^+$, and $CD34^{hi}$ cells may improve bone healing. $CD34^{hi}$ was a refined $Sca1^+CD51^+$ subpopulation that enriched for CFU-F formation.

This study has several limitations. We performed *in vitro* differentiation assays on osteogenesis and adipogenesis with selected populations, but not chondrogenesis in parallel due to insufficient cell density and large differences in differentiation conditions. It is surprising that periosteal cells undergo adipogenesis so readily given this is not seen *in vivo*, but is consistent with our recent studies of human periosteum (Cao et al., 2022). We performed a limited number of *in vivo* transplantation assays using subcutaneous transplantation with carrier cells. It is still unclear whether this assay, or others using different types of transplantation, accurately reflect the *in vivo* potential of cell populations. In addition, we only evaluated cell fate at a single time point so the $Sca1^-CD51^+$ derived ossicles can be either more immature, developing bone and marrow infiltration later than the other ossicles, or more osteogenic, never forming the same amount of stromal cells as the other populations. Our study clearly illustrates the challenges integrating data from *in vitro*, *in vivo* and *in situ* studies to understand the function and potential of stem and progenitor cell populations. It is still unclear how removing periosteal cells from their niche affects their behavior, presenting a limitation for any type of *ex vivo* or transplantation studies. The periosteum scratch injury avoids the direct infiltration of bone marrow cells as part of the callus, although these cells generally appear to make a very minor direct contribution (Colnot, 2009). Nonetheless, we cannot avoid some injury to the neighboring muscle during this process.

In conclusion, we have confirmed that local injury to the periosteum heals with a similar process to semi-stabilized fracture healing through endochondral ossification. Injury leads to expansion of various SSPC populations, and an overall increase in the frequency of CFU-Fs. $Sca1^-CD51^+$ cells are osteochondral progenitors resident specifically in the cambium layer of the periosteum that expand and contribute to bone and cartilage upon transplantation and likely do the same in the context of injury. $Sca1^+CD51^+$ cells could not be localized histologically, and despite high expansion and differentiation potential *in vitro* and following injury, they show poorer expansion or survival following transplantation making the utility of Sca1/CD51 combination in identifying periosteal SSPC populations uncertain without additional markers. Histologically Sca1 was primarily detectable in the outer fibrous layer of the periosteum that is not thought to house SSPCs. Further refinement and characterization of populations including $Sca1^-CD51^+$ and $CD34^{hi}$ cells is important in order to confirm their lineage hierarchy in the adult skeletal system, and ensure that mature cells like osteoblasts are excluded. Finally, our data suggests that skeletal progenitor cells may be more effective than stem cells for regenerative uses that do not require long-term engraftment.

Data availability statement

The raw data supporting the conclusion of this article will be made available by the authors, without undue reservation.

Ethics statement

The animal studies were approved by the University of Auckland Animal Ethics Committee and the UConn Health Institutional Animal Care and Use Committee. The study was conducted in accordance with the local legislation and institutional requirements.

Author contributions

YC, IK, and BM conceptualized the study; YC performed experiments; IK and BM assisted with experiments; YC performed data analysis; IK and BM funded the study; YC wrote the initial draft; All authors contributed to the article and approved the submitted version.

Funding

Funded by a Health Research Council of New Zealand Sir Charles Hercus Fellowship 17/050 to BM and NIAMS/NIH grant R01 AR055607 to IK. YC was supported by a University of Auckland Doctoral Scholarship.

Acknowledgments

We acknowledge the assistance of Thaize Chrometon with flow cytometry analysis, and Stephen Edgar and Evan Jellison for cell sorting. We thank Marcus Ground for assisting with figure assembly using BioRender.

Conflict of interest

The authors declare that the research was conducted in the absence of any commercial or financial relationships that could be construed as a potential conflict of interest.

Publisher's note

Supplementary material

The Supplementary Material for this article can be found online at: https://www.frontiersin.org/articles/10.3389/fphys.2023.1231352/full#supplementary-material

References

Abdallah, B. M., Al-Shammary, A., Skagen, P., Abu Dawud, R., Adjaye, J., Aldahmash, A., et al. (2015). CD34 defines an osteoprogenitor cell population in mouse bone marrow stromal cells. *Stem Cell. Res.* 15 (3), 449–458. doi:10.1016/j.scr.2015.09.005

Ball, M. D., Bonzani, I. C., Bovis, M. J., Williams, A., and Stevens, M. M. (2011). Human periosteum is a source of cells for orthopaedic tissue engineering: a pilot study. *Clin. Orthop. Relat. Res.* 469 (11), 3085–3093. doi:10.1007/s11999-011-1895-x

Baryawno, N., Przybylski, D., Kowalczyk, M. S., Kfoury, Y., Severe, N., Gustafsson, K., et al. (2019). A cellular taxonomy of the bone marrow stroma in homeostasis and leukemia. *Cell.* 177 (7), 1915–1932. doi:10.1016/j.cell.2019.04.040

Cao, Y., Bolam, S. M., Boss, A. L., Murray, H. C., Dalbeth, N., Brooks, A. E. S., et al. (2022). *Characterization of adult human skeletal cells in different tissues reveals a CD90+CD34+ periosteal stem cell population*. Cold Spring Harbor Laboratory.

Cao, Y., Buckels, E. J., and Matthews, B. G. (2020). Markers for identification of postnatal skeletal stem cells *in vivo*. *Curr. Osteoporos. Rep.* 18 (6), 655–665. doi:10.1007/s11914-020-00622-2

Chai, W. H., Hao, W. W., Liu, J. T., Han, Z. L., Chang, S. Y., Cheng, L. B., et al. (2023). Visualizing cathepsin K-Cre expression at the single-cell level with GFP reporters. *JBMR Plus* 7 (1), e10706. doi:10.1002/jbm4.10706

Chan, C. K. F., Chen, C. C., Luppen, C. A., Kim, J. B., DeBoer, A. T., Wei, K., et al. (2009). Endochondral ossification is required for haematopoietic stem-cell niche formation. *Nature* 457 (7228), 490–494. doi:10.1038/nature07547

Chan, C. K. F., Seo, E. Y., Chen, J. Y., Lo, D., McArdle, A., Sinha, R., et al. (2015). Identification and specification of the mouse skeletal stem cell. *Cell.* 160 (1-2), 285–298. doi:10.1016/j.cell.2014.12.002

Colnot, C. (2009). Skeletal cell fate decisions within periosteum and bone marrow during bone regeneration. *J. Bone Min. Res.* 24 (2), 274–282. doi:10.1359/jbmr.081003

Debnath, S., Yallowitz, A. R., McCormick, J., Lalani, S., Zhang, T., Xu, R., et al. (2018). Discovery of a periosteal stem cell mediating intramembranous bone formation. *Nature* 562 (7725), 133–139. doi:10.1038/s41586-018-0554-8

Dishowitz, M. I., Mutyaba, P. L., Takacs, J. D., Barr, A. M., Engiles, J. B., Ahn, J., et al. (2013). Systemic inhibition of canonical Notch signaling results in sustained callus inflammation and alters multiple phases of fracture healing. *PLoS One* 8(7), e68726-e68726. doi:10.1371/journal.pone.0068726

Dishowitz, M. I., Terkhorn, S. P., Bostic, S. A., and Hankenson, K. D. (2012). Notch signaling components are upregulated during both endochondral and intramembranous bone regeneration. *J. Orthop. Res.* 30 (2), 296–303. doi:10.1002/jor.21518

Duchamp de Lageneste, O., Julien, A., Abou-Khalil, R., Frangi, G., Carvalho, C., Cagnard, N., et al. (2018). Periosteum contains skeletal stem cells with high bone regenerative potential controlled by Periostin. *Nat. Commun.* 9 (1), 773. doi:10.1038/s41467-018-03124-z

Dyment, N. A., Jiang, X., Chen, L., Hong, S.-H., Adams, D. J., Ackert-Bicknell, C., et al. (2016). High-throughput, multi-image cryohistology of mineralized tissues. *J. Vis. Exp.* (115), e54468. doi:10.3791/54468

Grcevic, D., Pejda, S., Matthews, B. G., Repic, D., Wang, L., Li, H., et al. (2012). *In vivo* fate mapping identifies mesenchymal progenitor cells. *Stem Cells* 30 (2), 187–196. doi:10.1002/stem.780

Green, A. C., Tjin, G., Lee, S. C., Chalk, A. M., Straszkowski, L., Kwang, D., et al. (2021). The characterization of distinct populations of murine skeletal cells that have different roles in B lymphopoiesis. *Blood* 138 (4), 304–317. doi:10.1182/blood.2020005865

Hagiwara, Y., Dyment, N. A., Jiang, X., Ping, H. J., Ackert-Bicknell, C., Adams, D. J., et al. (2015). Fixation stability dictates the differentiation pathway of periosteal progenitor cells in fracture repair. *J. Orthop. Res.* 33 (7), 948–956. doi:10.1002/jor.22816

Julien, A., Perrin, S., Martínez-Sarrà, E., Kanagalingam, A., Carvalho, C., Luka, M., et al. (2022). Skeletal stem/progenitor cells in periosteum and skeletal muscle share a common molecular response to bone injury. *J. Bone Mineral Res.* 37 (8), 1545–1561. doi:10.1002/jbmr.4616

Kalajzic, Z., Liu, P., Kalajzic, I., Du, Z., Braut, A., Mina, M., et al. (2002). Directing the expression of a green fluorescent protein transgene in differentiated osteoblasts: comparison between rat type I collagen and rat osteocalcin promoters. *Bone* 31 (6), 654–660. doi:10.1016/s8756-3282(02)00912-2

Kawanami, A., Matsushita, T., Chan, Y. Y., and Murakami, S. (2009). Mice expressing GFP and CreER in osteochondro progenitor cells in the periosteum. *Biochem. Biophys. Res. Commun.* 386 (3), 477–482. doi:10.1016/j.bbrc.2009.06.059

Madisen, L., Zwingman, T. A., Sunkin, S. M., Oh, S. W., Zariwala, H. A., Gu, H., et al. (2010). A robust and high-throughput Cre reporting and characterization system for the whole mouse brain. *Nat. Neurosci.* 13 (1), 133–140. doi:10.1038/nn.2467

Marecic, O., Tevlin, R., McArdle, A., Seo, E. Y., Wearda, T., Duldulao, C., et al. (2015). Identification and characterization of an injury-induced skeletal progenitor. *Proc. Natl. Acad. Sci. U. S. A.* 112 (32), 9920–9925. doi:10.1073/pnas.1513066112

Matic, I., Matthews, B. G., Wang, X., Dyment, N. A., Worthley, D. L., Rowe, D. W., et al. (2016). Quiescent bone lining cells are a major source of osteoblasts during adulthood. *Stem Cells* 34 (12), 2930–2942. doi:10.1002/stem.2474

Matthews, B. G., Grcevic, D., Wang, L., Hagiwara, Y., Roguljic, H., Joshi, P., et al. (2014). Analysis of αSMA-labeled progenitor cell commitment identifies notch signaling as an important pathway in fracture healing. *J. Bone Min. Res.* 29 (5), 1283–1294. doi:10.1002/jbmr.2140

Matthews, B. G., Novak, S., Sbrana, F. V., Funnell, J. L., Cao, Y., Buckels, E. J., et al. (2021). Heterogeneity of murine periosteum progenitors involved in fracture healing. *eLife* 10, e58534. doi:10.7554/eLife.58534

Novak, S., Roeder, E., Sinder, B. P., Adams, D. J., Siebel, C. W., Grcevic, D., et al. (2020). Modulation of Notch1 signaling regulates bone fracture healing. *J. Orthop. Research®* 38 (11), 2350–2361. doi:10.1002/JOR.24650

Ortinau, L. C., Wang, H., Lei, K., Deveza, L., Jeong, Y., Hara, Y., et al. (2019). Identification of functionally distinct Mx1+αSMA+ periosteal skeletal stem cells. *Cell. Stem Cell.* 25 (6), 784–796. doi:10.1016/j.stem.2019.11.003

Pinho, S., Lacombe, J., Hanoun, M., Mizoguchi, T., Bruns, I., Kunisaki, Y., et al. (2013). PDGFRα and CD51 mark human nestin+ sphere-forming mesenchymal stem cells capable of hematopoietic progenitor cell expansion. *J. Exp. Med.* 210 (7), 1351–1367. doi:10.1084/jem.20122252

Sinder, B. P., Novak, S., Wee, N. K. Y., Basile, M., Maye, P., Matthews, B. G., et al. (2020). Engraftment of skeletal progenitor cells by bone directed transplantation improves osteogenesis imperfecta murine bone phenotype. *Stem Cells* 38 (4), 530–541. doi:10.1002/stem.3133

Tate, M. L. K., Ritzman, T. E., Schneider, E., and Knothe, U. R. (2007). Testing of a new one-stage bone-transport surgical procedure exploiting the periosteum for the repair of long-bone defects. *J. Bone Jt. Surgery-American* 89a (2), 307–316. doi:10.2106/Jbjs.E.00512

Tikhonova, A. N., Dolgalev, I., Hu, H., Sivaraj, K. K., Hoxha, E., Cuesta-Domínguez, Á., et al. (2019). The bone marrow microenvironment at single-cell resolution. *Nature* 569 (7755), 222–228. doi:10.1038/s41586-019-1104-8

Tournaire, G., Stegen, S., Giacomini, G., Stockmans, I., Moermans, K., Carmeliet, G., et al. (2020). Nestin-GFP transgene labels skeletal progenitors in the periosteum. *Bone* 133, 115259. doi:10.1016/j.bone.2020.115259

Viswanathan, S., Shi, Y., Galipeau, J., Krampera, M., Leblanc, K., Martin, I., et al. (2019). Mesenchymal stem versus stromal cells: international society for cell and gene therapy (ISCT®) mesenchymal stromal cell committee position statement on nomenclature. *Cytotherapy* 21 (10), 1019–1024. doi:10.1016/j.jcyt.2019.08.002

Wang, C. C., Inzana, J. A., Mirando, A. J., Ren, Y. S., Liu, Z. Y., Shen, J., et al. (2016). NOTCH signaling in skeletal progenitors is critical for fracture repair. *J. Clin. Investigation* 126 (4), 1471–1481. doi:10.1172/Jci80672

Wilk, K., Yeh, S. C. A., Mortensen, L. J., Ghaffarigarakani, S., Lombardo, C. M., Bassir, S. H., et al. (2017). Postnatal calvarial skeletal stem cells expressing PRX1 reside exclusively in the calvarial sutures and are required for bone regeneration. *Stem Cell. Rep.* 8 (4), 933–946. doi:10.1016/j.stemcr.2017.03.002

Zhang, X., Xie, C., Lin, A. S. P., Ito, H., Awad, H., Lieberman, J. R., et al. (2005). Periosteal progenitor cell fate in segmental cortical bone graft transplantations: implications for functional tissue engineering. *J. Bone Mineral Res.* 20 (12), 2124–2137. doi:10.1359/JBMR.050806

frontiers | Frontiers in Physiology

TYPE Original Research
PUBLISHED 20 September 2023
DOI 10.3389/fphys.2023.1221152

OPEN ACCESS

EDITED BY
Celine Colnot,
INSERM U955, France

REVIEWED BY
Noriaki Ono,
University of Texas Health Science Center at Houston, United States
Fanxin Long,
Children's Hospital of Philadelphia, United States
Xinping Zhang,
University of Rochester, United States

*CORRESPONDENCE
Emily R. Moore,
emily_moore@hsdm.harvard.edu

RECEIVED 11 May 2023
ACCEPTED 05 September 2023
PUBLISHED 20 September 2023

CITATION
Moore ER, Maridas DE, Gamer L, Chen G, Burton K and Rosen V (2023), A periosteum-derived cell line to study the role of BMP/TGFβ signaling in periosteal cell behavior and function.
Front. Physiol. 14:1221152.
doi: 10.3389/fphys.2023.1221152

A periosteum-derived cell line to study the role of BMP/TGFβ signaling in periosteal cell behavior and function

Emily R. Moore*, David E. Maridas, Laura Gamer, Gavin Chen, Kathryn Burton and Vicki Rosen

Department of Developmental Biology, Harvard School of Dental Medicine, Boston, MA, United States

The periosteum is a thin tissue surrounding each skeletal element that contains stem and progenitor cells involved in bone development, postnatal appositional bone growth, load-induced bone formation, and fracture repair. BMP and TGFβ signaling are important for periosteal activity and periosteal cell behavior, but thorough examination of the influence of these pathways on specific cell populations resident in the periosteum is lacking due to limitations associated with primary periosteal cell isolations and *in vitro* experiments. Here we describe the generation of a novel periosteum-derived clonal cell (PDC) line from postnatal day 14 mice and use it to examine periosteal cell behavior *in vitro*. PDCs exhibit key characteristics of periosteal cells observed during skeletal development, maintenance, and bone repair. Specifically, PDCs express established periosteal markers, can be expanded in culture, demonstrate the ability to differentiate into chondrocytes, osteoblasts, and adipocytes, and exhibit an osteogenic response to physical stimulation. PDCs also engage in BMP and/or TGFβ signaling when treated with the activating ligands BMP2 and TGFβ-1, and in response to mechanical stimulation via fluid shear. We believe that this PDC line will be useful for large-scale, long-term experiments that were not feasible when using primary periosteal cells. Anticipated future uses include advancing our understanding of the signaling interactions that occur during appositional bone growth and fracture repair and developing drug screening platforms to discover novel growth and fracture healing factors.

KEYWORDS

periosteum, cell line, BMP signaling, TGFβ signaling, mechanotransduction

Introduction

The periosteum is a thin tissue surrounding each skeletal element that contains stem and progenitor cells involved in bone development, postnatal appositional bone growth, load-induced bone formation, and fracture repair (Colnot, 2009; Wang et al., 2017; Moore et al., 2018a; Moore et al., 2018b; Duchamp De Lageneste et al., 2018; Moore et al., 2019; Ortinau et al., 2019; Moore et al., 2020; Xiao et al., 2020; Ono, 2022). In each of these contexts, bone morphogenetic protein (BMP) and/or transforming growth factor-β (TGFβ) signaling is required for periosteal cell function (Tsuji et al., 2006; Chen et al., 2012; Salazar et al., 2016; Wu et al., 2016; Salazar et al., 2019; Xia et al., 2020). Deficits in periosteal cell presence and activity are

linked to severe skeletal abnormalities, highlighting the periosteum's importance in skeletal health (Tsuji et al., 2006; Shi et al., 2017; Moore et al., 2018a; Duchamp De Lageneste et al., 2018; Moore et al., 2019; Salazar et al., 2019; Wang et al., 2019; Moore et al., 2020). The periosteum's superior regenerative potential has sparked efforts to identify stem/progenitor cells that can be targeted to generate bone where needed. This pursuit has been complicated by the surprising heterogeneity of stem/progenitor cell populations present in the periosteum (Matthews et al., 2021). Markers that have been utilized to identify periosteal stem/progenitor cells include *Prx1, αSMA, Gli1, Ctsk,* and *Pdgfrα* (Kawanami et al., 2009; Grcevic et al., 2012; Matthews et al., 2014; Shi et al., 2017; Debnath et al., 2018; Duchamp De Lageneste et al., 2018; Ortinau et al., 2019; Esposito et al., 2020; Brown et al., 2022; Jeffery et al., 2022; Xu et al., 2022). Genetic mouse models have been used to characterize cell populations resident in the periosteum, but a consensus has yet to be reached on the population dynamics of periosteal stem/progenitors.

One meaningful approach to analyzing periosteal stem/progenitor cells has been to isolate primary cells from whole periosteum and perform *in vitro* experiments. From these studies we have come to appreciate the heterogeneity of cells resident in the periosteum, and learned that periosteal stem/progenitor cells can be expanded in culture, are multipotent and mechanoresponsive, and have high regenerative potential when implanted *in vivo* (Moore et al., 2018b; Debnath et al., 2018; Moore et al., 2019; Perrin et al., 2021; Brown et al., 2022). However, there are several limitations when working with primary periosteal cells. First, isolating the periosteum is technically challenging. The periosteum is extremely thin and requires a microscope to visually detect and dissect. It is also intimately connected to muscle and connective tissues such that contamination of other cell types during isolation is essentially unavoidable. Second, the cellular yield from periosteal preparations pales in comparison to that of more traditional skeletal cell isolations, such as calvarial osteoblasts or bone marrow stromal cells. The periosteum becomes thinner and harder to physically separate from surrounding tissues with age, so isolating a substantial, purified population from adult mice is especially challenging. Third, the osteogenic behavior of periosteal stem/progenitor cells decreases significantly with just a few passages and survival of the various periosteal cell populations in culture remains uncharacterized (Brown et al., 2022). Lastly, depending on the chosen protocol and because of the periosteum's heterogeneity, isolations can vary significantly between sessions. Collectively, these limitations have made it difficult to conduct large-scale and long-term experiments investigating periosteal cells with a great degree of reproducibility.

Here, we present the establishment of a novel periosteum-derived clonal cell line that expresses classic periosteal cell markers, is multipotent *in vitro*, engages in BMP/TGFβ signaling, and is responsive to mechanical stimulation. These characteristics are stable with passaging, indicating this cell line can be utilized for large-scale *in vitro* experiments. We anticipate this cell line will greatly advance our understanding of periosteal cells in bone growth and regeneration, as well as the signaling mechanisms involved in these biological processes.

Materials and methods

Animals

Bmp2^{lacZ} mice were generated in the Rosen Lab and model characteristics and genotyping are previously described (Salazar et al., 2019). Experiments were performed in compliance with the Guide for the Care and Use of Laboratory Animals and were approved by the Harvard Medical Area Institutional Animal Care and Use Committee (IACUC). Mice were housed and cared for in accordance with IACUC standards in an AAALAC-accredited facility. Mice were euthanized via CO_2 inhalation and cervical dislocation as secondary confirmation in accordance with IACUC standards.

Periosteal cell isolation and culture

Femurs were dissected from two male and two female postnatal day 14 *Bmp2*^{lacZ} mice (see Figures 1A–D). Most of the muscle and connective tissue were removed before placing femurs in PBS on ice. Under a dissecting microscope, a scalpel was used to bisect the growth plates (perpendicular to the longitudinal axis of the femur) to remove most of the epiphyseal ends and associated connective tissue without exposing the bone marrow. Fine-tipped Dumont forceps (Fine Science Tools, 11203-23) were used to separate as much muscle and connective tissue from the femur as possible without disrupting the periosteum. These tissues were gently removed using a scalpel with a #10 blade in a cutting motion parallel to the periosteal surface to avoid pulling off the periosteum. At each epiphyseal end, the scalpel was used to make a single cut around the circumference of the femur 1 mm beneath the growth plate to avoid capturing perichondrium. The scalpel was then used to make a single cut in the periosteum from one epiphyseal end to the other and the periosteum was peeled from the femur using Dumont forceps. The resulting periosteal tissue was incubated in 1 mg/mL Collagenase type I (Millipore, scr103) in sterile PBS in a cell culture incubator (37°C, 5% CO_2) for 1 h. The digestion solution was then filtered through a 70 µm filter (Corning, 431751) and resulting cells were cultured in MEMα (Gibco, A10490-01) supplemented with 10% fetal bovine serum (FBS) and 1% PenStrep (Gibco, 15140122). Primary cells did not survive if cloned immediately after isolation, so extensive passaging was performed first to eliminate populations incapable of being immortalized. The cells isolated from all four mice were pooled together and passaged twenty times. Cell density never exceeded 80% confluence to avoid potential osteogenic differentiation. Passage 21 (P-21) cells were diluted and seeded at a density of one cell per well in one 96 well plate to establish individual clones. The plate was examined under a microscope to confirm no more than one cell was present in each well. After 2–3 weeks, twelve clones that were viable and proliferated to achieve a confluence greater than 50% were further cultured for two additional passages (P-22, P-23) to observe expansion and viability on a larger scale. Nearly a dozen other wells contained cells, but these populations were excluded based on evidence of cell death and a lack of

10.3389/fphys.2023.1221152

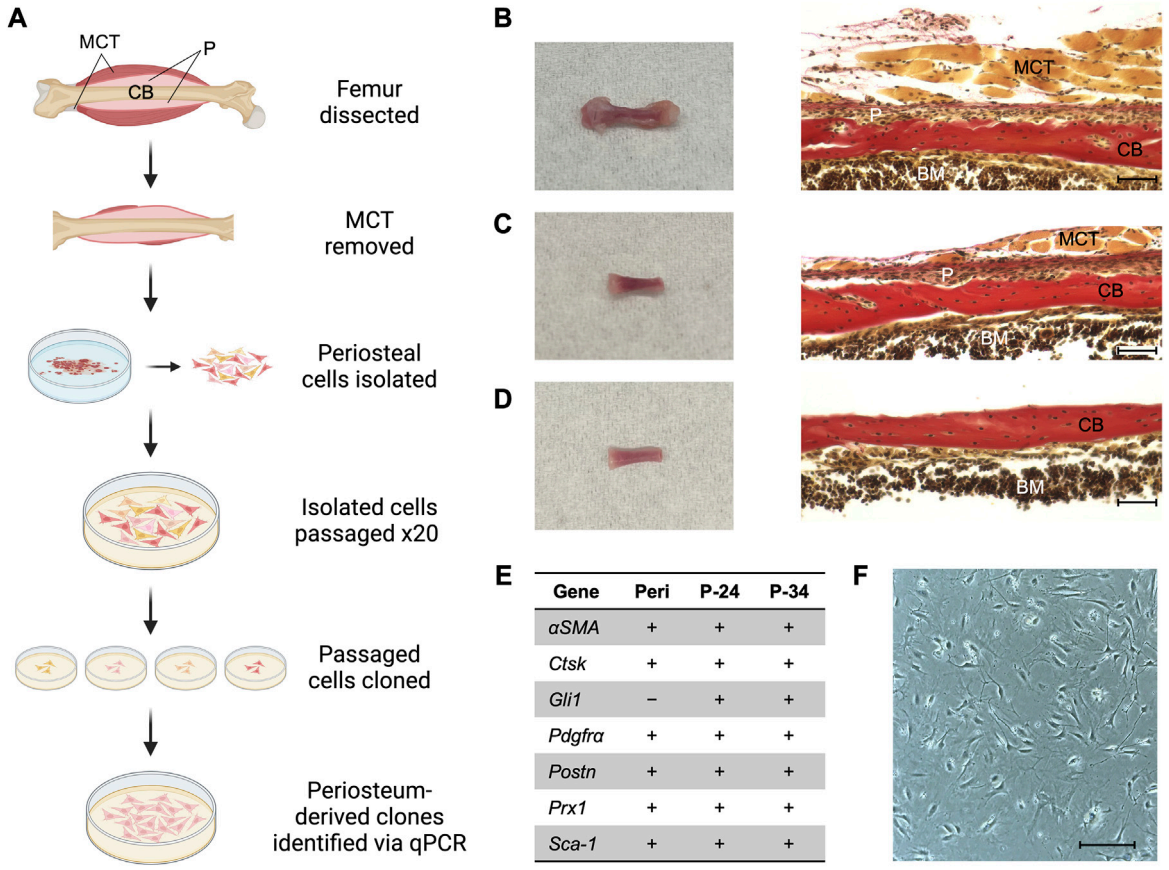

Gene	Peri	P-24	P-34
αSMA	+	+	+
Ctsk	+	+	+
Gli1	–	+	+
Pdgfra	+	+	+
Postn	+	+	+
Prx1	+	+	+
Sca-1	+	+	+

FIGURE 1
Generating a periosteum-derived cell line. **(A)** Schematic summarizing the steps to generate a line of periosteum-derived cells (PDCs). Created with BioRender.com. Abbreviations: periosteum (P), muscle and connective tissue (MCT), and cortical bone (CB). **(B)** Femur isolated from a P14 *Bmp2*^{LacZ} mouse and corresponding histology stained with Hematoxylin Van Gieson's to indicate P, MCT, CB, and bone marrow (BM). **(C)** Femur from **(B)** after the epiphyses and most of the MCT were removed under a dissecting microscope. **(D)** Femur from **(C)** after the periosteum was peeled under a dissecting microscope for the cell digest. Images were taken at ×20 magnification and scale bars indicate 100 μm. **(E)** mRNA expression of markers used to identify periosteum-derived clones. Expression was examined in freshly isolated periosteum (Peri) from P14 *Bmp2*^{LacZ} mice and candidate clones at passages 24 (P-24) and 34 (P-34). Denotes markers that are expressed (+) or not detected (–). *n* = 3–4 biological replicates for each group. **(F)** Cell morphology of the clone selected for the PDC line. Image was taken at ×10 magnification and scale bar indicates 100 μm.

proliferation. Four of the twelve selected clones proliferated at a comparatively staggering rate and exhibited extensive cell death, so these clones were excluded. The eight remaining candidate clones were reserved in stock vials and examined for mRNA markers of muscle, tendon, and periosteum (Supplementary Figure S1). Stock vials consist of approximately 1 million cells in culture media supplemented with 10% DMSO (Sigma-Aldrich, D2650) and are stored in liquid nitrogen.

Differentiation culture and staining

Experiments were conducted using both early (P-24–P-26) and later passages (P-32–P-34) to examine consistency. Osteogenic differentiation: media consisted of MEMα supplemented with 20% FBS, 1% PenStrep, 10 mM β-glycerophosphate (Sigma-Aldrich, G9422), and 100 μM Ascorbic acid (Sigma-Aldrich, A4544). Media was changed every 2–3 days and mineral deposition was detected after 3–4 weeks of treatment. Cells were fixed in 10% neutral-buffered formalin (Millipore, HT501128) for 20 min at ambient temperature and incubated in 1.5% Alizarin Red S (Sigma-Aldrich, A5533) solution to detect matrix deposition. Chondrogenic differentiation: periosteal cells were seeded at a density of 100,000 cells per 15 μL to create micromasses. Micromasses were differentiated using the Gibco StemPro Chondrogenesis Differentiation Kit (Gibco, A1007101). Media was changed every 2–3 days and matrix deposition was detected after 1–2 weeks of treatment. Cells were fixed in 4% paraformaldehyde (Electron Microscopy Sciences, 15710) for 15 min at ambient temperature and incubated in 1% Alcian Blue (Electron Microscopy Sciences, 10350) in 0.1 N HCl to detect cartilaginous matrix deposition. Adipogenic differentiation: periosteal cells were treated with DMEM High Glucose (Sigma-Aldrich, D5796) supplemented with 10% FBS, 1% PenStrep, 62.5 mM IBMX (Sigma-Aldrich, I5879), 1 mM Dexamethasone (Sigma-Aldrich, D4902), 20 mM Rosiglitazone (Cayman Chemical, 71742-10), and 2 mM Insulin (Sigma-Aldrich, I6634) for 4 days, followed by treatment with DMEM High Glucose

supplemented with 10% FBS, 1% PenStrep, 20 mM Rosiglitazone, and 2 mM Insulin for 3 days. Media was changed every 2 days and lipid formation was detected after 1 week of treatment. Cells were fixed in 10% neutral-buffered formalin for 45 min at ambient temperature and incubated in 0.35% Oil O Red (Sigma-Aldrich, O0625) in isopropanol solution to detect lipid accumulation. Cells were counterstained with 0.1% Crystal Violet (Sigma-Aldrich, C6158). Images were collected at 4X or ×10 magnification using a Keyence BZ-X710 microscope and stitched together using its associated software.

Ligand treatment

Experiments were conducted using both early (P-24–P-26) and later passages (P-32–P-34) to examine consistency. To detect changes in mRNA transcription: periosteal cells were incubated in MEMα alone for 2 h to synchronize cell activity. Cells were then incubated in MEMα containing 100 ng/mL BMP2 (Genetics Institute) or 1 ng/mL TGFβ-1 (Peprotech, 100-21C) and lysed after 4 h. For Western blotting: periosteal cells were incubated in MEMα alone for 6 h to synchronize cell signaling. Cells were then incubated in MEMα containing 100 ng/mL BMP2 or 1 ng/mL TGFβ-1 and lysed after 45 min of treatment.

Fluid shear

Experiments were conducted using both early (P-24–P-26) and later passages (P-32–P-34) to examine consistency. Periosteal cells were seeded on 75 × 38 × 1 mm glass slides (Corning, CLS294775X38) and exposed to fluid flow upon exceeding 80% confluence. Fluid shear was applied using a previously described parallel-plate oscillatory fluid flow apparatus (Moore et al., 2018b). Briefly, slides were inserted into chambers containing regular culture media, placed in a cell culture incubator for 30 min to acclimate, and exposed to 1 h of oscillatory fluid flow at 1 Hz with a peak shear stress of 10 dyn/cm^2. Static controls were similarly placed into chambers and incubated alongside fluid shear samples. Slides were removed from the chambers, rinsed with PBS, and lysed for RTqPCR or Western blotting at the conclusion of flow.

RTqPCR

RNA was isolated using TRIzol reagent (ThermoFisher, 15596018) and a RNeasy Kit (Qiagen, 74106). RNA was converted to cDNA using the High-Capacity cDNA Reverse Transcription Kit (ThermoFisher, 4368814). qPCR was performed using Faststart universal SYBR Green (Sigma-Aldrich, 4913850001) and a StepOnePlus Real-Time PCR System (Applied Biosciences). mRNA values were normalized to GAPDH or β-actin–housekeeping genes constitutively expressed at high levels–to account for general variability in mRNA expression between samples. Genes that were within 12 cycles of the cycle at which GAPDH reached the threshold for expression were considered expressed in the PDC line. Experimental groups are expressed as a fold change in relation to controls normalized to a value of "1". Primer sequences are available upon request.

Western blotting

Protein was isolated using RIPA Buffer (Cell Signaling Technology, 9806S) supplemented with protease and phosphatase inhibitors (ThermoFisher, 78440). Samples were examined by immunoblotting after SDS-PAGE using a 10% Bis-Tris gel (Invitrogen, WG1202BX10). Following transfer, membranes were blocked in TBST containing 5% non-fat dry milk and 5% bovine serum albumin and incubated overnight at 4°C in the following primary antibodies diluted in blocking buffer (1:1000): pSmad1 (Cell Signaling Technology, 13820S), Smad1 (Cell Signaling Technology, 9743S), Smad2/3 (Cell Signaling Technology, 8685S), pSmad2 (Cell Signaling Technology, 3108L), and β-actin (Cell Signaling Technology, 4967S). Membranes were then incubated for 1 h at ambient temperature in an anti-Rabbit IgG HRP-linked secondary antibody (Cell Signaling Technology, 7074S) diluted in blocking buffer (1:2000). Blots were developed using SuperSignal West Femto Maximum Sensitivity Substrate (ThermoFisher, 34095). Images were acquired with a PXi4 Chemiluminescent and Fluorescent Imaging System (Syngene, Bangalore, India) and quantification was performed using ImageJ software (National Institutes of Health).

Histology

Dissected femurs were fixed in 10% formalin overnight, decalcified in 0.5 M EDTA (VWR, 75800-470) for 1 week, dehydrated, embedded in paraffin, and sectioned in 5–10 µm slices. Slides were rehydrated and stained using Weigert's Iron Hematoxylin A (VWR, 26044-05), Weigert's Iron Hematoxylin B (VWR, 26044-15) and Van Gieson's Solution (VWR, cat #26046-05). Images were collected at ×20 magnification using a Keyence BZ-X710 microscope and its associated software.

Mycoplasma testing

The clonal cell lines used for this experiment were determined to be negative for *mycoplasma* using the MycoAlert™ *Mycoplasma* Detection Kit (Lonza, LT07-118). Clones were tested the first passage after thawing a stock vial (passage 24, P-24), at P-28 or P-29 during experimentation, and at the conclusion of experiments at P-34.

Karyotyping

PDCs at passage 28 (P-28) and P-33 were seeded at two different densities on 25 cm^2 flasks and shipped at ambient temperature overnight to KaryoLogic, Inc. in Durham, NC for karyotyping. Cytogenetic analysis was performed on twenty G-banded metaphase spreads and we consulted with a senior analyst to interpret the findings.

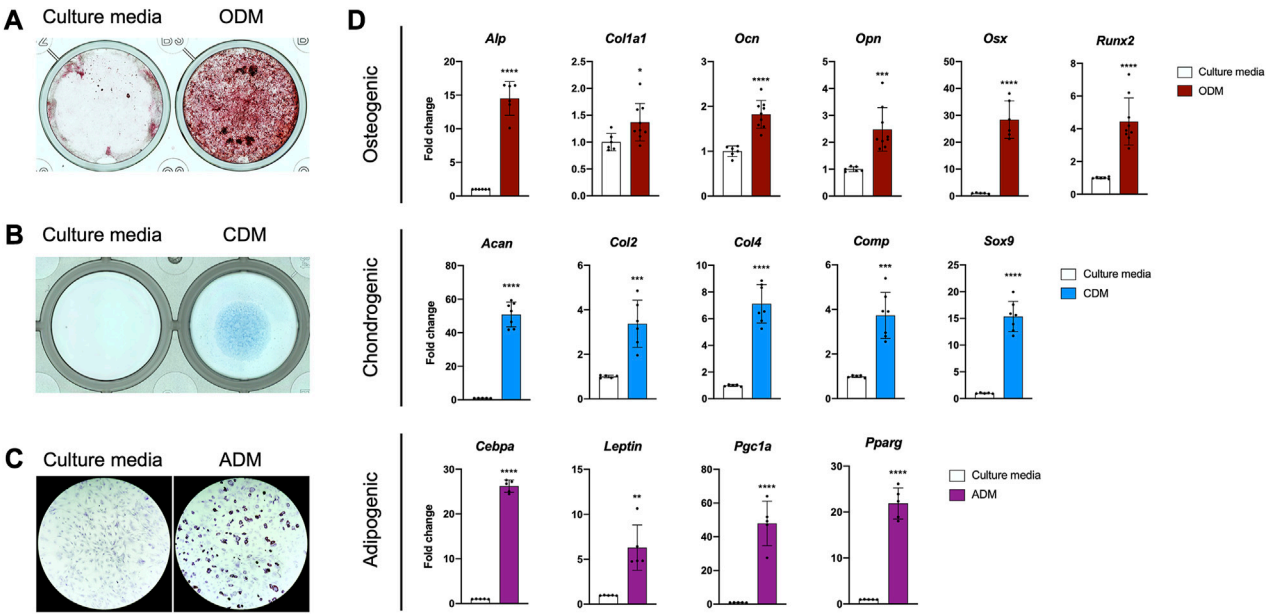

FIGURE 2
The PDC line is multipotent. **(A)** Alizarin Red staining of PDCs incubated in culture media and osteogenic differentiation media (ODM). **(B)** Alcian Blue staining of PDCs incubated in culture media and chondrogenic differentiation media (CDM). **(C)** Oil Red O staining of PDCs incubated in culture media and adipogenic differentiation media (ADM). Images were collected at ×4 magnification and $n = 3–4$ technical replicates in 3 biological replicates for each group in **(A–C)**. **(D)** mRNA expression of genes associated with differentiation. Values are represented as fold changes with DM treatment compared to regular culture media controls. Osteogenic and Chondrogenic values are normalized to *Gapdh* expression, Adipogenic values are normalized to *β-actin* expression. $*p < 0.05$, $**p < 0.01$, $***p < 0.001$, $****p < 0.0001$, n = 6-8 technical replicates in 3 biological replicates for each group. Replicates are represented as individual dots on bar graphs.

Statistics

Researchers were blinded to all data analysis. Differences between control and experimental groups were determined using a two-tailed Student's *t*-test. Values are reported as mean ± SEM, with $p < 0.05$ considered statistically significant. The sample size was selected to achieve a power of at least 80%. Statistical analysis was conducted using GraphPad Prism (San Diego, CA).

Results

Generating a periosteum-derived clonal cell (PDC) line

Primary periosteal cells were isolated from postnatal day 14 (P14) *Bmp2*^{LacZ} mice to maximize cell yield and to utilize X-gal staining to detect BMP2. Briefly, periosteal tissue from femurs was pooled and digested to extract primary cells (Figure 1). These cells were passaged 20 times to select for cells that exhibited high-passage potential and then seeded at a density of 1 cell per well to generate clones. Clones that survived and proliferated were examined for mRNA expression of published markers for periosteal (*αSMA*, *Gli1*, *Pdgfrα*, *Ctsk*, *Prx1*, *Pstn*, and *Sca-1*), skeletal muscle (*Mef2c*, *Myh2*, *Myod1*, and *Myog*), and connective tissue (*Scx*, *Tnmd*) cells (Colnot et al., 2012; Grcevic et al., 2012; Debnath et al., 2018; Duchamp De Lageneste et al., 2018; Jo et al., 2019; Matthews et al., 2021; Piasecka et al., 2021). We first examined these markers in freshly isolated periosteum from P14 *Bmp2*^{LacZ} mice. All periosteal markers except *Gli1* were detected and the muscle and connective tissue markers were not detected. Two candidate clones expressed all periosteal markers, and muscle and connective tissue markers were not detected (Supplementary Figure S1). In fact, none of the candidate clones examined expressed *Scx* or *Tnmd*. This mRNA expression profile remained consistent for 10 passages, suggesting the clones are stable with further passaging (Figure 1E). The following experiments were conducted using cells within the 10 passages examined for mRNA expression and findings at different passages were consistent. For simplicity, we highlight data for one clone to describe a periosteum-derived cell (PDC) line in this manuscript, but results were consistent for both clones (Supplementary Figure S2; Figure 1F).

The PDC line is multipotent *in vitro*

Periosteal stem and progenitor cell populations are known to differentiate into osteoblasts, chondrocytes, and adipocytes *in vitro*, so we examined the lineage potential of our line (De Bari et al., 2006; Arnsdorf et al., 2009a; Debnath et al., 2018; Perrin et al., 2021). PDCs incubated in osteogenic differentiation media deposited mineral in 3–4 weeks (Figure 2A). We detected cartilage matrix deposition in PDC micromasses incubated in chondrogenic differentiation media for 1–2 weeks (Figure 2B). Lipid accumulation was observed in PDCs treated with adipogenic differentiation media after 1 week (Figure 2C). mRNA markers for osteogenesis, chondrogenesis, and

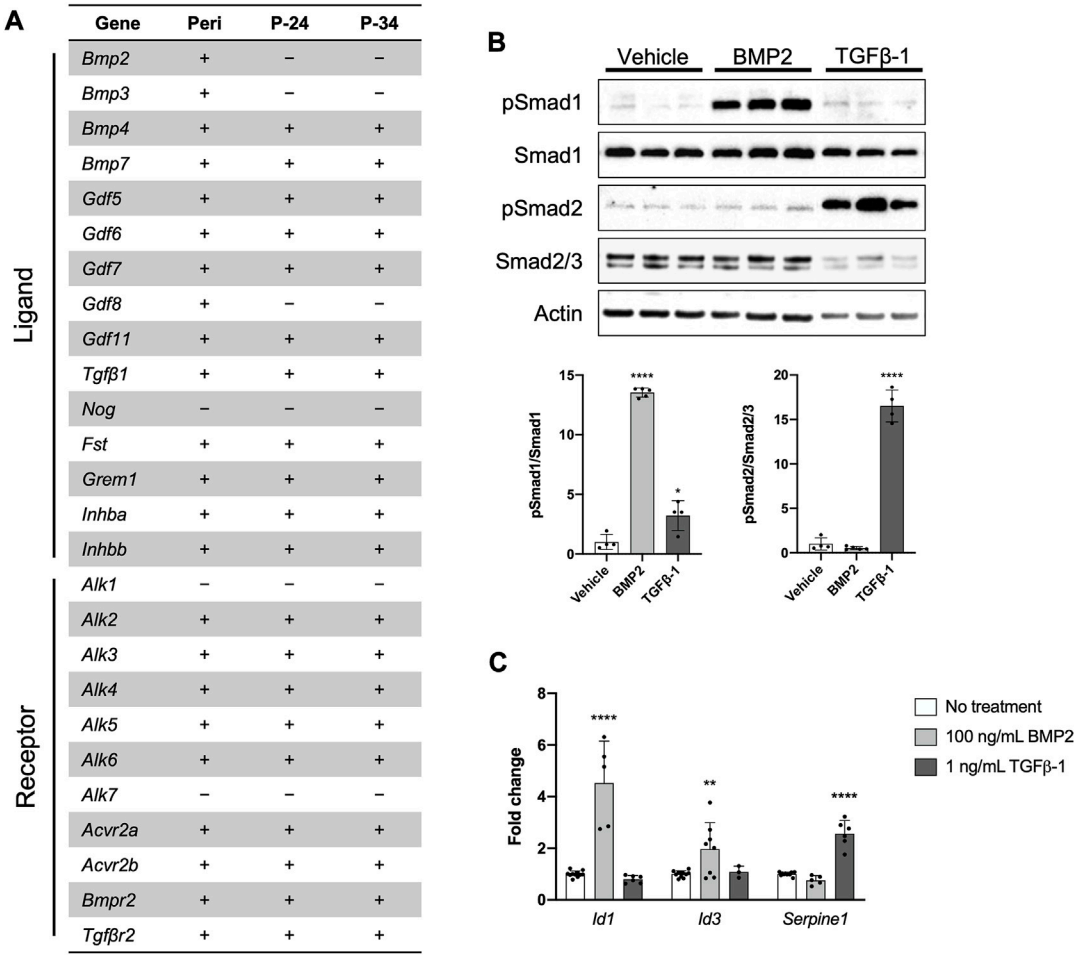

FIGURE 3
The PDC line engages in BMP/TGFβ signaling. **(A)** Expression of genes associated with the BMP/TGFβ superfamily in freshly isolated periosteum (Peri) from P14 *Bmp2*^{LacZ} mice and PDCs at passage 24 (P-24) and 34 (P-34). Denotes markers that are expressed (+) or not detected (–). n = 4–6 technical replicates in 3 biological replicates for each group. **(B)** Representative Western blot image and quantification of changes in total and phosphorylated (p) Smad1 and Smad2/3 with 100 ng/mL BMP2 or 1 ng/mL TGFβ-1 treatment. All values were normalized to Actin expression. *$p < 0.05$, ****$p < 0.0001$, n = 4-5 technical replicates in 3 biological replicates for each group. **(C)** Fold changes in mRNA expression of genes associated with activation of BMP and TGFβ signaling in PDCs treated with 100 ng/mL BMP2 or 1 ng/mL TGFβ-1. Changes in expression are represented as fold changes compared to static controls and all values are normalized to *Gapdh* expression. **$p < 0.01$, ****$p < 0.0001$, n = 3–4 technical replicates in 3 biological replicates for each group. Replicates are represented as individual dots on bar graphs.

adipogenesis were significantly upregulated in differentiated PDCs (Figure 2D). These studies indicate the PDC line is multipotent and differentiates into the lineages expected for a periosteal stem cell *in vitro*.

The PDC line engages in BMP/TGFβ signaling

Recent work indicates the importance of BMP and/or TGFβ signaling for normal periosteal activity during skeletal development, fracture repair, and load-induced bone formation (Tsuji et al., 2006; Chen et al., 2012; Salazar et al., 2016; Wu et al., 2016; Salazar et al., 2019; Xia et al., 2020). We therefore determined whether our PDC line could be utilized to study these signaling pathways *in vitro*. First, we examined mRNA expression of components in the TGFβ/BMP superfamily in freshly isolated periosteum and early and later passages of the PDC line (Figure 3A). Nearly all the associated components were expressed in the PDC line except for the ligands *Bmp2*, *Bmp3*, *Gdf8*, and *Nog*, and Type I receptors *Alk1* and *Alk7*. This expression profile was consistent between the early and later PDC passages, but we noted some inconsistencies with whole periosteum. Specifically, we detected *Bmp2*, *Bmp3*, and *Gdf8* expression in whole periosteum, which was absent in PDCs. We then examined BMP and TGFβ signaling in the PDC line by treating with ligands known to activate these pathways in periosteal cells. PDCs incubated in media containing recombinant BMP2 exhibited an increased ratio of phosphorylated Smad1 (pSmad1) to total Smad1 compared to vehicle controls, which is indicative of activated canonical BMP signaling (Figure 3B). The ratio of pSmad2/Smad2/3 was unchanged with BMP2 treatment compared to vehicle controls. PDCs incubated in media containing recombinant TGFβ-1 exhibited increased levels of pSmad2/Smad2/3, which is typically associated with activated canonical TGFβ signaling. Interestingly, pSmad1/Smad1 levels

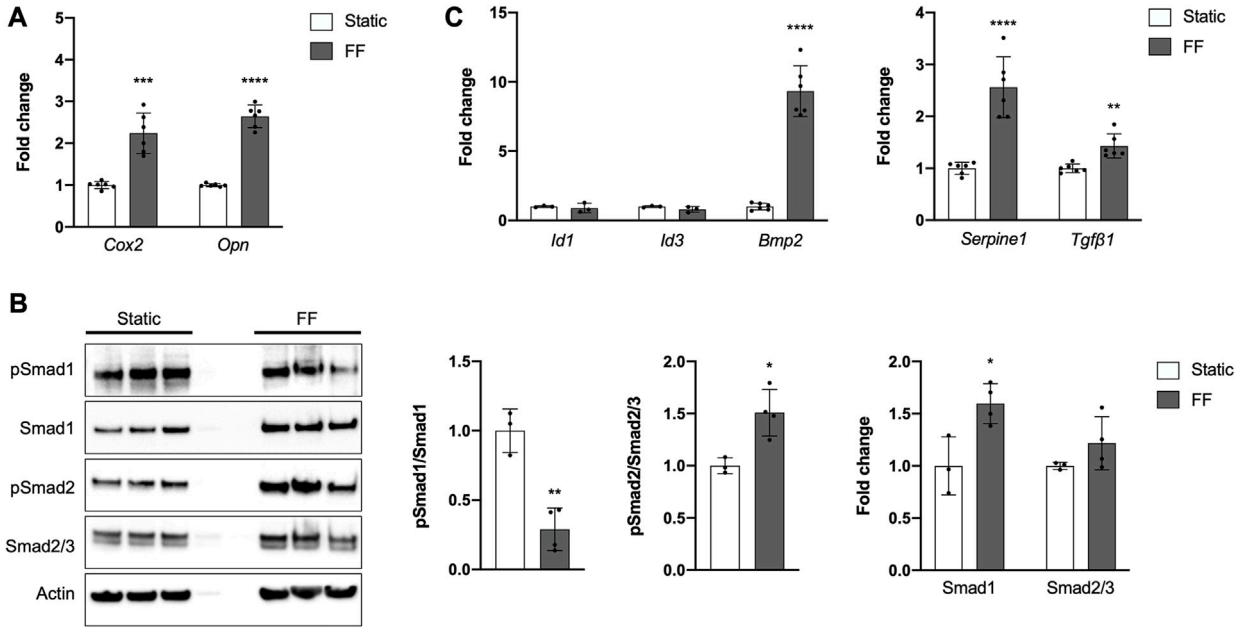

FIGURE 4
The PDC line is mechanoresponsive. **(A)** Fold change in mRNA expression of genes associated with mechanically-induced osteogenesis under static or fluid flow (FF) conditions. **(B)** Representative Western blot image and quantification of changes in total and phosphorylated (p) Smad1 and Smad2/3 under static or FF conditions. All values are normalized to Actin expression and fold changes are normalized to static controls. *$p < 0.05$, **$p < 0.01$, n = 3–4 technical replicates in 3 biological replicates for each group. **(C)** Fold change in mRNA expression of genes associated with BMP and TGFβ signaling. Changes in mRNA expression **(A,C)** are represented as fold changes compared to static controls and all values are normalized to *Gapdh* expression. n = 4–6 technical replicates in 3 biological replicates for all groups. **$p < 0.01$, ***$p < 0.001$, ****$p < 0.0001$. Replicates are represented as individual dots on bar graphs.

were also slightly elevated with TGFβ-1 treatment. When signaling is activated, pSmads bind Smad4 and translocate to the nucleus to trigger transcription of genes associated with canonical BMP (*Id1, Id3*) and TGFβ (*Serpine1*) signaling. We therefore examined changes in mRNA expression of these target genes with treatment (Figure 3C). Indeed, *Id1* and *Id3* were uniquely upregulated with BMP2 treatment and *Serpine1* was upregulated only by TGFβ-1 treatment.

The PDC line is mechanosensitive

Periosteal cells are known to be mechanosensitive and are important for load-induced bone formation (Arnsdorf et al., 2009a; Moore et al., 2018b; Moore et al., 2019; Xiao et al., 2020). We examined whether our PDC line was mechanosensitive using a custom fluid shear chamber device previously used to study primary periosteal cell mechanotransduction *in vitro* (Moore et al., 2018b). Indeed, PDCs exposed to fluid flow exhibited increases in *Cox2* and *Opn*, genes that are upregulated in bone cells in response to physical stimulation (Figure 4A) (Wadhwa et al., 2002; Ponik and Pavalko, 2004; Arnsdorf et al., 2009b; Hoey et al., 2012; Moore et al., 2018b). TGFβ signaling is believed to be important in periosteal cell mechanotransduction so we examined whether this pathway was upregulated in response to fluid flow (Figures 4B, C) (Raab-Cullen et al., 1994; Klein-Nulend et al., 1995; Nguyen et al., 2020). As expected, pSmad2/Smad2/3 levels increased with fluid flow and mRNA expression of the target genes *Serpine1* and *Tgfβ1* also increased. The role of BMP signaling in load-induced bone formation and periosteal cell mechanotransduction is less clear (Kopf et al., 2012; McBride-Gagyi et al., 2015). In our system, we found that pSmad1/Smad1 levels decreased in PDCs exposed to fluid flow and *Id1* and *Id3* expression was unchanged compared to static controls. However, *Bmp2* expression was significantly elevated with application of. The decreased pSmad1/Smad1 levels seen in PDCs exposed to fluid flow are in part due to a significant increase in total Smad1. Smad2/3 levels were comparable between static and fluid flow groups.

Chromosomal abnormalities in the PDC line

Standard G-banded karyotyping was performed on PDCs at P-28 and P-33 to determine what chromosomal abnormalities, which are expected for immortalized cell lines, were present (Stepanenko and Dmitrenko, 2015). Abnormal karyotypes were present in both passages, with several consistent observations between the varying spreads. At both passages multiple polysomies, or additional copies of chromosomes, were observed and only one copy of Chromosome 14 was present. P-28 cells exhibited a modal chromosome number of 72, ranging from 63 to 75 across the spreads. P-33 cells had a modal chromosome number of 72 ranging from 68 to 74 across spreads. Markers, or structurally abnormal chromosomes that cannot be unambiguously identified by conventional banding cytogenetics, were also detected. P-28 cells exhibited 2-6 markers among spreads and this range increased to 4-10 in P-33 cells. A single

dicentric chromosome was observed in two spreads of P-33 cells. As dicentrics can have difficulty passing through mitosis, it is recommended that the PDC line be used up to P-34, the highest passage we validated. Further validation is encouraged when using cells beyond P-34. X and Y sex chromosomes were present, indicating the PDC line was derived from a male mouse.

Discussion

In this work we present a new tool to study periosteal cell behavior and signaling *in vitro*. Our periosteum-derived clonal cell line expresses established periosteal markers, engages in signaling pathways known to be important for periosteal cell osteogenesis, and exhibits an osteogenic response to physical stimulation. More importantly, these characteristics are stable with extensive passaging. The features of PDCs address many of the issues associated with using primary periosteal cells for *in vitro* experiments. The purity and yield of primary periosteal cell isolations can vary drastically with animal age, approach, and personnel so a clonal line provides much needed standardization in the periosteum field. By creating a clonal line, we also avoided concerns with contamination of muscle or connective tissue cells. Osteogenic and chondrogenic behavior can become limited with passage in primary cell populations, but we found this behavior was consistent with passaging in the PDC line. Thus, the PDC line can be expanded for large-scale and long-term *in vitro* experiments, such as drug screens, bulk RNA sequencing, and allograft design. We therefore conclude that our PDC line can be utilized *in vitro* to better understand periosteal cell activity and inform *in vivo* studies.

We focused on key features to assess utility of our PDCs, but further experiments are required to fully characterize this line and determine its potential uses. Our PDCs are clonal, viable with extensive passaging, and multipotent, but this only confirms stem cell-like qualities *in vitro*. PDCs express mRNA for markers attributed to periosteal stem/progenitor cells such as *Sca-1*, *Cd29*, *Cd51*, and *Cd105* (Supplementary Figure S1D), but *in vivo* implantation studies and cell-surface marker analysis are necessary to determine whether this is truly a stem cell line (Debnath et al., 2018; Deveza et al., 2018; Duchamp De Lageneste et al., 2018; Bradaschia-Correa et al., 2019; Ortinau et al., 2019; Matthews et al., 2021; Jeffery et al., 2022; Julien et al., 2022; Perrin and Colnot, 2022). It is unknown if our PDCs represent an abundant or rare population found *in vivo*, and it is likely slowly dividing stem/progenitor cells were lost in the process of extensive passaging and cloning. Existing studies have focused on cells selected using a single periosteal marker, but our mRNA expression analysis indicates PDCs express many of these markers (Figure 1E). Considering the heterogenous nature of the periosteum, it is possible that periosteal cells express multiple markers at low levels *in vivo*. Through cloning, we may have captured a population enriched in several periosteal markers. It is equally possible that culturing itself altered transcription. Our mRNA analysis also showed that PDCs express *Gli1*, which was absent in periosteal tissue from which the PDC line was derived. We speculate this is due to enrichment in PDCs compared to whole periosteum. The presence of *Gli1*-expressing cells is known to diminish with age, so it is possible that by P14 there are too few cells for RTqPCR detection (Shi et al., 2017; Shi et al., 2021). One final limitation is that we only examined BMP and TGFβ signaling in PDCs. There are other signaling pathways involved in periosteal cell activation and differentiation that will require initial characterization before determining the full experimental utility of the line. We recognize that our line may not be appropriate for all periosteum studies, especially those that require a heterogenous population or slowly dividing periosteal stem/progenitor populations. However, we can conclude at this time that our PDC line will be useful for examining periosteal cell activation, differentiation, and BMP/TGFβ signaling, events central to appositional growth, fracture repair, and load-induced bone formation.

We examined BMP and TGFβ signaling in PDCs because these pathways are known to be important for periosteal cell activation and differentiation. Treatment with recombinant BMP2 and TGFβ-1 activated signaling and corresponding gene transcription (Figures 3B, C). BMP2 uniquely activated canonical BMP signaling. TGFβ-1 activated canonical TGFβ signaling as expected, but also slightly increased pSmad1/Smad1 levels which are typically associated with BMP signaling. However, this increase did not correspond with upregulated BMP signaling, as we observed no changes in *Id1* and *Id3* transcription. It is possible that PDCs can be activated by other ligands in the BMP/TGFβ pathway: we highlighted BMP2 and TGFβ-1 because their importance in the periosteum is established (Tsuji et al., 2006; Salazar et al., 2019; Nguyen et al., 2020).

Trends in mRNA expression of BMP/TGFβ pathway components in PDCs are consistent with what has been found in other skeletal cells (Salazar et al., 2016; Wu et al., 2016; Lademann et al., 2020). The PDC expression profile is largely consistent with that of whole periosteal tissue from which PDCs were derived, with a few exceptions. *Gdf8*, or Myostatin, is expressed in whole periosteum, but absent from PDCs. We attribute this to muscle contamination when isolating periosteum. In fact, 4 of the 8 candidate clones for the PDC line expressed muscle cell markers, highlighting the risk of muscle cell contamination in periosteal preps. *Bmp2* and *Bmp3* are expressed in whole periosteum but not detected in PDCs. *Bmp3* has been found to be highly expressed in osteoblasts and osteocytes but absent from bone marrow stromal cells and stem and progenitor cells in the periosteum (Kokabu and Rosen, 2018). Osteoblasts and their precursors are present near the periosteum-bone interface, especially during rapid postnatal appositional growth, so it is not surprising to see *Bmp3* expression in whole periosteum isolated at P14. We previously detected *Bmp2*-expressing cells residing in the cambium layer of the periosteum very near the bone surface (Salazar et al., 2019). We speculate these cells are differentiating cells committed to an osteogenic lineage. Thus, the lack of *Bmp2* and *Bmp3* expression combined with our multipotency data (Figure 2) suggests our PDCs are not committed to an osteogenic lineage and exhibit a degree of stemness.

Interestingly, we detected *Bmp2* mRNA expression in PDCs seeded for fluid flow studies (Figure 4C). We initially suspected the shift was due to increased cell density, but we did not detect *Bmp2* in PDCs seeded on tissue culture plates ranging from 50%–100% confluence (data not shown). Another possible explanation is PDCs respond to the increased substrate stiffness when seeded

on glass slides. Periosteal cells and other mechanoresponsive bone cells exhibit changes with increased substrate stiffness and osteocyte-like cells must be seeded on collagen-coated glass slides to prevent de-differentiation (Chen and Jacobs, 2013; Wang et al., 2022; Mattei et al., 2015; Zhang et al., 2017; Navarrete et al., 2017; K et al., 2010). *Bmp2* expression increased in PDCs exposed to fluid flow, further suggesting a role for BMP2 in PDC mechanosensation (Figure 4C). We derived the PDC line from heterozygous $Bmp2^{LacZ}$ mice so that X-gal staining could be used to visualize BMP2, for which there is no working antibody. In these mice, one copy of *Bmp2* is replaced with a LacZ cassette and mice develop normally with the remaining wildtype allele (Gamer et al., 2018; Salazar et al., 2019). We confirmed the PDCs contain the LacZ gene (Supplementary Figure S6) and X-gal staining can therefore be used to identify PDCs implanted *in vivo* or in co-cultures, as well as to visualize BMP2 secretion by PDCs, for example. Using this visual tool, we intend to further examine the role of periosteal BMP2 in the context of mechanotransduction.

We also evaluated BMP and TGFβ signaling in the context of PDC mechanotransduction. Canonical TGFβ signaling was activated in PDCs in response to fluid flow, which is consistent with existing *in vitro* and *in vivo* work examining mechanoresponsive skeletal cells (Figures 4B, C) (Raab-Cullen et al., 1994; Klein-Nulend et al., 1995; Sakai et al., 1998; Vermeulen et al., 2020; Monteiro et al., 2021). For canonical BMP signaling, pSmad1/Smad1 levels were downregulated and mRNA transcription of downstream targets was unchanged in response to fluid flow (Figures 4B, C). Interestingly, Smad1 levels and *Bmp2* expression increased in PDCs exposed to fluid flow, suggesting the cells are being primed for BMP signaling. Based on these results, we speculate that TGFβ signaling plays a role in mechanotransduction and activation of PDCs, and BMP signaling facilitates subsequent differentiation of PDCs. It is important to note that for fluid flow studies we did not serum-starve PDCs to synchronize the cells and deplete basal signaling like we did for the ligand treatment experiments (Figure 3B). It is possible that standard culture media elevates basal BMP signaling in PDCs such that our current setup cannot capture changes in response to fluid flow. Moreover, BMP signaling is time-sensitive and context-dependent such that protocol optimization is required to confidently detect cellular changes (Greenfeld et al., 2021; Komorowski, 2022). We tested PDCs using a protocol established for primary periosteal cell mechanotransduction studies, but this is not necessarily the optimal timing to observe BMP signaling. In future studies, we will interrogate signaling under different PDC culture conditions and at multiple timepoints to get a more accurate depiction of fluid flow-induced BMP signaling.

In addition to advancing our understanding of periosteal cell behavior and signaling in normal programs of skeletal development, growth, and repair, we anticipate the PDC line will be invaluable to address other questions regarding periosteal activity. We previously generated a genetic mouse model that dampens periosteal BMP signaling, resulting in disrupted appositional growth and a thin bone phenotype in mutants (Salazar et al., 2019). Primary periosteal cells isolated from these mice do not survive in culture, so we intend to utilize the PDC line and CRISPR/Cas9 tools to identify participating periosteal cell populations and mechanisms of osteogenic differentiation in appositional growth. The CRISPR/Cas9 system can further be used in PDCs to examine differences between periosteal stem and progenitor cell populations, as well as inform factors that drive intramembranous *versus* endochondral ossification. These two areas of investigation are critical to understanding the periosteum dynamics that direct unique cellular responses for different biological processes. During fracture repair, the periosteum expands and becomes the predominant source of chondrocytes and osteoblasts that direct reparative bone formation (Colnot, 2009; Duchamp De Lageneste et al., 2018). The PDC line expresses many of the markers thought to be indicative of periosteal stem/progenitor cells involved in repair (Figure 1E) and differentiates into chondrocytes and osteoblasts (Figure 2). Primary periosteal cells have been successfully transplanted in mouse models to study fracture repair *in vivo* (Perrin et al., 2021). We anticipate PDCs will not only successfully transplant *in vivo*, but having a standardized, consistent source of periosteal cells will greatly facilitate the technical aspects of fracture repair and non-union experiments in mouse models. Lastly, we expect the PDC line can be utilized for large-scale experiments like RNAseq and drug screens to provide further insight into periosteal cell behavior to identify targets for anabolic therapeutics that augment bone formation. Considering the wide range of potential uses, we believe this PDC line will significantly advance *in vitro* and *in vivo* investigation of the periosteum.

Data availability statement

The original contributions presented in the study are included in the article/Supplementary Material, further inquiries can be directed to the corresponding author.

Ethics statement

The animal study was approved by the Harvard Medical Area Institutional Animal Care and Use Committee. The study was conducted in accordance with the local legislation and institutional requirements.

Author contributions

EM, DM, LG, and VR contributed to conception and design of the study. EM, DM, LG, GC, and KB collected the data. EM and DM performed data and statistical analysis. EM wrote the first draft of the manuscript. EM, DM, LG, and VR wrote sections of the manuscript. All authors contributed to the article and approved the submitted version.

Funding

This work is supported by the National Institute of Arthritis and Musculoskeletal and Skin Diseases (NIAMS) grant R01AR077432.

Acknowledgments

We would like to thank Dr. Diana Carlone (Boston Children's Hospital, Boston, MA) and Dr. Francesca Gori (Harvard School of Dental Medicine, Boston, MA) for scientific conversations that facilitated generation of this cell line. We also thank Elizabeth Gonzalez, CEO and Senior Cytogeneticist at KaryoLogic, Inc., for her expertise in interpreting our karyotyping results.

Conflict of interest

The authors declare that the research was conducted in the absence of any commercial or financial relationships that could be construed as a potential conflict of interest.

Publisher's note

Supplementary material

The Supplementary Material for this article can be found online at: https://www.frontiersin.org/articles/10.3389/fphys.2023.1221152/full#supplementary-material

References

Arnsdorf, E. J., Jones, L. M., Carter, D. R., and Jacobs, C. R. (2009a). The periosteum as a cellular source for functional tissue engineering. *Tissue Eng. Part A* 15, 2637–2642. doi:10.1089/ten.TEA.2008.0244

Arnsdorf, E. J., Tummala, P., Kwon, R. Y., and Jacobs, C. R. (2009b). Mechanically induced osteogenic differentiation - the role of RhoA, ROCKII and cytoskeletal dynamics. *J. Cell Sci.* 122, 546–553. doi:10.1242/jcs.036293

Bradaschia-Correa, V., Leclerc, K., Josephson, A. M., Lee, S., Palma, L., Litwa, H. P., et al. (2019). Hox gene expression determines cell fate of adult periosteal stem/progenitor cells. *Sci. Rep.* 9, 5043. doi:10.1038/S41598-019-41639-7

Brown, S., Malik, S., Aljammal, M., O'Flynn, A., Hobbs, C., Shah, M., et al. (2022). The Prrx1eGFP mouse labels the periosteum during development and a subpopulation of osteogenic periosteal cells in the adult. *JBMR plus* 7, e10707. doi:10.1002/JBM4.10707

Chen, G., Deng, C., and Li, Y. P. (2012). TGF-B and BMP signaling in osteoblast differentiation and bone formation. *Int. J. Biol. Sci.* 8, 272–288. doi:10.7150/IJBS.2929

Chen, J. C., and Jacobs, C. R. (2013). Mechanically induced osteogenic lineage commitment of stem cells. *Stem Cell Res. Ther.* 4, 107. doi:10.1186/scrt318

Colnot, C. (2009). Skeletal cell fate decisions within periosteum and bone marrow during bone regeneration. *J. Bone Min. Res.* 24, 274–282. doi:10.1359/jbmr.081003

Colnot, C., Zhang, X., and Tate, M. L. K. (2012). Current insights on the regenerative potential of the periosteum: molecular, cellular, and endogenous engineering approaches. *J. Orthop. Res.* 30, 1869–1878. doi:10.1002/jor.22181

De Bari, C., Dell'Accio, F., Vanlauwe, J., Eyckmans, J., Khan, I. M., Archer, C. W., et al. (2006). Mesenchymal multipotency of adult human periosteal cells demonstrated by single-cell lineage analysis. *Arthritis Rheum.* 54, 1209–1221. doi:10.1002/art.21753

Debnath, S., Yallowitz, A. R., McCormick, J., Lalani, S., Zhang, T., Xu, R., et al. (2018). Discovery of a periosteal stem cell mediating intramembranous bone formation. *Nature* 562, 133–139. doi:10.1038/S41586-018-0554-8

Deveza, L., Ortinau, L., Lei, K., and Park, D. (2018). Comparative analysis of gene expression identifies distinct molecular signatures of bone marrow- and periosteal-skeletal stem/progenitor cells. *PLoS One* 13, e0190909. doi:10.1371/journal.pone.0190909

Duchamp De Lageneste, O., Julien, A., Abou-Khalil, R., Frangi, G., Carvalho, C., Cagnard, N., et al. (2018). Periosteum contains skeletal stem cells with high bone regenerative potential controlled by periostin. *Nat. Commun.* 9, 773. doi:10.1038/s41467-018-03124-z

Esposito, A., Wang, L., Li, T., Miranda, M., and Spagnoli, A. (2020). Role of prx1-expressing skeletal cells and prx1-expression in fracture repair. *Bone* 139, 115521. doi:10.1016/j.bone.2020.115521

Gamer, L. W., Pregizer, S., Gamer, J., Feigenson, M., Ionescu, A., Li, Q., et al. (2018). The role of Bmp2 in the maturation and maintenance of the murine knee joint. *J. Bone Min. Res.* 33, 1708–1717. doi:10.1002/JBMR.3441

Grcevic, D., Pejda, S., Matthews, B. G., Repic, D., Wang, L., Li, H., et al. (2012). *In vivo* fate mapping identifies mesenchymal progenitor cells. *Stem Cells* 30, 187–196. doi:10.1002/STEM.780

Greenfeld, H., Lin, J., and Mullins, M. C. (2021). The BMP signaling gradient is interpreted through concentration thresholds in dorsal–ventral axial patterning. *PLOS Biol.* 19, e3001059. doi:10.1371/JOURNAL.PBIO.3001059

Hoey, D. A., Tormey, S., Ramcharan, S., O'Brien, F. J., and Jacobs, C. R. (2012). Primary cilia-mediated mechanotransduction in human mesenchymal stem cells. *Stem Cells* 30, 2561–2570. doi:10.1002/stem.1235

Jeffery, E. C., Mann, T. L. A., Pool, J. A., Zhao, Z., and Morrison, S. J. (2022). Bone marrow and periosteal skeletal stem/progenitor cells make distinct contributions to bone maintenance and repair. *Cell Stem Cell* 29, 1547–1561.e6. doi:10.1016/J.STEM.2022.10.002

Jo, C. H., Lim, H. J., and Yoon, K. S. (2019). Characterization of tendon-specific markers in various human tissues, tenocytes and mesenchymal stem cells. *Tissue Eng. Regen. Med.* 16, 151–159. doi:10.1007/S13770-019-00182-2

Julien, A., Perrin, S., Martínez-Sarrà, E., Kanagalingam, A., Carvalho, C., Luka, M., et al. (2022). Skeletal stem/progenitor cells in periosteum and skeletal muscle share a common molecular response to bone injury. *J. Bone Min. Res.* 37, 1545–1561. doi:10.1002/JBMR.4616

Kato, Y., Windle, J. J., Koop, B. A., Mundy, G. R., and Bonewald, L. F. (2010). Establishment of an osteocyte-like cell line, MLO-Y4. *J. Bone Min. Res.* 12, 2014–2023. doi:10.1359/jbmr.1997.12.12.2014

Kawanami, A., Matsushita, T., Chan, Y. Y., and Murakami, S. (2009). Mice expressing GFP and CreER in osteochondro progenitor cells in the periosteum. *Biochem. Biophys. Res. Commun.* 386, 477–482. doi:10.1016/j.bbrc.2009.06.059

Klein-Nulend, J., Roelofsen, J., Sterck, J. G. H., Semeins, C. M., and Burger, E. H. (1995). Mechanical loading stimulates the release of transforming growth factor-? Activity by cultured mouse calvariae and periosteal cells. *J. Cell. Physiol.* 163, 115–119. doi:10.1002/jcp.1041630113

Kokabu, S., and Rosen, V. (2018). BMP3 expression by osteoblast lineage cells is regulated by canonical wnt signaling. *FEBS Open Bio* 8, 168–176. doi:10.1002/2211-5463.12347

Komorowski, M. (2022). Making sense of BMP signaling complexity. *Cell Syst.* 13, 349–351. doi:10.1016/J.CELS.2022.04.002

Kopf, J., Petersen, A., Duda, G. N., and Knaus, P. (2012). BMP2 and mechanical loading cooperatively regulate immediate early signalling events in the BMP pathway. *BMC Biol.* 10, 37. doi:10.1186/1741-7007-10-37

Lademann, F., Hofbauer, L. C., and Rauner, M. (2020). The bone morphogenetic protein pathway: the osteoclastic perspective. *Front. Cell Dev. Biol.* 8, 586031. doi:10.3389/fcell.2020.586031

Mattei, G., Ferretti, C., Tirella, A., Ahluwalia, A., and Mattioli-Belmonte, M. (2015). Corrigendum: decoupling the role of stiffness from other hydroxyapatite signalling cues in periosteal derived stem cell differentiation. *Sci. Rep.* 5, 14590. doi:10.1038/srep14590

Matthews, B. G., Grcevic, D., Wang, L., Hagiwara, Y., Roguljic, H., Joshi, P., et al. (2014). Analysis of AsMA-labeled progenitor cell commitment identifies notch signaling as an important pathway in fracture healing. *J. Bone Min. Res.* 29, 1283–1294. doi:10.1002/jbmr.2140

Matthews, B. G., Novak, S., Sbrana, F. V., Funnell, J. L., Cao, Y., Buckels, E. J., et al. (2021). Heterogeneity of murine periosteum progenitors involved in fracture healing. *Elife* 10, 585344–e58628. doi:10.7554/ELIFE.58534

McBride-Gagyi, S. H., McKenzie, J. A., Buettmann, E. G., Gardner, M. J., and Silva, M. J. (2015). Bmp2 conditional knockout in osteoblasts and endothelial cells does not impair bone formation after injury or mechanical loading in adult mice. *Bone* 81, 533–543. doi:10.1016/J.BONE.2015.09.003

Monteiro, D. A., Dole, N. S., Campos, J. L., Kaya, S., Schurman, C. A., Belair, C. D., et al. (2021). Fluid shear stress generates a unique signaling response by activating multiple TGFβ family type I receptors in osteocytes. *FASEB J.* 35, e21263. doi:10.1096/FJ.202001998R

Moore, E. R., Chen, J. C., and Jacobs, C. R. (2019). Prx1-Expressing progenitor primary cilia mediate bone formation in response to mechanical loading in mice. *Stem Cells Int.* 2019, 3094154. doi:10.1155/2019/3094154

Moore, E. R., Mathews, O. A., Yao, Y., and Yang, Y. (2020). Prx1-Expressing cells contributing to fracture repair require primary cilia for complete healing in mice. *Bone* 143, 115738. doi:10.1016/j.bone.2020.115738

Moore, E. R., Yang, Y., and Jacobs, C. R. (2018a). Primary cilia are necessary for prx1-expressing cells to contribute to postnatal skeletogenesis. *J. Cell Sci.* 131, jcs217828. doi:10.1242/jcs.217828

Moore, E. R., Zhu, Y. X., Ryu, H. S., and Jacobs, C. R. (2018b). Periosteal progenitors contribute to load-induced bone formation in adult mice and require primary cilia to sense mechanical stimulation. *Stem Cell Res. Ther.* 9, 190. doi:10.1186/s13287-018-0930-1

Navarrete, R. O., Lee, E. M., Smith, K., Hyzy, S. L., Doroudi, M., Williams, J. K., et al. (2017). Substrate stiffness controls osteoblastic and chondrocytic differentiation of mesenchymal stem cells without exogenous stimuli. *PLoS One* 12, e0170312. doi:10.1371/JOURNAL.PONE.0170312

Nguyen, J., Massoumi, R., and Alliston, T. (2020). CYLD, a mechanosensitive deubiquitinase, regulates TGFβ signaling in load-induced bone formation. *Bone* 131, 115148. doi:10.1016/J.BONE.2019.115148

Ono, N. (2022). The mechanism of bone repair: stem cells in the periosteum dedicated to bridging a large gap. *Cell Rep. Med.* 3, 100807. doi:10.1016/j.xcrm.2022.100807

Ortinau, L. C., Wang, H., Lei, K., Deveza, L., Jeong, Y., Hara, Y., et al. (2019). Identification of functionally distinct Mx1+αSMA+ periosteal skeletal stem cells. *Cell Stem Cell* 25, 784–796. doi:10.1016/j.stem.2019.11.003

Perrin, S., and Colnot, C. (2022). Periosteal skeletal stem and progenitor cells in bone regeneration. *Curr. Osteoporos. Rep.* 20, 334–343. doi:10.1007/S11914-022-00737-8

Perrin, S., Julien, A., de Lageneste, O. D., Abou-Khalil, R., and Colnot, C. (2021). Mouse periosteal cell culture, *in vitro* differentiation, and *in vivo* transplantationin tibial fractures. *Bio-protocol* 11, e4107. doi:10.21769/BIOPROTOC.4107

Piasecka, A., Sekrecki, M., Szcześniak, M. W., and Sobczak, K. (2021). MEF2C shapes the microtranscriptome during differentiation of skeletal muscles. *Sci. Rep.* 11, 3476–3514. doi:10.1038/s41598-021-82706-2

Ponik, S. M., and Pavalko, F. M. (2004). Formation of focal adhesions on fibronectin promotes fluid shear stress induction of COX-2 and PGE2 release in mc3t3-E1 osteoblasts. *J. Appl. Physiol.* 97, 135–142. doi:10.1152/JAPPLPHYSIOL.01260.2003

Raab-Cullen, D. M., Thiede, M. A., Petersen, D. N., Kimmel, D. B., and Recker, R. R. (1994). Mechanical loading stimulates rapid changes in periosteal gene expression. *Calcif. Tissue Int.* 55, 473–478. doi:10.1007/BF00298562

Sakai, K., Mohtai, M., and Iwamoto, Y. (1998). Fluid shear stress increases transforming growth factor beta 1 expression in human osteoblast-like cells: modulation by cation channel blockades. *Calcif. Tissue Int.* 63, 515–520. doi:10.1007/S002239900567

Salazar, V. S., Capelo, L. P., Cantù, C., Zimmerli, D., Gosalia, N., Pregizer, S., et al. (2019). Reactivation of a developmental Bmp2 signaling center is required for therapeutic control of the murine periosteal niche. *Elife* 8, e42386. doi:10.7554/eLife.42386

Salazar, V. S., Gamer, L. W., and Rosen, V. (2016). BMP signalling in skeletal development, disease and repair. *Nat. Rev. Endocrinol.* 12, 203–221. doi:10.1038/nrendo.2016.12

Shi, Y., He, G., Lee, W. C., McKenzie, J. A., Silva, M. J., and Long, F. (2017). Gli1 identifies osteogenic progenitors for bone formation and fracture repair. *Nat. Commun.* 8, 2043. doi:10.1038/S41467-017-02171-2

Shi, Y., Liao, X., Long, J. Y., Yao, L., Chen, J., Yin, B., et al. (2021). Gli1+ progenitors mediate bone anabolic function of teriparatide via hh and igf signaling. *Cell Rep.* 36, 109542. doi:10.1016/J.CELREP.2021.109542

Stepanenko, A. A., and Dmitrenko, V. V. (2015). HEK293 in cell biology and cancer research: phenotype, karyotype, tumorigenicity, and stress-induced genome-phenotype evolution. *Gene* 569, 182–190. doi:10.1016/J.GENE.2015.05.065

Tsuji, K., Bandyopadhyay, A., Harfe, B. D., Cox, K., Kakar, S., Gerstenfeld, L., et al. (2006). BMP2 activity, although dispensable for bone formation, is required for the initiation of fracture healing. *Nat. Genet.* 38, 1424–1429. doi:10.1038/ng1916

Vermeulen, S., Roumans, N., Honig, F., Carlier, A., Hebels, D. G. A. J., Eren, A. D., et al. (2020). Mechanotransduction is a context-dependent activator of TGF-β signaling in mesenchymal stem cells. *Biomaterials* 259, 120331. doi:10.1016/J.BIOMATERIALS.2020.120331

Wadhwa, S., Choudhary, S., Voznesensky, M., Epstein, M., Raisz, L., and Pilbeam, C. (2002). Fluid flow induces COX-2 expression in mc3t3-E1 osteoblasts via a PKA signaling pathway. *Biochem. Biophys. Res. Commun.* 297, 46–51. doi:10.1016/s0006-291x(02)02124-1

Wang, L., Tower, R. J., Chandra, A., Yao, L., Tong, W., Xiong, Z., et al. (2019). Periosteal mesenchymal progenitor dysfunction and extraskeletally-derived fibrosis contribute to atrophic fracture nonunion. *J. Bone Min. Res.* 34, 520–532. doi:10.1002/JBMR.3626

Wang, Q., Xie, J., Zhou, C., and Lai, W. (2022). Substrate stiffness regulates the differentiation profile and functions of osteoclasts via cytoskeletal arrangement. *Cell Prolif.* 55, e13172. doi:10.1111/CPR.13172

Wang, T., Zhang, X., and Bikle, D. D. (2017). Osteogenic differentiation of periosteal cells during fracture healing. *J. Cell. Physiol.* 232, 913–921. doi:10.1002/jcp.25641

Wu, M., Chen, G., and Li, Y. P. (2016). TGF-B and BMP signaling in osteoblast, skeletal development, and bone formation, homeostasis and disease. *Bone Res.* 4, 16009. doi:10.1038/BONERES.2016.9

Xia, C., Ge, Q., Fang, L., Yu, H., Zou, Z., Zhang, P., et al. (2020). TGF-β/Smad2 signalling regulates enchondral bone formation of Gli1+ periosteal cells during fracture healing. *Cell Prolif.* 53, e12904. doi:10.1111/cpr.12904

Xiao, H., Wang, L., Zhang, T., Chen, C., Chen, H., Li, S., et al. (2020). Periosteum progenitors could stimulate bone regeneration in aged murine bone defect model. *J. Cell. Mol. Med.* 24, 12199–12210. doi:10.1111/jcmm.15891

Xu, J., Wang, Y., Li, Z., Tian, Y., Li, Z., Lu, A., et al. (2022). PDGFRα reporter activity identifies periosteal progenitor cells critical for bone formation and fracture repair. *Bone Res.* 10, 7–15. doi:10.1038/s41413-021-00176-8

Zhang, T., Lin, S., Shao, X., Zhang, Q., Xue, C., Zhang, S., et al. (2017). Effect of matrix stiffness on osteoblast functionalization. *Cell Prolif.* 50, e12338. doi:10.1111/CPR.12338

frontiers | Frontiers in Physiology

TYPE Mini Review
PUBLISHED 09 October 2023
DOI 10.3389/fphys.2023.1232698

OPEN ACCESS

EDITED BY
Celine Colnot,
Institut National de la Santé et de la Recherche Medicale, INSERM U955, France

REVIEWED BY
Diane Wagner,
Indiana University-Purdue University Indianapolis, United States
John Brunski,
Stanford University, United States

*CORRESPONDENCE
Timothy O. Josephson,
toj@bu.edu

RECEIVED 01 June 2023
ACCEPTED 25 September 2023
PUBLISHED 09 October 2023

CITATION
Josephson TO and Morgan EF (2023), Harnessing mechanical cues in the cellular microenvironment for bone regeneration.
Front. Physiol. 14:1232698.
doi: 10.3389/fphys.2023.1232698

Harnessing mechanical cues in the cellular microenvironment for bone regeneration

Timothy O. Josephson[1,2]* and Elise F. Morgan[1,2,3]

[1]Biomedical Engineering, Boston University, Boston, MA, United States, [2]Center for Multiscale and Translational Mechanobiology, Boston University, Boston, MA, United States, [3]Mechanical Engineering, Boston University, Boston, MA, United States

At the macroscale, bones experience a variety of compressive and tensile loads, and these loads cause deformations of the cortical and trabecular microstructure. These deformations produce a variety of stimuli in the cellular microenvironment that can influence the differentiation of marrow stromal cells (MSCs) and the activity of cells of the MSC lineage, including osteoblasts, osteocytes, and chondrocytes. Mechanotransduction, or conversion of mechanical stimuli to biochemical and biological signals, is thus part of a multiscale mechanobiological process that drives bone modeling, remodeling, fracture healing, and implant osseointegration. Despite strong evidence of the influence of a variety of mechanical cues, and multiple paradigms proposed to explain the influence of these cues on tissue growth and differentiation, even a working understanding of how skeletal cells respond to the complex combinations of stimuli in their microenvironments remains elusive. This review covers the current understanding of what types of microenvironmental mechanical cues MSCs respond to and what is known about how they respond in the presence of multiple such cues. We argue that in order to realize the vast potential for harnessing the cellular microenvironment for the enhancement of bone regeneration, additional investigations of how combinations of mechanical cues influence bone regeneration are needed.

KEYWORDS

bone, mechanobiology, marrow stromal cells (MSCs), mechanical microenvironment, osteogenesis

1 Introduction

The response of skeletal cells to mechanical stimuli is fundamental to understanding, treating, and preventing orthopaedic injuries and diseases. The fact that bone is responsive to mechanical stimulation is well documented: athletes whose bodies experience more intense loading have increased bone mass (Bennell et al., 1997), while astronauts lose bone mass after spending time in low-gravity environments (Orwoll et al., 2013). Distraction osteogenesis, a surgical process of lengthening and reshaping a bone, improves healing outcomes in treatment of non-union by providing controlled levels of mechanical stimulation (Kanellopoulos and Soucacos, 2006; Fu et al., 2021), while metal implants can locally weaken bone due to stress shielding (Sumner, 2015; Augat and von Rüden, 2018). Mechanical cues also have a strong influence on the outcomes of fracture healing (Augat et al., 2021) and implant osseointegration (Mavrogenis et al., 2009). Bone responds to mechanical cues through multiple mechanisms, including osteocyte signaling, which plays an important

role in bone remodeling, and the differentiation of MSCs. In the context of bone regeneration, mechanobiologically driven differentiation of MSCs is particularly important, as it determines the cell and tissue types that will form as a fracture heals. There is a long standing belief that the mechanoresponsiveness of bone, if well understood, could be routinely harnessed for therapeutic benefit in many clinical contexts. Indeed, in the words of Julius Wolff more than a century ago, "the remodelling force is a therapeutic force of immeasurable magnitude" (Wolff, 1986).

The field of orthopaedics has sought to translate this therapeutic force in a variety of ways to enhance bone regeneration. As reviewed by Mavčič and Antolič (2012), Augat et al. (2021), and Huang et al. (2013), numerous studies have attempted to enhance healing by regulating the magnitude and frequency of loading at different stages of the healing process. While some studies have achieved promising results, these results have yet to be generalized to actionable guidelines for other scenarios, or even other patients, due to the complex dependence of the mechanical stimuli on parameters such as fracture geometry and location, as well as to other factors such as patient age and co-morbidities. The first of these causes—the complexity of the relevant mechanics—arises from the fact that similar loading of bones at the macroscale may result in distinctly different microenvironmental stimuli in different patients, in different regions of bone (Figure 1) and over time as the tissue microstructure changes with adaptation. When bones experience forces, whether through load bearing or muscle contraction, the cortical and trabecular microstructures deform. The same is true for the soft tissues and woven bone that form in the initial and intermediate stages of fracture healing, and in the periosteum (McBride et al., 2011). These deformations push and pull on the cells residing within the complex geometries of bone tissue (Vaughan et al., 2015) and drive the flow of marrow and extracellular fluid around cells (Metzger et al., 2015). These local stimuli—tissue strains, fluid-based stresses, and geometric cues—constitute the cellular mechanical microenvironment.

Hence, in order to understand how and why bones adapt and heal in the ways that they do, focus has shifted from the macroscale stimuli that whole bones receive to the microscale stimuli that skeletal cells experience. However, the relative influence and the optimal levels of the various microenvironmental stimuli are not well known, particularly in complex microenvironments with a variety of different stimuli. By reviewing the evidence for the influence of these specific stimuli, individually and in combination, on MSC differentiation and the prevailing theories of how combinations of them act to regulate bone regeneration, we aim to demonstrate the potential for further harnessing the mechanical microenvironment and to identify the critical questions that must be answered in order to do so. While this review will primarily focus on the microenvironmental stimuli that influence osteogenic differentiation of MSCs in the context of bone regeneration following trauma, chondrogenic differentiation of MSCs and chondrocyte-to-osteoblast transdifferentiation also play important roles in endochondral ossification and can both be regulated by many of the same types of microenvironmental stimuli as are discussed for osteogenic differentiation of MSCs (Wong et al., 2018; McDermott et al., 2019).

2 Individual microenvironmental stimuli

2.1 Exogenous mechanical stimulation

Exogenous stimuli are those induced by applied mechanical loads. These stimuli arise from both the solid and fluid compartments of bone, and include solid strain, fluid shear stress, and hydrostatic pressure. Applied loads are often transient in nature, so the microenvironment is characterized also by the frequency and loading history of these exogenous stimuli, not just the instantaneous magnitudes.

A large body of work provides evidence [as reviewed by Scott et al. (2008) and Steward and Kelly (2015)] that cyclic strains can influence MSC differentiation and that the magnitude and frequency of loading are relevant factors. MSCs are capable of sensing both tensile and compressive strains, and they respond to the two in distinct ways. Cyclic tensile strains have been frequently associated with osteogenic differentiation of MSCs on both 2D substrates (Qi et al., 2008; Kearney et al., 2010) and 3D soft scaffolds (Haudenschild et al., 2009; Yu et al., 2021) while cyclic compression of MSCs in 3D constructs has been shown to promote both osteogenesis (Schreivogel et al., 2019) and chondrogenesis (Pelaez et al., 2009). Additionally, stretch-activated cation channels (SACC) have been implicated as an important component of the response to tissue strain-based deformations of cells and have been associated with synthesis of both glycosaminoglycans [GAGs, McMahon et al. (2008)] and collagen I (Kearney et al., 2010). The synthesis of matrix components as downstream effect of mechanical stimulation is a main mechanism by which the mechano-responsiveness of MSCs and osteoblasts are regulated, as changes in the matrix will likely modulate the cellular microenvironment. This general type of regulatory loop is referred to as mechanomics (Knothe Tate et al., 2016). Haudenschild et al. (2009) identified that α- and β-catenin, which are relevant in cytoskeletal mechanics and the osteogenically important Wnt signaling pathway, are regulated differently by the type of strain, with α-catenin upregulated by compressive strains and β-catenin upregulated by tensile/distortional stretch.

Despite these findings, the optimal strain magnitudes and frequencies for promoting osteogenesis are difficult to ascertain in a broadly applicable manner. This can be attributed to two main causes: differences in experimental setups and measured outputs, and the presence of other stimuli that are not always accounted for. Studies often use different loading conditions (e.g., uniaxial, biaxial, bending-based stretch), different culture conditions (e.g., serum vs. serum-free media), study different cell types (e.g., MSCs, osteoblasts, osteoblast-like cells), and measure the expression of different osteogenic markers (e.g., RUNX2, osteopontin, osteocalcin). These differences make quantitative agreement and reproducibility across studies difficult to assess. The presence of confounding factors amplifies this challenge. Differences among substrates in regards to other cues that cells experience, such as stiffness and/or curvature present another barrier to comparing results across studies. Additionally, macroscale tensile or compressive loading of 3D structures like bone can easily result in cells experiencing combinations of both tension and compression at the microscale

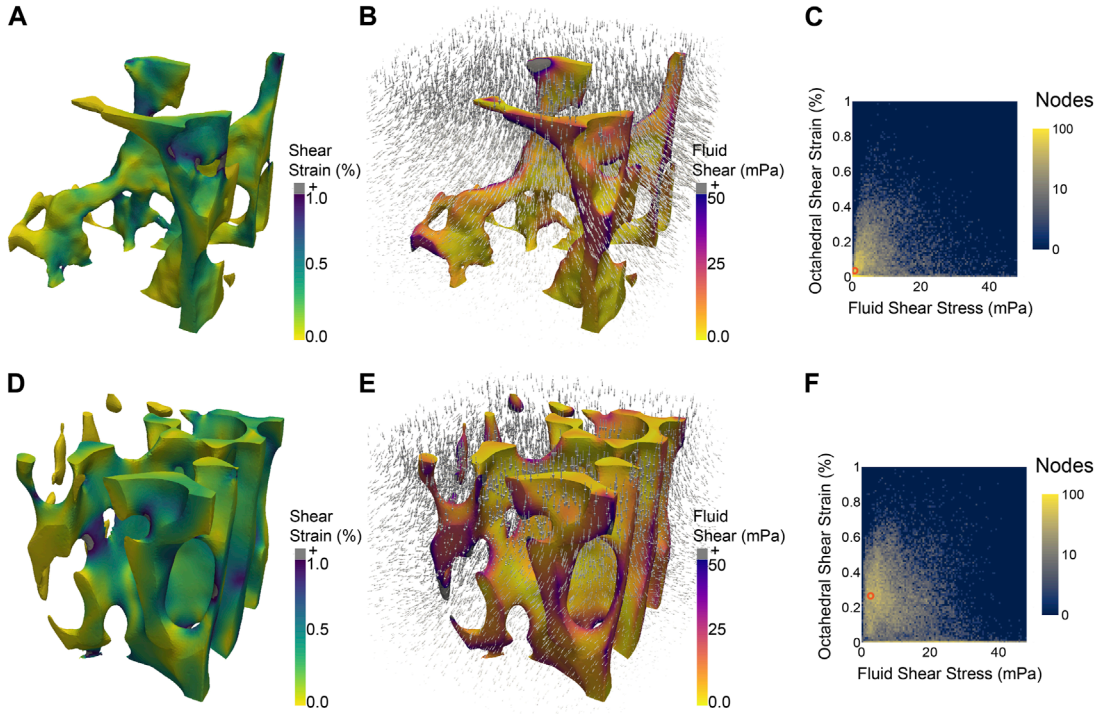

FIGURE 1
Two regions of trabecular bone from the same mouse vertebra, each subjected to the same simulated macroscale stimulus (uniaxial compression of 2,500 $\mu\epsilon$) experience different distributions of microscale stimuli, such as octahedral shear strain **(A,D)** induced by the applied compression and fluid shear stress **(B,E)** due to the flow of marrow induced by the compression. 2D histograms **(C,F)** illustrate the difference in distributions of shear strain and fluid shear stress between the two regions of bone. The most prevalent combination of the two micro-stimuli in each region is denoted by an orange circle at (0.75 mPa, 0.035%) **(C)** and (2.75 mPa, 0.265%) **(F)**.

(Niebur et al., 2000; Fields et al., 2010). Further, the fact that cells exist within aqueous environments means that strain-based stimulation doesn't occur independently of fluid-based stimuli; however, the latter are typically not accounted for when examining the influence of strain.

A variety of studies have emphasized the importance of fluid shear stress, due to both oscillatory flow and continuous unidirectional flow, in skeletal cell mechanobiology. Arnsdorf et al. (2009) demonstrated that oscillatory fluid flow promotes osteogenic differentiation of MSCs by activating RhoA, a regulator of ROCKII and subsequently cytoskeletal tension and organization. Corrigan et al. (2018) found that calcium channel transient receptor potential subfamily V member 4 (TRPV4) is critical for flow-based mechanotransduction in MSCs and is strongly associated with mechanosensitivity of the primary cilium. A variety of studies have demonstrated that parallel flow over a flat monolayer of MSCs can induce osteogenic behavior when the shear stress is on the order of 1 Pa in constant (Reich and Frangos, 1991; Yourek et al., 2010) and oscillatory (Li et al., 2004; Stavenschi et al., 2017) flow conditions, with both the magnitude and frequency of flow being influential factors (Stavenschi et al., 2017). Interestingly, studies that examine flow through 3D scaffolds report that much lower shear stresses, on the order of 1 mPa, are associated with increased osteogenesis while stresses above approximately 10 mPa are detrimental to cell viability (Porter et al., 2005; Melke et al., 2018). This discrepancy may be indicative of a broader difference between cell-microenvironment interactions in 2D vs. 3D contexts (Baker and Chen, 2012). In addition to regulation of MSC differentiation, fluid shear stress has been shown to induce immunomodulatory behavior in MSCs (Skibber et al., 2022). Along with changes in fluid shear stress, fluid flow is also associated with changes in hydrostatic pressure. High cyclically applied hydrostatic pressure (~100–1,000 kPa) has been associated with chondrogenic differentiation of MSCs (Wagner et al., 2008; Stavenschi and Hoey, 2019) while lower pressures (~10–300 kPa) have been associated with osteogenesis (Burger et al., 1992; Tang et al., 2017; Reinwald and El Haj, 2018).

Not only does fluid flow apply forces to cells, it also distributes nutrients. The flow of nutrient- and oxygen-carrying fluid helps to ensure the distribution of nutrients to cells throughout a 3D environment to maintain cell viability and enable proliferation and differentiation (Karande et al., 2004; Amini and Nukavarapu, 2014). Donahue et al. (2003) found that cells were significantly less responsive to shear stress in nutrient-free media, further demonstrating the difficulty of separating the effects of chemotransport and fluid flow.

2.2 Endogenous cues in the mechanical microenvironment

In the absence of externally applied loads, there are still physical cues endogenous to the microenvironment. These factors, which

include curvature as well as matrix/substrate stiffness, influence cell adhesion and cytoskeletal tension and are capable of driving MSC differentiation.

As reviewed by Werner et al. (2020), cells are capable of sensing curvatures at both a subcellular length scale (primarily through focal adhesion placement and growth) and length scales greater than or equal to the size of the cell (due to interactions between stress fibers and the nucleus). For MSCs cultured on hemispherical concave and convex surfaces, Werner et al. (2017) found that convex curvatures increased osteogenic gene expression while concave curvatures increased cell migration speeds. Werner et al. (2019) additionally introduced the notion of direction-dependent "perceived curvature" on non-spherical anisotropic curvatures (such as a cylindrical curvature). The perceived curvature acknowledges that cells oriented along the long axis of a cylinder experience a different amount of curvature and therefore undergo less bending than cells oriented perpendicular to the long axis; MSCs were observed to alter their migration behavior, ostensibly to avoid this bending. Callens et al. (2023) studied pre-osteoblasts on patterned substrates with a broader range of curvatures and found that groups of cells preferentially pattern surfaces with at least one negative principal curvature (i.e., concave-saddle), though over time groups of cells are able overcome convexities through cell-cell interactions that result in the formation of cell sheets that bridge unfavorable curvatures. Yang et al. (2022) found that saddle-like surfaces (triply periodic minimal surface-based scaffolds) promoted both osteogenesis and angiogenesis *in vivo*. The magnitude of curvature, in addition to the shape of curvature, is relevant to MSCs, with Swanson et al. (2022) finding that small spherical pores with curvatures in the range (16.0, 33.3) mm^{-1} maintained the stemness of MSCs while larger pores with curvatures in the range (4.7, 8.0) mm^{-1} promoted osteogenic differentiation, however there is a lack of thorough examination of how variations in curvature magnitude influence osteogenic behavior of MSCs, particularly when coupled with variations in curvature shape. The lack of consensus as to what constitutes an "optimal" curvature for osteogenesis may be attributable to the possibility that different processes are stimulated by different curvatures, for example, a curvature that promotes osteogenic differentiation may differ from a curvature that promotes tissue formation.

The curvature of a surface influences how cells attach to it, making surface curvature an important determinant of cell shape (Werner et al., 2017). McBeath et al. (2004) found that cell shape regulates RhoA, which in turn regulates the switch between adipogenic and osteogenic differentiation, with cells becoming osteoblasts when they were allowed to spread, and adipocytes when they were maintained as round. Similarly, Kilian et al. (2010) found that seeding MSCs on 2D islands of different shapes led to different lineage commitments, with shapes that had higher aspect ratios or concave subcellular curvatures generally found to increase cytoskeletal contractility and osteogenic differentiation. This association among curvature, cell shape, and the cytoskeleton emphasizes the mechanical nature of sensing of microenvironmental curvature. Through focal adhesions and cytoskeletal mechanics, MSCs are also able to sense the local stiffness of their microenvironment. When seeded on substrates of varying stiffnesses, MSCs were found to undergo morphological changes and exhibited neurogenic, myogenic, or osteogenic differentiation depending on substrate stiffness, further implicating cytoskeletal contractility as a key sensory mechanism of the physical microenvironment (Engler et al., 2006). There has been extensive study of the role of matrix/substrate stiffness and the interactions between MSCs and the extracellular matrix more generally, which have been reviewed by Assis-Ribas et al. (2018) and Lv et al. (2015).

2.3 Other factors

There are, of course, many non-mechanical factors that influence osteogenesis and bone regeneration. As reviewed by Hayrapetyan et al. (2015), there are various hormones, cytokines, and signaling pathways that are critical to osteogenic differentiation. Bone regeneration is also strongly coupled to other physiological processes, including angiogenesis which delivers oxygen and essential nutrients [as reviewed by Kanczler and Oreffo (2008)], the immune/inflammatory response which plays an essential role in initiating the repair process [as reviewed by Claes et al. (2012)], and the presence of extracellular matrix proteins which have also been shown to play a significant role in mediating the behavior of MSCs (Datta et al., 2006). The influence of nutrients can be particularly relevant *in vitro*, as the choice of media can strongly influence the differentiation of MSCs (Ho et al., 2011; Kyllönen et al., 2013). While these chemical and biological factors are indeed essential to the bone regeneration process, they too occur within the context of a mechanical environment and are coupled with the mechanobiological response of skeletal cells.

3 Combinations of stimuli in the mechanical microenvironment

The simultaneous presence of multiple stimuli in the microenvironments of skeletal cells *in vivo* (Moraes et al., 2011) makes it difficult to draw general conclusions about skeletal mechanobiology from examining only individual stimuli. Relatively few studies have attempted to directly quantify the effects of multiple mechanical cues acting concurrently, leaving open questions about how cells respond to combinations of cues.

Jiao et al. (2022) examined the synergistic effects of adhesion morphology and fluid shear stress by applying different levels of flow to cells seeded on differently shaped micro patterned substrates. Their results demonstrated that fluid shear stress and adhesion morphology could work cooperatively or antagonistically to regulate osteogenesis, with osteogenically favorable adhesion morphologies enhancing the osteogenic response induced by fluid flow and unfavorable morphologies blunting its influence. Further, they found that fluid shear stress had no effect on cell shape or spreading, indicating that the two cues regulate osteogenesis through different mechanisms.

Additional studies on the influence of multiple concurrent mechanical cues are based on observation of tissue differentiation *in vivo*, often in the context of bone regeneration following fracture. These studies have formulated hypotheses of how mechanical stimuli lead to local tissue differentiation into bone, cartilage, or

fibrous tissue. Different models have considered different pairings of tensile, compressive, and shear stresses and strains as well as fluid flow velocities and hydrostatic pressures. Prendergast et al. (1997), Carter et al. (1998), and Claes and Heigele (1999) each proposed paradigms to predict tissue differentiation within a healing fracture callus. A comparative analysis by Isaksson et al. (2006a) between the mechanoregulatory models of Carter et al. (1998), Claes and Heigele (1999), Lacroix and Prendergast (2002), and a model based on deviatoric strain by Isaksson et al. (2006b) and found that the model by Lacroix and Prendergast (2002), which is an extension of the model proposed by Prendergast et al. (1997) and postulates that tissue differentiation depends on combinations of shear strain and fluid flow velocity, was the most consistent with experimental data, matching those data in most, but not all, cases that were examined. Song et al. (2012) examined similar relationships between MSC lineage commitment and stress and strain by measuring local cellular deformations and the expression of lineage-associated genes. Despite efforts towards a working mechanobiological theory of bone regeneration, more work is needed to fully unify the influence of the various endogenous, exogenous, and non-mechanical factors into a robust and clinically translatable predictive model.

All of the aforementioned models consider how combinations of stimuli impact cell and tissue differentiation in regions such as a fracture callus where there is preliminary granulation tissue present. A different class of mechanobiological models considers how various cues promote the growth of new tissue into pore space, which is relevant in both bone remodeling and the osseointegration of bone tissue engineering scaffolds and other implants. A series of models by Geris and colleagues (Guyot et al., 2014; Guyot et al., 2016; Mehrian et al., 2018) predicts neotissue growth due to curvature, fluid shear stress, and metabolic factors (oxygen, glucose, pH) for scaffolds in perfusion bioreactors. Another growth model considers the growth and remodeling of trabecular bone (Aland et al., 2020) using both strain energy density and volumetric compression as possible strain-based remodeling stimuli. Both types of models describe important parts of the mechanobiological response of bone, but neither captures its full scope.

4 Discussion

The cellular microenvironment contains a variety of mechanical stimuli that both individually and collectively appear to regulate cellular activity and mediate osteogenesis during bone repair and regeneration. While the fact that these stimuli, including curvature, stiffness, strain, fluid shear stress, and hydrostatic pressure, are influential has been convincingly demonstrated, a thorough quantitative understanding of their influence at various magnitudes, frequencies, and durations is still lacking, particularly when multiple stimuli act concurrently. Such an understanding could enable new therapies for enhanced bone regeneration, patient-specific treatment plans, and improved design of orthopaedic implants. In the absence of that understanding, progress on these fronts is likely to be slow.

Mechanobiological considerations are increasingly being made in the treatment of bone fractures, as well as injuries in other tissues, as described for example, by the revised definition of the term "mechanotherapy" (Huang et al., 2013; Thompson et al., 2016). Several methods have been proposed to provide controlled levels of mechanical stimulation to skeletal cells, including low intensity vibration (LIV) and low intensity pulsed ultrasound (LIPUS), which have in at least some studies shown a potential for improving bone regeneration (Thompson et al., 2016); however, recent studies have questioned the efficacy of these treatments and called for additional investigation into the situations when such treatments may provide benefit, further demonstrating the need for a thorough understanding of how MSCs respond to microenvironmental stimuli (Lou et al., 2017; Searle et al., 2023). Using the mechanobiological model of Prendergast et al. (1997) and Miramini et al. (2015) demonstrated that different locking compression plate configurations can yield different mechanical microenvironments and tissue differentiation patterns, highlighting the potential of using enhanced understanding of mechanical microenvironments to impact specific approaches to fracture fixation.

Patient-specific treatments are particularly relevant in the context of aging-related changes to bone. The mechanoresponsiveness of bone has been shown to be altered by aging in both animals (Turner et al., 1995) and humans (Kohrt, 2001), though it remains unclear whether this alteration is due to diminished mechanosensitivity of cells or to microstructural changes that alter the microenvironmental stimuli that they receive. Furthering the understanding of both the microstructural changes associated with aging and the effects of aging on cell mechanoresponsiveness could support the development of treatments and activity guidelines for both improved fracture healing and maintenance of bone mass that are specific to an individual's age and health.

In surgical situations that call for the use of orthopaedic implants, the design of those implants offers an opportunity to apply the understanding of skeletal mechanobiology to custom-designed microenvironments. Among the most direct possible applications is in the design and development of bone tissue engineering scaffolds. Microenvironmentally-informed scaffold architectures could be used to regulate the stimuli that cells seeded on their surfaces perceive in order to enhance tissue growth. This could lead to the development of artificial bone grafts that are both safer and more effective than auto- or allografts. Other relevant applications include improving the osseointegration of joint replacement implants and developing fracture fixation implants that regulate the allowable motion of a fracture site to improve healing outcomes.

In order to fully realize the potential of harnessing the mechanical microenvironment, further work is needed. Future studies that assess the influence of individual or combinations of stimuli should quantify both the applied macroscale stimuli as well as the local microscale stimuli. This broader accounting of stimuli would enhance the applicability of findings and make them relevant beyond the scope of particular experimental setups. Additionally, efforts should be made to account for stimuli beyond those being directly investigated, for example, compression-induced fluid flow. To this end, computational simulation offers a powerful tool for analysis of microenvironments (Figure 1) that can be paired with experimental results (Schulte et al., 2013). Another step to improving the robustness and generalizability of studies

examining the effect of microenvironmental stimuli on osteogenesis is to examine multiple markers of osteogenic differentiation, with an eye towards developing a minimum standard set of readouts. Osteocalcin, osteopontin, and RUNX2 are all commonly used markers of osteogenic differentiation; however many studies examine only one, making it difficult to compare results between studies.

Overall, the importance of mechanical cues to bone regeneration highlights the importance of elucidating the mechanoresponsiveness of skeletal cells to combinations of microenvironmental stimuli. Doing so has the potential to address a variety of key clinical needs and answer major questions about the nature of skeletal mechanobiology.

Author contributions

TJ: Writing–Original Draft and Conceptualization. EM: Conceptualization, Writing–Reviewing and Editing, Supervision, and Funding acquisition. All authors contributed to the article and approved the submitted version.

Funding

The funding was provided by the National Institutes of Health/National Institute on Aging (Grant #AG073671 to EM).

Conflict of interest

The authors declare that the research was conducted in the absence of any commercial or financial relationships that could be construed as a potential conflict of interest.

Publisher's note

References

Aland, S., Stenger, F., Müller, R., Deutsch, A., and Voigt, A. (2020). A phase field approach to trabecular bone remodeling. *Front. Appl. Math. Statistics* 6, 12. doi:10.3389/fams.2020.00012

Amini, A. R., and Nukavarapu, S. P. (2014). Oxygen-tension controlled matrices for enhanced osteogenic cell survival and performance. *Ann. Biomed. Eng.* 42, 1261–1270. doi:10.1007/s10439-014-0990-z

Arnsdorf, E. J., Tummala, P., Kwon, R. Y., and Jacobs, C. R. (2009). Mechanically induced osteogenic differentiation - the role of RhoA, ROCKII and cytoskeletal dynamics. *J. Cell Sci.* 122, 546–553. doi:10.1242/jcs.036293

Assis-Ribas, T., Forni, M. F., Winnischofer, S. M. B., Sogayar, M. C., and Trombetta-Lima, M. (2018). Extracellular matrix dynamics during mesenchymal stem cells differentiation. *Dev. Biol.* 437, 63–74. doi:10.1016/j.ydbio.2018.03.002

Augat, P., Hollensteiner, M., and von Rüden, C. (2021). The role of mechanical stimulation in the enhancement of bone healing. *Injury* 52, S78–S83. doi:10.1016/j.injury.2020.10.009

Augat, P., and von Rüden, C. (2018). Evolution of fracture treatment with bone plates. *Injury* 49, S2–S7. doi:10.1016/S0020-1383(18)30294-8

Baker, B. M., and Chen, C. S. (2012). Deconstructing the third dimension-how 3D culture microenvironments alter cellular cues. *J. Cell Sci.* 125, 3015–3024. doi:10.1242/jcs.079509

Bennell, K. L., Malcolm, S. A., Khan, K. M., Thomas, S. A., Reid, S. J., Brukner, P. D., et al. (1997). Bone mass and bone turnover in power athletes, endurance athletes, and controls: A 12-month longitudinal study. *Bone* 20, 477–484. doi:10.1016/S8756-3282(97)00026-4

Burger, E. H., Klein-Nulend, J., and Veldhuijzen, J. P. (1992). Mechanical stress and osteogenesis *in vitro*. *J. Bone Mineral Res.* 7, S397–S401. doi:10.1002/jbmr.5650071406

Callens, S. J. P., Fan, D., van Hengel, I. A. J., Minneboo, M., Díaz-Payno, P. J., Stevens, M. M., et al. (2023). Emergent collective organization of bone cells in complex curvature fields. *Nat. Commun.* 14, 855. doi:10.1038/s41467-023-36436-w

Carter, D. R., Beaupré, G. S., Giori, N. J., and Helms, J. A. (1998). Mechanobiology of skeletal regeneration. *Clin. Orthop. Relat. Res.* 355, S41–S55. doi:10.1097/00003086-199810001-00006

Claes, L. E., and Heigele, C. A. (1999). Magnitudes of local stress and strain along bony surfaces predict the course and type of fracture healing. *J. Biomechanics* 32, 255–266. doi:10.1016/S0021-9290(98)00153-5

Claes, L., Recknagel, S., and Ignatius, A. (2012). Fracture healing under healthy and inflammatory conditions. *Nat. Rev. Rheumatol.* 8, 133–143. doi:10.1038/nrrheum.2012.1

Corrigan, M. A., Johnson, G. P., Stavenschi, E., Riffault, M., Labour, M. N., and Hoey, D. A. (2018). TRPV4-mediates oscillatory fluid shear mechanotransduction in mesenchymal stem cells in part via the primary cilium. *Sci. Rep.* 8, 3824. doi:10.1038/s41598-018-22174-3

Datta, N., Pham, Q. P., Sharma, U., Sikavitsas, V. I., Jansen, J. A., and Mikos, A. G. (2006). *In vitro* generated extracellular matrix and fluid shear stress synergistically enhance 3D osteoblastic differentiation. *Proc. Natl. Acad. Sci. U. S. A.* 103, 2488–2493. doi:10.1073/pnas.0505661103

Donahue, T. L., Haut, T. R., Yellowley, C. E., Donahue, H. J., and Jacobs, C. R. (2003). Mechanosensitivity of bone cells to oscillating fluid flow induced shear stress may be modulated by chemotransport. *J. Biomechanics* 36, 1363–1371. doi:10.1016/S0021-9290(03)00118-0

Engler, A. J., Sen, S., Sweeney, H. L., and Discher, D. E. (2006). Matrix elasticity directs stem cell lineage specification. *Cell* 126, 677–689. doi:10.1016/j.cell.2006.06.044

Fields, A. J., Lee, G. L., and Keaveny, T. M. (2010). Mechanisms of initial endplate failure in the human vertebral body. *J. Biomechanics* 43, 3126–3131. doi:10.1016/j.jbiomech.2010.08.002

Fu, R., Feng, Y., Liu, Y., and Yang, H. (2021). Mechanical regulation of bone regeneration during distraction osteogenesis. *Med. Nov. Technol. Devices* 11, 100077. doi:10.1016/j.medntd.2021.100077

Guyot, Y., Papantoniou, I., Chai, Y. C., Van Bael, S., Schrooten, J., and Geris, L. (2014). A computational model for cell/ECM growth on 3D surfaces using the level set method: a bone tissue engineering case study. *Biomechanics Model. Mechanobiol.* 13, 1361–1371. doi:10.1007/s10237-014-0577-5

Guyot, Y., Papantoniou, I., Luyten, F. P., and Geris, L. (2016). Coupling curvature-dependent and shear stress-stimulated neotissue growth in dynamic bioreactor cultures: a 3D computational model of a complete scaffold. *Biomechanics Model. Mechanobiol.* 15, 169–180. doi:10.1007/s10237-015-0753-2

Haudenschild, A. K., Hsieh, A. H., Kapila, S., and Lotz, J. C. (2009). Pressure and distortion regulate human mesenchymal stem cell gene expression. *Ann. Biomed. Eng.* 37, 492–502. doi:10.1007/s10439-008-9629-2

Hayrapetyan, A., Jansen, J. A., and Van Den Beucken, J. J. (2015). Signaling pathways involved in osteogenesis and their application for bone regenerative medicine. *Tissue Eng. - Part B Rev.* 21, 75–87. doi:10.1089/ten.teb.2014.0119

Ho, S. T. B., Tanavde, V. M., Hui, J. H., and Lee, E. H. (2011). Upregulation of adipogenesis and chondrogenesis in MSC serum-free culture. *Cell Med.* 2, 27–41. doi:10.3727/215517911x575984

Huang, C., Holfeld, J., Schaden, W., Orgill, D., and Ogawa, R. (2013). Mechanotherapy: revisiting physical therapy and recruiting mechanobiology for a new era in medicine. *Trends Mol. Med.* 19, 555–564. doi:10.1016/j.molmed.2013.05.005

Isaksson, H., van Donkellar, C. C., Huiskes, R., and Ito, K. (2006a). Corroboration of mechanoregulatory algorithms for tissue differentiation during fracture healing: comparison with *in vivo* results. *J. Orthop. Res.* 24, 898–907. doi:10.1002/jor.20118

Isaksson, H., Wilson, W., van Donkelaar, C. C., Huiskes, R., and Ito, K. (2006b). Comparison of biophysical stimuli for mechano-regulation of tissue differentiation

during fracture healing. *J. Biomechanics* 39, 1507–1516. doi:10.1016/j.jbiomech.2005.01.037

Jiao, F., Xu, J., Zhao, Y., Ye, C., Sun, Q., Liu, C., et al. (2022). Synergistic effects of fluid shear stress and adhesion morphology on the apoptosis and osteogenesis of mesenchymal stem cells. *J. Biomed. Mater. Res. - Part A* 110, 1636–1644. doi:10.1002/jbm.a.37413

Kanczler, J. M., and Oreffo, R. O. (2008). Osteogenesis and angiogenesis: the potential for engineering bone. *Eur. Cells Mater.* 15, 100–114. doi:10.22203/eCM.v015a08

Kanellopoulos, A. D., and Soucacos, P. N. (2006). Management of nonunion with distraction osteogenesis. *Injury* 37, S51–S55. doi:10.1016/j.injury.2006.02.041

Karande, T. S., Ong, J. L., and Agrawal, C. M. (2004). Diffusion in musculoskeletal tissue engineering scaffolds: design issues related to porosity, permeability, architecture, and nutrient mixing. *Ann. Biomed. Eng.* 32, 1728–1743. doi:10.1007/s10439-004-7825-2

Kearney, E. M., Farrell, E., Prendergast, P. J., and Campbell, V. A. (2010). Tensile strain as a regulator of mesenchymal stem cell osteogenesis. *Ann. Biomed. Eng.* 38, 1767–1779. doi:10.1007/s10439-010-9979-4

Kilian, K. A., Bugarija, B., Lahn, B. T., and Mrksich, M. (2010). Geometric cues for directing the differentiation of mesenchymal stem cells. *Proc. Natl. Acad. Sci. U. S. A.* 107, 4872–4877. doi:10.1073/pnas.0903269107

Knothe Tate, M. L., Gunning, P. W., and Sansalone, V. (2016). Emergence of form from function—mechanical engineering approaches to probe the role of stem cell mechanoadaptation in sealing cell fate. *BioArchitecture* 6, 85–103. doi:10.1080/19490992.2016.1229729

Kohrt, W. M. (2001). Aging and the osteogenic response to mechanical loading. *Int. J. Sport Nutr.* 11, S137–S142. doi:10.1123/ijsnem.11.s1.s137

Kyllönen, L., Haimi, S., Mannerström, B., Huhtala, H., Rajala, K. M., Skottman, H., et al. (2013). Effects of different serum conditions on osteogenic differentiation of human adipose stem cells *in vitro*. *Stem Cell Res. Ther.* 4, 17. doi:10.1186/scrt165

Lacroix, D., and Prendergast, P. J. (2002). A mechano-regulation model for tissue differentiation during fracture healing: analysis of gap size and loading. *J. Biomechanics* 35, 1163–1171. doi:10.1016/S0021-9290(02)00086-6

Li, Y. J., Batra, N. N., You, L., Meier, S. C., Coe, I. A., Yellowley, C. E., et al. (2004). Oscillatory fluid flow affects human marrow stromal cell proliferation and differentiation. *J. Orthop. Res.* 22, 1283–1289. doi:10.1016/j.orthres.2004.04.002

Lou, S., Lv, H., Li, Z., Zhang, L., and Tang, P. (2017). The effects of low-intensity pulsed ultrasound on fresh fracture: A meta-analysis. *Med. (United States)* 96, e8181. doi:10.1097/MD.0000000000008181

Lv, H., Li, L., Sun, M., Zhang, Y., Chen, L., Rong, Y., et al. (2015). Mechanism of regulation of stem cell differentiation by matrix stiffness. *Stem Cell Res. Ther.* 6, 103–111. doi:10.1186/s13287-015-0083-4

Mavčič, B., and Antolič, V. (2012). Optimal mechanical environment of the healing bone fracture/osteotomy. *Int. Orthop.* 36, 689–695. doi:10.1007/s00264-012-1487-8

Mavrogenis, A. F., Dimitriou, R., Parvizi, J., and Babis, G. C. (2009). Biology of implant osseointegration. *J Musculoskelet Neuronal Interact* 9, 61-71.

McBeath, R., Pirone, D. M., Nelson, C. M., Bhadriraju, K., and Chen, C. S. (2004). Cell shape, cytoskeletal tension, and RhoA regulate stem cell lineage commitment. *Dev. Cell* 6, 483–495. doi:10.1016/S1534-5807(04)00075-9

McBride, S. H., Dolejs, S., Brianza, S., Knothe, U., and Knothe Tate, M. L. (2011). Net change in periosteal strain during stance shift loading after surgery correlates to rapid de novo bone generation in critically sized defects. *Ann. Biomed. Eng.* 39, 1570–1581. doi:10.1007/s10439-010-0242-9

McDermott, A. M., Herberg, S., Mason, D. E., Collins, J. M., Pearson, H. B., Dawahare, J. H., et al. (2019). Recapitulating bone development through engineered mesenchymal condensations and mechanical cues for tissue regeneration. *Sci. Transl. Med.* 11, 7756. doi:10.1126/scitranslmed.aav7756

McMahon, L. A., Campbell, V. A., and Prendergast, P. J. (2008). Involvement of stretch-activated ion channels in strain-regulated glycosaminoglycan synthesis in mesenchymal stem cell-seeded 3D scaffolds. *J. Biomechanics* 41, 2055–2059. doi:10.1016/j.jbiomech.2008.03.027

Mehrian, M., Guyot, Y., Papantoniou, I., Olofsson, S., Sonnaert, M., Misener, R., et al. (2018). Maximizing neotissue growth kinetics in a perfusion bioreactor: an *in silico* strategy using model reduction and bayesian optimization. *Biotechnol. Bioeng.* 115, 617–629. doi:10.1002/bit.26500

Melke, J., Zhao, F., Rietbergen, B., Ito, K., and Hofmann, S. (2018). Localisation of mineralised tissue in a complex spinner flask environment correlates with predicted wall shear stress level localisation. *Eur. Cells Mater.* 36, 57–68. doi:10.22203/eCM.v036a05

Metzger, T. A., Schwaner, S. A., LaNeve, A. J., Kreipke, T. C., and Niebur, G. L. (2015). Pressure and shear stress in trabecular bone marrow during whole bone loading. *J. Biomechanics* 48, 3035–3043. doi:10.1016/j.jbiomech.2015.07.028

Miramini, S., Zhang, L., Richardson, M., Pirpiris, M., Mendis, P., Oloyede, K., et al. (2015). Computational simulation of the early stage of bone healing under different configurations of locking compression plates. *Comput. Methods Biomechanics Biomed. Eng.* 18, 900–913. doi:10.1080/10255842.2013.855729

Moraes, C., Sun, Y., and Simmons, C. A. (2011). Micro)managing the mechanical microenvironment. *Integr. Biol.* 3, 959–971. doi:10.1039/c1ib00056j

Niebur, G. L., Feldstein, M. J., Yuen, J. C., Chen, T. J., and Keaveny, T. M. (2000). High-resolution finite element models with tissue strength asymmetry accurately predict failure of trabecular bone. *J. Biomechanics* 33, 1575–1583. doi:10.1016/S0021-9290(00)00149-4

Orwoll, E. S., Adler, R. A., Amin, S., Binkley, N., Lewiecki, E. M., Petak, S. M., et al. (2013). Skeletal health in long-duration astronauts: nature, assessment, and management recommendations from the NASA bone summit. *J. Bone Mineral Res.* 28, 1243–1255. doi:10.1002/jbmr.1948

Pelaez, D., Charles Huang, C. Y., and Cheung, H. S. (2009). Cyclic compression maintains viability and induces chondrogenesis of human mesenchymal stem cells in fibrin gel scaffolds. *Stem Cells Dev.* 18, 93–102. doi:10.1089/scd.2008.0030

Porter, B., Zauel, R., Stockman, H., Guldberg, R., and Fyhrie, D. (2005). 3-D computational modeling of media flow through scaffolds in a perfusion bioreactor. *J. Biomechanics* 38, 543–549. doi:10.1016/j.jbiomech.2004.04.011

Prendergast, P. J., Huiskes, R., and Søballe, K. (1997). ESB Research Award 1996. Biophysical stimuli on cells during tissue differentiation at implant interfaces. *J. Biomechanics* 30, 539–548. doi:10.1016/S0021-9290(96)00140-6

Qi, M. C., Hu, J., Zou, S. J., Chen, H. Q., Zhou, H. X., and Han, L. C. (2008). Mechanical strain induces osteogenic differentiation: cbfa1 and ets-1 expression in stretched rat mesenchymal stem cells. *Int. J. Oral Maxillofac. Surg.* 37, 453–458. doi:10.1016/j.ijom.2007.12.008

Reich, K. M., and Frangos, J. A. (1991). Effect of flow on prostaglandin E2 and inositol trisphosphate levels in osteoblasts. *Am. J. Physiology - Cell Physiology* 261, C428–C432. doi:10.1152/ajpcell.1991.261.3.c428

Reinwald, Y., and El Haj, A. J. (2018). Hydrostatic pressure in combination with topographical cues affects the fate of bone marrow-derived human mesenchymal stem cells for bone tissue regeneration. *J. Biomed. Mater. Res. - Part A* 106, 629–640. doi:10.1002/jbm.a.36267

Schreivogel, S., Kuchibhotla, V., Knaus, P., Duda, G. N., and Petersen, A. (2019). Load-induced osteogenic differentiation of mesenchymal stromal cells is caused by mechano-regulated autocrine signaling. *J. Tissue Eng. Regen. Med.* 13, 1992–2008. doi:10.1002/term.2948

Schulte, F. A., Ruffoni, D., Lambers, F. M., Christen, D., Webster, D. J., Kuhn, G., et al. (2013). Local mechanical stimuli regulate bone formation and resorption in mice at the tissue level. *PLoS ONE* 8, e62172. doi:10.1371/journal.pone.0062172

Scott, A., Khan, K. M., Duronio, V., and Hart, D. A. (2008). Mechanotransduction in human bone: *in vitro* cellular physiology that underpins bone changes with exercise. *Sports Med.* 38, 139–160. doi:10.2165/00007256-200838020-00004

Searle, H. K., Lewis, S. R., Coyle, C., Welch, M., and Griffin, X. L. (2023). Ultrasound and shockwave therapy for acute fractures in adults. *Cochrane Database Syst. Rev.* 2023, CD008579. doi:10.1002/14651858.CD008579.pub4

Skibber, M. A., Olson, S. D., Prabhakara, K. S., Gill, B. S., and Cox, C. S. (2022). Enhancing mesenchymal stromal cell Potency: inflammatory licensing via mechanotransduction. *Front. Immunol.* 13, 874698. doi:10.3389/fimmu.2022.874698

Song, M. J., Brady-Kalnay, S. M., McBride, S. H., Phillips-Mason, P., Dean, D., and Tate, M. L. (2012). Mapping the mechanome of live stem cells using a novel method to measure local strain fields *in situ* at the fluid-cell interface. *PLOS ONE* 7, e43601. doi:10.1371/JOURNAL.PONE.0043601

Stavenschi, E., and Hoey, D. A. (2019). Pressure-induced mesenchymal stem cell osteogenesis is dependent on intermediate filament remodeling. *FASEB J.* 33, 4178–4187. doi:10.1096/fj.201801474RR

Stavenschi, E., Labour, M. N., and Hoey, D. A. (2017). Oscillatory fluid flow induces the osteogenic lineage commitment of mesenchymal stem cells: the effect of shear stress magnitude, frequency, and duration. *J. Biomechanics* 55, 99–106. doi:10.1016/j.jbiomech.2017.02.002

Steward, A. J., and Kelly, D. J. (2015). Mechanical regulation of mesenchymal stem cell differentiation. *J. Anat.* 227, 717–731. doi:10.1111/joa.12243

Sumner, D. R. (2015). Long-term implant fixation and stress-shielding in total hip replacement. *J. Biomechanics* 48, 797–800. doi:10.1016/j.jbiomech.2014.12.021

Swanson, W. B., Omi, M., Woodbury, S. M., Douglas, L. M., Eberle, M., Ma, P. X., et al. (2022). Scaffold Pore curvature influences μsc fate through differential cellular organization and YAP/TAZ activity. *Int. J. Mol. Sci.* 23, 4499. doi:10.3390/ijms23094499

Tang, X., Teng, S., Liu, C., and Jagodzinski, M. (2017). Influence of hydrodynamic pressure on the proliferation and osteogenic differentiation of bone mesenchymal stromal cells seeded on polyurethane scaffolds. *J. Biomed. Mater. Res. - Part A* 105, 3445–3455. doi:10.1002/jbm.a.36197

Thompson, W. R., Scott, A., Terry Loghmani, M., Ward, S. R., and Warden, S. J. (2016). Understanding mechanobiology: Physical therapists as a force in mechanotherapy and musculoskeletal regenerative rehabilitation. *Phys. Ther.* 96, 560–569. doi:10.2522/ptj.20150224

Turner, C. H., Takano, Y., and Owan, I. (1995). Aging changes mechanical loading thresholds for bone formation in rats. *J. Bone Mineral Res.* 10, 1544–1549. doi:10.1002/jbmr.5650101016

Vaughan, T. J., Voisin, M., Niebur, G. L., and McNamara, L. M. (2015). Multiscale modeling of trabecular bone marrow: understanding the micromechanical environment of mesenchymal stem cells during osteoporosis. *J. Biomechanical Eng.* 137. doi:10.1115/1.4028986

Wagner, D. R., Lindsey, D. P., Li, K. W., Tummala, P., Chandran, S. E., Smith, R. L., et al. (2008). Hydrostatic pressure enhances chondrogenic differentiation of human bone marrow stromal cells in osteochondrogenic medium. *Ann. Biomed. Eng.* 36, 813–820. doi:10.1007/s10439-008-9448-5

Werner, M., Blanquer, S. B., Haimi, S. P., Korus, G., Dunlop, J. W., Duda, G. N., et al. (2017). Surface curvature differentially regulates stem cell migration and differentiation via altered attachment morphology and nuclear deformation. *Adv. Sci.* 4, 1600347. doi:10.1002/advs.201600347

Werner, M., Kurniawan, N. A., and Bouten, C. V. (2020). Cellular geometry sensing at different length scales and its implications for scaffold design. *Materials* 13, 963. doi:10.3390/ma13040963

Werner, M., Petersen, A., Kurniawan, N. A., and Bouten, C. V. (2019). Cell-Perceived substrate curvature dynamically coordinates the direction, speed, and persistence of stromal cell migration. *Adv. Biosyst.* 3, e1900080. doi:10.1002/adbi.201900080

Wolff, J. (1986). *The law of bone remodelling*. Berlin: Springer. doi:10.1007/978-3-642-71031-5

Wong, S. A., Rivera, K. O., Miclau, T., Alsberg, E., Marcucio, R. S., and Bahney, C. S. (2018). Microenvironmental regulation of chondrocyte plasticity in endochondral repair-A new frontier for developmental engineering. *Front. Bioeng. Biotechnol.* 6, 58. doi:10.3389/fbioe.2018.00058

Yang, Y., Xu, T., Bei, H. P., Zhang, L., Tang, C. Y., Zhang, M., et al. (2022). Gaussian curvature-driven direction of cell fate toward osteogenesis with triply periodic minimal surface scaffolds. *Proc. Natl. Acad. Sci. U. S. A.* 119, e2206684119. doi:10.1073/pnas.2206684119

Yourek, G., McCormick, S. M., Mao, J. J., and Reilly, G. C. (2010). Shear stress induces osteogenic differentiation of human mesenchymal stem cells. *Regen. Med.* 5, 713–724. doi:10.2217/RME.10.60

Yu, W., Su, X., Li, M., Wan, W., Li, A., Zhou, H., et al. (2021). Three-dimensional mechanical microenvironment enhanced osteogenic activity of mesenchymal stem cells-derived exosomes. *Chem. Eng. J.* 417, 128040. doi:10.1016/j.cej.2020.128040

frontiers | Frontiers in Physiology

TYPE Review
PUBLISHED 17 October 2023
DOI 10.3389/fphys.2023.1233920

OPEN ACCESS

EDITED BY
Noriaki Ono,
University of Texas Health Science Center at Houston, United States

REVIEWED BY
Carla Palumbo,
Metaboli and Neurnal Sciences–University of Modena and Reggio Emilia, Italy
Yuki Matsushita,
Nagasaki University, Japan
Chia-Lung Wu,
University of Rochester Medical Center, United States

*CORRESPONDENCE
Alesha B. Castillo,
alesha.castillo@nyu.edu

†These authors have contributed equally to this work

RECEIVED 03 June 2023
ACCEPTED 02 October 2023
PUBLISHED 17 October 2023

CITATION
Atria PJ and Castillo AB (2023), Skeletal adaptation to mechanical cues during homeostasis and repair: the niche, cells, and molecular signaling.
Front. Physiol. 14:1233920.
doi: 10.3389/fphys.2023.1233920

Skeletal adaptation to mechanical cues during homeostasis and repair: the niche, cells, and molecular signaling

Pablo J. Atria[1†] and Alesha B. Castillo[1,2*†]

[1]Department of Orthopedic Surgery, New York University Grossman School of Medicine, New York, NY, United States, [2]Department of Biomedical Engineering, New York University Tandon School of Engineering, New York, NY, United States

Bones constantly change and adapt to physical stress throughout a person's life. Mechanical signals are important regulators of bone remodeling and repair by activating skeletal stem and progenitor cells (SSPCs) to proliferate and differentiate into bone-forming osteoblasts using molecular signaling mechanisms not yet fully understood. SSPCs reside in a dynamic specialized microenvironment called the *niche*, where external signals integrate to influence cell maintenance, behavior and fate determination. The nature of the niche in bone, including its cellular and extracellular makeup and regulatory molecular signals, is not completely understood. The mechanisms by which the niche, with all of its components and complexity, is modulated by mechanical signals during homeostasis and repair are virtually unknown. This review summarizes the current view of the cells and signals involved in mechanical adaptation of bone during homeostasis and repair, with an emphasis on identifying novel targets for the prevention and treatment of age-related bone loss and hard-to-heal fractures.

KEYWORDS

skeletal stem and progenitor cells, SSPCs, bone, mechanical loading, mechanical signals, fracture repair, niche

1 Introduction

The skeleton plays a crucial mechanical role in our daily lives by facilitating movement, providing support against gravitational forces, acting as an endocrine organ and protecting internal organs against blunt force trauma (Castillo and Leucht, 2015). The ability of bones to adapt and respond to the prevailing mechanical environment over one's lifetime is critical for maintaining skeletal health, mineral homeostasis and meeting mechanical demands of everyday activities (e.g., walking, running, jumping, etc.) (Li and Xie, 2005; Chen et al., 2013; Castillo and Leucht, 2015; Cabahug-Zuckerman et al., 2020).

Regular physical activity and exercise can stimulate bone growth and increase bone density, thereby reducing the risk of fracture. However, with aging and disease (e.g., rickets, Paget's disease, diabetes, malignancy, etc.) (Augat et al., 2005; Heilmeier et al., 2016), there is a diminishment in bones' ability to adapt to mechanical stress over time (Morgan et al., 2018), leading to bone fragility and increased fracture risk. One critical contribution to bony non-union is delayed or inhibited revascularization of the injury site, revascularization depends on appropriate biological and mechanical cues, and recent data suggest that osteoprogenitor (OPC)-endothelial cell (EC) crosstalk, playing a critical role in revascularization of the injury site (Kusumbe et al., 2014; Yang et al., 2022;

Biswas et al., 2023). Skeletal stem and progenitor cells (SSPCs) play a vital role in maintaining bone mass and repairing damaged bones. SSPCs reside in a specialized microenvironment known as the niche which acts as the central hub for maintaining cellular identity during quiescence and coordinating a response to mechanical and biological signals. In bone, SSPCs have been found in the periosteum, endosteum, marrow and growth plate (Méndez-Ferrer et al., 2010; Zhou et al., 2014; Coutu et al., 2017; Debnath et al., 2018; Matsushita et al., 2020a; Kurenkova et al., 2020).

Current FDA approved anabolic treatments that can prevent bone loss are Teriparatide, Abaloparatide and Romosozumab. The first two are PTH analogs, while Romosozumab is a sclerostin inhibitor. All of these medications suppress bone remodeling, and might have an effect on the cellular populations which line the bone surface (Leaffer et al., 1995; Hodsman et al., 2005), even though this process has not been fully understood. Therefore, understanding the mechanisms involved in SSPC niche regulation is crucial for developing therapeutic strategies to prevent and treat skeletal disease and injury.

This review focuses on the identity of murine SSPCs, their unique environment in different bone compartments, and their involvement in bone homeostasis and repair. We then describe the mechanical environment in bone, relying heavily on previous comprehensive reviews by the senior author, with emphasis placed on the interplay between the niche, SSPCs and their response to mechanical signals during homeostasis and repair.

2 Bone compartments and their skeletal stem and progenitor cells

Stem cells are defined as cells with the ability to (Castillo and Leucht, 2015) reconstitute an environment that supports hematopoiesis (Li and Xie, 2005); self-renew on the clonal level; and (Cabahug-Zuckerman et al., 2020) differentiate into multiple lineages (Wagner et al., 2005). SSPCs include skeletal stem cells and downstream progenitors and are located in the niche the periosteum, endosteum and within bone marrow (Bianco et al., 2001; Méndez-Ferrer et al., 2010; Zhou et al., 2014; Shi et al., 2017; Debnath et al., 2018; Duchamp de Lageneste et al., 2018; Seike et al., 2018; Ortinau et al., 2019; Matsushita et al., 2020b; Shen et al., 2021). However, the extent to which distinct SSPC populations contribute to bone repair is still a matter of debate, largely due to the lack of proper markers to distinguish between the different populations. To date, SSPC populations have been characterized using a variety of markers such as Mx1, Grem1, LepR, Cxcl12, Pdgfra, Pdgfrb and Prrx1, among others (Table 1). Additionally, only a handful of studies have made quantitative comparisons of the contribution of uniquely identified SSPC populations to bone repair, making it difficult to compare results between studies (Matsushita et al., 2020b; Shen et al., 2021; Jeffery et al., 2022). State-of-the-art technologies, such as single cell RNA-seq and spatial transcriptomics have helped elucidate transcriptional characteristics of different bone resident cell populations, but none of the aforementioned markers is restricted to a single population, making it challenging to investigate their distinct functions during skeletal growth, repair, aging and adaptation (Baccin et al., 2020).

TABLE 1 Markers and mouse lines labeling SSPCs in injury.

Marker		Location	Type of injury	Potential contribution to bone repair	Pathway
LepR Zhou et al. (2014)	*LepR-cre*	Periosteum	Monocortical injury		
Cxcl12 Matsushita et al. (2020b)	*Cxcl12-creER*	Bone marrow (perisinusoidal)	Monocortical injury	Differentiate into mature osteoblasts	Wnt/B-catenin signaling
Adipoq Zhong et al. (2020)	*Adipoq:Td*	Bone marrow	None	Unknown	Unknown
Adipoq Jeffery et al. (2022)	*Adipoq-cre*	Bone marrow	Monocortical injury	Proliferation, differentiation into mature osteoblasts	Unknown
Oln Shen et al. (2021)	Oln^{iCreER}	Bone marrow (periarteriolar)	None (just mechanical stimulation)	Unknown	Unknown
Prrx1 Duchamp de Lageneste et al. (2018)	*Prx1-Cre;mTmG*	Bone marrow and periosteum	Bicortical		Periostin
Gli1 Jeffery et al. (2022)	$GlicreER^{T2}$	Periosteum	Bicortical	Proliferation, differentiation into mature osteoblasts	Wnt/β-catenin
Gli1 Shi et al. (2017)	*Gli1-* $CreER^{T2}$*; Ai9*	Bone marrow and Periosteum	Bicortical	Proliferation and differentiation	
Fgfr3 Matsushita et al. (2023)	*Fgfr3-creER*	Endosteum	Monocortical injury	Expand and differentiate to osteoblasts in young bones	Wnt/B-catenin signaling
Mx1, aSMA Ortinau et al. (2019)	*Mx1-Cre; aSMA-GFP*	Periosteum	Monocortical injury	Supply the majority of callus-forming cells	
Pdgfra Julien et al. (2022)	$Pdgfra^{CreERT}$	Various tissues	Bicortical		BMP signalign
Ctsk Debnath et al. (2018)	*CTSK–mGFP*	Periosteum (marks also osteoclasts)	Bicortical	Proliferation, osteoblast differentiation	

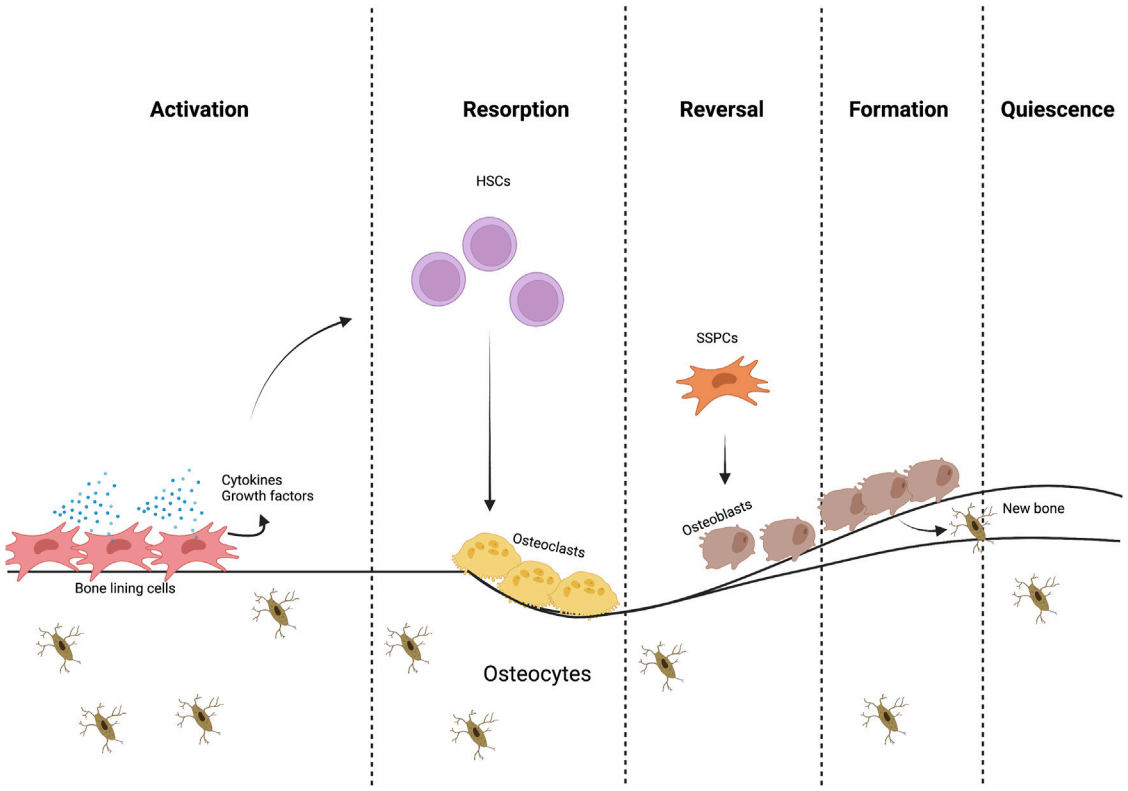

FIGURE 1
The bone remodeling process. Different cells and signaling molecules involved in the bone remodeling process, bone resorption by osteoclasts and formation by osteoblasts.

The most primitive SSPCs have reticular morphology and can be identified by leptin receptor (LepR) expression (Zhou et al., 2014). They also express high levels of CXC motif chemokine ligand 12 (Cxcl12) (Matsushita et al., 2020b) and stem cell factor (Scf), key factors maintaining the hematopoietic stem cell niche, hematopoietic stem cells (HSCs) and restricted progenitors (Zhou et al., 2014). This subpopulations will be discussed in details throughout this review.

SSPCs can originate from different bone compartments and even from adjacent skeletal muscle. Prx1+ SSPCs, a population that resides in the periosteum, bone marrow, and skeletal muscle, can form cartilage, adipose tissue and bone during bone healing (Julien et al., 2021). Lineage tracing and scRNA-seq showed that Prx1+ periosteal cells and mesenchymal progenitors in skeletal muscle are enriched in osteochondral progenitors, and contribute to endochondral ossification during fracture repair. Both populations transition to a fibrogenic state prior to chondrogenesis which is activated by BMP signaling (Sivaraj et al., 2021).

Cellular niches are dynamic microenvironments consisting of cellular and extracellular elements that regulate maintenance, self-renewal and differentiation of stem cells (Li and Xie, 2005; Kurenkova et al., 2020). These niches exist in different bone compartments (periosteal, endosteal and marrow), with the marrow containing trabecular bone in both metaphyseal and epiphyseal compartments. These different niches are influenced by a variety of metabolic products; for example, calcium and reactive oxygen species, have been shown to have a direct influence in stem cell behavior (Ito et al., 2004). Regarding mechanical stimulation, the response to mechanical cues in these distinct environments differs due to their unique makeup of cells and stroma (connective tissue, blood vessels, lymphatic vessels, and nerves) and calcified tissues of varying microstructure, which determines their mechanical properties (Robling et al., 2006; Gurkan and Akkus, 2008; Petzold and Gentleman, 2021). Presumably, each compartment contains distinct niches that vary in SSPC identity and heterogeneity. In the last year, there has been significant progress towards understanding the diversity of stromal cell populations owing to single-cell RNA seq and spatial transcriptomics (Baccin et al., 2020) (Figure 1).

Characterizing the location and composition of these niches, as well as understanding their response to mechanical signals and injury is important for developing effective therapeutic strategies to prevent and treat osteoporosis and fractures that are difficult to repair (Estell and Rosen, 2021). What is known presently is described below (Figure 2).

2.1 Periosteum

The periosteum is a thin external membrane of connective tissue that covers bones, it is composed of two layers: the outer fibrous layer and the inner cambium layer. The cambium layer contains stem and progenitor cells with chondrogenic and osteogenic capacity, which has been described elsewhere. (Lazzeri et al., 2009). Several markers, including Sca1, α-SMA, Prx1, Mx1, Ctsk, have been used to identify

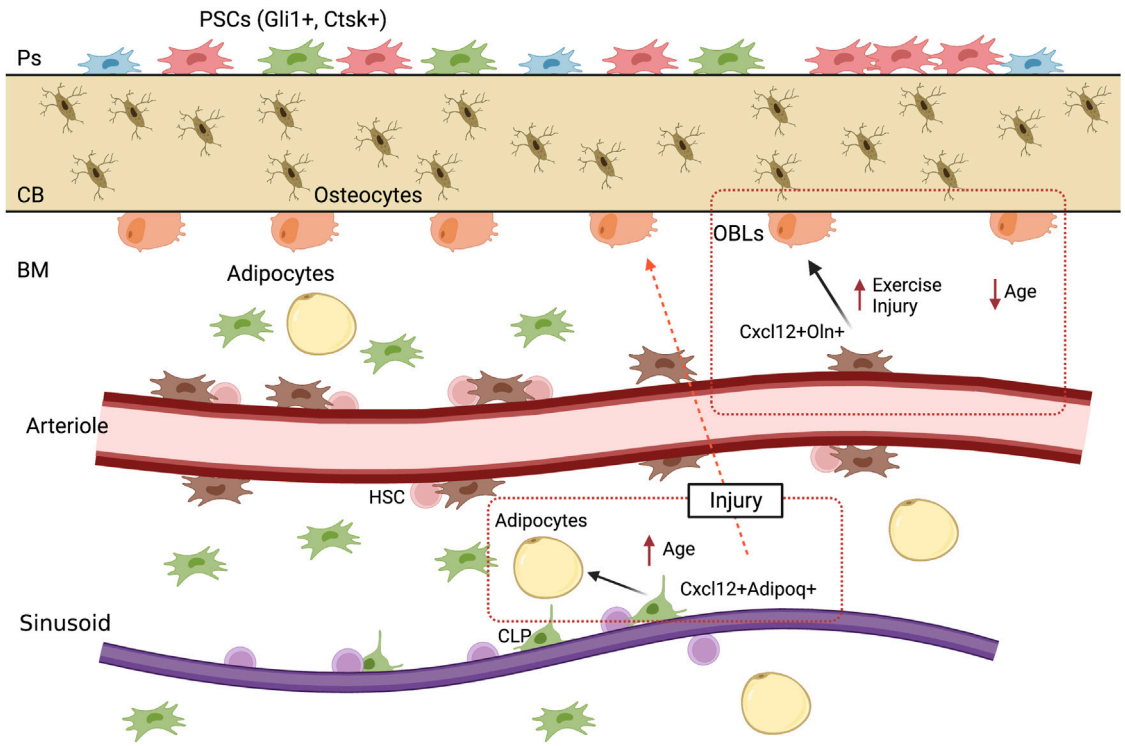

FIGURE 2
Bone compartments and their SSPCs. Something similar to Figure 1 generated before, the difference is that now it will describe periosteum, endosteum and bone marrow.

stem and progenitor population in the periosteum (Debnath et al., 2018; Duchamp de Lageneste et al., 2018; Ortinau et al., 2019; Matthews et al., 2021). Periosteal stem cells can regenerate bone tissues even in absence of bone marrow, which highlights their importance (Ortinau et al., 2019). Recently, a Ctsk+CD200+ population has been identified as periosteal stem cells (Debnath et al., 2018). This population can differentiate into osteogenic lineage cells, as well as into chondrocytes; however, Ctsk + cells do not express LepR (Colnot, 2009; Debnath et al., 2018). Rather, LepR + cells in the periosteum overlap with Gli1+ periosteal cells (Jeffery et al., 2022). Indeed, recent data show that in the adult periosteum, $Gli1^{creERT2}$ expression identifies periosteal SSPCs, while marrow SSPCs are identified by $LepR^{cre}$ and Adiponectin-cre/creER expression. Following bone injuries, both Gli1-creER+ and LepR + cells exhibit proliferation but contribute differently to the bone repair process (Jeffery et al., 2022). Gli1+ cells in the periosteum mainly contribute to endochondral ossification after bicortical fractures and give rise to bone marrow stromal cells residing in a perivascular niche after losing the expression of *Gli1* and acquiring expression of *LepR*, *Scf*, and *Cxcl12* (Jeffery et al., 2022). How these unique populations respond to mechanical cues both during homeostasis and fracture repair remains unknown.

2.2 Endosteum

During appositional bone growth, the endosteum is formed by the periosteum becoming trapped. The endosteum is a thin membrane, typically measuring only 10–40 μm in thickness, consisting of a loosely defined layer of connective tissue and a small number of cell layers.

The cells within the endosteum are arranged in a mosaic pattern, with formative, resting, and resorptive regions characterized by the presence of active osteoblasts, preosteoblasts, or osteoclasts, respectively (Frost, 1987). In terms of function, the endosteum contributes significantly to bone repair and reconstruction, as it houses osteoprogenitor cells like MSCs and preosteoblasts, much like the periosteum. The endosteum has been widely studied due to its importance as the site for hematopoietic stem cells (HSC) niche, and the characteristics of HSC compared to their central marrow counterparts (Haylock et al., 2007). It has been shown that HSCs residing in the endosteal region have different proliferative capacity and homing efficiency compared to central HSCs, highlighting the influence of site-specific niches (Sicl et al., 2013). SSPC niches are believed to exist in the metaphysis and endosteum, given the presence of cells expressing SSPC markers such as GLI family zinc finger 1 (Gli1), Gremlin 1 (Grem1), Leptin receptor (LepR), Nestin-GFP, Platelet-derived growth factor receptor a (PDGFRa), and PDGFRb. Recently, Matsushita et al. (2023) identified a novel SSPC population, which highly expresses *Fgfr3*, this population possesses osteoblast-chondrocyte transitional identity and diminishes with age.

However, the characteristics of these SSPC populations in the endosteum are not well-defined (Loopmans et al., 2022).

2.3 Marrow

The bone marrow contains hematopoietic stem cells (HSCs) which engage in hematopoiesis throughout the entire adult life. LepR+ and Cxcl12+ SSCs that are contained within the bone marrow space are essential components of the HSCs niche, due to the fact that they secrete essential factors for HSC maintenance (Zhou et al., 2014). Osteoblasts, are also important for the maintenance of the niche and some restricted progenitors, as they also provide important factors (Lévesque et al., 2010). In young and middle-aged C57BL/6 J mice, the percentage of LepR + cells in total bone marrow cells was reported to be between 0.7% and 11% (Kara et al., 2023). In postnatal mice, LepR + cells recovered 95% and 85% of all CFU-Fs from the bone marrow and femur shaft, respectively (Shu et al., 2021). Numerous single-cell RNA sequencing based studies have shown that LepR, Cxcl12 and Adipoq are expressed by the same cells in the adult bone marrow (Baryawno et al., 2019; Tikhonova et al., 2019; Matsushita et al., 2020b). Adipoq + cells are perivascular and are distributed throughout the bone marrow with similar location to LepR + cells (Jeffery et al., 2022). It has been shown that these Adipoq + cells do not contain lipid droplets, form a 3D network within the marrow space, and are essential in maintaining bone marrow vasculature, as well as playing an important role in regulating bone formation (Zhong et al., 2020).

If we analyze what has been reported regarding bone marrow SSPCs, LepR + largely overlap with Cxcl12+ cells (Zhou et al., 2014), this LepR + Cxcl12+ population could be divided into two different populations according to their specific location; LepR + Cxcl12+ periarteriolar cells and LepR + Cxcl12+ perisinusoidal cells (Baccin et al., 2020). It has been shown that LepR + cells that locate surrounding arterioles, can be further identified by the expression of Oln (Shen et al., 2021), this population is mechanosensitive, which means that is maintained by mechanical stimulation, as well as it has the ability to differentiate into mature osteoblasts (Shen et al., 2021). Additionally, perisinusoidal Cxcl12+ cells, are a quiescent cell population which are primed to become adipocytes, although, under special conditions can differentiate into mature osteoblast, this population also expresses Adipoq (Matsushita et al., 2020b).

Sivaraj and colleagues reported that bone marrow stromal cells (MSCs), which fall under the SSPC umbrella, found in the metaphysis (mpMSCs) and diaphysis (dpMSCs) are unique, that is, mpMSCs are PDGFRα$^{+}\beta^{+}$Hey1^{+} while dpMSCs are PDGFRα$^{+}\beta^{+}$Hey1^{-}, mpMSC can be efficiently differentiated to osteogenic, adipogenic, and chondrogenic lineage cells *in vitro,* and can also give rise to dpMSCs during bone development (Sivaraj et al., 2021). This highlights the substantial heterogeneity among MSCs, and illustrates the fundamental differences between distinct locations and microenvironments.

Besides both perivascular populations, it has also been identified a non-perivascular population with *in vivo* osteogenic and chondrogenic potential labeled by *Grem1,* although their contribution to adult bone is limited (Worthley et al., 2015).

3 Mechanical environment in bone

The skeleton is composed of cortical and trabecular bony architectures, differing both in mechanical characteristics and metabolic activity. The manner in which these tissues amalgamate to form complete bones is crucial in determining the overall mechanical properties of the organ. Additionally, factors such as size, shape, and cross-sectional area of the bone significantly influence its properties, and these features can be altered due to age-related changes or disease processes (Morgan et al., 2018). Differences between cortical and trabecular bone are mainly dictated by tissue porosity. Cortical bone has a porosity of 5%–15%, while trabecular bone has a porosity of 40%–95%. Cortical bone exhibits anisotropic behavior; that is, the longitudinal direction of the cortical bone, which is aligned with the diaphyseal axis, has greater strength and tensile/compressive modulus compared to the radial and circumferential directions (Morgan et al., 2018). Mechanical properties of trabecular bone at the apparent level - the level at which several trabeculae are observed at once - are mainly influenced by its porosity. Trabecular bone exhibits higher strength in compression compared to tension and is weakest in shear, although these variations diminish with decreasing apparent density. A more comprehensive review of this topic is found in Morgan, E. F., et al. (2018). "Bone mechanical properties in healthy and diseased states." (Morgan et al., 2018).

Bone adapts to mechanical cues as part of its homeostatic program. Physical activity, which transmits mechanical forces to the tissue, sends mechanical signals that affect cells at a molecular level, changing their gene expression, proliferation, differentiation, and apoptosis (Jacobs et al., 2010). Without these signals, bone undergoes increased resorption which translates into tissue loss. These changes in bone mass and architecture due to mechanical loading and unloading are described by a theory termed "the mechanostat" (Frost, 1987). The mechanostat theory classifies bone behavior based on mechanical strain and models the effect of influences on the skeleton through effector cells, osteocytes, osteoblasts, and osteoclasts (Frost, 1987).

Osteocytes are the most abundant cells in bone tissue, dispersed throughout the mineralized matrix, with their lacuna-canalicular system and dendritic connections, are the primary mechanosensors, mechanotransducers and major producers of some signaling proteins (Palumbo and Ferretti, 2021), able to detect metabolic changes, as well as detect and transmit mechanical cues to downstream signals that regulate bone cell activity. They can sense mechanical forces such as hydrostatic pressure, fluid shear stress, and direct deformation and convert them into biochemical and biological signaling events. This conversion involves four different elements: force transmission to cells, mechanosensing, signal transduction, and signal transmission (Carina et al., 2020). Specifically, SSPCs, osteoblasts, chondrocytes, and endothelial cells can respond directly to mechanical signals. Two recent reviews summarize molecular mechanisms underlying the transduction of mechanical cues into biochemical signals (Chen et al., 2013; Castillo and Leucht, 2015; Anani and Castillo, 2022).

The bone anabolic threshold refers to the minimum level of mechanical strain or deformation required to stimulate new bone formation. This threshold varies depending on a number of factors including age, sex, and genetic variability. If the strain magnitude exceeds the minimum strain threshold, bone formation is activated in those regions experiencing increased. The anabolic strain threshold (>1,050 microstrain) for initiating new bone formation *in vivo* (Turner et al., 1994) and for activating mechanoresponsive signaling pathways in bone cells (>10,000 microstrain) (You et al., 2000) has been estimated. During walking, tissue-level deformation or strain on bone surfaces can vary between 500 and 2,000 microstrain (Martelli et al., 2014), while strenuous activity can result in strains up to 10,000 microstrain (Milgrom et al., 2000). Whole bone strain plays a crucial role in facilitating fluid flow within the bony matrix, lacuna-canalicular space, and marrow (Piekarski and Munro, 1977; Birmingham et al., 2015). Additionally, fluid drag at cell attachment points along the osteocyte processes can amplify these strains, leading to osteocyte membrane strains estimated to be up to 30,000 microstrain (Verbruggen et al., 2012).

The fundamental principles governing the response of healthy, uninjured bone to mechanical signals have been established through seminal studies conducted both *in vivo* and *in vitro*, as reviewed in (34). These include (Castillo and Leucht, 2015): bone responds to dynamic loading (Li and Xie, 2005); bone responds only after distinct strain or strain rate thresholds are crossed (Cabahug-Zuckerman et al., 2020); the bone formation response correlates with strain magnitude and rate (Chen et al., 2013); bone responds to short loading periods (Augat et al., 2005); bone grows accustomed to routine mechanical signals (Heilmeier et al., 2016); bone is highly responsive to mechanical signals during growth and development (Morgan et al., 2018); aging results in a dysregulated bone response to mechanical signals (Castillo and Leucht, 2015). While these principles are important to consider and to think about, they do not explain the events that are occurring at the niche level, which means, understanding the SSPCs involved in the response, which autocrine or paracrine signals are involved in this response, and how different locations affect this response.

4 SSPCs in mechanoadaptation of bone

Riffault et al. (2020) investigated the effect of mechanical loading on bone marrow stromal/stem cells using LepR-cre; tdTomato + animals. *In vivo* axial compressive loading of the tibia did not result in proliferation of LepR-cre; tdTomato + stromal cells within the marrow or in the recruitment of these cells to the bone surface. The finding that LepR + cells did not significantly contribute to bone formation in adult mice is not unexpected, as previous research has shown that these cells only make up a small proportion of Col2.3+ cells in 2-month-old mice (3%–10%) and 10-month-old mice (10%–23%), with LepR + osteocytes only appearing at 10 months of age (Zhou et al., 2014). Instead, it suggests that these cells may play a supportive role in osteogenesis via cell non-autonomous effects or that LepR + cells already present along the bone surface are reactivated.

As mentioned before, Shen et al., showed that a specific LepR + subpopulation, which expresses exclusively Oln+, are located in the bone marrow, specifically in the peri-arteriolar niche, which is mechanosensitive. The peri-arteriolar niche contains unique cell populations that promote the growth and differentiation of both bone-forming cells and immune cells, specifically the LepR + Oln + cells, which are shown to be maintained by physical exercise, and their depletion directly affects the common lymphoid progenitor population, by decreasing its number. With regard to mechanism, removing Piezo1, a mechanosensitive ion channel protein (Ma et al., 2022), from Oln + cells led to lower bone mineral density, as well as reduced frequencies of Oln + cells and CLPs. Additionally, Piezo1 deletion resulted in a weakened response to sudden infection, which could be attributed to the close connection between Oln + cells and CLP (Shen et al., 2021).

Prrx1+ cells are primarily located in the periosteum and play a significant role in bone repair (Liu et al., 2019). Periosteal progenitors are a source for osteoblasts and become osteocytes in response to mechanical loading via a primary cilium-mediated process, but the exact mechanism is yet to be confirmed (Moore et al., 2019). The acute response of adult bone to loading involves expansion of Sca-1+Prrx1+ and Sca-1−Prrx1+ cells in the periosteum (Cabahug-Zuckerman et al., 2019). Both adult and aged mice exhibit load-induced periosteal bone formation, though the response is significantly attenuated with age (Cabahug-Zuckerman et al., 2019). The Sca-1+Prrx1+ population is targeted by loading, and loading activates proliferation of Prrx1+ cells in the periosteum as early as 2 days into a 4-consecutive-day loading protocol. Prrx1+ cells may play a key role in load-induced osteogenesis considering their presence in the periosteum, the primary site of load-induced cortical bone formation (Cabahug-Zuckerman et al., 2019). However, further research is needed to fully understand the role of Prrx1+ cells in load-induced bone formation.

Interestingly, recent studies seem to suggest that the origin of mature osteoblasts and adipocytes in homeostasis shifts between young (P21) and adult mice (18 M), they specifically identified a shift from Fgfr3+ cells to LepR + cells with age, which raises the question if the SSPCs population(s) involved in load-induce bone formation also undergoes this point of origin change (Matsushita et al., 2023).

In a separate study, Osx + cells or their progeny accounted for >98% of periosteal cells at sites of bone formation (Zannit and Silva, 2019). Approximately 30% of Osx + lineage cells arose via proliferation, and a recent study by the same group showed that ablation of proliferating osteoblast reduces lamellar bone formation, demonstrating that proliferating cells are necessary to achieve a maximal anabolic response to mechanical loading (Zannit et al., 2020). While these data suggest that recruitment and differentiation of more primitive osteoprogenitors is not required for the early response to acute anabolic loading, the origin and turnover of these periosteal-resident Osx + cells are still unclear.

5 SSPCs in bone repair

Jeffery and others (Jeffery et al., 2022) observed that periosteal SSPCs could be identified by Gli1creERT2 expression, whereas SSPCs in marrow were identified by LepR-cre and Adiponectin-cre/creER expression. After bone injuries, both SSPC populations underwent proliferation but contributed differently to the bone repair process. Gli1+ periosteal SSPCs were found to mainly contribute to endochondral ossification after bicortical fractures and gave rise to marrow SSPCs that lost Gli1 expression and acquired a perivascular localization with expression of LepR, Scf,

and Cxcl12. In contrast, LepR + Adipoq + cells only contributed to intramembranous repair. These findings underscore the distinctions between the two populations and their respective microenvironments (Jeffery et al., 2022).

LepR + Adipoq + cells, which are mainly found surrounding sinusoids and are fated to become adipocytes unless under specific conditions such as bone injury. These Adipoq + cells have distinct molecular signatures and respond differently to different types of signals compared to other SSPC populations; this cell population, which has been also referred as *MALPs*, has been shown to be critical for bone marrow regulation, including vasculature and bone formation (Zhong et al., 2020). It has been shown that ablating this Adipoq + population decreases the number of $Emcn^{+}CD31^{+}$ endothelial cells, as well as causing an increase in trabecular bone formation. Adipoq + cells have an important regulatory role since are the cell population that expresses *Csf1* the most, which encodes the macrophage colony-stimulating factor (M-CSF); this factor is paramount in the proliferation, differentiation, survival and function of myeloid lineage cells, including monocytes, macrophages, and osteoclasts (Inoue et al., 2023; Zhong et al., 2023).

As mentioned before, Jeffery et al. have shown that LepR + Adipoq + cells are located exclusively in the bone marrow compartment, are responsible for adult steady-state osteogenesis and actively participate in drill-hole injuries, which mean, injuries that heal via intramembranous repair (Jeffery et al., 2022).

Matsushita et al. (2020b) found that a specific type of quiescent bone marrow stem cell, marked by Cxcl12-creER, which correspond to perisinusoidal LepR + cells, can transition into a precursor cell state similar to skeletal stem cells during injury responses mediated by canonical Wnt signaling. These cells contribute to skeletal regeneration but do not participate in cortical bone osteoblast formation under homeostasis. Taken into consideration previous research, and the data from Matsushita et al. we believe that this Cxcl12-creER population corresponds to the LepR + Adipoq+ and MALPs population.

6 Summary and future approaches

As it was described, load induced bone formation during homeostasis and repair is a complex process which encompasses many biological events, which involve a variety of growth factors, the activation of niche specific SSPCs, differentiation and activation of osteolineage cells such as osteoblasts and osteoclasts, angiogenesis, among others (Figure 3).

The first need is to try to understand which SSPCs population or populations are involved in load-induced bone formation. This involvement can be either by activation and differentiation into mature osteoblasts, or it might be that some of these populations are acting as regulatory paracrine networks, providing the necessary signals and growth factors to either quiescent bone lining cells, stromal cells, or others. Whether these osteoblasts derive from one or several different sources remains to be elucidated.

We consider that the identification of more upstream therapeutic targets is relevant in injury and bone loss, due to

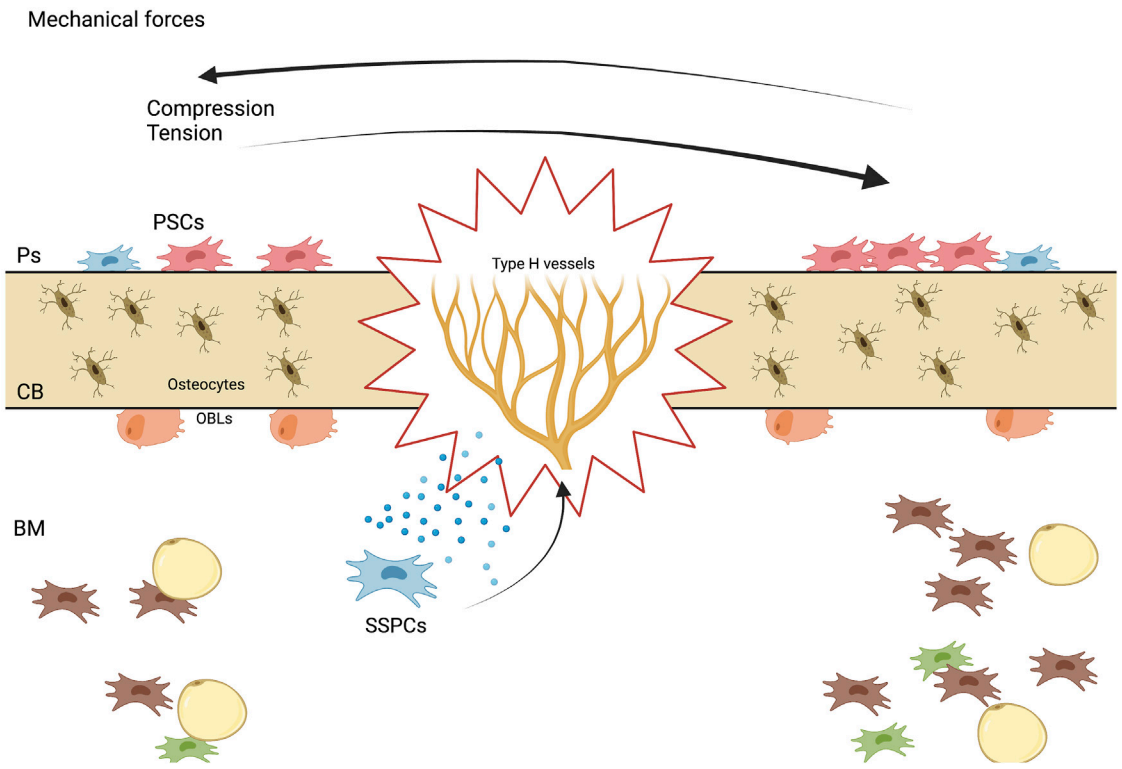

FIGURE 3
Mechanisms of stem cell-mediated bone regeneration. A diagram showing the various mechanisms by which stem cells promote bone regeneration, including differentiation into bone-forming cells, paracrine signaling to stimulate endogenous repair processes, and immunomodulatory effects.

the fact that it has been described, for aged individuals, that the SSPCs pool population declines with age; therefore, identifying potential factors that could aim to maintain the number and functionality of this multipotent cell populations might grant clinicians different treatment options depending on the clinical scenario.

Author contributions

PJA: Conceptualization, investigation, original draft, review & editing. ABC: Conceptualization, project administration, resources, supervision, validation, visualization, writing-original draft, writing-review.

Conflict of interest

The authors declare that the research was conducted in the absence of any commercial or financial relationships that could be construed as a potential conflict of interest.

Publisher's note

References

Anani, T., and Castillo, A. B. (2022). Mechanically-regulated bone repair. *Bone* 154, 116223. doi:10.1016/j.bone.2021.116223

Augat, P., Simon, U., Liedert, A., and Claes, L. (2005). Mechanics and mechano-biology of fracture healing in normal and osteoporotic bone. *Osteoporos. Int.* 16, S36–S43. doi:10.1007/s00198-004-1728-9

Baccin, C., Al-Sabah, J., Velten, L., Helbling, P. M., Grünschläger, F., Hernández-Malmierca, P., et al. (2020). Combined single-cell and spatial transcriptomics reveal the molecular, cellular and spatial bone marrow niche organization. *Nat. Cell Biol.* 22 (1), 38–48. doi:10.1038/s41556-019-0439-6

Baryawno, N., Przybylski, D., Kowalczyk, M. S., Kfoury, Y., Severe, N., Gustafsson, K., et al. (2019). A cellular taxonomy of the bone marrow stroma in homeostasis and leukemia. *Cell* 177 (7), 1915–1932. doi:10.1016/j.cell.2019.04.040

Bianco, P., Riminucci, M., Gronthos, S., and Robey, P. G. (2001). Bone marrow stromal stem cells: nature, biology, and potential applications. *Stem cells* 19 (3), 180–192. doi:10.1634/stemcells.19-3-180

Birmingham, E., Kreipke, T., Dolan, E., Coughlin, T., Owens, P., McNamara, L. M., et al. (2015). Mechanical stimulation of bone marrow *in situ* induces bone formation in trabecular explants. *Ann. Biomed. Eng.* 43, 1036–1050. doi:10.1007/s10439-014-1135-0

Biswas, L., Chen, J., De Angelis, J., Singh, A., Owen-Woods, C., Ding, Z., et al. (2023). Lymphatic vessels in bone support regeneration after injury. *Cell* 186 (2), 382–397.e24. doi:10.1016/j.cell.2022.12.031

Cabahug-Zuckerman, P., Liu, C., and Castillo, A. B. (2020). "Cells involved in mechanotransduction including mesenchymal stem cells," in *Encyclopedia of bone biology* (msterdam, Netherlands: Elsevier), 311–332.

Cabahug-Zuckerman, P., Liu, C., Cai, C., Mahaffey, I., Norman, S. C., Cole, W., et al. (2019). Site-specific load-induced expansion of Sca-1+ Prrx1+ and Sca-1− Prrx1+ cells in adult mouse long bone is attenuated with age. *JBMR plus* 3 (9), e10199. doi:10.1002/jbm4.10199

Carina, V., Della Bella, E., Costa, V., Bellavia, D., Veronesi, F., Cepollaro, S., et al. (2020). Bone's response to mechanical loading in aging and osteoporosis: molecular mechanisms. *Calcif. tissue Int.* 107 (4), 301–318. doi:10.1007/s00223-020-00724-0

Castillo, A. B., and Leucht, P. (2015). Bone homeostasis and repair: forced into shape. *Curr. Rheumatol. Rep.* 17, 58–8. doi:10.1007/s11926-015-0537-9

Chen, J., Castillo, A., and Jacobs, C. (2013). Chapter 20-cellular and molecular mechanotransduction in bone. *Osteoporos. fourth Ed.* 2013, 453–475. doi:10.1016/B978-0-12-415853-5.00020-0

Colnot, C. (2009). Skeletal cell fate decisions within periosteum and bone marrow during bone regeneration. *J. Bone Mineral Res.* 24 (2), 274–282. doi:10.1359/jbmr.081003

Coutu, D. L., Kokkaliaris, K. D., Kunz, L., and Schroeder, T. (2017). Three-dimensional map of nonhematopoietic bone and bone-marrow cells and molecules. *Nat. Biotechnol.* 35 (12), 1202–1210. doi:10.1038/nbt.4006

Debnath, S., Yallowitz, A. R., McCormick, J., Lalani, S., Zhang, T., Xu, R., et al. (2018). Discovery of a periosteal stem cell mediating intramembranous bone formation. *Nature* 562 (7725), 133–139. doi:10.1038/s41586-018-0554-8

Duchamp de Lageneste, O., Julien, A., Abou-Khalil, R., Frangi, G., Carvalho, C., Cagnard, N., et al. (2018). Periosteum contains skeletal stem cells with high bone regenerative potential controlled by Periostin. *Nat. Commun.* 9 (1), 773. doi:10.1038/s41467-018-03124-z

Estell, E. G., and Rosen, C. J. (2021). Emerging insights into the comparative effectiveness of anabolic therapies for osteoporosis. *Nat. Rev. Endocrinol.* 17 (1), 31–46. doi:10.1038/s41574-020-00426-5

Frost, H. M. (1987). The mechanostat: a proposed pathogenic mechanism of osteoporoses and the bone mass effects of mechanical and non mechanical agents. *Bone Min.* 2, 73–85.

Gurkan, U. A., and Akkus, O. (2008). The mechanical environment of bone marrow: a review. *Ann. Biomed. Eng.* 36, 1978–1991. doi:10.1007/s10439-008-9577-x

Haylock, D. N., Williams, B., Johnston, H. M., Liu, M. C., Rutherford, K. E., Whitty, G. A., et al. (2007). Hemopoietic stem cells with higher hemopoietic potential reside at the bone marrow endosteum. *Stem cells* 25 (4), 1062–1069. doi:10.1634/stemcells.2006-0528

Heilmeier, U., Cheng, K., Pasco, C., Parrish, R., Nirody, J., Patsch, J., et al. (2016). Cortical bone laminar analysis reveals increased midcortical and periosteal porosity in type 2 diabetic postmenopausal women with history of fragility fractures compared to fracture-free diabetics. *Osteoporos. Int.* 27, 2791–2802. doi:10.1007/s00198-016-3614-7

Hodsman, A. B., Bauer, D. C., Dempster, D. W., Dian, L., Hanley, D. A., Harris, S. T., et al. (2005). Parathyroid hormone and teriparatide for the treatment of osteoporosis: a review of the evidence and suggested guidelines for its use. *Endocr. Rev.* 26 (5), 688–703. doi:10.1210/er.2004-0006

Inoue, K., Qin, Y., Xia, Y., Han, J., Yuan, R., Sun, J., et al. (2023). Bone marrow Adipoq-lineage progenitors are a major cellular source of M-CSF that dominates bone marrow macrophage development, osteoclastogenesis, and bone mass. *Elife* 12, e82118. doi:10.7554/eLife.82118

Ito, K., Hirao, A., Arai, F., Matsuoka, S., Takubo, K., Hamaguchi, I., et al. (2004). Regulation of oxidative stress by ATM is required for self-renewal of haematopoietic stem cells. *Nature* 431 (7011), 997–1002. doi:10.1038/nature02989

Jacobs, C. R., Temiyasathit, S., and Castillo, A. B. (2010). Osteocyte mechanobiology and pericellular mechanics. *Annu. Rev. Biomed. Eng.* 12, 369–400. doi:10.1146/annurev-bioeng-070909-105302

Jeffery, E. C., Mann, T. L., Pool, J. A., Zhao, Z., and Morrison, S. J. (2022). Bone marrow and periosteal skeletal stem/progenitor cells make distinct contributions to bone maintenance and repair. *Cell Stem Cell* 29 (11), 1547–1561.e6. doi:10.1016/j.stem.2022.10.002

Julien, A., Kanagalingam, A., Martínez-Sarrà, E., Megret, J., Luka, M., Ménager, M., et al. (2021). Direct contribution of skeletal muscle mesenchymal progenitors to bone repair. *Nat. Commun.* 12 (1), 2860. doi:10.1038/s41467-021-22842-5

Julien, A., Perrin, S., Martínez-Sarrà, E., Kanagalingam, A., Carvalho, C., Luka, M., et al. (2022). Skeletal stem/progenitor cells in periosteum and skeletal muscle share a common molecular response to bone injury. *J. Bone Mineral Res.* 37 (8), 1545–1561. doi:10.1002/jbmr.4616

Kara, N., Xue, Y., Zhao, Z., Murphy, M. M., Comazzetto, S., Lesser, A., et al. (2023). Endothelial and Leptin Receptor+ cells promote the maintenance of stem cells and hematopoiesis in early postnatal murine bone marrow. *Dev. Cell* 58 (5), 348–360.e6. doi:10.1016/j.devcel.2023.02.003

Kurenkova, A. D., Medvedeva, E. V., Newton, P. T., and Chagin, A. S. (2020). Niches for skeletal stem cells of mesenchymal origin. *Front. Cell Dev. Biol.* 8, 592. doi:10.3389/fcell.2020.00592

Kusumbe, A. P., Ramasamy, S. K., and Adams, R. H. (2014). Coupling of angiogenesis and osteogenesis by a specific vessel subtype in bone. *Nature* 507 (7492), 323–328. doi:10.1038/nature13145

Lazzeri, D., Gatti, G. L., Romeo, G., Balmelli, B., and Massei, A. (2009). Bone regeneration and periosteoplasty: a 250-year-long history. *Cleft palate-craniofacial J.* 46 (6), 621–628. doi:10.1597/08-085.1

Leaffer, D., Sweeney, M., Kellerman, L. A., Avnur, Z., Krstenansky, J. L., Vickery, B. H., et al. (1995). Modulation of osteogenic cell ultrastructure by RS-23581, an analog of

human parathyroid hormone (PTH)-related peptide-(1-34), and bovine PTH-(1-34). *Endocrinology* 136 (8), 3624–3631. doi:10.1210/endo.136.8.7628402

Lévesque, J., Helwani, F., and Winkler, I. (2010). The endosteal "osteoblastic"niche and its role in hematopoietic stem cell homing and mobilization. *Leukemia* 24 (12), 1979–1992. doi:10.1038/leu.2010.214

Li, L., and Xie, T. (2005). Stem cell niche: structure and function. *Annu. Rev. Cell Dev. Biol.* 21, 605–631. doi:10.1146/annurev.cellbio.21.012704.131525

Liu, C., Cabahug-Zuckerman, P., Stubbs, C., Pendola, M., Cai, C., Mann, K. A., et al. (2019). Mechanical loading promotes the expansion of primitive osteoprogenitors and organizes matrix and vascular morphology in long bone defects. *J. Bone Mineral Res.* 34 (5), 896–910. doi:10.1002/jbmr.3668

Loopmans, S., Stockmans, I., Carmeliet, G., and Stegen, S. (2022). Isolation and *in vitro* characterization of murine young-adult long bone skeletal progenitors. *Front. Endocrinol.* 13, 930358. doi:10.3389/fendo.2022.930358

Ma, N., Chen, D., Lee, J.-H., Kuri, P., Hernandez, E. B., Kocan, J., et al. (2022). Piezo1 regulates the regenerative capacity of skeletal muscles via orchestration of stem cell morphological states. *Sci. Adv.* 8 (11), eabn0485. doi:10.1126/sciadv.abn0485

Martelli, S., Pivonka, P., and Ebeling, P. R. (2014). Femoral shaft strains during daily activities: implications for atypical femoral fractures. *Clin. Biomech.* 29 (8), 869–876. doi:10.1016/j.clinbiomech.2014.08.001

Matsushita, Y., Liu, J., Chu, A. K. Y., Tsutsumi-Arai, C., Nagata, M., Arai, Y., et al. (2023). Bone marrow endosteal stem cells dictate active osteogenesis and aggressive tumorigenesis. *Nat. Commun.* 14 (1), 2383. doi:10.1038/s41467-023-38034-2

Matsushita, Y., Nagata, M., Kozloff, K. M., Welch, J. D., Mizuhashi, K., Tokavanich, N., et al. (2020b). A Wnt-mediated transformation of the bone marrow stromal cell identity orchestrates skeletal regeneration. *Nat. Commun.* 11 (1), 332. doi:10.1038/s41467-019-14029-w

Matsushita, Y., Ono, W., and Ono, N. (2020a). Growth plate skeletal stem cells and their transition from cartilage to bone. *Bone* 136, 115359. doi:10.1016/j.bone.2020.115359

Matthews, B. G., Novak, S., Sbrana, F. V., Funnell, J. L., Cao, Y., Buckels, E. J., et al. (2021). Heterogeneity of murine periosteum progenitors involved in fracture healing. *Elife* 10, e58534. doi:10.7554/eLife.58534

Méndez-Ferrer, S., Michurina, T. V., Ferraro, F., Mazloom, A. R., MacArthur, B. D., Lira, S. A., et al. (2010). Mesenchymal and haematopoietic stem cells form a unique bone marrow niche. *nature* 466 (7308), 829–834. doi:10.1038/nature09262

Milgrom, C., Finestone, A., Levi, Y., Simkin, A., Ekenman, I., Mendelson, S., et al. (2000). Do high impact exercises produce higher tibial strains than running? *Br. J. sports Med.* 34 (3), 195–199. doi:10.1136/bjsm.34.3.195

Moore, E. R., Chen, J. C., and Jacobs, C. R. (2019). Prx1-expressing progenitor primary cilia mediate bone formation in response to mechanical loading in mice. *Stem cells Int.* 2019, 3094154. doi:10.1155/2019/3094154

Morgan, E. F., Unnikrisnan, G. U., and Hussein, A. I. (2018). Bone mechanical properties in healthy and diseased states. *Annu. Rev. Biomed. Eng.* 20, 119–143. doi:10.1146/annurev-bioeng-062117-121139

Ortinau, L. C., Wang, H., Lei, K., Deveza, L., Jeong, Y., Hara, Y., et al. (2019). Identification of functionally distinct Mx1+αSMA+ periosteal skeletal stem cells. *Cell Stem Cell* 25 (6), 784–796. doi:10.1016/j.stem.2019.11.003

Palumbo, C., and Ferretti, M. (2021). The osteocyte: from "prisoner" to "orchestrator". *J. Funct. Morphol. Kinesiol.* 6 (1), 28. doi:10.3390/jfmk6010028

Petzold, J., and Gentleman, E. (2021). Intrinsic mechanical cues and their impact on stem cells and embryogenesis. *Front. Cell Dev. Biol.* 9, 3112. doi:10.3389/fcell.2021.761871

Piekarski, K., and Munro, M. (1977). Transport mechanism operating between blood supply and osteocytes in long bones. *Nature* 269 (5623), 80–82. doi:10.1038/269080a0

Riffault, M., Johnson, G. P., Owen, M. M., Javaheri, B., Pitsillides, A. A., and Hoey, D. A. (2020). Loss of adenylyl cyclase 6 in leptin receptor-expressing stromal cells attenuates loading-induced endosteal bone formation. *JBMR plus* 4 (11), e10408. doi:10.1002/jbm4.10408

Robling, A. G., Castillo, A. B., and Turner, C. H. (2006). Biomechanical and molecular regulation of bone remodeling. *Annu. Rev. Biomed. Eng.* 8, 455–498. doi:10.1146/annurev.bioeng.8.061505.095721

Seike, M., Omatsu, Y., Watanabe, H., Kondoh, G., and Nagasawa, T. (2018). Stem cell niche-specific Ebf3 maintains the bone marrow cavity. *Genes and Dev.* 32 (5-6), 359–372. doi:10.1101/gad.311068.117

Shen, B., Tasdogan, A., Ubellacker, J. M., Zhang, J., Nosyreva, E. D., Du, L., et al. (2021). A mechanosensitive peri-arteriolar niche for osteogenesis and lymphopoiesis. *Nature* 591 (7850), 438–444. doi:10.1038/s41586-021-03298-5

Shi, Y., He, G., Lee, W.-C., McKenzie, J. A., Silva, M. J., and Long, F. (2017). Gli1 identifies osteogenic progenitors for bone formation and fracture repair. *Nat. Commun.* 8 (1), 2043. doi:10.1038/s41467-017-02171-2

Shu, H. S., Liu, Y. L., Tang, X. T., Zhang, X. S., Zhou, B., Zou, W., et al. (2021). Tracing the skeletal progenitor transition during postnatal bone formation. *Cell Stem Cell* 28 (12), 2122–2136.e3. doi:10.1016/j.stem.2021.08.010

Siclari, V. A., Zhu, J., Akiyama, K., Liu, F., Zhang, X., Chandra, A., et al. (2013). Mesenchymal progenitors residing close to the bone surface are functionally distinct from those in the central bone marrow. *Bone* 53 (2), 575–586. doi:10.1016/j.bone.2012.12.013

Sivaraj, K. K., Jeong, H.-W., Dharmalingam, B., Zeuschner, D., Adams, S., Potente, M., et al. (2021). Regional specialization and fate specification of bone stromal cells in skeletal development. *Cell Rep.* 36 (2), 109352. doi:10.1016/j.celrep.2021.109352

Tikhonova, A. N., Dolgalev, I., Hu, H., Sivaraj, K. K., Hoxha, E., Cuesta-Domínguez, Á., et al. (2019). The bone marrow microenvironment at single-cell resolution. *Nature* 569 (7755), 222–228. doi:10.1038/s41586-019-1104-8

Turner, C. H., Forwood, M., Rho, J. Y., and Yoshikawa, T. (1994). Mechanical loading thresholds for lamellar and woven bone formation. *J. bone mineral Res.* 9 (1), 87–97. doi:10.1002/jbmr.5650090113

Verbruggen, S. W., Vaughan, T. J., and McNamara, L. M. (2012). Strain amplification in bone mechanobiology: a computational investigation of the *in vivo* mechanics of osteocytes. *J. R. Soc. Interface* 9 (75), 2735–2744. doi:10.1098/rsif.2012.0286

Wagner, W., Wein, F., Seckinger, A., Frankhauser, M., Wirkner, U., Krause, U., et al. (2005). Comparative characteristics of mesenchymal stem cells from human bone marrow, adipose tissue, and umbilical cord blood. *Exp. Hematol.* 33 (11), 1402–1416. doi:10.1016/j.exphem.2005.07.003

Worthley, D. L., Churchill, M., Compton, J. T., Tailor, Y., Rao, M., Si, Y., et al. (2015). Gremlin 1 identifies a skeletal stem cell with bone, cartilage, and reticular stromal potential. *Cell* 160 (1), 269–284. doi:10.1016/j.cell.2014.11.042

You, J., Yellowley, C., Donahue, H., Zhang, Y., Chen, Q., and Jacobs, C. (2000). Substrate deformation levels associated with routine physical activity are less stimulatory to bone cells relative to loading-induced oscillatory fluid flow. *J. Biomech. Eng.* 122 (4), 387–393. doi:10.1115/1.1287161

Yang, C., Liu, Y., Wang, Z., Lin, M., and Liu, C. (2022). Controlled mechanical loading improves bone regeneration by regulating type H vessels in a S1Pr1-dependent manner. *FASEB J.* 36 (10), e22530. doi:10.1096/fj.202200339RRR

Zannit, H. M., Brodt, M. D., and Silva, M. J. (2020). Proliferating osteoblasts are necessary for maximal bone anabolic response to loading in mice. *FASEB J.* 34 (9), 12739–12750. doi:10.1096/fj.202000614R

Zannit, H. M., and Silva, M. J. (2019). Proliferation and activation of Osterix-lineage cells contribute to loading-induced periosteal bone formation in mice. *JBMR plus* 3 (11), e10227. doi:10.1002/jbm4.10227

Zhong, L., Lu, J., Fang, J., Yao, L., Yu, W., Gui, T., et al. (2023). Csf1 from marrow adipogenic precursors is required for osteoclast formation and hematopoiesis in bone. *Elife* 12, e82112. doi:10.7554/eLife.82112

Zhong, L., Yao, L., Tower, R. J., Wei, Y., Miao, Z., Park, J., et al. (2020). Single cell transcriptomics identifies a unique adipose lineage cell population that regulates bone marrow environment. *Elife* 9, e54695. doi:10.7554/eLife.54695

Zhou, B. O., Yue, R., Murphy, M. M., Peyer, J. G., and Morrison, S. J. (2014). Leptin-receptor-expressing mesenchymal stromal cells represent the main source of bone formed by adult bone marrow. *Cell stem Cell* 15 (2), 154–168. doi:10.1016/j.stem.2014.06.008

Frontiers in Physiology

Understanding how an organism's components work together to maintain a healthy state

The second most-cited physiology journal, promoting a multidisciplinary approach to the physiology of living systems - from the subcellular and molecular domains to the intact organism and its interaction with the environment.

Discover the latest Research Topics

See more →

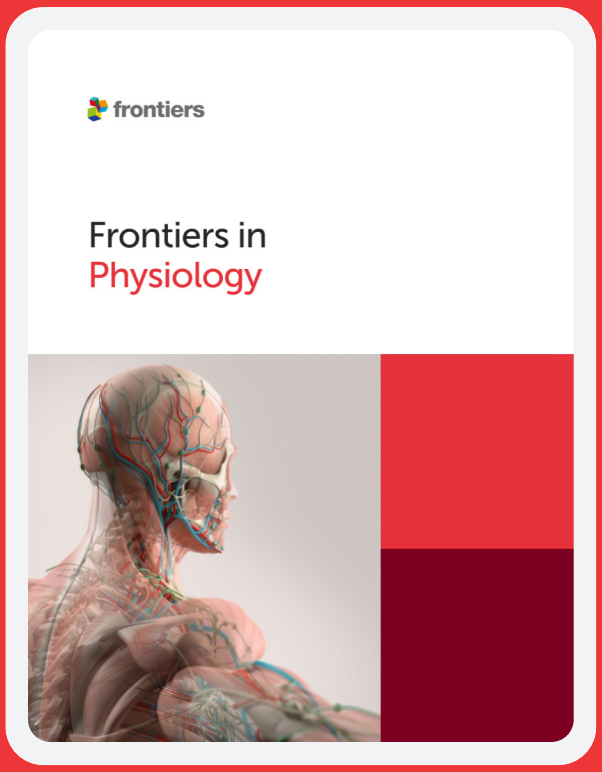

Frontiers

Avenue du Tribunal-Fédéral 34
1005 Lausanne, Switzerland
frontiersin.org

Contact us

+41 (0)21 510 17 00
frontiersin.org/about/contact